PPP2R1A Mutations in Gynaecologic Cancers: Functional Characterization and use in the Genomic Classification of Tumours

by

Melissa McConechy

B.Sc., Simon Fraser University, 2003

A THESIS SUBMITTED IN PARTIAL FULFILLMENT OF

THE REQUIREMENTS FOR THE DEGREE OF

Doctor of Philosophy

in

THE FACULTY OF GRADUATE AND POSTDOCTORAL STUDIES

(Pathology and Laboratory Medicine)

THE UNIVERSITY OF BRITISH COLUMBIA

(Vancouver)

April 2015

Abstract

Endometrial carcinoma is the most common gynaecological cancer in developed countries. The current pathologic classification system for endometrial cancer lacks reproducibility, which has hampered the development of new treatment approaches for these cancers. The PP2A phosphatase complexes are responsible for regulating many cellular pathways, and may play a large role in the deregulation of endometrial cancer-associated pathways.

Objectives: To determine the role of somatic *PPP2R1A* mutations in subtype specific classification of gynaecological tumours. In addition, mutational profiles from multiple genes will be used to improve the classification of the subtypes of endometrial carcinomas. Lastly, the functional effect of mutant PPP2R1A on PP2A subunit protein interactions will be determined, in the context of endometrial cancer cell lines.

Methods: Next-generation sequencing and Sanger sequencing was used to determine the presence of mutations in endometrial and ovarian carcinomas. PPP2R1A isogenic endometrial specific cell lines were generated using somatic cell gene knockout by homologous recombination. Co-immunoprecipitation coupled to mass spectrometry was used to determine the effects of the PPP2R1A W257L mutation on the ability to interact with PP2A subunits.

Results: Subtype-specific somatic *PPP2R1A* mutations were identified in endometrial serous carcinomas. Low-grade endometrial endometrioid carcinomas were defined by mutations in the genes: *ARID1A, PTEN, PIK3CA, CTNNB1*, and *KRAS*, whereas high-grade endometrioid also harbor *TP53* mutations. Endometrial serous carcinomas harbor mutations in *PPP2R1A, FBXW7, PIK3CA* and *TP53*. Consequently, the molecular profiles proved useful in assisting classification of seven tumours with overlapping morphological features that cause irreproducibility in diagnoses. Proteomic analysis of the isogenic cell lines determined that the PPP2R1A W257L mutation disrupts the interaction with PPP2R5C and PPP2R5D B subunits. In addition, PPP2R1A mutated protein caused an increased interaction with the endogenous PP2A inhibitor SET/I2PP2A.

Conclusions: The integration of mutational profiles and other genomic features will be used to improve clinical and pathological classification in endometrial tumours that are difficult to diagnose. *PPP2R1A* mutations are likely playing an important role in the transformation of gynaecological carcinoma, by disrupting PP2A subunit interactions with tumour suppressor functions. Increased interaction of mutant PPP2R1A with SET/I2PP2A adds another layer of

complexity to the tumour suppressive role of PP2A. In the future, targeting the PP2A complex with novel therapeutics could provide an alternative method for treating these gyneacological cancers with poor outcomes.

Preface

Chapter 2 is based on a published manuscript [1].

McConechy MK, Anglesio MS, Kalloger SE, Yang W, Senz J, Chow C, Heravi-Moussavi A, Morin GB, Mes-Masson AM, Australian Ovarian Cancer Study Group, Carey MS, McAlpine JN, Kwon JS, Prentice LM, Boyd N, Shah SP, Gilks CB, Huntsman DG, "Subtype-specific mutation of PPP2R1A in endometrial and ovarian carcinomas", The Journal of Pathology, 223(5), 567-573 © [2011] Pathological Society of Great Britain and Ireland, first published by John Wiley & Sons Ltd.

I was responsible for all experiments, writing, editing and coordination of the manuscript. MS Anglesio was a co-first author who contributed in interpretation, writing and editing of the manuscript. CB Gilks, DG Huntsman all assisted in experiment interpretation and manuscript writing. Dr. CB Gilks was also the primary pathologist to review all cases in this study. W Yang, J Senz, A Heravi-Moussavi, C Chow assisted with technical experimentation. SE Kalloger, AOCSG, AM Mes-Masson assisted with obtaining and collection of tissue. All other authors assisted in the interpretation and editing of the manuscript. All immunohistochemistry was performed at GPEC (Genetic Pathology Evalutation Centre) at the Jack Bell Research Centre, and scored with Dr. CB Gilks.

The Ethics and certificates involved in this study are the following:

BC Cancer Agency Research Ethics Board - H05-60119 The Gynaecological Cancer Tissue Bank

BC Cancer Agency Research Ethics Board - H02-61375 Immunohistochemical and Fluorescent In-Situ Hybridization (FISH) Studies of Cancer

BC Cancer Agency Research Ethics Board - H08-01411 NGS in Tumours

BC Cancer Agency Research Ethics Board - H09-02153 Validation Cohort Study

UBC Biosafety Committee – B14-0070 Huntsman Lab Biosafety

Chapter 3 is mostly based on a published manuscript [2]. There are portions of this chapter that are unpublished data.

McConechy MK, Ding J, Cheang MC, Wiegand KC, Senz J, Tone AA, Yang W, Prentice LM, Tse K, Zeng T, McDonald H, Schmidt AP, Mutch DG, McAlpine JN, Hirst M, Shah SP, Lee CH, Goodfellow PJ, Gilks CB, Huntsman DG, "Use of mutation profiles to refine the classification of endometrial carcinomas", The Journal of Pathology, 228(1), 20-30 © [2012] Pathological Society of Great Britain and Ireland, first published by John Wiley & Sons Ltd.

I was responsible for all aspects of the study including sample preparation for exon capture sequencing, all validation sequencing, data analysis, writing, editing, development of all manuscript figures, and coordination of the manuscript. J Ding was a co-first author who was responsible for the exon-capture sequencing analysis, writing and editing of the manuscript. MC Cheang performed the statistical analysis. KC Wiegand, J Senz, AA Tone, W Yang, LM Prentice, K Tse, T Zeng, H McDonald, all assisted in technical experimentation or study coordination. K Tse, T Zeng, H McDonald designed the exon capture probes and performed the capture and library sequencing. AP Schmidt, DG Mutch, JN McAlpine, PJ Goodfellow assisted with collection of samples. SP Shah, M Hirst, CH Lee, PJ Goodfellow, CB Gilks, DG Huntsman all assisted in experimental interpretation and manuscript editing. Dr. CB Gilks and Dr. CH Lee were the primary pathologists to review all cases in this study. All immunohistochemistry was performed at GPEC (Genetic Pathology Evaluation Centre) at the Jack Bell Research Centre, and scored with Dr. CB Gilks. Dr. H Horlings assisted with the immunohistochemistry scoring for C-Myc, and Samuel Leung calculated H-scores for the C-Myc TMA analysis.
I also performed the technical experiments and analysis of the additional unpublished sequencing in this chapter.

The ethics and certificates involved in this study are the following:
BC Cancer Agency Research Ethics Board - H05-60119 The Gynaecological Cancer Tissue Bank
BC Cancer Agency Research Ethics Board - H02-61375 Immunohistochemical and Fluorescent

In-Situ Hybridization (FISH) Studies of Cancer
BC Cancer Agency Research Ethics Board - H08-01411 NGS in Tumours
BC Cancer Agency Research Ethics Board - H09-02153 Validation Cohort Study
UBC Biosafety Committee – B14-0070 Huntsman Lab Biosafety

Chapter 4 is based on a published manuscript [3].

M.K. McConechy, J Ding, J Senz, W Yang, N Melnyk, A.A. Tone, L.M. Prentice, K Wiegand, J.N. McAlpine, S.P. Shah, C-H Lee, P.J. Goodfellow, C.B. Gilks, D.G. Huntsman, "Ovarian and endometrial endometrioid carcinomas have distinct CTNNB1 and PTEN mutation profiles", Modern Pathology (2014) (27), 128-134.

Chapter 4 is an extension of the Chapter 3 study. I was responsible for all aspects of the manuscript including sample preparation for exon capture sequencing, all validation sequencing, data analysis, writing, editing development of all manuscript figures, and coordination of the manuscript. J Ding, J Senz, W Yang, N Melnyk, A.A. Tone, L.M. Prentice, K Wiegand, performed technical experimentation or assisted with study coordination. J.N. McAlpine, S.P. Shah, C-H Lee, P.J. Goodfellow, C.B. Gilks, D.G. Huntsman assisted in experimental interpretation and manuscript editing. Dr. CB Gilks was also the primary pathologist to review all cases in this study.

The ethics and certificates involved in this study are the following:
BC Cancer Agency Research Ethics Board - H05-60119 The Gynaecological Cancer Tissue Bank
BC Cancer Agency Research Ethics Board - H08-01411 NGS in Tumours
BC Cancer Agency Research Ethics Board - H09-02153 Validation Cohort Study
UBC Biosafety Committee – B14-0070 Huntsman Lab Biosafety

Chapter 5 is unpublished material, and was performed in collaboration with Dr. James Brenton's laboratory at the University of Cambridge (Cambridge, UK). I designed and generated the PPP2R1A targeting vectors in Vancouver, and then traveled to Dr. James Brenton's lab in Cambridge to undergo the transduction and generation of the Hec1A isogenic knockout cell line. Dr. Jian Xian provided assistance and standard protocols for the somatic cell knockout technique in Dr. James Brenton's laboratory. The cell lines were then shipped back to Vancouver for analysis and further experiments. Natalyia Melnyk performed all FISH experiments, otherwise I designed and performed all other technical experiments and interpretation described in this Chapter.

The certificates involved in this study are the following:
UBC Biosafety Committee – B14-0070 Huntsman Lab Biosafety
UBC Biosafety Committee – B12-0017 PP2A protein serine/threonine phosphatase mutations in cancer. Alternative splicing and CLK inhibitors.

Chapter 6 is unpublished material, performed in collaborations with Dr. Gregg Morin's laboratory in the Genome Sciences Centre at the BC Cancer Research Centre. I performed all technical experiments and interpretation. The mass spectrometry experiments were ongoing optimization experiments over the course of my PhD studies with assistance from Dr. Annie Moradian, Dr. Vincent Chen and Dr. Christopher Hughes. The final mass spectrometry experiments and analysis presented in this thesis were performed in collaboration with Dr. Christopher Hughes. Statistical consultation was performed with Dr. Aline Talhouk.

The certificates involved in this study are the following:
UBC Biosafety Committee – B14-0070 Huntsman Lab Biosafety
UBC Biosafety Committee – B12-0017 PP2A protein serine/threonine phosphatase mutations in cancer. Alternative splicing and CLK inhibitors.

Chapter 7 is unpublished material and is written solely by myself.

Appendix D is based on published material that is currently available as an early view online version on the website for The Journal of Pathology: Clinical Research.

McConechy MK, Hoang LN, Chi MH, Senz J, Yang W, Rozenberg N, Mackenzie R, McAlpine JN, Huntsman DG, Clarke BA, Gilks, CB, Lee CH. "In-depth molecular profiling of the biphasic components of uterine carcinosarcomas", The Journal of Pathology: Clinical Research (2015). doi: 10.1002/cjp2.18.

Appendix D is an extension of the Chapter 2 carcinosarcoma study. I was responsible for all aspects of the manuscript including sample preparation for targeted gene sequencing, all validation sequencing, data analysis, writing, editing development of all manuscript figures, and coordination of the manuscript. L.N. Hoang is a co-first author responsible for all pathologic review of samples, coordination of the study, preparation of figures, editing and writing of the manuscript. M.H. Chi, J Senz, W Yang, N Rozenberg, R MacKenzie performed technical experimentation or assisted with study coordination. J.N. McAlpine, D.G Huntsman, B.A. Clarke C.B. Gilks, CH Lee D.G. assisted with review, editing and interpretation of data for the manuscript. CH Lee assisted with experimental design, supervision of the study, interpretation and final preparations of the manuscript including writing and editing.

The ethics and certificates involved in this study are the following:
BC Cancer Agency Research Ethics Board - H05-60119 The Gynaecological Cancer Tissue Bank
BC Cancer Agency Research Ethics Board - H08-01411 NGS in Tumours
BC Cancer Agency Research Ethics Board - H09-02153 Validation Cohort Study
UBC Biosafety Committee – B14-0070 Huntsman Lab Biosafety

Table of Contents

List of Tables

List of Figures

List of Symbols

α	alpha
β	beta
γ	gamma
δ	delta
ε	epsilon

List of Abbreviations

Ab	Antibody
AKT	V-AKT Murine Thymoma Viral Oncogene Homolog (Protein Kinase B Alpha)
ARID1A	AT Rich Interactive Domain 1A (SWI-like)
ATM	Ataxia Telangiectasia
BAC	Bacterial Artificial Chromosome
BRCA1	Breast Cancer 1, Early Onset
BRCA2	Breast Cancer 2, Early Onset
BRAF	V-Raf Muring Sarcoma Viral Oncogene Homolog B
BSO	Bilateral Salpingo -Oophorectomy
cDNA	copy DNA
CCNE1	Cyclin E
CDK12	Cyclin-dependent kinase 12
CDKN2A	Cyclin-dependent kinase inhibitor 2A
CHD4	Chromodomain Helicase DNA Binding Protein 4
C-MYC	V-Myc Avian Myelocytomatosis Viral Oncogene Homolog
CNA	Copy Number Analysis
COSMIC	Catalogue of Somatic Mutations in Cancer
CTNNB1	Catenin (cadherin-associated protein), Beta 1
Co-IP	Co-Immunoprecipitation
DNA	Deoxyribonucleic Acid
DTT	Dithiothreitol
EDM	Exonuclease Domain Mutations
EEC	Endometrial Endometrioid Carcinoma
EEC-3	High-grade (grade 3) Endometrial Endometrioid Carcinoma
EP300	E1A Binding Protein p300
ER	Estrogen Receptor
ESC	Endometrial Serous Carcinoma
FBS	Fetal Bovine Serum
FBXW7	F-box and WD repeat domain containing 7, E3 Ubiquitin Protein Ligase
FFPE	Formalin Fixed Paraffin Embedded

FIGO	International Federation of Gynecology and Obstetrics
FISH	Fluorescence In-Situ Hybridization
HEAT	Huntington Elongation-A subunit TOR
HEPES	4-(2-hydroxyethyl)-1-piperazineethanesulfonic acid
HGSC	High-Grade Serous Carcinoma- Ovarian Cancer
HPLC	High Performance Liquid Chromatography
IAA	Iodoacetamide
IGBP1	Immunoglobulin (CD79A) Binding Protein 1, Protein Alpha-4
IP	Immunoprecipitation
iTRAQ	Isobaric tags for relative and absolute quantitation
KO	Knockout
KRAS	Kirsten Rat Sarcoma Viral Oncogene Homolog
LOH	Loss of Heterozygosity
LS	Lynch Syndrome
M-FISH	Metaphase Fluorescence In-Situ Hybridization
MLH1	MutL Homolog 1
MMMT	Malignant Mixed Müllerian Tumour
MRM-MS	Multiple Reaction Monitoring-Mass Spectrometry
MSH2	MutS Homolog 2
MSH6	MutS Homolog 6
MSI	Microsatellite Instability
OCCC	Ovarian Clear Cell Carcinoma
OEC	Ovarian Endometrioid Carcinoma
PARP	Poly ADP Ribose Polymerase
PBS	Phosphate Buffered Saline
PCR	Polymerase Chain Reaction
PI3K	Phosphatidylinositol-4,5-bisphosphate 3-kinase
PIK3CA	Phosphatidylinositol-4,5-bisphosphate 3-kinase, Catalytic Subunit alpha
PIK3R1	Phosphoinositide-3-Kinase, Regulatroy Subunit 1 alpha
PIK3R2	Phosphoinositide-3-Kinase, Regulatory Subunit 2 beta
PMS2	PMS2 Post Meiotic Segregation Increased 2 (S. Cerevisiae)

POLE	Polymerase (DNA), epsilon, catalytic subunit
PP2A	Protein Phosphatase 2A
PPP2R1A	Protein Phosphatase 2, Regulatory Subunit A, alpha
PPP2R1B	Protein Phosphatase 2, Regulatory Subunit A, beta
PPP2CA	Protein Phosphatase 2, Catalytic Subunit C, alpha
PPP2CB	Protein Phosphatase 2, Catalytic Subunit C, beta
PPP2R2A	Protein Phosphatase 2, Regulatory Subunit B, alpha
PPP2R2B	Protein Phosphatase 2, Regulatory Subunit B, beta
PPP2R5A	Protein Phosphatase 2, Regulatory Subunit B', alpha
PPP2R5B	Protein Phosphatase 2, Regulatory Subunit B', beta
PPP2R5C	Protein Phosphatase 2, Regulatory Subunit B', gamma
PPP2R5D	Protein Phosphatase 2, Regulatory Subunit B', delta
PPP2R5E	Protein Phosphatase 2, Regulatory Subunit B', epsilon
PPP2R4	Protein Phosphatase 2A Activator, Regulatory Subunit 4 *(PTPA*)
PPME1	Protein Phosphatase Methyltransferase 1
PR	Progesterone Receptor
PRM	Parallel Reaction Monitoring
pSEPT	plasmid Synthetic Exon Promoter Trap
PTEN	Phosphatase and Tensin Homolog
RNA	Ribonucleic Acid
SCNA	Somatic Copy Number Analysis
SET	SET Nuclear Oncogene
SILAC	Stable Isotope Labeling of Amino Acids in Cell Culture
SNP	Single Nucleotide Polymorphism
SNV	Single Nucleotide Variant
SP3	Single-Pot Solid-Phase-enhanced Sample Preparation
SPOP	Speckle-Type POZ Protein
TAH	Total Abdominal Hysterectomy
TCGA	The Cancer Genome Atlas
TLH	Total Laparoscopic Hysterectomy
TMA	Tissue Microarray

TMT	Tandem Mass Tags
TP53	Tumour Protein p53
UCSC	University of California Santa Cruz
WHO	World Health Organization

Glossary

Allelic Fraction - sequencing term used to describe the variant read number over the total depth of that specific position. Also referred to as allele ratios.

Bilateral Salpingo –Oophorectomy – removal of cervix, both fallopian tubes, and ovaries

Carcinoma – cancer that arises from epithelial cells

Mesenchymal – cells that develop into lymphatic, circulatory and connective tissues such as bone and cartilage.

Myometrium – the uterine smooth muscle layer that is found between the epithelium and the serosa (outer layer) of the uterus.

Sarcoma – a tumour that arises from mesenchymal cells (bone, fat, cartilage, vascular cells)

Simple Hysterectomy – also referred to as total hysterectomy, which includes removal of the uterus and cervix.

Squamous - flat looking cells that make up an epithelium

Villoglandular – papillary pattern of tumour cells

Acknowledgements

I would first like to thank my supervisor Dr. David Huntsman for his utmost support throughout my PhD studies. From the start of my program, David believed in my technical abilities and allowed me to be a part of many different projects. This has allowed me to experience a wide range of research topics in science and medical fields. I feel very lucky to be a part of Dr. Huntsman's lab and the team of OvCaRe researchers. Thank you David for allowing me to have a work/life balance, where you were so supportive of my love for volleyball, snowboarding and family life. All of our meetings over the years have been invaluable, and I appreciate your always insightful advice and support regarding my future career as a scientist.

To my second mentor, Dr. Blake Gilks, thank you very much for always taking the time from your busy schedule to talk and teach from behind the microscope. You have given me so much valuable advice over the years with respect to career and life, which I appreciate a great deal. Thank you very much for all the assistance with my manuscripts, I could not have finished these projects with out your expertise.

Thank you to all my committee members, Dr. Gregg Morin, Dr. Sohrab Shah, and Dr. Mark Carey for your valuable input on my thesis research. Your different areas of expertise have allowed me to acquire a wide range of exposure to cancer genomics, proteomics and medicine. Also thank you to Dr. Haydn Pritchard for agreeing to be my committee chair, and your respected advice as a graduate advisor. I would also like to thank Dr. Kevin Bennewith who came to my rescue to act as my committee chair on a few different occasions. I am very grateful for your help.

I would like to give additional thanks to Dr. Gregg Morin for your support and assistance in the proteomics work of my thesis. It was a bumpy road for the both of us, but overall it was an important learning experience for my science career. Thank you to all of the GSC staff that has helped me along the way: Dr. Grace Cheng, Dr. Christopher Hughes, Dr. Vincent Chen, and Dr. Annie Moradian.

The collaborations I have had over the past 5 years have meant a great deal to me. Thank you to Dr. Jessica McAlpine, Dr. Cheng-Han Lee, and Dr. Lien Hoang for allowing me to be a part of all our collaborations. I have learned so much from our interactions over the years, and I appreciate your patience and time in meetings to finish up all of our exciting projects. Also, thank you to Dr. James Brenton for allowing me to visit your laboratory, and have an amazing

learning experience that was extremely important for the advancement of my science career. Your guidance along with Dr. Jian Xian's expertise was priceless in constructing the endometrial isogenic cell lines. Lastly, thank you to Dr. Paul Goodfellow who provided endometrial samples and guidance in this research.

Special thanks to all the members of the past and present Huntsman laboratory (Winnie, Janine, Alicia, Clara, Sarah, Samantha, Niki, Dawn, Michelle, Natalyia, Genny, Leah, Rob, Tony, Hugo, Mike, Kim, Satoshi), CTAG laboratory (Peggy, Julie, Ying, Amy, Julie, Sarah, Sylvia), GPEC laboratory (Christine, Sherman, Angela), the OvCaRe team (Jessica, Anna, Margaret, Karen), the Shah lab (Ali, Jiarui, Karey, Yikan) and the Aparicio lab (Adrian, Cherry). Thank you to all of your for assistance in all aspect of my research over the last five years. Special thanks to Dr. Alicia Tone, Winnie Yang, Janine Senz, Natalyia Meylnk, and Samantha Hansford for all the laughs, talks and shoulder to cry on. Also, thank you to Jiarui Ding who was instrumental for the completion of the exon capture sequencing analysis. I could not have done any of it without the support of so many great people.

I have been very fortunate over the period of my PhD research to be funded by many scholarships, travel funds and awards. I would like to thank the following organizations for their support of my PhD career: UBC, CIHR Masters and CIHR PhD Fellowships, Canadian Cancer Society, Ovarian Cancer Canada, and the Evelyn Martin Memorial Fund.

Last but not least, I would like to thank my family and friends for their utmost support in my Ph.D. endeavor. A very special thanks to my parents who have always supported me in my independence and academics. Dad and Mom, thank you for doing whatever you did to make me love school and want to further my education. Dad, thank you for attending my defence that meant a great deal to me. Thank you to my sisters and brothers for your support, especially to Kirstin who has been my number one supporter since the beginning of the crazy thought of starting a PhD. Finally, thank you to Thibault who has been my rock in keeping me grounded over the last few years. Thank you for your love and patience with my long workdays and studying, and especially for keeping me company at the lab during a few late-night experiments. You mean the world to me, and hope we can continue to support each other in our life adventures. I am very grateful for everyone's support.

Dedication

I dedicate this to my family, with special dedication to my sister Kirstin, and my supportive partner Thibault.

Chapter 1: Introduction

1.1 Endometrial Carcinoma

Endometrial cancer, or cancer of the uterus, is the most common gyneacological malignancy in developed countries, and is the sixth most commonly diagnosed cancer in women worldwide [4]. In 2011, an estimated 143,000 new cases of endometrial cancer were reported, causing death in about 33,000 women in developed countries, and this incidence is rising [4, 5]. This is likely due to a variety of factors including increased worldwide obesity, the growing aging population, and prior tamoxifen use [6]. The majority of endometrial cancers occur in post-menopausal women; 90% being sporadic and 10% with a hereditary nature [7]. Endometrial tumours are diagnosed as multiple histopathologic subtypes: endometrioid, serous, carcinosarcoma, clear cell and mucinous carcinoma. In 1983, Bokhman proposed the classical dualistic histopathological model separating this cancer into two broad types; estrogen-dependent endometrioid endometrial carcinoma (type 1), and non-endometrioid endometrial carcinoma (type II) [8]. Approximately 70-80% of endometrial tumours are diagnosed as low-grade, low-stage endometrial endometrioid carcinomas (EEC), which are generally confined to the body of the uterus, and can be cured by a simple hysterectomy [9]**.** In contrast, non-endometrioid carcinomas constitute 10-20% of the histopathological subtypes serous, clear cell and carcinosarcomas. These cancers are responsible for a disproportional majority of endometrial cancer deaths, as they are generally high-grade, aggressive, and present in older post menopausal women [10]. Endometrial serous carcinomas (ESC) also referred to as high-grade endometrial serous carcinoma, uterine papillary serous carcinoma, or uterine serous carcinoma, are aggressive and invasive, and tend to relapse with metastatic disease [11-13]. The 5-year overall survival for women with serous carcinoma was 45.9%, and those with stage III and stage IV disease were 37.3% and 19.9% respectively [14, 15]. Carcinosarcomas, also referred to as MMMT, and clear cell carcinomas are extremely rare high-grade endometrial subtypes, accounting for less than 5% of all endometrial cancers that tend to recur locally and can metastasize to distant areas [16]. For the purpose of this body of research, I will focus mainly on the histological subtypes endometrioid and serous carcinomas with brief mentions of carcinosarcomas.

In the current clinical setting, low-stage, low-grade EEC patients undergo hysterectomy by total laparoscopic hysterectomy (TLH) or total abdominal hysterectomy (TAH) with bilateral salpingo-oophorectomy (BSO). The hysterectomy and BSO involves removal of the uterus, cervix, fallopian tubes and ovaries. Histopathological diagnosis is extremely important in clinical management, as adjuvant radiation and chemotherapy regimes will be dependent on cell type (endometrioid or non-endometrioid), grade and stage. EECs with greater than stage 1B and grade 3 nuclei will generally undergo adjuvant radiotherapy and chemotherapy, and is always administered to women diagnosed with serous, carcinosarcomas and clear cell carcinomas with myometrial invasion. This will include cycles of chemotherapeutic agents carboplatin and paclitaxel, as this treatment has been shown to be efficacious with low toxicity in advanced or recurrent endometrial carcinoma [17, 18].

1.1.1 Histopathology of Endometrial Carcinoma Subtypes

Endometrial carcinoma originates from the epithelial lining of the uterus. In premenopausal women, endometrial glandular cells undergo a monthly cycle (average of 28 days) consisting of the menstrual phase, followed by proliferative and secretory phases [19]. The histopathologic definitions of endometrial tumours are guided by the international WHO (World Health Organization) classification of female reproductive organs [20] and FIGO (International Federation of Gynecology and Obstetrics) [21]. The morphology of low-grade EEC is distinct from that of high-grade serous carcinoma [22]. The epithelial tumour cells of grade 1 EEC are well differentiated with apparent glandular or villoglandular structure with less that 5% solid structure [20] (Figure 1.1). Generally, grade 2 EECs range from 6-50% solid growth patterns with moderate differentiation patterns. Tumour grade increases to grade 3 with the presence of more than 50% solid growth and cellular atypia, including atypical pleomorphic nuclei with poor differentiation.

Endometrial serous tumours are all grade 3 neoplasms with complex papillary and glandular structures, often with solid growth, and nuclear pleomorphism [20]. Serous carcinomas are characterized by the presence of many mitotic figures per field of view, and large prominent nucleoli (Figure 1.1). Epithelial cells in the myometrium indicate invasion, however the presence

of metastatic cells to sites outside the uterus may be evident even with lack of myometrial invasion [20].

High-grade endometrial adenocarcinomas can have overlapping morphological features, consequently making a pathologist's diagnoses challenging [22, 23]. Some serous tumours exhibit well-differentiated glandular structures that are characteristic of endometrioid

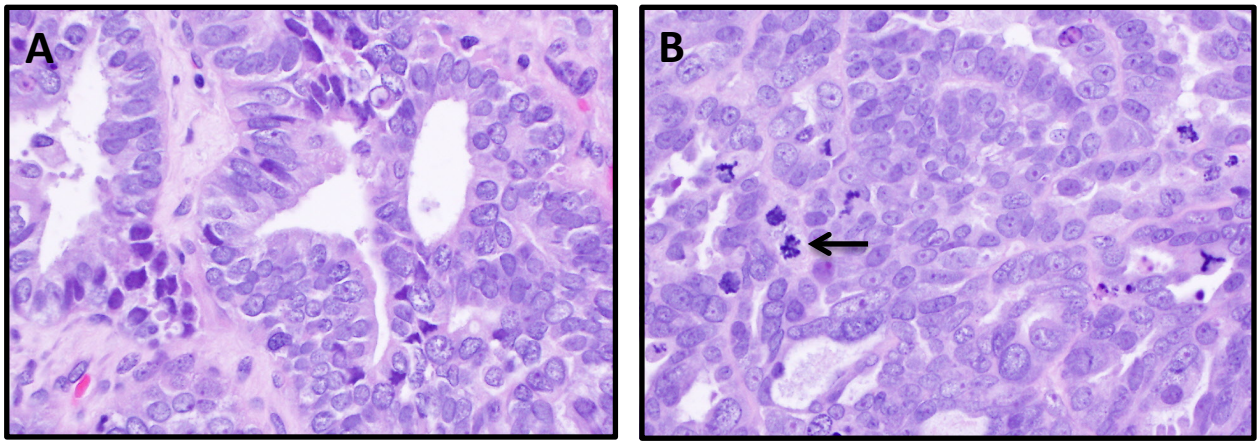

Figure 1.1 Histopathology of endometrial carcinomas
A. H&E (Hematoxylin and Eosin) staining of a low-grade endometrial endometrioid carcinoma with glandular structures. **B.** H&E staining of an endometrial serous carcinoma with solid pattern, pleomorphic nuclei and many mitotic figures (arrow).

carcinomas, and some high-grade endometrioid tumours have serous-like solid papillary growth patterns with a high mitotic index [22]. The apparent ambiguity of differentiation associated histologic features can make the process of differentiating serous from endometrioid cancers extremely challenging, which can ultimately affect the clinical management of patients. This is particularly difficult in cases with mixed histologic features (see Chapter 3 Figure 3.2 and Table 3.5).

Carcinosarcomas are biphasic high-grade tumours with carcinomatous (epithelial) and sarcomatous (mesenchymal) components, which can be found as tumours with separate distinct entities or with mixed cell-types [24]. Histologically, the epithelial component can appear with endometrioid or serous morphology, and the sarcomatous can include homologous and heterologous elements. Homologous elements include cell types that are derived from uterine

tissues, and heterologous elements include cell types derived outside the uterus (cartilage, skeletal muscle) such as rhabdomyosarcoma, chondrosarcoma, and osteosarcoma [25].

1.1.2 Molecular Genetics of Endometrial Carcinoma

1.1.2.1 Endometrial Endometrioid Carcinoma (EEC)

Endometrial endometrioid carcinomas have been molecularly characterized using immunohistochemistry and DNA sequencing, often on a small scale, by observing only one to two proteins or genes at a time. However, advances in next-generation sequencing technology have allowed investigation of whole genomes and targeted gene panel sequencing. EECs are characterized by microsatellite instability (MSI) (17-26%) [26], PI3K pathway alterations (80%) [27, 28], *ARID1A (40%)*, *KRAS (8-40%)*, *FGFR2 (5-16%)* and *CTNNB1 (2-45%)* mutations [2, 29, 30]. *PTEN* is the most frequently altered gene in EEC (26-80%); mostly due to mutations, rare copy number alteration events, deleted by promoter methylation, or protein degradation to ultimately cause activation of the PI3K pathway [31]. In the TCGA data set, *PTEN* gene abnormalities were seen in 66% of cases (153/232); of those 147/153 (96%) harbor mutations, 4/153 (3%) with homozygous deletions, 2/153 (1.3%) with homozygous deletions and concurrent mutations, 1/153 with an amplification alteration [32, 33]. Overall, EECs also have a high frequency (80%) of activating mutations in additional PI3K pathway genes; *PIK3CA* (30-50%), *PIK3R1* (20-40%), *PIK3R2* (5%) [27]. Mutations in *PIK3CA* and *PIK3R1* are generally mutually exclusive, however are often found concurrently with *PTEN* alterations [27, 28]. *ARID1A* mutations, a component of the SWI/SNF chromatin-remodeling complex, result in BAF250a protein loss, and are frequently found in low-grade and high-grade EEC [34, 35]. Mutations in *TP53* are infrequent in low-grade EECs, however high-grade EECs do harbor a higher frequency of *TP53* alterations.

The autosomal dominant hereditary condition, Lynch syndrome (LS), predisposes about 3% of women for EEC, and about 3% of all colorectal cancers [36, 37]. Women with LS have a 40-60% lifetime risk of acquiring endometrial cancer, and 10-12% risk for ovarian cancer [38], which is caused by germline mutations in mismatch repair (MMR) genes (*MLH1, MSH2, MSH6*, and *PMS2*) [39]. This genetic defect results in tumour microsatellite instability (MSI), and can be

detected by immunohistochemistry or DNA-based MSI analysis of tumours and germline tissue [39]. Clinical testing is performed on patients diagnosed with EEC, and can have benefits for both affected individuals, and at-risk family members with potential MMR germline mutations [38].

1.1.2.2 High-Grade Endometrial Carcinoma: Serous, Clear Cell, Carcinosarcoma

The endometrial high-grade subtypes characteristically do not harbor the same high frequency of mutations found in EECs, and are molecularly different than EECs [40]. Endometrial serous carcinomas are often aneuploid, with fewer mutational aberrations than EECs [41]. *TP53 (50-90%)* mutations are the most frequent molecular alteration, with *PPP2R1A (20-40%)* and *FBXW7 (20%)* mutations also present in a large proportion of serous carcinomas [1, 2, 29, 42]. The first exome sequencing of serous carcinomas identified mutations harbored in chromatin remodeling genes (*ARID1A, EP300, CHD4*) and ubiquitin ligase complex genes (*FBXW7, SPOP*) [43]. Most endometrial serous carcinomas exhibit high protein expression of p16, encoded by the gene *CDKN2A*, which is distinct from EEC [23]. This is also a distinct feature compared to ovarian high-grade serous carcinoma, as *CDKN2A* is frequently downregulated [44]. Conversely, Cyclin E (*CCNE1*) is overexpressed in a subset of poorly differentiated endometrial carcinomas, as measured by IHC [45], as well as exhibiting copy number amplifications [46], which is also a similar feature of ovarian high-grade serous carcinomas.

Endometrial clear cell carcinomas (CCC) are extremely rare tumours; therefore few molecular studies have been completed. Most of what is known about these rare tumours comes from observations of ovarian clear cell carcinomas (OCCC). Similar to OCCC, *ARID1A* and *PIK3CA* are frequently mutated [47, 48]. However in contrast to OCCC, *TP53* (33%) mutations can be identified in endometrial CCC. During my PhD studies, I assisted with a published study wherein 14 prototypical endometrial CCC tumours were sequenced with a targeted endometrial specific gene panel. Mutations were detected in genes involved in chromatin remodeling and transcriptional regulation (*ARID1A, ZFHX3, TSPYL2*), and ubiquitin-mediated proteolysis (*SPOP* and *FBXW7*) [49]. Furthermore, mutations in *TP53* (29%) and *PPP2R1A* (20%) were discovered, indicating these tumours have a mutational profile closely related to endometrial serous carcinomas.

Few comprehensive multi-gene studies have been performed to detect molecular alterations in carcinosarcomas, however low frequency mutations have been identified in *KRAS* and *PIK3CA* [50]. Defective MMR has been identified in 20% of carcinosarcomas, and a high frequency of *TP53* aberrations in both the carcinoma (68%) and sarcoma (64%) components [51]. Based on molecular alterations, Taylor *et al*. and others, has provided evidence to suggest that carcinosarcomas are of monoclonal origin; therefore proposing that the sarcomatous component is derived from the carcinomatous component through trans-differentiation [50]. This theory is still yet to be fully established, as more comprehensive molecular studies are needed.

I also performed targeted sequencing of 27 genes in 30 cases of endometrial carcinosarcomas [52] (Appendix D) as an extension to the work presented in Chapter 3. This involved sequencing the carcinoma and sarcoma components as separate entities, as well as metastatic sites when available. Sequencing mutational analysis illustrates *TP53* as the most frequently mutated gene in 24/30 (80%) carcinosarcomas, yet genes in the *PIK3CA* pathway (*PTEN, PIK3CA, PIK3R1*, and *PIK3R2*) were mutated in 20 of 30 (67%) of cases. The patterns of mutations can be categorized as serous-like mutation profiles, and endometrioid-like mutation profiles (Appendix D Figure D.4), which supports the observations in Chapter 3 of this thesis [2]. These mutation patterns also provides additional evidence to support the monoclonal theory of carcinosarcomas; the theory of trans-differentiation of the carcinoma to give rise to the sarcoma component of the tumour.

1.2 Controversies in High-Grade Endometrial Classification

Current endometrial classification is based solely on histological subtypes [53]. Although this classification works well for low-grade EECs, for high-grade subtypes (grade 3 EECs and serous carcinomas) there is poor pathological interobserver agreement rendering it of dubious utility [54]. The current grading system is also irreproducible, and there are inconsistencies in demonstrating its prognostic relevance. Serous carcinomas can often harbor endometrioid-like features and vise versa, which leads to some of this discordance. Due to the aggressive nature of serous carcinomas, misdiagnoses could change clinical management of the patient; therefore improved classification is much needed. The data presented in Chapter 3 suggests that mutational

profiles may provide useful information for improving the classification of difficult to diagnose endometrial carcinomas. Furthermore, an extension of my work presented in Chapter 3 attempted to correlate histotype and genotype in a subset of these problematic diagnoses [55]. Based purely on morphological cell type, the interobserver concordance of the diagnoses was very poor (K value =0.55). However, when immunostaining and genotype were considered, diagnostic reproducibility improved to K=0.68. This study shows that in the future, molecular and histological features will be needed for improving the diagnoses of difficult endometrial cases.

Many of the core driver mutations in endometrial cancers have been identified; The Cancer Genome Atlas (TCGA) project acquired 373 endometrial tumours to improve the definitions of endometrial genomes. Based on full exome sequencing and SNP arrays, mutations and copy number alterations (CNAs) were identified, leading to the classification of 4 categories of tumours: *POLE* ultra-mutated (232×10^{-6} mutations per Mb), MSI hypermutated (18×10^{-6} mutations per Mb) (most with MLH1 promoter methylation), copy-number low, and copy-number high [42]. Low-grade EECs were categorized into *POLE* ultra-mutated, MSI hypermutated, and copy-number low groups. Pathologically defined high-grade EECs were classified mostly into the *POLE* ultra-mutated and copy-number high categories, whereas serous carcinomas were placed primarily in the copy-number high group. Although this analysis did not result in the discovery of novel recurrently mutated genes, the *POLE* mutated tumours, which have a unique clinical phenotype is of great interest. The distribution of other known mutations in the TCGA defines subtypes of endometrial cancer [42] along with my own work of this disease [2], which predated TCGA is discussed in Chapter 4.

POLE encodes for the catalytic domain of DNA polymerase ε, with mutations identified in the protein exonuclease domain [42, 56, 57]. DNA polymerase ε is involved in DNA replication and repair; therefore exonuclease domain mutations (EDM) may cause inefficient proofreading for DNA replication and repair, thus resulting in the ultra-mutated phenotype. Additional studies and TCGA have identified the presence of *POLE* EDM mutations in 7-15% of EECs [42, 57, 58] with a frequency of 7-11%. Interestingly, in the TCGA cohort, patients with *POLE* mutations were shown to have an improved progression-free survival [42]. In a recent study by Meng *et al*., *POLE* mutations were identified in 15% of grade 3 EECs, and when data was analyzed

together with TCGA data, these patients were also significantly associated with improved progression-free survival [57]. Conversely, a separate study of 544 tumours, exhibited only 5.6% of EECs with *POLE* mutations and no improvement in progression-free survival [56]. To validate these observations in a large independent cohort of endometrial carcinomas, I have sequenced 406 tumours to identify 39 (9.6%) *POLE* somatic EDM mutations (Table E.8 (Appendix E)). Future analysis of this targeted sequencing study will be used to associate *POLE* mutations with progression-free survival, in order to verify the prognostic use of *POLE* mutation status and aid in classifying this group of endometrial patients. In addition, we will determine if *POLE* mutations are markers for overall good response to conventional treatment, or if this group of patients does well without the need for adjuvant treatment. This distinction is key to determining the clinical relevance of this discovery.

1.3 Ovarian Carcinoma

Epithelial ovarian carcinoma is the leading cause of gynaecological cancer deaths, and is the sixth leading cause of death of women in developed countries [4]. Similar to endometrial carcinomas, ovarian carcinomas have been histologically typed into two main groups: Type 1 consists of low-grade serous, endometrioid, clear cell, and Type II consists of high-grade serous carcinomas, and carcinosarcomas [59]. In contrast to uterine carcinomas, high-grade serous ovarian carcinoma (HGSC) is the most common ovarian subtype. HGSC is aggressive with metastatic spread to the peritoneum, and is often diagnosed late stage, thus 70% of patients will die of their disease. Original studies described ovarian cancer as a single disease, however today the view is that ovarian cancer encompasses many diseases, and may not originate from ovarian cells [60]. The cell of origin for HGSC was thought to be the ovarian surface epithelium; however there is a growing body of evidence to suggest the cell of origin is the fallopian tube epithelium [61]. In this hypothesis, the secretory epithelial cells of the distal fallopian tube (the fimbria) acquire *TP53* mutations then transform into serous tubal intraepithelial carcinoma (STICs), which shed onto the surface of the ovary and into the peritoneum [62]. These transformed cells attach to the peritoneal walls, the omentum, the fallopian tubes, and the surface of the ovary; therefore this disease is also referred to as high-grade pelvic serous carcinoma [63]. These tumours are usually treated with aggressive surgery to optimally de-bulk the patient of any residual tumour, and then followed by platinum-taxane chemotherapy. Unfortunately, platinum

resistance will be acquired in about 25% of all patients within six months, and in most other patients after subsequent courses of treatment [64]. New treatment options for HGSC, such as PARP inhibitors, are being tested in clinical trials.

Type I endometrioid and clear cell carcinomas account for only 15-20% of all ovarian cancers. Ovarian clear cell carcinomas (OCCC) diagnosed at a high stage have an extremely poor prognosis with the second leading cause of death from ovarian cancer [65], whereas ovarian endometrioid tumour (OEC) patients generally do quite well with conventional treatment [66]. There is now considerable evidence to suggest these tumours develop from an endometriotic cyst and not from ovarian surface epithelial cells [60]. The most accepted theory is that retrograde menstruation accounts for endometriosis, which is deposited in and on the ovary; therefore these cells would originate from the uterine epithelium [67]. This theory is supported by the morphological and molecular similarities of the tumours found in the uterus and the ovary.

1.3.1 Histopathology of Ovarian Carcinoma

Similar to endometrial tumours, ovarian tumours are also classified by the WHO and FIGO systems [20]. Ovarian endometrioid and clear cell carcinomas are morphologically similar to their endometrial counterparts, due to a common endometrial cell of origin, and are also similarly graded. These tumours harbor arrangements of glandular structures with villoglandular patterns and squamous differentiation in about 30-50% of cases (Figure 1.2) [68]. OCCC is histopathologically characterized by the presence of clear cells and “hobnail” cells [20].

High-grade serous carcinoma (HGSC), the most common type of epithelial ovarian carcinoma, is composed of solid papillary and glandular structures with often large, unusual-looking nuclei with prominent nucleoli (Figure 1.2). Mitotic and atypical mitotic figures are commonly found in large numbers within a field of view.

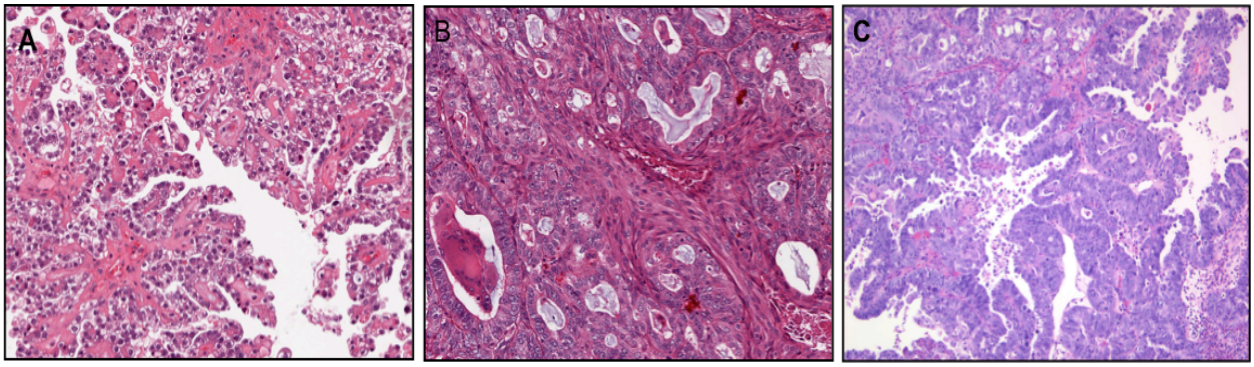

Figure 1.2 Histopathology of ovarian carcinomas
A. H&E of ovarian clear cell carcinoma **B.** H&E of ovarian endometrioid carcinoma. **C**. Ovarian high-grade serous carcinoma

The histological classification of ovarian cancer is now generally reproducible between pathologists, unlike high-grade endometrial carcinomas. Nevertheless, research and clinical management have historically lumped this disease into one uniform ovarian disease classification. The development of prognostic biomarkers (immunohistochemistry markers or mutations) has been unsuccessful; therefore stratification of the ovarian subtypes in research studies and clinical trials is needed for improvement in clinical treatment and care [69].

1.3.2 Molecular Genetics of Ovarian Carcinoma

1.3.2.1 Ovarian Endometrioid (OEC) and Clear Cell Carcinoma (OCCC)

Two landmark studies using whole exome and transcriptome sequencing discovered inactivating mutations in *ARID1A* in about 50% of OCCCs [70, 71]. About 7% of OCCCs also harbor mutations in *PPP2R1A*, which was the first study to report these mutations in ovarian cancer. The PI3K pathway is mutated at a high frequency, with mutations found in *PIK3CA* (50%) and deletion of *PTEN* (20%) [72, 73]. The PI3K pathway is also mutated in OECs (20%), along with the Wnt pathway [74], where the later is rare in OCCCs. OECs harbor mutations in *CTNNB1* (40%), which encodes for the protein β-catenin, and are associated with squamous differentiation, low tumour grade and favorable outcome [75].

Early molecular and histopathology studies, gave evidence to suggest an association of endometriosis with OEC and OCCC, by exhibiting LOH in the same chromosomal regions of the tumour and adjacent endometriosis [76]. Additionally, the discovery of *ARID1A* mutations in

clear cell carcinoma cells and adjacent atypical endometriosis, thus provides further evidence that endometriosis may be the precursor of OCCC [71]. Although OEC and OCCC may be derived from similar endometriotic precursors, these tumours are molecularly different, suggesting they evolve by different mechanisms. Genomic studies of these two cancers and their potential cells of origin are currently underway in our laboratory. The precursor of endometriosis is the endometrial epithelium; therefore it has been hypothesized that OEC and EEC have similar molecular features [29, 77]. In Chapter 4, I show the results of sequencing a panel of genes in endometrial endometrioid carcinoma and ovarian endometrioid carcinoma to determine if there are differences in mutation profiles.

1.3.2.2 Ovarian High Grade Serous Carcinoma (HGSC)

The mutation spectrum of HGSC is sparse, however these tumours are genomically unstable due to a high number of somatic copy number alterations (SCNA) [44]. It is striking that *TP53* mutations (>95%) are ubiquitous in HGSC, and harbors the highest frequency of *TP53* mutations found in any type of cancer [63]. Inactivation of *BRCA1* and *BRCA2* by mutation or hypermethylation of the promoter region has been demonstrated in about 30-50% of sporadic HGSC [44, 60], however is a characterizing feature of hereditary HGSC [78].

The TCGA analysis of HGSC identified previously described CNAs in *CCNE1*, *MYC, MAPK1* and *KRAS*. Low frequency recurrent somatic mutations were also demonstrated in the genes *NF1, BRCA1, BRCA2, RB1* and *CDK12* [44]. Pathway analysis identified alterations in RB (67%), PI3K/RAS (45%), NOTCH (22%), FOXM1 (84%) signaling, and alterations in homologous recombination (HR) proteins (51%) [44]. These deregulated pathways could potentially be targeted for improved treatment options for HGSC patients; hence is a focus of current research and clinical trials. An example of this research is the treatment of HGSC patients that are altered by HR defects, such as inactivation of BRCA1 and BRCA2 with PARP inhibitors in combination with DNA alkylators, which is considered a synthetic lethal treatment approach [79]. PARP inhibitors target DNA repair mechanisms, thus the cells that harbor homologous recombination defects have an inability to repair double stranded DNA breaks, and the cells undergo cell death [80]. Unfortunately, this targeted treatment can eventually drive

genetic reversion in *BRCA*-associated ovarian cancer causing drug resistance and tumour recurrence by [81].

1.4 Protein Phosphatase 2A (PP2A)

The heterotrimeric protein phosphatase 2A (PP2A) complex is the most abundant serine/threonine protein phosphatase complex, making up 1% of all cellular proteins [82]. It is a promiscuous protein complex involved in numerous cellular processes such as differentiation, development and growth [83, 84]. The core function of PP2A is to remove phosphate groups on signaling protein substrates, that may be activating or deactivating, which is a fundamental regulatory biological mechanism [85]. The core PP2A enzyme is composed of a 65kDa scaffolding A subunit, and a 36kDa catalytic C subunit. The third regulatory B subunit interacts with the core enzyme, to construct the fully functional heterotrimeric PP2A holoenzyme complex, and is the key component for substrate-specificity, cellular functions, and localization (Figure 1.3) [86]. The scaffolding A subunit is encoded by two isoforms: protein phosphatase regulatory Aα (*PPP2R1A*) or Aβ (*PPP2R1B*) genes which are 86% identical [87]. Studies have established that PPP2R1A is ubiquitously expressed, is 40 times more abundant than PPP2R1B [87], and represents about 0.1% of total protein in the cell [88]. The catalytic C subunit is also encoded by two isoforms: protein phosphatase catalytic 2A or 2B (*PPP2CA* and *PPP2CB*) [89]. The regulatory B subunits include about 15 different family members with multiple isoforms (Table 1.1) that could potentially compose around 200 different PP2A enzyme complexes [82, 90].

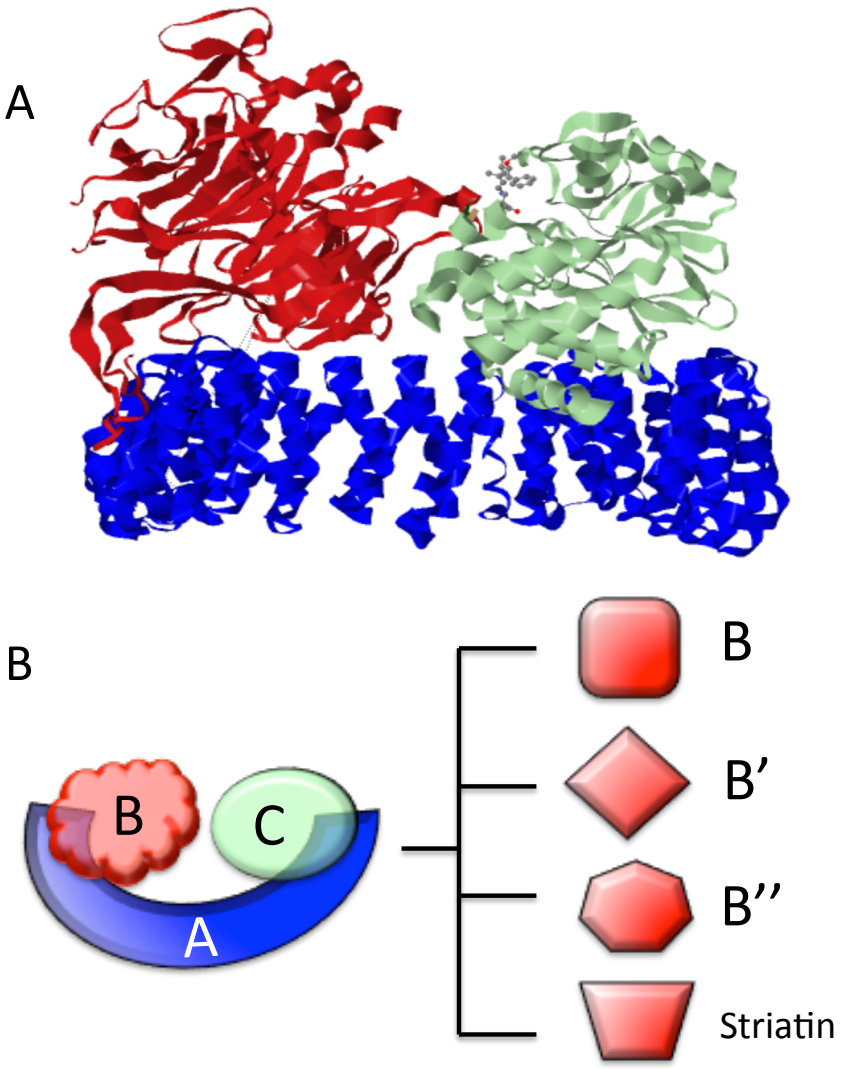

Figure 1.3 3D Structure of Protein Phosphatase 2A (PP2A)
A. The blue ribbon is the scaffold A subunit (PPP2R1A), the green ribbon is the catalytic C subunit (PPP2CA), and the red ribbon structure is the regulatory B55α subunit (PPP2R2A), as assessed from crystal structures. The orientation and colours were adjusted from the original PDB (Protein Data Bank) file (3DW8.pdb) [91]. **B.** Cartoon of PP2A subunits with choices of four different B subunit family members. The ability of each B subunit (including Striatin) to bind to the A subunit will compose a unique PP2A holoenzyme.

Gene Names	Additional Name	Family	Protein Size (kDa)
Scaffold A Subunit			
PPP2R1A, alpha isoform	PR65a, Aα	*A*	65
PPP2R1B, beta isoform	PR65b, Aβ	*A*	65
Catalytic C Subunit			
PPP2CA, alpha isoform	PP2Acα, Cα	*C*	36
PPP2CB, beta isoform	PP2Acβ, Cβ	*C*	36
Regulatory B Subunit			
PPP2R2A, B55 alpha isoform	PR55α, B55α, Bα	*B*	55
PPP2R2B, B55 beta isoform	PR55β, B55β, Bβ	*B*	55
PPP2R2C, B55 gamma isoform	PR55γ, B55γ, Bγ	*B*	55
PPP2R2D, B55 delta isoform	PR55δ, B55δ, Bδ	*B*	55
PPP2R5A B56 alpha isoform	PR61α, B56α, B′α	*B′*	56
PPP2R5B B56 beta isoform	PR61β, B55β, B′β	*B′*	56
PPP2R5C B56 gamma isoform	PR61γ, B56γ, B′γ	*B′*	56
PPP2R5D B56 delta isoform	PR61δ, B56δ, B′δ	*B′*	56
PPP2R5E B56 epsilon isoform	PR61ε, B56ε, B′ε	*B′*	56
PPP2R3A	PR130, B″α1	*B″*	130
PPP2R3A	PR72, B″α1	*B″*	72
PPP2R3B	PR70/48, B″β1	*B″*	70/48
PPP2R3B	PR70, B″β2	*B″*	70
PPP2R3C	G5PR, B″γ	*B″*	
PPP2R4	PR53, PTPA		53
STRN	PR110, Striatin		110
STRN3	PR93, SG2NA		93

Table 1.1 Heterotrimeric PP2A subunit components

The structure of PPP2R1A is composed of a curved, hook-like helical structure with 15 HEAT repeat motifs (**H**untingtin-**E**longation-**A** subunit-**T**OR; Huntingtin elongation factor 3, A subunit of protein phosphatase 2A, Target of Rapamycin 1) [92]. Each repeat is defined by two alpha helices that are connected by an intra-repeat loop [93]. Crystal structure studies (Figure 1.3) demonstrate that the HEAT repeats 2-8 (N-terminus) directly interacts with regulatory B subunits through hydrogen bonds [86, 94]. The A subunit HEAT repeats 11-15 (C-terminus) interacts with PP2A catalytic C subunits through hydrogen bonds and hydrophobic interactions

[86, 94]. Each regulatory B subunit has a unique structure, and may interact with the A and C subunits differently, enabling regulation of the high complexity of PP2A functions. Through a large mass spectrometry analysis of PP2A interactions, researchers discovered that additional proteins can replace B subunits, and C subunits can form heterodimers with proteins other than with the A subunit [95].

PP2A also plays a major role in mitosis and cell cycle regulation. The PP2A-B56δ complex has demonstrated an ability to dephosphorylate CDC25C, another major phosphatase regulator of mitosis, which prevents 14-3-3 release to ultimately trigger cells to enter mitosis [96]. At mitotic exit, the PP2A-B56δ complex is also responsible for the dephosphorylation of CDC25C to repress its phosphatase activity on CDK1, thus causing exit from mitosis. If B56δ is repressed, then CDC25C is hyperphosphorylated causing activation and dephosphorylation of CDK1 leading to a delay in mitotic exit [97]. In addition, the protein kinase Gwl (Greatwall) will associate and inhibit PP2A phosphatase activity in order to promote entry into mitosis [98]. Furthermore, PP2A-B56γ3 exhibits localization to the nucleus to dephosphorylate the p27 protein, which regulates cell cycle entry by delaying G1 to S phase [99]. Overexpression of B56γ3 increases its nuclear localization and delays G1 to S, thus decreasing cell proliferation. Conversely, knockdown of B56γ3 increases the G1 to S transition and increases cell proliferation. An elegant *in vitro* study using live-cell imaging demonstrated that PP2A-B55α is also important in regulating mitotic cell exit. Knockdown of B55α with siRNA significantly slowed mitotic cell cycle exit, delayed disassembly of spindle-pole-associated microtubules, and delayed post-mitotic chromosome decondensation [100]. These observations may be linked to the mitotic regulator kinase MASTL, which negatively regulates PP2A-B55α to delay mitotic exit. However, when CDK1 and MASTL are inhibited, PP2A-B55α and PP2A-B55δ will be activated to dephosphorylate substrates causing transition into mitotic exit [101]. PP2A is also implicated in the tight regulation of the cohesion complex which is important at centromeres for sister chromatid cohesion during mitosis and meiosis. PP2A was found to co-localize with the shugoshin complex at centromeres to ultimately de-phosphorylate cohesion which helps protect the protein complex [102]. This is important as phosphorylation of cohesion promotes dissociation from chromosomes, and shugoshin protects the centromere until the kinetochores

are ready to be captured by spindles in tight spatial and temporal regulation. Overall, distinctive PP2A complexes are crucial for the different stages of cell cycle regulation.

1.4.1 The Role of PP2A in Cancer

PP2A was first described as a tumour suppressor using the selective inhibitor okadaic acid, which leads to the formation of tumours in mice [103, 104]. However, other studies have found that PP2A is required for growth and survival, thus it is not a typical tumour suppressor protein [105]. Considering the PP2A holoenzyme is a multi-protein complex encoded by hundreds of PP2A molecules, this may not be a simple prototypical classification of a tumour suppressor or oncogene protein. Tissue specificity, cellular localization and substrate specificity may contribute to PP2A complex's functional role as a tumour suppressor or oncogene in different cellular contexts.

Tumour promoting virus proteins are able to alter PP2A activity in multiple ways; by mimicking B subunits and enabling binding to the A-C dimer complex, and altering PP2A substrate specificity by interacting directly with B subunits in the PP2A complex. It has been established that the polyoma small T (pyST), polyoma middle T (pyMT) antigen, simian virus SV40 small T (SV40ST), and E4orf4 antigens can form complexes with PP2A [106, 107]. Complete inhibition of PP2A activity leads to cellular death; therefore viral antigens control PP2A by inhibiting interaction with substrates, and altering targets for dephosphorylation. SV40ST binds PP2A to inhibit its phosphatase activity, thereby causing cellular transformation by activating specific cellular pathways [108]. Specifically, SV40ST was shown to interact with B56γ PP2A complexes, which drives cellular transformation and tumour formation [109]. In a later study, suppression of the B subunits B56α (PPP2R5A), B56γ (PPP2R5C), PR72/PR130 (PPP2R3A), and PTPA recapitulated the SV40ST cell transformation phenotype [110]. Deregulation of phosphatase activity induced by down regulating some of these PP2A B subunits, caused signaling changes in a subset of the Wnt, c-Myc and PI3K/Akt pathway to ultimately assist in transformation. An interesting study deciphered the crystal structure of B55α, and was subsequently able to demonstrate that E4orf4 binds to the substrate groove of B55α (PPP2R2A) to inhibit a specific interaction with p107 (RBL1) causing a dephosphorylation blockade. When high expression levels of E4orf4 infection are present, this causes an inability of

cell cycle progression substrates to be dephosphorylated by PP2A-B55α, thus causing cell death. Albeit at lower levels, E4orf4 recruits the substrates ASF/SF2/SRSF1 to enhance adenoviral replication [111].

PP2A B55 complexes have been implicated as partaking in both activating and inhibiting effects on the MAPK pathway, which is cell-type specific [82]. Dephosphorylation of the genes ERK, RAF1, KSR1, and c-SRC causes signaling in the MAPK pathway [112, 113], which is often deregulated in many cancers. Recently, the PP2A-B55α (PPP2R2A) complex was shown to specifically dephosphorylate the c-Jun T239 residue, which promotes binding with the AP-1 transcription complex to regulate tumour migration and invasion [114]. Additionally, in AML (Acute Myeloid Leukemia) patients, the protein levels of B55α were decreased compared to normal cells, and correlate with an increase in AKT T308 phosphorylation levels. The decreased B55α levels and increased AKT signaling was an adverse prognostic factor for these patients [115]. PP2A-B55β (PPP2R2B) targets cyclin E for dephosphorylation, which stabilizes the protein and protects it from ubiquitin-mediated degradation [116]. Thus, decreased levels of B55β cause overexpression of the cyclin E protein [116], which is correlated with aggressive tumours and poor patient outcome [117].

Functional studies of PP2A suggest that loss of the B56 (PR61) family is the most relevant event for tumourigenesis, however this is likely context dependent [82]. PP2A is important in controlling the accumulation of c-Myc, which is dysregulated in many cancers [118]. PP2A dephosphorylates the c-Myc S62 residue, resulting in protein instability and subsequent ubiquitination by the F-box E3-ubiquitin ligase protein, FBXW7, followed by 26S proteasome degradation [119, 120]. In a study by Arnold and Sears, knockdown of B56α (PPP2R5A) resulted in *c-myc* overexpression, increased levels of phospho-S62 and stability of the c-Myc protein, implicating the PP2A-B56α complex as an important regulator of c-Myc function [121]. Additionally, B56α has also been show to interact with the anti-apoptotic BCL2 protein at the mitochondrial membrane, causing dephosphorylation and inactivation of BCL2 [122]. Furthermore, the B56α-PP2A complex plays an indirect role in the regulation of p53, with opposing studies suggesting PP2A as a negative and a positive regulator of p53 signaling [82].

The expression of B56γ (PPP2R5C) is decreased in primary melanoma compared to non-transformed cells, conversely higher expression of PPP2R5C was found in melanoma cell lines compared to normal melanocytes [123]. In a separate study, PPP2R5C was overexpressed in lung cancer cell lines that lacked the endogenous protein expression, resulting in partial reversal of cell line tumourgenicity and suppressed cell proliferation, implicating levels of PP2A B56γ may be important in transformation behavior of human cancer cell lines [109]. Moreover, PP2A-B56γ is also important in Wnt signaling by inhibiting formation of the APC-Axin complex, which destabilizes β-catenin and inhibits transcription of Wnt pathway genes [124]. Lastly, a recent report has linked PP2A-B56delta (PPP2R5D) with selective dephosphorylation of BCL2 Ser70. BCL2 is overexpressed in many hematopoietic tumours and hyperphosphorylation of Ser70 causes anti-apoptotic activity [125].

Specific gene inhibitors of PP2A have also been implicated to play a role in cancer. The gene CIP2A (Cancerous Inhibitor of PP2A) inhibits PP2A induced de-phosphorylation of c-Myc S62 by direct interaction, thereby preventing c-Myc degradation [126]. A second endogenous PP2A inhibitor protein, the oncoprotein SET (I2PP2), can form an inhibitory protein complex with PP2A, thus causing changes in phosphatase regulation which ultimately contributes to tumourigenesis [127]. Targeting these PP2A inhibitory proteins by novel therapeutics has shown to increase PP2A activity by affecting the stability of c-Myc in breast and prostate cancer cell lines [128, 129]. Overexpression of CIP2A is present in head and neck squamous cell carcinoma (HNSCC) and colon cancer; therefore targeting overexpressed inhibitors of PP2A could be a novel way to treat cancers with this disease hallmark.

1.4.1.1 The Role of the PP2A A Subunits (*PPP2R1A* and *PPP2R1B*) in Cancer

The first somatic mutations in *PPP2R1A* were identified in multiple human tumour types albeit at low frequencies [130]. Calin *et al.* identified four different mutations in one case of lung carcinoma (E64D), one case of malignant melanoma (R418W), and two cases of breast carcinoma (E64G and a frameshift mutation). Additional studies using site-directed mutagenesis demonstrated that the few somatic mutations of *PPP2R1A* disrupt the binding of B and C subunits [90]. Specifically, the mutations were shown to disrupt binding with Bα, B'α and B''/PR72 B subunit family members. The introduction of these Aα (PPP2R1A) mutations into

non-transformed cell lines displayed defects in B subunit binding (B55α, all B56 family members), in particular for B56γ (PPP2R5C), which is a critical interaction in human cell transformation [131]. *PPP2R1A* is an essential gene, thus complete loss induces cell death [132]. Several studies have concluded that *PPP2R1A* mutations contribute to cell transformation by haploinsufficiency, and that the level of functional PPP2R1A is essential for the balance of cell death and transformation [131, 133]. The haploinsufficient levels of PPP2R1A act to create competition between B subunit binding for the formation of an active PP2A complex. In addition, Chen *et al.*, also found that suppression of Aα decreased phosphatase activity, and activated the AKT pathway. Furthermore, it has been discovered that 43% of human glioma harbor decreased expression of *PPP2R1A* [134].

Frequent loss of heterozygosity (LOH) on 11q22-24 was reported in ovarian carcinoma, which coincides with the *PPP2R1B* loci [135]. Upon closer inspection, the region of LOH involved the entire 11q arm, therefore was not only restricted to the *PPP2R1B* gene. Additionally, no somatic mutations of *PPP2R1B* were identified in ovarian carcinomas [135], resulting in the conclusion that *PPP2R1B* is not likely involved in ovarian tumourigenesis. Mutations in *PPP2R1B* (Aβ) were first identified in 15% of primary lung tumours, 6% of lung cell lines, and 15% of primary colon tumours [136]. Subsequent functional analysis established that some of the mutations, but not all, altered binding to the B"/PR72 and C subunits [137]. Interestingly, wild-type Aβ did not bind to the B-subunits Bα, B'α1 when compared to Aα binding. The B"/PR72 and C subunits bound at higher levels to Aβ, 30% and 15% respectively, although still significantly less binding compared to the Aα subunit. This may be due to differences in expression levels of the two A subunits, as the Aα subunit is 40X more abundant than Aβ [87]. One study has shown that Aβ, but not Aα, is responsible for the dephosphorylation of a small GTPase RalA, which is important in many cell processes [138]. In a lung cancer cell line that harbors an Aβ mutation there is constitutive phosphorylation of RalA promoting cell transformation. Taken together these two subunits likely have distinctive roles in growth control during tumourigenesis, and mutations in the two subunits can affect the binding of B subunits family members in the context of different diseases and tissues.

The majority of my thesis work has focused on assessing *PPP2R1A* mutations in all subtypes of endometrial and ovarian carcinomas. The discovery of *PPP2R1A* mutations is described in Chapter 1, which led to the work in Chapter 3 discussing full exon sequencing of *PPP2R1A* and eight other genes for the molecular classification of endometrial carcinomas. The prevalence of these *PPP2R1A* mutations in gynaecological cancers, also led to the studies presented in Chapter 5 and 6, showing how a specific endogenous mutation affects interactions between PP2A A and B subunit proteins to form the PP2A holoenzyme.

1.5 Omics Technology – Advances in DNA and Protein Sequencing

1.5.1 Next-Generation Sequencing Technology

Advances in next-generation sequencing (NGS) technology, also referred to as second-generation sequencing, have revolutionized our ability to sequence cancer genomes. Large international collaborations such as TCGA (The Cancer Genome Atlas) and the International Cancer Genome Consortium (ICGC) are completing sequencing efforts for almost every cancer type. NGS technology has dramatically decreased the cost of sequencing a human genome, although this is still expensive. The total time for sequencing has decreased, which subsequently increased throughput and the amount of data output. The mass amount of data generated has caused a computational challenge for analysis as well as for suitable data storage. The Illumina sequencers (HiSeq, MiSeq) use massively parallel sequencing by synthesis (SBS) on a chip, called a flowcell, and has become the leading NGS sequencing technology used for whole genome RNA-sequencing (RNA-seq), exomes, epigenetic, and targeting panel sequencing. Other sequencing platforms such as the Ion Torrent and Roche 454 sequencing use emulsion PCR, and are now mostly used for targeted sequencing. The newest Illumina HiSeq2500 can produce a whole genome in less than a week, and a whole exome in just a few days. New technology is constantly being released to enable higher throughput and lower sequencing costs. This is revolutionary considering the first human genome took 10 years to produce and cost billions of dollars. The first Illumina personal sequencer released in 2011, called the MiSeq, is now leading the field with targeted gene sequencing and “hotspot” sequencing for clinical applications and molecular pathology, although new sequencing chemistry can allow for exome and RNA sequencing. Sanger sequencing is still used as a gold standard in validation experiments, however the power of NGS comes from the ability to barcode DNA from one patient, then pool

multiple patient DNA into one large sequencing run. This also allows the ability to perform bidirectional sequencing of multiple regions and multiple patients in one run, whereas a single Sanger sequencing reaction is limited by one direction, one amplicon and one sample.

Analysis of NGS data can identify heritable SNPs, somatic mutations, copy number variations (CNVs), and structural aberrations. The enormous amounts of sequencing output data from whole genome sequencing, exomes, targeted sequencing, etc., are being used to discover cancer driver and passenger mutations, identify somatic mutation profiles, clonal evolution and cancer subclone populations [139-141]. The characterization of these cancer hallmarks is being used to progress and aid the fast growing area of personalized cancer genomics. For example, patient tumour and normal samples are sequenced with NGS technology to identify somatic mutations and alterations that may be used for clinical diagnosis, targets for novel therapeutics or response to specific treatments. Clinical trials and therapeutics are being designed based on the presence of specific mutations in the tumour genome; for example the *EGFR* mutation in lung cancer for treatment with gefitinib, and *BRCA1* and *BRCA2* mutated tumours with PARP inhibitors [142]. In this thesis work, I have focused mainly on using targeted gene sequencing with Illumina NGS technology, and Sanger sequencing to identify mutational profiles that will aid in molecular pathology and the classification of endometrial tumours.

1.5.2 Proteomics Technology

With the plethora of research and technology advancement in genomics, there is now a large need to decipher how these genetic aberrations affect the function and structure of proteins in cancer cells. The field of proteomics has emerged to address the analysis of global protein expression analysis in a complex biological sample, and to complement the massive genomic datasets. There is accumulating evidence to suggest there is a low correlation of mRNA expression change with the changes in protein counterpart expression, thus underscoring the importance of post-transcriptional modifications and the complexity of the biological system. However, proteomics technologies are plagued by a number of technical challenges, making this analysis very challenging [143]. In the case of genomic sequencing, we have the luxury of being able to amplify DNA and RNA using PCR, however there are no such amplification methods for proteins that are extracted from tissue or cells. Low abundance proteins are analyzed in their

physiological state, unless a large amount of starting material can be prepared. This may be feasible for some *in vitro* cell line experiments, but when you are working with small patient samples this can become problematic.

To overcome these challenges and to keep up with the incredible pace of advancing NGS technology, there was a sizeable need for sensitive, high-resolution mass spectrometer technology enabling the analysis of complex samples. The Orbitrap mass spectrometer (MS) was invented by Makarov in 1999-2000 based on a technology from the 1920's called the Kingdon trap [144]. The commercial Orbitrap MS was the first new MS instrument introduced in the last 20 years and has slowly revolutionized the world of proteomics [145]. In conjunction with HPLC (High Performance Liquid Chromatography), the Orbitrap MS has enabled the analysis of complex samples, and overcome some of the old issues of sensitivity, accuracy, and a need for high quantities of sample. In traditional "bottom-up proteomics", proteins are digested into peptides, ionized and fragmented in the MS, and lastly identified using known peptide databases. With the advent of the Orbitrap, ionizing intact proteins can now be performed using "top-down proteomics", which can allow for full protein characterization [146, 147]. This enables improvements in the study of post-translational modifications of proteins, which is not always supported using bottom-up proteomics due to inconsistent coverage of the many peptides that make up an individual protein. However, this type of analysis is still in the very early days of research, and is limited by hurdles in sample processing, instrumentation and analysis. Similar to NGS, proteins or processed peptides can be labeled (barcoded) using chemical labels after cell lysis (TMT, dimethyl or iTRAQ), or by *in vitro* labeling (SILAC) to enable pooling of samples and quantitation of protein levels. TMT (Tandem Mass Tags) and iTRAQ (Isobaric Tags for Relative and Absolute Quantitation) labeling methods allows peptides from different samples (up to 8 samples) to be simultaneously identified on the MS instrument [148, 149]. This allows for quantitation of the relative abundances from MS/MS analysis, resulting in the ability to perform differential protein expression in dynamic cellular systems. An advantage of this system is the ability to label and quantitate fixed and frozen patient proteomes. For analyzing cell lines, SILAC (Stable Isotope Labeling by Amino Acids in Cell Culture) uses "heavy" and "light" amino acids in the growth media which are incorporated into all of the endogenous proteins. Different cell lines or differing treatment of cell lines (i.e. drug treatments, or cell cycles) can

then be pooled for identification and quantitation by LC-MS/MS [150]. These proteomics analyses are slowly bringing genomics and proteomics together to enable mapping of the global changes in the cancer genome. In Chapter 6, I have also utilized challenging proteomics mass spectrometry technology, using TMT peptide labeling, in order to determine the effects of endometrial PPP2R1A mutations (identified in Chapter 2 and 3) on PP2A B subunit interactions.

1.6 Hypotheses

A) Hypothesis A (Chapter 2) Endometrial and ovarian carcinomas will harbor mutations in *PPP2R1A*, which will aid in defining the molecular profiles of the histological subtypes.

B) Hypothesis B (Chapter 3) The histopathological subtypes of endometrial tumours need assessment of specific gene mutation profiles to help classify and diagnose tumours.

C) Hypothesis C (Chapter 4) Mutation frequencies in specific genes and co-occurrence patterns, will differ in histologically similar tumours: ovarian endometrioid and endometrial endometrioid carcinomas.

D) Hypothesis D (Chapter 5 and 6) The PPP2R1A W257L mutation leads to changes in interactions with specific PP2A B subunits and additional PP2A binding proteins.

Chapter 2: Identification of Subtype-Specific *PPP2R1A* Mutations in Endometrial and Ovarian Carcinomas

2.1 Introduction

Low frequency *PPP2R1A* mutations were first described in 3/42 (7%) of clear cell carcinomas of the ovary [70]. Mutations in *PPP2R1A* have been described at very low frequency in other types of cancers [130], but not in any histological subtype of endometrial cancer or ovarian tumours. There are striking clinical and pathological similarities between endometrial and ovarian histopathological subtypes, therefore it is expected that there are molecular similarities. This is evident between high-grade serous carcinoma of the endometrium and ovary, and between endometrioid carcinoma of endometrium and ovary, however it is less clear whether tumours of comparable cell type arising in different organs are also similar with respect to underlying molecular abnormalities. This is an important consideration if treatments are based on tumour cell types rather than if the organ of origin is also being contemplated. Recently, there has been an effort to identify new markers to define patient groups that would benefit from alternative or aggressive treatments for both ovarian and endometrial cancers [69]. To accomplish this, molecular and mutational characterization is needed to better understand the carcinoma subtypes and their relationship within a spectrum of gynaecological malignancies.

The goal of this study was to sequence exon 5 and 6 of *PPP2R1A* in endometrial and ovarian high-grade serous and endometrioid tumours, to test the hypothesis that *PPP2R1A* mutations are present in other subtypes of ovarian and endometrial carcinomas. Herein, I present the novel finding that *PPP2R1A* is mutated in endometrioid-type endometrial and ovarian carcinomas and in a significantly higher percentage of high-grade serous endometrial carcinomas, but not high-grade serous carcinomas of the ovary.

2.2 Materials and Methods

2.2.1 Patient Samples

The tumour specimens analyzed in this study for DNA and RNA sequencing were collected via several tumour banks and tissue repositories at the BC Cancer Agency and Vancouver General Hospital (via OvCaRe), the Australian Ovarian Cancer Study (AOCS), and Montreal

tumour bank (Banque de Tissus et de Données, of the Réseau de Recherche sur le Cancer of the Fonds de la Recherche en Santé du Québec, affiliated with the Canadian Tumour Repository Network), see also Supplemental Table 2 (Appendix A). Patients were approached for written informed consent, before undergoing surgery; to donate tissue surplus to diagnostic requirements plus a blood sample, for use in a research ethics board (REB) approved research protocol. All patients were informed at the time of consent about the potential risks of loss of confidentiality arising from use of their samples in research and that none of the research study data would ever form part of the clinical record or be reported back to the care physicians. See also Wiegand *et al [71]*.

2.2.2 Whole Transcriptome Sequencing Analysis

Whole transcriptome data from Wiegand *et al.* (European Genome–Phenome Archive accession number, EGAS00000000075) was analyzed as previously described [71, 151].

2.2.3 DNA Extraction

DNA and RNA were extracted using standard methodologies, as previously described [71, 151].

2.2.4 PCR and Sanger Sequencing

PCR primer sets were designed to amplify exons 5 and 6 of *PPP2R1A*. Priming sites for -21M13 forward and -27M13 reverse were added to 5′ ends to allow direct Sanger sequencing of amplicons. *PPP2R1A* exons 5 and 6 forward primer 5'-ACAGAGAGGGGGTCATCACTT-3', reverse 5'-GCCTAATGGAAACCTCAGCTC-3'. FFPE samples were amplified using exon 5 forward 5'-AAAACCTGGACCCACACAAC-3', reverse 5'-TTGGAGAACATGGGGATGAT-3', and exon 6 using forward 5'-CTCTCCTCTCCCTAGGACTCG-3', reverse 5'-GTGTCAGTGTCCCCACCAGT-3'. For PCR reactions Platinum Taq DNA Polymerase High Fidelity (Invitrogen, Carlsbad, CA) reagents were used. After denaturation at 94ºC for 3 min, DNA was amplified 35-45 cycles (94ºC 45 sec, 64ºC 30sec, 72ºC 30 sec), final extension was at 72ºC for 5 min using a MJ Research Tetrad (Ramsey, MN). PCR products were purified using ExoSAP-IT® (USB® Products Affymetrix, Inc., Cleveland, OH) and amplified in both forward and reverse directions using M13 oligos (M13 forward 5'-TGTAAAACGACGGCCAGT-3',

M13 reverse 5'-CAGGAAACAGCTATGAC-3') and the ABI BigDye terminator v3.1 cycle sequencing kit (Applied Biosystems, Foster City, CA). Amplified products were then sequenced using an ABI Prism 3130xl Genetic Analyzer (Applied Biosystems, Foster City, CA). All capillary traces were visually inspected to confirm their presence in tumour and absence from germline traces by using Finch TV (Geospiza, Seattle, WA) and Mutation Surveyor (SoftGenetics LLC). All mutations were confirmed by duplicate PCR reactions.

2.2.5 Immunohistochemistry Staining

4 μm sections were processed using a Ventana Discovery XT automated system (Ventana Medical Systems, Tucson, AZ, USA) as per manufacturer's protocol with proprietary reagents. After baking at 60°C for 1 h, they were deparaffinized on the automated system with EZ Prep solution (Ventana). Heat induced antigen retrieval method was used in Cell Conditioning solution (CC1-Tris based EDTA buffer, pH 8.0, Ventana). The rabbit monoclonal ER (Estrogen Receptor), clone SP1 (cat#: RM-9101) antibody was obtained from Thermo Fisher Scientific (Ottawa, Ont, Canada), the mouse monoclonal p53, clone DO-7 (cat#: M7001) antibody, and mouse monoclonal WT-1 (Wilms Tumour 1), clone 6F-H2 (cat#: M3561) antibody both obtained from Dako (Burlington, Ont, Canada). All primary incubations were performed for 60 min with heat at a 1:25 dilution for ER, 1:400 dilution for p53, and 1:50 dilution for WT-1 in Ventana antibody diluents. The Ventana Universal Secondary Antibody was used for 32 min at 37°C. The detection system used was the Ventana DABMap kit, and slides were then counterstained with Hematoxylin and treated with a proprietary bluing agent (p53 and WT-1 used Ventana, ER used Tissue Tek Prisma). All washes were conducted with the Ventana Reaction Buffer, and dehydration steps and coverslip procedure were completed as per manufacturer's recommendations. Categorical scoring for WT-1 and ER was assessed as 0=no expression, 1=expression. Scores for p53 were as follows; 0=loss of expression, equivalent to deletion or nonsense mutation, 1=normal expression, 2=overexpression equivalent to missense mutation (Supplemental Table A.2 (Appendix A).

2.3 Results

From our whole transcriptome sequencing data [71] I identified and validated one mutation within exon 5 of *PPP2R1A,* corresponding to amino acid residue R183*,* in an ovarian clear cell

carcinoma (OCCC1). To determine if such mutations are present in other ovarian or endometrial carcinomas I used Sanger sequencing to analyze exons 5 and 6 of *PPP2R1A* in DNA extracted from 271 tumours (see Methods) (Table 2.1). The somatic status of *PPP2R1A* mutated cases was also assessed using germline DNA. Although mutations of exon 6 have not been previously described, it was included due to known interactions of amino acids P179, R183, R182 (coded within exon 5) and W257 (coded within exon 6) with the PP2A regulatory B subunits [86, 90, 152, 153]. Recurrent somatic mutations, not previously described within COSMIC [154], were identified in both ovarian and endometrial carcinomas. Mutations appeared to be subtype enriched (Fisher's Exact $p < 0.0001$): 40.8% (20 of 49 cases) of high-grade serous endometrial carcinomas compared to only 5.0% (3 of 60 cases) of endometrial endometrioid carcinomas and 12.2% (5 of 41 cases) within ovarian endometrioid carcinomas (Figure 2.1A, Table 2.1). Mutations were also observed at a lower frequency of 4.1% (2 of 49 cases) in ovarian clear cell carcinomas (Table 2.1; Supplemental Table A.1 (Appendix A)), including two distinct missense mutations observed in neighboring nucleotides resulting in two apparent amino acid changes in a single case of ovarian clear cell carcinoma (Table 2.1; Supplemental Table A.1 (Appendix A)). No other cases had more than a single mutation, and all mutations appeared heterozygous upon review of electropherograms. In 28 of the 31 cases, which tested positive for mutations in *PPP2R1A*, the normal germline DNA tested negative for *PPP2R1A* mutations, demonstrating that all mutations were somatic (Supplemental Table A.1 and A.2 (Appendix A)). Also to further assess the sensitivity of mutation detection by sequencing, the tumour cellularity was determined for the majority of endometrial and ovarian tumours (Supplemental Table A.2 (Appendix A)). I confirmed there were no significant cellularity differences between endometrial high-grade serous carcinomas with and without mutations (p-value >0.3, range [20%-90%]), giving good indication that it is possible to detect *PPP2R1A* mutations in tumours with low cellularity.

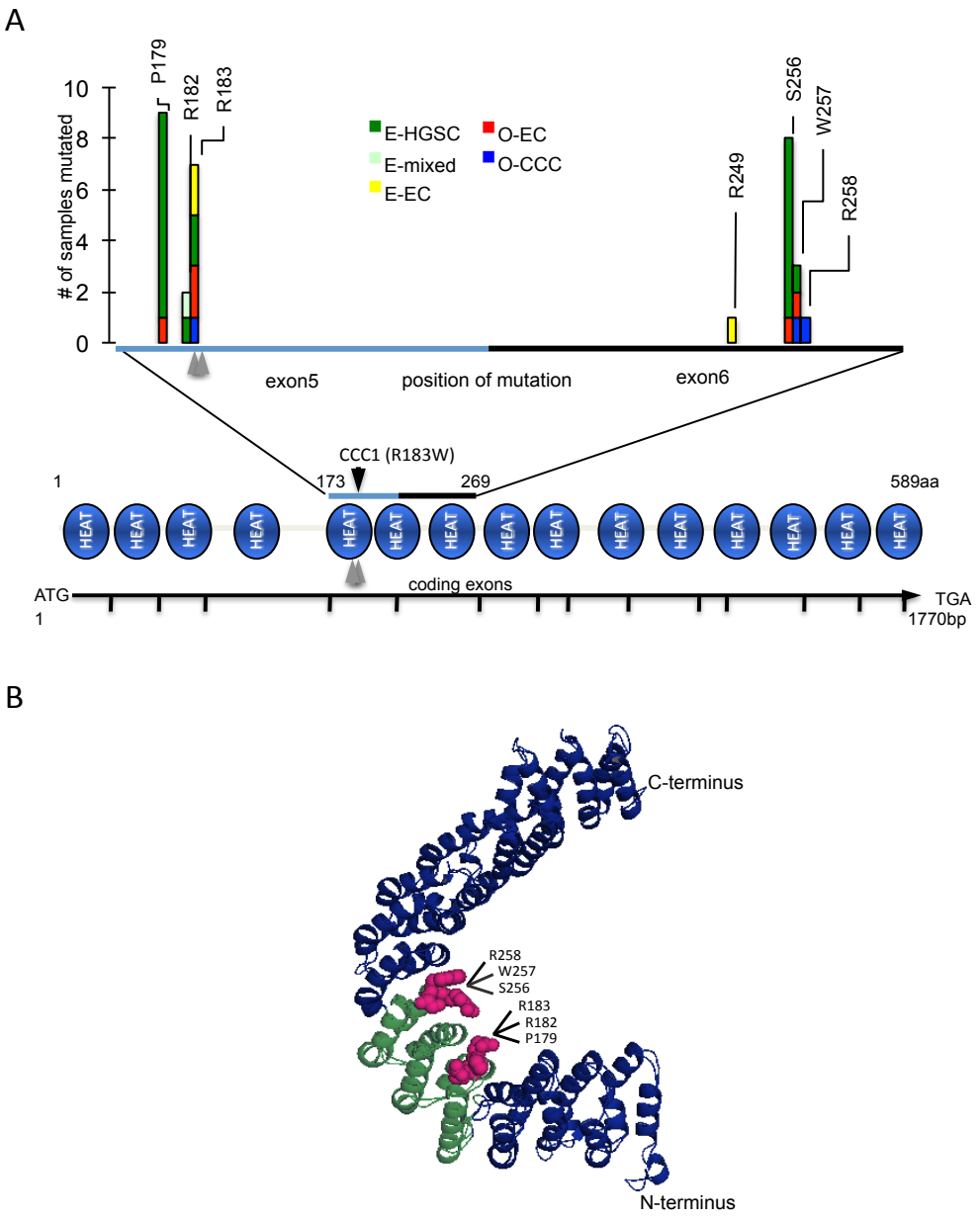

Figure 2.1 Schematic of mutations in PPP2R1A

(A) The lower panels represent the coding sequence and protein domain structure of PPP2R1A, grey arrows denote positions (corresponding to amino acids R182 and R183) of mutations described by Jones *et al*. [70], while the black arrow corresponds to the position of a single variant detected in whole transcriptome sequencing data of ovarian clear cell carcinomas from Wiegand *et al*. [71]. Upper panel denotes the position (amino acid residue), frequency, and subtype of mutations found across the cohort of ovarian and endometrial malignancies as a histogram. (B) Three dimensional protein structure of the PPP2R1A scaffolding Aα subunit of PP2A, with 15 repeat HEAT motifs (Model generated by SWISS-MODEL [155], and manipulated using PyMOL1.1). The HEAT 5 and 7 motifs coded by exons 5 and 6 are highlighted and amino acids affected by radical changes are annotated. Amino acid residues P179, R183 and W257 are know to interact with the regulatory B subunit of PP2A.

	Frequency (%)	Coding sequence changes (mutation occurrence)	Predicted amino acid changes
Endometrial Carcinoma			
High-Grade Serous	20/49 (40.8%)	c.536C>G (6)	p.Pro179Arg
		c.536C>T (3)	p.Pro179Leu
		c.544C>T (1)	p.Arg182Trp
		c.547C>T (2)	p.Arg183Trp
		c.767C>T (6)	p.Ser256Phe
		c.767C>A (1)	p.Ser256Tyr
		c.769T>G (1)	p.Trp257Gly
Clear Cell	0/1 (0%)	NA	NA
Endometrioid	3/60 (5.0%)	c.548G>A (2)	p.Arg183Gln
		c.746G>A (1)	pArg249His
Mixed	1/3 (33.3%)	c.544C>T (1)	p.Arg182Trp
Ovarian Carcinoma			
High-Grade Serous	0/50 (0%)	NA	NA
Low-Grade Serous	0/12 (0%)	NA	NA
Clear Cell	2/49 (4.1%)	c.547C>T (1)	p.Arg183Trp
		c.771G>T[§] (1)	p.Trp257Cys[§]
		c.772C>T[§] (1)	p.Arg258Cys[§]
Endometrioid	5/41 (12.2%)	c.536C>G (1)	p.Pro179Arg
		c.547C>T (2)	p.Arg183Trp
		c.767C>A (1)	p.Ser256Tyr
		c.769T>G (1)	p.Trp257Gly

Table 2.1 *PPP2R1A* mutation results with frequency, coding changes, and predicted amino acid changes
Sequence co-ordinates are given relative to the coding sequence, or translation, within the *PPP2R1A* transcript variant 1 (NM_014225.5), unique mutations observed for each subtype are listed (see also Figure 2.1A and Supplemental Table 1(Appendix A)).
[§]Two somatic mutations were found in side-by-side nucleotides resulting in two apparent codon changes in ovarian clear cell carcinoma sample OCCC2.

With the exception of mutations observed at R182 and R183, all other PPP2R1A mutations described in this study have not been found in other human cancers [154]. All mutations appear to be confined to intra-repeat regions of the PPP2R1A HEAT motifs, with mutations in exon 5 and 6 corresponding to HEAT 5 and 7 motifs, respectively (Figure 2.1B). These regions are known to loosely interact with the various isoforms of the regulatory B subunit of the PP2A holoenzyme [86, 94]. There was no correlation between the intra-repeat loop affected, carcinoma type or subtype. All except one of the observed mutations resulted in a predicted radical amino acid change (Supplemental Table A.1 (Appendix A)), and none of the mutations are predicted to result in premature termination or frameshifts.

To give some insight into the possible morphological differences within endometrial high-grade serous carcinomas with and without mutations, in conjunction with a histopathology expert, we assessed expression of p53, WT-1 (Wilms Tumour 1), and ER (Estrogen Receptor) by immunohistochemistry (IHC) (Supplemental Table A.2 (Appendix A)). The frequency of IHC staining of abnormal p53 (nuclear overexpression immunostaining or complete loss of protein expression) and ER immunoreactivity (IHC positive) was 87.8% (43 of 49 cases), and 79.6% (39 of 49 cases) of endometrial high-grade serous carcinomas, respectively. WT-1 positive IHC staining was also present in 28.6% (14 of 49 cases), which is consistent with the typical immunohistochemical profile of endometrial serous carcinomas [156]. There were no significant differences of expression (Pearson Chi-Square probability >0.15) of these molecules within the endometrial high-grade serous carcinomas that were mutation positive and mutation negative for *PPP2R1A*. Therefore, *PPP2R1A* mutations are independent from these already known molecular markers of endometrial high-grade serous carcinoma.

2.4 Discussion

As indicated in Chapter 1, endometrial serous carcinoma is a well-recognized aggressive variant of endometrial cancer, with a high propensity for extra-uterine metastasis [11, 12, 157]. I have identified a total of 31 missense mutations within exons 5 and 6 of *PPP2R1A*, with novel mutations most frequently (40.8%) found in endometrial serous carcinomas. No mutations were detected in either high-grade or low-grade serous ovarian carcinomas; however only a small number of the latter (n=12) were studied. Previous *PPP2R1A* mutational analysis had suggested that the mutated amino acids P179, R182, R183 and W257 are involved in the interaction with different B subunit family members [86, 137, 152, 153]. Mutation of residues 179, 182, and 183 to alanine results in variable loss (50-90%) of binding to B subunit family members, and of particular importance a W257A mutation completely abolishes binding of B subunit family members [153]. The A subunit residues P179, R183 and W257 are known to interact with B subunit residues at N206, E214 and L107 of the B' regulatory subunit B56γ1 (PPP2R5Cγ1), respectively [86, 94], suggesting that all of these residues may influence interactions with the regulatory B subunits. Additional *in silico* computation, by MutationAssessor [158], of these protein mutations results in a medium functional impact score adding further evidence to the importance of these amino acid residues. Furthermore, multiple studies have found polyomavirus

middle and small tumour (T) antigens and SV40 small t antigens can displace the regulatory B subunits [106, 107] resulting in increased phosphorylation of PP2A substrates and increasing cellular transformation [108]. Taken together this may indicate that mutations of the above noted regions of PPP2R1A could have a dominant-negative effect, modifying or eliminating proper interaction within the holoenzyme of regulatory B subunit family members. This may result in a change of the spectrum of PP2A scaffold, catalytic and regulatory subunit combinations in cells, and possible destabilization of the PP2A complex. In Chapter 6, the effect of a specific PPP2R1A mutation on B subunit interactions is determined using immunoprecipitation coupled with mass spectrometry.

Jones *et al.* suggested that since *PPP2R1A* mutations clustered in a small region, similar to the pattern of mutations seen in many well-described oncogenes, the mutations might be pro-oncogenic [70]. However, as previously described in the Introduction of this thesis (Chapter 1) the PP2A holoenzyme has mostly been described as a putative tumour suppresser and acts to regulate multiple cellular pathways [159-161]. The PP2A B subunits have been associated with negative regulation of multiple cancer-causing pathways including c-MYC, BCL2, p53, ERBB2, and AKT (reviewed in [82]). PP2A plays a role in the regulation of MAP kinase signalling and WNT pathways, possibly by stabilizing β-catenin, which can lead to proliferation and tumourigenesis [82, 162]. PP2A also plays a role in the G2-M cell cycle transition through direct interaction and dephosphorylation of CHK2 leading to cell cycle arrest [161, 163]. Additionally, the dysfunction of PP2A has been hypothesized to play a role in progression of serous borderline tumour cell lines [164]. Overall, the numerous studies of PP2A in the literature reflects the importance of this phosphatase complex for normal cellular functions and tumourigenesis.

Previous studies have highlighted the morphological similarities between high-grade serous carcinoma of the endometrium and ovary, starting with the first detailed description of serous carcinoma of the endometrium [11], however this study demonstrates an important molecular difference between them. Mutations in *PPP2R1A* were present in 40.8% of endometrial serous carcinomas, but were not seen in any high-grade serous carcinomas of the ovary. Although, this does not preclude the occurrence of low frequency *PPP2R1A* mutation in ovarian high-grade serous carcinomas, it does make them distinct. I have also shown IHC staining for the expression

of p53, WT-1 and ER, which is consistent with previous reports of molecular profiling of endometrial serous carcinomas [165]. These results also confirm distinct expression differences of WT-1 between endometrial and ovarian high-grade serous carcinomas, further strengthening the argument to caution against the common practice of regarding these as equivalent tumours.

Certainly the role of *PPP2R1A* in cancer has not been fully resolved; this study and future studies of full *PPP2R1A* sequencing may reveal further evidence supporting a role for *PPP2R1A* in endometrial and ovarian cancers. The identification of these subtype-specific mutations in endometrial serous carcinoma may have potentially significant treatment implications. These patients almost invariably receive adjuvant therapy, and remain at high risk for relapse and death, which underscores the need for further research. I hypothesize that mutations of *PPP2R1A* and thus the dysfunction of the PP2A holoenzyme may contribute to disease pathogenesis in a subtype specific manner, serve as a molecular marker and, upon further study, yield molecular druggable targets for high-grade serous carcinoma of the endometrium.

Chapter 3: Mutational Classification of Endometrial Carcinoma Subtypes

3.1 Introduction

Before the TCGA (The Cancer Genome Atlas) endometrial genomics characterization study [42], large-scale mutational profiling had been mostly confined to single gene or hotspot screening studies using Sanger-based sequencing. As described in the Introduction, advances in next-generation sequencing technologies in the last few years has allowed sequencing of multiple genes and samples simultaneously [166], making large mutational studies achievable.

Unlike ovarian subtype classification [69], no single gene is a sensitive or specific marker for endometrial carcinoma subtypes; therefore it is likely that the analysis of gene panels will be needed to guide subclassification. Ovarian subtype classification is considered reproducible, however recent reports have shown the current pathological classification and grading system of high-grade endometrial carcinomas is limited in both reproducibility and prognostic ability [23, 167-169]. My discovery of subtype-specific *PPP2R1A* mutations in endometrial serous tumours, described in Chapter 2, gives significant evidence to support mutational profiles aiding in stratifying endometrial subtypes. Therefore, herein I sought to determine the mutation profiles of a large series of endometrial carcinomas, using next-generation exon capture sequencing of 9 genes known to be important in carcinogenesis (*ARID1A, PTEN, PIK3CA, KRAS, CTNNB1, PPP2R1A, BRAF, TP53,* and *PPP2R5C)* in an attempt to improve the classification of endometrial carcinomas.

3.2 Methods

3.2.1 Patient Samples

I obtained 152 endometrial tumours, and 90 corresponding buffy coat specimens originating from the BC Cancer Agency and Vancouver General Hospital via the OvCaRe Tissue Biobank repository, Vancouver, BC, Canada. An additional 76 cases of endometrial serous carcinomas, corresponding to two TMAs were also obtained from the same institutions. Patients were informed for written consent, and research ethics approved as previously described [1]. An additional 260 endometrial tumour DNA samples were obtained from Washington University, St. Louis, Missouri. The endometrial subtype, grade and microsatellite instability data was

previously determined in these cases. All samples from both centers' have undergone review by gynaecological pathologists.

3.2.2 DNA Isolation

Genomic DNA, from the Vancouver cohort, was extracted from flash frozen tumours using the Ambion DNA extraction kit as per manufacturer's protocol (Ambion, Life Technologies). Genomic DNA, from the St. Louis cohort, was isolated using Proteinase K and phenol extraction or the DNeasy Tissue kit (Qiagen Inc.). For the additional endometrial serous cohort, fixed formalin paraffin embedded (FFPE) blocks were identified and extracted for DNA using the Qiagen FFPE kit as per manufacturers protocols.

3.2.3 Exon Sequencing

Genomic DNA (500ng) was used for indexed Illumina library construction [71], then underwent targeted enrichment using biotinylated RNA capture probes generated from cDNA clones or PCR amplicons [170] representing all exons of *ARID1A, PTEN, PIK3CA, KRAS, CTNNB1, PPP2R1A, BRAF, TP53,* and *PPP2R5C* (probe genomic locations can be found in Supplemental Table B.3 (Appendix B) and sequenced using Illumina (GAIIx).

3.2.4 Bioinformatics Analysis

Short reads were aligned to the human genome (hg18) using the BWA aligner v0.5.9 [171]. A Random Forest classifier (MutationSeq) trained on validated SNVs was used to remove false-positive calls [172]. SNVs in the Catalogue of Somatic Mutations in Cancer (COSMIC) [173] were considered to be true positives, so a 99% cutoff threshold was selected with a probability threshold cutoff of 0.2588 (Supplemental Figure B.1 (Appendix B)). Mean coverage was plotted for cases with and without mutations (Supplemental Figure B.2 (Appendix B)). Details found in Supplemental materials and methods (Appendix B).

3.2.5 DNA Validations

Select predicted SNVs were validated using Sanger sequencing as previously described [1]. Sanger sequencing validated a subset of the SNVs and indels called by bioinformatics' analysis. I validated 340 predicted positions that were present in all 9 genes tested. 330/340 (97%)

positions were validated as true positive, and 10/340 (2.9%) were considered false positive. The majority of these false positives have low allelic fraction reads (<10%), therefore Sanger sequencing may not be sensitive enough to identify these mutations if tumour cellularity is low. Validation was performed on a range of called mutations with low and high frequency and probability. All others were considered true positive unless otherwise indicated.

3.2.6 Targeted Fluidigm-MiSeq Sequencing of *PPP2R1A, FBXW7, TP53*

Targeted primers were designed to cover the full exon regions of the genes (*PPP2R1A, FBXW7, TP53*) and synthesized by IDT Technologies. All primers were tested and re-synthesized if no amplification product was present. In brief, primer sets were designed using Primer 3 to amplify the specific gene regions, and tagged with CS1 (5'-ACACTGACGACATGGTTCTACA-3') and CS2 (5'-TACGGTAGCAGAGACTTGGTCT-3') sequencing tags. PCR products (150-200bp) were amplified using the Fluidigm 48X48 Access Arrays, as per manufacturers protocol, with input of 100ng for FFPE derived DNA, and 50ng for high-quality DNA from buffy coat or frozen tumour DNA. DNA was sequenced originating from 89 endometrial serous tumours with 40 from frozen tumours, and 49 from FFPE tissue. DNA barcodes (10bp) with Illumina cluster-generating adapters were added to the libraries post-Fluidigm harvest as previously described [174], and cleaned-up using Agencourt AMpure XP beads (Beckman Coulter). Barcoded PCR product pools were then quantified using the high sensitivity DNA assay and Qubit fluorometer (Life Technologies) and pooled to one total library by normalizing to equal amounts of PCR product. In total, 96 samples were pooled, denatured according to Illumina standard protocols, and sequenced using a MiSeq 300 cycle V2 kit on the Illumina MiSeq for ultra-deep validations. Uni-directional barcode sequencing was performed. All bam and VCF files were generated using Illumina MiSeq reporter. Analysis was performed using the VCF files generated by the somatic variant caller 3.2.3.0, then filtered based on reads passing filter, non-synonymous, and >5% variant allele frequency. All potential mutations were then manually interrogated and filtered using the Integrated Genome Viewer (IGV). For validations, repeat Fluidigm-MiSeq sequencing was performed along with select Sanger sequencing, however CS1 and CS2 primers were used as a universal sequencing primers on the ABI 3130xl Genetic Analyzer (Applied Biosystems) and analyzed as previously described [1]. Normal DNA was also sequenced to check somatic status.

3.2.7 Identifying Outlier Cases

Outliers were identified by observing mutation profiles that did not fit the original diagnosed histological subtype; defined as ESC with *PTEN* and/or *ARID1A* mutations, and low-grade EECs with only *TP53* and/or *PPP2R1A* mutations. With the goal of comparing mutational outliers with immuno-profiles, formalin-fixed embedded paraffin blocks were only available for 147/156 Vancouver cases, for the construction of a Tissue Microarray (TMA). These cases were used for the characterization of mutational outliers, by correlating with morphology and immunohistochemistry (IHC), and retrospectively reviewed by two independent pathologists, using the full hysterectomy case, without knowledge of mutation or IHC data.

3.2.8 TMA and Immunohistochemistry

To construct the endometrial TMA, tumours were annotated by a pathologist (BG) and two 0.6mm cores per case were arrayed. TMAs were cut at 4μm thickness onto Superfrost+ glass slides, and were processed using the Ventana Discovery XT, and the Ventana Benchmark XT automated system (Ventana Medical Systems) as per manufacturer's protocol with proprietary reagents. After slides were baked at 60°C for 1 h, they were deparaffinized on the automated system with EZ Prep solution (Ventana). Heat induced antigen retrieval method was used in Cell Conditioning solution (CC1-Tris based EDTA buffer, pH 8.0, Ventana). The rabbit monoclonal ER, clone SP1 (cat#: RM-9101) antibody was obtained from Thermo Fisher Scientific, the mouse monoclonal p53, clone DO-7 (cat#: M7001) antibody obtained from Dako, the rabbit monoclonal PR, clone 1E2 (cat#790-2223) antibody obtained from Ventana, the rabbit monoclonal PTEN, clone 138G6 (cat#9559) antibody obtained from Cell Signaling, the mouse monoclonal p16, clone E6H4 (cat#9517) antibody obtained from mtm Laboratories, the rabbit monoclonal c-myc, clone Y69 (cat# ab3072) antibody obtained from Abcam. Primary incubations for ER were performed for 60 min with heat at a 1:25 dilution, 32 min with heat at 1:800 dilution for p53, 8 min with heat and neat for PR, 60 min without heat at 1:25 dilution for PTEN, and 32 min with heat at 1:3 dilution for p16, all using Ventana antibody diluents. The Ventana Universal Secondary Antibody was used for 32 min at 37°C. The detection system used was the Ventana DABMap kit (ER, PR), Ventana UltraMap DAB kit (PTEN), Ventana OptiView DAB kit (p16, p53), and slides were then counterstained with Hematoxylin and treated

with a proprietary bluing agent (Ventana). All washes were conducted with the Ventana Reaction Buffer, and dehydration steps and coverslip procedure were completed as per manufacturer's recommendations. Categorical scoring for ER, PR, PTEN, p16 was assessed as 0=no expression (loss of expression for PTEN), 1=expression. Scores for p53 were as follows: 0=loss of expression, equivalent to deletion or nonsense mutation, 1=normal expression, 2=overexpression equivalent to missense mutation (Supplemental Table B.5 (Appendix B)). The c-myc IHC was scored as intensity =0/1/2, and nuclear expression 0-100%. The final scoring resulted from the maximum H-score between duplicate TMA cores calculated as intensity multiplied by percent nuclear positivity.

3.2.9 Microsatellite Instability (MSI) Assay

The analysis of tumour MSI was performed as previously described [175]. I used the Bethesda Markers; Bat 25, Bat 26, DI7S250, D5S346, and D2S123 to assess the MSI status. MSI-high is reported if 2 or more markers have MSI, one or less markers with MSI were considered MSI-low, and MSS (Microsatellite Stable) indicates no markers were positive. Cases reported as N/A, did not have sufficient normal available to assess the MSI status of these tumours (Supplemental Table B.4 (Appendix B)).

3.2.10 Statistical Analysis

Fisher exact tests and multivariable logistic regression analysis were used to test the significance of associations between mutations within subtypes. All tests were two-tailed and p-value < 0.05 were considered significant. Fisher exact tests were not adjusted for multiple comparisons. The multivariable logistic regression model used step-wise selection based on the likelihood ratio test, with all genes included. The Hosmer-Lemeshow test was used to assess the goodness-of-fit of the estimated logistic regression models.

3.3 Results

To determine the mutation frequencies in various subtypes of endometrial carcinomas, exon capture sequencing was performed for *ARID1A, PTEN, PIK3CA, KRAS, CTNNB1, PPP2R1A, BRAF, TP53,* and *PPP2R5C*. This resulted in the detection of somatic nonsynonymous missense, truncating, indels (insertions/deletions), and splice site mutations in 90.1% (353/392) of cases. The characteristics of the endometrial carcinomas, with histology subtypes and grade, are summarized in Table 3.1. These carcinomas were stratified into low-grade (grade 1 and 2) EECs, EEC-3, ESC, carcinosarcoma, mixed, and undifferentiated, based on routine histopathological assessment, to determine the differences in mutational profiles. All mutational data are summarized in Supplemental Table B.4 (Appendix B). The mutation frequencies of *ARID1A, PTEN, PIK3CA, PPP2R1A, TP53*, and *CTNNB1* are significantly different across four subtypes of endometrial carcinomas (Table 3.2).

3.3.1 High-Grade and Low-Grade Endometrioid Carcinomas have Similar Mutation Profiles but Differ in Frequencies of *TP53* Mutations

Low-grade EECs have mutations in *PTEN* (67%), *ARID1A* (47%), *PIK3CA* (38%), and *CTNNB1* (24%) (Table 3.2), with higher frequencies of mutations in *PTEN* (90%), *ARID1A* (60%), *PIK3CA* (57%), *KRAS* (27%), *PPP2R1A* (10%) and *TP53* (30%) seen in EEC-3s (Table 3.2). The comparison of mutations in low-grade EEC and EEC-3 showed that *PTEN* ($p=0.0111$) and *TP53* ($p=0.0046$) mutation frequencies are significantly different (Table 3.3). Multivariable logistic regression model fitting suggested *PTEN* ($p=0.007$) and *TP53* ($p<0.001$) mutations as disguising features (Table 3.4).

All Subtypes	
Endometrioid	306
Grade 1	169
Grade 2	107
Grade 3	30
Serous	37
Mixed*	4
Undifferentiated	3
Carcinosarcoma	42
Total	392

Table 3.1 Summary of all endometrial carcinoma subtypes
***** Includes one cases as mixed serous and endometrioid carcinoma, one case mixed G2 and G3 endometrioid and clear cell carcinoma, and two cases as mixed serous and clear cell carcinoma.

	Low-Grade Endometrioid (G1 and 2) (n=276)	High-Grade Endometrioid (G3) (n=30)	Serous (n=37)	Carcinosarcoma (n=42)	p-value across all subtypes (chi-squared test)
PTEN	185 (67.0%)	27 (90.0%)	1 (2.7%)	14 (33.3%)	**4.63E-17**
PIK3CA	105 (38.0%)	17 (56.7%)	10 (27.0%)	12 (28.6%)	**0.0480**
ARID1A	129 (46.7%)	18 (60.0%)	4 (10.8%)	10 (23.8%)	**5.77E-06**
KRAS	46 (16.6%)	8 (26.7%)	3 (8.1%)	7 (16.7%)	0.2434
CTNNB1	66 (23.8%)	6 (20.0%)	1 (2.7%)	2 (4.8%)	**1.19E-03**
PPP2R1A	19 (6.9%)	3 (10.0%)	16 (43.2%)	9 (21.4%)	**1.50E-09**
TP53	28 (10.1%)	9 (30.0%)	25 (67.6%)	27 (64.3%)	**2.79E-23**
BRAF	8 (2.9%)	2 (6.7%)	2 (5.4%)	1 (2.4%)	0.6186
PPP2R5C	1 (0.4%)	2 (6.7%)	0 (0%)	0 (0%)	**0.002**

Table 3.2 The frequency of mutations within all endometrial subtypes
Bold indicates significant p-values <0.05

	Low-Grade Endometrioid vs. High-Grade Endometrioid	Low-Grade Endometrioid vs. Serous	High-Grade Endometrioid vs. Serous	High-Grade Endometrioid vs. Carcinosarcoma	Serous vs. Carcinosarcoma
PTEN	**0.0111**	**6.58E-15**	**2.57E-14**	**1.09E-06**	**4.30E-04**
PIK3CA	0.0522	0.2091	**0.0235**	**0.0276**	1.0000
ARID1A	0.1826	**1.38E-05**	**2.42E-05**	**0.0030**	0.1522
KRAS	0.2000	0.2328	0.0525	0.3814	0.3215
CTNNB1	0.8211	**1.23E-03**	**0.0394**	0.0602	1.0000
PPP2R1A	0.4630	**4.96E-08**	**2.95E-03**	0.3365	0.0526
TP53	**4.62E-03**	**8.56E-14**	**3.17E-03**	**0.0080**	0.8151
BRAF	0.2555	0.3352	1.0000	0.5669	0.5972
PPP2R5C	**0.0263**	1.0000	0.1967	0.1702	NA

Table 3.3 Univariate Fisher exact test (p-values) to show significant differences between mutation profiles of each endometrial carcinoma subtypes.

3.3.2 Endometrial Serous Carcinomas Show a Distinct Mutation Profile

Of 37 ESCs, high frequencies of mutations were found in *TP53*, *PPP2R1A*, and *PIK3CA* (Table 3.2). *TP53* and/or *PPP2R1A* mutations were found in 28/37 (75.7%) of ESCs, accounting for the majority of aberrations in this subtype (Figure 3.1). The comparison of EEC-3 to ESC revealed significantly different mutation frequencies for *ARID1A, PTEN, PIK3CA, CTNNB1, PPP2R1A,* and *TP53* ($p < 0.05$) (Table 3.3). Low frequencies to zero mutation events were noted for some genes common in both ESCs and EEC-3. In an attempt to keep all the multivariable analyses consistent across the subtype comparisons, the statistician and I included the same list of genes in the logistic regression model building between EEC-3 and ESC. As a result, there was no one reliable multivariable logistic regression model built, based on the mutation markers, to distinguish between these two subtypes (Table 3.4). As expected, the mutational profiles of low-grade EEC and ESC are significantly different (Table 3.3). Multivariable logistic regression shows, *PTEN* ($p < 0.001$) with a trend of *ARID1A* ($p=0.08$) mutations associated with low-grade EEC, whereas *PPP2R1A* and *TP53* ($p < 0.001$) are associated with ESC (Table 3.4). Additional testing in a separate cohort would need to be performed to validate these results.

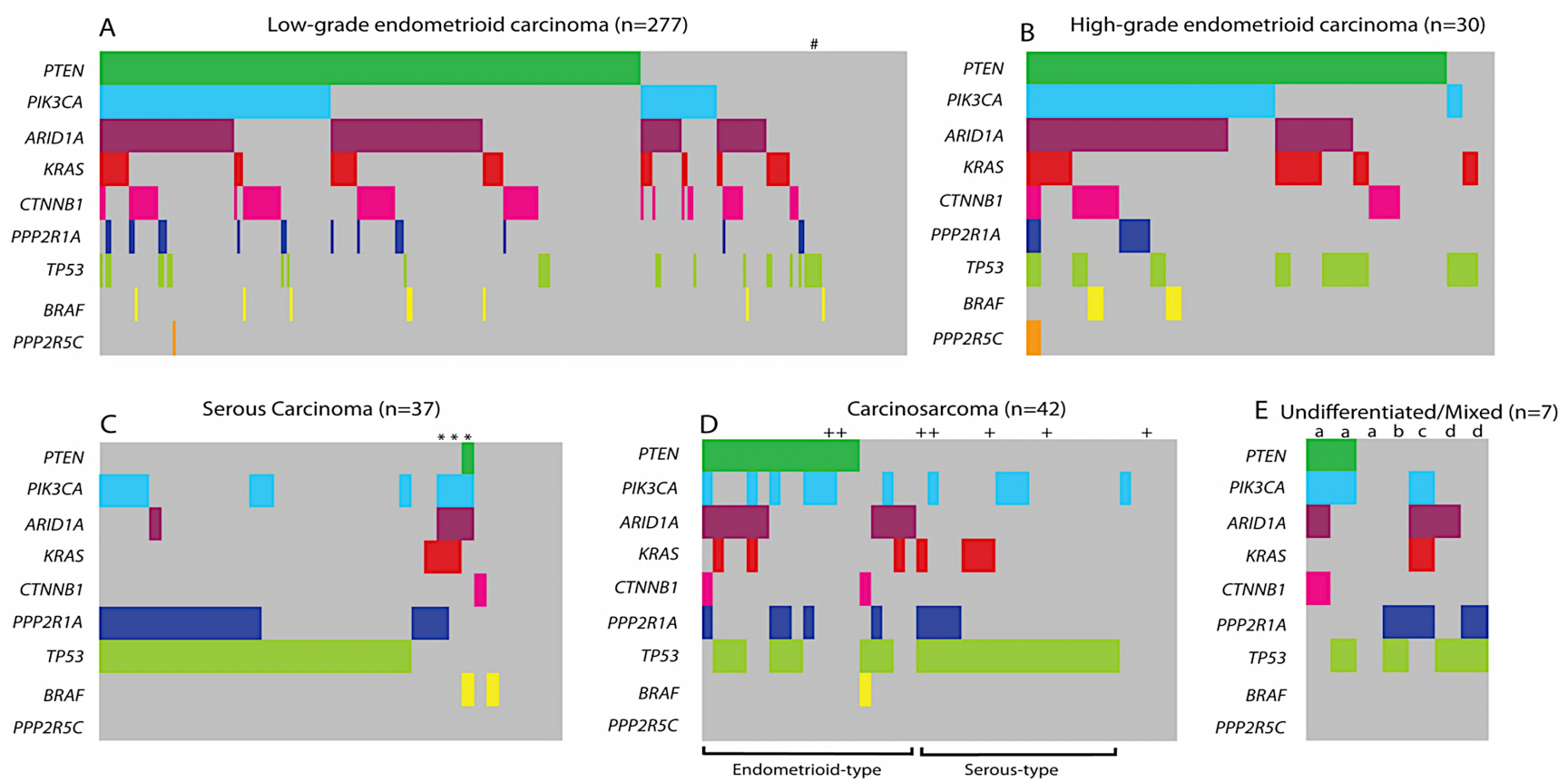

Figure 3.1 Mutation profiles of endometrial subtypes

A. Low-grade endometrioid carcinoma, including grade 1 and 2 tumours (n=276); **B.** High-grade endometrioid carcinoma, grade 3 tumours (n=30); **C.** Serous carcinoma (n=37); **D.** Carcinosarcoma (n=42), (+) indicates carcinosarcomas with heterologous differentiation elements; **E.** Undifferentiated and mixed histology subtypes, (a) undifferentiated carcinomas, (b) mixed low-grade EEC with serous carcinoma, (c) mixed endometrioid and clear cell carcinoma, (d) mixed serous and clear cell carcinoma. Rows indicate genes, columns represent tumour cases. Coloured bars indicate mutations' including; missense, truncating, indels and splice site mutations. Grey bars indicate no mutations were detected. (*) indicates serous carcinoma outliers with *ARID1A* mutations; (#) indicates low-grade EECs and EEC-3s mutation outliers with serous-type mutations (*TP53* or *PPP2R1A*).

Gene (Marker)	Low-grade Endometrioid (n=276) vs. High-grade Endometrioid (n=30)		Low-grade Endometrioid (n=276) vs. Serous (n=37)		High-grade Endometrioid (n=30) vs. Serous (n=37)		High-grade Endometrioid (n=30) vs. Carcinosarcoma (n=42)		Serous (n=37) vs. Carcinosarcoma (n=42)	
	p-value	Odds ratio* to high-grade endometrioid	p-value	Odds ratio* to serous	p-value	Odds ratio* to serous	p-value	Odds ratio* to carcinosarcoma	p-value	Odds ratio* to carcinosarcoma
PTEN	0.007	5.61 (1.6-19.7)	1.89E-04	0.02 (0.002-0.14)			3.75E-05	0.05 (0.01-0.22)	6.24E-03	19.41 (2.3-162.6)
PIK3CA										
ARID1A			0.080	0.3 (0.08-1.2)						
KRAS										
CTNNB1										
PPP2R1A			2.7E-04	13.28 (3.3-53.4)			0.0736	5.12 (0.86-30.7)	0.0446	0.32 (0.1-0.97)
TP53	7.04E-04	4.95 (2.0-12.5)	7.64E-05	7.64 (2.8-20.9)						
BRAF			1.40E-02	18.9 (1.8-196.7)						
PPP2R5C										

Table 3.4 Multivariable logistic regression analysis of gene mutations between endometrial carcinoma subtypes.
Reported values are only the most significant genes selected by the step-wise selection method based on the Likelihood ratio test. *Odds ratio (95% CI).

3.3.3 Cases with Discordant Morphological Diagnosis and Mutational Profiles

As discussed, ESCs were found to have a high frequency of mutations in *TP53* and *PPP2R1A* (Figure 3.1). From the mutation profiles, I identified three histology-defined ESC cases with *ARID1A* and *PTEN* mutations and lacked *TP53* mutations, a profile more indicative of EECs (Figure 3.1). Other studies have not found *ARID1A* or *PTEN* mutations in ESCs, however there have been limited studies testing for *ARID1A* mutations in endometrial carcinomas [31, 34, 176]. On independent histopathological review of these three cases, all were mixed tumours consisting predominantly of ESC, but with minor components of low-grade EEC in two cases, and EEC-3 with clear cell carcinoma in one case (Table 3.5). For the two mixed ESC and low-grade EEC cases, I confirmed the section of tumour sample used for DNA extraction and subsequent sequencing exclusively contained the ESC component (Figure 3.2); however it

ID	841	1120	220	895	511	1034	611
Original Subtype	Serous carcinoma	Serous carcinoma	Serous carcinoma	Low-grade endometrioid carcinoma	Low-grade endometrioid carcinoma	Low-grade endometrioid carcinoma	Low-grade endometrioid carcinoma
Review	mixed serous (80%) and low-grade endometrioid carcinoma, with adjacent endometrium showing focal complex atypical hyperplasia	mixed serous (60%) and low-grade endometrioid carcinoma, with adjacent endometrium showing complex atypical hyperplasia	Grade 3 endometrioid with clear cell changes	Grade 2 endometrioid (extensively myometrial-invasive and LVI)	Grade 3 endometrioid	Mixed low-grade (G2) endometrioid and serous carcinoma	Serous carcinoma
p53-IHC[a]	1	1	1	2	2	2	2
ER-IHC[b]	0	1	0	1	1	1	1
P16-IHC[b]	0	0	0	0	0	1	1
PR-IHC[b]	0	1	0	1	1	1	NA
PTEN-IHC[c]	1	1	0	0	0	0	0
ARID1A	p.Q420*, p.R1335*	p.Q2176fs	p.Q548fs, p.G1847fs				
PTEN			p.L265fs			splice site acceptor	
PIK3CA	p.G106V, p.V344M	p.Q546K, p.H1047Y	Y1021C				
KRAS	p.G13D	p.G12A					
PPP2R1A	p.R182W				p.P179L		
TP53				p.R282W	p.H193L	p.R248Q	p.S241F
CTNNB1							
BRAF			p.A526V, p.P403fs				
PPP2R5C							

Table 3.5 Outlier cases with pathological review, IHC and mutation profile.

[a]Scoring; 0= loss of expression, 1= normal expression, 2= over-expression

[b]Scoring; 0= no expression, 1= over-expression, [c]Scoring; 1=normal expression, 0= loss of expression

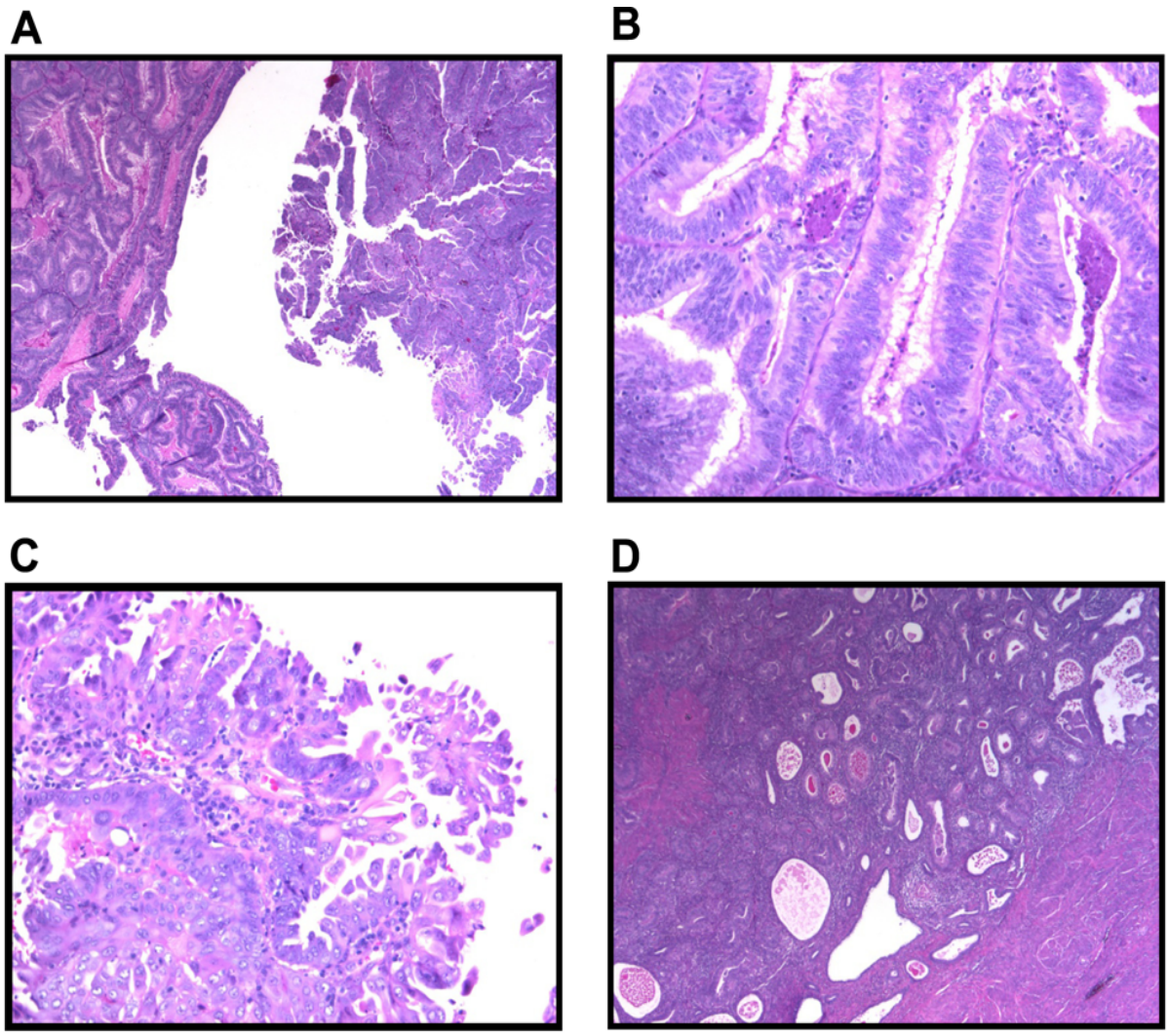

Figure 3.2 A case originally diagnosed as serous carcinoma, but with an *ARID1A* mutation and no *TP53* mutation, is a mixed low-grade endometrioid and serous carcinoma (case #1120).
A. A mix of a grade 1 endometrioid (left half) and high-grade serous (right half) carcinoma, 40X magnification; **B**. High power (100X) image of histologically distinct low-grade endometrioid carcinoma; **C**. High power (100X) images of serous carcinoma component, of which the sampling of tumour was used for mutation sequencing; **D**. Atypical complex hyperplasia in the background endometrium (40X magnification) harbored mutations with an endometrioid profile. Immunostaining is recommended for use in diagnostically problematic cases [22], although not universally used. These three cases showed a non-serous IHC profile; p53 normal expression and p16 negative expression, while one expressed ER and PR (Table 3.5).

harbored mutations with an endometrioid profile. Immunostaining is recommended for use in diagnostically problematic cases [22], although not universally used. These three cases showed a non-serous IHC profile; p53 normal expression and p16 negative expression, while one expressed ER and PR (Table 3.5).

I also identified four outlier low-grade EECs that contained *TP53* mutations and lacked *PTEN* mutations, which were also diagnostically challenging cases. Upon review, two cases showed morphological features of serous, and one case was re-classified from low-grade EEC to EEC-3. One outlier remained classified as low-grade EEC, however it was noted that this case showed extensive myometrial invasion and widespread lymphovascular invasion. By IHC, abnormal p53 expression was confirmed in all cases. All were, however, ER-positive with PTEN loss of expression, features found primarily in EECs. In two of these cases, p16 was strongly expressed (Table 3.5). In summary, these seven outlier cases showed features intermediate between ESC and EEC in morphological, IHC and genetic analysis (Table 3.5, Table B.5, Figure B.3 (Appendix B)).

I also performed unsupervised hierarchical clustering analysis on the 147 cases with IHC and mutational status (Figure B.3, Table B.5, Supplemental methods (Appendix B)). This shows most low-grade EEC and EEC-3 subtypes cluster together, while the remaining EEC-3, serous and mixed cases are scattered. The mutational outliers with the diagnosed subtype are indicated, as well as the new classification.

3.3.4 Carcinosarcomas Show Either an Endometrioid or Serous Mutation Profile

Endometrial carcinosarcomas are relatively rare, and their classification as an endometrial carcinoma subtype or as a distinct entity is under debate [177]. In my analysis of carcinosarcomas I found mutations in *TP53*, *PTEN*, *PIK3CA*, *ARID1A*, and *PPP2R1A* (Table 3.2). Two subgroups of carcinosarcomas were identified; one group characterized by mutations in *PTEN* and *ARID1A* (endometrioid-type), and a second group with *TP53* and *PPP2R1A* mutations more similar to ESC (Figure 3.1). Heterologous differentiation of the sarcomatous component was observed in a subset of tumors from both groups. Histopathological reviews of cases were not available; therefore it was not possible to correlate morphological features and mutational profiles of endometrioid-like or serous-like in the epithelial components of these tumours.

3.3.5 Mutations Involving Signalling Pathways in Endometrial Carcinomas

By mutational analysis of multiple genes, it is possible to identify different mutations involving a single signalling pathway that may be functionally equivalent, and to examine the relationship between mutations involving different genes/pathways. Mutations in the PI3K and MAPK signalling pathways are known to be important in EECs, therefore I further examined the prevalence of mutations in *PTEN, PIK3CA, KRAS, ARID1A* and *CTNNB1*. I found 211/276 (76.5%) low-grade EECs have *PTEN* and/or *PIK3CA* mutations (Figure 3.1). Co-existent *PTEN* and *PIK3CA* mutations were identified in 79/276 (28.6%) low-grade EECs, and 16/30 (53.3%) EEC-3s (p=0.0112). *AR1D1A* mutations have recently been identified in low-grade EECs; however the relationship of these mutations with other pathways such as PI3K and WNT has not been examined [34]. Of the low-grade EECs with *ARID1A* mutations, 112/129 (86.8%) have mutations within *PTEN* and/or *PIK3CA* (p=0.0002). EEC-3s with *ARID1A* mutations (n=18) all have *PTEN* mutations, and 13/18 (72.2%) also have *PIK3CA* mutations. Thus there is a significant association between *ARID1A* and *PTEN/PIK3CA* mutations.

3.3.6 Microsatellite Instability

MSI is a feature of the endometrioid subtype, therefore I determined the MSI status of 241/276 low-grade EECs and 13/30 EEC-3s. I found 97/241 (40.2%) of the low-grade EECs were MSI positive, compared to 8/13 (61.5%) of EEC-3 (Supplemental Table B.4 (Appendix B)). Considering all 110 cases of EECs with MSI, only 39/110 (35%) harbor concurrent *PTEN* and *PIK3CA* mutations, and 25/110 (23%) have co-occurring mutation in *PTEN, PIK3CA* and *ARID1A*.

3.3.7 Analysis of *PPP2R1A* and *FBXW7* Mutations in Endometrial Serous Carcinomas

The endometrial TCGA analysis in cBioPortal (www.cbioportal.org) [32, 33], revealed similar frequencies of *PPP2R1A* (23%) and *FBXW7* (22%) mutations in the copy-number high (serous-like n=60) group of tumours (Figure 3.3A). Of interest, these two genes with the highest frequency of mutations, not including *TP53* alterations, showed a trend towards mutual exclusivity, although not statistically significant. This led to the investigation of *PPP2R1A* and *FBXW7* mutation mutual exclusivity in a validation cohort of endometrial serous carcinoma cases (89 cases). Targeted exon sequencing (involving all exons) revealed mutations in 33/89

(36%) *PPP2R1A*, 15/89 (17%) *FBXW7*, 57/89 (64%) *TP53* (Figure 3.3B, Table B.6 (Appendix B)). However, 6/89 (7%) cases harbored mutations in both *PPP2R1A* and *FBXW7*, which did not support statistically significant mutation mutual exclusivity in these cases. Further analysis of this cohort with c-Myc immunohistochemistry revealed that there is no significant association of *FBXW7* or *PPP2R1A* mutations with high c-Myc expression. However, there is a significant association of high c-Myc expression (H-score >60) when both *FBXW7* and *PPP2R1A* are mutated together (Fisher exact test, $p<0.0011$) (Table B.6 (Appendix B)).

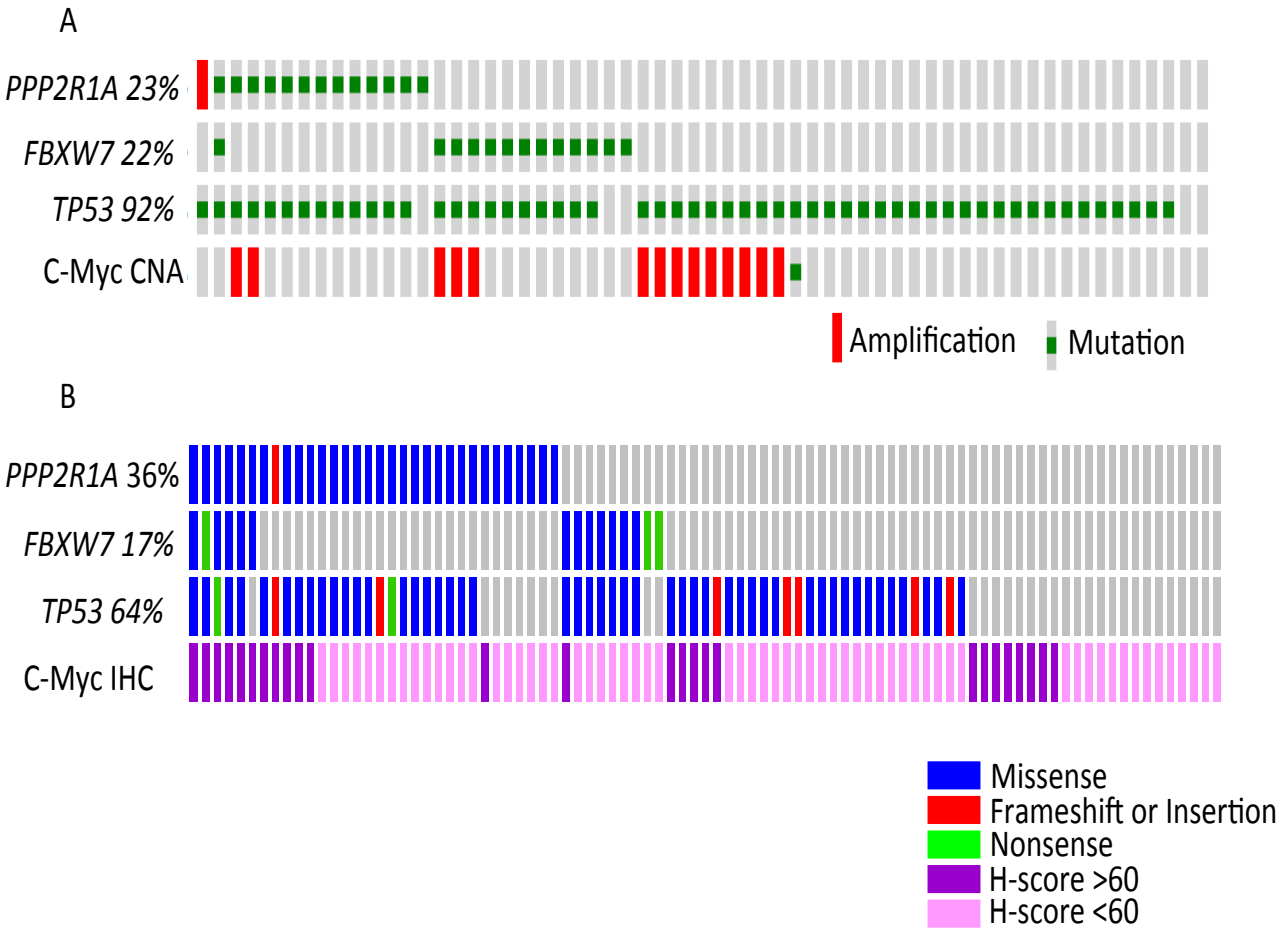

Figure 3.3 Mutation profiles of endometrial serous carcinomas
A. TCGA endometrial carcinoma OncoPrint copy number high (serous-like) (n=60) mutations and copy number alterations (CNA) data from cBioPortal. **B.** Vancouver endometrial serous carcinoma validation samples (n=89) mutations and c-Myc IHC data. Rows indicate altered genes, and columns indicate patient tumours. Grey bars indicate no mutation was detected. See Appendix B Table 8.6 for mutation and IHC details.

3.4 Discussion

Endometrial carcinoma is a heterogeneous disease, comprised of multiple subtypes with differing risk factors, precursor lesions, and outcomes. Lack of reproducibility in histopathological diagnosis of endometrial carcinoma subtypes has hindered progress. For example, while some studies have found that EEC-3 and ESC have different outcomes [178], other studies have not [23]. This difference may reflect inclusion of different cases, based on subtly different diagnostic criteria, within these cohorts. Robust and reproducible diagnostic categories are an important first step in moving towards subtype-specific treatment, which is proceeding in ovarian carcinoma [179, 180]. However in the case of endometrial carcinoma, it is likely that molecular markers will be needed to improve the suboptimal performance of conventional histopathological assessment [181]. With the advent of next-generation sequencing technologies, the molecular profiles of many tumour cell types are being extensively characterized. These mutation profiles can potentially be used diagnostically for subclassification, and to identify relevant targets for the development/deployment of targeted therapeutics. In this study, exon capture sequencing of nine genes was performed in two large cohorts of endometrial carcinomas, revealing differing mutational landscapes for endometrial carcinoma subtypes.

As demonstrated in previous studies, I identified high frequencies of mutations within *PTEN, PIK3CA, ARID1A, KRAS* and *CTNNB1*, and lack of *TP53* mutations in low-grade EECs. EEC-3s demonstrate a similar pattern of mutations, but with a significantly increased frequency of *TP53* mutations. High frequencies of *PTEN* mutations in EECs confirm this is an early driver event in tumour progression. My results show that the frequency of MSI cases is similar in low-grade EEC and EEC-3, which supports the view that the majority of EEC-3s have progressed from low-grade EEC [23].

Recent studies identified a high frequency of concurrent *PTEN* and *PIK3CA* mutations in endometrial carcinomas [27, 182], but not in any other tumour type investigated to date [27]. In this study, this phenomenon was also observed in low-grade EECs and EEC-3s, but not in ESC or carcinosarcoma. I have determined that in low-grade EECs and EEC-3s, *ARID1A* mutations

are significantly associated with concurrent mutations in *PTEN* and *PIK3CA*, a novel finding suggesting a cooperative role of these pathways in EEC tumourigenesis.

ESCs have frequent *TP53* and *PPP2R1A* mutations, and lack mutations in *PTEN, ARID1A* and *CTNNB1,* a mutational profile distinct from that of EECs. While it was not possible to classify tumours solely based on this nine gene mutation panel, I was able to use the mutation profile as a diagnostic adjunct for morphological subclassification in individual cases. This is an attractive prospect given the significant problems in distinguishing EEC-3 and ESC highlighted in recent studies [22, 53, 168, 169, 183, 184]. There were mutational outliers where the original diagnosis did not fit the mutation profile, specifically ESC cases with *ARID1A* mutations, and low-grade EECs with only *TP53* mutations. In the seven outlier cases, retrospective review by two independent pathologists resulted in reclassification, agreeing with the subtype-specific mutation patterns rather than the original diagnosis.

It has previously been proposed that ESC may arise through two different tumourigenic pathways, i.e. from progression through hyperplasia and low-grade EEC, or arising via high-grade endometrial intraepithelial carcinoma, in an estrogen-independent pathway [185]. In this study, I observed two tumours initially diagnosed as ESC that showed an endometrioid mutation profile. On retrospective review the diagnosis for both was changed to mixed serous and endometrioid. This observation is not novel but does give further support to ESCs arising in some cases by an alternative molecular pathway, rather than the classical Type 2 pathway (Figure 3.4, Figure 3.5) [186]. This further suggests that the classification of endometrial carcinomas cannot be encompassed by a simple dualistic model. In particular, the high-grade subtypes show considerable heterogeneity not reflected adequately in a Type 1 versus Type 2 model. Future studies will be required to address the following issues: 1. How reproducible is molecularly supported subtype diagnoses? 2. If diagnoses can be made reproducibly, do subtypes show significant differences in stage at diagnosis, pattern of spread, prognosis or response to treatment? Only after those questions are addressed can subtype-specific management move forward, and mutation-based treatment decisions can be made for challenging diagnoses.

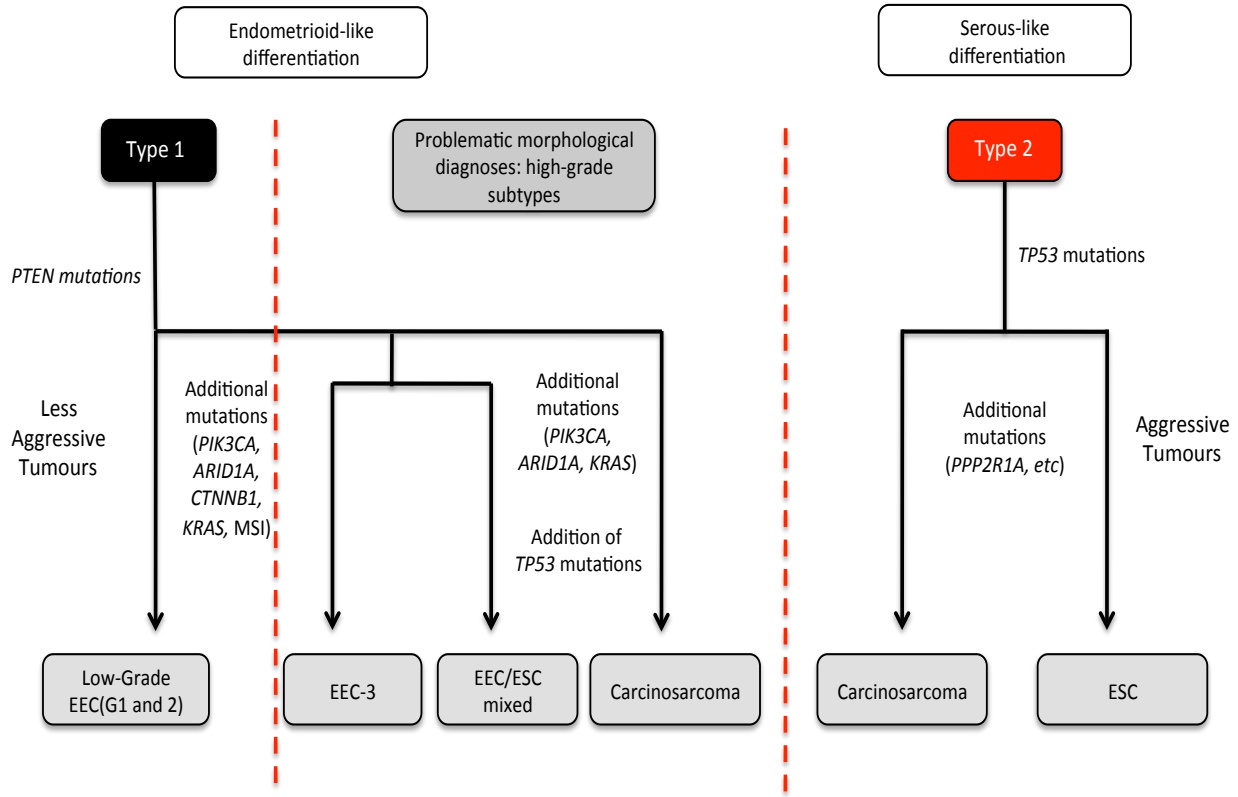

Figure 3.4 An intermediate type of high-grade endometrial carcinomas is not encompassed in the Type 1 and Type 2 model. Problematic morphological diagnoses of high-grade endometrial carcinomas are an intermediate subtype and may be further subclassified by mutational profiles.

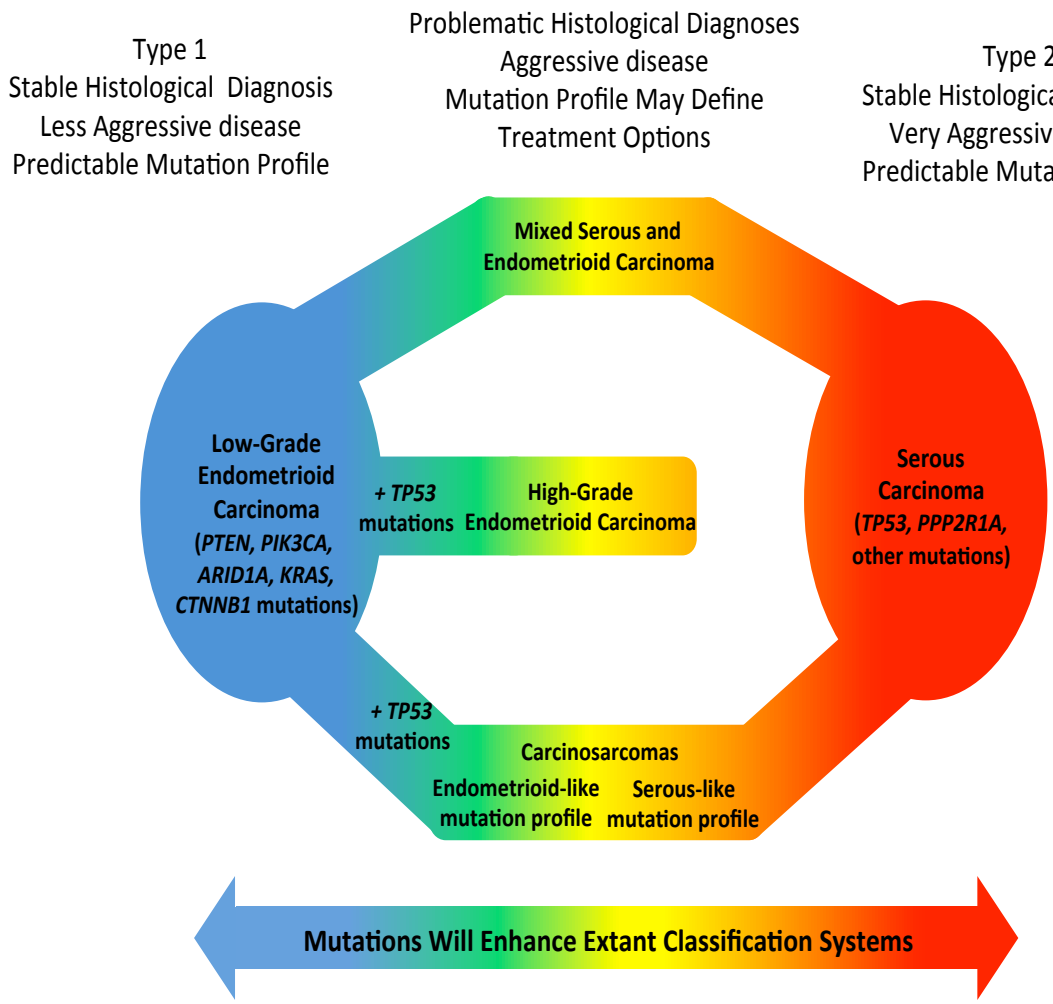

Figure 3.5 Mutational analysis may be an effective tool to classify morphologically problematic cases into biologically relevant treatment groups

Intermediate high-grade cell types tend to be diagnostically challenging cases, often with multiple morphological features of endometrioid and/or serous carcinomas. The addition of mutation profiles can lead to reproducible diagnosis and the future of mutation-based treatment decisions for targeted therapeutics. Blue and red colours indicate distinct mutation profiles for low-grade EEC and serous carcinomas. Yellow indicates the cases were the mutational profiles will aid in separating out the appropriate histological subtype and dictate appropriate treatment options for patients.

I also investigated the molecular profiles of carcinosarcomas. These tumours are generally rare with poor prognosis [187], and are composed of a mixture of carcinomatous and sarcomatous elements [188]. While previous studies have not identified a high number of mutations in this subtype [189], I have shown a moderate frequency of mutations in the majority of genes sequenced. This discrepancy may be due to limited exon sequencing in previous studies; in the current study all exons of these genes were interrogated. Two patterns of mutations were observed; an endometrioid-type mutation profile (*ARID1A, PTEN, PIK3CA*, *KRAS*) or a serous mutation profile (*TP53*, *PPP2R1A)*. This suggests a dualistic molecular evolution of carcinosarcomas with an endometrioid-like or serous-like mutation pattern, however this analysis is limited by the 9-gene panel and may underestimate the mutation patterns (Figure 3.4). Larger gene panels, whole exome, or whole genome sequencing would be useful to validate these endometrial mutation patterns in carcinosarcomas. Further validation studies will also be necessary to determine if these molecular profiles are associated with different morphological features in the carcinomatous or sarcomatous components, or are associated with outcome differences.

I acknowledge that there are limitations of this study; the pathologist and I were unable to perform full histopathological reviews of many cases, including all carcinosarcomas. There were also limited numbers of cases of EEC-3 and ESC in this study, therefore independent validation studies, linked with outcome [30], will be needed in these tumour types. There is also uncertainty about the sensitivity of the exon capture method, and false negatives are likely to be present in this data set. The TCGA endometrial sequencing effort will prove to be useful in validating the observations of this study.

After the publication of this body of work, I completed an in-depth sequencing analysis of *PPP2R1A*, *FBXW7* and *TP53* mutations in a large number (n=89) of endometrial serous cases. The mutation frequency of *PPP2R1A* was 36% in this cohort as compared to the TCGA data (23%), although my results aligned with Chapter 2 results (40% of cases with *PPP2R1A* mutations). Mutations in *TP53* were slightly lower than what was observed by TCGA. This could be due to differences in sequencing methods and the population of the cohort. Although, this difference is likely due to sequencing FFPE material, which caused a significant amount

sequencing noise due to deamination (G to A and C to T) events. This resulted in areas that were difficult to confirm the presence of mutations. In addition, a second limitation of the *TP53* sequencing was that exon 5 and 11 primers did not reliably amplify in some samples; therefore all *TP53* exons were not always sequenced efficiently. To resolve this problem, the use of immunohistochemistry could be used to determine if aberrations are present in the tumours.

This sequencing experiment was based on the analysis of TCGA data, where there appeared to be a near mutual exclusive trend of mutations in *PPP2R1A* and *FBXW7*, independent of *TP53* mutations. It has been previously shown that the PP2A pathway acts by dephosphorylating c-Myc at S62 [121], and PP2A-B56δ acts to dephosphorylate GSK3β to enable phosphorylation of c-Myc [190]. In addition, FBXW7 acts to negatively regulate c-Myc by ubiquitination and proteasome-dependent degradation [119], therefore it is possible that the mutual exclusive pattern of mutations could lead to two different pathways of activation, and converge on c-Myc. Deregulation of PP2A phosphatase activity induced by a *PPP2R1A* mutation could potentially increase c-Myc activity by increasing the phosphorylation levels of c-Myc, thus stabilizing the protein. Alternatively, a mutation in *FBXW7,* a E3 ubiquitin ligase, could disrupt its ability to ubiquitinate c-Myc, resulting in protein stabilization and lack of protein degradation. This has been demonstrated in a mouse model of leukemia where *FBXW7* R465C mutation is incapable of c-Myc ubiquitination and leads to increased c-Myc protein levels [191]. However, in this cohort of 89 serous carcinomas there was no significant associations of *PPP2R1A* or *FBXW7* mutation with the accumulation of c-Myc as assessed by IHC. There was however a significant association of high c-Myc expression when both genes, *PPP2R1A* and *FBXW7* are mutated, although the number of cases are small. It is possible that in this specific system, deregulation of both genes is needed for the stabilization of c-Myc protein levels. Previous studies have shown that PP2A B56α (PPP2R5A) specifically regulates the phosphorylation level of c-Myc at S62, which leads to stabilization and protein accumulation [121]. This was tested in the cell line HEK-293 model, therefore it is possible that *PPP2R1A* mutations in endometrial carcinomas do not specifically affect the B56α interaction, or there are cell context specific differences. A second study using HEK-293 cells has also shown that a feedback loop wherein c-Myc can induce transcriptional upregulation of PPP2R5D (B56δ), which can then participate in the dephosphorylation of GSK3β–S9. This dephosphorylation causes activation of GSK3β enabling the phosphorylation

of c-Myc to enable degradation [190]. Additional studies of these proteins with *PPP2R1A* mutations, B subunit alterations and B subunit interactions are needed in context-specific disease models. It is likely that the overall biological system may differ in each disease type. Overall, the mutational analysis of these genes in endometrial serous carcinomas are important, as they define the disease to aid in classification, and may be used to design patient targeted therapies.

Chapter 4: Differences in the Mutation Profiles of Ovarian Endometrioid and Endometrial Endometrioid Carcinomas

4.1 Introduction

Ovarian endometrioid carcinomas are histologically similar to endometrial endometrioid carcinomas. There is accumulating evidence that OECs arise from transformed endometriosis [192], which would link a common cell of origin; endometrial epithelial cells that line the uterine cavity. The molecular features of OECs and EECs have been characterized in many studies using immunohistochemistry markers and mutational analysis by DNA sequencing (reviewed in [29, 60, 77, 193]). There have been studies that infer differences in mutation frequencies in OECs and EECs [74], however to the best of my knowledge, no prior studies have directly compared endometrial and ovarian endometrioid mutation frequencies with a uniform technical approach in a large cohort of tumors. In the previous Chapter, the mutation profiles from a panel of nine genes was investigated in the various subtypes of endometrial carcinoma [2]. Herein, I have also performed the same exon capture sequencing method and applied this to a cohort of ovarian endometrioid carcinomas. The goal of this study was to directly compare the mutation frequencies of seven specific genes in low-grade EECs and low-grade OECs to determine differences in molecular features. These features may be useful in ovarian and endometrioid classification and targets for targeted therapeutics.

4.2 Materials and Methods

4.2.1 Patient Samples

I obtained frozen tumor tissue from 129 EECs and 33 OECs, for exon capture sequencing, originating from the OvCaRe Tissue Biobank repository, Vancouver, BC, Canada. Patients provided informed consent, and research ethics was approved, and DNA extracted as previously described [1]. An additional 178 EEC tumor DNA samples, with grade information available, were obtained from Washington University, St. Louis, Missouri. All samples from both centers have undergone histological review by gynaecological pathologists. All subtype and mutational data for all endometrial carcinomas have been previously reported [2]. An additional 20 OEC cases (18 frozen tumors, 2 Formalin-Fixed Paraffin Embedded were obtained from the OvCaRe Tissue Biobank repository to test *CTNNB1* mutation status, so that a total of 53 OECs were

tested for mutation in this gene only, and 33 OECs were tested for the other genes in the panel. Normal germline DNA, when available, was used for testing somatic status from mutation positive cases only from the OvCaRe Tissue Biobank.

4.2.2 Mutation Analysis

Genomic DNA (500ng) was used for indexed Illumina library construction, then underwent targeted enrichment using biotinylated RNA capture probes generated from cDNA clones or PCR amplicons representing exons of *ARID1A, PTEN, PIK3CA, KRAS, CTNNB1, PPP2R1A, TP53, BRAF* and *PPP2R5C* and sequenced using the Illumina (GAIIx). All sequencing validation methods and primers used are previously described [2]. The two genes *BRAF* and *PPP2R5C* were excluded from subsequent analysis due to only one mutation found in *BRAF* and no mutations in *PPP2R5C* in the OEC cases. To validate the differences in *CTNNB1* mutation frequencies, I re-sequenced the hotspot exon 3 of *CTNNB1* by Sanger sequencing from all 178 low-grade endometrial endometrioid DNA obtained from Washington University. Additional Sanger sequencing validations for the hotspot exon 3 of *CTNNB1* were also performed on 20 low-grade OEC cases that were not included in the original select exon capture sequencing set.

4.2.3 Bioinformatics Analysis

Short reads were aligned to the human genome (hg18) using the BWA aligner v0.5.9 [171]. A Random Forest classifier trained on validated single nucleotide variants was used to remove false-positive calls [172]. Single nucleotide variants in the Catalogue of Somatic Mutations in Cancer (COSMIC) [173] were considered to be true positives, with a probability threshold cutoff for selecting positive SNVs of 0.2588 (Figure B.1 (Appendix B)). All analysis was performed as previously described [2], and can be found in Chapter 3 materials and methods and Appendix B Supplemental methods.

4.2.4 Statistical Analysis

Fisher exact tests were used to test the significance of associations between mutations within subtypes. All tests were two-tailed and p-value < 0.05 were considered significant. The Benjamini-Hochberg [194] method was used to adjust p-values to account for multiple comparisons (R stats package).

4.3 Results

To determine the differences in somatic mutation frequencies between endometrial and ovarian endometrioid carcinomas, I used select gene exon capture sequencing of *ARID1A, PTEN, PIK3CA, KRAS, CTNNB1, PPP2R1A,* and *TP53*. This was performed using 33 cases of ovarian endometrioid and 307 cases of EECs (Supplemental Table C.7 (Appendix C)). Comparison of the mutational frequencies of low-grade (grade 1 and 2) EECs to low-grade (grade 1 and 2) OECs showed a significant difference for *PTEN* (adjusted $p<0.0007$) and *CTNNB1* (adjusted $p=0.02$) mutations (Table 4.1, Figure 4.1). *PTEN* mutations were found in 67% of low-grade EECs, while 17% of low-grade OECs harbor *PTEN* mutations. Mutations of *CTNNB1* were identified in 53% of OECs, and only 28% of EECs. This frequency of *CTNNB1* mutations in EECs is slightly higher than previously published [2] due to additional validations of mutations using Sanger sequencing and select exon capture sequencing. To further verify the high *CTNNB1* mutation frequency found in OECs, I acquired an additional 20 low-grade OECs cases and tested for hotspot *CTNNB1* mutations using direct Sanger sequencing. I found that 45% (9 of 20) of these cases contained hotspot *CTNNB1* mutations, bringing the overall frequency to 50% (25 of 50) *CTNNB1* mutations in low-grade OECs (Supplemental Table C.7 (Appendix C)). The mutation frequencies of *PIK3CA, ARID1A, PPP2R1A,* and *TP53* are not significantly different between low-grade EECs and OECs. There is a trend towards more *KRAS* mutations in low-grade OECs (33%) compared to low-grade EECs (18%), however this is not significant after multiple comparison adjustments (Table 4.1).

	Low-Grade Ovarian Endometrioid (Grade 1 and 2) (n=30)	Low-Grade Endometrial Endometrioid (Grade 1 and 2) (n=276)	Fisher Exact Test (p-value)	Adjusted p-value*
PTEN	5 (16.6%)	185 (67.0%)	**1.08e-07**	**0.001**
PIK3CA	12 (40.0%)	107 (38.7%)+	1	1
ARID1A	9 (30.0%)	129 (46.7%)	0.086	0.120
KRAS	10 (33.3%)	50 (18.1%)+	0.055	0.120
CTNNB1	16 (53.3%)	76 (27.5%)+	**0.006**	**0.020**
PPP2R1A	5 (16.6%)	19 (6.9%)	0.071	0.120
TP53	2 (6.6%)	28 (10.1%)	1	1

Table 4.1 Comparison of mutation frequencies in low-grade OECs and low-grade EECs
*p-values are adjusted using the B-H method
+ additional mutations have been verified by Sanger sequencing post-original publication.

The comparisons of high-grade (grade 3) EECs with high-grade OECs cannot be statistically compared, as this is limited by the rarity of high-grade OECs (n=3). Each high-grade OECs case harbors different mutations in different genes. Similarly to low-grade EECs, high-grade EECs also have a high frequency of *PTEN* mutations (87%), and a lower frequency of *CTNNB1* mutations (19%) (Table 4.2).

	High-Grade Ovarian Endometrioid (Grade 3) (n=3)	**High-Grade Endometrial Endometrioid (Grade 3) (n=31)**
PTEN	1 (33.3%)	27 (87.1%)
PIK3CA	1 (33.3%)	17 (54.8%)
ARID1A	0 (0%)	18 (58.1%)
KRAS	1 (33.3%)	8 (25.8%)
CTNNB1	1 (33.3%)	6 (19.4%)
PPP2R1A	0 (0%)	4 (12.9%)
TP53	1 (33.3%)	10 (32.2%)

Table 4.2 The mutation frequencies of high-grade OECs and high-grade EECs.

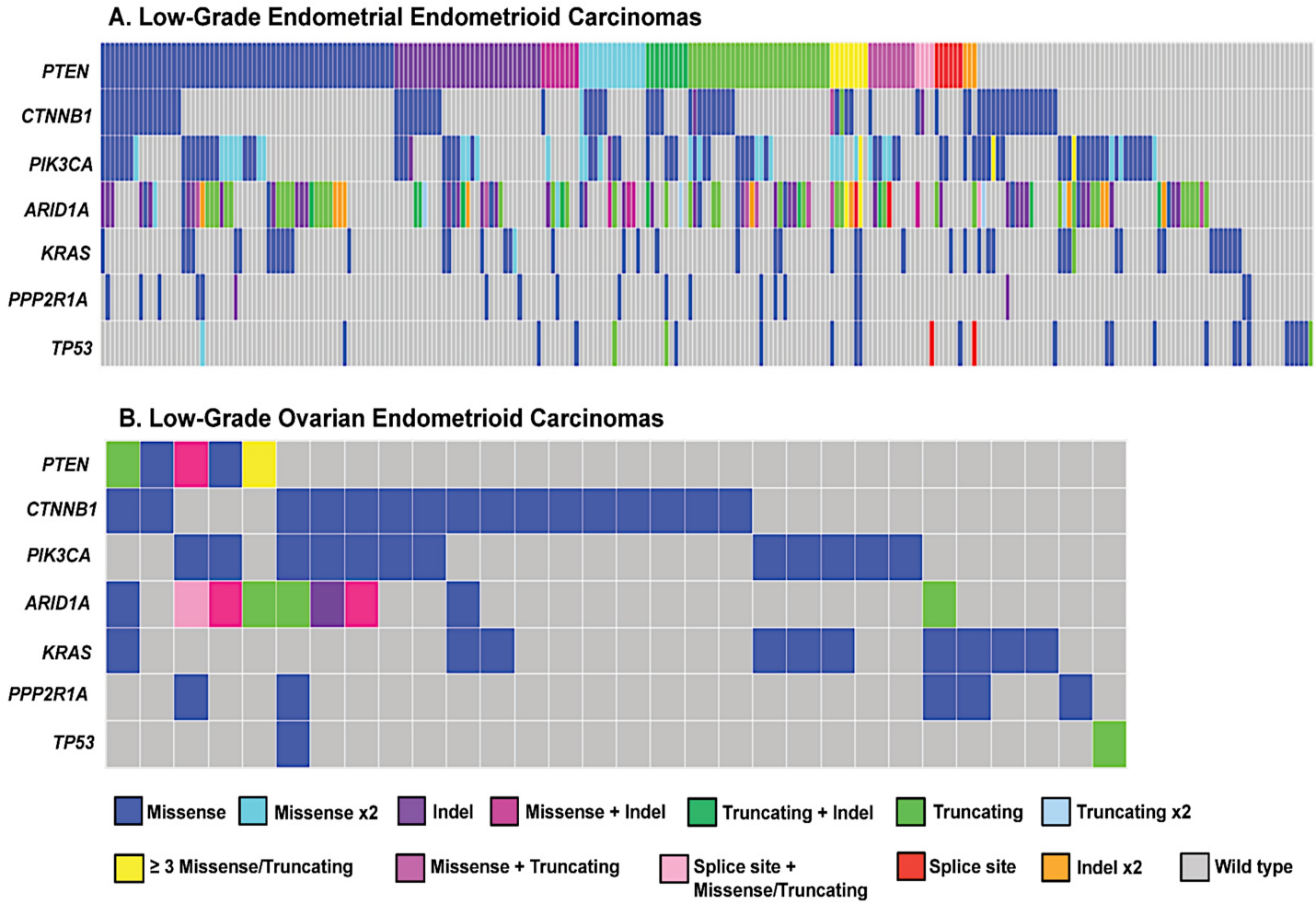

Figure 4.1 Low-grade ovarian and endometrial endometrioid mutation profiles.
A. Low-grade endometrial endometrioid carcinomas (EEC) including grade 1 and 2 (n=276). **B.** Low-grade ovarian endometrioid carcinomas (OEC) including grade 1 and 2 (n=30). Individual columns designate one tumor case, and rows indicate genes. All colored boxes specify a genetic alteration such as missense, truncating, indels, splice site mutations and combinations of these mutations. Grey boxes indicate no mutations were identified by sequencing. These colors are specifically shown in the color legend.

Most *CTNNB1* mutations found in both OECs and EECs involve known phospho-acceptor sites. In OECs, 16 of 25 (64%) contain *CTNNB1* mutations that affect serine (S33 and S37) or threonine (T41) amino acid residues, which are phosphorylation targets for glycogen synthase kinase 3-beta (GSK3β). Similarly in low-grade EECs, 43 of 76 (57%) of the *CTNNB1* mutations are located at serine (S33, S37, S45) and threonine (T41) residues (Appendix C Table C.7). Our analysis of all *CTNNB1* coding sequences also revealed additional somatic mutations outside the hotspot serine/threonine residues.

4.4 Discussion

The distinct molecular abnormalities of endometrial and ovarian carcinoma subtypes will be the basis for subtype specific treatment, and may become an essential component of stratified management strategies. Standard treatment options for ovarian and endometrial carcinomas have not yet changed, but a shift towards subtype-specific clinical trials highlights the need to better understand the molecular abnormalities and potential therapeutic targets in the different subtypes [195]. The same subtypes at different sites in the gynaecological tract, endometrial endometrioid carcinomas and ovarian endometrioid carcinomas, have indistinguishable morphology, clinical similarities, and share at least some genetic abnormalities. I have directly compared the mutation frequencies in the same gene set, using the same technology, in low-grade ovarian and endometrial endometrioid carcinomas. This has shown that there are similar mutations patterns but there are also two distinct differences.

Previous literature often refers to endometrial and ovarian endometrioid carcinomas as having similar molecular alterations [196, 197]. The same genes are often mutated, however some suggest that OECs and EECs have similar frequencies of *CTNNB1* [74] and *PTEN* mutations [198], but do not directly compare the two tumor types in the same study. In this study, *PTEN* mutations are found at higher frequencies in low-grade EECs compared to low-grade OECs, and *CTNNB1* mutations at higher frequencies in OECs compared to EECs. One limitation of this study is the small number of low-grade OECs (n=30) OECs. Previous studies have reported low-grade OECs with *CTNNB1* mutation frequencies between 16-54% [75, 199-204], with an average frequency of 40-50%. This range of *CTNNB1* mutation frequency is due to varying

methods of detection and limited exon sequencing. *PTEN* mutations are reported in only about 20% of ovarian endometrioid carcinomas [73, 205]. All these studies also assessed small cohorts of OECs, and reported similar mutation frequencies for both *CTNNB1* and *PTEN.*

Recently, our group [2] and others [27, 28, 30] have reported mutation frequencies in a large number of EECs. *Byron et al.* report a 19% *CTNNB1* mutation frequency from 466 endometrial endometrioid tumors [30]. In this study I report a slightly higher *CTNNB1* mutation frequency of 28% from 276 low-grade EECs. This difference is most probably due to differences in sequencing (hotspot vs. all exons) and analysis methods used. The current study included 25 EECs tumor samples also analyzed by Byron et al.; there were 66 *CTNNB1* and 46 *KRAS* mutations reported in the original paper [2], whereas I have now identified 76 *CTNNB1* and 50 *KRAS* mutations in these same tumours, all validated by Sanger sequencing, indicating a low false negative rate in the earlier study. This does not change the conclusions of that study [2] but does indicate that there was an underestimation of mutation frequencies. In conclusion, this study confirms observations from other studies suggesting there are differences in *PTEN* and *CTNNB1* mutation rates in OECs and EECs. Similarly, ovarian and endometrial serous carcinoma subtypes are morphologically equivalent and were often thought to have similar mutation patterns, with both showing a high frequency of *TP53* mutations. However, more detailed sequencing analyses of these tumor types have revealed mutational profile differences. Mutations of *PPP2R1A* are found at high frequencies in endometrial serous carcinomas but are rarely found in ovarian high-grade serous carcinomas [1, 206]. More recent studies have identified high frequencies of other gene mutations (i.e. *FBXW7, CHD4*) [43, 46], in endometrial serous carcinomas but not in ovarian serous carcinomas [44].

The majority of OECs are believed to arise from endometriosis [60, 76]. Although ovarian and EECs may develop from the same cell type, namely the endometrial epithelial cell, these two tumor types are exposed to different microenvironments that may reflect differences in the evolution of their mutation profiles. Endometrial endometrioid carcinomas frequently occur in postmenopausal women with unopposed estrogen [207]; exposure to high estrogen and low progesterone levels have been found to increase proliferation of endometrial cells thus increasing the risk of tumourigenesis [208]. Endometriosis is thought to occur via retrograde menstruation,

where endometrial epithelial cells travel from the uterus through the fallopian tubes and can establish as an endometriotic cyst within the ovary [67]. This creates a unique microenvironment where menstruation-like blood and necrotic tissue is trapped within the cyst, resulting in high concentrations of iron in a confined space [209], causing oxidative stress and a hypoxic environment leading to DNA damage and mutation accumulation [210, 211]. The cells that embed in the ovary are then exposed to a proliferative microenvironment known to be an inflammatory milieu where malignant transformation can occur [212]. Chromosomal aberrations have been identified at a high frequency in ovarian endometriotic cysts compared to extra-gonadal endometriosis [213]. The different selection pressures found in the uterus compared to the ovary are likely factors in the evolution of the tumourigenic cells. The mutational analysis of a small number of endometriosis lesions has mostly been confined to a subset of genes, *PTEN, CTNNB1* and *KRAS* with only a small number of somatic mutations found in *PTEN* [73], and *KRAS* [214]. It will be important to determine the malignant transformation pathways of endometriosis to ovarian endometrioid carcinomas, and in so doing, identify the genetic differences between the precursors of endometrial and ovarian endometrioid carcinomas and from endometriosis with low potential for transformation. In addition to considering the microenvironment the impact that these mutations have on different cell context must be considered. The use of endometriosis derived cell lines as opposed to endometrial cell lines may be of critical importance for studying the origins of these cancers [215].

Based on the mutation frequencies found in this study, *CTNNB1* mutations in the ovary and *PTEN* mutations in the endometrium are characteristic features of these diseases. Mutations in *CTNNB1* and deregulation of the Wnt pathway are a well-established pathway in cancer signaling first characterized in colorectal cancers [216, 217]. As seen in our study, the majority of *CTNNB1* mutations change the phospho-serine/threonine sites, which affects the ability of GSK3β to phosphorylate β-catenin to signal degradation. Lack of β-catenin phosphorylation results in nuclear accumulation causing expression of cell proliferation and inflammatory genes (reviewed in [218]) (Figure 4.2). Ovarian carcinomas with an accumulation of nuclear β-catenin,

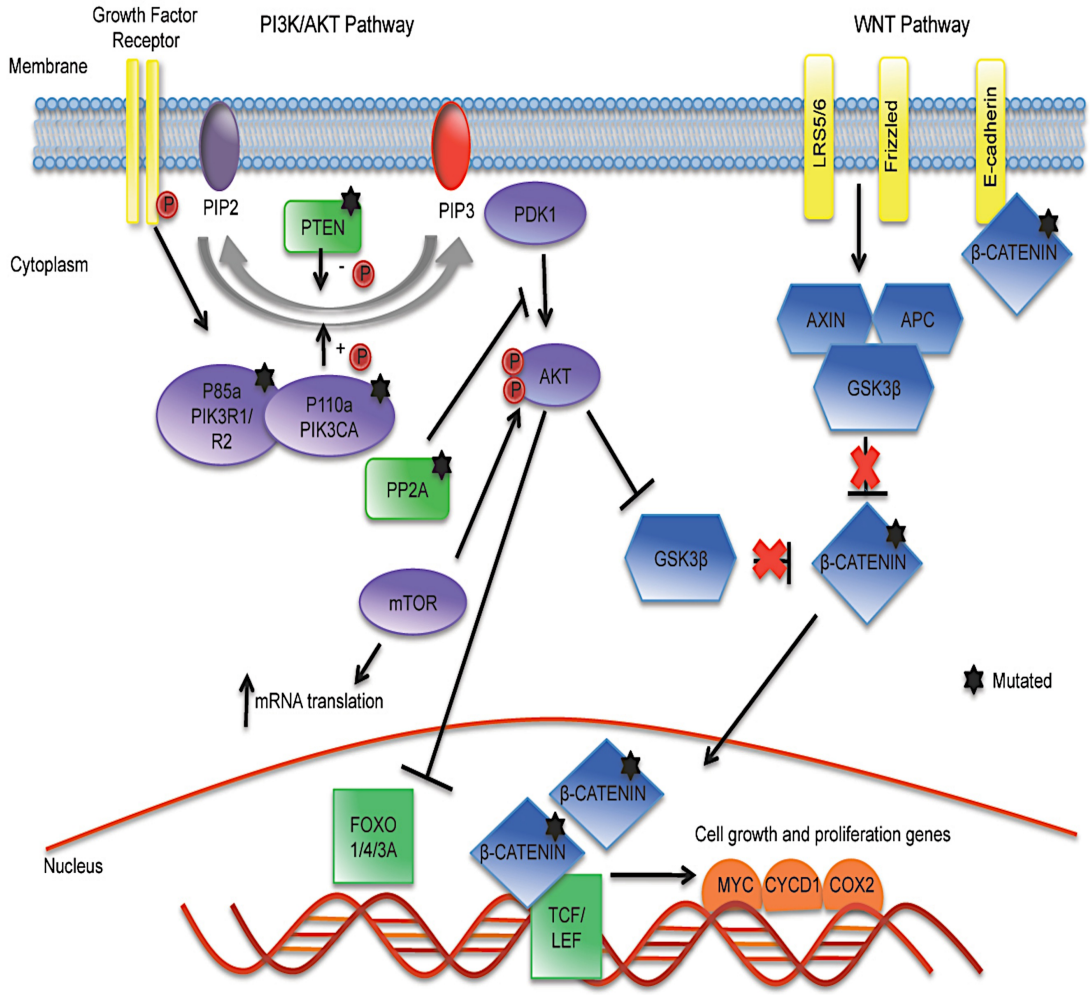

Figure 4.2 PI3K/AKT and WNT signaling pathways.
These two signaling pathways show convergence on GSK3β and β-catenin. Genetic alterations caused by mutations in both pathways can result in the transcription of cell growth and proliferation genes. Mutations are indicated by black stars and are found in both ovarian and endometrial endometrioid tumor

either due to *CTNNB1* mutations or deregulation of other Wnt family member like APC or Axin, is an indicator of good prognosis [75]. Similar to the Wnt pathway, PI3K signaling is also one of the most commonly altered cancer pathways [219]. PTEN acts as a negative regulator of the PI3K pathway by dephosphorylating the signaling lipid molecule PIP3 to PIP2; where PIK3CA (p110α) together with PIK3R1 (p85α) acts to phosphorylate PIP2 to PIP3, thus allowing signaling to proceed through AKT and mTOR. Mutations in both *PTEN* and *PIK3CA* can act to maintain constitutively activated PI3K signaling (reviewed in [220]). This activation leads to the degradation of GSK3β, and thus allows β-catenin nuclear translocation [221]. The PI3K and Wnt pathways do not occur linearly, and are interactive within their own signal transduction networks as well as with other pathways, which is shown by convergence on GSK3β (Figure 4.2). There are however many other gene regulation events resulting through the activation of PI3K/AKT/mTOR pathway that are not activated through the Wnt pathway. Therefore, in OECs that do not respond to standard treatments, it may be beneficial to target both the Wnt pathway, to inhibit β-catenin and the PI3K pathway when *PI3KCA* is mutated. In the case of EECs, *PTEN* and *PIK3CA* are both frequently mutated, likely leading to the up-regulation of PI3K signaling, thus targeting the PI3K pathway may be of benefit. Additionally, there is no mutual exclusivity of *CTNNB1*, *PTEN* or *PIK3CA* mutations in EECs and OECs (Figure 4.1), indicating that they are not functionally equivalent, therefore when both pathways are mutated; simultaneously targeting the PI3K and Wnt pathways may be appropriate. Careful consideration will be needed when deciding which molecules to target in one or multiple pathways, as well as the specific cellular context.

Ovarian and endometrial endometrioid carcinomas share obvious histogenic connections and are morphologically similar, however there are genomic differences, as shown by *CTNNB1* and *PTEN* mutation frequencies. The occurrence of these mutations may reflect different environmental niches during oncogenesis, and ultimately point toward different routes of distinct targeted therapeutics.

Chapter 5: Construction of Endometrial Hec1A Isogenic PPP2R1A Cell Lines

5.1 Introduction

The most definitive way to assess gene function is by targeting the endogenous genome [222]. Gene overexpression and knockdown approaches of genes in cell lines or mouse models have traditionally been the approach of molecular functional studies. Overexpressing genes has given insight into how mutations or genes may affect the biology of the cell, however this is often an artificial system, and is frequently performed in cell lines or models that do not have any relevance to disease or cell type. Knockdown approaches have mostly been accomplished using small interfering RNA (siRNA) technologies, however this technique has limitations with high non-specific effects and incomplete inactivation of the gene of interest [223, 224]. These approaches, although have been useful, cannot compare genetic variants and do not recapitulate the naturally occurring genetic variants found in specific cell types or diseases [225].

Knockout (KO) and knockin technology in mammalian cells was traditionally very difficult and inefficient. Nevertheless, Fred Bunz and Bert Vogelstein at Johns Hopkins University utilized the recombinant adeno-associated virus (rAAV) to enable efficient somatic cell knockout by homologous recombination into mammalian cells [222, 226]. This rAAV infection approach was found to be 25-fold more efficient than transfection of plasmids for homologous recombination into the same exon. The rAAV technology exploits endogenous homologous recombination to insert a specific promoter-trap targeting construct into the endogenous gene. Thus allowing the targeted insertion of mutations or deletions into one allele or the knockout of a specific allele. The promoter-trap requires integration of a promoterless construct into the proximity of an active gene promoter to drive expression, and has been used to successfully target human loci [227]. The two diploid colorectal cancer cell lines (HCT116, DLD1) have been mostly used for this technology as they are mismatch repair (MMR) deficient thus allowing for homologous recombination to occur. Most diploid or near diploid cell lines are MMR-deficient with stable chromosomes [228]. The inactivation of MMR genes leads to the accumulation of many mutations in cancer genes, called a mutator phenotype, and the development of cancer [229]. The rAAV method has been used to target many genes including *CTNNB1* [226] and *PIK3CA* [230] loci.

Previous molecular studies of *PPP2R1A* mutations have been based on a few very low frequency cancer mutations and experiments were performed in unrelated disease cell types [90, 131, 153]. In Chapters 2 and 3, I have presented data where I discovered a high frequency of *PPP2R1A* mutations in multiple types of endometrial carcinomas (serous, endometrioid, carcinosarcoma) [1, 2]. It is therefore important to study these mutations in the context of endometrial or ovarian specific cell types. To overcome the limitations of overexpressing genes, in this Chapter, I describe the generation of isogenic endometrial-derived cell lines using rAAV somatic cell knockout technology to further study an endogenous *PPP2R1A* mutation. As part of the endometrial exon capture analysis utilized in Chapter 3, four endometrial derived cell lines (Hec1A, KLE, ECC1, Hec50) were also sequenced (data not shown). There were two endometrial cell lines that harbor *PPP2R1A* mutations: the Hec1A cell line with a heterozygous W257L mutation, and the Hec50 cell line with a homozygous R183W mutation. The Hec1A cell lines originates from a human endometrial adenocarcinoma [231], is mostly diploid and MMR-deficient with a *PMS2* nonsense mutation [232], which allows for homologous recombination utilized by the rAAV somatic cell knockout technique. Since this cell line is MMR-deficient it harbors a hyper-mutator phenotype, with mutations in almost every gene, and could be classified with the MSI group according the TCGA classification [42]. Using the Hec1A cell line, *PPP2R1A* mutant and wild-type alleles can be targeted using the rAAV somatic cell knockout system, and be used to determine the effects of *PPP2R1A* mutations on cell proliferation and migration. The Hec50 cell line with a homozygous R183W mutation is not MMR deficient, therefore was not a good candidate cell line for somatic cell gene knockout or knockin. The generation of the Hec1A isogenic *PPP2R1A* cell line clones is described in this Chapter 5, and was crudely characterized for cell proliferation and migration characteristics. The main purpose of generating these isogenic cell lines was not to characterize a new cell line, but to use as a cell-context specific model for PPP2R1A interactions studies presented in Chapter 6. This includes performing immunoprecipitation coupled with mass spectrometry experiments to determine how the PPP2R1A mutation affects binding of PP2A B subunits and other known PP2A interactors.

5.2 Materials and Methods

5.2.1 Cell Culture Maintenance

Endometrial Hec1A cells [231] were grown in McCoy's 5A media (Hyclone) with 10% fetal bovine serum (FBS). All cell lines were maintained at 37^0C with 5% CO_2.

5.2.2 Creation of Somatic Cell Knockout Hec1A Cell Lines

5.2.2.1 Cloning PPP2R1A Exon 3 and Exon 4 Regions into the Targeting Vectors pSEPT and pAAV-MCS

The endometrial cell line Hec1A containing an endogenous missense W257L (c.770 G>T) mutation (present in exon 6) was chosen for somatic cell knockout, to isolate isogeneic cell lines that express only mutant or wild-type PPP2R1A. The construct design is based on using recombinant adeno-associated viral vector (rAAV) system described in two publications [222, 226]. The synthetic exon promoter trap pSEPT (plasmid synthetic exon promoter trap) vector was obtained from Dr. Fred Bunz's lab at Johns Hopkins Medicine, USA [226]. Two separate pSEPT constructs were designed to target exon 3 and exon 4 of *PPP2R1A*. This will enable incorporation of the knockout construct upstream of the mutation that is present in exon 6, causing loss of expression of the targeted allele. To clone the *PPP2R1A* regions of interest into the pSEPT vector, primers were designed to incorporate *PPP2R1A* homology regions (HA) and restriction enzyme sites. Using the Clontech Online In-Fusion primer design tools (http://www.clontech.ca), two homology arms (left and right) were designed for each of PPP2R1A exon 3 and 4.

Primer Name	Primer Sequence	RE	RE sequence
PPP2R1Ax3_LHA1_F	**CCGCGGTGGCGGCCGC**AAGGAAGAGG CAGAGATACTAACC	NotI	GCGGCCGC
PPP2R1Ax3_LHA1_R	**ATCCACTAGTTCTAGA**CAGCACTCAGT TCTTCCATCC	XbaI	TCTAGA
PPP2R1Ax3_RHA1_F	**GCATATGTATGAATTC**GGAACCTTCAC TACCCTGGTG	EcoR1	GAATTC
PPP2R1Ax3_RHA1_R	**GCTTGATATCGAATTC**GCGGCCGCTCA AATCCCAAGATCCCAAC	EcoRI, Not1	GCGGCCGC
PPP2R1Ax4_LHA_F	**ACCGCGGTGGCGGCCGC**CCTGTCAGCC CAAGTTGAAT	NotI	GCGGCCGC
PPP2R1Ax4_LHA_R	**ATCCACTAGTTCTAGA**CCTATTACCCAT CCCGACCT	XbaI	TCTAGA
PPP2R1Ax4_RHA_F	**GCATATGTATGAATTC**GGACAAGGCAG TGGAGTCCT	EcoR1	GAATTC
PPP2R1Ax4_RHA_R	**GCTTGATATCGAATTC**GCGGCCGCAGG CAGGTCTAGAGCCACAG	EcoRI, Not1	GCGGCCGC

Table 5.1 Homology arm primers for cloning *PPP2R1A* exon 3 and 4 into pSEPT
The primers for LHA: left homology arm, RHA: right homology arm with restriction enzyme sites (RE) and RE sequence. The bold primer sequence contains pSEPT vector-specific sequences with restriction enzyme sequences.

Each HA was PCR amplified from Hec1A DNA using iPROOF High-fidelity polymerase (BioRAD) and purified using the PCR purification kit (Qiagen). Each HA was cloned stepwise into the pSEPT vector (Figure 5.1), using the Clontech In-Fusion Cloning kit as per manufacturer's protocol. The targeting cassette was sequenced, using Sanger sequencing, off the pSEPT backbone to make sure the cloning was efficient and to check for possible errors in the sequence. The HA targeting *PPP2R1A* cassette was then excised from the pSEPT vector backbone using Not1, then purified using the QIAquick gel purification kit (Qiagen). Finally, the pAAV-MCS vector was also linearized with Not1 and purified to allow cloning of the HA targeting *PPP2R1A* cassette into the vector backbone using T4 ligase. The final vector with the targeting cassette was sequenced using Sanger sequencing.

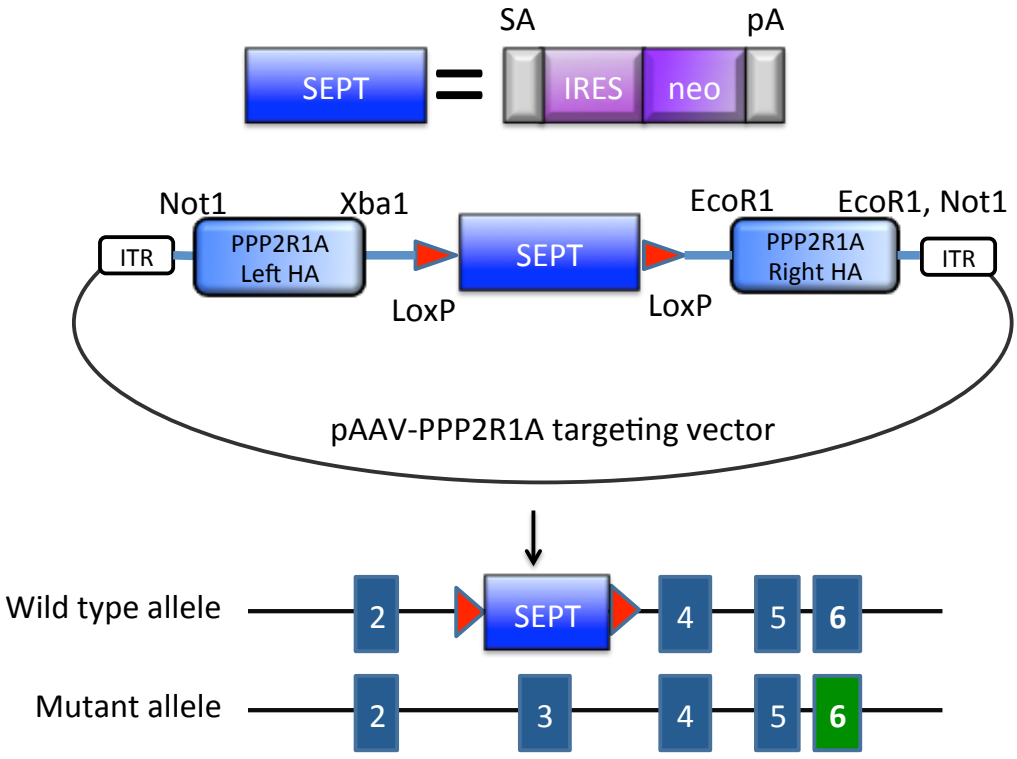

Figure 5.1 pAAV-PPP2R1A exon 3 targeting vector
The SEPT cassette includes a splice acceptor (SA), Internal Ribosomal Entry Site (IRES), neomycin selection (neo), polyadenylation site (pA). The red arrows indicate LoxP sites. The pAAV-P*PP2R1A* targeting vector was utilized to make adenovirus in AAV-293 cells, then harvested to transduce into the Hec1A parental cell line to target the *PPP2R1A* exon 3 or exon 4 locus.

5.2.2.2 Generating *PPP2R1A* Exon 3 and 4 Hec1A KO Cell Lines

The final pAAV-*PPP2R1A* exon 3 and 4 targeting vector (Figure 5.1) was then transfected into AAV-293 cells to package the recombinant virus using the AAV-Helper-Free System (Agilent) as per manufacturer's protocol. The virus was harvested and transduced into the Hec1A cell lines according to Rago *et al* [225]. For single cell selection, the cells were harvested, diluted to low concentrations and seeded into 10 X 96 well plates with 1200ug/mL G418 selection media (Geneticin, Life Technologies). Once the colonies had grown to cover the majority of a single well of a 96 well plate, (3-5 weeks) (Figure 5.2), the cells were transferred to larger tissue culture vessels, and tested for integration of the knockout allele.

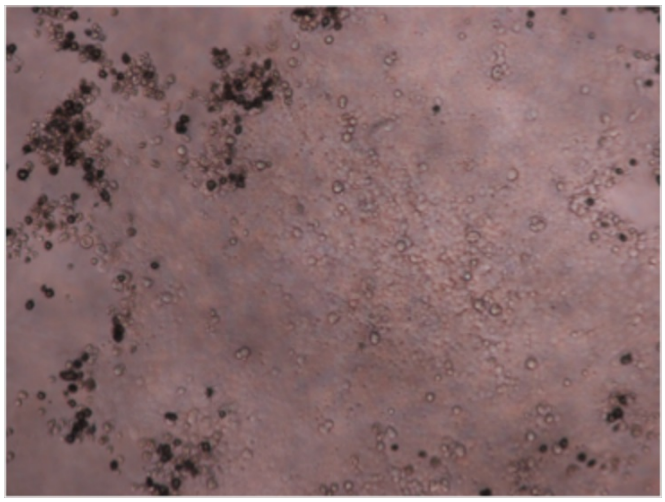

Figure 5.2 pAAV-PPP2R1A exon 3 targeted Hec1A single cell colony
Bright field image of a single cell colony after 6 days on selection, and 8 days on selection medium. The black cells are dead cells that are found mostly surrounding the growing colony.

5.2.2.3 Sanger Sequencing of Hec1A Single Cell Knockout Colonies

To determine which *PPP2R1A* allele was targeted in the single cell Hec1A clones, RNA was extracted from cell pellets using the QIAamp mini RNA extraction kit (Qiagen) as per manufacturer's protocol. The cDNA was synthesized using First Strand cDNA synthesis kit (Invitrogen), and proceeded as per manufacturers protocols. The *PPP2R1A* exon 6 region surrounding the W257L (c.796-771) mutation was amplified using cDNA specific primers (PPP2R1A_c381F CTTTGTGCCGCTAGTGAAGC, PPP2R1A_c889R CGGCCTCACAGTCTTTCATC), then sequenced using the same primers on the ABI 3130xl capillary sequencer in the forward and reverse directions. Sequences were analyzed using the Applied Biosystems Sequencing Analysis 5.2 software, BLAST, and visualized using FinchTV (Geospiza, Inc). Once positively targeted clones were identified, Cre recombinase was utilized to excise the neomycin cassette (pSEPT) flanked by LoxP sites (see Figure 5.1). Ad-CMV-Cre (Cre Recombinase Adenovirus) (Vector Biolabs) was used for excision of the pSEPT construct as per Rago *et al* [225]. Phenotypic screening using with the same concentration of Geneticin in which they were first selected, resulted in choosing positive clones that had undergone correct pSEPT excision.

5.2.2.4 Ion Torrent Sequencing of *PPP2R1A* Exon 6 in Hec1A Cell Line

To determine how many alleles of mutant *PPP2R1A* W257L (c.769-771) were expressed in the parental Hec1A cells, RNA was extracted and cDNA was synthesized as described in the Sanger sequencing methods. Targeting primers were designed using Primer 3, and Ion Torrent adapter sequences were added to the target sequence and synthesized by IDT (Integrated DNA Technologies). For bidirectional sequencing, two sets of primers were synthesized and used for amplification (Table 5.2). PCR was performed using the BioRAD iPROOF Hi-fidelity enzyme, as per manufacturer's protocol. The amplified products were checked on a 1% agarose gel, cleaned with magnetic Ampure beads, and then spiked into an existing Ion Torrent library at 1/100 dilution. The final library was loaded onto an Ion 316™ chip and sequenced on the Personal Genome Machine™ (PGM) Ion Torrent sequencer (Life Technologies).

Primer Name	Adapter	Full Primer Sequence
PPP2R1A_ex6_F_A	CCATCTCATCCCTGCGTG TCTCCGACTCAG	CCATCTCATCCCTGCGTGTCTCCGACTC AGTCTGCCCCAGGAGGATCT
PPP2R1A_ex6_R_trP1	CCTCTCTATGGGCAGTC GGTGAT	CCTCTCTATGGGCAGTCGGTGATCACC AGTGGGACAATGTCAA
PPP2R1A_ex6_F_trP1	CCTCTCTATGGGCAGTC GGTGAT	CCTCTCTATGGGCAGTCGGTGATTCTG CCCCAGGAGGATCT
PPP2R1A_ex6_R_A	CCATCTCATCCCTGCGTG TCTCCGACTCAG	CCATCTCATCCCTGCGTGTCTCCGACTC AGCACCAGTGGGACAATGTCAA

Table 5.2 Primer sets for amplifying PPP2R1A cDNA for Ion Torrent sequencing.

5.2.3 M-FISH and FISH

Metaphase cells for M-FISH and FISH were prepared by using colcemid (Sigma) treatment for 10 min, then fixed with methanol/acetic acid and stored at 4°C. To label endometrial Hec1A cells for M-FISH analysis, the MetaSystem multi-colour probe kit – 24XCyte and the MetaSystem B-tect kit was used as per manufacturer's protocol. Imaging and analysis was performed using the MetaSystem analysis software on a Zeiss Axioplan epifluorescent microscope. For Hec1A FISH analysis, the probes were generated using BAC (bacterial artificial chromosomes) clones selected from the UCSC Human Genome Browser. BAC DNA was isolated using the rapid alkaline lysis miniprep method, then labeled with a nick translation kit as per manufacturer's protocol (Abbott Molecular, Illinois, USA) using SpectrumOrange-11-dUTP or SpectrumGreen-11-dUTP. The specific probes to label chromosome 19 centromere and

PPP2R1A loci are as follows respectively: RP11-317K24 and RP11-13M19 at 19p12 (SpectrumGreen, Centromere region), RP11-890J19 at 19q13.33 (SpectrumOrange, *PPP2R1A*).

5.2.4 Cell Proliferation Assays

To assess cell proliferation by using the crystal violet assay, cells were seeded at various densities 10,000 cells/well, 20,000 cells/well, 40,000 cells/well in 6 replicates (number of wells =6) for each cell line into 12-well plates. Cells were plated for assessment from 0-9 days. At each time point, the cells were washed three times with PBS, fixed with 4% formalin for 10 min, then washed another three times with PBS. Plates were stored at 4^{o}C, and all plates were simultaneously fixed and stained with 0.1% crystal violet solution for 30 min at room temperature. The crystal violet solution was washed off with distilled water and allowed to dry at room temperature. To extract dye from the cells, 2mL of 30% methanol and 10% acetic acid was added to each well and shaken for uniform colour. For each well, 150uL of solution was transferred to a 96-well plate and the absorbance was read at 590nm on a UV spectrometer plate reader. The absorbance readings were averaged with standard deviations reported. The automated Incucyte^{TM} (Essen Biosciences) was also used to determine cell proliferation by monitoring cell confluence over a defined time period. Cells were seeded at different densities (5,000 cells/well and 10,000 cells/well) in a 96-well tissue culture plate (number of wells=4). Each well was then monitored, by taking an image with a 10X lens, every 6 hours for 4-5 days. Final analysis was performed and images viewed using the Incucyte^{TM} ZOOM software. At each time point, the average cell confluence for each cell line was reported with standard errors reported.

5.2.5 Migration (Scratch-Wound) Assay

Each of the cell line clones (mut/mut clones: 9-14, 9-15, 33-1, 33-4; mut/wt clones: 10-23-45-3, 10-23-45-6, 10-23-60-17, 10-23-45-24) were plated at 100% confluence (~20,000cells/well) (number of wells=6) into a 96-well Essen ImageLock microplate, and allowed to grow and attach overnight. The next day, a sterile Essen 96-well WoundMaker^{TM} was used to make a consistent wound through the middle of each well. All media was aspirated off, and carefully washed twice with culture media to get rid of any loose cells. Cell media (100uL) was added back to each well, and wells were then monitored for 4 days, every 4 hours, or until the wounds were healed using the Incucyte^{TM} (Essen Biosciences). This protocol was adapted

from Essen Bioscience's CellPlayer™ 96-well cell migration assay protocol. Final analysis, images and videos were performed using the Incucyte™ ZOOM software.

5.3 Results

5.3.1 Isolation of PPP2R1A Exon 3 and 4 Knockout Isogenic Hec1A Cell Lines

To generate Hec1A isogenic *PPP2R1A* cell lines, somatic cell knockout of *PPP2R1A* exon 3 and 4 was performed. Using this somatic cell technique, two different cell lines clones could potentially be isolated that express only the PPP2R1A L257 mutation or only the wild-type protein. The first round of transduction with the *PPP2R1A* targeting exon 3 in Hec1A cells resulted in 53 single colonies (Figure 5.2). The targeting of exon 4 was less efficient and resulted in 30 colonies. To test the efficiency of the knockout construct, the cDNA of all colonies was sequenced to determine which *PPP2R1A* allele was targeted. Three single cell colonies were isolated from the exon 3 knockout construct that expressed only the PPP2R1A (-) mutant L257 allele (clone #9, 33 and 37) (Figure 5.3). No mutants were isolated from the exon 4 knockout construct. There were also no single cell colonies that expressed only the wild-type allele. To try to isolate the *PPP2R1A* (wt) wild-type (W257) only expressing Hec1A cell line, two more rounds of transducing the *PPP2R1A* exon 3 targeting construct was completed. This resulted in an additional 95 single colonies being tested for the knockout of the *PPP2R1A* mutant or wild-type allele. No wild-type only colonies were identified, however 5 additional mutant only expressing cell colonies were isolated.

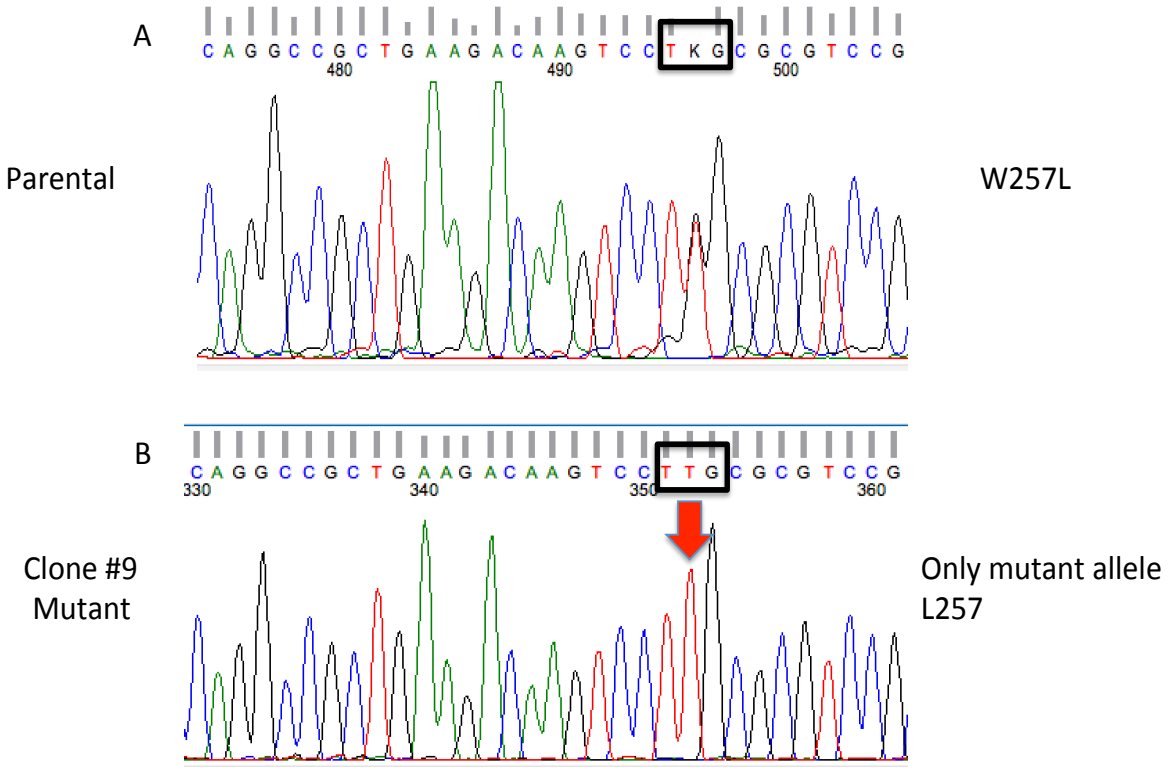

Figure 5.3 Sanger Sequencing Traces for Hec1A KO
A. Sanger sequencing trace for the parental Hec1A cell line cDNA with an endogenous W257L (G to T) mutation. B. Sanger sequencing trace for the cDNA of the mutant clone #9 with only the T nucleotide present (L257).

It was possible that the Hec1A cells are not actually diploid at the *PPP2R1A* locus (chr19: 52,190,039-52,229,533); therefore to determine a digital count of the allele frequency of the mutation, Hec1A cDNA was sequenced at the *PPP2R1A* locus using the PGM™ Ion Torrent next generation sequencer. This may give insight into the lack of isolation of the wild-type only expressing cell lines. This analysis revealed a digital count of 62% T mutant reads and 38% G reference reads giving a 2:1 mutant:wild-type allele expression of the *PPP2R1A* (G to T) W257L mutation in the Hec1A cell lines (Figure 5.4). To determine if this was due to chromosome ploidy changes, M-FISH and FISH for the *PPP2R1A* gene region was performed using the Hec1A parental cell line (Figure 5.5). The M-FISH assay showed the parental Hec1A cell line as diploid at chromosome 19, however there was also a small piece of chromosome 19 that had been translocated to chromosome 17, as depicted by the purple on the aqua chromosome 17 (Figure 5.5A). FISH specific for the *PPP2R1A* region of chromosome 19 shows one normal chromosome and one chromosome with 2 regions of PPP2R1A similar to an isochromosome (Figure 5.5B). Therefore, together these results show that Hec1A parental cell line actually

contains 3 *PPP2R1A* alleles; two PPP2R1A (T) L257 mutated alleles, and one PPP2R1A (G) W257 wild-type allele, designated as (mut/mut/wt). The knockout of one wild-type allele generates a cell with 2 *PPP2R1A* (mut/mut) mutant alleles, and the targeted knockout of one mutant allele generates a heterozygous *PPP2R1A* (mut/wt) cell.

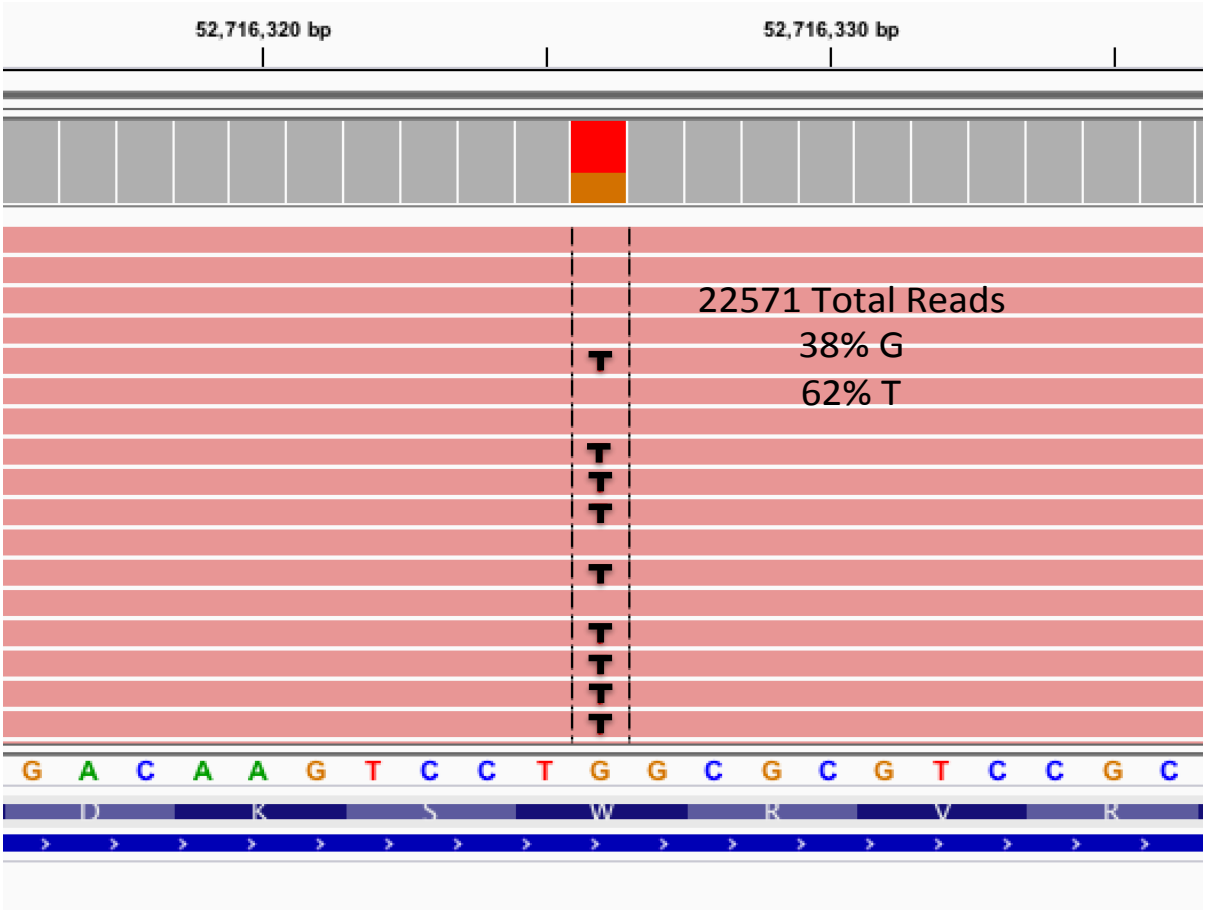

Figure 5.4 Ion torrent sequencing of the parental Hec1A cell line for W257L mutation
Integrated Genome Viewer (IGV) panel depicting the total reads for PPP2R1A cDNA exon 6. Each row indicates one sequencing read, with the total reads shown for each variant.

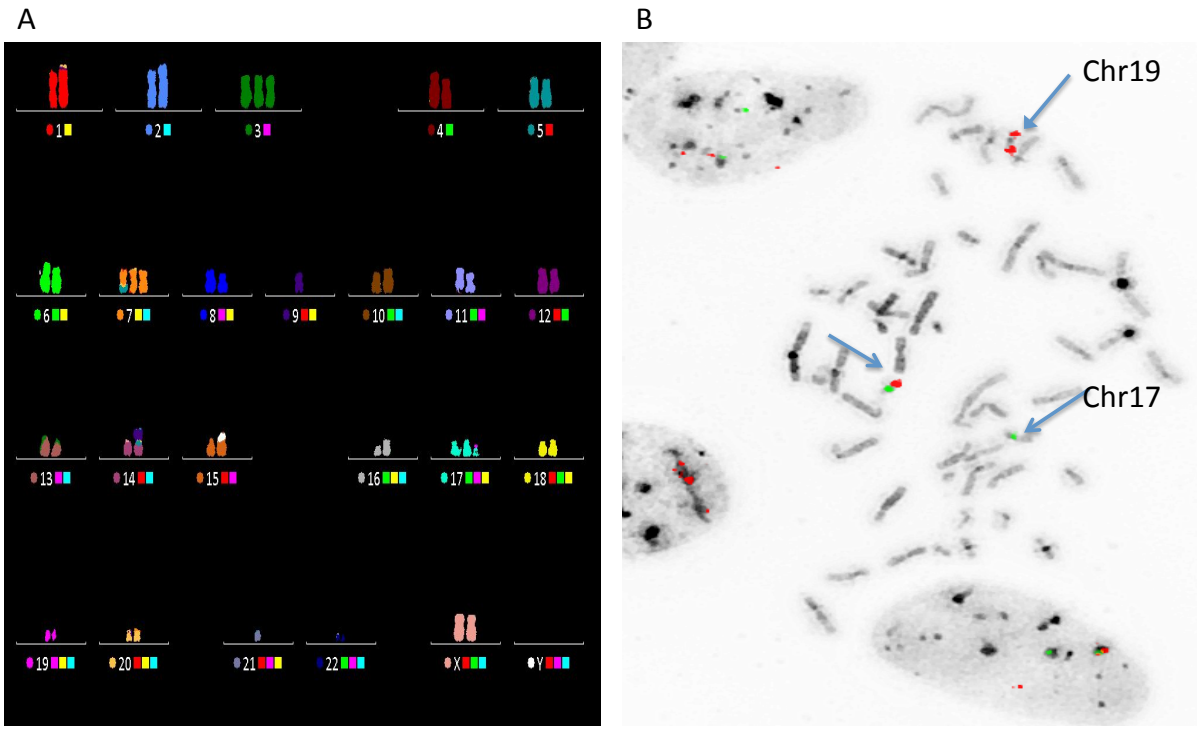

Figure 5.5 M-FISH and FISH for Hec1A cells
A. M-FISH results of the Hec1A parental cell line. B. *PPP2R1A* specific FISH in metaphase Hec1A cells. The red probe is specific for the *PPP2R1A* locus (RP11-890J19 at 19q13.33), the green probe is specific for the chromosome 19 region (RP11-317K24, RP11-13M19 at 19p12).

In light of these results, the isolation of a wild-type only cell line could potentially be generated from the heterozygous single colonies isolated from the first round of targeted selection. A single Hec1A cell line (clone 10-23) that had undergone the Cre excision of the exon 3 targeting pSEPT vector, was used for a second round of targeting. A total of about 46 colonies were screened, and no 100% wild-type colonies were identified. All the cell clones screened had detectable levels of the *PPP2R1A* mutant L257 allele. The resulting cell line clones have equal to less mutant allele being expressed, pre-targeting, however are still mostly equivalent to a heterozygous *PPP2R1A* (mut/wt) W257L mutation. The resulting Hec1A *PPP2R1A* isogenic cell lines are shown in Figure 5.6. My inability to produce a pure wild-type isogenic line from Hec1A cells may be due to an inability of the wild-type cell clones to survive after selection.

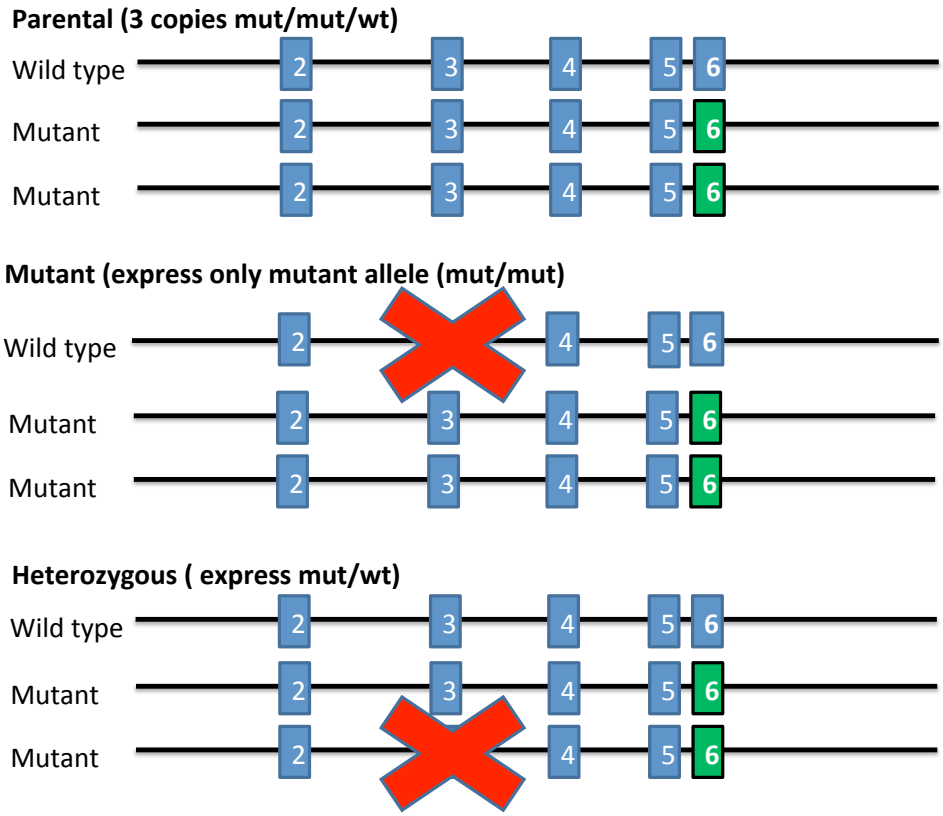

Figure 5.6 Resulting Hec1A *PPP2R1A* isogenic knockout cell lines
Blue boxes depict the wild-type exons, and the green exon 6 boxes encode a mutation (G>T). The red cross indicates which allele is being targeted by the pSEPT targeting construct, and thus not expressed in the cell line.

5.3.2 Growth Characteristics of Isogenic Cell Lines

To determine if the *PPP2R1A* mutation affects cell growth, two different methods were used to assess the cell proliferation of the isogenic cell lines. First, cell nuclei were stained using crystal violet dye, which is proportional to the number of live cells present. After 9 days of cell growth, starting with 10,000 cells/well, I discovered that the parental line proliferates at a faster rate than three clones of the mutant only expressing clones (#9, 33 and 37) (Figure 5.7A). This was replicated when the cells were seeded at a higher confluence of 40,000 cells/well, however the mutant clone #33 appears to proliferate at a faster rate than the other two mutant clones (Figure 5.7B). The heterozygous cell lines were not tested with this method because they were still in the process of being isolated and screened.

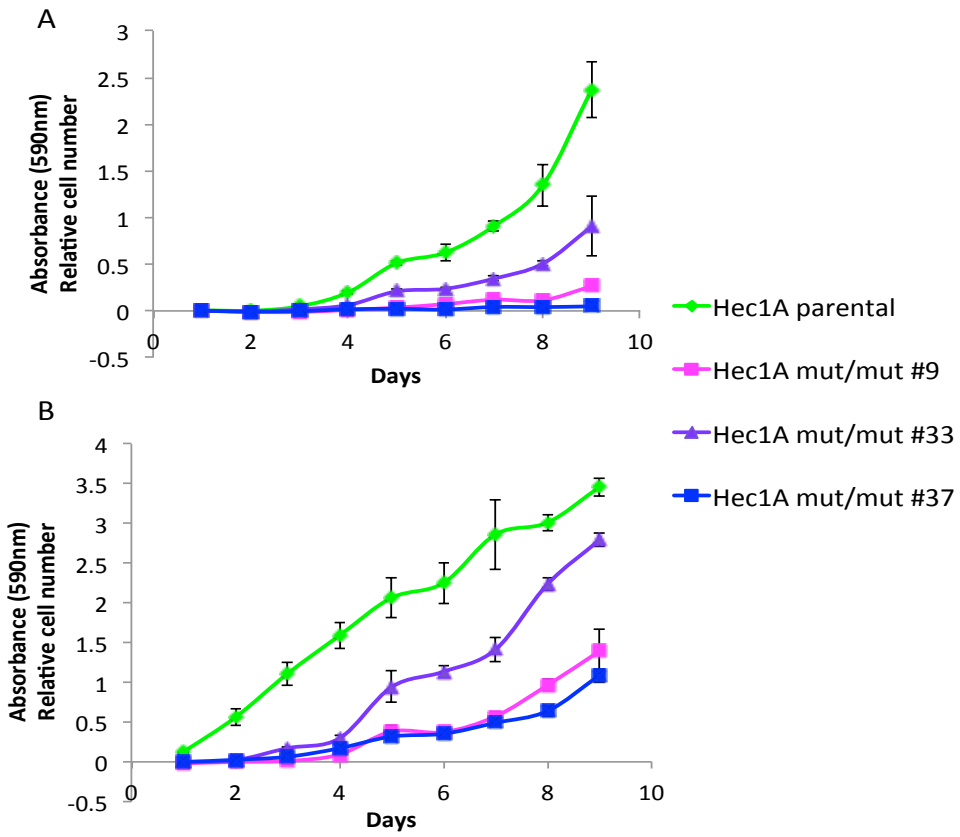

Figure 5.7 Cell proliferation of Hec1A mutant/mutant expressing cell lines using the crystal violet assay
A. A total of 10,000 cells were plated (n=6) on Day1 and assessed every day for 9 days. **B.** A total of 40,000 cells were also plated (n=6) on Day 1 and assayed every day 9 days. The absorbance readings from n=6 for each cell line were averaged, with the error bars indicating standard deviation.

A second method of analyzing cell proliferation, based on cell confluence as measured by the Incucyte™, also shows that after 4.5 days of cell growth, all of the mutant cells line clones proliferate slower than the parental and the heterozygous cell lines (Figure 5.8A). A closer look at only three of the cell lines (Figure 5.8B) reveals that one of the heterozygous cell clones may proliferate faster than the parental line. However, this is confounded by increased confluence of the heterozygous cell line, compared to the other two cell lines, at the beginning of the assay (time=0). When the changes in cell growth rates are compared; the parental and heterozygous cell lines show almost identical changes in growth rate (Figure 5.8C). Conversely, the mutated cell line demonstrations a slower rate of change over time compared to the other two cell lines.

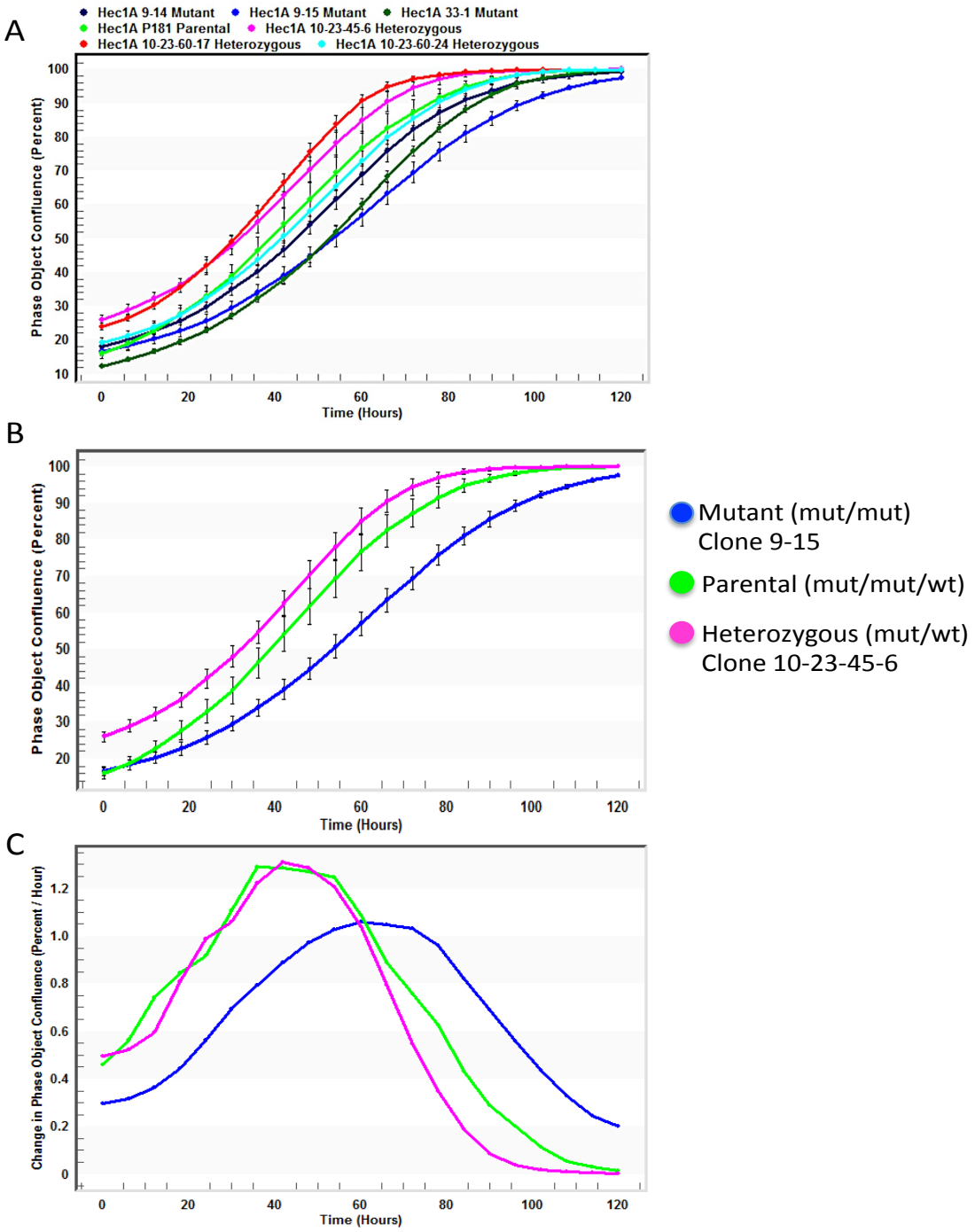

Figure 5.8 Cell proliferation of Hec1A *PPP2R1A* isogenic cell lines with differing expression of mutant PPP2R1A.

A. Cell proliferation, represented by phase cell confluence, of all cell lines (10,000cells/well) as monitored by the Incucyte™ over 120 hours. **B.** Cell proliferation of only one each of the parental, mutant and heterozygous cell line clones over time is shown. **C.** The rates of change of phase confluence as measured by the Incucyte™ to show the change in rate of proliferation of the trio of isogenic cell lines. Error bars indicate standard error.

To determine the effects of growth factors on the proliferation of the different isogenic cell lines in triplicate, I assayed cells with varying concentrations of FBS (Fetal Bovine Serum). The concentration of FBS did not seem to affect the growth characteristics of the parental and heterozygous (clone 10-23-45-6) cell lines, however there were differences in growth patterns for the mutant cells (clone 9-14) (Figure 5.9). At low levels (1% and 0.1%) of FBS, the rate of proliferation of the mutant cell line (clone 9-14) was different than the regular growth conditions (10% FBS).

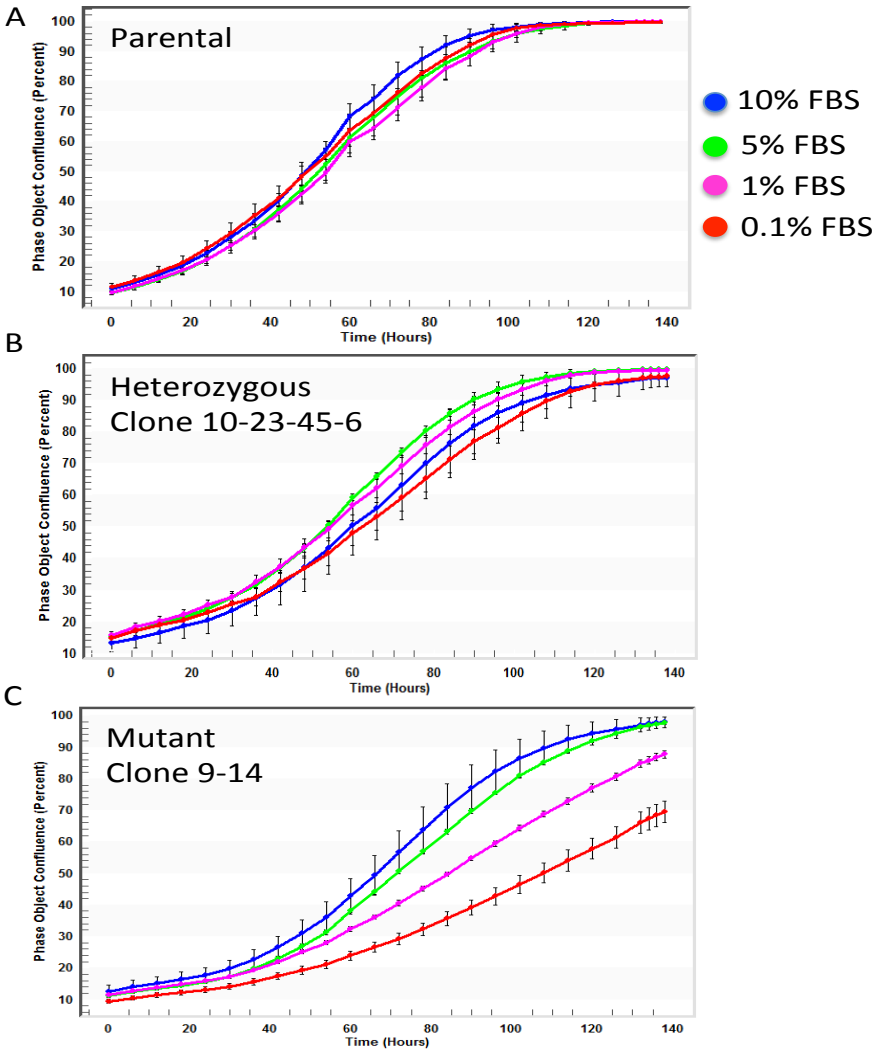

Figure 5.9 Effect of different FBS concentration on the proliferation of Hec1A *PPP2R1A* isogenic cell lines.
Panels A, B and C depict cell proliferation over time for each of the each of the Hec1A *PPP2R1A* isogenic cell line clones in triplicate with varying levels of FBS. Error bars indicate standard error.

The migration characteristics of the Hec1A *PPP2R1A* isogenic cell lines were also assayed using the scratch, or wound, assay. Over a 4-day period, the different cells lines clones (parental, mut/mut clones: 9-14, 9-15, 33-1, 33-4, mut/wt clones: 10-23-45-3, 10-23-45-6, 10-23-60-17, 10-23-60-24) were monitored to determine the rate of movement into the scratched area, however only one of each clone is shown (Figure 5.10 and 5.11). The results are consistent with the previously observed cell proliferation rates, where the parental and the heterozygous cells grow and migrate into the scratch at similar rates. In addition, the mutant cells are significantly impeded from migrating into the scratch area (Figure 5.10 and 5.11). After 72 hours, the mutant cells are not able to fully close the wound, whereas both the parental and heterozygous cell lines are able to migrate to close the full scratch area. The mutant cells appear to spread into the scratch area by growing on top of the cells at the scratch boundary instead of moving into the unoccupied areas, which is how the parental and heterozygous cells seem to grow.

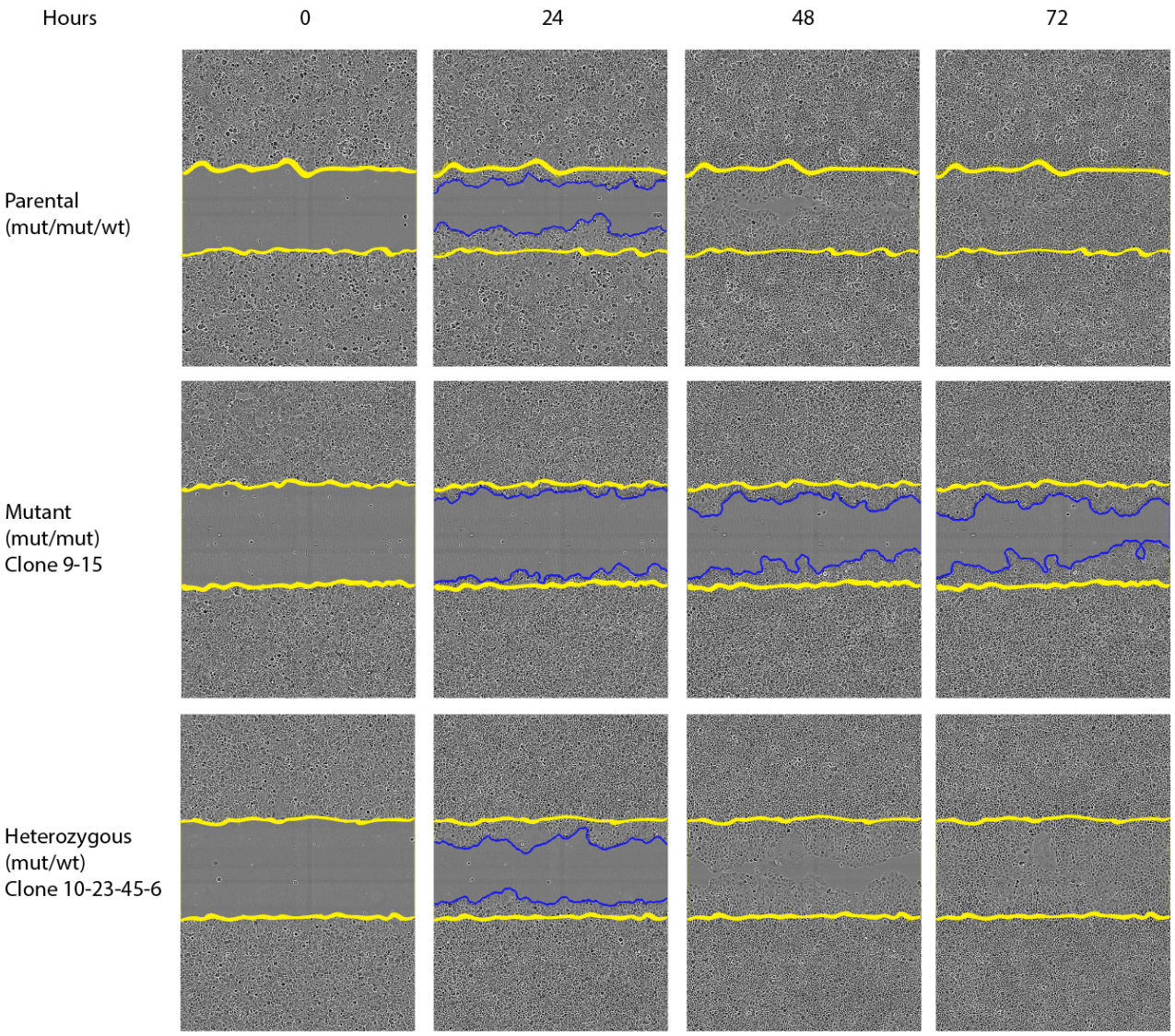

Figure 5.10 Images of the scratch (wound) assay over time

The three rows show time-lapse images of the migration rates of the different isogenic cell lines. The yellow lines indicate the starting scratched area boundary (wound outline). As the cells migrate into the cleared wound area, the blue line indicates the new boundary of the cells. For the parental and heterozygous cell lines, the blue line disappears after 48 hours indicating the wound area has been closed from migrating cells. For the mutant cell line, the blue lines indicate that the cells were not able to move into the scratch area to close the wound after 72 hours. The changes in the density of these areas are shown in Figure 5.11.

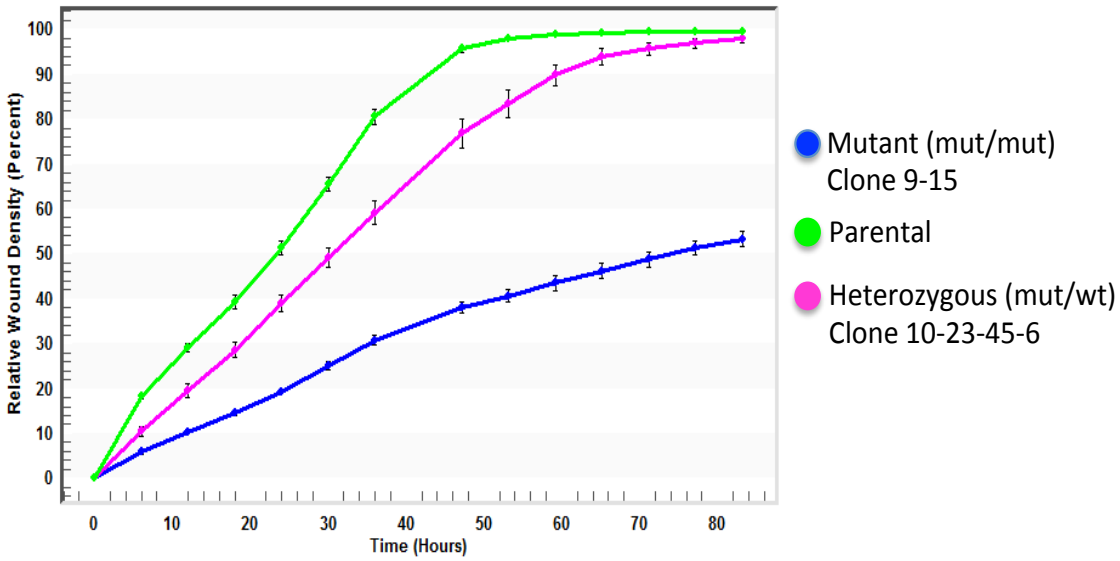

Figure 5.11 Relative wound density over time of Hec1A *PPP2R1A* isogenic cell lines
A graphical figure showing the differences in migration characteristics of the isogenic cell lines (n=6) using a scratch or wound assay. The relative wound density is plotted over time to show the rate of cell movement into the scratch area. Error bars indicate standard error.

5.4 Discussion

Overexpression cell line models and gene knockout by shRNA (small hairpin interfering RNA) experiments, in many different cell lines, has been previously performed by many groups [90, 110, 131]. The use of shRNA to knockdown *PPP2R1A* was not used in my PhD project experiments, as it has been previously shown that *PPP2R1A* knockout to less than 30-37% of endogenous levels leads to cellular apoptosis and death [131, 132]. Instead, I utilized the endometrial Hec1A cell line with an endogenously expressing PPP2R1A W257L mutation and pAAV somatic cell KO methodology, to establish the first context-specific disease cell line models. This model will be used to determine the effect of endogenous *PPP2R1A* mutations on PP2A formation and activity in endometrial carcinoma. The establishment of these endometrial Hec1A *PPP2R1A* isogenic cell lines was challenging. I was able to isolate a mutant only expressing PPP2R1A (mut/mut) L257 cell line, however the unanticipated presence of an extra PPP2R1A mutant allele in the Hec1A genome, made isolating an wild-type only expressing cell line unsuccessful. Therefore, the final Hec1A trio isogenic cell lines consists of the parental PPP2R1A (mut/mut/wt) W257L cells, mutant only PPP2R1A (mut/mut) L257 cells, and heterozygous PPP2R1A (mut/wt) cells.

After isolating the isogenic cell lines, I next determined if the PPP2R1A mutation had any effect on the growth characteristics of the cells. I therefore, utilized various methods of determining cell proliferation and cell migration. The results of the different cell proliferation assays showed consistently that the different *PPP2R1A* (mut/mut) cell lines clones demonstrated an *in vitro* decrease in cell proliferation over time, compared to both the parental (mut/mut/wt) and heterozygous (mut/wt) cell line clones. Both the parental and heterozygous lines exhibited similar cell proliferation characteristics. In addition, there were large differences in the migration characteristics of the mutant (mut/mut) cells compared to the parental or heterozygous cell lines. The time-lapse scratch assay dramatically shows the extent of migration inhibition in the mutant expressing cell lines. Taken together, these results demonstrate that the one allele expressing PPP2R1A L257 mutation has inhibitory effects on cell growth and migration. However, both the W257L mutated cell lines (parental and heterozygous) proliferate quickly and have an ability to migrate. This is consistent with patient endometrial tumours, as somatic *PPP2R1A* mutations are usually found as heterozygous missense mutations, and rarely found as homozygous mutations [1, 206].

Each of the isogenic mutant and heterozygous and cell lines were single cell cloned after the initial *PPP2R1A* pSEPT targeting vector transduction. Once the mutant and heterozygous lines were identified an additional Cre-recombinase step was utilized to excise out the SEPT cassette which resulting clones were also single cell cloned. Therefore, each mutant and heterozygous cell clone could potentially have different genetic backgrounds. The multiple single cell cloning is one explanation for the differences in cell proliferation for each mutant and heterozygous cell line clones. It was important to assay multiple clones for each genotype as biological replicates, however each of the different clones had a similar trend of proliferation. A second explanation for the differences in cell proliferation is that the Hec1A is an MMR deficient cell with a hyper-mutator phenotype. It is entirely possible that there is heterogeneity within the original Hec1A cell line; therefore each single cell clone may have a slightly different mutational background. Furthermore, over time the cell lines may acquire additional mutations contributing to the different isogenic backgrounds.

PPP2R1A has been described as a haploinsufficient and a dominant negative tumour suppressor [105, 131, 160]. The functional level of PPP2R1A (PP2A Aα) has been described to be an important modulator of cell transformation [133]. The haploinsufficiency model, and the levels of PPP2R1A to sustain cell growth are consistent with the growth characteristics of the isogenic cell lines. The balance of PP2A levels are extremely important for keeping the cells in a transformed or normal state. The Hec1A (mut/wt) cells with one mutant *PPP2R1A* allele and one wild-type *PPP2R1A* are viable due to the typical haploinsufficient phenotype, and proliferate similar to the parental PPP2R1A (mut/mut/wt) W257L cells (Figure 5.8). The Hec1A (mut/mut) mutant only expressing cell line is likely viable because it provides enough semi-functional PP2A to allow the cells to keep proliferating, however at a slower rate. The expression of the mutant PPP2R1A has likely changed the ability of the PP2A core complex to interact with B subunits, and also alters B subunit substrate interactions, resulting in changes in functional PP2A to keep the cells in a transformed state. This is supported by established literature wherein SV40ST can bind to PPP2R1A, thus inactivating PP2A by blocking B subunit binding, to induce cellular transformation [107]. Transformation can also occur when specific B subunits are knocked down [110], which may mimic *PPP2R1A* mutations that disrupt binding of the B subunits to form functional PP2A phosphatases. Interestingly, the knockdown of PP2A-B56γ (PPP2R5C), in conjunction with sh-p53 and mutant CDK4 was used to transform human fallopian tube secretory epithelial cells (FTSEC) that mimic ovarian high-grade serous carcinoma [233]. This is an important observation, as high-grade serous of the ovary and endometrium are histologically similar, however differ in some landscapes of somatic genotypes. *PPP2R1A* mutations are an example of one of these differences, however it is possible that PP2A is being alternatively disrupted in the ovary compared to the endometrium.

There are a few hypotheses that may explain why the isolation of a wild-type only expressing cell line was unsuccessful. 1) This may be due to unspecific targeting of the pSEPT vector into non-PPP2R1A sites, which would allow for selection of drug resistant clones, but would not result in the knockout of PPP2R1A exon 3. 2) The haploinsufficiency model, and the ability of PP2A to cause cellular transformation may also explain the lack of isolation of the wild-type only cell line. It is possible that the wild-type only expressing PPP2R1A cell clones are not able to survive and thus die during selection. This may be a phenomenon of the balance of a *PPP2R1A*

mutation providing a survival advantage, to keep the cells growing in a transformed state in culture. If this transformed state is disrupted, the cells can no longer survive. A previous study has shown that the overexpression of one allele of wild-type functional PPP2R1A into cells that lack less than 50% of endogenous PPP2R1A, inhibited cell proliferation and reversed the ability of cells to form tumours [131]. In the case of the potential Hec1A wild-type only expressing cell line, it would express only one copy of the wild-type allele, which may be at a threshold of functional PP2A needed to overcome the transformed state and revive the tumour suppressor function, thus causing cell death. This may also be supported by a study assessing mutational inactivation of the *BAX* frameshift mutation in the MMR-deficient human colon cell line HCT-116 [234]. Ionov *et al.,* found that single cell cloning of HCT-116 cells isolated two populations of cells: heterozygous mutated BAX (+/-), and homozygous mutated BAX (-/-). These populations of cells were inoculated in nude mice and the resulting tumours were tested to find the BAX (+/-) population composed of subclonal populations of BAX (-/-) and (+/-), but never BAX (+/+) cells. The BAX (-/-) population never produced tumours with wild-type BAX expression. The authors show that wild-type *BAX* alleles can acquire a mutation, however the reversion of a mutation to wild-type was not observed. These results support evidence that *BAX* inactivation provides a survival advantage for tumour progression. There is also evidence to support this theory in the studies of the re-expression of wild-type p53. In this well-studied tumour suppressor, which is mutated in many different cancers including endometrial and ovarian serous carcinoma, studies have shown that the reversion of mutated p53 or the introduction of wild-type p53 can cause tumour cell death [235].

The production of these Hec1A PPP2R1A isogenic cell lines using the rAAV method was an intensive, time-consuming procedure. While the rAAV somatic cell knockout eliminates the limitations of an overexpression system, there are certainly limitations to this method. Of note, the neomycin (neo) resistance coding sequence found in the targeting vector, can have unintended consequences on the target gene and surrounding genes [236, 237]. The neomycin resistance gene has cryptic splice acceptors, which could be used by target genes, therefore it is recommended to remove the neo gene by Cre-recombination if long-term culture is required. Geneticin (G418) selection of the single cell clones containing the neomycin targeting cassette takes a few weeks to a month to enable clones to grow to a significant size for long-term storage,

passage and further cre-exision. It is indeed possible that these aberrant effects of the neomycin gene described, could have enough time to cause unintentional consequences.

To overcome some of these limitations, in recent years there have been advances in other genome-editing technologies to allow the generation of endogenous gene targeting systems in mammalian cells. The zinc finger nucleases (ZFN) [238, 239], TALENs (transcription activator-like effector nucleases) [240] and most recently the CRISPR (clustered regularly interspaced short palindromic repeats) [241, 242] systems have enabled increased success for creating somatic *in vitro* cell knockout and knockin models. The ZFNs and TALENs work by inducing loci-specific double strand breaks that are repaired by error-prone non-homologous end joining (NHEJ) and homology-directed repair (HDR) [243, 244]. This produces small insertions and deletions at break spots, which disrupt the target gene ultimately causing endogenous gene knockout. These genetic engineering technologies are groundbreaking and are replacing methods that rely on inefficient homologous recombination like the rAAV somatic cell knockout method. The ZFN and TALEN systems are however limited by their genetic delivery methods that rely on inefficient plasmid DNA, viral vectors or *in vitro* transcribed mRNA. *Gaj et al*, has shown that purified ZFN proteins can cross cell membranes and induce endogenous gene disruption [245]. This may overcome some of the limitations of gene-based delivery systems and reduce off target effects of viral and plasmid vectors.

CRISPR has emerged as a more efficient alternative to ZFNs and TALENs for genome editing, as it utilizes the bacterial adaptive immune system to perform RNA-guided DNA cleavage by Cas9 nucleases [241, 246]. This system has now been applied as a whole-genome scale knockout screening method in mammalian cells [247], and been successful in many studies and cell types [248, 249]. The field of CRISPR gene editing has exploded in a very short amount of time with a plethora of online resources and protocols for using the CRISPR technique [250], and is thought to replace ZFN and TALENs as the method of choice for genome editing [251]. For future studies, I would recommend utilizing the CRISPR system to generate improved and different isogenic cell lines to study the role of *PPP2R1A* mutations in gynaecological cancers. The endometrial cell lines that could not be utilized for the rAAV pSEPT somatic cell knockout, due to MSI stability, would be ideal candidates to introduce or knockout *PPP2R1A* mutations

into the endogenous genome using CRISPR. Our in-house collection of cell line candidates are the endometrial Hec50 cell line derived from the peritoneal fluid of a high-grade endometrioid carcinoma with a homozygous PPP2R1A mutation, and the KLE cell line derived from a poorly differentiated endometrial carcinoma (no histology defined) that does not harbor endogenous *PPP2R1A* mutations. The importance of using disease specific model cell lines is extremely important, therefore one could argue that the Hec1A, Hec50 or KLE cell lines are not perfect models for investigating the function of *PPP2R1A* mutations due to the lower frequency of *PPP2R1A* mutations in the cell line derived histological subtypes. Endometrial serous carcinoma harbors the highest frequency of *PPP2R1A* mutations as shown in Chapter 2 and 3, therefore an *in vitro* endometrial serous cell line would be the most ideal *in vitro* model. However, these cell lines are rare and our own attempts at making these cell lines from primary endometrial serous tumour tissue has failed. I have acquired only one endometrial serous carcinoma derived cell line SPAC-1-L from Japan [231], however my own sequencing of the PPP2R1A gene revealed no endogenous mutation. In the future, this cell line would be an ideal cell line for the introduction of a PPP2R1A mutation(s) to derive isogenic cell lines by CRISPR.

In conclusion, the establishment of the endometrial Hec1A trio isogenic PPP2R1A cell lines is an important contribution to the endometrial model resources. These model cell lines will be used to determine the how this *PPP2R1A* mutation affects the binding of PP2A B-subunits to form a functional PP2A holoenzyme. The majority of previous PP2A studies have been performed in non-relevant cell lines and disease models, therefore these cell lines will be one of the first to take into account *PPP2R1A* mutations in a context-specific disease model.

Chapter 6: Proteomics Analysis of PPP2R1A Mutations in Model Cell Lines

6.1 Introduction

PP2A and PPP2R1A have been extensively studied over many years, however the complexity of these proteins and involvement in many protein interactions makes this a very difficult protein complex to study. To determine interactions of each of the B subunits to the core enzyme (A and C subunits), *in vitro* overexpressing constructs with single mutations and or deletions in *PPP2R1A* have been utilized [90, 153]. Ruediger *et al.,* was the first to determine how *PPP2R1A* mutations (E64D, E64G and R418W) identified in various cancers disrupt the formation of PP2A. The authors employed EE-tagged (EEEEYMPME) mutant *PPP2R1A* constructs with *in vitro* synthesized radiolabeled B subunits, supplemented unlabeled PPP2CA, and finally coupled immunoprecipitation to determine if a PP2A complex was formed [90]. The study concluded that E64 mutant constructs affected the binding of the B'α subunit (PPP2R5A) only. In an earlier study, the same authors found that mutating the amino acid position P179A caused disruption in the binding of the B55α (PPP2R2A) and B'α (PPP2R5A) B subunits [153], and hypothesized that this amino acid would likely be mutated in some cancers. It was not until my study of endometrial serous carcinomas, where I discovered that this specific amino acid change (P179R) can be found in nature and is a *PPP2R1A* cancer mutation hotspot [1]. In addition, a separate study has utilized transformed HEK (human embryonic kidney) cells expressing large T, hTERT and H-RAS (HEK TER) with mutant *PPP2R1A* constructs to determine the effects of the E64D, E64G and R418W mutations on B subunit binding [131]. Similar to past studies, these mutations were found to disrupt binding of B55α and some members of the B' subunit to the Aα subunit [131].

Many of the first functional experiments that indicate PPP2R1A mutations disrupt binding of particular PP2A B-subunits were performed using IP-Western experiments [90, 131]. This method is limited by a need for multiple antibodies for each of the PP2A subunits (>15), and many of these subunits have many alternative transcript products. This results in many non-specific bands detected by a western blot, and is often a guess to determine which band is the specific band of interest. There is also high similarity between the B-subunit family members making it difficult for specific antibody detection and production. Previous studies have

generated their own antibodies [109, 110], which is time consuming and costly. Testing multiple antibodies for IP-western experiments is also costly, especially when investigating multi-protein complexes involved in many protein-protein interactions. To avoid this problem, researchers have overexpressed constructs with tags (FLAG, HA), which eliminates the need for multiple B subunit antibodies [114, 252, 253]. However, the process of quantifying differences on a western blot can be subjective and inaccurate, and has also been the subject of manuscript retractions due to manipulated western blot images [254, 255]. In my own experience (data not shown), the antibodies for the specific B subunits did not show consistent results, and often the bands detected on a western blot were not the same as the predicted molecular weight. This becomes problematic to try to detect small differences in the binding of B subunits to the PP2A core protein complex.

Proteomics experiments using mass spectrometry can avoid these limitations of antibodies and western blots [256], and have been used to determine the PP2A holoenzyme complexes and PP2A interaction networks [95, 257]. These studies are imperative for understanding the complexity of the PP2A protein network, however they are limited by cell context. The cell lines that were primarily used are easy to grow and easily transfected; HEK293 (transformed human embryonic kidney cells) and HeLa (cervical carcinoma) cells. Although these cell lines are useful for initial biochemical studies, the overexpressed mutated constructs transfected into these types of cells do not take into account the disease of which the mutations are found. PP2A subunit expression and biological role may be different in tissue and cell types; therefore this needs to be taken into account for disease-specific studies. It is also apparent from previous work, and Chapter 5, that the balance of PP2A levels are important.

Overall, studies have shown that a few *PPP2R1A* mutations (E64A, E64G, R418W, and 171-589 deletion) identified in one case of lung carcinoma, one case of melanoma and breast carcinoma, can disrupt the binding of specific B subunit proteins to form a functional PP2A phosphatase holoenzyme complex [90, 131]. However, there have been no studies to date on how the specific *PPP2R1A* mutations (P179R, R183W, R182W, S256F/W, W257G/L/C, R258C), discovered in endometrial and ovarian carcinomas [1, 2, 70, 206], can disrupt the binding of the B subunits in the context of gynaecological cancer. The last goal for my thesis research was to

utilize the endometrial carcinoma derived Hec1A isogenic PPP2R1A cell lines, as described in Chapter 5, to study the effect of the PPP2R1A mutation at endogenous levels and in a context-specific model. I hypothesized that the Hec1A endogenous PPP2R1A W257L mutation affects the interaction of PP2A B subunit family members; this was tested by isolating the PP2A complex using co-IP (co-immunoprecipitation) then coupled with proteomics technology and analysis. State of the art proteomics technology was utilized to allow insight into the relative differences in B subunit protein interactions in the Hec1A isogenic cell lines.

6.2 Methods

6.2.1 Co-Immunoprecipitation

For all co-immunoprecipitation (co-IP) and western blots, the rat monoclonal PPP2R1A 6F9 (Covance) was used. To covalently link the PPP2R1A antibody (Ab) to agarose beads, the Pierce co-IP kit was used as per manufacturers protocols (Thermo Scientific, Pierce, IL, USA). A control normal rat IgG antibody (Santa Cruz Biotechnology) was also covalently attached to agarose beads using the same protocol. In brief, 100ug of PPP2R1A Ab or normal rat IgG Ab was covalently bound to the AminoLink Plus Coupling Resin (aldehyde-activated beaded agarose). Hec1A cells from 6 X 15cm plates were cross-linked on plastic using 1% paraformaldehyde in serum-free media for 7 min, then quenched with 250nM glycine for at least one minute. The cells were washed twice with approximately 5-8mL cold PBS, then lysed and scraped off the tissue culture dishes using 10mL of cold Pierce IP lysis buffer with 1 tablet of cOmplete Protease Inhibitor Cocktail tablets (Roche). The cells were scraped on ice, then centrifuged at 16,000Xg for 15min to clear the lysate. The Pierce BCA assay was used as per manufacturer's protocol to quantitate the total protein concentration. In total 20mg of cell lysate was used for each co-IP reaction. The bound Ab-bead mixture was added to the cell lysate and incubated at 4^{o}C with rocking for about 2 hours. The protein complexes and beads were spun down at 1000Xg for 5min, then applied to a small spin column to allow washing and eluting. Once all the beads were applied to the column, the beads were washed 2X with cold PBS, then eluted with 60uL of Pierce Elution Buffer. The Elution buffer was allowed to incubate on the beads for 5min at room temperature, then eluted at 1000Xg for 1min. This elution was repeated for a total of 120uL of eluted IP proteins. The antibody-bead resin was then regenerated using

Pierce 1X Coupling Buffer, and added back to the cell lysate to repeat the co-IP. This co-IP was repeated for an additional two times, for a total of 3 sequential co-IP elutions. After all elutions were complete, the samples were pooled to a total of 320uL, and stored at -80^{o}C.

6.2.2 Western Blots

To determine if the PPP2R1A co-IP was successful, 10uL of each co-IP reaction was subjected to analysis on a 10% SDS-PAGE gel. Proteins were transferred to a nitrocellulose membrane and then washed in TBST (0.1% Tween-20). The blots were blocked using 5% skim milk with TBST for either 1hr at room temp or overnight at 4^{o}C. The primary PPP2R1A Ab (Covance) was incubated for 1-2hrs at room temp, or overnight at 4^{o}C, using 1/4000 dilution in 5% skim milk + TBST solution. The secondary anti-rat HRP-labeled antibody was used at 1/20,000 dilution in 5% skim milk +TBST. The chemiluminescence kit (Millipore) was used for detection, and exposed at various times and developed using x-ray film.

6.2.3 Sample Digestion for Mass Spectrometry Analysis

Each of the IP samples was split into 3 aliquots. The first 100uL samples were prepared with no heating for de-crosslinking, the second 100uL aliquots were heated for de-crosslinking at 68^{o}C overnight, and the last 300uL were de-fixed at 95^{o}C for 10min. To then digest the IP samples, 100uL of the each pooled IP sample was used for reduction and alkylation. The samples were first reduced by using 5uL per 100uL volume of 200mM DTT in 50mM HEPES pH8.5, and then incubated at 45^{o}C for 30min. This was followed by the addition of 10uL per 100uL volume of 400mM IAA in 50mM HEPES pH8.5 then incubated at 30min at 24^{o}C in the dark. To quench the reaction 10uL per 100uL volume of 200mM DTT in 50mM HEPES pH8.5 was added and mixed. To proceed with protein cleanup and trypsin digestion, the paramagnetic SP3 beads were utilized as per protocols cited in Hughes *et al.* [258]. Samples were digested overnight with 80ng sequencing grade Trypsin (Promega) at 37^{o}C with the presence of SP3 beads. At the peptide level, 4 TMT labels (TMT^{6}-126, TMT^{6}-127, TMT^{6}-128, TMT^{6}-129) (Thermo Scientific) were used to pool samples (Table 6.1), as per Hughes *et al.* [258] and manufacturer's protocol. In brief, 20ug of each TMT label was added to the peptide-bead mix and incubated at room temp for 30min. This step was repeated and incubated for a further 30min. The samples were quenched for 5min at room temp then washed with acetonitrile. To pool samples, 10uL of 2% DMSO was

used to resuspend one sample, then transferred to the next sample for incorporation into the pool, and repeated until all four samples were pooled in 10uL total. The pools (Table 6.1) were then acidified to final 0.1% formic acid, and run directly on the LC coupled to the mass spectrometer.

PPP2R1A-IP Pool	TMT^6-126 (mut/mut/wt)	TMT^6-127 (mut/mut)	TMT^6-128 (mut/wt)	TMT^6-129 (mut/mut/wt ctl)
Pool 1	Parental P145	9-15 mutant	10-23-45-6 het	Parental P145 IgG-IP
Pool 2	Parental P146	9-14 mutant	10-23-60-17 het	Parental P146 IgG-IP
Pool 3	Parental P147	33-1 mutant	10-23-60-24 het	Parental P147 IgG-IP

Table 6.1 Hec1A isogenic cell line IP TMT pools for mass spectrometry analysis
P145, P146, P147 indicates passage number. For the mutant and heterozygous cell, the number indicates the clone ID.

6.2.4 Mass Spectrometry Data Acquisition

The pools of IP TMT labeled samples were analyzed on a Fusion Orbitrap system (Thermo Scientific) coupled with an EASY-nLC 1000 (Thermo Scientific) liquid chromatography system. A total of 4uL for each pooled peptide sample was loaded onto the LC with 10uL/min flow into a reverse phase C18 column. The samples were eluted from the column with a gradient flow of 250nL/min, for a total of 120 min. The gradient parameters are as follows: 1min at 2% Buffer B, 91min at 22% Buffer B, 14min at 30% Buffer B, 14min 80% Buffer B (Buffer A: 0.5% formic acid in water, Buffer B 0.5% formic acid in acetonitrile). Data acquisition on the Fusion Orbitrap was programed using the Thermo Scientific software and workflow template. The first MS scan was used for precursor selection, then MS2 fragmentation in the CID (collisional induced fragmentation), with a cycle time of 3sec. At this point the top 10 fragments were selected for MS3 in the Orbitrap HCD, to allow fragmentation for TMT label quantitation. The survey scans were used at a mass range of 380-1200(m/z), with the Orbitrap resolution set at 120,000.

6.2.5 Mass Spectrometry Data Analysis

To perform peptide and protein identification, as well as TMT quantitation, the Thermo Proteome Discoverer 1.4.1.14 software (Thermo Scientific) was utilized. All MS runs for each pool were searched together using the protein databases Mascot and Sequest HT. The analysis workflow was set up to search and group peptides into proteins, which also assigned a FDR

(0.05). A medium peptide confidence filter was utilized, and the raw data was extracted for subsequent analysis in the stats package RStudio Version 0.98.1074. To first filter the raw peptide data in each individual pools, peptides were removed if duplicate peptides were present, and if missing values were present in any of the TMT126, TMT127 and TMT128 labeled samples. The resulting peptides from each of the 3 pools were then merged, to allow quantile normalization [259]. Normalization of the cell lines is shown before and after normalization (Figure 6.1). The Negative control Ig-G IP values were not used in the downstream analysis. Each of the pools was then collapsed into proteins (based on accession groups), which takes the mean of the peptides for each protein and collapses into the protein group. An accession group list of PP2A subunits and PP2A interacting proteins found in the raw data (PPP2R1A, PPP2CA, PPP2CB, PPP2R2A, PPP2R5A, PPP2R5C, PPP2R5D, PPP2R5E, PPP2R4, SET, IGBP1, PPME1) were used to extract proteins of interest for additional statistical analysis. The peptide list and intensities associated with these proteins can be found in Table F.9 (Appendix F). Proteins were included in additional analysis only if they were identified in 2 of the 3 pools. This removed only one of the B subunits (PPP2R5A) from the analysis, as it was only detected in one of the 3 IP pools. To determine significant changes for these proteins of interest, the fold changes for each individual replicate were calculated. To calculate unadjusted p-values, the Limma R package [260] was used for each cell line comparison (n=3) within each protein group. The adjusted p-values were then calculated based on all the tests performed using the B-H method [194].

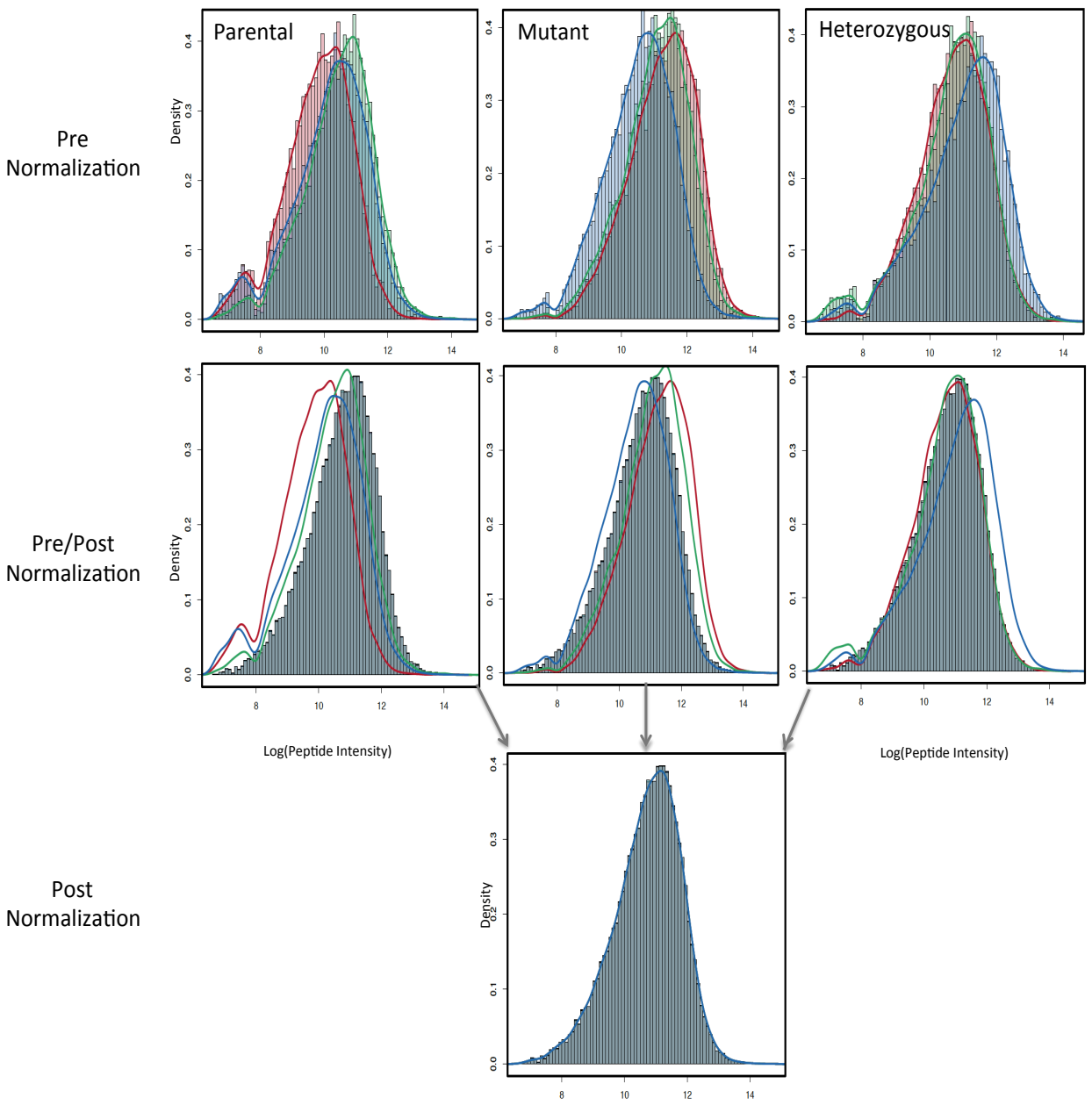

Figure 6.1 Pre and post normalization of all peptides identified in the IP-MS pools.
Histograms for pre and post normalization by quantile normalization analysis are shown. The histograms depict peptide density (y-axis) by the log of the peptide intensity (x-axis). The first row of panels indicate pre-normalization, the middle row panels show log peptide intensities with normalization as the histogram and the smoothed lines indicate pre-normalization levels for each of the 3 pools. Red lines indicate pool 1, green as pool 2, and blue as pool 3. The post normalization histogram is the finalized normalized data for the parental, mutant and heterozygous samples.

6.3 Results

To determine the changes in endogenous PPP2R1A interactions in the trio of Hec1A isogenic cell lines harboring the PPP2R1A mutation, immunoprecipitation were employed for analysis by western blot and mass spectrometry. A previous study had determined that the PPP2R1A 6F9 antibody enabled the isolation of the endogenous PP2A heterotrimeric complex using sequential immunoprecipitation [261]. Therefore, by performing sequential PPP2R1A co-IPs of the Hec1A parental and isogenic cell lines, I was able to isolate the endogenous PP2A complex in each IP (Figure 6.2).

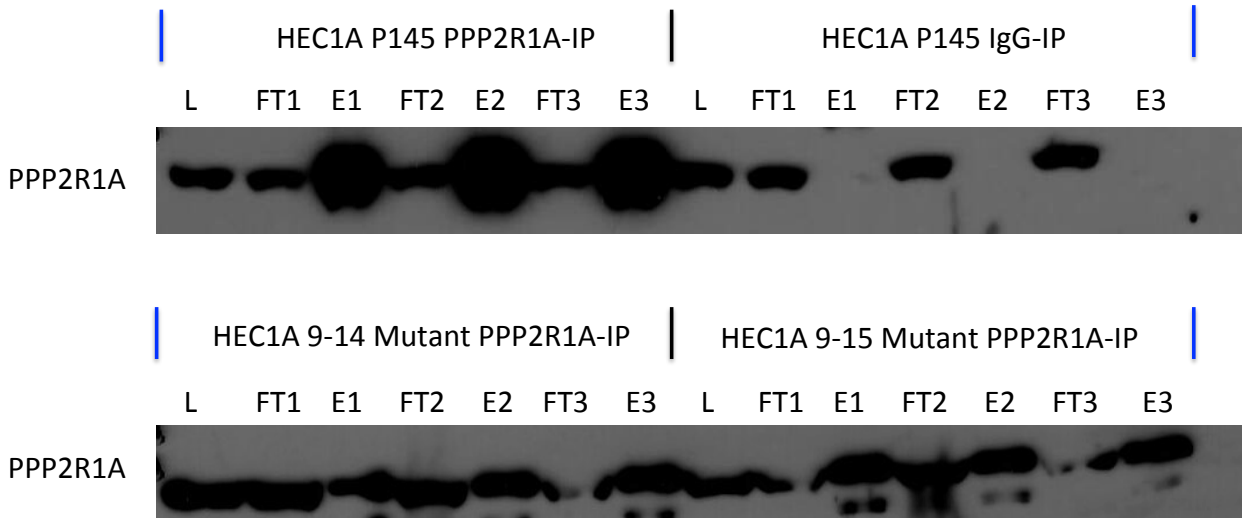

Figure 6.2 PPP2R1A-IP samples with immunoblot (IB) for PPP2R1A
Sequential PPP2R1A-IPs from Hec1A lysates and PPP2R1A-IB shown by Western blot. L=total lysate, FT=Flow-Through, E= Elution. The IgG negative control shows that there was no PPP2R1A pull down through immunoprecipitation.

The monomeric PPP2R1A protein or the core subunit bound to the catalytic subunit is very abundant in the cell, however, I found that the B subunits were in limiting amounts, and difficult to detect by IP-western analysis. I also found it difficult to detect B subunit protein interaction with PPP2R1A without chemical cross-linking. I therefore utilized chemical crosslinking to allow isolation of an intact PP2A holoenzyme, and sequential IPs from each cell line were needed in order to maximize the number of PPP2R1A protein molecules and PP2A complexes binding to the PPP2R1A-IP antibody. Sequential IP's were performed by using the unbound fraction to carry into the next IP using the agarose-conjugated PPP2R1A antibody. Even after three sequential co-IPs, the levels of PPP2R1A were not 100% depleted from the cell lysate, as

PPP2R1A was still present in the flow-through after the third immunoprecipitation reaction (Figure 6.2). However, there was sufficient PPP2R1A and interacting proteins in the elutions to perform mass spectrometry.

To acquire a complete analysis of the possible PPP2R1A-IP interactions, I used the sensitive Fusion Orbitrap mass spectrometer to analyze the three PPP2R1A-IP pools of isogenic cell lines containing triplicate biological replicates (three different mutant clones, heterozygous clones and different passages of the parental cell line). For the purposes of this study, I was interested in only the PP2A subunits and known interactors with PP2A, therefore the analysis was directed at only these specific proteins. In all of the samples, I was able to detect both C subunits (PPP2CA, PPP2CB), five of the B subunit family members (PPP2R2A, PPP2R5A, PPP2R5C, PPP2R5D, PPP2R5E), and four additional known PP2A interactors (PPP2R4, PPME1, IGBP1 (alpha4), and SET) (Table 6.2). Peptides from PPP2R1B, along with the other B55, B56' and B'' subunit family members (including Striatin (STRN)), and an additional PP2A inhibitor CIP2A were not detected in any of the IP samples.

By comparing the IP pools of Hec1A PPP2R1A mutant (mut/mut) clones with Hec1A PPP2R1A heterozygous (mut/wt) cell lines clones, there were significant differential interactions of the B subunits PPP2R5C, PPP2R5D and the PP2A inhibitor SET (p-value 0.035, 0.043, 0.043 respectively) (Table 6.2, Figure 6.3). PPP2R5C and PPP2R5D peptides were found at lower intensities in the mutant cells compared to the heterozygous cell lines. Conversely, the endogenous PP2A inhibitor, SET, was found at higher intensities in the mutant cell lines. This implies that there was an increased interaction of SET with PPP2R1A in the mutant cells compared to the heterozygous cells. There was a trend for decreased interaction of PPP2R2A and PPP2R5E with mutant PPP2R1A, however this was not significant after multiple p-value corrections (Table 6.2).

The comparison of the parental (mut/mut/wt) with the mutant cell line clones also shows significant differential interaction with PPP2R5C and PPP2R5D (Figure 6.3). However, PPP2R1A levels were also found to be significantly different in the parental cells compared to the mutant and the heterozygous cell lines. This may be explained by the difference in the

number of PPP2R1A expressing alleles in the isogenic cell lines; the parental cell line harbors three expressed PPP2R1A alleles compared to only two alleles in the mutant and heterozygous cell lines. Therefore, assessing the differences in interactions between the mutant cells and the heterozygous cells was a more suitable comparison to account for the number of alleles expressing PPP2R1A. There were no other significant differences between the PPP2R1A-IP samples from the parental and heterozygous cell lines (Figure 6.3). There were also no significant effects of the PPP2R1A mutation on the catalytic C subunit (PPP2CA or PPP2CB) binding in any of the cell lines. In addition, the PPP2R1A mutation did not seem to show an interaction difference with the PP2A interacting proteins PPP2R4, IGBP1 or PPME1.

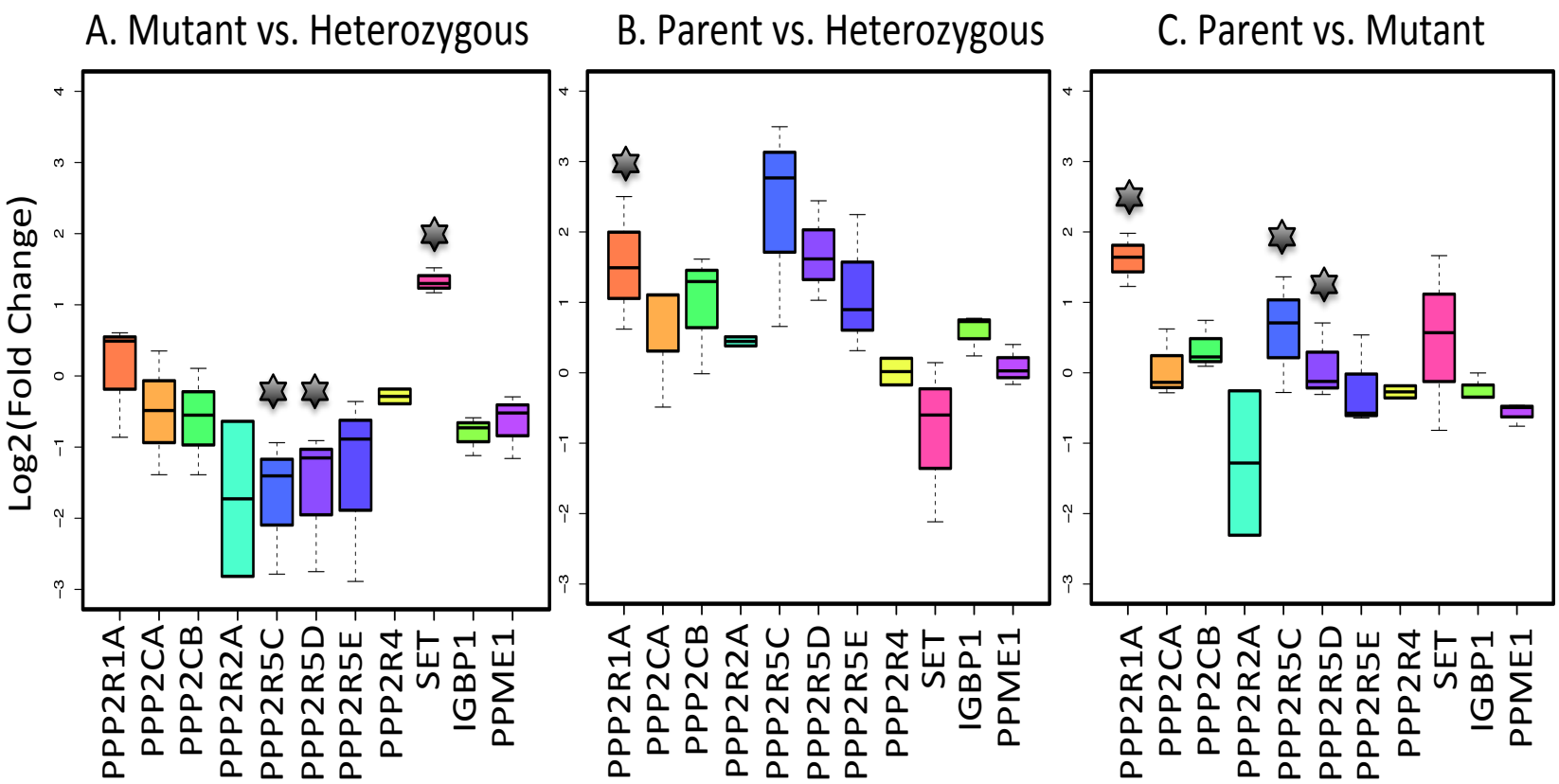

Figure 6.3 Quantitative analysis of PPP2R1A-IP TMT labeled pools using mass spectrometry.
Each panel shows the comparison between the isogenic cell lines. Box plots reveal the variation of the detection of each protein in the three IP pools. Black stars indicate significant adjusted p-values.

Protein Name	PPP2R1A	PPP2CA	PPP2CB	PPP2R2A	PPP2R5C	PPP2R5D	PPP2R5E	PPP2R4	SET	IGBP1	PPME1
Protein Groups	P30153	P67775	P62714	E5RFR9	H0YJU0	Q14738	Q16537	A6PVN9	Q01105	P78318	Q9Y570
Parental-t126a	433000	384000	169000	2980	12300	46300	32600	20200	173000	16100	28000
Parental-t126b	327000	456000	167000	NA	15300	100000	6710	13200	94000	9760	24500
Parental-t126c	262000	352000	106000	16100	5950	48000	17220	NA	50100	9190	21600
Mutant-t127a	76400	179000	55100	2090	1090	8510	6860	22800	156000	9420	21200
Mutant-t127b	116000	212000	68000	NA	2250	32600	5400	11400	142000	8270	27400
Mutant-t127c	170000	493000	107000	12400	3770	23500	9250	NA	217000	5550	21200
Het-t128a	139000	468000	144000	14800	7540	57300	50800	25900	54500	20500	47300
Het-t128b	82900	297000	99600	NA	5960	61200	9980	15000	63300	12400	33600
Het-t128c	112000	387000	99100	19300	7220	52300	11900	NA	88200	9200	30400
MutVHet a	-0.86	-1.39	-1.39	-2.82	-2.79	-2.75	-2.89	-0.18	1.52	-1.12	-1.16
MutVHet b	0.49	-0.49	-0.55	NA	-1.40	-0.91	-0.89	-0.39	1.17	-0.59	-0.29
MutVHet c	0.61	0.35	0.11	-0.64	-0.94	-1.15	-0.36	NA	1.30	-0.73	-0.52
ParVHet a	1.64	-0.28	0.22	-2.31	0.71	-0.31	-0.64	-0.36	1.66	-0.35	-0.76
ParVHet b	1.98	0.62	0.74	NA	1.36	0.71	-0.57	-0.19	0.57	-0.35	-0.46
ParVHet c	1.23	-0.14	0.09	-0.26	-0.28	-0.12	0.54	NA	-0.82	0.00	-0.49
ParVMut a	2.50	1.10	1.61	0.51	3.49	2.44	2.25	-0.17	0.14	0.77	0.40
ParVMut b	1.49	1.11	1.30	NA	2.77	1.62	0.31	0.21	-0.60	0.24	-0.17
ParVMut c	0.62	-0.49	-0.01	0.38	0.66	1.03	0.90	NA	-2.12	0.73	0.03
MutVHet pvalue	0.87	0.30	0.21	**0.03**	**0.01**	**0.01**	**0.03**	0.60	**0.01**	0.08	0.15
ParVHet pvalue	0.00	0.84	0.28	0.05	0.15	0.79	0.53	0.50	0.33	0.46	0.09
ParVMut pvalue	0.00	0.23	0.05	0.44	**0.0001**	**0.001**	**0.022**	0.98	0.08	0.22	0.85
MutVHet pAdj	0.90	0.45	0.38	0.09	**0.04**	**0.04**	0.09	0.71	**0.04**	0.19	0.30
ParVHet pAdj	**0.01**	0.90	0.44	0.14	0.30	0.89	0.65	0.63	0.48	0.60	0.19
ParVMut pAdj	**0.03**	0.38	0.14	0.60	**0.003**	**0.02**	0.09	0.98	0.19	0.38	0.90

Table 6.2 Mass spectrometry data at the protein level after normalization
The TMT values (126-128) in the first nine rows show the normalized protein intensities for each pool. The comparison rows (MutVHet, ParVHet, ParVMut) show the ratio of the log intensities for each protein. The unadjusted and adjusted p-value is also shown for each comparison.

6.4 Discussion

This is the first study to determine the effects of an endometrial endogenous PPP2R1A mutation on the interactions with PP2A B subunits. In an attempt to perform protein interaction experiments without the use of multiple antibodies, I utilized sequential co-immunoprecipitation of endogenous PPP2R1A in isogenic Hec1A cell lines, coupled with proteomic mass spectrometry analysis. As shown in Chapter 5, each of the mutant and heterozygous cell line clones had slightly different cell proliferation profiles, however all proliferate similarly within the same isogenic background. For example, the mutant clonal cell lines all proliferate slower than the parental, and the heterozygous cell clones proliferate similarly to the parental cell line. To potentially mitigate these slight variations of one particular clone, three different mutant and heterozygous clones were utilized for the IPs and combined for the overall peptide data analysis. By comparing the different PPP2R1A isogenic cell lines, I was able to show that there are significant differences in some PP2A B' subunit interactions with mutant PPP2R1A.

Of particular interest, the Hec1A PPP2R1A mutant (mut/mut) cell clones demonstrate a significant decrease in interaction with the B56 family members PPP2R5C and PPP2R5D when compared to the heterozygous and parental cell lines. Due to the unbalanced PPP2R1A allele levels of the parental (mut/mut/wt) compared to the mutant (mut/mut) and heterozygous (mut/wt) cell lines, there was a significant difference in PPP2R1A levels detected by mass spectrometry analysis. However, it was acceptable to compare the pooled mutant and heterozygous cell lines clones (both express two PPP2R1A alleles) to determine if the mutation had an affect on B subunit binding. The intensity of the PPP2R1A peptides detected in the mutant and heterozygous cell line IP samples were not significantly different. The IP-MS analysis demonstrated the novel discovery that the PPP2R1A L257 mutation affected the interaction of both PPP2R5C and PPP2R5D. These two proteins have been previously reported as being important regulators of tumourigenesis and cellular transformation.

The crystal structure studies of PP2A revealed that the specific B'γ subunit (PPP2R5C) interacts with the A subunit (PPP2R1A) via HEAT domains. These interactions are over a large surface area, however the overall interaction is low involving only a few key amino acid

residues. Xu *et al.*, showed that a small interaction area involves the B subunit HEAT repeat 2 with the A subunit HEAT repeat 7 and 8, where W257 directly hydrogen bonds with the L107 residue on the B subunit [86, 94]. In addition, amino acid residue L107 and the surrounding residues are highly conserved amino acids in all family members of the B' family [86]. This provides further evidence that the W257 mutation found in PPP2R1A can cause disruption of the hydrogen bond that links the whole B' family to the A subunit of PP2A. This structure interaction also provides additional validity to my observation of decreased protein interactions involving PPP2R5C and PPP2R5D with PPP2R1A that harbors the W257L mutation.

As previously described, the suppression of PPP2R5C has induced cellular transformation [109, 133]; therefore it is not surprising to find that this particular Hec1A PPP2R1A mutation (W257L) can affect the binding of PPP2R5C to potentially induce endometrial transformation. The knockdown of PPP2R5C, to replace SV40ST, has exhibited an ability to fully transform cell lines that express SV40LT, hTERT, and Ras-V12 [262]. The capability of PPP2R5C knockout to transform cells, explains the use of this knockout construct for the construction of the human fallopian tube secretory epithelial cell model in mice [233], also giving evidence to show this protein is extremely important in tumourigenesis. My observed results were also consistent with the report by Chen *et al.,* where the authors show that PPP2R5C (B56γ) interaction is lost when a PPP2R1A E64D/G mutation is overexpressed. Loss of PPP2R5C interaction with PPP2R1A was also observed when PPP2R1A was downregulated with the use of shRNA [131]. PPP2R5C and also all B56 family members have been reported to directly inhibit the formation of the APC-Axin complex, which leads to the destabilization of β-catenin [263]. Moreover, functional PP2A complexes containing PPP2R5C can dephosphorylate p53 at Thr55, thus preventing its degradation and inhibiting cell proliferation [264]. In the tumour cell, if PP2A-PPP2R5C complexes cannot effectively dephosphorylate p53, hyperphosphorylation of p53 occurs leading to it's degradation by the proteasome and thus kept at low levels to allow cell proliferation and tumourigenesis. In the context of endometrial serous carcinomas *TP53* is almost ubiquitously mutated [42], however it is possible that *PPP2R1A* mutations that cause disruption of PPP2R5C interaction may provide an alternative "safe keeping" suppression of p53 by lack of Thr55 dephosphorylation. One PPP2R5C mutation (F395C) described in lung cancer has been previously found to disrupt the ability of PP2A to dephosphorylate Thr55 on p53 [265]. In

Chapter 3, I also sequenced PPP2R5C in a large cohort of endometrial carcinomas, and found this gene to be rarely mutated (n=3), therefore it is unlikely that *PPP2R5C* DNA mutations are playing a large role in tumourigenesis. It is however possible that perturbed binding of PPP2R5C to PPP2R1A or alternative post-translational modifications causes disruption of PP2A-PPP2R5C specific substrate dephosphorylation to promote endometrial tumourigenesis.

My discovery of the PPP2R1A Hec1A mutation disrupting interaction with PPP2R5D is interesting in the context of endometrial carcinoma. Firulli *et al.,* demonstrated that B56δ-containing PP2A complexes interacts with the bHLH factors HAND1 and HAND2 [266] to reduce levels of HAND1 phosphorylation. The HAND transcription factors are required for heart, vascular, embryonic and placental development [267], and phosphorylation is required for nucleolar release, dimerization and biological function [268]. A recent publication presented evidence associating hypermethylation of HAND2 in >90% of endometrial endometrioid carcinomas, which is also correlated with the downregulation of mRNA expression [269]. The *PPP2R5D* gene was also noted to be hypermethylated in these endometrial carcinomas. HAND2 is expressed in the normal endometrial stroma, is regulated by progesterone and aids in progesterone suppression of estrogen induced pathways [270]. In mice that lack HAND2, epithelial proliferation is maintained by induction of fibroblast growth factors and stimulation of estrogen pathways [270]. This is fitting as the majority of endometrial endometrioid carcinomas are estrogen-dependent tumours, and the loss of HAND2 and PPP2R5D protein expression by gene hypermethylation could be an important contributor to endometrial carcinogenesis. Taken together, the deregulation of PPP2R5D in endometrial carcinoma seems to be an important mechanism of tumourigenesis and warrants further investigation. It would be interesting to determine if PPP2R1A mutations and hypermethylation of PPP2R5D and HAND2 are leading to the same pathways for promotion of tumourigenesis and cell proliferation. In addition, PP2A-PPP2R5D complexes have been found to be an important regulator of CDC25C in mitotic exit [97]. If PPP2R5D cannot dephosphorylate CDC25C in mitosis, this will lead to prolonged activation, and subsequent activation of CDK1 to delay exit from mitosis [97].

The mutated PPP2R1A cell lines also demonstrated a statistically significant increased interaction with the PP2A inhibitor SET (I2PP2A). At this time, it is unclear if SET can interact

more efficiently with the mutant-containing PPP2R1A-PP2A holoenzymes, or that the disruption of B subunit interactions by the PPP2R1A mutation has caused an unbalance of available free PP2A, which can then bind to SET. Earlier studies have shown that SET/I2PP2A likely interacts with the PP2A catalytic subunit [127, 271]. With respect to the structure of PP2A, if mutated PPP2R1A causes loss of hydrogen bonds that act to facilitate A and B subunit interactions, it is possible that the pool of A-C dimers (without B subunit interaction) may be more available to interact with SET through the catalytic domain. In other words, the SET protein may be able to mimic the B subunit and interact with the A-C core PP2A protein. It is also possible that mutant PPP2R1A could cause "loose" interactions of B subunits resulting in a conformational change in PP2A, which could then allow for efficient SET interaction with the catalytic subunit. These theories are purely speculative, as these types of structure studies need to be performed in the future to determine how mutant PPP2R1A affects SET interaction.

The SET oncoprotein has been identified as overexpressed in many cancer types including B-cell chronic lymphocytic leukemia (CLL), non-Hodgkin lymphoma [272], and breast cancers [273]. In addition SET overexpression was correlated with decreased PP2A activity in chronic myelogenous leukemia (CML) cells [252]. In CML, BCR/ABL induces expression of SET to inactivate the dephosphorylation activity of PP2A, however re-activation of PP2A causes growth suppression and apoptosis. Interestingly, the inactivation of SET or CIP2A has been the subject of a few recent studies, these show that a SET inhibitor (OP449) can significantly reduce the tumourigenic potential in pancreatic cell lines and breast cancer cell lines [128, 129]. Furthermore, ceramides have exhibited antiproliferative properties, with an ability to increase PP2A activity by directly binding to SET/I2PP2A in lung cancer models [274, 275]. An FDA approved spingolipid analogue drug, FTY720, has recently been shown to directly target SET to activate PP2A, causing cell death and lung tumour suppression [268]. The importance of SET in gynaecological cancers is yet to be determined, although in light of these results this warrants further research and drug testing in endometrial cancer models.

It was interesting to note that the PPP2R1A mutation does not cause complete loss of binding of any of the observed B subunits. This may be due to the importance of the fine balance of PP2A activity for the cell's growth, survival and death. If there is complete loss of PP2A activity

this will lead to cell death, therefore for the tumour cell to survive, it must not eliminate all functional PP2A activity. As described previously, mutations in PPP2R1A seem to function by disrupting B subunit binding which likely partakes in cellular transformation and tumourigenesis. From these results, I propose that the W257L PPP2R1A mutation is affecting the PP2A holoenzyme in three ways: 1) to disrupt efficient binding of particular B subunits, 2) disrupting B subunit substrate interaction for effective phosphatase activity 3) allowing the PP2A inhibitor SET to interact with PP2A (containing mutated PPP2R1A) to thus inhibit PP2A activity.

The use of mass spectrometry analysis enabled the simultaneous identification of a number of protein interactions in the PPP2R1A-IP cell line lysates. Currently, these interaction results have not been validated, and traditionally the "gold standard" would be to perform a number of western blots. As stated previously, western blots are not quantitative, and are dependent on reliable antibodies for each protein of interest. Aebersold *et al.,* recently advocated that targeted proteomics techniques should be used to perform quantitative protein analysis and for validating mass spectrometry results, instead of the western blot [256]. These techniques, such as SRM/MRM (selected reaction monitoring/multiple reaction monitoring) or PRM (parallel reaction monitoring) [276], are extremely accurate as they provide quantitative information from multiple peptides per protein, multiple transitions per peptide with multiple measures of each signal. This level of analysis would be equivalent to performing hundreds to thousands of western blots to potentially validate the interactions of PP2A. For future studies, I will likely utilize the PRM methodology to validate the results from this study.

In conclusion, the immunoprecipitation of endogenously mutated PPP2R1A and subsequent analysis by sensitive mass spectrometry identified many subtle differences in the interaction of regulatory B subunits to PPP2R1A. I have presented a novel discovery wherein the endogenous PP2A inhibitor, SET oncoprotein, can interact with mutated PPP2R1A. Additional studies will be needed to determine if this increased interaction contributes to the suppression of PP2A activity. Overall, these findings suggest that the PPP2R1A mutation is likely playing a large role in cellular tumourigenesis by disrupting the balance of B subunit interactions. It will be interesting to study additional cell lines and patient samples for changes in PP2A subunits to determine if all hotspot PPP2R1A mutations act similarly. Future studies should also include

assessing the changes in B subunit substrate dephosphorylation events. Finally, targeting PP2A for targeted therapeutics may be an efficient way to inhibit tumourigenesis in gyneacological carcinomas.

Chapter 7: Conclusion

7.1 Overall Significance of My Thesis Research

7.1.1 *PPP2R1A* Mutations in Endometrial Carcinomas

My publication on the discovery of *PPP2R1A* mutations in endometrial carcinomas, described in Chapter 2, has lead to a number of other researchers validating and publishing their sequencing results of *PPP2R1A* mutations. The validation of these results by separate international groups is of immense importance that reflects the validity of the finding. It was especially important to validate the hypothesis and discovery of *PPP2R1A* mutations specific to endometrial serous carcinoma, and not ovarian serous carcinomas [206]. As this suggests that these cancers are molecularly distinct and thus should not be bundled as a single entity in clinical trials. Multiple groups including the TCGA consortium have validated this observation, there are, of course exceptions and *PPP2R1A* mutations have now been described in ovarian serous carcinoma, albeit at very low frequencies (1%) [33]. *PPP2R1A* mutations are not only found in endometrial serous carcinomas, as I also identified varying mutation frequencies in endometrial and ovarian endometrioid carcinomas. These two subtypes are thought to originate from the same endometrial epithelial precursor cell, however it is apparent from their differences in the frequency of *PPP2R1A* mutations that they evolve by different tumourigenic pathways.

7.1.2 Mutational Profiling of Endometrial Carcinomas

My work presented in Chapter 3, identified distinct molecular profiles that may aid in improving endometrial carcinoma classification leading to increased reproducibility of diagnoses. This publication was an important stepping-stone for the TCGA endometrial carcinoma study. The TCGA study used whole exome sequencing and other genomic technologies; therefore they were able to perform a more comprehensive analysis for classifying the genetic landscape of these tumours. Although my study did not have larger genomic view of the tumour, I was still able to demonstrate that there was a molecular difference between the histologically defined endometrioid and serous cases. In addition, I was able to pinpoint the misclassified cases using mutation profiles. This is important, as the subset of cases that can appear as intermediate subtypes (Figure 3.4), mixed endometrioid and serous, are in particular

need of subclassification, and mutational profiling seems to distinguish these challenging cases. In addition, the TCGA study was also able to show misclassified cases based on their genomic data [42]. Although endometrial carcinoma subtype diagnoses and grade are currently used in guiding patient management, mutational analysis is emerging as a realistic option in clinical practice. In the future, I predict that the mutational classification of endometrial carcinomas will become an important tool in diagnosis, and guiding mutation-based targeted treatment decisions. Mutation profiles are already being applied in other cancers for selecting targeted therapeutics, for example BRAF inhibitors in malignant melanoma [277] and BRAF and EGFR targeting in colorectal cancers [278, 279]. Determination of the role of mutational analysis in assessment of endometrial carcinomas will require additional study, with careful comparison of molecular versus conventional subclassification.

In Chapter 3, I also proposed that the traditional dualistic model of endometrial cancer that divides this cancer into type I and type II should be avoided, as it is too simple and does not capture the important distinctions between the subtypes of endometrial cancer. The very first small epidemiological study of endometrial cancers did show that risk factors were different between endometrioid and serous histologies [280], however a recent large case control study indicates that the risk factors may be similar for both types [281]. This large study also supports the notion that the type I and type II terminology should not be used, and should not be grouped separately based on histology alone, as there may be a common etiologic pathway. A recent review by Murali *et al.,* also recommended the elimination of the dualistic type I and type II model as it does not encompass the heterogeneity of the endometrial tumours [282]. In the future, this terminology will be filtered out of mainstream publications due to the recommendations from these new studies.

7.1.3 *PPP2R1A* Isogenic Cell Line Models

The generation of the *PPP2R1A* isogenic endometrial cell lines, described in Chapter 5, provides an important model for the PP2A research community. This is the first endogenously expressing *PPP2R1A* mutant only cell line in a relevant disease specific model. These cell lines could be used in future studies of drug screens to assess the ability of drugs to selectively target tumours with *PPP2R1A* aberrations. To determine the downstream effects of the PPP2R1A

mutation and disruption of PP2A B subunit binding, it will be interesting to use these cell lines in additional assays, for example, phospho-proteomic, global proteomics and cell cycle regulation and mitotic checkpoint assays. This may aid in the discovery of novel targetable proteins or pathways that could be used for endometrial-specific therapeutics and diagnostic tools. These cell lines may also provide a model for the assessment of drugs that target PPP2R1A and/or the SET protein. Overall, my research has generated the first set of isogenic PPP2R1A endometrial specific cell lines for one particular mutation, therefore it will be important to generate additional cell lines to determine the effect of the other hotspot mutations identified in endometrial and ovarian cancers.

7.1.4 Impact of *PPP2R1A* Mutations on PP2A Holoenzyme Composition

The work presented in Chapter 6 is the first study to perform the assessment of an endogenous *PPP2R1A* mutation in a disease-specific cell line model system. I was able to show using sensitive mass spectrometry analysis, that the PPP2R1A W257L mutation causes changes in the interactions of PP2A B subunits PPP2R5C and PPP2R5D. There were also subtle differences in the interaction of PPP2R2A and PPP2R5E although these did not reach statistical significance. Many additional studies will be needed to determine the effects of the interaction disruption, however previous studies have shown that these particular interactions are crucial for cellular transformation. The experiments I performed in Chapter 6 only indicate changes in B subunit interactions with the PPP2R1A mutant. At this point in time I can only speculate on how these changes can affect tumourigenesis, although, literature suggests that both PPP2R5C and PPP2R5D play important roles in cancer [82, 131]. In 2011, Ruediger *et al.,* performed an elegant knockout and knockin mouse model study [283] to determine the effects of a low frequency *PPP2R1A* E64G/D mutation previously found in one breast and one lung carcinoma [130]. The authors show that mutant heterozygous mice have an increased incidence of lung tumours, and there was a partial reduction of B' holoenzymes. These results suggest that the reduction of B' holoenzymes leads to increased cancer incidence, and PP2A acts as haploinsufficient tumour suppressor in this mouse model. Surprisingly, the mouse model with both altered *PPP2R1A* alleles (Δ5-6/E64D) was viable, even with no expression of wild-type PPP2R1A, and gave rise to mice presenting with multiple tumours [283]. This also provides

support for the viability of the mutant only expressing PPP2R1A L257 Hec1A cell lines I generated for this thesis research presented in Chapter 5 and 6.

It is interesting to note that in a normal cell PPP2R5C-induces dephosphorylation of p53 Thr55, and this is important to inhibit p53 degradation and promotes its tumour suppressor function. TP53 is considered a gatekeeper of the cell to inhibit tumour formation, however if PPP2R5C is deregulated and cannot efficiently dephosphorylate p53, this may promote p53 degradation to promote tumourigenesis. There is evidence to suggest that the PP2A-PPP2R5C complex and TP53 could be working together to suppress tumour promotion, therefore when one protein or the other is de-regulated this could lead to tumour progression. In light of this, I also hypothesize that when both p53 and PPP2R1A are mutated, for example in the specific case of endometrial serous and some high-grade endometrioid carcinomas, the tumour cells have evolved an extra mechanism to suppress both PP2A and TP53 tumour suppressor function. This may contribute to the level of aggressiveness to aid tumour cell growth and survival.

There has been limited evidence to support the role of PPP2R5D in cancer, however recent evidence suggests that a PPP2R5D substrate, *HAND2*, is frequently hypermethylated in endometrial cancer. The study also found that *PPP2R5D* is frequently hypermethylated in these endometrial endometrioid tumours [269]. The downregulation of both PPP2R5D and HAND2 proteins by epigenetic regulation may lead to endometrial tumourigenesis. This study did not investigate the epigenetic regulation of the aggressive serous carcinomas, however, it is possible that PPP2R1A mutations causing disruption in the interaction of PPP2R5D may also function similarly to DNA hypermethylation to cause downregulation of gene expression.

The discovery of the PPP2R1A mutation allowing for increased interaction with the PP2A inhibitor SET is interesting and novel. This is the first report to my knowledge, which describes this phenomenon of the ability of SET to interact with mutant PPP2R1A. However, as mentioned in the discussion of Chapter 6, SET is reported to interact with the catalytic subunit and not the A regulatory subunit [127, 271]. This could indicate that SET interacts with the A-C core protein complex, without B subunits present due to the inability to interact efficiently with the mutant A subunit. Thus, the ability to immunoprecipitate SET with PPP2R1A was due to the PPP2CA/B

interaction. A second possibility is that the B subunits may loosely interact with the A-C complex, which can allow SET to interact with the C subunit. This may be reflected in the observation that B subunit interaction was not completely abolished by the presence of the mutation, likely attributing to the need for some PP2A protein function in the tumour. Future studies would be needed to determine this exact mechanism.

Targeting endogenous PP2A inhibitors, like SET, have been recently described to be effective in cancers with SET overexpression [128, 284]. These new exogenous SET inhibitors have been found to be effective in breast, prostate, CML, and CLL cancers, which has resulted in a plethora of recent publications [128, 129, 272, 284-286]. This may indicate new significance for targeting this protein for novel therapeutics, and may provide an alternative way to target endometrial tumours with PPP2R1A mutations to increase PP2A tumour suppressor activity.

7.2 Limitations of Study Designs

The genomic studies completed in Chapters 2, 3 and 4 were limited by targeted gene sequencing experiments without the use of whole genome or exome sequencing. However, full exon sequencing of *PPP2R1A* in Chapter 3 did not result in the discovery of additional hotspot mutations outside of exon 5 and 6. In Chapter 3, I was able to show that endometrial carcinomas can be classified on the basis of mutational profile, however this does not improve clinical practice or have any benefit to the patients. This work was a stepping-stone for additional molecular studies to dive deeper into endometrial molecular classifications that may stratify patients for predictive markers or targeted therapeutics. The important study by the endometrial TCGA group [42], allowed an improved subclassification of endometrial tumours, however the genomic techniques used to display these classifications are also limited by the ease of use in standard cancer care. The use of targeted gene panels in clinical diagnosis and care is still in early stages however will likely become standard practice in the future.

The functional proteomic studies of PPP2R1A mutations identified in gynaecological malignancies were also limited by the analysis of a single cell line with one PPP2R1A mutation. Unfortunately, the isolation of the isogenic cell lines and subsequent proteomics experiments were time consuming, which limited the proteomics analysis of different PPP2R1A mutations.

Although, I was only able to provide evidence that one PPP2R1A mutation causes disruption of a few B subunit interactions, I can only speculate that the lack of these particular B subunits interacting with PPP2R1A can cause tumourigenesis. However, literature evidence suggests a very strong link. The use of additional cell line models will be needed to validate these results, and determine if other hotspot mutations cause similar disruptions.

The use of the Hec1A MMR deficient cell line was a limitation for using the somatic cell knockout technique. This technique had previously been validated to work well in cell lines with MMR (ref), however it was uncertain when I started these experiments if other cell lines could be utilized. Therefore the Hec1A cells with the endogenous hotspot PPP2R1A W257L mutation seemed like the most reasonable cell line to start assessing a specific PPP2R1A endogenous mutation. As discussed throughout Chapter 5 and 6, the cell and disease context of the cell line models should be taken into consideration. The Hec1A cells originated from a primary endometrial endometrioid cancer with MMR deficiency and a hyper-mutator phenotype. *PPP2R1A* mutations are found in all subtypes of endometrial tumours, however most frequently in endometrial serous carcinomas as identified in Chapter 2 and 3. Of course, the ideal model for assessing PPP2R1A mutations would be in the context of endometrial serous carcinoma, however cell lines originating from primary endometrial serous tumours are not easily obtained. Through our laboratory's in-house practice of establishing new cell lines from endometrial and ovarian primary tissue, we have been unsuccessful with establishing an endometrial serous cell line. I have now obtained a cell line, SPAC-1-L originating from Japan [287] that is a reported to have originated from a primary endometrial serous adenocarcinoma, however this cell line did not harbor a *PPP2R1A* mutation as assessed by Sanger sequencing (data not shown). In the future, researchers and future graduate students in our laboratory could use the CRISPR technique to introduce different PPP2R1A mutations into different endometrial and ovarian cell lines. These will be important future experiments as mutations could be assessed in a stable (non mutator phenotype) background, and a wild-type comparison is already available as the parental cell line. The SPAC-1-L cell line, targeted with CRISPR to make PPP2R1A isogenic cell lines, would be a superior context-specific disease model to assess how the hotspot PPP2R1A mutations affect PP2A binding and substrate dephosphorylation, compared to the current Hec1A isogenic model. Furthermore there are a few endometrial and ovarian cell lines; Hec50

(endometrial endometrioid cell line with a homozygous R183W), RMG2 (ovarian clear cell carcinoma, heterozygous R183W) that harbor *PPP2R1A* mutations that could be targeted with CRISPR to generate additional model cell lines for these diseases. These new genomic engineering approaches and use of different cell lines to assess the function of PPP2R1A mutations in gynaecological cancers pose a new set of experimental challenges and limitations.

7.3 Challenges in Studying Protein Complexes

A phosphatase review in 2009 stated that a major challenge for the future would be to find ways to identify the complex phosphatase network. The traditional approach for identifying a phospho-protein and its phosphatase is slow, incomplete and often relies heavily on serendipity [288]. The majority of cellular signaling through phosphorylation acts on serine/threonine residues, of which involves about 428 Ser/Thr kinase genes, and only about 40 phosphatase genes, a disproportion that is perhaps staggering [289]. The difference in the number of genes for kinases compared to phosphatases, underscores the complexity of how phosphatases use a low number of proteins to build multi-protein complexes for specific processes. The complex nature of PP2A emphasizes this point, and has been the source of major challenges throughout this thesis work to identify how *PPP2R1A* mutations identified in endometrial cancers affects the PP2A composition and thus phosphorylation levels of cellular proteins. The complexity of PP2A does not lie solely in the formation of the heterotrimeric holoenzyme with the A/B/C complexes, but also in the ability of the A and C subunits to bind to multiple other proteins. This adds another layer of finite phosphatase regulation. These noncanonical PP2A complexes involve binding of the C subunit to α4 (IGBP1), PTPA, PME1, which are competing with the A subunit to bind and activate the catalytic subunit [290]. PP2A composition is still widely unknown in different cell types, and yeast studies to understand the stoichiometry have provided conflicting results [291, 292].

The increased use and advances in proteomic technology, especially with the use of Orbitrap technology, will provide large–scale global phospho-protein and protein interaction analysis. The use of AP-MS (affinity purification-mass spectrometry), which is essentially IP-MS, have advanced the ability of proteomics to acquire high-throughput interaction data [293]. These techniques will enable application to *in vitro* cell models, and importantly, directly from tumours

and other human disease tissue. Large-scale PP2A interaction studies have been performed *in vitro* and suggest that the PP2A interaction network is large [95]. A chemical cross-link study of PP2A interactions identified 176 interprotein and 570 intraprotein crosslinks linking PP2A complexes, giving additional evidence to the complexity of the PP2A network [257].

7.4 Future Directions

7.4.1 Classification of Endometrial Carcinomas

Many studies have shown that the classifications of endometrial carcinomas are in need of a major overhaul. The morphological heterogeneity of the tumours can cause misclassification and irreproducibility in diagnosis [23, 53, 54]. My study along with the TCGA study used molecular markers to try to define and classify endometrial tumours, however there is still much work to be completed. The intermediate, high-risk groups of tumours are very heterogeneous and should be classified with clinical markers to aid in diagnosis and clinical management. The use of *POLE* mutations for future endometrial classification could be profoundly useful, as many of these tumours with *POLE* mutations tend to be high-grade endometrioid cases (Table E.8 (Appendix E). The patients with these types of tumours are often thought to do just as poorly as serous carcinomas, however these women tend to have near absolute favorable outcomes [42, 57]. These studies could indicate *POLE* as a prognostic marker for good outcome in a heterogeneous population of endometrial tumours. TCGA has also used copy number as a classification scheme for endometrial cancers, however this type of analysis is very expensive and needs technical expertise. In a clinical pathology setting, it is unlikely that this type of analysis can be performed on a day-to-day basis; therefore a different method or marker would need to be utilized as a surrogate for copy number changes. These types of research are currently underway in our laboratory and others. Lastly, the integration of histological, molecular, and clinical features of endometrial carcinomas has been proposed to improve the future classifications of endometrial cancers [282].

7.4.2 PP2A Aberrations in Gynaecological and Breast Carcinomas

The copy number high (serous-like) endometrial TCGA cBioPortal data suggests most of the PP2A B subunits are not frequently mutated, however *PPP2R2A* homozygous deletion occurs in

about 10% of copy-number high (serous-like) cases, with a trend towards mutual exclusivity with other B subunits (Figure 7.1) [32, 33]. In Chapter 6, there was a trend towards loss of PPP2R2A interaction with the W257L mutation, however this was not statistically significant in this assay. This phosphatase complex could be a very important part of endometrial serous carcinoma tumour biology, and it could be possible that other *PPP2R1A* mutations could cause significant disruption of PPP2R2A interaction. This would be very interesting, as it would mean that PPP2R1A mutations and deletion of the PPP2R2A could be assisting in driving aggressive endometrial tumours. Although other B-subunit aberrations are not present in the TCGA data, there is the possibility of epigenetic regulation or post-translational modifications. Therefore further work should be performed to determine the validity of this observation, which could potentially be assessed in the cohort of 89 endometrial serous carcinomas where the mutational status is known for *PPP2R1A* and *FBXW7* (Chapter3, Figure 3.3). It would also be interesting to determine if *PPP2R2A* deletion is responsible for causing stability of c-Myc in this tissue type. In previous studies, PPP2R5A was responsible for the activation of GSK3β, which de-phosphorylates the S9 residue to allow phosphorylation of c-Myc and ultimately c-Myc degradation [121]. This could be explained by the importance of cell-type context for specific B subunit function, however one study has shown that the deletion of PPP2R2A is not involved in affecting c-Myc levels as assessed by an RNAi screen [121]. Conversely, another study has shown evidence that PPP2R5D is responsible for dephosphorylating GSK3β-S9 which subsequently can phosphorylate c-Myc to cause degradation [190]. Knockdown of PPP2R5D resulted in the accumulation of c-Myc. However, in my study of *PPP2R1A* mutations with c-Myc IHC in Chapter 3, this did not show any significant association of *PPP2R1A* mutations with up-regulated c-Myc protein expression. It is possible that not all PPP2R1A mutations cause disruption of PPP2R2A or PPP2R5D equally, which could explain the lack of association of *PPP2R1A* mutations with high c-Myc expression.

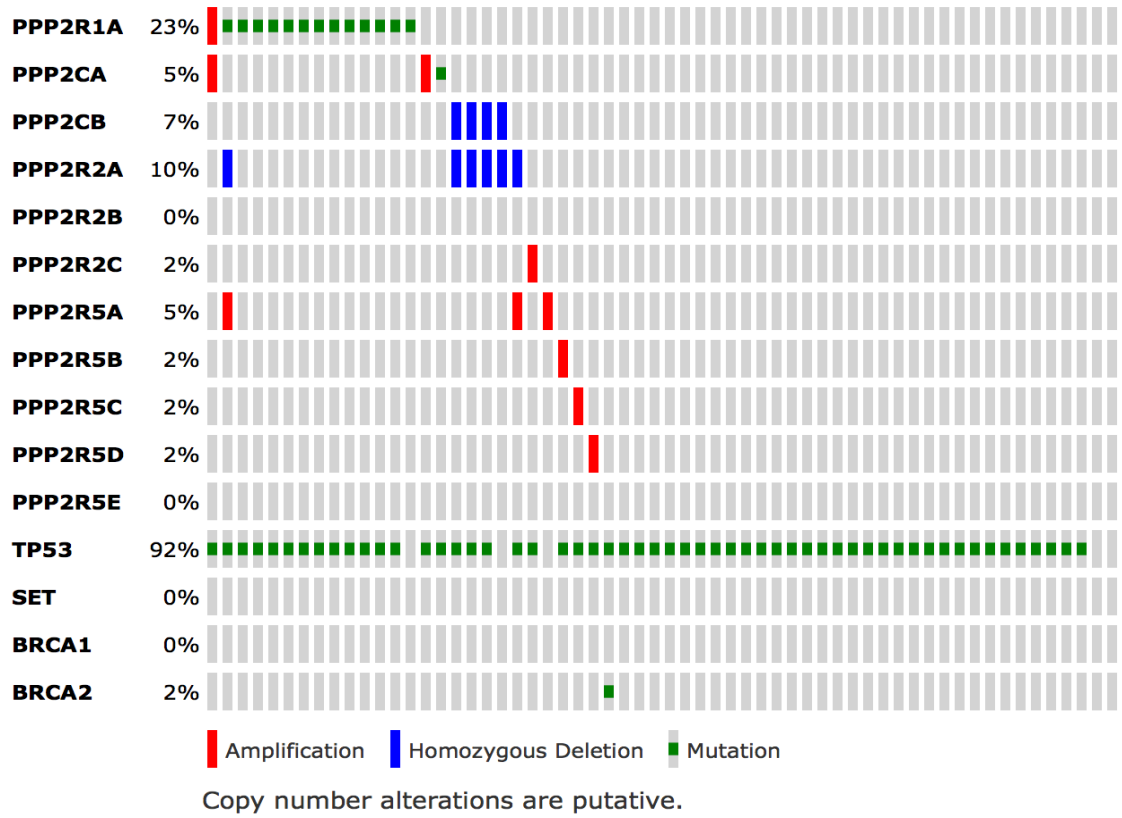

Figure 7.1 TCGA endometrial copy number high (serous-like) group (n=60)
The cBioPortal TCGA OncoPrint shows each column indicates an individual patient. Coloured lines indicate a DNA aberration. The grey bars indicate no DNA aberration identified.

Analysis of the TCGA ovarian serous carcinoma data set (n=316), *PPP2R1A* alterations (including CNA amplification, deletions, mutations) are rare (3%), but are mutually exclusive to 5% of *PPP2R2A* alterations (mostly consisting of homozygous deletions, and the rare amplification and mutation) (Figure 7.2). Other PP2A regulatory B subunits are also altered in this disease including: 4% CNA amplifications and mutations in *PPP2R3A*, 2% *PPP2R2C*, 3% *PPP2R5C*, 5% *PPP2R5D*, and 2% deletions in *PPP2R5E* (Figure 7.2). There is a trend towards mutual exclusivity, however the numbers of cases that are altered are small. Interestingly, these genomic aberrations also show a trend towards mutually exclusivity with 12% of *BRCA1* and *BRCA2* alterations. Endometrial serous and ovarian serous carcinomas harbor different altered genetic profiles, however histological similarities warrant investigation of PP2A alterations in this cancer type. It has also been established that about 4-7% of ovarian clear carcinoma and 12% of ovarian endometrioid carcinomas harbor PPP2R1A mutations [1, 2, 70].

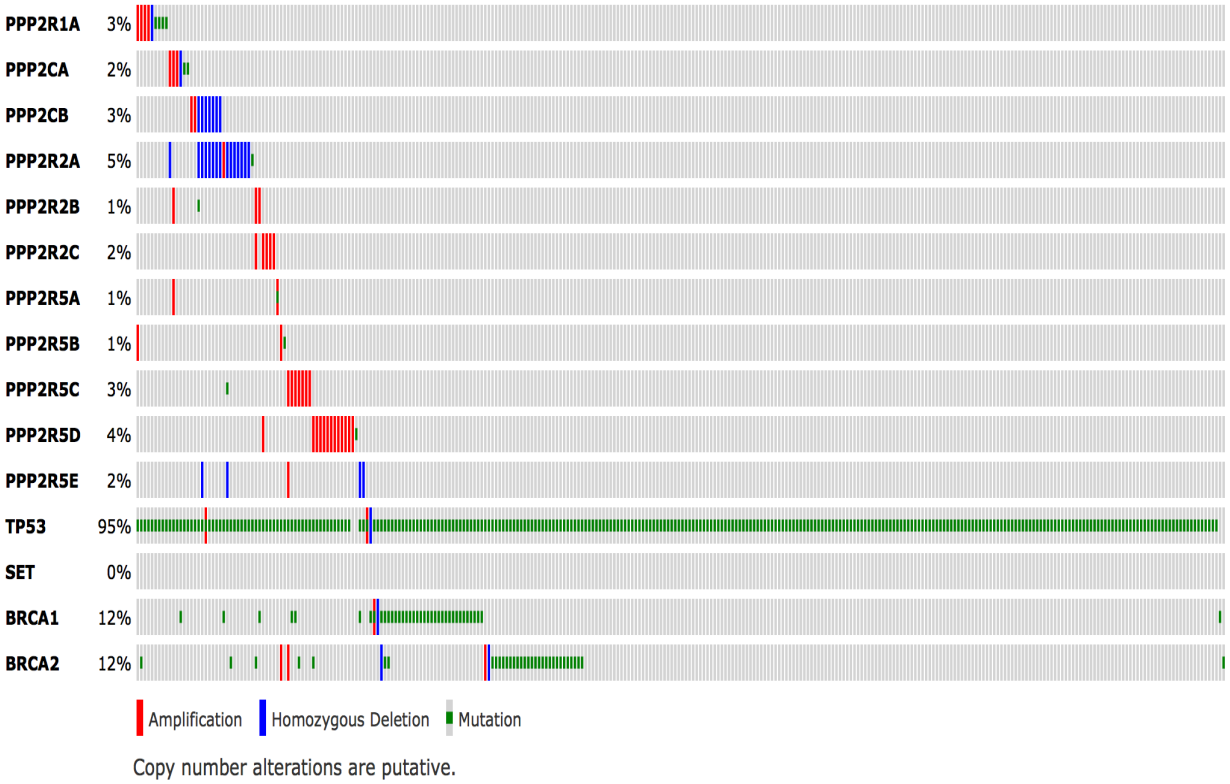

Figure 7.2 TCGA ovarian serous carcinoma (n=316)
The cBioPortal TCGA OncoPrint shows each column indicates an individual patient. Coloured lines indicate a DNA aberration. The grey bars indicate no DNA aberration identified.

Additionally, the cBioPortal TCGA breast data (n=466) also shows the same trend of mutual exclusivity between 2% *PPP2R1A* and 2% *PPP2R2A* alterations (Figure 7.3). The difference lies in that *PPP2R1A* is not mutated but putatively amplified. Additional evidence that PP2A alterations may play an important role in breast carcinomas is the discovery of ER-positive Luminal B-type breast cancers with PPP2R2A deletions [294]. The investigation of these deletions and how this plays are role in substrate dephosphorylation in the cancer cell is needed.

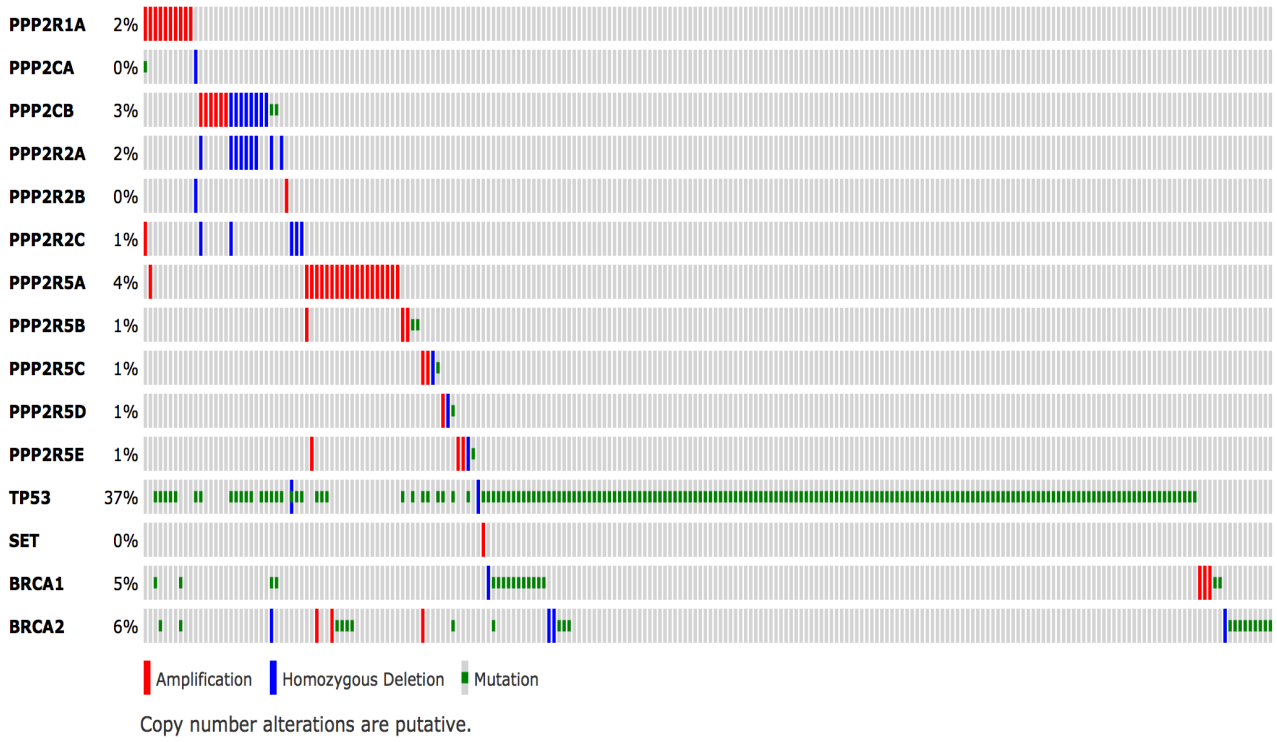

Figure 7.3 TCGA breast carcinomas (all subtypes n=466)
The cBioPortal TCGA OncoPrint shows each column indicates an individual patient.
Coloured lines indicate a DNA aberration. The grey bars indicate no DNA aberration identified.

From the TCGA ovarian serous and all breast subtype mutation profiles, there appears to be a trend towards mutual exclusivity of *BRCA1* and *BRCA2* mutations and PP2A subunit aberrations. *BRCA1* and *BRCA2* are important genes for homologous recombination, and the TCGA ovarian data suggests that 50% of all ovarian serous carcinomas have defects in the homologous recombination pathway [44]. I can speculate that the mutual exclusive pattern of BRCA1/2 mutations with PP2A genes may indicate that PP2A genes are also affecting double strand break repair via homologous recombination. Kalev *et al*., has reported on the PP2A genes PPP2R2A, PPP2R2D, PPP2R5A and PPP2R3C involvement in double strand break repair mechanisms. Loss of function of these genes inhibited homologous recombination by increasing phosphorylation levels of ATM, thus sensitizing cells to PARP inhibition [295]. Additional analysis of the TCGA ovarian data also found that a recurrently mutated tumour suppressor gene, *CDK12* (9 of 316 (3%) of tumours) [44], trended towards mutually exclusivity (7 of 9 tumours) with *BRCA1* and *BRCA2* mutations [296]. Similar to PP2A B subunits loss of function,

knockdown of CDK12 lead to suppression of DNA repair mechanisms via homologous recombination, reduced expression of BRCA1, and also sensitized cells to PARP inhibition [296]. Future studies of the effect of PP2A alterations on DNA repair by homologous recombination in gyneacological and breast carcinomas are needed to define the relationship of these proteins. It is possible that these proteins together or separate are biomarkers for patients that may benefit from PARP inhibitors.

7.4.3 Proteomic Studies of Endometrial Cancer Patient Samples

The proteomics finding that PPP2R1A mutations causes disruption of B subunit interactions implies that the specific dephosphorylation events induced by these specific PP2A holoenzyme complex will be decreased. Additional studies of the Hec1A isogenic cell lines could be used as a model to discover the differences in phosphorylation events caused by the PPP2R1A mutation. These studies could potentially lead to alternative deregulated pathways that may be targeted by novel therapeutics. Additional MS experiments using total IP-MS and PRM for specific PP2A interacting proteins would be useful in additional gynaecological cell lines and patient samples. The integration of proteomics analysis in endometrial tumour patient samples would provide insight into the effect of PPP2R1A mutations on the PP2A complex in human tumours. However, the tools for these types of proteomics studies are slowly catching up with the field of genomics to enable proteomics profiling of patient tumours. The first draft of the human proteome was only published in May 2014 [297], which is more than 10 years behind the release of the first human genome. The integration of clinical, genomics and proteomics will be an exciting new field for cancer research.

7.4.4 Novel Therapeutic Options for Targeting PP2A Altered Cancers

Endometrial serous carcinomas are characterized almost exclusively with mutations in the tumour suppressor *TP53*, and a subset of these with *PPP2R1A* mutations. Since *TP53* is also frequently mutated in many other types of cancers, there have been concentrated efforts to target p53 with novel therapeutics. Earlier studies have shown that restoring p53 alone is sufficient to cause regression of lymphomas, sarcomas, and liver carcinomas in mouse models [235, 298]. Therefore restoring the function of p53 could be an attractive therapeutic strategy for many tumours. Viruses, small molecule inhibitors, and protein chaperones are now being used in

clinical trials in an attempt to restore the wild-type function of p53 in tumour cells [299]. A novel potential synthetic lethal approach for targeting endometrial and perhaps ovarian serous carcinoma, includes therapeutics to restore wild-type p53 and wild-type PPP2R1A or B subunits to restore the function of PP2A. The inhibition of PP2A can kill cancerous cells, however since this is an essential gene, inhibition would also kill normal cells. Overexpression of wild-type PPP2R1A has been shown to decrease cell proliferation and tumour growth [131]. In addition, multiple PP2A inhibitors (okadaic acid, calyculin A) are potent tumour promoters, and viruses that bind to PP2A to increase cellular transformation [300]. From my own experiments in Chapter 5, I have also shown that my attempts of isolating Hec1A isogenic cell lines with one copy of wild-type PPP2R1A were unsuccessful. This was likely due to slow growth with no growth advantage; therefore the wild-type cells are not selected. A synthetic lethal approach to target two major tumour suppressor genes by restoring wild-type function could be an "out of the box" solution for targeting the tumour cells and leaving the normal cells alone. This would essentially restore the function of p53 and PP2A to bring the tumour cells back to a "normal" like state, which would not allow abnormal growth and proliferation.

Currently, there is a FDA approved drug for use in multiple sclerosis, FTY720, a sphingosine analogue drug that is an activator of PP2A [300], and has shown to be well tolerated in humans [301, 302]. This drug demonstrates an antitumour effect in leukemia and mouse xenographs with no toxicity [303]. Studies also suggest that prostate cancer cells are more sensitive to the drug than normal stromal cells [304]. It is interesting to note that FTY720 acts to bind and target the PP2A inhibitor SET, to induce reactivation of PP2A [284]. The use of an additional SET peptide inhibitor (OP449) significantly reduces proliferation and cell survival signaling [128, 129]. OP449 acts to antagonize SET inhibition of PP2A, and has been reported to be efficacious *in vitro* and *in vivo* in chronic myeloid leukemia (CML) and acute myeloid leukemia (AML) when used in combination with tyrosine kinase inhibitors [286]. Furthermore, the mass spectrometry results, presented in Chapter 6, illustrate an increased affinity of the PPP2R1A L257 mutation with the PP2A inhibitor SET. It would be useful to test the efficacy of these drugs on endometrial cell lines and patient derived mouse xenographs with known PP2A aberrations (*PPP2R1A* mutations or *PPP2R2A* deletions), to determine if this could be a useful targeted

therapy. In conclusion, future studies of targeting SET to reactivate PP2A could provide an additional way to treat PP2A disrupted cancers for novel therapeutics.

Bibliography

1. McConechy, M.K., Anglesio, M.S., Kalloger, S.E., Yang, W., Senz, J., Chow, C., Heravi-Moussavi, A., Morin, G.B., Mes-Masson, A.M., Carey, M.S., et al. (2011). Subtype-specific mutation of PPP2R1A in endometrial and ovarian carcinomas. The Journal of pathology *223*, 567-573.
2. McConechy, M.K., Ding, J., Cheang, M.C., Wiegand, K.C., Senz, J., Tone, A.A., Yang, W., Prentice, L.M., Tse, K., Zeng, T., et al. (2012). Use of mutation profiles to refine the classification of endometrial carcinomas. The Journal of pathology *228*, 20-30.
3. McConechy, M.K., Ding, J., Senz, J., Yang, W., Melnyk, N., Tone, A.A., Prentice, L.M., Wiegand, K.C., McAlpine, J.N., Shah, S.P., et al. (2014). Ovarian and endometrial endometrioid carcinomas have distinct CTNNB1 and PTEN mutation profiles. Modern Pathol *27*, 128-134.
4. Jemal, A., Bray, F., Center, M.M., Ferlay, J., Ward, E., and Forman, D. (2011). Global cancer statistics. CA Cancer J Clin *61*, 69-90.
5. Ferlay, J., Shin, H.R., Bray, F., Forman, D., Mathers, C., and Parkin, D.M. (2010). GLOBOCAN 2008 v1.2, Cancer Incidence and Mortality Worldwide: IARC CancerBase No. 10 Lyon, France, http://globocan.iarc.fr. In International Agency for Research on Cancer.
6. Evans, T., Sany, O., Pearmain, P., Ganesan, R., Blann, A., and Sundar, S. (2011). Differential trends in the rising incidence of endometrial cancer by type: data from a UK population-based registry from 1994 to 2006. Br J Cancer *104*, 1505-1510.
7. Okuda, T., Sekizawa, A., Purwosunu, Y., Nagatsuka, M., Morioka, M., Hayashi, M., and Okai, T. (2010). Genetics of endometrial cancers. Obstet Gynecol Int *2010*, 984013.
8. Bokhman, J.V. (1983). Two pathogenetic types of endometrial carcinoma. Gynecol Oncol *15*, 10-17.
9. Eltabbakh, G.H., Piver, M.S., Hempling, R.E., and Shin, K.H. (1997). Excellent long-term survival and absence of vaginal recurrences in 332 patients with low-risk stage I endometrial adenocarcinoma treated with hysterectomy and vaginal brachytherapy without formal staging lymph node sampling: report of a prospective trial. International journal of radiation oncology, biology, physics *38*, 373-380.
10. Hamilton, C.A., Cheung, M.K., Osann, K., Chen, L., Teng, N.N., Longacre, T.A., Powell, M.A., Hendrickson, M.R., Kapp, D.S., and Chan, J.K. (2006). Uterine papillary serous and clear cell carcinomas predict for poorer survival compared to grade 3 endometrioid corpus cancers. Br J Cancer *94*, 642-646.
11. Hendrickson, M., Ross, J., Eifel, P., Martinez, A., and Kempson, R. (1982). Uterine papillary serous carcinoma: a highly malignant form of endometrial adenocarcinoma. Am J Surg Pathol *6*, 93-108.
12. Chan, J.K., Loizzi, V., Youssef, M., Osann, K., Rutgers, J., Vasilev, S.A., and Berman, M.L. (2003). Significance of comprehensive surgical staging in noninvasive papillary serous carcinoma of the endometrium. Gynecol Oncol *90*, 181-185.
13. Goff, B.A., Kato, D., Schmidt, R.A., Ek, M., Ferry, J.A., Muntz, H.G., Cain, J.M., Tamimi, H.K., Figge, D.C., and Greer, B.E. (1994). Uterine papillary serous carcinoma: patterns of metastatic spread. Gynecol Oncol *54*, 264-268.

14. Kato, D.T., Ferry, J.A., Goodman, A., Sullinger, J., Scully, R.E., Goff, B.A., Fuller, A.F., Jr., and Rice, L.W. (1995). Uterine papillary serous carcinoma (UPSC): a clinicopathologic study of 30 cases. Gynecol Oncol *59*, 384-389.
15. Slomovitz, B.M., Burke, T.W., Eifel, P.J., Ramondetta, L.M., Silva, E.G., Jhingran, A., Oh, J.C., Atkinson, E.N., Broaddus, R.R., Gershenson, D.M., et al. (2003). Uterine papillary serous carcinoma (UPSC): a single institution review of 129 cases. Gynecol Oncol *91*, 463-469.
16. Jonson, A.L., Bliss, R.L., Truskinovsky, A., Judson, P., Argenta, P., Carson, L., Dusenbery, K., and Downs, L.S., Jr. (2006). Clinical features and outcomes of uterine and ovarian carcinosarcoma. Gynecol Oncol *100*, 561-564.
17. Hoskins, P.J., Swenerton, K.D., Pike, J.A., Wong, F., Lim, P., Acquino-Parsons, C., and Lee, N. (2001). Paclitaxel and carboplatin, alone or with irradiation, in advanced or recurrent endometrial cancer: a phase II study. Journal of clinical oncology : official journal of the American Society of Clinical Oncology *19*, 4048-4053.
18. Carey, M.S., Gawlik, C., Fung-Kee-Fung, M., Chambers, A., Oliver, T., and Cancer Care Ontario Practice Guidelines Initiative Gynecology Cancer Disease Site, G. (2006). Systematic review of systemic therapy for advanced or recurrent endometrial cancer. Gynecol Oncol *101*, 158-167.
19. Widmaier, E.P., Raff, H., Strang, K.T., and Vander, A.J. (2014). Vander's human physiology : the mechanisms of body function, Thirteenth edition / Edition, (New York: McGraw-Hill).
20. Kurman, R.J., International Agency for Research on Cancer., and World Health Organization. (2014). WHO classification of tumours of female reproductive organs, 4th Edition, (Lyon: International Agency for Research on Cancer).
21. Benedet, J.L., Bender, H., Jones, H., 3rd, Ngan, H.Y., and Pecorelli, S. (2000). FIGO staging classifications and clinical practice guidelines in the management of gynecologic cancers. FIGO Committee on Gynecologic Oncology. International journal of gynaecology and obstetrics: the official organ of the International Federation of Gynaecology and Obstetrics *70*, 209-262.
22. Darvishian, F., Hummer, A.J., Thaler, H.T., Bhargava, R., Linkov, I., Asher, M., and Soslow, R.A. (2004). Serous endometrial cancers that mimic endometrioid adenocarcinomas: a clinicopathologic and immunohistochemical study of a group of problematic cases. Am J Surg Pathol *28*, 1568-1578.
23. Alkushi, A., Kobel, M., Kalloger, S.E., and Gilks, C.B. (2010). High-grade endometrial carcinoma: serous and grade 3 endometrioid carcinomas have different immunophenotypes and outcomes. Int J Gynecol Pathol *29*, 343-350.
24. Norris, H.J., and Taylor, H.B. (1966). Mesenchymal tumors of the uterus. 3. A clinical and pathologic study of 31 carcinosarcomas. Cancer *19*, 1459-1465.
25. McCluggage, W.G. (2002). Uterine carcinosarcomas (malignant mixed Mullerian tumors) are metaplastic carcinomas. Int J Gynecol Cancer *12*, 687-690.
26. Risinger, J.I., Berchuck, A., Kohler, M.F., Watson, P., Lynch, H.T., and Boyd, J. (1993). Genetic instability of microsatellites in endometrial carcinoma. Cancer research *53*, 5100-5103.
27. Cheung, L.W., Hennessy, B.T., Li, J., Yu, S., Myers, A.P., Djordjevic, B., Lu, Y., Stemke-Hale, K., Zhang, F., Ju, Z., et al. (2011). High Frequency of PIK3R1 and PIK3R2

Mutations in Endometrial Cancer Elucidates a Novel Mechanism for Regulation of PTEN Protein Stability. Cancer discovery *1*, 170-185.
28. Urick, M.E., Rudd, M.L., Godwin, A.K., Sgroi, D., Merino, M., and Bell, D.W. (2011). PIK3R1 (p85{alpha}) Is Somatically Mutated at High Frequency in Primary Endometrial Cancer. Cancer research *71*, 4061-4067.
29. O'Hara, A.J., and Bell, D.W. (2012). The genomics and genetics of endometrial cancer. Advances in Genomics and Genetics *2*, 33-47.
30. Byron, S.A., Gartside, M., Powell, M.A., Wellens, C.L., Gao, F., Mutch, D.G., Goodfellow, P.J., and Pollock, P.M. (2012). *FGFR2* Point Mutations in 466 Endometrioid Endometrial Tumors: Relationship with MSI, *KRAS*, *PIK3CA, CTNNB*1 Mutations and Clinicopathological Features. PloS one *7*, e30801.
31. Sun, H., Enomoto, T., Fujita, M., Wada, H., Yoshino, K., Ozaki, K., Nakamura, T., and Murata, Y. (2001). Mutational analysis of the PTEN gene in endometrial carcinoma and hyperplasia. Am J Clin Pathol *115*, 32-38.
32. Cerami, E., Gao, J., Dogrusoz, U., Gross, B.E., Sumer, S.O., Aksoy, B.A., Jacobsen, A., Byrne, C.J., Heuer, M.L., Larsson, E., et al. (2012). The cBio Cancer Genomics Portal: An Open Platform for Exploring Multidimensional Cancer Genomics Data. Cancer discovery *2*, 401-404.
33. Gao, J., Aksoy, B.A., Dogrusoz, U., Dresdner, G., Gross, B., Sumer, S.O., Sun, Y., Jacobsen, A., Sinha, R., Larsson, E., et al. (2013). Integrative Analysis of Complex Cancer Genomics and Clinical Profiles Using the cBioPortal. Science Signaling *6*, pl1-pl1.
34. Guan, B., Mao, T.L., Panuganti, P.K., Kuhn, E., Kurman, R.J., Maeda, D., Chen, E., Jeng, Y.M., Wang, T.L., and Shih Ie, M. (2011). Mutation and loss of expression of ARID1A in uterine low-grade endometrioid carcinoma. Am J Surg Pathol *35*, 625-632.
35. Wiegand, K.C., Lee, A.F., Al-Agha, O.M., Chow, C., Kalloger, S.E., Scott, D.W., Steidl, C., Wiseman, S.M., Gascoyne, R.D., Gilks, B., et al. (2011). Loss of BAF250a (ARID1A) is frequent in high-grade endometrial carcinomas. The Journal of pathology *224*, 328-333.
36. Hampel, H., Frankel, W., Panescu, J., Lockman, J., Sotamaa, K., Fix, D., Comeras, I., La Jeunesse, J., Nakagawa, H., Westman, J.A., et al. (2006). Screening for Lynch syndrome (hereditary nonpolyposis colorectal cancer) among endometrial cancer patients. Cancer research *66*, 7810-7817.
37. Lynch, H.T., Lynch, P.M., and Harris, R.E. (1978). Minimal genetic findings and their cancer control implications. A family with the cancer family syndrome. Jama *240*, 535-538.
38. Schmeler, K.M., Lynch, H.T., Chen, L.-m., Munsell, M.F., Soliman, P.T., Clark, M.B., Daniels, M.S., White, K.G., Boyd-Rogers, S.G., Conrad, P.G., et al. (2006). Prophylactic Surgery to Reduce the Risk of Gynecologic Cancers in the Lynch Syndrome. New England Journal of Medicine *354*, 261-269.
39. Geurts-Giele, W.R., Leenen, C.H., Dubbink, H.J., Meijssen, I.C., Post, E., Sleddens, H.F., Kuipers, E.J., Goverde, A., van den Ouweland, A.M., van Lier, M.G., et al. (2014). Somatic aberrations of mismatch repair genes as a cause of microsatellite-unstable cancers. J Pathol.

40. Lax, S.F., Kendall, B., Tashiro, H., Slebos, R.J., and Hedrick, L. (2000). The frequency of p53, K-ras mutations, and microsatellite instability differs in uterine endometrioid and serous carcinoma: evidence of distinct molecular genetic pathways. Cancer *88*, 814-824.
41. Pradhan, M., Abeler, V.M., Danielsen, H.E., Trope, C.G., and Risberg, B.A. (2006). Image cytometry DNA ploidy correlates with histological subtypes in endometrial carcinomas. Mod Pathol *19*, 1227-1235.
42. Kandoth, C., Schultz, N., Cherniack, A.D., Akbani, R., Liu, Y., Shen, H., Robertson, A.G., Pashtan, I., Shen, R., Benz, C.C., et al. (2013). Integrated genomic characterization of endometrial carcinoma. Nature *497*, 67-73.
43. Gallo, M.L., O'Hara, A.J., Rudd, M.L., Urick, M.E., Hansen, N.F., O'Neil, N.J., Price, J.C., Zhang, S., England, B.M., Godwin, A.K., et al. (2012). Exome sequencing of serous endometrial tumors identifies recurrent somatic mutations in chromatin-remodeling and ubiquitin ligase complex genes. Nature genetics.
44. Cancer Genome Atlas Research, N. (2011). Integrated genomic analyses of ovarian carcinoma. Nature *474*, 609-615.
45. Cassia, R., Moreno-Bueno, G., Rodriguez-Perales, S., Hardisson, D., Cigudosa, J.C., and Palacios, J. (2003). Cyclin E gene (CCNE) amplification and hCDC4 mutations in endometrial carcinoma. J Pathol *201*, 589-595.
46. Kuhn, E., Wu, R.C., Guan, B., Wu, G., Zhang, J., Wang, Y., Song, L., Yuan, X., Wei, L., Roden, R.B., et al. (2012). Identification of Molecular Pathway Aberrations in Uterine Serous Carcinoma by Genome-wide Analyses. J Natl Cancer Inst.
47. Fadare, O., Gwin, K., Desouki, M.M., Crispens, M.A., Jones, H.W., 3rd, Khabele, D., Liang, S.X., Zheng, W., Mohammed, K., Hecht, J.L., et al. (2013). The clinicopathologic significance of p53 and BAF-250a (ARID1A) expression in clear cell carcinoma of the endometrium. Mod Pathol *26*, 1101-1110.
48. Kuo, K.T., Mao, T.L., Jones, S., Veras, E., Ayhan, A., Wang, T.L., Glas, R., Slamon, D., Velculescu, V.E., Kuman, R.J., et al. (2009). Frequent activating mutations of PIK3CA in ovarian clear cell carcinoma. The American journal of pathology *174*, 1597-1601.
49. Hoang, L.N., Han, G., McConechy, M., Lau, S., Chow, C., Gilks, C.B., Huntsman, D.G., Kobel, M., and Lee, C.H. (2013). Immunohistochemical characterization of prototypical endometrial clear cell carcinoma-diagnostic utility of HNF-1beta and oestrogen receptor. Histopathology.
50. Kobayashi, H., Uekuri, C., Akasaka, J., Ito, F., Shigemitsu, A., Koike, N., and Shigetomi, H. (2013). The biology of uterine sarcomas: A review and update. Molecular and clinical oncology *1*, 599-609.
51. Taylor, N.P., Zighelboim, I., Huettner, P.C., Powell, M.A., Gibb, R.K., Rader, J.S., Mutch, D.G., Edmonston, T.B., and Goodfellow, P.J. (2006). DNA mismatch repair and TP53 defects are early events in uterine carcinosarcoma tumorigenesis. Mod Pathol *19*, 1333-1338.
52. McConechy, M.K., Hoang, L.N., Chui, M.H., Senz, J., Yang, W., Rozenberg, N., Mackenzie, R., McAlpine, J.N., Huntsman, D.G., Clarke, B.A., et al. (2015). In-depth molecular profiling of the biphasic components of uterine carcinosarcomas. The Journal of Pathology: Clinical Research, n/a-n/a.
53. Clarke, B.A., and Gilks, C.B. (2010). Endometrial carcinoma: controversies in histopathological assessment of grade and tumour cell type. J Clin Pathol *63*, 410-415.

54. Gilks, C.B., Oliva, E., and Soslow, R. (2011). Poor Interobserver Reproducibility in the Diagnosis of High-Grade Endometrial Carcinoma. Modern Pathol *24*, 248A-248A.
55. Hoang, L.N., McConechy, M.K., Kobel, M., Han, G., Rouzbahman, M., Davidson, B., Irving, J., Ali, R.H., Leung, S., McAlpine, J.N., et al. (2013). Histotype-genotype correlation in 36 high-grade endometrial carcinomas. Am J Surg Pathol *37*, 1421-1432.
56. Billingsley, C.C., Cohn, D.E., Mutch, D.G., Stephens, J.A., Suarez, A.A., and Goodfellow, P.J. (2014). Polymerase varepsilon (POLE) mutations in endometrial cancer: Clinical outcomes and implications for Lynch syndrome testing. Cancer.
57. Meng, B., Hoang, L.N., McIntyre, J.B., Duggan, M.A., Nelson, G.S., Lee, C.H., and Kobel, M. (2014). POLE exonuclease domain mutation predicts long progression-free survival in grade 3 endometrioid carcinoma of the endometrium. Gynecol Oncol *134*, 15-19.
58. Church, D.N., Briggs, S.E., Palles, C., Domingo, E., Kearsey, S.J., Grimes, J.M., Gorman, M., Martin, L., Howarth, K.M., Hodgson, S.V., et al. (2013). DNA polymerase epsilon and delta exonuclease domain mutations in endometrial cancer. Human molecular genetics *22*, 2820-2828.
59. Kurman, R.J., and Shih Ie, M. (2010). The origin and pathogenesis of epithelial ovarian cancer: a proposed unifying theory. Am J Surg Pathol *34*, 433-443.
60. Kurman, R.J., and Shih Ie, M. (2011). Molecular pathogenesis and extraovarian origin of epithelial ovarian cancer--shifting the paradigm. Human pathology *42*, 918-931.
61. Lee, Y., Miron, A., Drapkin, R., Nucci, M.R., Medeiros, F., Saleemuddin, A., Garber, J., Birch, C., Mou, H., Gordon, R.W., et al. (2007). A candidate precursor to serous carcinoma that originates in the distal fallopian tube. J Pathol *211*, 26-35.
62. Crum, C.P., Drapkin, R., Kindelberger, D., Medeiros, F., Miron, A., and Lee, Y. (2007). Lessons from BRCA: the tubal fimbria emerges as an origin for pelvic serous cancer. Clinical medicine & research *5*, 35-44.
63. Ahmed, A.A., Etemadmoghadam, D., Temple, J., Lynch, A.G., Riad, M., Sharma, R., Stewart, C., Fereday, S., Caldas, C., Defazio, A., et al. (2010). Driver mutations in TP53 are ubiquitous in high grade serous carcinoma of the ovary. The Journal of pathology *221*, 49-56.
64. Miller, D.S., Blessing, J.A., Krasner, C.N., Mannel, R.S., Hanjani, P., Pearl, M.L., Waggoner, S.E., and Boardman, C.H. (2009). Phase II evaluation of pemetrexed in the treatment of recurrent or persistent platinum-resistant ovarian or primary peritoneal carcinoma: a study of the Gynecologic Oncology Group. Journal of clinical oncology : official journal of the American Society of Clinical Oncology *27*, 2686-2691.
65. Kobel, M., Kalloger, S.E., Huntsman, D.G., Santos, J.L., Swenerton, K.D., Seidman, J.D., Gilks, C.B., and Cheryl Brown Ovarian Cancer Outcomes Unit of the British Columbia Cancer Agency, V.B.C. (2010). Differences in tumor type in low-stage versus high-stage ovarian carcinomas. Int J Gynecol Pathol *29*, 203-211.
66. Kumar, A., Le, N., Tinker, A.V., Santos, J.L., Parsons, C., and Hoskins, P.J. (2014). Early-stage endometrioid ovarian carcinoma: population-based outcomes in British Columbia. Int J Gynecol Cancer *24*, 1401-1405.
67. Giudice, L.C. (2010). Endometriosis. New England Journal of Medicine *362*, 2389-2398.
68. Brescia, R.J., Dubin, N., and Demopoulos, R.I. (1989). Endometrioid and clear cell carcinoma of the ovary. Factors affecting survival. Int J Gynecol Pathol *8*, 132-138.

69. Kobel, M., Kalloger, S.E., Boyd, N., McKinney, S., Mehl, E., Palmer, C., Leung, S., Bowen, N.J., Ionescu, D.N., Rajput, A., et al. (2008). Ovarian carcinoma subtypes are different diseases: implications for biomarker studies. PLoS Med *5*, e232.
70. Jones, S., Wang, T.L., Shih Ie, M., Mao, T.L., Nakayama, K., Roden, R., Glas, R., Slamon, D., Diaz, L.A., Jr., Vogelstein, B., et al. (2010). Frequent mutations of chromatin remodeling gene ARID1A in ovarian clear cell carcinoma. Science *330*, 228-231.
71. Wiegand, K.C., Shah, S.P., Al-Agha, O.M., Zhao, Y., Tse, K., Zeng, T., Senz, J., McConechy, M.K., Anglesio, M.S., Kalloger, S.E., et al. (2010). ARID1A mutations in endometriosis-associated ovarian carcinomas. The New England journal of medicine *363*, 1532-1543.
72. Campbell, I.G., Russell, S.E., Choong, D.Y., Montgomery, K.G., Ciavarella, M.L., Hooi, C.S., Cristiano, B.E., Pearson, R.B., and Phillips, W.A. (2004). Mutation of the PIK3CA gene in ovarian and breast cancer. Cancer research *64*, 7678-7681.
73. Sato, N., Tsunoda, H., Nishida, M., Morishita, Y., Takimoto, Y., Kubo, T., and Noguchi, M. (2000). Loss of Heterozygosity on 10q23.3 and Mutation of the Tumor Suppressor Gene PTEN in Benign Endometrial Cyst of the Ovary: Possible Sequence Progression from Benign Endometrial Cyst to Endometrioid Carcinoma and Clear Cell Carcinoma of the Ovary. Cancer research *60*, 7052-7056.
74. Catasus, L., Bussaglia, E., Rodrguez, I., Gallardo, A., Pons, C., Irving, J.A., and Prat, J. (2004). Molecular genetic alterations in endometrioid carcinomas of the ovary: similar frequency of beta-catenin abnormalities but lower rate of microsatellite instability and PTEN alterations than in uterine endometrioid carcinomas. Human pathology *35*, 1360-1368.
75. Gamallo, C., Palacios, J., Moreno, G., Calvo de Mora, J., Suarez, A., and Armas, A. (1999). beta-catenin expression pattern in stage I and II ovarian carcinomas : relationship with beta-catenin gene mutations, clinicopathological features, and clinical outcome. The American journal of pathology *155*, 527-536.
76. Jiang, X., Morland, S.J., Hitchcock, A., Thomas, E.J., and Campbell, I.G. (1998). Allelotyping of endometriosis with adjacent ovarian carcinoma reveals evidence of a common lineage. Cancer research *58*, 1707-1712.
77. Bell, D.A. (2005). Origins and molecular pathology of ovarian cancer. Modern pathology : an official journal of the United States and Canadian Academy of Pathology, Inc *18 Suppl 2*, S19-32.
78. Stratton, J.F., Gayther, S.A., Russell, P., Dearden, J., Gore, M., Blake, P., Easton, D., and Ponder, B.A.J. (1997). Contribution of BRCA1 Mutations to Ovarian Cancer. New England Journal of Medicine *336*, 1125-1130.
79. Audeh, M.W., Carmichael, J., Penson, R.T., Friedlander, M., Powell, B., Bell-McGuinn, K.M., Scott, C., Weitzel, J.N., Oaknin, A., Loman, N., et al. (2010). Oral poly(ADP-ribose) polymerase inhibitor olaparib in patients with BRCA1 or BRCA2 mutations and recurrent ovarian cancer: a proof-of-concept trial. The Lancet *376*, 245-251.
80. Fong, P.C., Yap, T.A., Boss, D.S., Carden, C.P., Mergui-Roelvink, M., Gourley, C., De Greve, J., Lubinski, J., Shanley, S., Messiou, C., et al. (2010). Poly(ADP)-ribose polymerase inhibition: frequent durable responses in BRCA carrier ovarian cancer correlating with platinum-free interval. Journal of clinical oncology : official journal of the American Society of Clinical Oncology *28*, 2512-2519.

81. Bouwman, P., and Jonkers, J. (2012). The effects of deregulated DNA damage signalling on cancer chemotherapy response and resistance. Nat Rev Cancer *12*, 587-598.
82. Eichhorn, P.J., Creyghton, M.P., and Bernards, R. (2009). Protein phosphatase 2A regulatory subunits and cancer. Biochimica et biophysica acta *1795*, 1-15.
83. Zhou, J., Pham, H.T., and Walter, G. (2003). The formation and activity of PP2A holoenzymes do not depend on the isoform of the catalytic subunit. The Journal of biological chemistry *278*, 8617-8622.
84. Virshup, D.M. (2000). Protein phosphatase 2A: a panoply of enzymes. Current opinion in cell biology *12*, 180-185.
85. Hunter, T. (1995). Protein kinases and phosphatases: the yin and yang of protein phosphorylation and signaling. Cell *80*, 225-236.
86. Xu, Y., Xing, Y., Chen, Y., Chao, Y., Lin, Z., Fan, E., Yu, J.W., Strack, S., Jeffrey, P.D., and Shi, Y. (2006). Structure of the protein phosphatase 2A holoenzyme. Cell *127*, 1239-1251.
87. Hemmings, B.A., Adams-Pearson, C., Maurer, F., Muller, P., Goris, J., Merlevede, W., Hofsteenge, J., and Stone, S.R. (1990). alpha- and beta-forms of the 65-kDa subunit of protein phosphatase 2A have a similar 39 amino acid repeating structure. Biochemistry *29*, 3166-3173.
88. Ruediger, R., Van Wart Hood, J.E., Mumby, M., and Walter, G. (1991). Constant expression and activity of protein phosphatase 2A in synchronized cells. Molecular and cellular biology *11*, 4282-4285.
89. Arino, J., Woon, C.W., Brautigan, D.L., Miller, T.B., Jr., and Johnson, G.L. (1988). Human liver phosphatase 2A: cDNA and amino acid sequence of two catalytic subunit isotypes. Proc Natl Acad Sci U S A *85*, 4252-4256.
90. Ruediger, R., Pham, H.T., and Walter, G. (2001). Disruption of protein phosphatase 2A subunit interaction in human cancers with mutations in the A alpha subunit gene. Oncogene *20*, 10-15.
91. Xu, Y., Chen, Y., Zhang, P., Jeffrey, P.D., and Shi, Y. (2008). Structure of a protein phosphatase 2A holoenzyme: insights into B55-mediated Tau dephosphorylation. Molecular cell *31*, 873-885.
92. Groves, M.R., Hanlon, N., Turowski, P., Hemmings, B.A., and Barford, D. (1999). The structure of the protein phosphatase 2A PR65/A subunit reveals the conformation of its 15 tandemly repeated HEAT motifs. Cell *96*, 99-110.
93. Ruediger, R., Roeckel, D., Fait, J., Bergqvist, A., Magnusson, G., and Walter, G. (1992). Identification of binding sites on the regulatory A subunit of protein phosphatase 2A for the catalytic C subunit and for tumor antigens of simian virus 40 and polyomavirus. Molecular and cellular biology *12*, 4872-4882.
94. Cho, U.S., and Xu, W. (2007). Crystal structure of a protein phosphatase 2A heterotrimeric holoenzyme. Nature *445*, 53-57.
95. Goudreault, M., D'Ambrosio, L.M., Kean, M.J., Mullin, M.J., Larsen, B.G., Sanchez, A., Chaudhry, S., Chen, G.I., Sicheri, F., Nesvizhskii, A.I., et al. (2009). A PP2A phosphatase high density interaction network identifies a novel striatin-interacting phosphatase and kinase complex linked to the cerebral cavernous malformation 3 (CCM3) protein. Molecular & cellular proteomics : MCP *8*, 157-171.
96. Margolis, S.S., Perry, J.A., Forester, C.M., Nutt, L.K., Guo, Y., Jardim, M.J., Thomenius, M.J., Freel, C.D., Darbandi, R., Ahn, J.H., et al. (2006). Role for the PP2A/B56delta

phosphatase in regulating 14-3-3 release from Cdc25 to control mitosis. Cell *127*, 759-773.
97. Forester, C.M., Maddox, J., Louis, J.V., Goris, J., and Virshup, D.M. (2007). Control of mitotic exit by PP2A regulation of Cdc25C and Cdk1. Proc Natl Acad Sci U S A *104*, 19867-19872.
98. Gharbi-Ayachi, A., Labbe, J.C., Burgess, A., Vigneron, S., Strub, J.M., Brioudes, E., Van-Dorsselaer, A., Castro, A., and Lorca, T. (2010). The substrate of Greatwall kinase, Arpp19, controls mitosis by inhibiting protein phosphatase 2A. Science *330*, 1673-1677.
99. Lee, T.Y., Lai, T.Y., Lin, S.C., Wu, C.W., Ni, I.F., Yang, Y.S., Hung, L.Y., Law, B.K., and Chiang, C.W. (2010). The B56gamma3 regulatory subunit of protein phosphatase 2A (PP2A) regulates S phase-specific nuclear accumulation of PP2A and the G1 to S transition. The Journal of biological chemistry *285*, 21567-21580.
100. Schmitz, M.H., Held, M., Janssens, V., Hutchins, J.R., Hudecz, O., Ivanova, E., Goris, J., Trinkle-Mulcahy, L., Lamond, A.I., Poser, I., et al. (2010). Live-cell imaging RNAi screen identifies PP2A-B55alpha and importin-beta1 as key mitotic exit regulators in human cells. Nature cell biology *12*, 886-893.
101. Manchado, E., Guillamot, M., de Cárcer, G., Eguren, M., Trickey, M., García-Higuera, I., Moreno, S., Yamano, H., Cañamero, M., and Malumbres, M. (2010). Targeting Mitotic Exit Leads to Tumor Regression In Vivo: Modulation by Cdk1, Mastl, and the PP2A/B55α,δ Phosphatase. Cancer Cell *18*, 641-654.
102. Kitajima, T.S., Sakuno, T., Ishiguro, K., Iemura, S., Natsume, T., Kawashima, S.A., and Watanabe, Y. (2006). Shugoshin collaborates with protein phosphatase 2A to protect cohesin. Nature *441*, 46-52.
103. Suganuma, M., Fujiki, H., Suguri, H., Yoshizawa, S., Hirota, M., Nakayasu, M., Ojika, M., Wakamatsu, K., Yamada, K., and Sugimura, T. (1988). Okadaic acid: an additional non-phorbol-12-tetradecanoate-13-acetate-type tumor promoter. Proc Natl Acad Sci U S A *85*, 1768-1771.
104. Takai, A., Bialojan, C., Troschka, M., and Ruegg, J.C. (1987). Smooth muscle myosin phosphatase inhibition and force enhancement by black sponge toxin. FEBS letters *217*, 81-84.
105. Schonthal, A.H. (2001). Role of serine/threonine protein phosphatase 2A in cancer. Cancer Lett *170*, 1-13.
106. Walter, G., Ruediger, R., Slaughter, C., and Mumby, M. (1990). Association of protein phosphatase 2A with polyoma virus medium tumor antigen. Proc Natl Acad Sci U S A *87*, 2521-2525.
107. Pallas, D.C., Shahrik, L.K., Martin, B.L., Jaspers, S., Miller, T.B., Brautigan, D.L., and Roberts, T.M. (1990). Polyoma small and middle T antigens and SV40 small t antigen form stable complexes with protein phosphatase 2A. Cell *60*, 167-176.
108. Rodriguez-Viciana, P., Collins, C., and Fried, M. (2006). Polyoma and SV40 proteins differentially regulate PP2A to activate distinct cellular signaling pathways involved in growth control. Proc Natl Acad Sci U S A *103*, 19290-19295.
109. Chen, W., Possemato, R., Campbell, K.T., Plattner, C.A., Pallas, D.C., and Hahn, W.C. (2004). Identification of specific PP2A complexes involved in human cell transformation. Cancer Cell *5*, 127-136.

110. Sablina, A.A., Hector, M., Colpaert, N., and Hahn, W.C. (2010). Identification of PP2A complexes and pathways involved in cell transformation. Cancer research *70*, 10474-10484.
111. Mui, M.Z., Kucharski, M., Miron, M.J., Hur, W.S., Berghuis, A.M., Blanchette, P., and Branton, P.E. (2013). Identification of the adenovirus E4orf4 protein binding site on the B55alpha and Cdc55 regulatory subunits of PP2A: Implications for PP2A function, tumor cell killing and viral replication. PLoS pathogens *9*, e1003742.
112. Eichhorn, P.J., Creyghton, M.P., Wilhelmsen, K., van Dam, H., and Bernards, R. (2007). A RNA interference screen identifies the protein phosphatase 2A subunit PR55gamma as a stress-sensitive inhibitor of c-SRC. PLoS Genet *3*, e218.
113. Ory, S., Zhou, M., Conrads, T.P., Veenstra, T.D., and Morrison, D.K. (2003). Protein phosphatase 2A positively regulates Ras signaling by dephosphorylating KSR1 and Raf-1 on critical 14-3-3 binding sites. Current biology : CB *13*, 1356-1364.
114. Gilan, O., Diesch, J., Amalia, M., Jastrzebski, K., Chueh, A., Verrills, N.M., Pearson, R.B., Mariadason, J.M., Tulchinsky, E., Hannan, R.D., et al. (2014). PR55alpha-containing protein phosphatase 2A complexes promote cancer cell migration and invasion through regulation of AP-1 transcriptional activity. Oncogene *0*.
115. Ruvolo, P.P., Qui, Y.H., Coombes, K.R., Zhang, N., Ruvolo, V.R., Borthakur, G., Konopleva, M., Andreeff, M., and Kornblau, S.M. (2011). Low expression of PP2A regulatory subunit B55alpha is associated with T308 phosphorylation of AKT and shorter complete remission duration in acute myeloid leukemia patients. Leukemia *25*, 1711-1717.
116. Tan, Y., Sun, D., Jiang, W., Klotz-Noack, K., Vashisht, A.A., Wohlschlegel, J., Widschwendter, M., and Spruck, C. (2014). PP2A-B55beta antagonizes cyclin E1 proteolysis and promotes its dysregulation in cancer. Cancer research *74*, 2006-2014.
117. Keyomarsi, K., Tucker, S.L., Buchholz, T.A., Callister, M., Ding, Y., Hortobagyi, G.N., Bedrosian, I., Knickerbocker, C., Toyofuku, W., Lowe, M., et al. (2002). Cyclin E and survival in patients with breast cancer. The New England journal of medicine *347*, 1566-1575.
118. Meyer, N., and Penn, L.Z. (2008). Reflecting on 25 years with MYC. Nat Rev Cancer *8*, 976-990.
119. Welcker, M., Orian, A., Jin, J., Grim, J.E., Harper, J.W., Eisenman, R.N., and Clurman, B.E. (2004). The Fbw7 tumor suppressor regulates glycogen synthase kinase 3 phosphorylation-dependent c-Myc protein degradation. Proc Natl Acad Sci U S A *101*, 9085-9090.
120. Yeh, E., Cunningham, M., Arnold, H., Chasse, D., Monteith, T., Ivaldi, G., Hahn, W.C., Stukenberg, P.T., Shenolikar, S., Uchida, T., et al. (2004). A signalling pathway controlling c-Myc degradation that impacts oncogenic transformation of human cells. Nature cell biology *6*, 308-318.
121. Arnold, H.K., and Sears, R.C. (2006). Protein phosphatase 2A regulatory subunit B56alpha associates with c-myc and negatively regulates c-myc accumulation. Molecular and cellular biology *26*, 2832-2844.
122. Ruvolo, P.P., Clark, W., Mumby, M., Gao, F., and May, W.S. (2002). A functional role for the B56 alpha-subunit of protein phosphatase 2A in ceramide-mediated regulation of Bcl2 phosphorylation status and function. The Journal of biological chemistry *277*, 22847-22852.

123. Deichmann, M., Polychronidis, M., Wacker, J., Thome, M., and Naher, H. (2001). The protein phosphatase 2A subunit Bgamma gene is identified to be differentially expressed in malignant melanomas by subtractive suppression hybridization. Melanoma research *11*, 577-585.
124. Polakis, P. (2000). Wnt signaling and cancer. Genes & development *14*, 1837-1851.
125. Low, I.C., Loh, T., Huang, Y., Virshup, D.M., and Pervaiz, S. (2014). Ser70 phosphorylation of Bcl-2 by selective tyrosine nitration of PP2A-B56delta stabilizes its antiapoptotic activity. Blood *124*, 2223-2234.
126. Junttila, M.R., Puustinen, P., Niemela, M., Ahola, R., Arnold, H., Bottzauw, T., Ala-aho, R., Nielsen, C., Ivaska, J., Taya, Y., et al. (2007). CIP2A inhibits PP2A in human malignancies. Cell *130*, 51-62.
127. Li, M., Makkinje, A., and Damuni, Z. (1996). The myeloid leukemia-associated protein SET is a potent inhibitor of protein phosphatase 2A. The Journal of biological chemistry *271*, 11059-11062.
128. Janghorban, M., Farrell, A.S., Allen-Petersen, B.L., Pelz, C., Daniel, C.J., Oddo, J., Langer, E.M., Christensen, D.J., and Sears, R.C. (2014). Targeting c-MYC by antagonizing PP2A inhibitors in breast cancer. Proceedings of the National Academy of Sciences *111*, 9157-9162.
129. Farrell, A.S., Allen-Petersen, B., Daniel, C.J., Wang, X., Wang, Z., Rodriguez, S., Impey, S., Oddo, J., Vitek, M.P., Lopez, C., et al. (2014). Targeting inhibitors of the tumor suppressor PP2A for the treatment of pancreatic cancer. Molecular cancer research : MCR *12*, 924-939.
130. Calin, G.A., di Iasio, M.G., Caprini, E., Vorechovsky, I., Natali, P.G., Sozzi, G., Croce, C.M., Barbanti-Brodano, G., Russo, G., and Negrini, M. (2000). Low frequency of alterations of the alpha (PPP2R1A) and beta (PPP2R1B) isoforms of the subunit A of the serine-threonine phosphatase 2A in human neoplasms. Oncogene *19*, 1191-1195.
131. Chen, W., Arroyo, J.D., Timmons, J.C., Possemato, R., and Hahn, W.C. (2005). Cancer-associated PP2A Aalpha subunits induce functional haploinsufficiency and tumorigenicity. Cancer research *65*, 8183-8192.
132. Strack, S., Cribbs, J.T., and Gomez, L. (2004). Critical role for protein phosphatase 2A heterotrimers in mammalian cell survival. The Journal of biological chemistry *279*, 47732-47739.
133. Westermarck, J., and Hahn, W.C. (2008). Multiple pathways regulated by the tumor suppressor PP2A in transformation. Trends Mol Med *14*, 152-160.
134. Colella, S., Ohgaki, H., Ruediger, R., Yang, F., Nakamura, M., Fujisawa, H., Kleihues, P., and Walter, G. (2001). Reduced expression of the Aalpha subunit of protein phosphatase 2A in human gliomas in the absence of mutations in the Aalpha and Abeta subunit genes. Int J Cancer *93*, 798-804.
135. Campbell, I.G., and Manolitsas, T. (1999). Absence of PPP2R1B gene alterations in primary ovarian cancers. Oncogene *18*, 6367-6369.
136. Wang, S.S., Esplin, E.D., Li, J.L., Huang, L., Gazdar, A., Minna, J., and Evans, G.A. (1998). Alterations of the PPP2R1B gene in human lung and colon cancer. Science *282*, 284-287.
137. Ruediger, R., Pham, H.T., and Walter, G. (2001). Alterations in protein phosphatase 2A subunit interaction in human carcinomas of the lung and colon with mutations in the A beta subunit gene. Oncogene *20*, 1892-1899.

138. Sablina, A.A., Chen, W., Arroyo, J.D., Corral, L., Hector, M., Bulmer, S.E., DeCaprio, J.A., and Hahn, W.C. (2007). The tumor suppressor PP2A Abeta regulates the RalA GTPase. Cell *129*, 969-982.
139. Mwenifumbo, J.C., and Marra, M.A. (2013). Cancer genome-sequencing study design. Nat Rev Genet *14*, 321-332.
140. Cancer Genome Atlas Research, N., Weinstein, J.N., Collisson, E.A., Mills, G.B., Shaw, K.R., Ozenberger, B.A., Ellrott, K., Shmulevich, I., Sander, C., and Stuart, J.M. (2013). The Cancer Genome Atlas Pan-Cancer analysis project. Nat Genet *45*, 1113-1120.
141. Thomas, R.K., Baker, A.C., Debiasi, R.M., Winckler, W., Laframboise, T., Lin, W.M., Wang, M., Feng, W., Zander, T., MacConaill, L., et al. (2007). High-throughput oncogene mutation profiling in human cancer. Nat Genet *39*, 347-351.
142. Doroshow, J.H., and Kummar, S. (2014). Translational research in oncology[mdash]10 years of progress and future prospects. Nature reviews. Clinical oncology *11*, 649-662.
143. Aebersold, R., and Cravatt, B.F. (2002). Proteomics – advances, applications and the challenges that remain. Trends in biotechnology *20*, s1-s2.
144. Makarov, A. (2000). Electrostatic axially harmonic orbital trapping: a high-performance technique of mass analysis. Analytical chemistry *72*, 1156-1162.
145. Perry, R.H., Cooks, R.G., and Noll, R.J. (2008). Orbitrap mass spectrometry: instrumentation, ion motion and applications. Mass spectrometry reviews *27*, 661-699.
146. Macek, B., Waanders, L.F., Olsen, J.V., and Mann, M. (2006). Top-down Protein Sequencing and MS3 on a Hybrid Linear Quadrupole Ion Trap-Orbitrap Mass Spectrometer. Molecular & Cellular Proteomics *5*, 949-958.
147. Tran, J.C., Zamdborg, L., Ahlf, D.R., Lee, J.E., Catherman, A.D., Durbin, K.R., Tipton, J.D., Vellaichamy, A., Kellie, J.F., Li, M., et al. (2011). Mapping intact protein isoforms in discovery mode using top-down proteomics. Nature *480*, 254-258.
148. Thompson, A., Schäfer, J., Kuhn, K., Kienle, S., Schwarz, J., Schmidt, G., Neumann, T., and Hamon, C. (2003). Tandem Mass Tags: A Novel Quantification Strategy for Comparative Analysis of Complex Protein Mixtures by MS/MS. Analytical chemistry *75*, 1895-1904.
149. Zieske, L.R. (2006). A perspective on the use of iTRAQ reagent technology for protein complex and profiling studies. Journal of experimental botany *57*, 1501-1508.
150. Ong, S.E., Blagoev, B., Kratchmarova, I., Kristensen, D.B., Steen, H., Pandey, A., and Mann, M. (2002). Stable isotope labeling by amino acids in cell culture, SILAC, as a simple and accurate approach to expression proteomics. Molecular & cellular proteomics : MCP *1*, 376-386.
151. Shah, S.P., Kobel, M., Senz, J., Morin, R.D., Clarke, B.A., Wiegand, K.C., Leung, G., Zayed, A., Mehl, E., Kalloger, S.E., et al. (2009). Mutation of FOXL2 in granulosa-cell tumors of the ovary. The New England journal of medicine *360*, 2719-2729.
152. Ruediger, R., Hentz, M., Fait, J., Mumby, M., and Walter, G. (1994). Molecular model of the A subunit of protein phosphatase 2A: interaction with other subunits and tumor antigens. Journal of virology *68*, 123-129.
153. Ruediger, R., Fields, K., and Walter, G. (1999). Binding specificity of protein phosphatase 2A core enzyme for regulatory B subunits and T antigens. Journal of virology *73*, 839-842.
154. Forbes, S.A., Tang, G., Bindal, N., Bamford, S., Dawson, E., Cole, C., Kok, C.Y., Jia, M., Ewing, R., Menzies, A., et al. (2010). COSMIC (the Catalogue of Somatic Mutations

in Cancer): a resource to investigate acquired mutations in human cancer. Nucleic Acids Res *38*, D652-657.
155. Arnold, K., Bordoli, L., Kopp, J., and Schwede, T. (2006). The SWISS-MODEL workspace: a web-based environment for protein structure homology modelling. Bioinformatics *22*, 195-201.
156. Al-Hussaini, M., Stockman, A., Foster, H., and McCluggage, W.G. (2004). WT-1 assists in distinguishing ovarian from uterine serous carcinoma and in distinguishing between serous and endometrioid ovarian carcinoma. Histopathology *44*, 109-115.
157. Abeler, V.M., and Kjorstad, K.E. (1990). Serous papillary carcinoma of the endometrium: a histopathological study of 22 cases. Gynecol Oncol *39*, 266-271.
158. Reva, B., Antipin, Y., and Sander, C. (2007). Determinants of protein function revealed by combinatorial entropy optimization. Genome Biol *8*, R232.
159. Janssens, V., Goris, J., and Van Hoof, C. (2005). PP2A: the expected tumor suppressor. Current opinion in genetics & development *15*, 34-41.
160. Bialojan, C., and Takai, A. (1988). Inhibitory effect of a marine-sponge toxin, okadaic acid, on protein phosphatases. Specificity and kinetics. The Biochemical journal *256*, 283-290.
161. Kawabe, T. (2004). G2 checkpoint abrogators as anticancer drugs. Molecular cancer therapeutics *3*, 513-519.
162. Zhang, W., Yang, J., Liu, Y., Chen, X., Yu, T., Jia, J., and Liu, C. (2009). PR55 alpha, a regulatory subunit of PP2A, specifically regulates PP2A-mediated beta-catenin dephosphorylation. The Journal of biological chemistry *284*, 22649-22656.
163. Dozier, C., Bonyadi, M., Baricault, L., Tonasso, L., and Darbon, J.M. (2004). Regulation of Chk2 phosphorylation by interaction with protein phosphatase 2A via its B' regulatory subunit. Biology of the cell / under the auspices of the European Cell Biology Organization *96*, 509-517.
164. Woo, M.M., Salamanca, C.M., Symowicz, J., Stack, M.S., Miller, D.M., Leung, P.C., Gilks, C.B., and Auersperg, N. (2008). SV40 early genes induce neoplastic properties in serous borderline ovarian tumor cells. Gynecol Oncol *111*, 125-131.
165. Hirschowitz, L., Ganesan, R., and McCluggage, W.G. (2009). WT1, p53 and hormone receptor expression in uterine serous carcinoma. Histopathology *55*, 478-482.
166. Watson, I.R., Takahashi, K., Futreal, P.A., and Chin, L. (2013). Emerging patterns of somatic mutations in cancer. Nat Rev Genet *14*, 703-718.
167. Soslow, R.A. (2010). Endometrial carcinomas with ambiguous features. Seminars in Diagnostic Pathology *27*, 261-273.
168. Sidhu, D., Duggan, M., Clement, P., Ewanowich, C., Arseneau, J., Cesari, M., Kobel, M., and Han, G. (2012). Interobserver Agreement on High-Grade Endometrial Carcinoma and Correlation with ER, p53 and p16 Expression. Modern Pathology *25*, 296A-297A.
169. Gilks, C.B., Oliva, E., and Soslow, R. (2011). Poor Interobserver Reproducibility in the Diagnosis of High-Grade Endometrial Carcinoma. In USCAP. (San Antonio, TX, USA).
170. Morin, R.D., Mendez-Lago, M., Mungall, A.J., Goya, R., Mungall, K.L., Corbett, R.D., Johnson, N.A., Severson, T.M., Chiu, R., Field, M., et al. (2011). Frequent mutation of histone-modifying genes in non-Hodgkin lymphoma. Nature *476*, 298-303.
171. Li, H., and Durbin, R. (2009). Fast and accurate short read alignment with Burrows-Wheeler transform. Bioinformatics *25*, 1754-1760.

172. Ding, J., Bashashati, A., Roth, A., Oloumi, A., Tse, K., Zeng, T., Haffari, G., Hirst, M., Marra, M.A., Condon, A., et al. (2012). Feature-based classifiers for somatic mutation detection in tumour-normal paired sequencing data. Bioinformatics *28*, 167-175.
173. Forbes, S.A., Bindal, N., Bamford, S., Cole, C., Kok, C.Y., Beare, D., Jia, M., Shepherd, R., Leung, K., Menzies, A., et al. (2011). COSMIC: mining complete cancer genomes in the Catalogue of Somatic Mutations in Cancer. Nucleic Acids Res *39*, D945-950.
174. Forshew, T., Murtaza, M., Parkinson, C., Gale, D., Tsui, D.W., Kaper, F., Dawson, S.J., Piskorz, A.M., Jimenez-Linan, M., Bentley, D., et al. (2012). Noninvasive identification and monitoring of cancer mutations by targeted deep sequencing of plasma DNA. Science translational medicine *4*, 136ra168.
175. Goodfellow, P.J., Buttin, B.M., Herzog, T.J., Rader, J.S., Gibb, R.K., Swisher, E., Look, K., Walls, K.C., Fan, M.-Y., and Mutch, D.G. (2003). Prevalence of defective DNA mismatch repair and MSH6 mutation in an unselected series of endometrial cancers. Proceedings of the National Academy of Sciences *100*, 5908-5913.
176. Tashiro, H., Blazes, M.S., Wu, R., Cho, K.R., Bose, S., Wang, S.I., Li, J., Parsons, R., and Ellenson, L.H. (1997). Mutations in PTEN are frequent in endometrial carcinoma but rare in other common gynecological malignancies. Cancer research *57*, 3935-3940.
177. D'Angelo, E., and Prat, J. (2011). Pathology of mixed Müllerian tumours. Best Practice & Research Clinical Obstetrics & Gynaecology *25*, 705-718.
178. Soslow, R.A., Bissonnette, J.P., Wilton, A., Ferguson, S.E., Alektiar, K.M., Duska, L.R., and Oliva, E. (2007). Clinicopathologic analysis of 187 high-grade endometrial carcinomas of different histologic subtypes: similar outcomes belie distinctive biologic differences. Am J Surg Pathol *31*, 979-987.
179. Kobel, M., Kalloger, S.E., Baker, P.M., Ewanowich, C.A., Arseneau, J., Zherebitskiy, V., Abdulkarim, S., Leung, S., Duggan, M.A., Fontaine, D., et al. (2010). Diagnosis of ovarian carcinoma cell type is highly reproducible: a transcanadian study. Am J Surg Pathol *34*, 984-993.
180. Anglesio, M.S., Carey, M.S., Kobel, M., Mackay, H., and Huntsman, D.G. (2011). Clear cell carcinoma of the ovary: a report from the first Ovarian Clear Cell Symposium, June 24th, 2010. Gynecol Oncol *121*, 407-415.
181. Alkushi, A., Clarke, B.A., Akbari, M., Makretsov, N., Lim, P., Miller, D., Magliocco, A., Coldman, A., van de Rijn, M., Huntsman, D., et al. (2007). Identification of prognostically relevant and reproducible subsets of endometrial adenocarcinoma based on clustering analysis of immunostaining data. Modern Pathol *20*, 1156-1165.
182. Oda, K., Stokoe, D., Taketani, Y., and McCormick, F. (2005). High frequency of coexistent mutations of PIK3CA and PTEN genes in endometrial carcinoma. Cancer research *65*, 10669-10673.
183. Voss, M.A., Ganesan, R., Ludeman, L., McCarthy, K., Gornall, R., Schaller, G., Wei, W., and Sundar, S. (2011). Should grade 3 endometrioid endometrial carcinoma be considered a type 2 cancer-A clinical and pathological evaluation. Gynecologic oncology.
184. Zannoni, G., Vellone, V., Arena, V., Prisco, M., Scambia, G., Carbone, A., and Gallo, D. (2010). Does high-grade endometrioid carcinoma (grade 3 FIGO) belong to type I or type II endometrial cancer? A clinical–pathological and immunohistochemical study. Virchows Archiv *457*, 27-34.

185. Crum, C.P., Lee, Kenneth R., Genest, David R. (2006). Adenocarcinoma, carcinosarcoma and other epithelial tumors of the endometrium. In Diagnostic gynecologic and obstetric pathology, Volume
, 1st Edition, K.R.L. Christopher P. Crum, ed. (Philadelphia, PA: Saunders/Elsevier), p. 1182 p.
186. Catasus, L., Gallardo, A., and Prat, J. (2009). Molecular genetics of endometrial carcinoma. *15*, 554-563.
187. Amant, F., Cadron, I., Fuso, L., Berteloot, P., de Jonge, E., Jacomen, G., Van Robaeys, J., Neven, P., Moerman, P., and Vergote, I. (2005). Endometrial carcinosarcomas have a different prognosis and pattern of spread compared to high-risk epithelial endometrial cancer. Gynecologic oncology *98*, 274-280.
188. Chiyoda, T., Tsuda, H., Tanaka, H., Kataoka, F., Nomura, H., Nishimura, S., Takano, M., Susumu, N., Saya, H., and Aoki, D. (2012). Expression profiles of carcinosarcoma of the uterine corpus—are these similar to carcinoma or sarcoma? Genes, Chromosomes and Cancer *51*, 229-239.
189. Murray, S., Linardou, H., Mountzios, G., Manoloukos, M., Markaki, S., Eleutherakis-Papaiakovou, E., Dimopoulos, M.A., and Papadimitriou, C.A. (2010). Low frequency of somatic mutations in uterine sarcomas: a molecular analysis and review of the literature. Mutat Res *686*, 68-73.
190. Liu, L., and Eisenman, R.N. (2012). Regulation of c-Myc Protein Abundance by a Protein Phosphatase 2A-Glycogen Synthase Kinase 3beta-Negative Feedback Pathway. Genes & cancer *3*, 23-36.
191. King, B., Trimarchi, T., Reavie, L., Xu, L., Mullenders, J., Ntziachristos, P., Aranda-Orgilles, B., Perez-Garcia, A., Shi, J., Vakoc, C., et al. (2013). The ubiquitin ligase FBXW7 modulates leukemia-initiating cell activity by regulating MYC stability. Cell *153*, 1552-1566.
192. Prowse, A.H., Manek, S., Varma, R., Liu, J., Godwin, A.K., Maher, E.R., Tomlinson, I.P.M., and Kennedy, S.H. (2006). Molecular genetic evidence that endometriosis is a precursor of ovarian cancer. International Journal of Cancer *119*, 556-562.
193. Samarnthai, N., Hall, K., and Yeh, I.T. (2010). Molecular profiling of endometrial malignancies. Obstet Gynecol Int *2010*, 162363.
194. Benjamini, Y., and Hochberg, Y. (1995). Controlling the False Discovery Rate - a Practical and Powerful Approach to Multiple Testing. J Roy Stat Soc B Met *57*, 289-300.
195. Stuart, G.C.E., Kitchener, H., Bacon, M., duBois, A., Friedlander, M., Ledermann, J., Marth, C., Thigpen, T., Trimble, E., and OCCC, t.O.C.C.C. (2011). 2010 Gynecologic Cancer InterGroup (GCIG) Consensus Statement on Clinical Trials in Ovarian Cancer Report From the Fourth Ovarian Cancer Consensus Conference. Int J Gynecol Cancer *21*, 750-755.
196. Geyer, J.T., Lopez-Garcia, M.A., Sanchez-Estevez, C., Sarrio, D., Moreno-Bueno, G., Franceschetti, I., Palacios, J., and Oliva, E. (2009). Pathogenetic pathways in ovarian endometrioid adenocarcinoma: a molecular study of 29 cases. Am J Surg Pathol *33*, 1157-1163.
197. McCluggage, W.G. (2011). Morphological subtypes of ovarian carcinoma: a review with emphasis on new developments and pathogenesis. Pathology *43*, 420-432.
198. Shedden, K.A., Kshirsagar, M.P., Schwartz, D.R., Wu, R., Yu, H., Misek, D.E., Hanash, S., Katabuchi, H., Ellenson, L.H., Fearon, E.R., et al. (2005). Histologic type, organ of origin, and Wnt pathway status: effect on gene expression in ovarian and uterine

carcinomas. Clinical cancer research : an official journal of the American Association for Cancer Research *11*, 2123-2131.
199. Palacios, J., and Gamallo, C. (1998). Mutations in the beta-catenin gene (CTNNB1) in endometrioid ovarian carcinomas. Cancer research *58*, 1344-1347.
200. Wu, R., Zhai, Y., Fearon, E.R., and Cho, K.R. (2001). Diverse mechanisms of beta-catenin deregulation in ovarian endometrioid adenocarcinomas. Cancer research *61*, 8247-8255.
201. Wright, K., Wilson, P., Morland, S., Campbell, I., Walsh, M., Hurst, T., Ward, B., Cummings, M., and Chenevix-Trench, G. (1999). beta-catenin mutation and expression analysis in ovarian cancer: exon 3 mutations and nuclear translocation in 16% of endometrioid tumours. Int J Cancer *82*, 625-629.
202. Saegusa, M., and Okayasu, I. (2001). Frequent nuclear beta-catenin accumulation and associated mutations in endometrioid-type endometrial and ovarian carcinomas with squamous differentiation. The Journal of pathology *194*, 59-67.
203. Sagae, S., Kobayashi, K., Nishioka, Y., Sugimura, M., Ishioka, S., Nagata, M., Terasawa, K., Tokino, T., and Kudo, R. (1999). Mutational analysis of beta-catenin gene in Japanese ovarian carcinomas: frequent mutations in endometrioid carcinomas. Jpn J Cancer Res *90*, 510-515.
204. Moreno-Bueno, G., Gamallo, C., Perez-Gallego, L., de Mora, J.C., Suarez, A., and Palacios, J. (2001). beta-Catenin expression pattern, beta-catenin gene mutations, and microsatellite instability in endometrioid ovarian carcinomas and synchronous endometrial carcinomas. Diagn Mol Pathol *10*, 116-122.
205. Obata, K., Morland, S.J., Watson, R.H., Hitchcock, A., Chenevix-Trench, G., Thomas, E.J., and Campbell, I.G. (1998). Frequent PTEN/MMAC Mutations in Endometrioid but not Serous or Mucinous Epithelial Ovarian Tumors. Cancer research *58*, 2095-2097.
206. Shih Ie, M., Panuganti, P.K., Kuo, K.T., Mao, T.L., Kuhn, E., Jones, S., Velculescu, V.E., Kurman, R.J., and Wang, T.L. (2011). Somatic mutations of PPP2R1A in ovarian and uterine carcinomas. The American journal of pathology *178*, 1442-1447.
207. Siiteri, P.K., Schwarz, B.E., and MacDonald, P.C. (1974). Estrogen receptors and the estrone hypothesis in relation to endometrial and breast cancer. Gynecologic oncology *2*, 228-238.
208. Key, T.J.A., and Pike, M.C. (1988). The Dose-Effect Relationship between Unopposed Estrogens and Endometrial Mitotic Rate - Its Central Role in Explaining and Predicting Endometrial Cancer Risk. Brit J Cancer *57*, 205-212.
209. Yamaguchi, K., Mandai, M., Toyokuni, S., Hamanishi, J., Higuchi, T., Takakura, K., and Fujii, S. (2008). Contents of endometriotic cysts, especially the high concentration of free iron, are a possible cause of carcinogenesis in the cysts through the iron-induced persistent oxidative stress. Clinical Cancer Research *14*, 32-40.
210. Van Langendonckt, A., Casanas-Roux, F., Dolmans, M.M., and Donnez, J. (2002). Potential involvement of hemoglobin and heme in the pathogenesis of peritoneal endometriosis. Fertil Steril *77*, 561-570.
211. Kobayashi, H., Kajiwara, H., Kanayama, S., Yamada, Y., Furukawa, N., Noguchi, T., Haruta, S., Yoshida, S., Sakata, M., Sado, T., et al. (2009). Molecular pathogenesis of endometriosis-associated clear cell carcinoma of the ovary (Review). Oncol Rep *22*, 233-240.

212. Fleming, J.S., Beaugie, C.R., Haviv, I., Chenevix-Trench, G., and Tan, O.L. (2006). Incessant ovulation, inflammation and epithelial ovarian carcinogenesis: revisiting old hypotheses. Mol Cell Endocrinol *247*, 4-21.
213. Korner, M., Burckhardt, E., and Mazzucchelli, L. (2006). Higher frequency of chromosomal aberrations in ovarian endometriosis compared to extragonadal endometriosis: A possible link to endometrioid adenocarcinoma. Modern pathology : an official journal of the United States and Canadian Academy of Pathology, Inc *19*, 1615-1623.
214. Vestergaard, A.L., Thorup, K., Knudsen, U.B., Munk, T., Rosbach, H., Poulsen, J.B., Guldberg, P., and Martensen, P.M. (2011). Oncogenic events associated with endometrial and ovarian cancers are rare in endometriosis. Molecular Human Reproduction *17*, 758-761.
215. Lawrenson, K., Lee, N., Torres, H.A., Lee, J.M., Brueggmann, D., Rao, P.N., Noushmehr, H., and Gayther, S.A. (2014). Src as a novel therapeutic target for endometriosis. Gynecol Oncol *135*, 100-107.
216. Su, L.K., Vogelstein, B., and Kinzler, K.W. (1993). Association of the APC tumor suppressor protein with catenins. Science *262*, 1734-1737.
217. Rubinfeld, B., Souza, B., Albert, I., Muller, O., Chamberlain, S.H., Masiarz, F.R., Munemitsu, S., and Polakis, P. (1993). Association of the APC gene product with beta-catenin. Science *262*, 1731-1734.
218. Klaus, A., and Birchmeier, W. (2008). Wnt signalling and its impact on development and cancer. Nature reviews. Cancer *8*, 387-398.
219. Samuels, Y., Wang, Z., Bardelli, A., Silliman, N., Ptak, J., Szabo, S., Yan, H., Gazdar, A., Powell, S.M., Riggins, G.J., et al. (2004). High frequency of mutations of the PIK3CA gene in human cancers. Science *304*, 554.
220. Cully, M., You, H., Levine, A.J., and Mak, T.W. (2006). Beyond PTEN mutations: the PI3K pathway as an integrator of multiple inputs during tumorigenesis. Nature reviews. Cancer *6*, 184-192.
221. McCubrey, J.A., Steelman, L.S., Chappell, W.H., Abrams, S.L., Montalto, G., Cervello, M., Nicoletti, F., Fagone, P., Malaponte, G., Mazzarino, M.C., et al. (2012). Mutations and Deregulation of Ras/Raf/MEK/ERK and PI3K/PTEN/Akt/mTOR Cascades. Oncotarget *3*, 954-987.
222. Kohli, M., Rago, C., Lengauer, C., Kinzler, K.W., and Vogelstein, B. (2004). Facile methods for generating human somatic cell gene knockouts using recombinant adeno-associated viruses. Nucleic Acids Res *32*, e3.
223. Hannon, G.J. (2002). RNA interference. Nature *418*, 244-251.
224. Bridge, A.J., Pebernard, S., Ducraux, A., Nicoulaz, A.L., and Iggo, R. (2003). Induction of an interferon response by RNAi vectors in mammalian cells. Nat Genet *34*, 263-264.
225. Rago, C., Vogelstein, B., and Bunz, F. (2007). Genetic knockouts and knockins in human somatic cells. Nat Protoc *2*, 2734-2746.
226. Topaloglu, O., Hurley, P.J., Yildirim, O., Civin, C.I., and Bunz, F. (2005). Improved methods for the generation of human gene knockout and knockin cell lines. Nucleic Acids Res *33*, e158.
227. Hanson, K.D., and Sedivy, J.M. (1995). Analysis of biological selections for high-efficiency gene targeting. Molecular and cellular biology *15*, 45-51.

228. Lengauer, C., Kinzler, K.W., and Vogelstein, B. (1998). Genetic instabilities in human cancers. Nature *396*, 643-649.
229. Kolodner, R. (1996). Biochemistry and genetics of eukaryotic mismatch repair. Genes & development *10*, 1433-1442.
230. Samuels, Y., Diaz Jr, L.A., Schmidt-Kittler, O., Cummins, J.M., DeLong, L., Cheong, I., Rago, C., Huso, D.L., Lengauer, C., Kinzler, K.W., et al. (2005). Mutant PIK3CA promotes cell growth and invasion of human cancer cells. Cancer Cell *7*, 561-573.
231. Kuramoto, H., Tamura, S., and Notake, Y. (1972). Establishment of a cell line of human endometrial adenocarcinoma in vitro. American journal of obstetrics and gynecology *114*, 1012-1019.
232. Risinger, J.I., Umar, A., Barrett, J.C., and Kunkel, T.A. (1995). A hPMS2 Mutant Cell Line Is Defective in Strand-specific Mismatch Repair. Journal of Biological Chemistry *270*, 18183-18186.
233. Karst, A.M., Levanon, K., and Drapkin, R. (2011). Modeling high-grade serous ovarian carcinogenesis from the fallopian tube. Proc Natl Acad Sci U S A *108*, 7547-7552.
234. Ionov, Y., Yamamoto, H., Krajewski, S., Reed, J.C., and Perucho, M. (2000). Mutational inactivation of the proapoptotic gene BAX confers selective advantage during tumor clonal evolution. Proc Natl Acad Sci U S A *97*, 10872-10877.
235. Ventura, A., Kirsch, D.G., McLaughlin, M.E., Tuveson, D.A., Grimm, J., Lintault, L., Newman, J., Reczek, E.E., Weissleder, R., and Jacks, T. (2007). Restoration of p53 function leads to tumour regression in vivo. Nature *445*, 661-665.
236. Meyers, E.N., Lewandoski, M., and Martin, G.R. (1998). An Fgf8 mutant allelic series generated by Cre- and Flp-mediated recombination. Nat Genet *18*, 136-141.
237. Olson, E.N., Arnold, H.H., Rigby, P.W., and Wold, B.J. (1996). Know your neighbors: three phenotypes in null mutants of the myogenic bHLH gene MRF4. Cell *85*, 1-4.
238. Porteus, M.H., and Baltimore, D. (2003). Chimeric nucleases stimulate gene targeting in human cells. Science *300*, 763.
239. Porteus, M.H., and Carroll, D. (2005). Gene targeting using zinc finger nucleases. Nature biotechnology *23*, 967-973.
240. Christian, M., Cermak, T., Doyle, E.L., Schmidt, C., Zhang, F., Hummel, A., Bogdanove, A.J., and Voytas, D.F. (2010). Targeting DNA double-strand breaks with TAL effector nucleases. Genetics *186*, 757-761.
241. Cong, L., Ran, F.A., Cox, D., Lin, S., Barretto, R., Habib, N., Hsu, P.D., Wu, X., Jiang, W., Marraffini, L.A., et al. (2013). Multiplex Genome Engineering Using CRISPR/Cas Systems. Science *339*, 819-823.
242. Mali, P., Yang, L., Esvelt, K.M., Aach, J., Guell, M., DiCarlo, J.E., Norville, J.E., and Church, G.M. (2013). RNA-Guided Human Genome Engineering via Cas9. Science *339*, 823-826.
243. Gaj, T., Gersbach, C.A., and Barbas, C.F., 3rd (2013). ZFN, TALEN, and CRISPR/Cas-based methods for genome engineering. Trends in biotechnology *31*, 397-405.
244. Wood, A.J., Lo, T.W., Zeitler, B., Pickle, C.S., Ralston, E.J., Lee, A.H., Amora, R., Miller, J.C., Leung, E., Meng, X., et al. (2011). Targeted genome editing across species using ZFNs and TALENs. Science *333*, 307.
245. Gaj, T., Guo, J., Kato, Y., Sirk, S.J., and Barbas, C.F., 3rd (2012). Targeted gene knockout by direct delivery of zinc-finger nuclease proteins. Nature methods *9*, 805-807.

246. Brouns, S.J.J., Jore, M.M., Lundgren, M., Westra, E.R., Slijkhuis, R.J.H., Snijders, A.P.L., Dickman, M.J., Makarova, K.S., Koonin, E.V., and van der Oost, J. (2008). Small CRISPR RNAs Guide Antiviral Defense in Prokaryotes. Science *321*, 960-964.
247. Shalem, O., Sanjana, N.E., Hartenian, E., Shi, X., Scott, D.A., Mikkelsen, T.S., Heckl, D., Ebert, B.L., Root, D.E., Doench, J.G., et al. (2014). Genome-scale CRISPR-Cas9 knockout screening in human cells. Science *343*, 84-87.
248. Canver, M.C., Bauer, D.E., Dass, A., Yien, Y.Y., Chung, J., Masuda, T., Maeda, T., Paw, B.H., and Orkin, S.H. (2014). Characterization of Genomic Deletion Efficiency Mediated by Clustered Regularly Interspaced Palindromic Repeats (CRISPR)/Cas9 Nuclease System in Mammalian Cells. Journal of Biological Chemistry *289*, 21312-21324.
249. Kennedy, E.M., Kornepati, A.V., Goldstein, M., Bogerd, H.P., Poling, B.C., Whisnant, A.W., Kastan, M.B., and Cullen, B.R. (2014). Inactivation of the Human Papillomavirus E6 or E7 Gene in Cervical Carcinoma Cells by Using a Bacterial CRISPR/Cas RNA-Guided Endonuclease. Journal of virology *88*, 11965-11972.
250. Ran, F.A., Hsu, P.D., Wright, J., Agarwala, V., Scott, D.A., and Zhang, F. (2013). Genome engineering using the CRISPR-Cas9 system. Nat Protoc *8*, 2281-2308.
251. Pennisi, E. (2013). The CRISPR craze. Science *341*, 833-836.
252. Neviani, P., Santhanam, R., Trotta, R., Notari, M., Blaser, B.W., Liu, S., Mao, H., Chang, J.S., Galietta, A., Uttam, A., et al. (2005). The tumor suppressor PP2A is functionally inactivated in blast crisis CML through the inhibitory activity of the BCR/ABL-regulated SET protein. Cancer Cell *8*, 355-368.
253. Chen, G.I., and Gingras, A.C. (2007). Affinity-purification mass spectrometry (AP-MS) of serine/threonine phosphatases. Methods *42*, 298-305.
254. Katavic, V. (2014). Retractions of scientific publications: responsibility and accountability. Biochemia medica *24*, 217-222.
255. Marcus A, O.I. (2012). Can We Trust Western Blots? In Lab Times, Volume 2. (Germany: Lab Times), p. 41.
256. Aebersold, R., Burlingame, A.L., and Bradshaw, R.A. (2013). Western blots versus selected reaction monitoring assays: time to turn the tables? Molecular & cellular proteomics : MCP *12*, 2381-2382.
257. Herzog, F., Kahraman, A., Boehringer, D., Mak, R., Bracher, A., Walzthoeni, T., Leitner, A., Beck, M., Hartl, F.U., Ban, N., et al. (2012). Structural probing of a protein phosphatase 2A network by chemical cross-linking and mass spectrometry. Science *337*, 1348-1352.
258. Hughes, C.S., Foehr, S., Garfield, D.A., Furlong, E.E., Steinmetz, L.M., and Krijgsveld, J. (2014). Ultrasensitive proteome analysis using paramagnetic bead technology. Molecular Systems Biology *10*, n/a-n/a.
259. Bolstad, B.M., Irizarry, R.A., Astrand, M., and Speed, T.P. (2003). A comparison of normalization methods for high density oligonucleotide array data based on variance and bias. Bioinformatics *19*, 185-193.
260. Smyth, G.K. (2005). Limma: linear models for microarray data, (New York: Springer).
261. Kremmer, E., Ohst, K., Kiefer, J., Brewis, N., and Walter, G. (1997). Separation of PP2A core enzyme and holoenzyme with monoclonal antibodies against the regulatory A subunit: abundant expression of both forms in cells. Molecular and cellular biology *17*, 1692-1701.

262. Moreno, C.S., Ramachandran, S., Ashby, D.G., Laycock, N., Plattner, C.A., Chen, W., Hahn, W.C., and Pallas, D.C. (2004). Signaling and Transcriptional Changes Critical for Transformation of Human Cells by Simian Virus 40 Small Tumor Antigen or Protein Phosphatase 2A B56γ Knockdown. Cancer research *64*, 6978-6988.
263. Seeling, J.M., Miller, J.R., Gil, R., Moon, R.T., White, R., and Virshup, D.M. (1999). Regulation of beta-catenin signaling by the B56 subunit of protein phosphatase 2A. Science *283*, 2089-2091.
264. Li, H.H., Cai, X., Shouse, G.P., Piluso, L.G., and Liu, X. (2007). A specific PP2A regulatory subunit, B56gamma, mediates DNA damage-induced dephosphorylation of p53 at Thr55. The EMBO journal *26*, 402-411.
265. Shouse, G.P., Nobumori, Y., and Liu, X. (2010). A B56gamma mutation in lung cancer disrupts the p53-dependent tumor-suppressor function of protein phosphatase 2A. Oncogene *29*, 3933-3941.
266. Firulli, B.A., Howard, M.J., McDaid, J.R., McIlreavey, L., Dionne, K.M., Centonze, V.E., Cserjesi, P., Virshup, D.M., and Firulli, A.B. (2003). PKA, PKC, and the protein phosphatase 2A influence HAND factor function: a mechanism for tissue-specific transcriptional regulation. Molecular cell *12*, 1225-1237.
267. Scott, I.C., Anson-Cartwright, L., Riley, P., Reda, D., and Cross, J.C. (2000). The HAND1 basic helix-loop-helix transcription factor regulates trophoblast differentiation via multiple mechanisms. Molecular and cellular biology *20*, 530-541.
268. Martindill, D.M., Risebro, C.A., Smart, N., Franco-Viseras Mdel, M., Rosario, C.O., Swallow, C.J., Dennis, J.W., and Riley, P.R. (2007). Nucleolar release of Hand1 acts as a molecular switch to determine cell fate. Nature cell biology *9*, 1131-1141.
269. Jones, A., Teschendorff, A.E., Li, Q., Hayward, J.D., Kannan, A., Mould, T., West, J., Zikan, M., Cibula, D., Fiegl, H., et al. (2013). Role of DNA methylation and epigenetic silencing of HAND2 in endometrial cancer development. PLoS Med *10*, e1001551.
270. Li, Q., Kannan, A., DeMayo, F.J., Lydon, J.P., Cooke, P.S., Yamagishi, H., Srivastava, D., Bagchi, M.K., and Bagchi, I.C. (2011). The Antiproliferative Action of Progesterone in Uterine Epithelium Is Mediated by Hand2. Science *331*, 912-916.
271. Li, M., Makkinje, A., and Damuni, Z. (1996). Molecular identification of I1PP2A, a novel potent heat-stable inhibitor protein of protein phosphatase 2A. Biochemistry *35*, 6998-7002.
272. Christensen, D.J., Chen, Y., Oddo, J., Matta, K.M., Neil, J., Davis, E.D., Volkheimer, A.D., Lanasa, M.C., Friedman, D.R., Goodman, B.K., et al. (2011). SET oncoprotein overexpression in B-cell chronic lymphocytic leukemia and non-Hodgkin lymphoma: a predictor of aggressive disease and a new treatment target. Blood *118*, 4150-4158.
273. Janghorban, M., Farrell, A.S., Allen-Petersen, B.L., Pelz, C., Daniel, C.J., Oddo, J., Langer, E.M., Christensen, D.J., and Sears, R.C. (2014). Targeting c-MYC by antagonizing PP2A inhibitors in breast cancer. Proc Natl Acad Sci U S A *111*, 9157-9162.
274. Mukhopadhyay, A., Saddoughi, S.A., Song, P., Sultan, I., Ponnusamy, S., Senkal, C.E., Snook, C.F., Arnold, H.K., Sears, R.C., Hannun, Y.A., et al. (2009). Direct interaction between the inhibitor 2 and ceramide via sphingolipid-protein binding is involved in the regulation of protein phosphatase 2A activity and signaling. FASEB journal : official publication of the Federation of American Societies for Experimental Biology *23*, 751-763.

275. Ponnusamy, S., Meyers-Needham, M., Senkal, C.E., Saddoughi, S.A., Sentelle, D., Selvam, S.P., Salas, A., and Ogretmen, B. (2010). Sphingolipids and cancer: ceramide and sphingosine-1-phosphate in the regulation of cell death and drug resistance. Future oncology *6*, 1603-1624.
276. Gallien, S., Duriez, E., Crone, C., Kellmann, M., Moehring, T., and Domon, B. (2012). Targeted proteomic quantification on quadrupole-orbitrap mass spectrometer. Molecular & cellular proteomics : MCP *11*, 1709-1723.
277. Chapman, P.B., Hauschild, A., Robert, C., Haanen, J.B., Ascierto, P., Larkin, J., Dummer, R., Garbe, C., Testori, A., Maio, M., et al. (2011). Improved Survival with Vemurafenib in Melanoma with BRAF V600E Mutation. New England Journal of Medicine *364*, 2507-2516.
278. Prahallad, A., Sun, C., Huang, S., Di Nicolantonio, F., Salazar, R., Zecchin, D., Beijersbergen, R.L., Bardelli, A., and Bernards, R. (2012). Unresponsiveness of colon cancer to BRAF(V600E) inhibition through feedback activation of EGFR. Nature *483*, 100-103.
279. Corcoran, R.B., Ebi, H., Turke, A.B., Coffee, E.M., Nishino, M., Cogdill, A.P., Brown, R.D., Pelle, P.D., Dias-Santagata, D., Hung, K.E., et al. (2012). EGFR-Mediated Reactivation of MAPK Signaling Contributes to Insensitivity of BRAF-Mutant Colorectal Cancers to RAF Inhibition with Vemurafenib. Cancer discovery.
280. Sherman, M.E., Sturgeon, S., Brinton, L.A., Potischman, N., Kurman, R.J., Berman, M.L., Mortel, R., Twiggs, L.B., Barrett, R.J., and Wilbanks, G.D. (1997). Risk factors and hormone levels in patients with serous and endometrioid uterine carcinomas. Mod Pathol *10*, 963-968.
281. Setiawan, V.W., Yang, H.P., Pike, M.C., McCann, S.E., Yu, H., Xiang, Y.B., Wolk, A., Wentzensen, N., Weiss, N.S., Webb, P.M., et al. (2013). Type I and II endometrial cancers: have they different risk factors? Journal of clinical oncology : official journal of the American Society of Clinical Oncology *31*, 2607-2618.
282. Murali, R., Soslow, R.A., and Weigelt, B. (2014). Classification of endometrial carcinoma: more than two types. Lancet Oncol *15*, e268-278.
283. Ruediger, R., Ruiz, J., and Walter, G. (2011). Human cancer-associated mutations in the Aalpha subunit of protein phosphatase 2A increase lung cancer incidence in Aalpha knock-in and knockout mice. Molecular and cellular biology *31*, 3832-3844.
284. Saddoughi, S.A., Gencer, S., Peterson, Y.K., Ward, K.E., Mukhopadhyay, A., Oaks, J., Bielawski, J., Szulc, Z.M., Thomas, R.J., Selvam, S.P., et al. (2013). Sphingosine analogue drug FTY720 targets I2PP2A/SET and mediates lung tumour suppression via activation of PP2A-RIPK1-dependent necroptosis. EMBO molecular medicine *5*, 105-121.
285. Neviani, P., Harb, J.G., Oaks, J.J., Santhanam, R., Walker, C.J., Ellis, J.J., Ferenchak, G., Dorrance, A.M., Paisie, C.A., Eiring, A.M., et al. (2013). PP2A-activating drugs selectively eradicate TKI-resistant chronic myeloid leukemic stem cells. The Journal of Clinical Investigation *123*, 4144-4157.
286. Agarwal, A., MacKenzie, R.J., Pippa, R., Eide, C.A., Oddo, J., Tyner, J.W., Sears, R., Vitek, M.P., Odero, M.D., Christensen, D.J., et al. (2014). Antagonism of SET Using OP449 Enhances the Efficacy of Tyrosine Kinase Inhibitors and Overcomes Drug Resistance in Myeloid Leukemia. Clinical Cancer Research *20*, 2092-2103.

287. Hirai, Y., Kawaguchi, T., Hasumi, K., Kitagawa, T., and Noda, T. (1994). Establishment and characterization of human cell lines from a serous papillary adenocarcinoma of the endometrium. Gynecol Oncol *54*, 184-195.
288. Virshup, D.M., and Shenolikar, S. (2009). From promiscuity to precision: protein phosphatases get a makeover. Molecular cell *33*, 537-545.
289. Moorhead, G.B., Trinkle-Mulcahy, L., and Ulke-Lemee, A. (2007). Emerging roles of nuclear protein phosphatases. Nat Rev Mol Cell Biol *8*, 234-244.
290. Sents, W., Ivanova, E., Lambrecht, C., Haesen, D., and Janssens, V. (2013). The biogenesis of active protein phosphatase 2A holoenzymes: a tightly regulated process creating phosphatase specificity. The FEBS journal *280*, 644-661.
291. Gentry, M.S., and Hallberg, R.L. (2002). Localization of Saccharomyces cerevisiae protein phosphatase 2A subunits throughout mitotic cell cycle. Molecular biology of the cell *13*, 3477-3492.
292. Ghaemmaghami, S., Huh, W.K., Bower, K., Howson, R.W., Belle, A., Dephoure, N., O'Shea, E.K., and Weissman, J.S. (2003). Global analysis of protein expression in yeast. Nature *425*, 737-741.
293. Gingras, A.C., Gstaiger, M., Raught, B., and Aebersold, R. (2007). Analysis of protein complexes using mass spectrometry. Nat Rev Mol Cell Biol *8*, 645-654.
294. Curtis, C., Shah, S.P., Chin, S.F., Turashvili, G., Rueda, O.M., Dunning, M.J., Speed, D., Lynch, A.G., Samarajiwa, S., Yuan, Y., et al. (2012). The genomic and transcriptomic architecture of 2,000 breast tumours reveals novel subgroups. Nature *486*, 346-352.
295. Kalev, P., Simicek, M., Vazquez, I., Munck, S., Chen, L., Soin, T., Danda, N., Chen, W., and Sablina, A. (2012). Loss of PPP2R2A inhibits homologous recombination DNA repair and predicts tumor sensitivity to PARP inhibition. Cancer research *72*, 6414-6424.
296. Bajrami, I., Frankum, J.R., Konde, A., Miller, R.E., Rehman, F.L., Brough, R., Campbell, J., Sims, D., Rafiq, R., Hooper, S., et al. (2014). Genome-wide profiling of genetic synthetic lethality identifies CDK12 as a novel determinant of PARP1/2 inhibitor sensitivity. Cancer research *74*, 287-297.
297. Kim, M.S., Pinto, S.M., Getnet, D., Nirujogi, R.S., Manda, S.S., Chaerkady, R., Madugundu, A.K., Kelkar, D.S., Isserlin, R., Jain, S., et al. (2014). A draft map of the human proteome. Nature *509*, 575-581.
298. Xue, W., Zender, L., Miething, C., Dickins, R.A., Hernando, E., Krizhanovsky, V., Cordon-Cardo, C., and Lowe, S.W. (2007). Senescence and tumour clearance is triggered by p53 restoration in murine liver carcinomas. Nature *445*, 656-660.
299. Hoe, K.K., Verma, C.S., and Lane, D.P. (2014). Drugging the p53 pathway: understanding the route to clinical efficacy. Nat Rev Drug Discov *13*, 217-236.
300. Kurimchak, A., and Grana, X. (2012). PP2A Counterbalances Phosphorylation of pRB and Mitotic Proteins by Multiple CDKs: Potential Implications for PP2A Disruption in Cancer. Genes & cancer *3*, 739-748.
301. Neviani, P., Santhanam, R., Oaks, J.J., Eiring, A.M., Notari, M., Blaser, B.W., Liu, S., Trotta, R., Muthusamy, N., Gambacorti-Passerini, C., et al. (2007). FTY720, a new alternative for treating blast crisis chronic myelogenous leukemia and Philadelphia chromosome-positive acute lymphocytic leukemia. J Clin Invest *117*, 2408-2421.
302. Liu, Q., Zhao, X., Frissora, F., Ma, Y., Santhanam, R., Jarjoura, D., Lehman, A., Perrotti, D., Chen, C.S., Dalton, J.T., et al. (2008). FTY720 demonstrates promising preclinical

activity for chronic lymphocytic leukemia and lymphoblastic leukemia/lymphoma. Blood *111*, 275-284.
303. Wallington-Beddoe, C.T., Don, A.S., Hewson, J., Qiao, Q., Papa, R.A., Lock, R.B., Bradstock, K.F., and Bendall, L.J. (2012). Disparate in vivo efficacy of FTY720 in xenograft models of Philadelphia positive and negative B-lineage acute lymphoblastic leukemia. PloS one *7*, e36429.
304. Wang, J.D., Takahara, S., Nonomura, N., Ichimaru, N., Toki, K., Azuma, H., Matsumiya, K., Okuyama, A., and Suzuki, S. (1999). Early induction of apoptosis in androgen-independent prostate cancer cell line by FTY720 requires caspase-3 activation. The Prostate *40*, 50-55.
305. Li, H., Handsaker, B., Wysoker, A., Fennell, T., Ruan, J., Homer, N., Marth, G., Abecasis, G., and Durbin, R. (2009). The Sequence Alignment/Map format and SAMtools. Bioinformatics *25*, 2078-2079.
306. McKenna, A., Hanna, M., Banks, E., Sivachenko, A., Cibulskis, K., Kernytsky, A., Garimella, K., Altshuler, D., Gabriel, S., Daly, M., et al. (2010). The Genome Analysis Toolkit: a MapReduce framework for analyzing next-generation DNA sequencing data. Genome Res *20*, 1297-1303.
307. Shah, S.P., Morin, R.D., Khattra, J., Prentice, L., Pugh, T., Burleigh, A., Delaney, A., Gelmon, K., Guliany, R., Senz, J., et al. (2009). Mutational evolution in a lobular breast tumour profiled at single nucleotide resolution. Nature *461*, 809-U867.
308. Shah, S.P., Roth, A., Goya, R., Oloumi, A., Ha, G., Zhao, Y., Turashvili, G., Ding, J., Tse, K., Haffari, G., et al. (2012). The clonal and mutational evolution spectrum of primary triple-negative breast cancers. Nature.
309. Reva, B., Antipin, Y., and Sander, C. (2011). Predicting the functional impact of protein mutations: application to cancer genomics. Nucleic Acids Res *39*, e118.

Appendices

Appendix A Chapter 2 Supplemental Tables

Sample No.	Subtype	Mutation	Genomic Location (hg18)	Exon	Amino Acid Change Polarity	Mutation Status
OCCC1	Ovarian clear cell carcinoma	C547T (R183W)	57407794	5	Radical	Somatic
OCCC2	Ovarian clear cell carcinoma	G771T (W257C) C772T (R258C)	57408139 57408140	6	Radical Radical	Somatic
EOC1	Endometrioid ovarian carcinoma	C536G (P179R)	57407783	5	Radical	Somatic
EOC2	Endometrioid ovarian carcinoma	C547T (R183W)	57407794	5	Radical	Somatic
EOC4	Endometrioid ovarian carcinoma	C547T (R183W)	57407794	5	Radical	Somatic
EOC5	Endometrioid ovarian carcinoma	C767A (S256Y)	57408135	6	Radical	Somatic
EOC3	Endometrioid ovarian carcinoma	T769G (W257G)	57408137	6	Radical	Somatic
UtEC1	Endometrioid Uterine Carcinoma	G548A (R183Q)	57407795	5	Radical	Somatic
UtEC3	Endometrioid Uterine Carcinoma	G548A (R183Q)	57407795	5	Radical	Somatic
UtEC2	Endometrioid Uterine Carcinoma	G746A (R249H)	57408114	6	Conservative	Somatic
UtM1	Mixed Uterine Carcinoma	C544T (R182W)	57407791	5	Radical	Somatic
UtHGS1	High-grade serous uterine carcinoma	C536G (P179R)	57407783	5	Radical	Somatic
UtHGS2	High-grade serous uterine carcinoma	C536G (P179R)	57407783	5	Radical	Somatic
UtHGS3	High-grade serous uterine carcinoma	C536G (P179R)	57407783	5	Radical	Somatic
UtHGS19	High-grade serous uterine carcinoma	C536G (P179R)	57407783	5	Radical	Somatic
UtHGS20	High-grade serous uterine carcinoma	C536G (P179R)	57407783	5	Radical	Somatic
UtHGS4	High-grade serous uterine carcinoma	C536T (P179L)	57407783	5	Radical	Somatic
UtHGS5	High-grade serous uterine carcinoma	C536T (P179L)	57407783	5	Radical	Somatic
UtHGS11	High-grade serous uterine carcinoma	C536T (P179L)	57407783	5	Radical	Somatic
UtHGS13	High-grade serous uterine carcinoma	C536G (P179R)	57407783	5	Radical	ND (normal
UtHGS6	High-grade serous uterine carcinoma	C544T (R182W)	57407791	5	Radical	Somatic
UtHGS7	High-grade serous uterine carcinoma	C547T (R183W)	57407794	5	Radical	Somatic
UtHGS17	High-grade serous uterine carcinoma	C547T (R183W)	57407794	5	Radical	Somatic
UtHGS8	High-grade serous uterine carcinoma	C767T (S256F)	57408135	6	Radical	ND (normal
UtHGS9	High-grade serous uterine carcinoma	C767T (S256F)	57408135	6	Radical	Somatic
UtHGS10	High-grade serous uterine carcinoma	C767T (S256F)	57408135	6	Radical	Somatic
UtHGS12	High-grade serous uterine carcinoma	C767T (S256F)	57408135	6	Radical	ND (normal
UtHGS14	High-grade serous uterine carcinoma	C767T (S256F)	57408135	6	Radical	Somatic
UtHGS16	High-grade serous uterine carcinoma	C767T (S256F)	57408135	6	Radical	Somatic
UtHGS18	High-grade serous uterine carcinoma	C767A (S256Y)	57408135	6	Radical	Somatic
UtHGS15	High-grade serous uterine carcinoma	T769G (W257G)	57408137	6	Radical	Somatic

Table A.1 *PPP2R1A* mutations by sample
Identification of *PPP2R1A* mutations by subtype, genomic location, mutation type in cDNA and amino acid changes. The change in amino acid polarity and somatic status is also represented. ND, Not Determined

Sample No.	Tissue	Tumour Type	Tested for PPP2R1A	Mutation Status	Cellularity	p53 IHC score	WT-1 IHC score	ER IHC score	Tumour DNA source	Germline DNA source	Origin
UtHGS1	Endometrial	ESC	Y	Positive - Somatic	70	2	0	1	Froze	FFPE-normal	OvCare Tumour Bank
UtHGS2	Endometrial	ESC	Y	Positive - Somatic	60	2	0	1	Froze	Buffy Coat	OvCare Tumour Bank
UtHGS3	Endometrial	ESC	Y	Positive - Somatic	30	2	0	2	Froze	Buffy Coat	OvCare Tumour Bank
UtHGS4	Endometrial	ESC	Y	Positive - Somatic	90	2	1	2	Froze	Buffy Coat	OvCare Tumour Bank
UtHGS5	Endometrial	ESC	Y	Positive - Somatic	25	2	0	2	Froze	Buffy Coat	OvCare Tumour Bank
UtHGS6	Endometrial	ESC	Y	Positive - Somatic	75	1	0	0	Froze	Buffy Coat	OvCare Tumour Bank
UtHGS7	Endometrial	ESC	Y	Positive - Somatic	50	0	0	1	Froze	FFPE-normal	OvCare Tumour Bank
UtHGS8	Endometrial	ESC	Y	Positive - ND	85	2	0	2	Froze	no normal	OvCare Tumour Bank
UtHGS9	Endometrial	ESC	Y	Positive - Somatic	70	0	0	1	Froze	Buffy Coat	OvCare Tumour Bank
UtHGS10	Endometrial	ESC	Y	Positive - Somatic	85	2	0	2	FFPE	FFPE-normal	VGH Archives
UtHGS11	Endometrial	ESC	Y	Positive - Somatic	90	2	0	1	FFPE	FFPE-normal	VGH Archives
UtHGS12	Endometrial	ESC	Y	Positive - ND	80	0	1	1	FFPE	no normal	VGH Archives
UtHGS13	Endometrial	ESC	Y	Positive - ND	75	2	0	1	FFPE	no normal	VGH Archives
UtHGS14	Endometrial	ESC	Y	Positive - Somatic	80	0	0	1	FFPE	FFPE-normal	VGH Archives
UtHGS15	Endometrial	ESC	Y	Positive - Somatic	80	2	0	2	FFPE	FFPE-normal	VGH Archives
UtHGS16	Endometrial	ESC	Y	Positive - Somatic	75	2	1	1	FFPE	FFPE-normal	VGH Archives
UtHGS17	Endometrial	ESC	Y	Positive - Somatic	65	2	0	0	FFPE	FFPE-normal	VGH Archives
UtHGS18	Endometrial	ESC	Y	Positive - Somatic	90	0	1	1	FFPE	FFPE-normal	VGH Archives
UtHGS19	Endometrial	ESC	Y	Positive - Somatic	85	2	0	1	FFPE	FFPE-normal	VGH Archives
UtHGS20	Endometrial	ESC	Y	Positive - Somatic	85	2	0	2	FFPE	FFPE-normal	VGH Archives
UtHGS21	Endometrial	ESC	Y	Negative	70	2	0	1	FFPE	ND	VGH Archives
UtHGS22	Endometrial	ESC	Y	Negative	85	1	1	1	Froze	ND	OvCare Tumour Bank
UtHGS23	Endometrial	ESC	Y	Negative	30	2	0	2	Froze	ND	OvCare Tumour Bank
UtHGS24	Endometrial	ESC	Y	Negative	85	0	0	0	Froze	ND	OvCare Tumour Bank
UtHGS25	Endometrial	ESC	Y	Negative	80	2	0	1	Froze	ND	OvCare Tumour Bank
UtHGS26	Endometrial	ESC	Y	Negative	30	1	0	2	Froze	ND	OvCare Tumour Bank
UtHGS27	Endometrial	ESC	Y	Negative	90	1	0	1	Froze	ND	OvCare Tumour Bank
UtHGS28	Endometrial	ESC	Y	Negative	90	2	0	1	Froze	ND	OvCare Tumour Bank
UtHGS29	Endometrial	ESC	Y	Negative	75	2	0	1	Froze	ND	OvCare Tumour Bank
UtHGS30	Endometrial	ESC	Y	Negative	40	2	1	0	Froze	ND	OvCare Tumour Bank
UtHGS31	Endometrial	ESC	Y	Negative	20	2	0	1	Froze	ND	OvCare Tumour Bank
UtHGS32	Endometrial	ESC	Y	Negative	55	0	0	1	Froze	ND	OvCare Tumour Bank
UtHGS33	Endometrial	ESC	Y	Negative	50	2	0	1	FFPE	ND	VGH Archives
UtHGS34	Endometrial	ESC	Y	Negative	90	1	0	0	FFPE	ND	VGH Archives
UtHGS35	Endometrial	ESC	Y	Negative	85	0	1	1	FFPE	ND	VGH Archives
UtHGS36	Endometrial	ESC	Y	Negative	90	2	1	2	FFPE	ND	VGH Archives
UtHGS37	Endometrial	ESC	Y	Negative	70	2	0	0	FFPE	ND	VGH Archives

Sample No.	Tissue	Tumour Type	Tested for PPP2R1A	Mutation Status	Cellularity	p53 IHC score	WT-1 IHC score	ER IHC score	Tumour DNA source	Germline DNA source	Origin
UtHGS38	Endometrial	ESC	Y	Negative	90	2	0	0	FFPE	ND	VGH Archives
UtHGS39	Endometrial	ESC	Y	Negative	80	2	1	1	FFPE	ND	VGH Archives
UtHGS40	Endometrial	ESC	Y	Negative	80	2	1	1	FFPE	ND	VGH Archives
UtHGS41	Endometrial	ESC	Y	Negative	50	2	1	2	FFPE	ND	VGH Archives
UtHGS42	Endometrial	ESC	Y	Negative	80	1	0	0	FFPE	ND	VGH Archives
UtHGS43	Endometrial	ESC	Y	Negative	85	2	0	1	FFPE	ND	VGH Archives
UtHGS44	Endometrial	ESC	Y	Negative	35	2	1	1	FFPE	ND	VGH Archives
UtHGS45	Endometrial	ESC	Y	Negative	60	2	0	0	FFPE	ND	VGH Archives
UtHGS46	Endometrial	ESC	Y	Negative	60	0	1	1	FFPE	ND	VGH Archives
UtHGS47	Endometrial	ESC	Y	Negative	60	2	0	2	FFPE	ND	VGH Archives
UtHGS48	Endometrial	ESC	Y	Negative	80	2	0	0	FFPE	ND	VGH Archives
UtHGS49	Endometrial	ESC	Y	Negative	50	2	1	2	FFPE	ND	VGH Archives
UtEC1	Endometrial	EEC	Y	Positive - Somatic	30	ND	ND	ND	Froze	Buffy Coat	OvCare Tumour Bank
UtEC2	Endometrial	EEC	Y	Positive - Somatic	90	ND	ND	ND	Froze	Buffy Coat	OvCare Tumour Bank
UtEC3	Endometrial	EEC	Y	Positive - Somatic	25	ND	ND	ND	Froze	Buffy Coat	OvCare Tumour Bank
UtEC4	Endometrial	EEC	Y	Negative	15	ND	ND	ND	Froze	ND	OvCare Tumour Bank
UtEC5	Endometrial	EEC	Y	Negative	70	ND	ND	ND	Froze	ND	OvCare Tumour Bank
UtEC6	Endometrial	EEC	Y	Negative	25	ND	ND	ND	Froze	ND	OvCare Tumour Bank
UtEC7	Endometrial	EEC	Y	Negative	80	ND	ND	ND	Froze	ND	OvCare Tumour Bank
UtEC8	Endometrial	EEC	Y	Negative	80	ND	ND	ND	Froze	ND	OvCare Tumour Bank
UtEC9	Endometrial	EEC	Y	Negative	25	ND	ND	ND	Froze	ND	OvCare Tumour Bank
UtEC10	Endometrial	EEC	Y	Negative	40	ND	ND	ND	Froze	ND	OvCare Tumour Bank
UtEC11	Endometrial	EEC	Y	Negative	30	ND	ND	ND	Froze	ND	OvCare Tumour Bank
UtEC12	Endometrial	EEC	Y	Negative	80	ND	ND	ND	Froze	ND	OvCare Tumour Bank
UtEC13	Endometrial	EEC	Y	Negative	60	ND	ND	ND	Froze	ND	OvCare Tumour Bank
UtEC14	Endometrial	EEC	Y	Negative	40	ND	ND	ND	Froze	ND	OvCare Tumour Bank
UtEC15	Endometrial	EEC	Y	Negative	40	ND	ND	ND	Froze	ND	OvCare Tumour Bank
UtEC16	Endometrial	EEC	Y	Negative	90	ND	ND	ND	Froze	ND	OvCare Tumour Bank
UtEC17	Endometrial	EEC	Y	Negative	65	ND	ND	ND	Froze	ND	OvCare Tumour Bank
UtEC18	Endometrial	EEC	Y	Negative	50	ND	ND	ND	Froze	ND	OvCare Tumour Bank
UtEC19	Endometrial	EEC	Y	Negative	75	ND	ND	ND	Froze	ND	OvCare Tumour Bank
UtEC20	Endometrial	EEC	Y	Negative	85	ND	ND	ND	Froze	ND	OvCare Tumour Bank
UtEC21	Endometrial	EEC	Y	Negative	80	ND	ND	ND	Froze	ND	OvCare Tumour Bank
UtEC22	Endometrial	EEC	Y	Negative	80	ND	ND	ND	Froze	ND	OvCare Tumour Bank
UtEC23	Endometrial	EEC	Y	Negative	80	ND	ND	ND	Froze	ND	OvCare Tumour Bank
UtEC24	Endometrial	EEC	Y	Negative	80	ND	ND	ND	Froze	ND	OvCare Tumour Bank
UtEC25	Endometrial	EEC	Y	Negative	40	ND	ND	ND	Froze	ND	OvCare Tumour Bank

Sample No.	Tissue	Tumour Type	Tested for PPP2R1A	Mutation Status	Cellularity	p53 IHC score	WT-1 IHC score	ER IHC score	Tumour DNA source	Germline DNA source	Origin
UtEC26	Endometrial	EEC	Y	Negative	30	ND	ND	ND	Froze	ND	OvCare Tumour Bank
UtEC27	Endometrial	EEC	Y	Negative	35	ND	ND	ND	Froze	ND	OvCare Tumour Bank
UtEC28	Endometrial	EEC	Y	Negative	60	ND	ND	ND	Froze	ND	OvCare Tumour Bank
UtEC29	Endometrial	EEC	Y	Negative	55	ND	ND	ND	Froze	ND	OvCare Tumour Bank
UtEC30	Endometrial	EEC	Y	Negative	75	ND	ND	ND	Froze	ND	OvCare Tumour Bank
UtEC31	Endometrial	EEC	Y	Negative	85	ND	ND	ND	Froze	ND	OvCare Tumour Bank
UtEC32	Endometrial	EEC	Y	Negative	80	ND	ND	ND	Froze	ND	OvCare Tumour Bank
UtEC33	Endometrial	EEC	Y	Negative	15	ND	ND	ND	Froze	ND	OvCare Tumour Bank
UtEC34	Endometrial	EEC	Y	Negative	40	ND	ND	ND	Froze	ND	OvCare Tumour Bank
UtEC35	Endometrial	EEC	Y	Negative	65	ND	ND	ND	Froze	ND	OvCare Tumour Bank
UtEC36	Endometrial	EEC	Y	Negative	35	ND	ND	ND	Froze	ND	OvCare Tumour Bank
UtEC37	Endometrial	EEC	Y	Negative	30	ND	ND	ND	Froze	ND	OvCare Tumour Bank
UtEC38	Endometrial	EEC	Y	Negative	75	ND	ND	ND	Froze	ND	OvCare Tumour Bank
UtEC39	Endometrial	EEC	Y	Negative	70	ND	ND	ND	Froze	ND	OvCare Tumour Bank
UtEC40	Endometrial	EEC	Y	Negative	55	ND	ND	ND	Froze	ND	OvCare Tumour Bank
UtEC41	Endometrial	EEC	Y	Negative	70	ND	ND	ND	Froze	ND	OvCare Tumour Bank
UtEC42	Endometrial	EEC	Y	Negative	85	ND	ND	ND	Froze	ND	OvCare Tumour Bank
UtEC43	Endometrial	EEC	Y	Negative	90	ND	ND	ND	Froze	ND	OvCare Tumour Bank
UtEC44	Endometrial	EEC	Y	Negative	85	ND	ND	ND	Froze	ND	OvCare Tumour Bank
UtEC45	Endometrial	EEC	Y	Negative	45	ND	ND	ND	Froze	ND	OvCare Tumour Bank
UtEC46	Endometrial	EEC	Y	Negative	25	ND	ND	ND	Froze	ND	OvCare Tumour Bank
UtEC47	Endometrial	EEC	Y	Negative	45	ND	ND	ND	Froze	ND	OvCare Tumour Bank
UtEC48	Endometrial	EEC	Y	Negative	85	ND	ND	ND	Froze	ND	OvCare Tumour Bank
UtEC49	Endometrial	EEC	Y	Negative	15	ND	ND	ND	Froze	ND	OvCare Tumour Bank
UtEC50	Endometrial	EEC	Y	Negative	45	ND	ND	ND	Froze	ND	OvCare Tumour Bank
UtEC51	Endometrial	EEC	Y	Negative	85	ND	ND	ND	Froze	ND	OvCare Tumour Bank
UtEC52	Endometrial	EEC	Y	Negative	40	ND	ND	ND	Froze	ND	OvCare Tumour Bank
UtEC53	Endometrial	EEC	Y	Negative	15	ND	ND	ND	Froze	ND	OvCare Tumour Bank
UtEC54	Endometrial	EEC	Y	Negative	25	ND	ND	ND	Froze	ND	OvCare Tumour Bank
UtEC55	Endometrial	EEC	Y	Negative	30	ND	ND	ND	Froze	ND	OvCare Tumour Bank
UtEC56	Endometrial	EEC	Y	Negative	50	ND	ND	ND	Froze	ND	OvCare Tumour Bank
UtEC57	Endometrial	EEC	Y	Negative	40	ND	ND	ND	Froze	ND	OvCare Tumour Bank
UtEC58	Endometrial	EEC	Y	Negative	60	ND	ND	ND	Froze	ND	OvCare Tumour Bank
UtEC59	Endometrial	EEC	Y	Negative	35	ND	ND	ND	Froze	ND	OvCare Tumour Bank
UtEC60	Endometrial	EEC	Y	Negative	20	ND	ND	ND	Froze	ND	OvCare Tumour Bank
UtHNPC	Endometrial	HNPCC	Y	Negative	80	ND	ND	ND	Froze	ND	OvCare Tumour Bank
UtM1	Endometrial	Mixed carcinoma	Y	Positive - Somatic	50	ND	ND	ND	Froze	Buffy Coat	OvCare Tumour Bank

Sample No.	Tissue	Tumour Type	Tested for PPP2R1A	Mutation Status	Cellularity	p53 IHC score	WT-1 IHC score	ER IHC score	Tumour DNA source	Germline DNA source	Origin
UtM2	Endometrial	Mixed carcinoma	Y	Negative	40	ND	ND	ND	Froze	ND	OvCare Tumour Bank
UtM3	Endometrial	Mixed carcinoma	Y	Negative	60	ND	ND	ND	Froze	ND	OvCare Tumour Bank
UtCC1	Endometrial	Clear cell	Y	Negative	80	ND	ND	ND	Froze	ND	OvCare Tumour Bank
UtUnd1	Endometrial	Undifferentiated	Y	Negative	70	ND	ND	ND	Froze	ND	OvCare Tumour Bank
UtUnd2	Endometrial	Undifferentiated	Y	Negative	95	ND	ND	ND	Froze	ND	OvCare Tumour Bank
OCCC1	Ovarian	OCCC	Y	Positive - Somatic	90	ND	ND	ND	Froze	FFPE Normal	OvCare Tumour Bank
OCCC2	Ovarian	OCCC	Y	Positive - Somatic	80	ND	ND	ND	Froze	FFPE Normal	OvCare Tumour Bank
OCCC4	Ovarian	OCCC	Y	Negative	85	ND	ND	ND	Froze	ND	OvCare Tumour Bank
OCCC5	Ovarian	OCCC	Y	Negative	80	ND	ND	ND	Froze	ND	OvCare Tumour Bank
OCCC6	Ovarian	OCCC	Y	Negative	60	ND	ND	ND	Froze	ND	OvCare Tumour Bank
OCCC7	Ovarian	OCCC	Y	Negative	90	ND	ND	ND	Froze	ND	OvCare Tumour Bank
OCCC8	Ovarian	OCCC	Y	Negative	80	ND	ND	ND	Froze	ND	OvCare Tumour Bank
OCCC9	Ovarian	OCCC	Y	Negative	35	ND	ND	ND	Froze	ND	OvCare Tumour Bank
OCCC10	Ovarian	OCCC	Y	Negative	50	ND	ND	ND	Froze	ND	OvCare Tumour Bank
OCCC11	Ovarian	OCCC	Y	Negative	50	ND	ND	ND	Froze	ND	OvCare Tumour Bank
OCCC12	Ovarian	OCCC	Y	Negative	60	ND	ND	ND	Froze	ND	OvCare Tumour Bank
OCCC13	Ovarian	OCCC	Y	Negative	65	ND	ND	ND	Froze	ND	OvCare Tumour Bank
OCCC14	Ovarian	OCCC	Y	Negative	65	ND	ND	ND	Froze	ND	OvCare Tumour Bank
OCCC15	Ovarian	OCCC	Y	Negative	50	ND	ND	ND	Froze	ND	OvCare Tumour Bank
OCCC16	Ovarian	OCCC	Y	Negative	70	ND	ND	ND	Froze	ND	OvCare Tumour Bank
OCCC17	Ovarian	OCCC	Y	Negative	75	ND	ND	ND	Froze	ND	OvCare Tumour Bank
OCCC18	Ovarian	OCCC	Y	Negative	65	ND	ND	ND	Froze	ND	OvCare Tumour Bank
OCCC19	Ovarian	OCCC	Y	Negative	85	ND	ND	ND	Froze	ND	OvCare Tumour Bank
OCCC20	Ovarian	OCCC	Y	Negative	85	ND	ND	ND	Froze	ND	OvCare Tumour Bank
OCCC21	Ovarian	OCCC	Y	Negative	90	ND	ND	ND	Froze	ND	OvCare Tumour Bank
OCCC22	Ovarian	OCCC	Y	Negative	80	ND	ND	ND	Froze	ND	OvCare Tumour Bank
OCCC23	Ovarian	OCCC	Y	Negative	75	ND	ND	ND	Froze	ND	OvCare Tumour Bank
OCCC24	Ovarian	OCCC	Y	Negative	70	ND	ND	ND	Froze	ND	OvCare Tumour Bank
OCCC25	Ovarian	OCCC	Y	Negative	85	ND	ND	ND	Froze	ND	OvCare Tumour Bank
OCCC26	Ovarian	OCCC	Y	Negative	70	ND	ND	ND	Froze	ND	OvCare Tumour Bank
OCCC27	Ovarian	OCCC	Y	Negative	75	ND	ND	ND	Froze	ND	OvCare Tumour Bank
OCCC28	Ovarian	OCCC	Y	Negative	60	ND	ND	ND	Froze	ND	OvCare Tumour Bank
OCCC29	Ovarian	OCCC	Y	Negative	85	ND	ND	ND	Froze	ND	OvCare Tumour Bank
OCCC30	Ovarian	OCCC	Y	Negative	60	ND	ND	ND	Froze	ND	OvCare Tumour Bank
OCCC31	Ovarian	OCCC	Y	Negative	40	ND	ND	ND	Froze	ND	OvCare Tumour Bank
OCCC32	Ovarian	OCCC	Y	Negative	65	ND	ND	ND	Froze	ND	OvCare Tumour Bank
OCCC33	Ovarian	OCCC	Y	Negative	ND	ND	ND	ND	Cell	ND	OvCare Tumour Bank

Sample No.	Tissue	Tumour Type	Tested for PPP2R1A	Mutation Status	Cellularity	p53 IHC score	WT-1 IHC score	ER IHC score	Tumour DNA source	Germline DNA source	Origin
OCCC34	Ovarian	OCCC	Y	Negative	ND	ND	ND	ND	Froze	ND	OvCare Tumour Bank
OCCC35	Ovarian	OCCC	Y	Negative	ND	ND	ND	ND	Froze	ND	OvCare Tumour Bank
OCCC36	Ovarian	OCCC	Y	Negative	ND	ND	ND	ND	WG	ND	Montreal Tumour
OCCC37	Ovarian	OCCC	Y	Negative	ND	ND	ND	ND	WG	ND	Montreal Tumour
OCCC38	Ovarian	OCCC	Y	Negative	ND	ND	ND	ND	WG	ND	Montreal Tumour
OCCC39	Ovarian	OCCC	Y	Negative	ND	ND	ND	ND	WG	ND	Montreal Tumour
OCCC40	Ovarian	OCCC	Y	Negative	ND	ND	ND	ND	WG	ND	Montreal Tumour
OCCC41	Ovarian	OCCC	Y	Negative	ND	ND	ND	ND	WG	ND	Montreal Tumour
OCCC42	Ovarian	OCCC	Y	Negative	ND	ND	ND	ND	WG	ND	Montreal Tumour
OCCC43	Ovarian	OCCC	Y	Negative	>50	ND	ND	ND	WG	ND	AOCS
OCCC44	Ovarian	OCCC	Y	Negative	>50	ND	ND	ND	WG	ND	AOCS
OCCC45	Ovarian	OCCC	Y	Negative	>50	ND	ND	ND	WG	ND	AOCS
OCCC46	Ovarian	OCCC	Y	Negative	>50	ND	ND	ND	WG	ND	AOCS
OCCC47	Ovarian	OCCC	Y	Negative	>50	ND	ND	ND	WG	ND	AOCS
OCCC48	Ovarian	OCCC	Y	Negative	>50	ND	ND	ND	WG	ND	AOCS
OCCC49	Ovarian	OCCC	Y	Negative	>50	ND	ND	ND	WG	ND	AOCS
OCCC50	Ovarian	OCCC	Y	Negative	>50	ND	ND	ND	WG	ND	AOCS
EOC1	Ovarian	OEC	Y	Positive - Somatic	50	ND	ND	ND	Froze	FFPE Normal	OvCare Tumour Bank
EOC2	Ovarian	OEC	Y	Positive - Somatic	60	ND	ND	ND	Froze	FFPE Normal	OvCare Tumour Bank
EOC3	Ovarian	OEC	Y	Positive - Somatic	65	ND	ND	ND	Froze	FFPE Normal	OvCare Tumour Bank
EOC4	Ovarian	OEC	Y	Positive - Somatic	80	ND	ND	ND	Froze	Buffy Coat	OvCare Tumour Bank
EOC5	Ovarian	OEC	Y	Positive - Somatic	70	ND	ND	ND	Froze	Buffy Coat	OvCare Tumour Bank
EOC7	Ovarian	OEC	Y	Negative	80	ND	ND	ND	Froze	ND	OvCare Tumour Bank
EOC8	Ovarian	OEC	Y	Negative	85	ND	ND	ND	Froze	ND	OvCare Tumour Bank
EOC9	Ovarian	OEC	Y	Negative	65	ND	ND	ND	Froze	ND	OvCare Tumour Bank
EOC10	Ovarian	OEC	Y	Negative	65	ND	ND	ND	Froze	ND	OvCare Tumour Bank
EOC11	Ovarian	OEC	Y	Negative	70	ND	ND	ND	Froze	ND	OvCare Tumour Bank
EOC12	Ovarian	OEC	Y	Negative	85	ND	ND	ND	Froze	ND	OvCare Tumour Bank
EOC13	Ovarian	OEC	Y	Negative	60	ND	ND	ND	Froze	ND	OvCare Tumour Bank
EOC14	Ovarian	OEC	Y	Negative	70	ND	ND	ND	Froze	ND	OvCare Tumour Bank
EOC15	Ovarian	OEC	Y	Negative	30	ND	ND	ND	Froze	ND	OvCare Tumour Bank
EOC16	Ovarian	OEC	Y	Negative	60	ND	ND	ND	Froze	ND	OvCare Tumour Bank
EOC17	Ovarian	OEC	Y	Negative	55	ND	ND	ND	Froze	ND	OvCare Tumour Bank
EOC18	Ovarian	OEC	Y	Negative	75	ND	ND	ND	Froze	ND	OvCare Tumour Bank
EOC19	Ovarian	OEC	Y	Negative	80	ND	ND	ND	Froze	ND	OvCare Tumour Bank
EOC20	Ovarian	OEC	Y	Negative	60	ND	ND	ND	Froze	ND	OvCare Tumour Bank
EOC21	Ovarian	OEC	Y	Negative	55	ND	ND	ND	Froze	ND	OvCare Tumour Bank

Sample No.	Tissue	Tumour Type	Tested for PPP2R1A	Mutation Status	Cellularity	p53 IHC score	WT-1 IHC score	ER IHC score	Tumour DNA source	Germline DNA source	Origin
EOC22	Ovarian	OEC	Y	Negative	80	ND	ND	ND	Froze	ND	OvCare Tumour Bank
EOC23	Ovarian	OEC	Y	Negative	60	ND	ND	ND	Froze	ND	OvCare Tumour Bank
EOC24	Ovarian	OEC	Y	Negative	80	ND	ND	ND	Froze	ND	OvCare Tumour Bank
EOC25	Ovarian	OEC	Y	Negative	75	ND	ND	ND	Froze	ND	OvCare Tumour Bank
EOC26	Ovarian	OEC	Y	Negative	80	ND	ND	ND	Froze	ND	OvCare Tumour Bank
EOC27	Ovarian	OEC	Y	Negative	85	ND	ND	ND	Froze	ND	OvCare Tumour Bank
EOC28	Ovarian	OEC	Y	Negative	60	ND	ND	ND	Froze	ND	OvCare Tumour Bank
EOC29	Ovarian	OEC	Y	Negative	50	ND	ND	ND	Froze	ND	OvCare Tumour Bank
EOC30	Ovarian	OEC	Y	Negative	55	ND	ND	ND	Froze	ND	OvCare Tumour Bank
EOC31	Ovarian	OEC	Y	Negative	65	ND	ND	ND	Froze	ND	OvCare Tumour Bank
EOC32	Ovarian	OEC	Y	Negative	70	ND	ND	ND	Froze	ND	OvCare Tumour Bank
EOC34	Ovarian	OEC	Y	Negative	40	ND	ND	ND	Froze	ND	OvCare Tumour Bank
EOC35	Ovarian	OEC	Y	Negative	50	ND	ND	ND	Froze	ND	OvCare Tumour Bank
EOC36	Ovarian	OEC	Y	Negative	40	ND	ND	ND	Froze	ND	OvCare Tumour Bank
EOC37	Ovarian	OEC	Y	Negative	60	ND	ND	ND	Froze	ND	OvCare Tumour Bank
EOC38	Ovarian	OEC	Y	Negative	75	ND	ND	ND	Froze	ND	OvCare Tumour Bank
EOC39	Ovarian	OEC	Y	Negative	55	ND	ND	ND	Froze	ND	OvCare Tumour Bank
EOC40	Ovarian	OEC	Y	Negative	80	ND	ND	ND	Froze	ND	OvCare Tumour Bank
EOC41	Ovarian	OEC	Y	Negative	55	ND	ND	ND	Froze	ND	OvCare Tumour Bank
EOC42	Ovarian	OEC	Y	Negative	80	ND	ND	ND	Froze	ND	OvCare Tumour Bank
EOC43	Ovarian	OEC	Y	Negative	85	ND	ND	ND	Froze	ND	OvCare Tumour Bank
OHGS1	Ovarian	OHGSC	Y	Negative	85	ND	ND	ND	Froze	ND	OvCare Tumour Bank
OHGS2	Ovarian	OHGSC	Y	Negative	65	ND	ND	ND	Froze	ND	OvCare Tumour Bank
OHGS3	Ovarian	OHGSC	Y	Negative	70	ND	ND	ND	Froze	ND	OvCare Tumour Bank
OHGS4	Ovarian	OHGSC	Y	Negative	30	ND	ND	ND	Froze	ND	OvCare Tumour Bank
OHGS5	Ovarian	OHGSC	Y	Negative	90	ND	ND	ND	Froze	ND	OvCare Tumour Bank
OHGS6	Ovarian	OHGSC	Y	Negative	80	ND	ND	ND	Froze	ND	OvCare Tumour Bank
OHGS7	Ovarian	OHGSC	Y	Negative	85	ND	ND	ND	Froze	ND	OvCare Tumour Bank
OHGS8	Ovarian	OHGSC	Y	Negative	85	ND	ND	ND	Froze	ND	OvCare Tumour Bank
OHGS9	Ovarian	OHGSC	Y	Negative	70	ND	ND	ND	Froze	ND	OvCare Tumour Bank
OHGS10	Ovarian	OHGSC	Y	Negative	90	ND	ND	ND	Froze	ND	OvCare Tumour Bank
OHGS11	Ovarian	OHGSC	Y	Negative	70	ND	ND	ND	Froze	ND	OvCare Tumour Bank
OHGS12	Ovarian	OHGSC	Y	Negative	80	ND	ND	ND	Froze	ND	OvCare Tumour Bank
OHGS13	Ovarian	OHGSC	Y	Negative	90	ND	ND	ND	Froze	ND	OvCare Tumour Bank
OHGS14	Ovarian	OHGSC	Y	Negative	90	ND	ND	ND	Froze	ND	OvCare Tumour Bank
OHGS15	Ovarian	OHGSC	Y	Negative	85	ND	ND	ND	Froze	ND	OvCare Tumour Bank
OHGS16	Ovarian	OHGSC	Y	Negative	80	ND	ND	ND	Froze	ND	OvCare Tumour Bank

Sample No.	Tissue	Tumour Type	Tested for PPP2R1A	Mutation Status	Cellularity	p53 IHC score	WT-1 IHC score	ER IHC score	Tumour DNA source	Germline DNA source	Origin
OHGS17	Ovarian	OHGSC	Y	Negative	70	ND	ND	ND	Froze	ND	OvCare Tumour Bank
OHGS18	Ovarian	OHGSC	Y	Negative	75	ND	ND	ND	Froze	ND	OvCare Tumour Bank
OHGS19	Ovarian	OHGSC	Y	Negative	70	ND	ND	ND	Froze	ND	OvCare Tumour Bank
OHGS20	Ovarian	OHGSC	Y	Negative	65	ND	ND	ND	Froze	ND	OvCare Tumour Bank
OHGS21	Ovarian	OHGSC	Y	Negative	80	ND	ND	ND	Froze	ND	OvCare Tumour Bank
OHGS22	Ovarian	OHGSC	Y	Negative	25	ND	ND	ND	Froze	ND	OvCare Tumour Bank
OHGS23	Ovarian	OHGSC	Y	Negative	70	ND	ND	ND	Froze	ND	OvCare Tumour Bank
OHGS24	Ovarian	OHGSC	Y	Negative	80	ND	ND	ND	Froze	ND	OvCare Tumour Bank
OHGS25	Ovarian	OHGSC	Y	Negative	55	ND	ND	ND	Froze	ND	OvCare Tumour Bank
OHGS26	Ovarian	OHGSC	Y	Negative	80	ND	ND	ND	Froze	ND	OvCare Tumour Bank
OHGS27	Ovarian	OHGSC	Y	Negative	65	ND	ND	ND	Froze	ND	OvCare Tumour Bank
OHGS28	Ovarian	OHGSC	Y	Negative	75	ND	ND	ND	Froze	ND	OvCare Tumour Bank
OHGS29	Ovarian	OHGSC	Y	Negative	80	ND	ND	ND	Froze	ND	OvCare Tumour Bank
OHGS30	Ovarian	OHGSC	Y	Negative	60	ND	ND	ND	Froze	ND	OvCare Tumour Bank
OHGS31	Ovarian	OHGSC	Y	Negative	35	ND	ND	ND	Froze	ND	OvCare Tumour Bank
OHGS32	Ovarian	OHGSC	Y	Negative	80	ND	ND	ND	Froze	ND	OvCare Tumour Bank
OHGS33	Ovarian	OHGSC	Y	Negative	85	ND	ND	ND	Froze	ND	OvCare Tumour Bank
OHGS34	Ovarian	OHGSC	Y	Negative	70	ND	ND	ND	Froze	ND	OvCare Tumour Bank
OHGS35	Ovarian	OHGSC	Y	Negative	80	ND	ND	ND	Froze	ND	OvCare Tumour Bank
OHGS36	Ovarian	OHGSC	Y	Negative	80	ND	ND	ND	Froze	ND	OvCare Tumour Bank
OHGS37	Ovarian	OHGSC	Y	Negative	75	ND	ND	ND	Froze	ND	OvCare Tumour Bank
OHGS38	Ovarian	OHGSC	Y	Negative	90	ND	ND	ND	Froze	ND	OvCare Tumour Bank
OHGS39	Ovarian	OHGSC	Y	Negative	50	ND	ND	ND	Froze	ND	OvCare Tumour Bank
OHGS40	Ovarian	OHGSC	Y	Negative	60	ND	ND	ND	Froze	ND	OvCare Tumour Bank
OHGS41	Ovarian	OHGSC	Y	Negative	70	ND	ND	ND	Froze	ND	OvCare Tumour Bank
OHGS42	Ovarian	OHGSC	Y	Negative	55	ND	ND	ND	Froze	ND	OvCare Tumour Bank
OHGS43	Ovarian	OHGSC	Y	Negative	55	ND	ND	ND	Froze	ND	OvCare Tumour Bank
OHGS44	Ovarian	OHGSC	Y	Negative	65	ND	ND	ND	Froze	ND	OvCare Tumour Bank
OHGS45	Ovarian	OHGSC	Y	Negative	70	ND	ND	ND	Froze	ND	OvCare Tumour Bank
OHGS46	Ovarian	OHGSC	Y	Negative	80	ND	ND	ND	Froze	ND	OvCare Tumour Bank
OHGS47	Ovarian	OHGSC	Y	Negative	75	ND	ND	ND	Froze	ND	OvCare Tumour Bank
OHGS48	Ovarian	OHGSC	Y	Negative	70	ND	ND	ND	Froze	ND	OvCare Tumour Bank
OHGS49	Ovarian	OHGSC	Y	Negative	60	ND	ND	ND	Froze	ND	OvCare Tumour Bank
OHGS50	Ovarian	OHGSC	Y	Negative	70	ND	ND	ND	FFPE	ND	VGH Archives
OLGS1	Ovarian	OLGSC	Y	Negative	ND	ND	ND	ND	Cell	ND	Cell Line
OLGS2	Ovarian	OLGSC	Y	Negative	65	ND	ND	ND	Froze	ND	OvCare Tumour Bank
OLGS3	Ovarian	OLGSC	Y	Negative	55	ND	ND	ND	Froze	ND	OvCare Tumour Bank

Sample No.	Tissue	Tumour Type	Tested for PPP2R1A	Mutation Status	Cellularity	p53 IHC score	WT-1 IHC score	ER IHC score	Tumour DNA source	Germline DNA source	Origin
OLGS4	Ovarian	OLGSC	Y	Negative	70	ND	ND	ND	Froze	ND	OvCare Tumour Bank
OLGS5	Ovarian	OLGSC	Y	Negative	75	ND	ND	ND	Froze	ND	OvCare Tumour Bank
OLGS6	Ovarian	OLGSC	Y	Negative	25	ND	ND	ND	Froze	ND	OvCare Tumour Bank
OLGS7	Ovarian	OLGSC	Y	Negative	90	ND	ND	ND	Froze	ND	OvCare Tumour Bank
OLGS8	Ovarian	OLGSC	Y	Negative	75	ND	ND	ND	Froze	ND	OvCare Tumour Bank
OLGS9	Ovarian	OLGSC	Y	Negative	50	ND	ND	ND	Froze	ND	OvCare Tumour Bank
OLGS10	Ovarian	OLGSC	Y	Negative	50	ND	ND	ND	Froze	ND	OvCare Tumour Bank
OLGS11	Ovarian	OLGSC	Y	Negative	60	ND	ND	ND	Froze	ND	OvCare Tumour Bank
OLGS12	Ovarian	OLGSC	Y	Negative	50	ND	ND	ND	Froze	ND	OvCare Tumour Bank

Table A.2 Endometrial and ovarian carcinomas dataset information
Identification of all endometrial and ovarian cases showing subtype, tumour type, mutation status, cellularity, IHC scoring (if applicable), tumour DNA source, germline DNA source, and origin. Scores for IHC staining are as follows: p53 (0= no staining, truncating mutation, 1=normal, 2=high staining, missense mutation), WT-1 (0=no staining, 1= positive staining), ER (0=no staining, 1=greater than 1% staining, 2=greater than 50% staining).

Appendix B Chapter 3 Supplemental Materials and Methods, Tables and Figures

B.1 Materials and Methods

Bioinformatics Analysis

Image analysis, base-calling and error calibration were performed using SCS 2.6 and 2.8 and RTA 1.5 through 1.8 analysis pipelines (Illumina). The exon capture libraries were sequenced using the Illumina Genome Analyzer (GAIIx) as 76bp pair-end reads. These short reads were aligned to the human genome (hg18) using the BWA aligner version v0.5.9 [171]. Subsequent analysis such as sam/bam file format conversation, sorting and indexing was conducted by Samtools version v0.16 [305].

Reads around indels were realigned using the full Smith-Waterman alignment algorithm implemented in the Genome Analysis Toolkit (GATK) version v1.0.5543M [306]. Indels were called by the Samtools pileup command, and were reported if a minimum of 10% of all reads aligned to the position containing the indel, and the minimum local realignment score was larger than or equal to 300.

Duplicate fragments from polymerase chain reaction (PCR) were removed by Picard v1.44 (http://picard.sourceforge.net/). SNVs were initially called by binomial exact test as previously described in [307]. To remove artifacts, we used a Random Forest classifier trained on validated SNVs as in [172]. Only a subset of the tumours had matched normal DNA, therefore a pairwise analysis could not be performed. Instead, only the forty features constructed from the tumours [172]was used to train a classifier on about 1000 validated somatic mutations and about 2000 wild-type positions from triple negative breast cancer exome capture data [308]. This classifier provides a probability of each site being a variant, therefore an optimal threshold was set to separate true SNVs from false positive predictions. We assumed the predicted positions, also in the COSMIC database [173], are true positives and selected a threshold so 99% of the true positives could be kept (Figure S1). The probability distribution of these SNVs was fitted by a Gaussian distribution, and the threshold was the mean minus 1.98 standard deviations of the estimated Gaussian distribution. The predicted SNVs were filtered through dbSNP, 1000 Genome (http://www.1000genomes.org/) and the control normals to remove germline

polymorphisms. All SNVs were profiled by MutationAssessor [309], which predicts the functional impact of each missense mutation. The SNVs were also annotated by snpEff (http://snpeff.sourceforge.net/) to find splice site mutations. All silent mutations were removed. The indels were also filtered by the control normals and then profiled by Oncotator (http://www.broadinstitute.org/oncotator/). Thirty-eight of the total 392 cases did not have mutations detected from this gene panel. To determine if these are false negatives, we investigated the mean coverage of the 9 genes (Figure 0.2), with and without mutations, across all tumour cases. We then removed any cases (n=20) whose maximum mean coverage across all the genes was less than 10 reads, to account for poor DNA used for sequencing.

DNA Validation

A subset of the SNVs and indels called by bioinformatics' analysis were validated by Sanger sequencing. We validated 340 predicted positions that were present in all 9 genes tested. 330/340 (97%) positions were validated as true positive, and 10/340 (2.9%) were considered false positive. The majority of these false positives have low-frequency reads (<10%), therefore Sanger sequencing may not be sensitive enough to identify these mutations if tumour cellularity is low. We validated a range of called mutations with low and high frequency and probability. All others were considered true positive unless otherwise indicated.

Primer List

Gene Name	Exon	Primer Sequence (with M13F and M13R)
PTEN-exon1-F	1	TGTAAAACGACGGCCAGTCAAGTCCAGAGCCATTTCCATCCT
PTEN-exon1-R	1	CAGGAAACAGCTATGACTTTCGCATCCGTCTACTCCCACGTT
PTEN-EXON2-F	2	TGTAAAACGACGGCCAGTTCTCATATACCTGAATACTGTCCATGTG
PTEN-EXON2-R	2	CAGGAAACAGCTATGACGAAGTCCATTAGGTACGGTAAGCC
PTEN-EXON3-F	3	TGTAAAACGACGGCCAGTACATGATTACTACTCTAAACCCATAGAAGG
PTEN-EXON3-R	3	CAGGAAACAGCTATGACGCTCTTGGACTTCTTGACTTAATCGG
PTEN-exon7-F	7	TGTAAAACGACGGCCAGTGCTTGAGATCAAGATTGCAGATACAG
PTEN-exon7-R	7	CAGGAAACAGCTATGACGTCTCACCAATGCCAGAGTAAGCA
PTEN-exon8-F	8	TGTAAAACGACGGCCAGTTGCAACAGATAACTCAGATTGCCT
PTEN-exon8-R	8	CAGGAAACAGCTATGACGCAAGTTCTTCATCAGCTGTACTCC
PTEN-EXON9-F	9	TGTAAAACGACGGCCAGTCCTCTTAAAGATCATGTTTGTTACAGTGCT
PTEN-EXON9-R	9	CAGGAAACAGCTATGACTCTGACACAATGTCCTATTGCCA
ARID1A_x4F	4	TGTAAAACGACGGCCAGTCAGTCCCATAACCCTTTCACA
ARID1A_x4R	4	CAGGAAACAGCTATGACAGTCAGCCTTTAAGTTCCTTGA
ARID1A_x6F	6	TGTAAAACGACGGCCAGTGGGAGGTACTTGGCCTCTTC
ARID1A_x6R	6	CAGGAAACAGCTATGACAATTTGCTGCAGGGATTGTC

Gene Name	Exon	Primer Sequence (with M13F and M13R)
ARID1A_x7F	7	TGTAAAACGACGGCCAGTTCCCAGGATAAGGATGGAGA
ARID1A_x7R	7	CAGGAAACAGCTATGACCTTGCCTTGCCCTACTTCAG
ARID1A_x8F	8	TGTAAAACGACGGCCAGTCCCTTTTTCTCATGGCGATA
ARID1A_x8R	8	CAGGAAACAGCTATGACTTGCACTGACACCCTCTCTG
ARID1A_x12F	12	TGTAAAACGACGGCCAGTCTTATGGGCAGGAAAACCAG
ARID1A_x12R	12	CAGGAAACAGCTATGACTGTTAAGCCCTGTGGTAGGG
ARID1A_x13_14F	13_14	TGTAAAACGACGGCCAGTCACTGTCATGCCAAGCAAAC
ARID1A_x13_14R	13_14	CAGGAAACAGCTATGACCATTTCACTGGCCCTGTCTT
ARID1A_x16_17F	16	TGTAAAACGACGGCCAGTCCCAGCACCCTGAAGCTAT
ARID1A_x16_17R	16	CAGGAAACAGCTATGACCTAGTTTTCAAGGCGAACCTG
ARID1A_x20set1F	20_1	TGTAAAACGACGGCCAGTGCAAGTTTCCATTTGGCATT
ARID1A_x20set1R	20_1	CAGGAAACAGCTATGACCACATTGTTGTCCTGGATGC
ARID1A_x20set2F	20_2	TGTAAAACGACGGCCAGTCGCAGAGACTGGTCTTGGA
ARID1A_x20set2R	20_2	CAGGAAACAGCTATGACGCATAAATAAAGGGCAACAGTCA
ARID1A_20_F	20	TGTAAAACGACGGCCAGTGCAACTCTGCCTCTCCCAACTGAT
ARID1A_20_R	20	CAGGAAACAGCTATGACAGGGTCACCCACCTCATACTCCTTT
ARID1A_18_F	18	TGTAAAACGACGGCCAGTAACAAGCTGCCCAGCCTTCC
ARID1A_18_R	18	CAGGAAACAGCTATGACAGCCCATCATTTGTGGTGGCATGTT
ARID1A_18_F	18	TGTAAAACGACGGCCAGTAATTATGCCAACAGGCAGAGCACG
ARID1A_18_R	18	CAGGAAACAGCTATGACAGGGCTGGTAGTTAGATGGAGGG
ARID1A_19_F	19	TGTAAAACGACGGCCAGTCGGGTAATGATGTCCCTCAAGTCT
ARID1A_19_R	19	CAGGAAACAGCTATGACAGAGAAAGAGAAAGACCAAGGTGGC
ARID1A_5_F	5	TGTAAAACGACGGCCAGTATTTCCAGCAGCCAAGGAGAGCA
ARID1A_5_R	5	CAGGAAACAGCTATGACATCACCTTTCCCTCTCCCTAAAGCC
KRAS_Forward	2	TGTAAAACGACGGCCAGTAAAAGGTACTGGTGGAGTATTTGA
KRAS_Reverse	2	CAGGAAACAGCTATGACTTGAAACCCAAGGTACATTTCA
KRAS_ex3_F	3	TGTAAAACGACGGCCAGTCCAGACTGTGTTTCTCCCTTC
KRAS_ex3_R	3	CAGGAAACAGCTATGACCTGCTCTAATCCCCCAAGAA
KRAS ex4_F	4	TGTAAAACGACGGCCAGTTGACAAAAGTTGTGGACAGGT
KRAS ex4_R	4	CAGGAAACAGCTATGACAAGAAGCAATGCCCTCTCAA
BRAF_ex1_F	1	TGTAAAACGACGGCCAGT CTAGCGTCCTTCCCCCAAT
BRAF_ex1_R	1	CAGGAAACAGCTATGAC CCGCCTCTTTCCAAAATAAA
BRAF_ex3_F	3	TGTAAAACGACGGCCAGTACCCTATCAACTGGTGAAAAGA
BRAF_ex3_R	3	CAGGAAACAGCTATGACTGCCTCTATTTGCATGACCTC
BRAF_ex4_F	4	TGTAAAACGACGGCCAGTTTGCTCCCTTTACCTCTTATCA
BRAF_ex4_R	4	CAGGAAACAGCTATGACTTTCAATTCCCTAGGTTTTGG
BRAF_ex7_F	7	TGTAAAACGACGGCCAGTGAAGCTTCTGGGTTTTGCAC
BRAF_ex7_R	7	CAGGAAACAGCTATGACTTGGGGAAAAAGTCCTTAATTT
BRAF_ex13_F	13	TGTAAAACGACGGCCAGTCCGACAGACTACTTTGGTTCTC
BRAF_ex13_R	13	CAGGAAACAGCTATGACCCAAAAGAATAGCAGCCAAAA
BRAF_ex15_F	15	TGTAAAACGACGGCCAGTTGCTTGCTCTGATAGGAAAATG
BRAF_ex15_R	15	CAGGAAACAGCTATGACAGTAACTCAGCAGCATCTCAGG
BRAF_ex17_F	17	TGTAAAACGACGGCCAGTGGGTTTCCCACCATCTATGA

Gene Name	Exon	Primer Sequence (with M13F and M13R)
BRAF_ex17_R	17	CAGGAAACAGCTATGACTTCTTTTGGATAGCATGAAGC
CTNNB1_ex3_F	3	TGTAAAACGACGGCCAGTCCCTGGCTATCATTCTGCTT
CTNNB1_ex3_R	3	CAGGAAACAGCTATGACTCAAAACTGCATTCTGACTTTCA
CTNNB1_ex4_F	4	TGTAAAACGACGGCCAGTAGGTAAATGCTGAACTGTGGA
CTNNB1_ex4_R	4	CAGGAAACAGCTATGACTGGTATTGGGTAGACATTCTGAAA
CTNNB1_ex5_F	5	TGTAAAACGACGGCCAGTAACGATGTTTCTGAATTCCTGT
CTNNB1_ex5_R	5	CAGGAAACAGCTATGACTCCAATGCTCCATGAAAACC
CTNNB1_ex7_F	7	TGTAAAACGACGGCCAGTTGGCTCTTCTCAGACATGTGAT
CTNNB1_ex7_R	7	CAGGAAACAGCTATGACTGGCTGCAAACTGAATAGGA
CTNNB1_ex8_9_F	8_9	TGTAAAACGACGGCCAGTGAAGGACACCTCCTAAGGCTA
CTNNB1_ex8_9_R	8_9	CAGGAAACAGCTATGACTGCTTCATTTTCAATTCTGCAA
CTNNB1_ex10_F	10	TGTAAAACGACGGCCAGTGTGTGGTGGGAATTTTAGGG
CTNNB1_ex10_R	10	CAGGAAACAGCTATGACGCTCTTCAGGAAGACGGATG
PIK3CA_ex2_F	2	TGTAAAACGACGGCCAGTTGCTTTGGGACAACCATACA
PIK3CA_ex2_R	2	CAGGAAACAGCTATGACCTAAGTCATCCCACAAATGACA
PIK3CA_ex5_F	5	TGTAAAACGACGGCCAGTTTTGATTGATCTTGTGCTTCAA
PIK3CA_ex5_R	5	CAGGAAACAGCTATGACTGGATGTTCTCCTAACCATCTG
PIK3CA_ex6_F	6	TGTAAAACGACGGCCAGTATTAGTGGATGAAGGCAGCA
PIK3CA_ex6_R	6	CAGGAAACAGCTATGACAATGGGGTCTTGCTTTGTTG
PIK3CA_ex8_F	8	TGTAAAACGACGGCCAGTCTCATGCTTGCTTTGGTTCA
PIK3CA_ex8_R	8	CAGGAAACAGCTATGACTTGGCATGCTCTTCAATCAC
PIK3CA_ex11_F	11	TGTAAAACGACGGCCAGTTCCATTTGCATTTTCCTTTTG
PIK3CA_ex11_R	11	CAGGAAACAGCTATGACTGTGGACTTTCTGAGAGAAAACA
PIK3CA_ex12_F	12	TGTAAAACGACGGCCAGTGGCAGTGTTTTAGATGGCTCA
PIK3CA_ex12_R	12	CAGGAAACAGCTATGACCAAATCAGGGTCAGTTTCTGC
PIK3CA_ex15_F	15	TGTAAAACGACGGCCAGTACACAGTGCTGCCAGTCTTG
PIK3CA_ex15_R	15	CAGGAAACAGCTATGACTTGAGGGTAGGAGAATGAGAGA
PPP2R5C_ex2_F	2	TGTAAAACGACGGCCAGTTTGTTTACCCCACCCATCTC
PPP2R5C_ex2_R	2	CAGGAAACAGCTATGACTCAGAACTGGGACACACTGG
PPP2R5C_ex6_F	6	TGTAAAACGACGGCCAGTGATCAAGCAGATGGAGCACA
PPP2R5C_ex6_R	6	CAGGAAACAGCTATGACGGCAGCTGGACTCAATGAA
PPP2R5C_ex8_F	8	TGTAAAACGACGGCCAGTAATGCCCGTTAATCACACAA
PPP2R5C_ex8_R	8	CAGGAAACAGCTATGACGAATGGCAATTTGGTGAAGC

Statistical Plots and Cluster Analysis

The R package (2.14.2) was used to plot the probability distribution (Figure B.1), and the mean-coverage plots (Figure B.2). Unsupervised hierarchical clustering of mutations used Hammings distance and single linkage analysis (Figures B.3). The mutations were binarized into 0=no mutation, 1=with mutation, IHC scores were 0 and 1, however for p53 scoring, 0, 1, 2 was used

B.2 **Supplemental Tables**

Chromosome	Probe genomic location start (hg18)	Probe genomic location end (hg18)	Gene Name	Exon
chr3	180399230	180399659	PIK3CA	Exon001
chr3	180400171	180400381	PIK3CA	Exon002
chr3	180401771	180402022	PIK3CA	Exon003
chr3	180404025	180404271	PIK3CA	Exon004
chr3	180404984	180405070	PIK3CA	Exon005
chr3	180410076	180410182	PIK3CA	Exon006
chr3	180410667	180410820	PIK3CA	Exon007
chr3	180410912	180411047	PIK3CA	Exon008
chr3	180418691	180418816	PIK3CA	Exon009
chr3	180419677	180419759	PIK3CA	Exon010
chr3	180420052	180420217	PIK3CA	Exon011
chr3	180420430	180420534	PIK3CA	Exon012
chr3	180421467	180421639	PIK3CA	Exon013
chr3	180424562	180424669	PIK3CA	Exon014
chr3	180425181	180425303	PIK3CA	Exon015
chr3	180426443	180426522	PIK3CA	Exon016
chr3	180429753	180429924	PIK3CA	Exon017
chr3	180430485	180430603	PIK3CA	Exon018
chr3	180430706	180430858	PIK3CA	Exon019
chr3	180434575	180434928	PIK3CA	Exon020
chr3	180399230	180399659	PIK3CA	Exon001
chr3	180400171	180400381	PIK3CA	Exon002
chr3	180401771	180402022	PIK3CA	Exon003
chr3	180404025	180404271	PIK3CA	Exon004
chr3	180404984	180405070	PIK3CA	Exon005
chr3	180410076	180410182	PIK3CA	Exon006
chr3	180410667	180410820	PIK3CA	Exon007
chr3	180410912	180411047	PIK3CA	Exon008
chr3	180418691	180418816	PIK3CA	Exon009
chr3	180419677	180419759	PIK3CA	Exon010
chr3	180420052	180420217	PIK3CA	Exon011
chr3	180420430	180420534	PIK3CA	Exon012
chr3	180421467	180421639	PIK3CA	Exon013
chr3	180424562	180424669	PIK3CA	Exon014
chr3	180425181	180425303	PIK3CA	Exon015
chr3	180426443	180426522	PIK3CA	Exon016
chr3	180429753	180429924	PIK3CA	Exon017

Chromosome	Probe genomic location start (hg18)	Probe genomic location end (hg18)	Gene Name	Exon
chr3	180430485	180430603	PIK3CA	Exon018
chr3	180430706	180430858	PIK3CA	Exon019
chr3	180434575	180434922	PIK3CA	Exon020
chr7	140080825	140081039	BRAF	Exon001
chr7	140086080	140086215	BRAF	Exon002
chr7	140095555	140095687	BRAF	Exon003
chr7	140099543	140099662	BRAF	Exon004
chr7	140100455	140100502	BRAF	Exon005
chr7	140123180	140123357	BRAF	Exon006
chr7	140124259	140124344	BRAF	Exon007
chr7	140127844	140127962	BRAF	Exon008
chr7	140129289	140129426	BRAF	Exon009
chr7	140133816	140133853	BRAF	Exon010
chr7	140140576	140140736	BRAF	Exon011
chr7	140146630	140146750	BRAF	Exon012
chr7	140147680	140147829	BRAF	Exon013
chr7	140154228	140154331	BRAF	Exon014
chr7	140155160	140155264	BRAF	Exon015
chr7	140180877	140181141	BRAF	Exon016
chr7	140196379	140196481	BRAF	Exon017
chr7	140270834	140270994	BRAF	Exon018
chr7	140080822	140081039	BRAF	Exon001
chr7	140086080	140086215	BRAF	Exon002
chr7	140095555	140095687	BRAF	Exon003
chr7	140099543	140099662	BRAF	Exon004
chr7	140100455	140100502	BRAF	Exon005
chr7	140123180	140123357	BRAF	Exon006
chr7	140124259	140124344	BRAF	Exon007
chr7	140127844	140127962	BRAF	Exon008
chr7	140129289	140129426	BRAF	Exon009
chr7	140133816	140133853	BRAF	Exon010
chr7	140140576	140140736	BRAF	Exon011
chr7	140146630	140146750	BRAF	Exon012
chr7	140147680	140147829	BRAF	Exon013
chr7	140154228	140154331	BRAF	Exon014
chr7	140155160	140155264	BRAF	Exon015
chr7	140180877	140181141	BRAF	Exon016
chr7	140196379	140196481	BRAF	Exon017
chr7	140270834	140270994	BRAF	Exon018
chr10	89613369	89613840	PTEN	Exon001
chr10	89613841	89614285	PTEN	Exon002
chr10	89643761	89643846	PTEN	Exon003
chr10	89675249	89675294	PTEN	Exon004
chr10	89680782	89680826	PTEN	Exon005
chr10	89682749	89682988	PTEN	Exon006
chr10	89701854	89701996	PTEN	Exon007
chr10	89707589	89707756	PTEN	Exon008
chr10	89710630	89710855	PTEN	Exon009
chr10	89715023	89715219	PTEN	Exon010
chr10	89715219	89715496	PTEN	Exon011
chr17	7512463	7512896	P53	Exon001

Chromosome	Probe genomic location start (hg18)	Probe genomic location end (hg18)	Gene Name	Exon
chr17	7512897	7513733	P53	Exon002
chr17	7514651	7514758	P53	Exon003
chr17	7517577	7517651	P53	Exon004
chr17	7517743	7517880	P53	Exon005
chr17	7518223	7518333	P53	Exon006
chr17	7518901	7519014	P53	Exon007
chr17	7519095	7519279	P53	Exon008
chr17	7520036	7520315	P53	Exon009
chr17	7520424	7520446	P53	Exon010
chr17	7520563	7520665	P53	Exon011
chr17	7531419	7531511	P53	Exon012
chr3	41216015	41216165	CTNNB1	Exon001
chr3	41240515	41240576	CTNNB1	Exon002
chr3	41241020	41241248	CTNNB1	Exon003
chr3	41241448	41241702	CTNNB1	Exon004
chr3	41241828	41242067	CTNNB1	Exon005
chr3	41242154	41242356	CTNNB1	Exon006
chr3	41243702	41243847	CTNNB1	Exon007
chr3	41249835	41249939	CTNNB1	Exon008
chr3	41250023	41250362	CTNNB1	Exon009
chr3	41250633	41250792	CTNNB1	Exon010
chr3	41252218	41252338	CTNNB1	Exon011
chr3	41252843	41252994	CTNNB1	Exon012
chr3	41253082	41253204	CTNNB1	Exon013
chr3	41254510	41254571	CTNNB1	Exon014
chr3	41255628	41256481	CTNNB1	Exon015
chr3	41256481	41256609	CTNNB1	Exon016
chr3	41256609	41256938	CTNNB1	Exon017
chr12	25253378	25254112	KRAS	Exon001
chr12	25269814	25269974	KRAS	Exon002
chr12	25271434	25271613	KRAS	Exon003
chr12	25289474	25289596	KRAS	Exon004
chr12	25294951	25295087	KRAS	Exon005
chr1	26895108	26896618	ARID1A	Exon001
chr1	26928728	26928941	ARID1A	Exon002
chr1	26930229	26930682	ARID1A	Exon003
chr1	26931753	26931870	ARID1A	Exon004
chr1	26959933	26960174	ARID1A	Exon005
chr1	26960461	26960551	ARID1A	Exon006
chr1	26961229	26961397	ARID1A	Exon007
chr1	26962050	26962363	ARID1A	Exon008
chr1	26965298	26965444	ARID1A	Exon009
chr1	26965534	26965644	ARID1A	Exon010
chr1	26966867	26967077	ARID1A	Exon011
chr1	26970196	26970404	ARID1A	Exon012
chr1	26971577	26971710	ARID1A	Exon013
chr1	26971889	26972065	ARID1A	Exon014
chr1	26972423	26972574	ARID1A	Exon015
chr1	26972657	26972795	ARID1A	Exon016
chr1	26972879	26972976	ARID1A	Exon017
chr1	26973406	26974298	ARID1A	Exon018

Chromosome	Probe genomic location start (hg18)	Probe genomic location end (hg18)	Gene Name	Exon
chr1	26974654	26974785	ARID1A	Exon019
chr1	26978100	26981188	ARID1A	Exon020
chr19	57385161	57385239	PPP2R1A	Exon001
chr19	57397008	57397099	PPP2R1A	Exon002
chr19	57401027	57401128	PPP2R1A	Exon003
chr19	57406324	57406557	PPP2R1A	Exon004
chr19	57407750	57407898	PPP2R1A	Exon005
chr19	57408019	57408175	PPP2R1A	Exon006
chr19	57410843	57410958	PPP2R1A	Exon007
chr19	57411068	57411139	PPP2R1A	Exon008
chr19	57411593	57411728	PPP2R1A	Exon009
chr19	57414755	57414929	PPP2R1A	Exon010
chr19	57415253	57415314	PPP2R1A	Exon011
chr19	57416043	57416198	PPP2R1A	Exon012
chr19	57417163	57417306	PPP2R1A	Exon013
chr19	57420781	57420873	PPP2R1A	Exon014
chr19	57421029	57421046	PPP2R1A	Exon015
chr14	101346032	101346126	PPP2R5C	Exon001
chr14	101392775	101392975	PPP2R5C	Exon002
chr14	101418250	101418361	PPP2R5C	Exon003
chr14	101419346	101419439	PPP2R5C	Exon004
chr14	101419521	101419652	PPP2R5C	Exon005
chr14	101426326	101426386	PPP2R5C	Exon006
chr14	101429089	101429198	PPP2R5C	Exon007
chr14	101430596	101430650	PPP2R5C	Exon008
chr14	101437808	101437979	PPP2R5C	Exon009
chr14	101442491	101442623	PPP2R5C	Exon010

Table B.3 Exon capture probe design with genomic locations

ID	Gene	Original diagnosed subtype	Review Subtype	Grade	MSI Status	AA variant	Location (hg18)	Frequency	Probability	Type	Func. Impact	Sanger Validated	Normal available	Grade 3 Solid vs. Cytologic Atypia
92	KRAS	EEC		3	N/A	p.D33E	12,25289487,A,T	0.986	0.737	Missense	medium	Validated		Solid
92	TP53	EEC		3	N/A	p.R175H	17,7519131,C,T	0.970	0.690	Missense	high	Validated		Solid
148	ARID1A	EEC		3	N/A	p.F597fs	26930669			Frame_Shift_Del				Solid
148	PTEN	EEC		3	N/A	p.Y336*	10,89710837,C,A	0.246	0.439	Truncating		Validated		Solid
148	PTEN	EEC		3	N/A	p.R130G	10,89682884,C,G	0.415	0.624	Missense	high	Validated		Solid
148	TP53	EEC		3	N/A	p.A276D	17,7517836,G,T	0.667	0.685	Missense	high			Solid
181	PIK3CA	EEC		1	N/A	p.H1047R	3,180434779,A,G	0.421	0.696	Missense	low	Validated		
181	PTEN	EEC		1	N/A	p.D107V	10,89682816,A,T	0.338	0.367	Missense	medium	Validated		
220	ARID1A	ESC	EEC(G3) with clear cell changes	N/A(3)	N/A	p.G1847fs	26978517			Frame_Shift_Del				
220	ARID1A	ESC	EEC (G3) with clear cell changes	N/A(3)	N/A	p.Q548fs	26930523			Frame_Shift_Ins				
220	BRAF	ESC	EEC (G3) with clear cell changes	N/A(3)	N/A	p.A526V	7,140123298,G,A	0.308	0.650	Missense		Validated		
220	BRAF	ESC	EEC (G3) with clear cell changes	N/A(3)	N/A	p.P403fs	140129395			Frame_Shift_Del				
220	PIK3CA	ESC	EEC (G3) with clear cell changes	N/A(3)	N/A	p.Y1021C	3,180434701,A,G	0.347	0.735	Missense	medium	Validated		
220	PTEN	ESC	EEC (G3) with clear cell changes	N/A(3)	N/A	p.L265fs	89707749			Frame_Shift_Del				
267	KRAS	EEC		3	N/A	p.G13D	12,25289548,C,T	0.183	0.646	Missense	high	Validated		
267	PTEN	EEC		3	N/A	p.Q87*	10,89682755,C,T	0.265	0.679	Truncating		Validated		
267	TP53	EEC		3	N/A	p.P72fs	7520195			Frame_Shift_Del		Validated		
454	ARID1A	EEC		2	N/A	p.G1450fs	26973654			Frame_Shift_Del				
454	PIK3CA	EEC		1	N/A	p.R88Q	3,180399570,G,A	0.286	0.602	Missense	medium	Validated		
454	PTEN	EEC		1	N/A	p.E114*	10,89682836,G,T	0.815	0.700	Truncating		Validated		
458	ARID1A	EEC		2	N/A	p.P726fs	26960477			Frame_Shift_Del				
458	CTNNB1	EEC		1	N/A	p.S37F	3,41241117,C,T	0.299	0.428	Missense	high			
458	PIK3CA	EEC		1	N/A	p.Y343F	3,180404240,A,T	0.310	0.386	Missense	low	Validated		
458	PIK3CA	EEC		1	N/A	p.H1047R	3,180434779,A,G	0.313	0.726	Missense	low	Validated		
458	PTEN	EEC		1	N/A	p.M1I	10,89614209,G,T	0.336	0.627	Missense	medium	Validated		

ID	Gene	Original diagnosed subtype	Review Subtype	Grade	MSI Status	AA variant	Location (hg18)	Frequency	Probability	Type	Func. Impact	Sanger Validated	Normal available	Grade 3 Solid vs. Cytologic Atypia
458	PTEN	EEC		1	N/A	p.R130L	10,89682885,G,T	0.400	0.716	Missense	high	Validated		
465	ARID1A	EEC		2	N/A	p.G768S	1,26961280,G,A	0.420	0.617	Missense	low			
465	ARID1A	EEC		2	N/A	p.A273V	1,26896299,C,T	0.389	0.623	Missense	low			
465	ARID1A	EEC		2	N/A	p.R1722	1,26978140,C,T	0.431	0.630	Truncating				
465	ARID1A	EEC		2	N/A	p.R2232W	1,26979670,C,T	0.380	0.678	Missense	low			
465	KRAS	EEC		2	N/A	p.D69G	12,25271519,T,C	0.411	0.524	Missense	high	Validated		
465	PIK3CA	EEC		2	N/A	p.R992Q	3,180434614,G,A	0.294	0.350	Missense	medium	Validated		
465	PIK3CA	EEC		2	N/A	p.R1023Q	3,180434707,G,A	0.411	0.544	Missense	low	Validated		
465	PIK3CA	EEC		2	N/A	p.R612*	3,180420140,C,T	0.500	0.550	Truncating		Validated		
465	PPP2R1A	EEC		2	N/A	p.R48Q	19,57397073,G,A	0.441	0.587	Missense	medium	Validated		
465	PTEN	EEC		2	N/A	p.R173C	10,89701879,C,T	0.242	0.459	Missense	high	Validated		
465	PTEN	EEC		2	N/A	p.D107V	10,89682816,A,T	0.375	0.497	Missense	medium	Validated		
465	PTEN	EEC		2	N/A	p.G20V	10,89614265,G,T	0.337	0.538	Missense	medium	Validated		
465	PTEN	EEC		2	N/A	p.F341C	10,89710851,T,G	0.550	0.584	Missense	medium	Validated		
465	PTEN	EEC		2	N/A	p.E7*	10,89614225,G,T	0.436	0.700	Truncating		Validated		
465	TP53	EEC		2	N/A	p.S240R	17,7518286,A,C	0.438	0.494	Missense	high	Validated		
472	PIK3CA	ESC		N/A(3)	N/A	p.E542K	3,180418776,G,A	0.116	0.397	Missense	low	Validated		
472	PPP2R1A	ESC		N/A(3)	N/A	p.S256F	19,57408135,C,T	0.457	0.536	Missense	medium	Validated		
472	PPP2R1A	ESC		N/A(3)	N/A	p.T102K	19,57406359,C,A	0.434	0.547	Missense	medium	Validated		
472	TP53	ESC		N/A(3)	N/A	p.C124R	17,7520042,A,G	0.895	0.714	Missense	medium	Validated		
474	no mut	EEC		2	N/A	no mut								
477	ARID1A	EEC		2	N/A	p.D2277fs	26979805			Frame_Shift_Del				
477	PTEN	EEC		2	N/A	p.R233*	10,89707652,C,T	0.654	0.841	Truncating		Validated		
478	ARID1A	EEC		1	N/A	p.P1876fs	26978603			Frame_Shift_Del				
478	CTNNB1	EEC		1	N/A	p.G34E	3,41241108,G,A	0.321	0.367	Missense	medium			
478	PIK3CA	EEC		1	N/A	p.R88Q	3,180399570,G,A	0.333	0.602	Missense	medium	Validated		
478	PPP2R1A	EEC		1	N/A	p.S256F	19,57408135,C,T	0.244	0.381	Missense	medium	Validated		
478	PTEN	EEC		1	N/A	p.R130Q	10,89682885,G,A	0.784	0.575	Missense	high	Validated		
501	BRAF	EEC		1	N/A	p.D594G	7,140099623,T,C	0.528	0.721	Missense	high	Validated		
501	KRAS	EEC		1	N/A	p.G12S	12,25289552,C,T	0.340	0.527	Missense	high	Validated		
501	PTEN	EEC		1	N/A	p.G127fs	89682876			Frame_Shift_Ins				
511	PPP2R1A	EEC	EEC (G3)	2	N/A	p.P179L	19,57407783,C,T	0.490	0.466	Missense	medium	Validated		
511	TP53	EEC	EEC (G3)	2	N/A	p.H193L	17,7518996,T,A	0.550	0.625	Missense	high	Validated		
531	KRAS	EEC		2	N/A	p.V7G	12,25289566,A,C	0.354	0.392	Missense	high	Validated		
538	ARID1A	EEC		1	N/A	p.R1335	1,26972794,C,T	0.188	0.773	Truncating				
538	ARID1A	EEC		1	N/A	p.Q1420fs	26973564			Frame_Shift_Ins				
538	PTEN	EEC		1	N/A	p.R130G	10,89682884,C,G	0.523	0.624	Missense	high	Validated		
570	CTNNB1	EEC		1	MSS	p.G34R	3,41241107,G,C	0.175	0.525	Missense	medium	Validated	Yes	

ID	Gene	Original diagnosed subtype	Review Subtype	Grade	MSI Status	AA variant	Location (hg18)	Frequency	Probability	Type	Func. Impact	Sanger Validated	Normal available	Grade 3 Solid vs. Cytologic Atypia
570	PIK3CA	EEC		1	MSS	p.V344A	3,180404243,T,C	0.273	0.452	Missense	medium	Validated	Yes	
570	PTEN	EEC		1	MSS	p.P96S	10,89682782,C,T	0.453	0.478	Missense	high	Validated	Yes	
575	CTNNB1	EEC		2	MSS	p.S37F	3,41241117,C,T	0.208	0.438	Missense	high	Validated	Yes	
575	PIK3CA	EEC		2	MSS	p.C420R	3,180410674,T,C	0.370	0.561	Missense	medium	Validated	Yes	
577	PIK3CA	EEC		1	MSI-high	p.G1049A	3,180434785,G,C	0.152	0.534	Missense	low	Validated	Yes	
577	PIK3CA	EEC		1	MSI-high	p.R38C	3,180399419,C,T	0.255	0.641	Missense	medium	Validated	Yes	
577	PPP2R1A	EEC		1	MSI-high	p.R183Q	19,57407795,G,A	0.457	0.538	Missense	medium	Validated	Yes	
577	PTEN	EEC		1	MSI-high	p.R233*	10,89707652,C,T	0.297	0.623	Truncating		Validated	Yes	
577	TP53	EEC		1	MSI-high	p.R267W	17,7517864,G,A	0.273	0.673	Missense	high		Yes	
578	PIK3CA	EEC		1	MSS	p.E545G	3,180418786,A,G	0.407	0.502	Missense	low	Validated	Yes	
584	ARID1A	EEC		2	MSI-high	p.G1847fs	26978517			Frame_Shift_Ins			Yes	
584	KRAS	EEC		2	MSI-high	p.G12V	12,25289551,C,A	0.284	0.462	Missense	high	Validated	Yes	
584	PPP2R1A	EEC		2	MSI-high	p.R183W	19,57407794,C,T	0.415	0.524	Missense	medium	Validated	Yes	
584	PTEN	EEC		2	MSI-high	p.G129*	10,89682881,G,T	0.961	0.681	Truncating		Validated	Yes	
585	no mut	undifferentiated				no mut							Yes	
587	ARID1A	EEC		1	MSS	p.P729fs	26960485			Frame_Shift_Del			Yes	
587	ARID1A	EEC		1	MSS	p.S730fs	26960490			Frame_Shift_Del			Yes	
587	PIK3CA	EEC		1	MSS	p.E542K	3,180418776,G,A	0.357	0.456	Missense	low	Validated	Yes	
587	PTEN	EEC		1	MSS	p.G127*	10,89682875,G,T	0.541	0.563	Truncating		Validated	Yes	
588	PIK3CA	EEC		2	MSI-high	p.N345K	3,180404247,T,A	0.327	0.425	Missense	medium	Validated	Yes	
588	PPP2R1A	EEC		2	MSI-high	p.R183W	19,57407794,C,T	0.159	0.717	Missense	medium		Yes	
588	PTEN	EEC		2	MSI-high	p.H123Y	10,89682863,C,T	0.444	0.498	Missense	high	Validated	Yes	
588	PTEN	EEC		2	MSI-high	p.R130Q	10,89682885,G,A	0.362	0.594	Missense	high	Validated	Yes	
607	ARID1A	EEC		3	MSI-high	p.L573V	1,26930596,C,G	0.302	0.655	Missense	low		Yes	Cytologic Atypia
607	ARID1A	EEC		3	MSI-high	p.P568fs	26930583			Frame_Shift_Del			Yes	Cytologic Atypia
607	BRAF	EEC		3	MSI-high	p.D594G	7,140099623,T,C	0.391	0.652	Missense	high	Validated	Yes	Cytologic Atypia
607	PIK3CA	EEC		3	MSI-high	p.Q546R	3,180418789,A,G	0.182	0.344	Missense	low	Validated	Yes	Cytologic Atypia
607	PTEN	EEC		3	MSI-high	p.31_37NIIAMGF>I	89643773			In_Frame_Del			Yes	Cytologic Atypia
608	ARID1A	EEC		1	N/A	p.Q844*	1,26962161,C,T	0.379	0.680	Truncating				
608	PIK3CA	EEC		1	N/A	p.E545K	3,180418785,G,A	0.500	0.385	Missense	low	Validated		
608	PTEN	EEC		1	N/A	p.T131fs	89682887			Frame_Shift_Del				
608	PTEN	EEC		1	N/A	p.L318fs	89710783			Frame_Shift_Ins				

ID	Gene	Original diagnosed subtype	Review Subtype	Grade	MSI Status	AA variant	Location (hg18)	Frequency	Probability	Type	Func. Impact	Sanger Validated	Normal available	Grade 3 Solid vs. Cytologic Atypia
608	TP53	EEC		1	N/A	SPLICE_SITE_DONOR	7520036,C,T	0.610	0.737	SPLICE_SITE_DONOR				
611	TP53	EEC	ESC	2	MSI-low	p.S241F	17,7518284,G,A	0.561	0.633	Missense	high		Yes	
612	ARID1A	EEC		2	N/A	p.G731fs	26960492			Frame_Shift_Del				
612	ARID1A	EEC		2	N/A	p.W2049fs	26979121			Frame_Shift_Del				
612	CTNNB1	EEC		2	N/A	p.G34E	3,41241108,G,A	0.268	0.437	Missense	medium			
612	PTEN	EEC		2	N/A	p.R142W	10,89682920,C,T	0.455	0.568	Missense	medium	Validated		
612	PTEN	EEC		2	N/A	p.R130*	10,89682884,C,T	0.295	0.745	Truncating		Validated		
612	PTEN	EEC		2	N/A	p.R173H	10,89701880,G,A	0.633	0.818	Missense	medium	Validated		
615	ARID1A	EEC		1	MSI-low	p.R1461*	1,26973686,C,T	0.106	0.614	Truncating			Yes	
615	PIK3CA	EEC		1	MSI-low	p.H1047R	3,180434779,A,G	0.190	0.810	Missense	low	Validated	Yes	
615	PTEN	EEC		1	MSI-low	p.R130Q	10,89682885,G,A	0.206	0.506	Missense	high	Validated	Yes	
625	ARID1A	EEC		2	MSS	p.E2255*	1,26979739,G,T	0.297	0.748	Truncating			Yes	
625	CTNNB1	EEC		2	MSS	p.W383G	3,41249901,T,G	0.193	0.379	Missense	medium	Validated	Yes	
625	PTEN	EEC		2	MSS	SPLICE_SITE_ACCEPTOR	89710630,G,T	0.556	0.687	SPLICE_SITE_ACCEPTOR	high		Yes	
625	PTEN	EEC		2	MSS	p.R130*	10,89682884,C,T	0.212	0.822	Truncating		Validated	Yes	
632	ARID1A	EEC		1	N/A	p.A2235fs	26979679			Frame_Shift_Del				
632	KRAS	EEC		1	N/A	p.G12A	12,25289551,C,G	0.380	0.557	Missense	high	Validated		
632	PIK3CA	EEC		1	N/A	p.H1047R	3,180434779,A,G	0.242	0.788	Missense	low	Validated		
632	PTEN	EEC		1	N/A	p.K313fs	89710767			Frame_Shift_Del				
640	ARID1A	EEC		2	MSS	p.A2097S	1,26979265,G,T	0.359	0.712	Missense	medium		Yes	
640	ARID1A	EEC		2	MSS	p.S2096fs	26979262			Frame_Shift_Ins			Yes	
640	CTNNB1	EEC		2	MSS	p.S45F	3,41241141,C,T	0.317	0.465	Missense	medium	Validated	Yes	
640	PTEN	EEC		2	MSS	SPLICE_SITE_ACCEPTOR	89707588,A,G	0.343	0.317	SPLICE_SITE_ACCEPTOR			Yes	
640	PTEN	EEC		2	MSS	p.M134fs	89682898			Frame_Shift_Del			Yes	
642	no mutation	EEC		1	MSS	no mutation							Yes	
645	ARID1A	EEC		2	MSI-high	p.Q1631fs	26974198			Frame_Shift_Ins			Yes	
645	KRAS	EEC		2	MSI-high	p.G12D	12,25289551,C,T	0.182	0.504	Missense	high	Validated	Yes	
645	PTEN	EEC		2	MSI-high	p.Y178D	10,89701894,T,G	0.412	0.545	Missense	medium	Validated	Yes	
645	PTEN	EEC		2	MSI-high	p.R130G	10,89682884,C,G	0.461	0.599	Missense	high	Validated	Yes	
647	ARID1A	EEC		1	MSI-high	p.G1847fs	26978517			Frame_Shi			Yes	

ID	Gene	Original diagnosed subtype	Review Subtype	Grade	MSI Status	AA variant	Location (hg18)	Frequency	Probability	Type	Func. Impact	Sanger Validated	Normal available	Grade 3 Solid vs. Cytologic Atypia
										ft_Del				
647	PTEN	EEC		1	MSI-high	p.G143fs	89682925			Frame_Shift_Ins			Yes	
653	ARID1A	EEC		1	MSS	p.W2091*	1,26979249,G,A	0.271	0.560	Truncating			Yes	
653	PTEN	EEC		1	MSS	p.R130P	10,89682885,G,C	0.250	0.627	Missense	high	Validated	Yes	
653	PTEN	EEC		1	MSS	p.I203fs	89701971			Frame_Shift_Del			Yes	
658	CTNNB1	EEC		1	MSS	p.T41I	3,41241129,C,T	0.298	0.480	Missense	medium	Validated	Yes	
658	PTEN	EEC		1	MSS	p.EDLDQWLS106del	89682809			In_Frame_Del			Yes	
659	ARID1A	EEC		1	N/A	p.Q1188*	1,26971912,C,T	0.311	0.502	Truncating				
659	KRAS	EEC		1	N/A	p.G13D	12,25289548,C,T	0.375	0.530	Missense	high	Validated		
659	PTEN	EEC		1	N/A	p.R130Q	10,89682885,G,A	0.320	0.475	Missense	high	Validated		
659	PTEN	EEC		1	N/A	p.N212fs	89707591			Frame_Shift_Del				
661	ARID1A	EEC		3	N/A	p.V1982fs	26978922			Frame_Shift_Del			Yes	Solid
661	PIK3CA	EEC		3	N/A	p.P104L	3,180399618,C,T	0.338	0.506	Missense	low	Validated	Yes	Solid
661	PIK3CA	EEC		3	N/A	p.V344M	3,180404242,G,A	0.273	0.576	Missense	medium	Validated	Yes	Solid
661	PIK3CA	EEC		3	N/A	p.1066V	3,180434836,C,T	0.257	0.739	Missense	low	Not Validated		Solid
661	PTEN	EEC		3	N/A	p.H196fs	89701950			Frame_Shift_Del			Yes	Solid
668	CTNNB1	EEC		1	N/A	p.S37Y	3,41241117,C,A	0.400	0.571	Missense	high	Validated		
668	PIK3CA	EEC		1	N/A	p.H1047R	3,180434779,A,G	0.364	0.594	Missense	low	Validated		
668	PTEN	EEC		1	N/A	p.R130*	10,89682884,C,T	0.748	0.565	Truncating		Validated		
672	CTNNB1	EEC		2	N/A	p.S33F	3,41241105,C,T	0.220	0.453	Missense	medium	Validated		
674	ARID1A	EEC		2	MSI-low	p.R1528*	1,26973887,C,T	0.093	0.486	Truncating			Yes	
674	KRAS	EEC		2	MSI-low	p.G13D	12,25289548,C,T	0.121	0.507	Missense	high	Validated	Yes	
674	PTEN	EEC		2	MSI-low	p.H93Q	10,89682775,T,G	0.138	0.729	Missense	high		Yes	
694	PIK3CA	EEC		1	N/A	p.E545K	3,180418785,G,A	0.086	0.362	Missense	low	Validated		
694	PTEN	EEC		1	N/A	p.R130*	10,89682884,C,T	0.171	0.833	Truncating		Validated		
694	PTEN	EEC		1	N/A	p.D371fs	89715109			Frame_Shift_Del				
699	ARID1A	EEC		3	N/A	p.S764fs	26961268			Frame_Shift_Del				Solid
699	ARID1A	EEC		3	N/A	p.T2138fs	26979390			Frame_Shift_Del				Solid
699	PIK3CA	EEC		3	N/A	p.Y1021C	3,180434701,A,G	0.323	0.761	Missense	medium	Validated		Solid
699	PPP2R5C	EEC		3	N/A	SPLICE_SITE_ACCEPTOR	101392774,A,G	0.396	0.562	SPLICE_SITE_ACCEPTOR				Solid

ID	Gene	Original diagnosed subtype	Review Subtype	Grade	MSI Status	AA variant	Location (hg18)	Frequency	Probability	Type	Func. Impact	Sanger Validated	Normal available	Grade 3 Solid vs. Cytologic Atypia
699	PTEN	EEC		3	N/A	p.L265fs	89707749			Frame_Shift_Ins				Solid
699	TP53	EEC		3	N/A	p.R273C	17,7517846,G,A	0.333	0.741	Missense	high	Validated		Solid
699	TP53	EEC		3	N/A	p.R273H	17,7517845,C,T	0.202	0.761	Missense	high	Validated		Solid
700	KRAS	EEC		2	MSI-high	p.K117N	12,25269914,T,A	0.390	0.416	Missense	high	Validated	Yes	
700	PIK3CA	EEC		2	MSI-high	p.C420R	3,180410674,T,C	0.292	0.419	Missense	medium	Validated	Yes	
700	PIK3CA	EEC		2	MSI-high	p.R38C	3,180399419,C,T	0.402	0.600	Missense	medium	Validated	Yes	
700	PPP2R1A	EEC		2	MSI-high	p.VE99del	57406347			In_Frame_Del			Yes	
700	PTEN	EEC		2	MSI-high	p.L345P	10,89715031,T,C	0.194	0.448	Missense	medium	Validated	Yes	
701	ARID1A	EEC		2	MSI-high	SPLICE_SITE_ACCEPTOR	26962049,A,G	0.132	0.358	SPLICE_SITE_ACCEPTOR			Yes	
701	ARID1A	EEC		2	MSI-high	p.R1074W	1,26970218,C,T	0.150	0.712	Missense	medium		Yes	
701	CTNNB1	EEC		2	MSI-high	p.R190C	3,41241901,C,T	0.157	0.818	Missense	low	Validated	Yes	
701	KRAS	EEC		2	MSI-high	p.A146T	12,25269829,C,T	0.152	0.392	Missense	high		Yes	
701	PIK3CA	EEC		2	MSI-high	p.E81K	3,180399548,G,A	0.069	0.365	Missense	medium	Validated	Yes	
707	ARID1A	EEC		1	MSS	p.Q269*	1,26896286,C,T	0.714	0.541	Truncating				
707	CTNNB1	EEC		1	MSS	p.S37F	3,41241117,C,T	0.137	0.571	Missense	high	Validated		
707	PTEN	EEC		1	MSS	SPLICE_SITE_ACCEPTOR	89701854,G,A	0.809	0.630	SPLICE_SITE_ACCEPTOR				
712	ARID1A	EEC		3	N/A	p.R2158*	1,26979448,C,T	0.188	0.629	Truncating				Solid
712	ARID1A	EEC		3	N/A	p.E119G	1,26895837,A,G	0.625	0.639	Missense	low			Solid
712	ARID1A	EEC		3	N/A	p.T1302fs	26972695			Frame_Shift_Ins				Solid
712	CTNNB1	EEC		3	N/A	p.N287S	3,41242280,A,G	0.505	0.627	Missense	neutral			Solid
712	PIK3CA	EEC		3	N/A	p.E110del	180399631			In_Frame_Del				Solid
712	PTEN	EEC		3	N/A	p.I135V	10,89682899,A,G	0.723	0.558	Missense	low	Validated		Solid
712	TP53	EEC		3	N/A	p.K132R	17,7519260,T,C	0.340	0.469	Missense	high	Validated		Solid
721	PTEN	EEC		1	MSS	p.R130G	10,89682884,C,G	0.158	0.490	Missense	high	Validated	Yes	
733	PIK3CA	EEC		2	MSI-low	p.H1047R	3,180434779,A,G	0.114	0.781	Missense	low	Validated	Yes	
733	PTEN	EEC		2	MSI-low	p.D92G	10,89682771,A,G	0.342	0.331	Missense	high	Validated	Yes	
737	PIK3CA	ESC		N/A(3)	N/A	p.H1047Y	3,180434778,C,T	0.284	0.694	Missense	low	Validated		
737	TP53	ESC		N/A(3)	N/A	p.R248Q	17,7518263,C,T	0.577	0.718	Missense	high			
742	PPP2R1A	mixed ESC (60%), G2 EEC		3	MSS	p.P179R	19,57407783,C,G	0.364	0.486	Missense	medium	Validated	Yes	
742	TP53	mixed ESC (60%), G2 EEC		3	MSS	p.G245S	17,7518273,C,T	0.639	0.757	Missense	medium		Yes	

ID	Gene	Original diagnosed subtype	Review Subtype	Grade	MSI Status	AA variant	Location (hg18)	Frequency	Probability	Type	Func. Impact	Sanger Validated	Normal available	Grade 3 Solid vs. Cytologic Atypia
743	PTEN	EEC		1	MSS	p.R130G	10,89682884,C,G	0.106	0.391	Missense	high	Validated	Yes	
745	CTNNB1	EEC		1	MSS	p.S33C	3,41241105,C,G	0.122	0.773	Missense	medium	Validated	Yes	
745	PTEN	EEC		1	MSS	p.R130G	10,89682884,C,G	0.157	0.588	Missense	high	Validated	Yes	
750	KRAS	EEC		1	MSS	p.G12V	12,25289551,C,A	0.130	0.414	Missense	high	Validated	Yes	
750	PTEN	EEC		1	MSS	p.D24H	10,89614276,G,C	0.095	0.401	Missense	high		Yes	
750	PTEN	EEC		1	MSS	p.G129R	10,89682881,G,A	0.208	0.560	Missense	high	Validated	Yes	
771	ARID1A	EEC		2	MSI-high	p.T2138fs	26979390			Frame_Shift_Del			Yes	
771	CTNNB1	EEC		2	MSI-high	p.D32Y	3,41241101,G,T	0.162	0.653	Missense	medium		Yes	
771	PTEN	EEC		2	MSI-high	p.Q17*	10,89614255,C,T	0.207	0.556	Truncating		Validated	Yes	
771	PTEN	EEC		2	MSI-high	p.E307fs	89710750			Frame_Shift_Ins			Yes	
772	ARID1A	EEC		2	MSS	p.V2244G	1,26979707,T,G	0.071	0.262	Missense	low		Yes	
772	CTNNB1	EEC		2	MSS	p.D32A	3,41241102,A,C	0.303	0.573	Missense	medium	Validated	Yes	
772	PTEN	EEC		2	MSS	p.R130G	10,89682884,C,G	0.177	0.562	Missense	high	Validated	Yes	
778	ARID1A	EEC		1	MSS	p.R1989*	1,26978941,C,T	0.367	0.587	Truncating				
778	CTNNB1	EEC		1	MSS	p.E77*	3,41241236,G,T	0.109	0.621	Truncating		Validated		
778	PIK3CA	EEC		1	MSS	p.E563K	3,180419700,G,A	0.100	0.266	Missense	low	Validated		
778	PIK3CA	EEC		1	MSS	p.Y1021C	3,180434701,A,G	0.360	0.645	Missense	medium	Validated		
778	PTEN	EEC		1	MSS	p.R130Q	10,89682885,G,A	0.310	0.527	Missense	high	Validated		
778	PTEN	EEC		1	MSS	p.E7*	10,89614225,G,T	0.114	0.778	Truncating				
778	PTEN	EEC		1	MSS	p.E99*	10,89682791,G,T	0.203	0.789	Truncating		Validated		
780	CTNNB1	EEC		1	MSS	p.D32Y	3,41241101,G,T	0.450	0.615	Missense	medium		Yes	
780	PIK3CA	EEC		1	MSS	p.H1047R	3,180434779,A,G	0.333	0.621	Missense	low	Validated	Yes	
780	PTEN	EEC		1	MSS	p.L194fs	89701944			Frame_Shift_Del			Yes	
795	PIK3CA	ESC		N/A(3)	N/A	p.M1043I	3,180434768,G,A	0.393	0.549	Missense	low	Validated		
795	PPP2R1A	ESC		N/A(3)	N/A	p.S256F	19,57408135,C,T	0.370	0.411	Missense	medium	Validated		
795	TP53	ESC		N/A(3)	N/A	p.N239T	17,7518290,T,G	0.460	0.519	Missense	high	Validated		
799	no mut	EEC		1	MSI-High	no mu							Yes	
804	CTNNB1	EEC		3	MSI-low	p.S33P	3,41241104,T,C	0.438	0.544	Missense	medium	Validated	Yes	
804	PTEN	EEC		3	MSI-low	p.Q298*	10,89710721,C,T	0.912	0.806	Truncating		Validated	Yes	
806	KRAS	EEC		1	N/A	p.G12V	12,25289551,C,A	0.102	0.513	Missense	high	Validated		
806	PTEN	EEC		1	N/A	SPLICE_SITE_ACCEPTOR	89710629,A,T	0.271	0.338	SPLICE_SITE_ACCEPTOR	high			
807	PIK3CA	ESC		N/A(3)	MSS	p.H1047R	3,180434779,A,G	0.527	0.689	Missense	low	Validated	Yes	
807	PPP2R1A	ESC		N/A(3)	MSS	p.P179R	19,57407783,C,G	19,57407783,C,G		Missense	medium	Validated	Yes	
807	TP53	ESC		N/A(3)	MSS	p.G244C	17,7518276,C,A	0.767	0.715	Missense	high		Yes	
810	CTNNB1	EEC		2	MSI-low	p.S45P	3,41241140,T,C	0.301	0.464	Missense	medium	Validated		

ID	Gene	Original diagnosed subtype	Review Subtype	Grade	MSI Status	AA variant	Location (hg18)	Frequency	Probability	Type	Func. Impact	Sanger Validated	Normal available	Grade 3 Solid vs. Cytologic Atypia
810	PIK3CA	EEC		2	MSI-low	p.T1025A	3,180434712,A,G	0.085	0.268	Missense	low	Validated		
810	PTEN	EEC		2	MSI-low	p.G129R	10,89682881,G,A	0.547	0.575	Missense	high	Validated		
815	ARID1A	EEC		1	MSS	SPLICE_SITE_ACCEPTOR	26930229,G,T	0.182	0.466	SPLICE_SITE_ACCEPTOR			Yes	
815	PIK3CA	EEC		1	MSS	p.F83S	3,180399555,T,C	0.113	0.449	Missense	low	Validated	Yes	
815	PIK3CA	EEC		1	MSS	p.R88Q	3,180399570,G,A	0.143	0.498	Missense	medium	Validated	Yes	
815	PTEN	EEC		1	MSS	p.R130Q	10,89682885,G,A	0.221	0.609	Missense	high	Validated	Yes	
815	PTEN	EEC		1	MSS	p.E99*	10,89682791,G,T	0.151	0.615	Truncating		Validated	Yes	
819	no mut	EEC		2	MSI-High	no mut							Yes	
823	PIK3CA	EEC		3	MSI-high	p.H1047R	3,180434779,A,G	0.128	0.787	Missense	low	Validated	Yes	Solid
823	PTEN	EEC		3	MSI-high	p.R233*	10,89707652,C,T	0.124	0.809	Truncating			Yes	Solid
824	CTNNB1	EEC		2	MSI-high	p.S33P	3,41241104,T,C	0.397	0.494	Missense	medium	Validated	Yes	
824	PTEN	EEC		2	MSI-high	p.E242*	10,89707679,G,T	0.339	0.381	Truncating		Validated	Yes	
831	PIK3CA	EEC		2	MSI-low	p.E545K	3,180418785,G,A	0.122	0.293	Missense	low	Validated	Yes	
831	PTEN	EEC		2	MSI-low	p.R130G	10,89682884,C,G	0.077	0.529	Missense	high	Not Validated	Yes	
831	PTEN	EEC		2	MSI-low	p.E18*	10,89614258,G,T	0.110	0.676	Truncating			Yes	
832	PTEN	EEC		2	MSI-high	p.R130*	10,89682884,C,T	0.337	0.727	Truncating		Validated	Yes	
839	ARID1A	EEC		3	MSI-high	p.Q2115fs	26979319			Frame_Shift_Del			Yes	Solid
839	PIK3CA	EEC		3	MSI-high	p.R88Q	3,180399570,G,A	0.089	0.408	Missense	medium	Validated	Yes	Solid
839	PTEN	EEC		3	MSI-high	p.R130G	10,89682884,C,G	0.283	0.473	Missense	high	Validated	Yes	Solid
841	ARID1A	ESC	mixed - 80% ESC, 20% EEC	N/A(3)	MSI-high	p.R1335*	1,26972794,C,T	0.228	0.670	Truncating			Yes	
841	ARID1A	ESC	mixed - 80% ESC, 20% EEC	N/A(3)	MSI-high	p.Q420*	1,26928849,C,T	0.179	0.730	Truncating			Yes	
841	KRAS	ESC	mixed - 80% ESC, 20% EEC	N/A(3)	MSI-high	p.G13D	12,25289548,C,T	0.250	0.448	Missense	high	Validated	Yes	
841	PIK3CA	ESC	mixed - 80% ESC, 20% EEC	N/A(3)	MSI-high	p.G106V	3,180399624,G,T	0.225	0.432	Missense	medium	Validated	Yes	
841	PIK3CA	ESC	mixed - 80% ESC, 20% EEC	N/A(3)	MSI-high	p.V344M	3,180404242,G,A	0.172	0.596	Missense	medium	Validated	Yes	
841	PPP2R1A	ESC	mixed - 80% ESC, 20% EEC	N/A(3)	MSI-high	p.R182W	19,57407794,C,T			Missense	medium	Validated	Yes	
843	ARID1A	EEC		1	MSI-high	p.Q1142*	1,26971595,C,T	0.410	0.473	Truncating			Yes	
843	PIK3CA	EEC		1	MSI-high	p.D746V	3,180424612,A,T	0.406	0.599	Missense	low	Validated	Yes	

ID	Gene	Original diagnosed subtype	Review Subtype	Grade	MSI Status	AA variant	Location (hg18)	Frequency	Probability	Type	Func. Impact	Sanger Validated	Normal available	Grade 3 Solid vs. Cytologic Atypia
843	PPP2R1A	EEC		2	MSI-high	p.R249H	19, 57408114,G,A					Validated	Yes	
843	PTEN	EEC		1	MSI-high	p.E150*	10,89682944,G,T	0.185	0.808	Truncating			Yes	
843	PTEN	EEC		1	MSI-high	p.T321fs	89710791			Frame_Shift_Ins			Yes	
843	TP53	EEC		1	MSI-high	p.R196*	17,7518988,G,A	0.400	0.552	Truncating		Validated	Yes	
844	BRAF	EEC		1	N/A	p.S323L	7,140146643,G,A	0.386	0.553	Missense	low	Validated		
844	CTNNB1	EEC		1	N/A	p.T41A	3,41241128,A,G	0.431	0.684	Missense	medium	Validated		
844	PIK3CA	EEC		1	N/A	p.H1047R	3,180434779,A,G	0.346	0.595	Missense	low	Validated		
844	PTEN	EEC		1	N/A	p.R130Q	10,89682885,G,A	0.353	0.438	Missense	high	Validated		
849	PTEN	Carcinosarcoma - with ESC		N/A(3)	MSS	p.V317fs	89710778			Frame_Shift_Del			Yes	
849	TP53	Carcinosarcoma - with ESC		N/A(3)	MSS	p.D281H	17,7517822,C,G	0.382	0.680	Missense	high		Yes	
852	ARID1A	EEC		3	MSI-high	p.E1935*	1,26978779,G,T	0.438	0.661	Truncating			Yes	Cytologic Atypia
852	ARID1A	EEC		3	MSI-high	p.A1517fs	26973854			Frame_Shift_Del			Yes	Cytologic Atypia
852	KRAS	EEC		3	MSI-high	p.G12D	12,25289551,C,T	0.396	0.515	Missense	high	Validated	Yes	Cytologic Atypia
852	PTEN	EEC		3	MSI-high	p.R130*	10,89682884,C,T	0.733	0.839	Truncating		Validated	Yes	Cytologic Atypia
852	TP53	EEC		3	MSI-high	p.K382fs	7513687			Frame_Shift_Del			Yes	Cytologic Atypia
858	ARID1A	EEC		3	MSS	p.R1989*	1,26978941,C,T	0.125	0.467	Truncating			Yes	Solid
858	ARID1A	EEC		3	MSS	p.R693Q	1,26960091,G,A	0.215	0.664	Missense	low		Yes	Solid
858	ARID1A	EEC		3	MSS	p.K1106N	1,26970316,G,T	0.127	0.816	Missense	medium		Yes	Solid
858	ARID1A	EEC		3	MSS	p.E896*	1,26962317,G,T	0.127	0.827	Truncating			Yes	Solid
858	BRAF	EEC		3	MSS	p.L190I	7,140155201,G,T	0.104	0.496	Missense	medium	Validated	Yes	Solid
858	CTNNB1	EEC		3	MSS	p.E334K	3,41243766,G,A	0.090	0.465	Missense	medium	Validated	Yes	Solid
858	CTNNB1	EEC		3	MSS	p.D104Y	3,41241517,G,T	0.074	0.657	Missense	low	Validated	Yes	Solid
858	PIK3CA	EEC		3	MSS	p.R88Q	3,180399570,G,A	0.091	0.414	Missense	medium	Validated	Yes	Solid
858	PIK3CA	EEC		3	MSS	p.H1048N	3,180434781,C,A	0.079	0.435	Missense	low	Not Validated	Yes	Solid
858	PIK3CA	EEC		3	MSS	p.M1043V	3,180434766,A,G	0.149	0.504	Missense	low	Validated	Yes	Solid
858	PTEN	EEC		3	MSS	p.E299*	10,89710724,G,T	0.098	0.634	Truncating			Yes	Solid
863	ARID1A	EEC		2	N/A	p.S764fs	26961268			Frame_Shift_Del		Validated		
863	ARID1A	EEC		2	N/A	p.2233_2236RAAR>R	26979675			In_Frame_Del		Validated		
863	PTEN	EEC		2	N/A	p.R130G	10,89682884,C,G	0.480	0.589	Missense	high	Validated		

ID	Gene	Original diagnosed subtype	Review Subtype	Grade	MSI Status	AA variant	Location (hg18)	Frequency	Probability	Type	Func. Impact	Sanger Validated	Normal available	Grade 3 Solid vs. Cytologic Atypia
863	TP53	EEC		2	N/A	p.Q331H	17,7517578,C,A	0.075	0.401	Missense	medium	Validated		
872	ARID1A	EEC		2	N/A	p.S530fs	26930467			Frame_Shift_Del		Validated		
872	ARID1A	EEC		2	N/A	p.Y1324fs	26972762			Frame_Shift_Del		Validated		
872	CTNNB1	EEC		2	N/A	p.V22G	3,41241072,T,G	0.131	0.349	Missense	medium			
872	PIK3CA	EEC		2	N/A	p.E545K	3,180418785,G,A	0.250	0.323	Missense	low	Validated		
872	PIK3CA	EEC		2	N/A	p.E81K	3,180399548,G,A	0.362	0.521	Missense	medium	Validated		
872	PTEN	EEC		2	N/A	p.G129R	10,89682881,G,A	0.329	0.551	Missense	high	Validated		
872	PTEN	EEC		2	N/A	p.E307fs	89710750			Frame_Shift_Del				
874	PTEN	EEC		1	N/A	p.R130G	10,89682884,C,G	0.265	0.605	Missense	high	Validated		
874	PTEN	EEC		1	N/A	p.R308fs	89710751			Frame_Shift_Del				
874	TP53	EEC		1	N/A	p.R110C	17,7520084,G,A	0.258	0.577	Missense	medium	Validated		
876	ARID1A	EEC		2	N/A	p.Y222fs	26896146			Frame_Shift_Del				
876	PIK3CA	EEC		2	N/A	p.C420R	3,180410674,T,C	0.404	0.455	Missense	medium	Validated		
876	PTEN	EEC		2	N/A	p.G20*	10,89614264,G,T	0.229	0.448	Truncating				
876	TP53	EEC		2	N/A	p.T231P	17,7518315,T,G	0.103	0.434	Missense	high			
879	ARID1A	EEC		1	N/A	p.E119*	1,26895836,G,T	0.118	0.430	Truncating				
879	ARID1A	EEC		1	N/A	p.Q708P	1,26960136,A,C	0.400	0.572	Missense	low	Validated		
879	PIK3CA	EEC		1	N/A	p.R93W	3,180399584,C,T	0.075	0.276	Missense	medium	Not Validated		
879	PTEN	EEC		1	N/A	p.Q214*	10,89707595,C,T	0.095	0.395	Truncating				
882	no mutations	EEC		2	N/A	no mutation								
883	PTEN	EEC		3	N/A	p.W111*	10,89682829,G,A	0.143	0.505	Truncating		Validated		Solid
883	PTEN	EEC		3	N/A	p.R130G	10,89682884,C,G	0.179	0.605	Missense	high	Validated		Solid
887	ARID1A	EEC		2	MSS	p.G2087R	1,26979235,G,A	0.267	0.453	Missense	medium		Yes	
887	PIK3CA	EEC		2	MSS	p.H1047R	3,180434779,A,G	0.346	0.572	Missense	low	Validated	Yes	
888	ARID1A	mixed G2 & G3 EEC(70%) and clear cell		3	MSI-high	p.S2123T	1,26979344,G,C	0.185	0.613	Missense	low		Yes	
888	ARID1A	mixed G2 & G3 EEC(70%) and clear cell		3	MSI-high	p.T2138fs	26979390			Frame_Shift_Del			Yes	
888	KRAS	mixed G2 & G3 EEC(70%		3	MSI-high	p.V14I	12,25289546,C,T	0.092	0.557	Missense	high	Validated	Yes	

ID	Gene	Original diagnosed subtype	Review Subtype	Grade	MSI Status	AA variant	Location (hg18)	Frequency	Probability	Type	Func. Impact	Sanger Validated	Normal available	Grade 3 Solid vs. Cytologic Atypia
		) and clear cell												
888	PIK3CA	mixed G2 & G3 EEC(70%) and clear cell		3	MSI-high	p.R88Q	3,180399570,G,A	0.153	0.553	Missense	medium	Validated	Yes	
888	PPP2R1A	mixed G2 & G3 EEC(70%) and clear cell		3	MSI-high	p.R183Q	19,57407791,C,T			Missense		Validated	Yes	
892	PPP2R1A	ESC		N/A(3)	N/A	p.R183W	19,57407794,C,T	0.568	0.791	Missense	medium	Validated		
892	TP53	ESC		N/A(3)	N/A	SPLICE_SITE_DONOR	7520035,A,G	0.574	0.690	SPLICE_SITE_DONOR				
895	TP53	EEC	EEC (G2) with myometrial invasion	2	MSS	p.R282W	17,7517819,G,A	0.117	0.463	Missense	high	Validated	Yes	
896	no mut	ESC		N/A (3)	MSS	no mut							Yes	
913	ARID1A	EEC		2	MSI-high	p.R1989*	1,26978941,C,T	0.072	0.378	Truncating				
913	PIK3CA	EEC		2	MSI-high	p.M1043I	3,180434768,G,T	0.060	0.304	Missense	low	Validated		
913	PTEN	EEC		2	MSI-high	p.F278L	10,89710663,C,A	0.072	0.446	Missense	medium			
913	PTEN	EEC		2	MSI-high	p.R173C	10,89701879,C,T	0.146	0.767	Missense	high			
913	TP53	EEC		2	MSI-high	p.R213*	17,7518937,G,A	0.107	0.559	Truncating		Validated		
918	PIK3CA	EEC		1	N/A	p.H1047R	3,180434779,A,G	0.099	0.757	Missense	low	Validated		
918	PTEN	EEC		1	N/A	p.172_174 RRY>N	89701876			In_Frame_ Del				
920	KRAS	EEC		1	N/A	p.G12V	12,25289551,C,A	0.064	0.358	Missense	high	Not Validated		
920	no mut	EEC		1	N/A	no mut								
920	PTEN	EEC		1	N/A	p.Y178*	10,89701896,T,A	0.121	0.440	Truncating		Not Validated		
926	ARID1A	EEC		1	MSS	p.R1074W	1,26970218,C,T	0.259	0.618	Missense	medium		Yes	
926	PPP2R1A	EEC		2	MSS	p.R183Q	19,57407791,C,T			Missense		Validated	Yes	
926	PTEN	EEC		1	MSS	p.R233*	10,89707652,C,T	0.292	0.553	Truncating		Validated	Yes	
928	CTNNB1	EEC		1	MSI-low	p.S37F	3,41241117,C,T	0.339	0.576	Missense	high	Validated	Yes	
928	PIK3CA	EEC		1	MSI-low	p.H1047R	3,180434779,A,G	0.340	0.749	Missense	low	Validated	Yes	
928	PTEN	EEC		1	MSI-low	p.R130*	10,89682884,C,T	0.371	0.700	Truncating		Validated	Yes	
931	ARID1A	EEC		1	MSS	p.Q1856*	1,26978542,C,T	0.120	0.558	Truncating			Yes	
931	PIK3CA	EEC		1	MSS	p.E453K	3,180410773,G,A	0.114	0.385	Missense	medium	Validated	Yes	
931	PIK3CA	EEC		1	MSS	p.N1044S	3,180434770,A,G	0.111	0.510	Missense	low	Validated	Yes	

ID	Gene	Original diagnosed subtype	Review Subtype	Grade	MSI Status	AA variant	Location (hg18)	Frequency	Probability	Type	Func. Impact	Sanger Validated	Normal available	Grade 3 Solid vs. Cytologic Atypia
931	PTEN	EEC		1	MSS	p.R130G	10,89682884,C,G	0.180	0.566	Missense	high	Validated	Yes	
936	no mut	EEC		2	MSI-low	no mut							Yes	
938	ARID1A	EEC		3	MSI-high	p.P1325S	1,26972764,C,T	0.260	0.447	Missense	medium		Yes	Solid
938	ARID1A	EEC		3	MSI-high	p.A1872T	1,26978590,G,A	0.431	0.711	Missense	low	Validated	Yes	Solid
938	ARID1A	EEC		3	MSI-high	p.S1604Y	1,26974116,C,A	0.343	0.760	Missense	low		Yes	Solid
938	CTNNB1	EEC		3	MSI-high	SPLICE_SITE_ACCEPTOR	41250023,G,T	0.395	0.523	SPLICE_SITE_ACCEPTOR			Yes	Solid
938	CTNNB1	EEC		3	MSI-high	p.Q130H	3,41241597,G,T	0.107	0.734	Missense	medium	Validated	Yes	Solid
938	PIK3CA	EEC		3	MSI-high	p.E600K	3,180420104,G,A	0.429	0.376	Missense	high	Validated	Yes	Solid
938	PIK3CA	EEC		3	MSI-high	p.R88Q	3,180399570,G,A	0.216	0.456	Missense	medium	Validated	Yes	Solid
938	PTEN	EEC		3	MSI-high	p.E40*	10,89643800,G,T	0.260	0.718	Truncating		Validated	Yes	Solid
939	CTNNB1	EEC		3	MSI-high	p.S37C	3,41241117,C,G	0.156	0.731	Missense	high	Validated	Yes	Cytologic Atypia
939	PTEN	EEC		3	MSI-high	p.L325R	10,89710803,T,G	0.222	0.526	Missense	medium		Yes	Cytologic Atypia
941	no mut	EEC		1	MSS	no mut							Yes	
941	PTEN	EEC		1	MSS	p.R130G	10,89682884,C,G	0.080	0.551	Missense	high	Not Validated	Yes	
947	PTEN	EEC		3	N/A	p.V317fs	89710778			Frame_Shift_Del				Solid
955	ARID1A	EEC		3	N/A	p.G149D	1,26895927,G,A	0.232	0.516	Missense				Solid
955	ARID1A	EEC		3	N/A	p.R1989*	1,26978941,C,T	0.150	0.606	Truncating		Validated		Solid
955	ARID1A	EEC		3	N/A	p.E626*	1,26931826,G,T	0.103	0.778	Truncating		Validated		Solid
955	PIK3CA	EEC		3	N/A	p.N345S	3,180404246,A,G	0.148	0.443	Missense	medium	Validated		Solid
955	PIK3CA	EEC		3	N/A	p.R88Q	3,180399570,G,A	0.178	0.582	Missense	medium	Validated		Solid
955	PTEN	EEC		3	N/A	p.Y177*	10,89701893,T,G	0.101	0.548	Truncating				Solid
955	PTEN	EEC		3	N/A	p.R130Q	10,89682885,G,A	0.257	0.556	Missense	high	Validated		Solid
957	ARID1A	EEC		3	N/A	p.G275A	1,26896305,G,C	0.484	0.453	Missense	low			Solid
957	ARID1A	EEC		3	N/A	p.T1438fs	26973619			Frame_Shift_Del		Validated		Solid
957	ARID1A	EEC		3	N/A	p.A1517fs	26973854			Frame_Shift_Del		Validated		Solid
957	KRAS	EEC		3	N/A	p.G12D	12,25289551,C,T	0.432	0.629	Missense	high	Validated		Solid
957	PTEN	EEC		3	N/A	p.G129R	10,89682881,G,A	0.449	0.536	Missense	high	Validated		Solid
957	PTEN	EEC		3	N/A	p.S170I	10,89701871,G,T	0.467	0.581	Missense	high	Validated		Solid
960	ARID1A	EEC		2	MSS	p.S1985P	1,26978929,T,C	0.086	0.391	Missense	medium		Yes	
960	CTNNB1	EEC		2	MSS	p.S33C	3,41241105,C,G	0.129	0.748	Missense	medium	Validated	Yes	
961	no mutations	EEC		1	MSS	no mutation							Yes	
965	no mutations	EEC		2	MSI-low	no mutation							Yes	
977	PIK3CA	ESC		N/A(3)	N/A	p.R115L	3,180399651,G,T	0.259	0.695	Missense	low	Validated		

ID	Gene	Original diagnosed subtype	Review Subtype	Grade	MSI Status	AA variant	Location (hg18)	Frequency	Probability	Type	Func. Impact	Sanger Validated	Normal available	Grade 3 Solid vs. Cytologic Atypia
977	PPP2R1A	ESC		N/A(3)	N/A	p.S256F	19,57408135,C,T	0.327	0.459	Missense	medium	Validated		
983	ARID1A	EEC		1	MSI-high	p.S1807fs	26978396			Frame_Shift_Ins			Yes	
983	PIK3CA	EEC		1	MSI-high	p.R88Q	3,180399570,G,A	0.368	0.560	Missense	medium	Validated	Yes	
983	PIK3CA	EEC		1	MSI-high	p.H1047Y	3,180434778,C,T	0.176	0.764	Missense	low	Validated	Yes	
983	PTEN	EEC		1	MSI-high	p.I135K	10,89682900,T,A	0.696	0.650	Missense	high	Validated	Yes	
987	no mutations	EEC		1	MSS	no mutation							Yes	
996	PIK3CA	EEC		3	MSS	p.E545K	3,180418785,G,A	0.200	0.318	Missense	low	Validated	Yes	Solid
996	PTEN	EEC		3	MSS	p.R130G	10,89682884,C,G	0.483	0.569	Missense	high	Validated	Yes	Solid
998	no mut	EEC		1	MSS	no mut							Yes	
1000	ARID1A	EEC		1	N/A	p.H1581R	1,26974047,A,G	0.087	0.784	Missense	medium			
1000	ARID1A	EEC		1	N/A	p.G64fs	26895673			Frame_Shift_Ins				
1000	PIK3CA	EEC		1	N/A	p.E110del	180399631			In_Frame_Del				
1000	PTEN	EEC		1	N/A	p.R130G	10,89682884,C,G	0.472	0.570	Missense	high	Validated		
1000	PTEN	EEC		1	N/A	p.D92Y	10,89682770,G,T	0.467	0.590	Missense	high	Validated		
1002	no mut	EEC		1	MSS	no mut							Yes	
1002	PTEN	EEC		1	MSS	p.R130G	10,89682884,C,G	0.070	0.331	Missense	high	Not Validated		
1004	CTNNB1	EEC		1	MSS	p.D32Y	3,41241101,G,T	0.405	0.576	Missense	medium		Yes	
1004	PTEN	EEC		1	MSS	p.G127V	10,89682876,G,T	0.286	0.591	Missense	high	Validated	Yes	
1004	PTEN	EEC		1	MSS	p.T319fs	89710785			Frame_Shift_Del			Yes	
1007	no mut	EEC		1	N/A	no mut							Yes	
1009	no mut	ESC		N/A (3)	MSS	no mut							Yes	
1010	PIK3CA	undifferentiated			MSI-high	p.P609H	3,180420132,C,A	0.158	0.502	Missense	low		Yes	
1010	PTEN	undifferentiated			MSI-high	p.R130G	10,89682884,C,G	0.506	0.574	Missense	high	Validated	Yes	
1010	TP53	undifferentiated			MSI-high	p.A138D	17,7519242,G,T	0.108	0.470	Missense	medium	Validated	Yes	
1015	ARID1A	EEC		2	MSI-high	p.R911M	1,26962363,G,T	0.222	0.379	Missense	medium		Yes	
1015	KRAS	EEC		2	MSI-high	p.G12D	12,25289551,C,T	0.174	0.313	Missense	high	Validated	Yes	
1015	PIK3CA	EEC		2	MSI-high	p.C378R	3,180405057,T,C	0.381	0.588	Missense	medium	Validated	Yes	
1015	PTEN	EEC		2	MSI-high	p.R130*	10,89682884,C,T	0.638	0.733	Truncating		Validated	Yes	
1020	PIK3CA	EEC		1	N/A	p.H1047L	3,180434779,A,T	0.200	0.614	Missense	low	Validated		
1020	PTEN	EEC		1	N/A	p.EDGFDL18del	89614256			In_Frame_Del				
1024	ARID1A	EEC		3	N/A	p.A1682fs	26974706			Frame_Shift_Del		Validated		Solid

ID	Gene	Original diagnosed subtype	Review Subtype	Grade	MSI Status	AA variant	Location (hg18)	Frequency	Probability	Type	Func. Impact	Sanger Validated	Normal available	Grade 3 Solid vs. Cytologic Atypia
1024	KRAS	EEC		3	N/A	p.G13D	12,25289548,C,T	0.360	0.631	Missense	high	Validated		Solid
1024	PIK3CA	EEC		3	N/A	p.R88Q	3,180399570,G,A	0.514	0.584	Missense	medium	Validated		Solid
1024	PTEN	EEC		3	N/A	p.F37fs	89643792			Frame_Shift_Ins				Solid
1024	PTEN	EEC		3	N/A	p.37_38insMGL	89643793			In_Frame_Ins				Solid
1030	PPP2R1A	ESC		N/A(3)	MSS	p.P179R	19,57407783,C,G			Missense	medium	Validated	Yes	
1030	TP53	ESC		N/A(3)	MSS	p.D281E	17,7517820,G,T	0.423	0.519	Missense	high		Yes	
1034	PTEN	EEC	mixed low-grade EEC and ESC	2	N/A	SPLICE_SITE_ACCEPTOR	89707589,G,C	0.518	0.678	SPLICE_SITE_ACCEPTOR				
1034	TP53	EEC	mixed low-grade EEC and ESC	2	N/A	p.R248Q	17,7518263,C,T	0.371	0.474	Missense	high			
1040	no mu	EEC		2	MSS	no mut							Yes	
1046	CTNNB1	EEC		1	N/A	p.D32Y	3,41241101,G,T	0.111	0.431	Missense	medium	Validated		
1046	PTEN	EEC		1	N/A	p.I300fs	89710728			Frame_Shift_Del				
1046	PTEN	EEC		1	N/A	p.D331fs	89710822			Frame_Shift_Ins				
1047	PPP2R1A	ESC		N/A(3)	MSS	p.P179L	19, 57407783,C,T			Missense	medium	Validated	Yes	
1047	TP53	ESC		N/A(3)	MSS	p.R273H	17,7517845,C,T	0.561	0.749	Missense	high		Yes	
1055	CTNNB1	EEC		2	MSS	p.G34V	3,41241108,G,T	0.394	0.677	Missense	medium		Yes	
1055	PTEN	EEC		2	MSS	p.E43*	10,89643809,G,T	0.385	0.465	Truncating		Validated	Yes	
1055	PTEN	EEC		2	MSS	p.E91fs	89682768			Frame_Shift_Ins			Yes	
1058	ARID1A	EEC		3	N/A	p.A1466fs	26973703			Frame_Shift_Del				Solid
1058	ARID1A	EEC		3	N/A	p.G1847fs	26978517			Frame_Shift_Del				Solid
1058	KRAS	EEC		3	N/A	p.G13D	12,25289548,C,T	0.226	0.677	Missense	high	Validated		Solid
1058	PTEN	EEC		3	N/A	p.E285*	10,89710682,G,T	0.348	0.559	Truncating		Validated		Solid
1058	PTEN	EEC		3	N/A	p.G293V	10,89710707,G,T	0.257	0.639	Missense	medium	Validated		Solid
1059	TP53	ESC		N/A(3)	MSS	p.K132R	17,7519260,T,C	0.231	0.383	Missense	high	Validated		
1069	ARID1A	EEC		2	MSS	p.T991fs	26965628			Frame_Shift_Del			Yes	
1069	ARID1A	EEC		2	MSS	p.K1830fs	26978466			Frame_Shift_Ins			Yes	
1069	PIK3CA	EEC		2	MSS	p.H1047R	3,180434779,A,G	0.254	0.659	Missense	low	Validated	Yes	
1069	PPP2R1A	EEC		2	MSS	p.R183Q	19,57407795,G,A			Missense	medium	Validated	Yes	
1069	PTEN	EEC		2	MSS	p.R130Q	10,89682885,G,A	0.274	0.517	Missense	high	Validated	Yes	
1069	TP53	EEC		2	MSS	p.G279E	17,7517827,C,T	0.250	0.411	Missense	high		Yes	
1069	TP53	EEC		2	MSS	p.R175H	17,7519131,C,T	0.303	0.649	Missense	high	Validated	Yes	

ID	Gene	Original diagnosed subtype	Review Subtype	Grade	MSI Status	AA variant	Location (hg18)	Frequency	Probability	Type	Func. Impact	Sanger Validated	Normal available	Grade 3 Solid vs. Cytologic Atypia
1073	ARID1A	EEC		1	MSS	p.R1446*	1,26973641,C,T	0.111	0.483	Truncating			Yes	
1073	ARID1A	EEC		1	MSS	p.Q1404*	1,26973515,C,T	0.114	0.624	Truncating			Yes	
1073	CTNNB1	EEC		1	MSS	p.S33F	3,41241105,C,T	0.089	0.501	Missense	medium	Validated	Yes	
1073	PTEN	EEC		1	MSS	p.R172fs	89701877			Frame_Shift_Del			Yes	
1074	ARID1A	EEC		3	MSS	p.R1461*	1,26973686,C,T	0.469	0.548	Truncating			Yes	Solid
1074	ARID1A	EEC		3	MSS	p.A1517fs	26973854			Frame_Shift_Ins			Yes	Solid
1074	PIK3CA	EEC		3	MSS	p.R108H	3,180399630,G,A	0.340	0.619	Missense	medium	Validated	Yes	Solid
1074	PPP2R1A	EEC		3	MSS	p.R182W	19,57407791,C,T	0.341	0.598	Missense	medium	Validated	Yes	Solid
1074	PTEN	EEC		3	MSS	p.R130G	10,89682884,C,G	0.920	0.642	Missense	high	Validated	Yes	Solid
1075	CTNNB1	EEC		2	MSS	p.D32Y	3,41241101,G,T	0.349	0.628	Missense	medium		Yes	
1075	PIK3CA	EEC		2	MSS	p.T1025N	3,180434713,C,A	0.306	0.401	Missense	low	Validated	Yes	
1075	PTEN	EEC		2	MSS	p.R130G	10,89682884,C,G	0.291	0.567	Missense	high	Validated	Yes	
1075	PTEN	EEC		2	MSS	p.D24V	10,89614277,A,T	0.462	0.604	Missense	high	Validated	Yes	
1081	no mut	ESC		N/A (3)	MSS	no mut							Yes	
1082	TP53	ESC		N/A(3)	MSS	p.A138V	17,7519242,G,A	0.510	0.692	Missense	high	Validated	Yes	
1086	ARID1A	EEC		3	N/A	p.N1070fs	26970208			Frame_Shift_Del				Solid
1086	ARID1A	EEC		3	N/A	p.S1316fs	26972738			Frame_Shift_Del				Solid
1086	KRAS	EEC		3	N/A	p.G12V	12,25289551,C,A	0.351	0.594	Missense	high	Validated		Solid
1086	PIK3CA	EEC		3	N/A	p.R88Q	3,180399570,G,A	0.318	0.539	Missense	medium	Validated		Solid
1086	PTEN	EEC		3	N/A	p.R130G	10,89682884,C,G	0.635	0.530	Missense	high	Validated		Solid
1087	no mut	EEC		1	MSI-low	no mut							Yes	
1090	ARID1A	EEC		3	N/A	p.R1598C	1,26974097,C,T	0.341	0.536	Missense	medium			Solid
1090	PTEN	EEC		3	N/A	p.T319fs	89710784			Frame_Shift_Del				Solid
1090	TP53	EEC		3	N/A	p.G187S	17,7519015,C,T	0.789	0.563	Missense	medium	Validated		Solid
1090	TP53	EEC		3	N/A	SPLICE_SITE_ACCEPTOR	7519015,C,T	0.789	0.563	SPLICE_SITE_ACCEPTOR				Solid
1094	ARID1A	EEC		3	N/A	p.S2211N	1,26979608,G,A	0.074	0.573	Missense	low			Solid
1094	ARID1A	EEC		3	N/A	p.Q1342*	1,26972899,C,T	0.146	0.621	Truncating				Solid
1094	ARID1A	EEC		3	N/A	p.W1973*	1,26978895,G,A	0.108	0.625	Truncating				Solid
1094	ARID1A	EEC		3	N/A	p.H1384Y	1,26973455,C,T	0.167	0.775	Missense	medium			Solid
1094	CTNNB1	EEC		3	N/A	p.I423S	3,41250106,T,G	0.124	0.608	Missense	medium	Validated		Solid
1094	KRAS	EEC		3	N/A	p.G138E	12,25269852,C,T	0.089	0.490	Missense	high	Validated		Solid
1094	PIK3CA	EEC		3	N/A	p.T1025A	3,180434712,A,G	0.113	0.589	Missense	low	Validated		Solid
1094	PIK3CA	EEC		3	N/A	p.R88Q	3,180399570,G,A	0.077	0.604	Missense	medium	Validated		Solid
1094	PPP2R1A	EEC		3	N/A	p.R221W	19,57408029,C,T	0.125	0.818	Missense	medium	Validated		Solid
1094	PPP2R5C	EEC		3	N/A	p.T282M	14,101430643,C,T	0.182	0.588	Missense	medium			Solid

ID	Gene	Original diagnosed subtype	Review Subtype	Grade	MSI Status	AA variant	Location (hg18)	Frequency	Probability	Type	Func. Impact	Sanger Validated	Normal available	Grade 3 Solid vs. Cytologic Atypia
1094	PTEN	EEC		3	N/A	p.K128Q	10,89682878,A,C	0.067	0.366	Missense	high	Validated		Solid
1094	PTEN	EEC		3	N/A	p.R142W	10,89682920,C,T	0.111	0.542	Missense	medium			Solid
1094	PTEN	EEC		3	N/A	p.E7*	10,89614225,G,T	0.105	0.677	Truncating		Validated		Solid
1094	TP53	EEC		3	N/A	p.R196*	17,7518988,G,A	0.118	0.591	Truncating		Validated		Solid
1094	TP53	EEC		3	N/A	p.Y163C	17,7519167,T,C	0.159	0.814	Missense	medium	Validated		Solid
1095	PIK3CA	EEC		3	N/A	p.E545G	3,180418786,A,G	0.108	0.319	Missense	low	Validated		Solid
1095	PTEN	EEC		3	N/A	p.V317fs	89710778			Frame_Shift_Del				Solid
1099	ARID1A	EEC		1	MSI-high	p.R1551H	1,26973957,G,A	0.209	0.738	Missense	medium	Validated	Yes	
1099	PTEN	EEC		1	MSI-high	p.V119fs	89682851			Frame_Shift_Ins			Yes	
1100	PIK3CA	EEC		3	MSS	p.H1047R	3,180434779,A,G	0.607	0.534	Missense	low	Validated	Yes	
1100	TP53	EEC		3	MSS	p.C182fs	7519110			Frame_Shift_Del			Yes	
1102	PTEN	EEC		3	N/A	p.L25fs	89614279			Frame_Shift_Del			Yes	Solid
1104	no mut	EEC		2	MSS	no mut							Yes	
1109	ARID1A	EEC		3	MSI-low	p.E1767*	1,26978275,G,T	0.211	0.693	Truncating			Yes	Cytologic Atypia
1109	PIK3CA	EEC		3	MSI-low	p.R54K	3,180399468,G,A	0.180	0.525	Missense	low	Validated	Yes	Cytologic Atypia
1109	PIK3CA	EEC		3	MSI-low	p.R1023*	3,180434706,C,T	0.206	0.580	Truncating		Validated	Yes	Cytologic Atypia
1109	PIK3CA	EEC		3	MSI-low	p.R38C	3,180399419,C,T	0.147	0.609	Missense	medium	Validated	Yes	Cytologic Atypia
1109	PIK3CA	EEC		3	MSI-low	p.L339I	3,180404227,C,A	0.108	0.684	Missense	medium	Validated	Yes	Cytologic Atypia
1109	PIK3CA	EEC		3	MSI-low	p.Y1021C	3,180434701,A,G	0.096	0.774	Missense	medium	Validated	Yes	Cytologic Atypia
1109	PPP2R1A	EEC		3	MSI-low	p.R183W	19,57407794,C,T	0.198	0.819	Missense	medium	Validated	Yes	Cytologic Atypia
1109	PTEN	EEC		3	MSI-low	p.G20*	10,89614264,G,T	0.340	0.485	Truncating		Validated	Yes	Cytologic Atypia
1109	PTEN	EEC		3	MSI-low	p.R130Q	10,89682885,G,A	0.304	0.546	Missense	high	Validated	Yes	Cytologic Atypia
1111	no mut	EEC		3	MSS	no mut							Yes	Solid
1115	no mut	Carcinosarcoma		N/A (3)	MSS	no mut								
1118	PIK3CA	ESC		N/A(3)	MSS	p.H1047R	3,180434779,A,G	0.495	0.701	Missense	low	Validated	Yes	
1118	PPP2R1A	ESC		N/A(3)	MSS	p.P179R	19,57407783,C,G			Missense	medium		Yes	
1118	TP53	ESC		N/A(3)	MSS	p.M237I	17,7518295,C,T	0.273	0.746	Missense	high		Yes	
1119	ARID1A	undifferentiated			MSS	p.R1721*	1,26978137,C,T	0.411	0.489	Truncating		Validated	Yes	
1119	ARID1A	undiffere			MSS	p.S607*	1,26931770,C,A	0.533	0.717	Truncating			Yes	

ID	Gene	Original diagnosed subtype	Review Subtype	Grade	MSI Status	AA variant	Location (hg18)	Frequency	Probability	Type	Func. Impact	Sanger Validated	Normal available	Grade 3 Solid vs. Cytologic Atypia
		ntiated												
1119	CTNNB1	undifferentiated			MSS	p.D32N	3,41241101,G,A	0.402	0.557	Missense	medium	Validated	Yes	
1119	CTNNB1	undifferentiated			MSS	p.R200H	3,41241932,G,A	0.426	0.699	Missense	medium		Yes	
1119	PIK3CA	undifferentiated			MSS	p.R88Q	3,180399570,G,A	0.333	0.414	Missense	medium	Validated	Yes	
1119	PIK3CA	undifferentiated			MSS	p.H1047Q	3,180434780,T,G	0.422	0.684	Missense	low	Validated	Yes	
1119	PTEN	undifferentiated			MSS	SPLICE_SITE_DONOR	89710857,T,G	0.455	0.514	SPLICE_SITE_DONOR			Yes	
1119	PTEN	undifferentiated			MSS	p.K6N	10,89614224,A,C	0.427	0.572	Missense	medium	Validated	Yes	
1119	PTEN	undifferentiated			MSS	p.F81C	10,89680815,T,G	0.533	0.614	Missense	high		Yes	
1120	ARID1A	ESC	mixed - 60% ESC 40% low-grade EEC	3	N/A	p.Q2176fs	26979502			Frame_Shift_Del				
1120	KRAS	ESC	mixed - 60% ESC 40% low-grade EEC	3	N/A	p.G12A	12,25289551,C,G	0.174	0.580	Missense	high	Validated		
1120	PIK3CA	ESC	mixed - 60% ESC 40% low-grade EEC	3	N/A	p.H1047Y	3,180434778,C,T	0.058	0.336	Missense	low	Validated		
1120	PIK3CA	ESC	mixed - 60% ESC 40% low-grade EEC	3	N/A	p.Q546K	3,180418788,C,A	0.162	0.382	Missense	low	Validated		
1134	ARID1A	EEC		2	N/A	p.R1989*	1,26978941,C,T	0.088	0.551	Truncating				
1134	KRAS	EEC		2	N/A	p.S89*	12,25271459,G,T	0.144	0.506	Truncating		Validated		
1134	PIK3CA	EEC		2	N/A	p.R357Q	3,180404995,G,A	0.157	0.370	Missense	medium	Validated		
1134	PIK3CA	EEC		2	N/A	p.R88Q	3,180399570,G,A	0.140	0.566	Missense	medium	Validated		
1134	PIK3CA	EEC		2	N/A	p.K111N	3,180399640,G,T	0.085	0.583	Missense	medium	Validated		
1135	ARID1A	EEC		1	N/A	p.G89fs	26895747			Frame_Shift_Del				
1135	PTEN	EEC		1	N/A	p.R15*	10,89614249,A,T	0.101	0.613	Truncating		Not Validated		
1142	PTEN	EEC		1	MSS	p.G36R	10,89643788,G,A	0.121	0.370	Missense	high	Validated	Yes	
1142	PTEN	EEC		1	MSS	p.Q245*	10,89707688,C,T	0.259	0.610	Truncating		Validated	Yes	
1203	ARID1A	Carcinosarcoma		N/A (3)	MSS	p.R1658W	1,26974277,C,T	0.143	0.522	Missense				

ID	Gene	Original diagnosed subtype	Review Subtype	Grade	MSI Status	AA variant	Location (hg18)	Frequency	Probability	Type	Func. Impact	Sanger Validated	Normal available	Grade 3 Solid vs. Cytologic Atypia
1203	CTNNB1	Carcinosarcoma		N/A (3)	MSS	p.M243T	3,41242061,T,C	0.350	0.646	Missense				
1203	PIK3CA	Carcinosarcoma		N/A (3)	MSS	p.E81A	3,180399549,A,C	0.229	0.405	Missense				
1203	PIK3CA	Carcinosarcoma		N/A (3)	MSS	p.R88Q	3,180399570,G,A	0.258	0.431	Missense	medium			
1203	PIK3CA	Carcinosarcoma		N/A (3)	MSS	p.L239R	3,180401925,T,G	0.214	0.614	Missense				
1203	PPP2R1A	Carcinosarcoma		N/A (3)	MSS	p.V229M	19,57408053,G,A	0.364	0.571	Missense	medium			
1203	PTEN	Carcinosarcoma		N/A (3)	MSS	p.R130Q	10,89682885,G,A	0.241	0.307	Missense	high			
1203	PTEN	Carcinosarcoma		N/A (3)	MSS	p.E7*	10,89614225,G,T	0.295	0.713	Truncating				
1208	TP53	Carcinosarcoma		N/A (3)	MSS	p.E171*	17,7519144,C,A	0.625	0.730	Truncating				
1227	no mut	ESC		N/A (3)	MSS	no mut								
1239	ARID1A	Carcinosarcoma		N/A (3)	MSS	p.R2236C	1,26979682,C,T	0.229	0.462	Missense				
1241	PIK3CA	Carcinosarcoma		N/A (3)	MSI-High	p.E39K	3,180399422,G,A	0.419	0.567	Missense	medium			
1241	PTEN	Carcinosarcoma		N/A (3)	MSI-High	p.Y16*	10,89614254,T,G	0.225	0.475	Truncating				
1241	PTEN	Carcinosarcoma		N/A (3)	MSI-High	p.G129E	10,89682882,G,A	0.683	0.687	Missense	high			
1262	no mut	Carcinosarcoma		N/A (3)	MSS	no mut								
1272	ARID1A	EEC		1	MSS	p.T294P	1,26896361,A,C	0.333	0.347	Missense	low			
1272	ARID1A	EEC		1	MSS	p.R1989	1,26978941,C,T	0.300	0.684	Truncating				
1272	PIK3CA	EEC		1	MSS	p.D1029Y	3,180434724,G,T	0.350	0.734	Missense	medium	Validated		
1272	PIK3CA	EEC		1	MSS	p.T1025A	3,180434712,A,G	0.350	0.748	Missense	low	Validated		
1272	PPP2R5C	EEC		1	MSS	p.L168V	14,101419525,T,G	0.444	0.626	Missense				
1272	PTEN	EEC		1	MSS	p.E299	10,89710724,G,T	0.524	0.724	Truncating				
1274	CTNNB1	EEC		1	MSS	p.D32Y	3,41241101,G,T	0.273	0.733	Missense	medium			
1274	PIK3CA	EEC		1	MSS	p.H1047R	3,180434779,A,G	0.455	0.634	Missense	low	Validated		
1281	PIK3CA	EEC		2	MSS	p.H1047R	3,180434779,A,G	0.533	0.736	Missense	low	Validated		
1293	ARID1A	EEC		1	MSI-High	p.G1847fs	26978517			Frame_Shift_Del				
1293	KRAS	EEC		1	MSI-High	p.G12V	12,25289551,C,A	0.214	0.640	Missense	high			
1293	PIK3CA	EEC		1	MSI-High	p.E418K	3,180410668,G,A	0.350	0.588	Missense	low			
1293	PTEN	EEC		1	MSI-	p.G129E	10,89682882,G,A	0.353	0.685	Missense	high			

ID	Gene	Original diagnosed subtype	Review Subtype	Grade	MSI Status	AA variant	Location (hg18)	Frequency	Probability	Type	Func. Impact	Sanger Validated	Normal available	Grade 3 Solid vs. Cytologic Atypia
					High									
1294	PTEN	EEC		2	MSS	p.Q17	10,89614255,C,T	0.300	0.636	Truncating				
1297	ARID1A	EEC		2	MSI-High	p.C884	1,26962283,T,A	0.220	0.656	Truncating				
1297	ARID1A	EEC		2	MSI-High	p.R1335	1,26972794,C,T	0.220	0.686	Truncating				
1297	KRAS	EEC		2	MSI-High	p.G12D	12,25289551,C,T	0.500	0.683	Missense	high			
1297	PIK3CA	EEC		2	MSI-High	p.R88Q	3,180399570,G,A	0.261	0.736	Missense	medium			
1300	PTEN	EEC		1	MSS	p.R130Q	10,89682885,G,A	0.267	0.679	Missense	high			
1317	ARID1A	EEC		1	MSI-High	p.E1904fs	26978686			Frame_Shift_Del				
1317	CTNNB1	EEC		1	MSI-High	p.S33Y	3,41241105,C,A	0.214	0.664	Missense	medium			
1317	KRAS	EEC		1	MSI-High	p.G12C	12,25289552,C,A	0.412	0.669	Missense	high			
1317	PIK3CA	EEC		1	MSI-High	p.E542K	3,180418776,G,A	0.500	0.486	Missense	low	Validated		
1317	PTEN	EEC		1	MSI-High	p.F195S	10,89701946,T,C	0.813	0.845	Missense	low			
1332	CTNNB1	EEC		2	MSS	p.S33C	3,41241105,C,G	0.265	0.736	Missense	medium			
1332	PPP2R1A	EEC		2	MSS	p.R183W	19,57407794,C,T	0.273	0.373	Missense	medium			
1332	PTEN	EEC		2	MSS	p.R130G	10,89682884,C,G	0.889	0.674	Missense	high			
1338	PPP2R1A	Carcinosarcoma		N/A (3)	MSS	p.P179R	19,57407783,C,G	0.250	0.377	Missense	medium			
1338	TP53	Carcinosarcoma		N/A (3)	MSS	p.C176S	17,7519129,A,T	0.776	0.834	Missense	high			
1339	PTEN	EEC		1	MSS	SPLICE_SITE_ACCEPTOR	89710629,A,T	0.600	0.432	SPLICE_SITE_ACCEPTOR	high			
1354	PIK3CA	Carcinosarcoma		N/A (3)	MSS	p.H1047L	3,180434779,A,T	0.710	0.726	Missense	low			
1354	PPP2R1A	Carcinosarcoma		N/A (3)	MSS	p.P179R	19,57407783,C,G	0.438	0.476	Missense	medium			
1354	TP53	Carcinosarcoma		N/A (3)	MSS	p.E51*	17,7520261,C,A	0.667	0.748	Truncating				
1362	BRAF	EEC		2	MSS	p.A747D	7,140080927,G,T	0.375	0.480	Missense				
1375	ARID1A	EEC		2	MSS	p.L2134fs	26979376			Frame_Shift_Del				
1375	PTEN	EEC		2	MSS	p.H93D	10,89682773,C,G	0.560	0.678	Missense	medium			
1376	ARID1A	EEC		1	MSI-High	p.R1335	1,26972794,C,T	0.463	0.674	Truncating				
1376	TP53	EEC		1	MSI-	p.R213Q	17,7518936,C,T	0.190	0.436	Missense	high			

ID	Gene	Original diagnosed subtype	Review Subtype	Grade	MSI Status	AA variant	Location (hg18)	Frequency	Probability	Type	Func. Impact	Sanger Validated	Normal available	Grade 3 Solid vs. Cytologic Atypia
					High									
1378	PTEN	EEC		2	MSI-low	p.G132V	10,89682891,G,T	0.206	0.661	Missense	high			
1378	PTEN	EEC		2	MSI-low	p.R130Q	10,89682885,G,A	0.161	0.705	Missense	high			
1392	ARID1A	EEC		1	MSI-High	p.I1954fs	26978837			Frame_Shift_Del				
1392	ARID1A	EEC		1	MSI-High	p.K1962del	26978859			In_Frame_Del				
1392	PTEN	EEC		1	MSI-High	p.R130G	10,89682884,C,G	0.414	0.703	Missense	high			
1401	ARID1A	EEC		1	MSI-High	SPLICE_SITE_ACCEPTOR	26930229,G,A	0.333	0.562	SPLICE_SITE_ACCEPTOR				
1401	KRAS	EEC		1	MSI-High	p.G13D	12,25289548,C,T	0.450	0.669	Missense	high			
1401	PIK3CA	EEC		1	MSI-High	p.G106D	3,180399624,G,A	0.278	0.679	Missense				
1401	PIK3CA	EEC		1	MSI-High	p.R88Q	3,180399570,G,A	0.276	0.751	Missense	medium			
1401	PPP2R1A	EEC		1	MSI-High	p.R183W	19,57407794,C,T	0.625	0.810	Missense	medium			
1401	PTEN	EEC		1	MSI-High	p.V166A	10,89701859,T,C	0.455	0.565	Missense	medium			
1401	PTEN	EEC		1	MSI-High	p.L152R	10,89682951,T,G	0.448	0.689	Missense				
1401	PTEN	EEC		1	MSI-High	p.K147	10,89682935,A,T	0.577	0.713	Truncating				
1401	TP53	EEC		1	MSI-High	p.R283H	17,7517815,C,T	0.381	0.694	Missense	medium			
1402	CTNNB1	EEC		1	MSS	p.G34E	3,41241108,G,A	0.333	0.624	Missense	medium			
1402	PIK3CA	EEC		1	MSS	p.M1043I	3,180434768,G,T	0.429	0.691	Missense	low	Validated		
1402	PIK3CA	EEC		1	MSS	p.R88Q	3,180399570,G,A	0.500	0.696	Missense	medium			
1402	PTEN	EEC		1	MSS	p.K6T	10,89614223,A,C	0.292	0.690	Missense				
1402	PTEN	EEC		1	MSS	p.R130Q	10,89682885,G,A	0.393	0.712	Missense	high			
1409	PIK3CA	EEC		1	MSI-High	p.H1065Y	3,180434832,C,T	0.273	0.608	Missense	low			
1409	PIK3CA	EEC		1	MSI-High	p.R88Q	3,180399570,G,A	0.368	0.644	Missense	medium			
1409	TP53	EEC		1	MSI-High	p.R158H	17,7519182,C,T	0.211	0.655	Missense	high			
1413	ARID1A	Carcinosarcoma		N/A (3)	MSS	p.P120R	1,26895840,C,G	0.933	0.828	Missense				
1413	PPP2R1A	Carcinosarcoma		N/A (3)	MSS	p.W257C	19,57408139,G,T	0.353	0.375	Missense	medium			
1413	TP53	Carcinosarcoma		N/A (3)	MSS	SPLICE_SITE_DO	7520035,A,C	0.895	0.815	SPLICE_SITE_DON				

ID	Gene	Original diagnosed subtype	Review Subtype	Grade	MSI Status	AA variant	Location (hg18)	Frequency	Probability	Type	Func. Impact	Sanger Validated	Normal available	Grade 3 Solid vs. Cytologic Atypia
						NOR				OR				
1415	ARID1A	EEC		1	MSS	p.Y2254fs	26979736			Frame_Shift_Del				
1415	PTEN	EEC		1	MSS	p.R130G	10,89682884,C,G	0.710	0.806	Missense	high			
1416	PTEN	EEC		1	MSI-low	p.R130G	10,89682884,C,G	0.264	0.658	Missense	high			
1418	TP53	EEC		1	MSS	p.E285K	17,7517810,C,T	0.917	0.816	Missense	medium			
1421	ARID1A	EEC		1	MSS	p.Q548fs	26930523			Frame_Shift_Ins				
1421	CTNNB1	EEC		1	MSS	p.S33C	3,41241105,C,G	0.625	0.705	Missense	medium			
1423	ARID1A	EEC		2	MSS	p.F1606fs	26974122			Frame_Shift_Del				
1423	CTNNB1	EEC		2	MSS	p.G34V	3,41241108,G,T	0.389	0.745	Missense	medium			
1424	ARID1A	EEC		2	MSS	p.P2095fs	26979261			Frame_Shift_Del				
1424	PTEN	EEC		2	MSS	p.C124S	10,89682867,G,C	0.760	0.825	Missense	high			
1430	no mut	EEC		2	MSS	no mut								
1438	no mut	ESC		N/A (3)	MSS	no mut								
1440	PTEN	EEC		2	MSS	p.T319fs	89710784			Frame_Shift_Del				
1459	PTEN	EEC		1	MSS	p.Q214	10,89707595,C,T	0.500	0.731	Truncating				
1461	no mut	Carcinosarcoma		N/A (3)	MSS	no mut								
1467	KRAS	Carcinosarcoma		N/A (3)	MSS	p.G12C	12,25289552,C,A	0.875	0.633	Missense	high			
1467	PPP2R1A	Carcinosarcoma		N/A (3)	MSS	p.S256F	19,57408135,C,T	0.600	0.590	Missense	medium			
1467	TP53	Carcinosarcoma		N/A (3)	MSS	p.T18fs	7520585			Frame_Shift_Del				
1469	PIK3CA	Carcinosarcoma		N/A (3)	MSS	p.R88Q	3,180399570,G,A	0.310	0.464	Missense	medium			
1469	PTEN	Carcinosarcoma		N/A (3)	MSS	p.N48K	10,89643826,C,A	0.400	0.463	Missense	medium			
1469	PTEN	Carcinosarcoma		N/A (3)	MSS	p.R142fs	89682922			Frame_Shift_Del				
1489	PTEN	EEC		1	MSS	p.L295fs	89710712			Frame_Shift_Del				
1491	PTEN	Carcinosarcoma		N/A (3)	MSS	p.D252V	10,89707710,A,T	0.240	0.369	Missense	high			
1491	PTEN	Carcinosarcoma		N/A (3)	MSS	p.Q298	10,89710721,C,T	0.267	0.505	Truncating				
1494	PTEN	EEC		1	MSS	p.Y16*	10,89614254,T,G	0.121	0.462	Truncating				
1494	PTEN	EEC		1	MSS	p.R130Q	10,89682885,G,A	0.176	0.618	Missense	high			
1497	ARID1A	EEC		1	MSI-	p.R1461	1,26973686,C,T	0.290	0.632	Truncating				

ID	Gene	Original diagnosed subtype	Review Subtype	Grade	MSI Status	AA variant	Location (hg18)	Frequency	Probability	Type	Func. Impact	Sanger Validated	Normal available	Grade 3 Solid vs. Cytologic Atypia
					High									
1497	ARID1A	EEC		1	MSI-High	p.M1220T	1,26972009,T,C	0.292	0.703	Missense				
1497	PIK3CA	EEC		1	MSI-High	p.R38H	3,180399420,G,A	0.195	0.636	Missense	medium			
1497	PTEN	EEC		1	MSI-High	p.R130*	10,89682884,C,T	0.342	0.614	Truncating				
1502	CTNNB1	EEC		2	MSS	p.S37P	3,41241116,T,C	0.333	0.721	Missense	high			
1502	TP53	EEC		2	MSS	p.S149Y	17,7519209,G,T	0.121	0.572	Missense	medium			
1509	ARID1A	EEC		1	MSS	p.R1721	1,26978137,C,T	0.286	0.654	Truncating				
1509	CTNNB1	EEC		1	MSS	p.S33C	3,41241105,C,G	0.444	0.768	Missense	medium			
1509	PIK3CA	EEC		1	MSS	p.E453K	3,180410773,G,A	0.286	0.694	Missense	medium			
1509	PIK3CA	EEC		1	MSS	p.R88Q	3,180399570,G,A	0.289	0.744	Missense	medium			
1509	PPP2R1A	EEC		1	MSS	p.H87Y	19,57401117,C,T	0.286	0.590	Missense	low			
1509	PTEN	EEC		1	MSS	p.W111	10,89682829,G,A	0.607	0.683	Truncating				
1513	no mut	EEC		1	MSS	no mut								
1522	ARID1A	EEC		1	MSS	p.R1989*	1,26978941,C,T	0.278	0.662	Truncating				
1522	ARID1A	EEC		1	MSS	p.S2262L	1,26979761,C,T	0.115	0.733	Missense				
1522	PIK3CA	EEC		1	MSS	p.Y1021C	3,180434701,A,G	0.333	0.689	Missense	medium	Validated		
1522	PPP2R1A	EEC		1	MSS	p.S219L	19,57408024,C,T	0.250	0.647	Missense				
1522	PTEN	EEC		1	MSS	p.R130Q	10,89682885,G,A	0.333	0.689	Missense	high			
1524	ARID1A	EEC		2	MSI-High	p.R1722	1,26978140,C,T	0.407	0.492	Truncating				
1524	ARID1A	EEC		2	MSI-High	p.M1613I	1,26974144,G,A	0.405	0.696	Missense	low			
1524	CTNNB1	EEC		2	MSI-High	p.R661*	3,41253109,C,T	0.286	0.505	Truncating				
1524	CTNNB1	EEC		2	MSI-High	p.A230V	3,41242022,C,T	0.432	0.637	Missense				
1524	KRAS	EEC		2	MSI-High	p.G12D	12,25289551,C,T	0.294	0.684	Missense	high			
1524	PIK3CA	EEC		2	MSI-High	p.R38C	3,180399419,C,T	0.326	0.712	Missense	medium			
1524	PIK3CA	EEC		2	MSI-High	p.L1006F	3,180434655,C,T	0.350	0.716	Missense				
1524	PTEN	EEC		2	MSI-High	p.R233*	10,89707652,C,T	0.208	0.583	Truncating				
1524	PTEN	EEC		2	MSI-High	p.R130*	10,89682884,C,T	0.385	0.703	Truncating				
1524	PTEN	EEC		2	MSI-High	p.P246L	10,89707692,C,T	0.348	0.747	Missense	medium			
1524	TP53	EEC		2	MSI-High	p.R181C	17,7519114,G,A	0.413	0.511	Missense	medium			

ID	Gene	Original diagnosed subtype	Review Subtype	Grade	MSI Status	AA variant	Location (hg18)	Frequency	Probability	Type	Func. Impact	Sanger Validated	Normal available	Grade 3 Solid vs. Cytologic Atypia
1525	PTEN	EEC		1	MSS	p.R130L	10,89682885,G,T	0.233	0.654	Missense	high			
1526	KRAS	EEC		2	MSI-High	p.G13D	12,25289548,C,T	0.600	0.789	Missense	high			
1526	PTEN	EEC		2	MSI-High	p.L265fs	89707749			Frame_Shift_Ins				
1529	CTNNB1	EEC		1	MSI-High	p.R200C	3,41241931,C,T	0.182	0.637	Missense				
1529	PIK3CA	EEC		1	MSI-High	p.R38H	3,180399420,G,A	0.154	0.662	Missense	medium			
1529	PTEN	EEC		1	MSI-High	p.Y155fs	89682961			Frame_Shift_Ins				
1533	KRAS	EEC		1	MSS	p.G12V	12,25289551,C,A	0.313	0.609	Missense	high			
1536	no mut	EEC		1	MSS	no mut								
1537	ARID1A	EEC		1	MSS	p.R1989	1,26978941,C,T	0.167	0.545	Truncating				
1537	ARID1A	EEC		1	MSS	p.I1294T	1,26972672,T,C	0.385	0.697	Missense				
1538	KRAS	EEC		2	MSS	p.G12D	12,25289551,C,T	0.313	0.731	Missense	high			
1538	TP53	EEC		2	MSS	p.F270S	17,7517854,A,G	0.778	0.885	Missense	medium			
1549	ARID1A	EEC		1	MSS	p.Q1200	1,26971948,C,T	0.333	0.721	Truncating				
1549	BRAF	EEC		1	MSS	p.E26D	7,140270895,C,A	0.500	0.695	Missense	low			
1550	ARID1A	EEC		1	MSI-High	p.Q1330	1,26972779,C,T	0.444	0.708	Truncating				
1551	ARID1A	EEC		1	MSS	p.Q1579	1,26974040,C,T	0.239	0.705	Truncating				
1551	ARID1A	EEC		1	MSS	p.R2158	1,26979448,C,T	0.260	0.806	Truncating				
1551	PTEN	EEC		1	MSS	p.R233	10,89707652,C,T	0.261	0.491	Truncating				
1551	PTEN	EEC		1	MSS	p.V317fs	89710778			Frame_Shift_Del				
1563	ARID1A	EEC		1	MSS	p.Q435	1,26928894,C,T	0.214	0.644	Truncating				
1563	PTEN	EEC		1	MSS	p.R130fs	89682884			Frame_Shift_Del				
1572	ARID1A	EEC		1	MSS	p.E1767	1,26978275,G,T	0.279	0.672	Truncating				
1572	ARID1A	EEC		1	MSS	p.G2087fs	26979237			Frame_Shift_Del				
1572	PIK3CA	EEC		1	MSS	p.H1065Y	3,180434832,C,T	0.345	0.675	Missense	low			
1572	PTEN	EEC		1	MSS	p.R11*	10,89614237,A,T	0.273	0.456	Truncating				
1572	PTEN	EEC		1	MSS	p.R130G	10,89682884,C,G	0.214	0.624	Missense	high			
1574	PIK3CA	EEC		2	MSI-High	p.R93W	3,180399584,C,T	0.435	0.699	Missense	medium			
1575	ARID1A	EEC		1	MSS	p.M872T	1,26962246,T,C	0.596	0.798	Missense				
1575	ARID1A	EEC		1	MSS	p.A1517fs	26973854			Frame_Shift_Ins				
1575	PTEN	EEC		1	MSS	p.R130Q	10,89682885,G,A	0.241	0.571	Missense	high			
1575	PTEN	EEC		1	MSS	p.R130G	10,89682884,C,G	0.148	0.768	Missense	high			
1576	ARID1A	EEC		2	MSI-	p.A1517fs	26973854			Frame_Shi				

ID	Gene	Original diagnosed subtype	Review Subtype	Grade	MSI Status	AA variant	Location (hg18)	Frequency	Probability	Type	Func. Impact	Sanger Validated	Normal available	Grade 3 Solid vs. Cytologic Atypia
					High					ft_Del				
1576	KRAS	EEC		2	MSI-High	p.G13D	12,25289548,C,T	0.647	0.784	Missense	high			
1576	PTEN	EEC		2	MSI-High	p.R130Q	10,89682885,G,A	0.587	0.792	Missense	high			
1577	TP53	ESC		N/A (3)	MSS	p.K120E	17,7520054,T,C	0.619	0.710	Missense	medium			
1580	TP53	EEC		1	MSS	p.R248Q	17,7518263,C,T	0.154	0.683	Missense	high			
1583	ARID1A	EEC		1	MSS	p.Q1098	1,26970290,C,T	0.245	0.694	Truncating				
1583	CTNNB1	EEC		1	MSS	p.S37F	3,41241117,C,T	0.244	0.634	Missense	high			
1583	PTEN	EEC		1	MSS	p.R130*	10,89682884,C,T	0.684	0.819	Truncating				
1585	BRAF	ESC		N/A (3)	MSS	p.E26D	7,140270895,C,A	0.556	0.695	Missense	low			
1595	ARID1A	Carcinosarcoma		N/A (3)	MSS	p.P1627A	1,26974184,C,G	0.629	0.729	Missense	low			
1595	PIK3CA	Carcinosarcoma		N/A (3)	MSS	p.E453K	3,180410773,G,A	0.379	0.442	Missense	medium			
1595	TP53	Carcinosarcoma		N/A (3)	MSS	p.V272L	17,7517849,C,A	0.500	0.499	Missense	medium			
1596	ARID1A	Carcinosarcoma		N/A (3)	MSS	p.Q1328	1,26972773,C,T	0.318	0.706	Truncating				
1596	PTEN	Carcinosarcoma		N/A (3)	MSS	p.R130Q	10,89682885,G,A	0.515	0.623	Missense	high			
1596	TP53	Carcinosarcoma		N/A (3)	MSS	SPLICE_SITE_ACCEPTOR	7519280,C,T	0.294	0.336	SPLICE_SITE_ACCEPTOR				
1596	TP53	Carcinosarcoma		N/A (3)	MSS	p.N131del	7519259			In_Frame_Del				
1624	CTNNB1	ESC		N/A (3)	MSS	SPLICE_SITE_ACCEPTOR	41256313,G,T	0.086	0.376	SPLICE_SITE_ACCEPTOR				
1630	TP53	Carcinosarcoma		N/A (3)	MSS	SPLICE_SITE_ACCEPTOR	7518334,C,T	0.364	0.497	SPLICE_SITE_ACCEPTOR				
1643	no mut	Carcinosarcoma		N/A (3)	MSI-low	no mut								
1647	KRAS	ESC		N/A (3)	MSS	p.G12D	12,25289551,C,T	0.316	0.588	Missense	high			
1647	PPP2R1A	ESC		N/A (3)	MSS	p.P179R	19,57407783,C,G	0.333	0.436	Missense	medium			
1667	ARID1A	EEC		1	MSS	p.Q172fs	26895997			Frame_Shift_Del				
1667	ARID1A	EEC		1	MSS	p.Q176fs	26896009			Frame_Shift_Del				
1667	PIK3CA	EEC		1	MSS	p.D725N	3,180421625,G,A	0.458	0.631	Missense				

ID	Gene	Original diagnosed subtype	Review Subtype	Grade	MSI Status	AA variant	Location (hg18)	Frequency	Probability	Type	Func. Impact	Sanger Validated	Normal available	Grade 3 Solid vs. Cytologic Atypia
1667	TP53	EEC		1	MSS	p.R158S	17,7519183,G,T	0.058	0.368	Missense	high			
1675	KRAS	EEC		2	MSI-High	p.G12C	12,25289552,C,A	0.311	0.666	Missense	high			
1675	PIK3CA	EEC		2	MSI-High	p.R38S	3,180399419,C,A	0.440	0.676	Missense	medium			
1675	PIK3CA	EEC		2	MSI-High	p.E542G	3,180418777,A,G	0.412	0.690	Missense	low	Validated		
1675	PTEN	EEC		2	MSI-High	p.T277R	10,89710659,C,G	0.548	0.678	Missense				
1680	ARID1A	EEC		1	MSI-High	p.R693	1,26960090,C,T	0.277	0.464	Truncating				
1680	ARID1A	EEC		1	MSI-High	p.G1847fs	26978517			Frame_Shift_Del				
1680	KRAS	EEC		1	MSI-High	p.G12C	12,25289552,C,A	0.200	0.652	Missense	high			
1684	ARID1A	EEC		1	MSI-High	p.Q1212	1,26971984,C,T	0.486	0.682	Truncating				
1684	PTEN	EEC		1	MSI-High	p.R130G	10,89682884,C,G	0.883	0.691	Missense	high			
1687	ARID1A	EEC		1	MSI-High	p.Q920fs	26965326			Frame_Shift_Del				
1687	ARID1A	EEC		1	MSI-High	p.T2138fs	26979390			Frame_Shift_Del				
1687	BRAF	EEC		1	MSI-High	p.P403fs	140129395			Frame_Shift_Ins				
1687	PTEN	EEC		1	MSI-High	p.R130G	10,89682884,C,G	0.467	0.675	Missense	high			
1689	ARID1A	Carcinosarcoma		N/A (3)	MSI-High	p.T2138fs	26979390			Frame_Shift_Del				
1689	PTEN	Carcinosarcoma		N/A (3)	MSI-High	p.G132S	10,89682890,G,A	0.855	0.749	Missense	high			
1690	TP53	Carcinosarcoma		N/A (3)	MSS	p.I195T	17,7518990,A,G	0.697	0.776	Missense	high			
1698	KRAS	Carcinosarcoma		N/A (3)	MSS	p.G13C	12,25289549,C,A	0.348	0.466	Missense	high			
1698	TP53	Carcinosarcoma		N/A (3)	MSS	p.E294*	17,7517783,C,A	0.792	0.763	Truncating				
1700	TP53	ESC		N/A (3)	MSS	p.R273C	17,7517846,G,A	0.842	0.837	Missense	high			
1706	ARID1A	ESC		N/A (3)	MSS	p.P120S	1,26895839,C,T	0.385	0.543	Missense				
1706	PPP2R1A	ESC		N/A (3)	MSS	p.V162M	19,57406538,G,A	0.655	0.848	Missense	low			
1706	TP53	ESC		N/A (3)	MSS	p.H179Y	17,7519120,G,A	0.600	0.739	Missense	high			

ID	Gene	Original diagnosed subtype	Review Subtype	Grade	MSI Status	AA variant	Location (hg18)	Frequency	Probability	Type	Func. Impact	Sanger Validated	Normal available	Grade 3 Solid vs. Cytologic Atypia
1714	ARID1A	EEC		1	MSS	p.E896	1,26962317,G,T	0.304	0.687	Truncating				
1714	CTNNB1	EEC		1	MSS	p.K335T	3,41243770,A,C	0.250	0.663	Missense				
1714	PIK3CA	EEC		1	MSS	p.N345T	3,180404246,A,C	0.273	0.453	Missense	medium			
1714	PIK3CA	EEC		1	MSS	p.R88Q	3,180399570,G,A	0.319	0.652	Missense	medium			
1714	PTEN	EEC		1	MSS	p.L247S	10,89707695,T,C	0.226	0.509	Missense	medium			
1714	PTEN	EEC		1	MSS	p.D107Y	10,89682815,G,T	0.425	0.570	Missense	medium			
1714	PTEN	EEC		1	MSS	p.Y346	10,89715035,C,A	0.321	0.610	Truncating				
1717	ARID1A	EEC		2	MSS	p.I1635fs	26974208			Frame_Shift_Del				
1717	PIK3CA	EEC		2	MSS	p.P539R	3,180418768,C,G	0.429	0.501	Missense	medium	Validated		
1720	ARID1A	EEC		2	MSS	p.E2255	1,26979739,G,T	0.240	0.788	Truncating				
1720	PIK3CA	EEC		2	MSS	p.H1047R	3,180434779,A,G	0.844	0.669	Missense	low	Validated		
1724	ARID1A	EEC		1	MSS	p.R750	1,26960548,C,T	0.811	0.827	Truncating				
1724	PTEN	EEC		1	MSS	p.R130G	10,89682884,C,G	0.354	0.687	Missense	high			
1726	ARID1A	EEC		2	MSI-High	p.Y222fs	26896146			Frame_Shift_Del				
1726	PIK3CA	EEC		2	MSI-High	p.E453K	3,180410773,G,A	0.210	0.632	Missense	medium			
1726	PTEN	EEC		2	MSI-High	SPLICE_SITE_ACCEPTOR	89710629,A,T	0.867	0.767	SPLICE_SITE_ACCEPTOR				
1727	ARID1A	EEC		1	MSI-High	p.Q2115	1,26979319,C,T	0.248	0.781	Truncating				
1727	KRAS	EEC		1	MSI-High	p.G12D	12,25289551,C,T	0.246	0.732	Missense	high			
1727	PTEN	EEC		1	MSI-High	p.R130Q	10,89682885,G,A	0.473	0.643	Missense	high			
1728	KRAS	Carcinosarcoma		N/A (3)	MSS	p.G12D	12,25289551,C,T	0.286	0.447	Missense	high			
1728	TP53	Carcinosarcoma		N/A (3)	MSS	p.K132N	17,7519259,C,A	0.786	0.893	Missense	high			
1729	ARID1A	EEC		1	MSI-High	p.Q548fs	26930523			Frame_Shift_Del				
1729	PIK3CA	EEC		1	MSI-High	p.E545K	3,180418785,G,A	0.286	0.484	Missense	low	Validated		
1729	PTEN	EEC		1	MSI-High	p.H185fs	89701917			Frame_Shift_Del				
1730	ARID1A	EEC		2	MSI-High	p.Q909fs	26962356			Frame_Shift_Del				
1730	ARID1A	EEC		2	MSI-High	p.A1517fs	26973854			Frame_Shift_Ins				
1730	PIK3CA	EEC		2	MSI-High	p.N345I	3,180404246,A,T	0.632	0.701	Missense	medium			
1732	PTEN	EEC		2	MSS	p.N212*	10,89701997,G,C	0.533	0.742	Reference				

ID	Gene	Original diagnosed subtype	Review Subtype	Grade	MSI Status	AA variant	Location (hg18)	Frequency	Probability	Type	Func. Impact	Sanger Validated	Normal available	Grade 3 Solid vs. Cytologic Atypia
										allele: A				
1732	PTEN	EEC		2	MSS	SPLICE_SITE_DONOR	89701997,G,C	0.533	0.742	SPLICE_SITE_DONOR				
1732	TP53	EEC		2	MSS	SPLICE_SITE_DONOR	7520036,C,A	0.533	0.700	SPLICE_SITE_DONOR				
1733	PPP2R1A	ESC		N/A (3)	MSS	p.P179R	19,57407783,C,G	0.400	0.397	Missense	medium			
1733	TP53	ESC		N/A (3)	MSS	p.C242F	17,7518281,C,A	0.308	0.344	Missense	high			
1735	TP53	ESC		N/A (3)	MSS	p.Q165*	17,7519162,G,A	0.593	0.792	Truncating				
1751	ARID1A	EEC		1	MSI-High	p.A2205fs	26979590			Frame_Shift_Del				
1751	CTNNB1	EEC		1	MSI-High	p.T41A	3,41241128,A,G	0.425	0.591	Missense	medium			
1751	PIK3CA	EEC		1	MSI-High	p.G364R	3,180405015,G,A	0.400	0.487	Missense	medium	Validated		
1751	PTEN	EEC		1	MSI-High	p.C136Y	10,89682903,G,A	0.833	0.816	Missense	high			
1753	PPP2R1A	ESC_(metastatic_to_ovary)		N/A (3)	MSS	p.P179R	19,57407783,C,G	0.579	0.805	Missense	medium			
1753	TP53	ESC_(metastatic_to_ovary)		N/A (3)	MSS	p.R249G	17,7518261,T,C	0.375	0.618	Missense	high			
1756	ARID1A	EEC		1	MSS	p.L2073fs	26979194			Frame_Shift_Ins				
1756	CTNNB1	EEC		1	MSS	p.S37C	3,41241117,C,G	0.400	0.591	Missense	high			
1757	PTEN	EEC		2	MSS	p.V317fs	89710778			Frame_Shift_Del				
1762	ARID1A	EEC		1	MSI-High	p.Y430*	1,26928881,C,A	0.333	0.719	Truncating				
1762	ARID1A	EEC		1	MSI-High	p.S2249fs	26979722			Frame_Shift_Del				
1762	CTNNB1	EEC		1	MSI-High	p.G34E	3,41241108,G,A	0.133	0.635	Missense	medium			
1762	PTEN	EEC		1	MSI-High	p.D24fs	89614278			Frame_Shift_Del				
1765	TP53	Carcinosarcoma		N/A (3)	MSS	p.D281V	17,7517821,T,A	0.813	0.809	Missense	high			
1767	ARID1A	EEC		1	MSS	p.H1960fs	26978856			Frame_Shift_Del				
1767	PIK3CA	EEC		1	MSS	p.Q546R	3,180418789,A,G	0.294	0.444	Missense	low	Validated		

ID	Gene	Original diagnosed subtype	Review Subtype	Grade	MSI Status	AA variant	Location (hg18)	Frequency	Probability	Type	Func. Impact	Sanger Validated	Normal available	Grade 3 Solid vs. Cytologic Atypia
1767	PIK3CA	EEC		1	MSS	p.E600K	3,180420104,G,A	0.300	0.650	Missense	high	Validated		
1767	PTEN	EEC		1	MSS	p.R130G	10,89682884,C,G	0.205	0.766	Missense	high			
1767	PTEN	EEC		1	MSS	p.R130fs	89682884			Frame_Shift_Del				
1768	KRAS	EEC		1	MSS	p.G12C	12,25289552,C,A	0.244	0.691	Missense	high			
1768	PIK3CA	EEC		1	MSS	p.G106V	3,180399624,G,T	0.246	0.434	Missense	medium			
1768	PIK3CA	EEC		1	MSS	p.R88Q	3,180399570,G,A	0.276	0.729	Missense	medium			
1780	ARID1A	EEC		1	MSI-High	p.S1247F	1,26972448,C,T	0.549	0.731	Missense				
1780	KRAS	EEC		1	MSI-High	p.G12D	12,25289551,C,T	0.282	0.757	Missense	high			
1780	PIK3CA	EEC		1	MSI-High	p.M1043V	3,180434766,A,G	0.302	0.602	Missense	low	Validated		
1780	PTEN	EEC		1	MSI-High	p.L265fs	89707749			Frame_Shift_Del				
1781	TP53	EEC		1	MSS	p.Q165*	17,7519162,G,A	0.902	0.786	Truncating				
1782	PPP2R1A	ESC		N/A (3)	MSS	p.P179R	19,57407783,C,G	0.500	0.646	Missense	medium			
1782	TP53	ESC		N/A (3)	MSS	p.W91*	17,7520139,C,T	0.467	0.669	Truncating				
1783	ARID1A	EEC		1	MSS	p.Q2176*	1,26979502,C,T	0.333	0.636	Truncating				
1783	PTEN	EEC		1	MSS	p.R130G	10,89682884,C,G	0.235	0.653	Missense	high			
1796	CTNNB1	EEC		1	MSS	p.S37F	3,41241117,C,T	0.185	0.776	Missense	high			
1796	PTEN	EEC		1	MSS	p.L23*	10,89614274,T,G	0.250	0.549	Truncating				
1804	PTEN	EEC		1	MSI-High	p.I135V	10,89682899,A,G	0.175	0.770	Missense	low			
1806	ARID1A	EEC		1	MSS	p.R1335	1,26972794,C,T	0.077	0.361	Truncating				
1806	ARID1A	EEC		1	MSS	p.Q588*	1,26930641,C,T	0.525	0.671	Truncating				
1806	CTNNB1	EEC		1	MSS	p.S37F	3,41241117,C,T	0.417	0.583	Missense	high			
1806	PIK3CA	EEC		1	MSS	p.H1047L	3,180434779,A,T	0.407	0.567	Missense	low	Validated		
1811	ARID1A	EEC		2	MSI-low	p.G1255R	1,26972471,G,A	0.258	0.644	Missense				
1811	ARID1A	EEC		2	MSI-low	p.D1738G	1,26978189,A,G	0.116	0.754	Missense				
1811	ARID1A	EEC		2	MSI-low	p.R1989	1,26978941,C,T	0.264	0.793	Truncating				
1811	CTNNB1	EEC		2	MSI-low	p.S37F	3,41241117,C,T	0.082	0.549	Missense	high			
1811	PTEN	EEC		2	MSI-low	p.L112P	10,89682831,T,C	0.289	0.698	Missense	high			
1811	PTEN	EEC		2	MSI-low	p.F104V	10,89682806,T,G	0.260	0.726	Missense				
1811	PTEN	EEC		2	MSI-low	p.R142W	10,89682920,C,T	0.293	0.786	Missense	medium			
1816	CTNNB1	EEC		1	MSS	p.R212C	3,41241967,C,T	0.389	0.632	Missense	high			
1816	PIK3CA	EEC		1	MSS	p.K711T	3,180421584,A,C	0.357	0.597	Missense	medium	Validated		
1816	PIK3CA	EEC		1	MSS	p.M1043I	3,180434768,G,T	0.478	0.723	Missense	low	Validated		
1816	PTEN	EEC		1	MSS	p.C218*	10,89707609,C,A	0.286	0.717	Truncating				
1816	PTEN	EEC		1	MSS	p.Y177H	10,89701891,T,C	0.550	0.758	Missense	high			

ID	Gene	Original diagnosed subtype	Review Subtype	Grade	MSI Status	AA variant	Location (hg18)	Frequency	Probability	Type	Func. Impact	Sanger Validated	Normal available	Grade 3 Solid vs. Cytologic Atypia
1817	PIK3CA	EEC		2	MSI-High	p.Y1021C	3,180434701,A,G	0.455	0.704	Missense	medium	Validated		
1818	ARID1A	EEC		2	MSS	p.R1276	1,26972534,C,T	0.250	0.636	Truncating				
1818	KRAS	EEC		2	MSS	p.R68S	12,25271521,C,G	0.148	0.622	Missense	high			
1818	PTEN	EEC		2	MSS	p.R130G	10,89682884,C,G	0.214	0.635	Missense	high			
1821	ARID1A	EEC		1	MSI-High	p.T2138fs	26979390			Frame_Shift_Del				
1821	ARID1A	EEC		1	MSI-High	p.F2251fs	26979729			Frame_Shift_Ins				
1821	KRAS	EEC		1	MSI-High	p.G12V	12,25289551,C,A	0.300	0.676	Missense	high			
1821	PIK3CA	EEC		1	MSI-High	p.H1047Y	3,180434778,C,T	0.312	0.714	Missense	low	Validated		
1828	TP53	Carcinosarcoma		N/A (3)	MSS	p.C238Y	17,7518293,C,T	1.000	0.874	Missense	high			
1829	CTNNB1	EEC		1	MSS	p.S33C	3,41241105,C,G	0.400	0.578	Missense	medium			
1829	PTEN	EEC		1	MSS	p.A126S	10,89682872,G,T	0.351	0.550	Missense	high			
1829	PTEN	EEC		1	MSS	p.H259P	10,89707731,A,C	0.500	0.598	Missense				
1832	KRAS	EEC		1	MSS	p.G12C	12,25289552,C,A	0.500	0.517	Missense	high			
1832	PTEN	EEC		1	MSS	p.I5N	10,89614220,T,A	0.233	0.603	Missense				
1832	PTEN	EEC		1	MSS	p.R233*	10,89707652,C,T	0.429	0.632	Truncating				
1840	PIK3CA	EEC		2	MSI-High	p.R38C	3,180399419,C,T	0.167	0.613	Missense	medium			
1850	ARID1A	Carcinosarcoma		N/A (3)	MSS	p.A1539fs	26973920			Frame_Shift_Del				
1850	KRAS	Carcinosarcoma		N/A (3)	MSS	p.G13D	12,25289548,C,T	0.667	0.847	Missense	high			
1850	PIK3CA	Carcinosarcoma		N/A (3)	MSS	p.Q546K	3,180418788,C,A	0.800	0.826	Missense	low			
1850	PTEN	Carcinosarcoma		N/A (3)	MSS	p.R130G	10,89682884,C,G	0.353	0.724	Missense	high			
1852	ARID1A	EEC		2	MSI-High	p.Y1324fs	26972762			Frame_Shift_Del				
1852	CTNNB1	EEC		2	MSI-High	p.S33A	3,41241104,T,G	0.294	0.723	Missense	medium			
1852	PPP2R1A	EEC		2	MSI-High	p.181_182insV	57407785			In_Frame_Ins				
1853	ARID1A	EEC		1	MSI-High	p.R1528	1,26973887,C,T	0.386	0.538	Truncating				
1853	PIK3CA	EEC		1	MSI-High	p.H1047Y	3,180434778,C,T	0.282	0.727	Missense	low	Validated		
1853	PTEN	EEC		1	MSI-High	p.L98R	10,89682789,T,G	0.700	0.789	Missense				
1855	ARID1A	EEC		2	MSS	p.P726fs	26960478			Frame_Shi				

ID	Gene	Original diagnosed subtype	Review Subtype	Grade	MSI Status	AA variant	Location (hg18)	Frequency	Probability	Type	Func. Impact	Sanger Validated	Normal available	Grade 3 Solid vs. Cytologic Atypia
										ft_Del				
1855	ARID1A	EEC		2	MSS	p.R727fs	26960480			Frame_Shift_Del				
1855	ARID1A	EEC		2	MSS	p.Q2188fs	26979540			Frame_Shift_Ins				
1855	KRAS	EEC		2	MSS	p.G12V	12,25289551,C,A	0.339	0.603	Missense	high			
1856	CTNNB1	EEC		2	MSI-High	p.D32N	3,41241101,G,A	0.481	0.639	Missense	medium			
1856	KRAS	EEC		2	MSI-High	p.G12D	12,25289551,C,T	0.370	0.744	Missense	high			
1856	PIK3CA	EEC		2	MSI-High	p.R93Q	3,180399585,G,A	0.122	0.525	Missense	medium			
1856	PIK3CA	EEC		2	MSI-High	p.K111E	3,180399638,A,G	0.222	0.554	Missense	medium			
1856	PIK3CA	EEC		2	MSI-High	p.Y1021C	3,180434701,A,G	0.310	0.699	Missense	medium	Validated		
1866	CTNNB1	EEC		1	MSS	p.S37F	3,41241117,C,T	0.304	0.760	Missense	high			
1867	ARID1A	EEC		1	MSS	p.Q492fs	26930355			Frame_Shift_Del				
1867	CTNNB1	EEC		1	MSS	p.D32G	3,41241102,A,G	0.450	0.709	Missense	medium			
1871	ARID1A	EEC		2	MSS	p.NLAQGD2173del	26979491			In_Frame_Del				
1871	KRAS	EEC		2	MSS	p.G12V	12,25289551,C,A	0.364	0.706	Missense	high			
1871	PTEN	EEC		2	MSS	p.T321fs	89710791			Frame_Shift_Ins				
1873	CTNNB1	EEC		1	MSI-High	p.S45F	3,41241141,C,T	0.206	0.558	Missense	medium			
1873	KRAS	EEC		1	MSI-High	p.G12V	12,25289551,C,A	0.297	0.737	Missense	high			
1873	PIK3CA	EEC		1	MSI-High	p.H1047R	3,180434779,A,G	0.310	0.705	Missense	low	Validated		
1873	PTEN	EEC		1	MSI-High	p.P89fs	89682762			Frame_Shift_Del				
1873	PTEN	EEC		1	MSI-High	p.E288fs	89710691			Frame_Shift_Del				
1874	ARID1A	EEC		1	MSS	p.R1721P	1,26978138,G,C	0.380	0.512	Missense	medium			
1874	ARID1A	EEC		1	MSS	p.S1992L	1,26978951,C,T	0.291	0.741	Missense				
1874	PPP2R1A	EEC		1	MSS	p.R183Q	19,57407795,G,A	0.556	0.722	Missense	medium			
1874	PTEN	EEC		1	MSS	p.R130G	10,89682884,C,G	0.317	0.698	Missense	high			
1874	PTEN	EEC		1	MSS	p.V317fs	89710778			Frame_Shift_Del				
1875	PTEN	EEC		1	MSI-High	SPLICE_SITE_ACCEPTOR	89710630,G,A	0.313	0.353	SPLICE_SITE_ACCEPTOR				

ID	Gene	Original diagnosed subtype	Review Subtype	Grade	MSI Status	AA variant	Location (hg18)	Frequency	Probability	Type	Func. Impact	Sanger Validated	Normal available	Grade 3 Solid vs. Cytologic Atypia
1875	PTEN	EEC		1	MSI-High	p.Y177fs	89701892			Frame_Shift_Del				
1893	KRAS	EEC		1	MSS	p.G12D	12,25289551,C,T	0.243	0.636	Missense	high			
1895	PIK3CA	Carcinosarcoma		N/A (3)	MSS	p.K111E	3,180399638,A,G	0.429	0.672	Missense	medium			
1896	KRAS	EEC		1	MSI-High	p.F156L	12,25254095,G,C	0.154	0.587	Missense				
1896	KRAS	EEC		1	MSI-High	p.G12C	12,25289552,C,A	0.219	0.682	Missense	high			
1896	PTEN	EEC		1	MSI-High	p.A121fs	89682857			Frame_Shift_Del				
1897	ARID1A	EEC		2	MSI-High	p.R1335	1,26972794,C,T	0.525	0.578	Truncating				
1897	ARID1A	EEC		2	MSI-High	p.P687S	1,26960072,C,T	0.400	0.764	Missense	medium			
1897	PPP2R1A	EEC		2	MSI-High	p.Q237R	19,57408078,A,G	0.333	0.420	Missense				
1897	PTEN	EEC		2	MSI-High	p.Y16fs	89614253			Frame_Shift_Del				
1898	ARID1A	EEC		1	MSI-High	p.C1723	1,26978145,C,A	0.500	0.729	Truncating				
1900	ARID1A	EEC		1	MSI-High	p.2171_2172insL	26979483			In_Frame_Ins				
1900	PIK3CA	EEC		1	MSI-High	p.G463R	3,180410803,G,A	0.400	0.405	Missense	low			
1904	no mut	EEC		1	MSS	no mut								
1910	PIK3CA	Carcinosarcoma		N/A (3)	MSS	p.L422W	3,180410681,T,G	0.313	0.549	Missense		Validated		
1910	TP53	Carcinosarcoma		N/A (3)	MSS	p.R273H	17,7517845,C,T	0.733	0.838	Missense	high			
1913	ARID1A	EEC		2	MSI-High	p.A1466fs	26973703			Frame_Shift_Del				
1913	PTEN	EEC		2	MSI-High	p.E288*	10,89710691,G,T	0.889	0.842	Truncating				
1915	PTEN	EEC		1	MSI-low	p.V217D	10,89707605,T,A	0.286	0.524	Missense	medium			
1916	PTEN	EEC		1	MSS	p.R130L	10,89682885,G,T	0.571	0.645	Missense	high			
1921	TP53	ESC		N/A (3)	MSS	p.W146	17,7519217,C,T	0.692	0.875	Truncating				
1922	ARID1A	EEC		1	MSS	p.Y2148*	1,26979420,T,G	0.361	0.635	Truncating				
1922	ARID1A	EEC		1	MSS	p.G1847fs	26978517			Frame_Shift_Ins				
1922	CTNNB1	EEC		1	MSS	p.G34V	3,41241108,G,T	0.235	0.623	Missense	medium			
1928	KRAS	EEC		2	MSS	p.G12A	12,25289551,C,G	0.263	0.574	Missense	high			
1928	PTEN	EEC		2	MSS	p.Y177*	10,89701893,T,A	0.364	0.650	Truncating				

ID	Gene	Original diagnosed subtype	Review Subtype	Grade	MSI Status	AA variant	Location (hg18)	Frequency	Probability	Type	Func. Impact	Sanger Validated	Normal available	Grade 3 Solid vs. Cytologic Atypia
1928	PTEN	EEC		2	MSS	p.I33del	89643775			In_Frame_Del				
1931	no mut	EEC		1	MSS	no mut								
1933	ARID1A	EEC		1	MSI-High	p.A861T	1,26962212,G,A	0.520	0.731	Missense	low			
1934	PIK3CA	Carcinosarcoma		N/A (3)	MSS	p.E245*	3,180401942,G,T	0.075	0.538	Truncating				
1934	PPP2R1A	Carcinosarcoma		N/A (3)	MSS	p.P179R	19,57407783,C,G	0.195	0.687	Missense	medium			
1934	PTEN	Carcinosarcoma		N/A (3)	MSS	p.R130G	10,89682884,C,G	0.280	0.629	Missense	high			
1934	TP53	Carcinosarcoma		N/A (3)	MSS	p.P151R	17,7519203,G,C	0.208	0.503	Missense	high			
1936	PTEN	EEC		2	MSI-High	p.R130fs	89682884			Frame_Shift_Del				
1939	PIK3CA	Carcinosarcoma		N/A (3)	MSS	p.E365K	3,180405018,G,A	0.179	0.653	Missense	medium	Validated		
1939	PIK3CA	Carcinosarcoma		N/A (3)	MSS	p.R38C	3,180399419,C,T	0.455	0.667	Missense	medium			
1939	PPP2R1A	Carcinosarcoma		N/A (3)	MSS	p.N312H	19,57411080,A,C	0.550	0.770	Missense				
1939	PTEN	Carcinosarcoma		N/A (3)	MSS	p.E299*	10,89710724,G,T	0.375	0.556	Truncating				
1939	PTEN	Carcinosarcoma		N/A (3)	MSS	p.R130Q	10,89682885,G,A	0.318	0.667	Missense	high			
1940	PIK3CA	EEC		1	MSS	p.T1025A	3,180434712,A,G	0.368	0.659	Missense	low	Validated		
1940	PIK3CA	EEC		1	MSS	p.E365K	3,180405018,G,A	0.636	0.723	Missense	medium	Validated		
1940	PTEN	EEC		1	MSS	p.R11I	10,89614238,G,T	0.417	0.710	Missense				
1944	PTEN	EEC		1	MSS	p.G293*	10,89710706,G,T	0.750	0.827	Truncating				
1948	no mut	EEC		1	MSS	no mut								
1949	ARID1A	Carcinosarcoma		N/A (3)	MSI-High	p.Y1324fs	26972762			Frame_Shift_Ins				
1949	PTEN	Carcinosarcoma		N/A (3)	MSI-High	p.K266*	10,89707751,A,T	0.462	0.650	Truncating				
1949	TP53	Carcinosarcoma		N/A (3)	MSI-High	p.R342*	17,7514728,G,A	0.545	0.742	Truncating				
1955	ARID1A	EEC		1	MSS	p.Q575fs	26930603			Frame_Shift_Del				
1955	KRAS	EEC		1	MSS	p.G12D	12,25289551,C,T	0.167	0.621	Missense	high			
1955	PIK3CA	EEC		1	MSS	p.H1047L	3,180434779,A,T	0.357	0.755	Missense	low	Validated		
1955	PTEN	EEC		1	MSS	p.R130G	10,89682884,C,G	0.250	0.711	Missense	high			
1957	ARID1A	EEC		1	MSS	p.E1836	1,26978482,G,T	0.533	0.726	Truncating				
1957	ARID1A	EEC		1	MSS	p.R1528fs	26973889			Frame_Shift_Del				

ID	Gene	Original diagnosed subtype	Review Subtype	Grade	MSI Status	AA variant	Location (hg18)	Frequency	Probability	Type	Func. Impact	Sanger Validated	Normal available	Grade 3 Solid vs. Cytologic Atypia
1957	PIK3CA	EEC		1	MSS	p.I1058L	3,180434811,A,C	0.611	0.787	Missense		Validated		
1957	PIK3CA	EEC		1	MSS	p.R38H	3,180399420,G,A	0.800	0.802	Missense	medium			
1957	PTEN	EEC		1	MSS	p.D301fs	89710730			Frame_Shift_Del				
1961	KRAS	EEC		2	MSS	p.G12V	12,25289551,C,A	0.278	0.627	Missense	high			
1962	TP53	ESC		N/A (3)	MSS	p.R110C	17,7520084,G,A	0.133	0.616	Missense	medium			
1965	KRAS	Carcinosarcoma		N/A (3)	MSS	p.G12C	12,25289552,C,A	0.537	0.775	Missense	high			
1965	TP53	Carcinosarcoma		N/A (3)	MSS	p.P47S	17,7520273,G,A	0.864	0.781	Missense	neutral			
1965	TP53	Carcinosarcoma		N/A (3)	MSS	p.V216M	17,7518928,C,T	0.833	0.814	Missense	high			
1967	no mut	EEC		1	MSS	no mut								
1975	PTEN	EEC		1	MSS	p.E291fs	89710700			Frame_Shift_Ins				
1975	TP53	EEC		1	MSS	p.R282W	17,7517819,G,A	0.917	0.832	Missense	high			
1978	no mut	EEC		1	MSS	no mut								
1980	PIK3CA	Carcinosarcoma		N/A (3)	MSS	p.Q546R	3,180418789,A,G	0.769	0.737	Missense	low			
1980	TP53	Carcinosarcoma		N/A (3)	MSS	p.C238R	17,7518294,A,G	0.870	0.837	Missense	high			
1985	PTEN	EEC		1	MSS	p.Y16*	10,89614254,T,A	0.500	0.443	Truncating				
1988	ARID1A	EEC		1	MSS	p.R1989*	1,26978941,C,T	0.238	0.481	Truncating				
1988	PIK3CA	EEC		1	MSS	p.Y1021C	3,180434701,A,G	0.364	0.679	Missense	medium			
1989	PIK3CA	EEC		2	MSI-High	p.H1047R	3,180434779,A,G	0.385	0.515	Missense	low	Validated		
1989	PIK3CA	EEC		2	MSI-High	p.E81K	3,180399548,G,A	0.538	0.640	Missense	medium			
1989	PTEN	EEC		2	MSI-High	p.R233*	10,89707652,C,T	0.800	0.450	Truncating				
1992	no mut	EEC		1	MSS	no mut								
1994	ARID1A	EEC		1	MSI-High	p.W1686	1,26974719,G,A	0.571	0.615	Truncating				
1994	PIK3CA	EEC		1	MSI-High	p.H1047R	3,180434779,A,G	0.286	0.406	Missense	low	Validated		
1995	PTEN	EEC		1	MSS	p.C136R	10,89682902,T,C	0.450	0.696	Missense	high			
1996	ARID1A	EEC		1	MSS	p.R2158*	1,26979448,C,T	0.243	0.751	Truncating				
1996	PTEN	EEC		1	MSS	p.R130Q	10,89682885,G,A	0.514	0.631	Missense	high			
2019	ARID1A	EEC		2	MSI-High	p.P1478S	1,26973737,C,T	0.304	0.701	Missense				
2019	PTEN	EEC		2	MSI-High	p.R130Q	10,89682885,G,A	0.800	0.884	Missense	high			
2022	ARID1A	EEC		2	MSS	p.R1989*	1,26978941,C,T	0.444	0.663	Truncating				

ID	Gene	Original diagnosed subtype	Review Subtype	Grade	MSI Status	AA variant	Location (hg18)	Frequency	Probability	Type	Func. Impact	Sanger Validated	Normal available	Grade 3 Solid vs. Cytologic Atypia
2022	PIK3CA	EEC		2	MSS	p.R88Q	3,180399570,G,A	0.308	0.650	Missense	medium			
2022	PIK3CA	EEC		2	MSS	p.E81K	3,180399548,G,A	0.400	0.702	Missense	medium			
2022	PTEN	EEC		2	MSS	p.R130Q	10,89682885,G,A	0.500	0.635	Missense	high			
2022	PTEN	EEC		2	MSS	p.E7*	10,89614225,G,T	0.273	0.655	Truncating				
2024	KRAS	EEC		2	MSI-High	p.R68S	12,25271521,C,A	0.208	0.619	Missense	high			
2028	no mut	EEC		1	MSI-High	no mut								
2031	BRAF	Carcinosarcoma		N/A (3)	MSS	p.A712T	7,140081033,C,T	0.460	0.408	Missense	medium			
2031	CTNNB1	Carcinosarcoma		N/A (3)	MSS	p.S37F	3,41241117,C,T	0.339	0.544	Missense	high			
2031	TP53	Carcinosarcoma		N/A (3)	MSS	p.M237I	17,7518295,C,T	0.444	0.561	Missense	high			
2032	PTEN	EEC		2	MSS	p.R15I	10,89614250,G,T	0.192	0.604	Missense	high			
2040	PIK3CA	EEC		1	MSI-High	p.R88Q	3,180399570,G,A	0.571	0.747	Missense	medium			
2044	CTNNB1	EEC		1	MSS	p.D32Y	3,41241101,G,T	0.500	0.777	Missense	medium			
2044	PTEN	EEC		1	MSS	p.R130G	10,89682884,C,G	0.261	0.613	Missense	high			
2044	PTEN	EEC		1	MSS	p.C136Y	10,89682903,G,A	0.500	0.692	Missense	high			
2045	KRAS	EEC		1	MSS	p.G12V	12,25289551,C,A	0.500	0.671	Missense	high			
2045	TP53	EEC		1	MSS	p.R273H	17,7517845,C,T	0.471	0.748	Missense	high			
2046	CTNNB1	EEC		1	MSS	p.S33F	3,41241105,C,T	0.286	0.398	Missense	medium			
2046	PIK3CA	EEC		1	MSS	p.E418K	3,180410668,G,A	0.462	0.622	Missense	low			
2046	PIK3CA	EEC		1	MSS	p.T1025S	3,180434712,A,T	0.450	0.693	Missense	low	Validated		
2046	PTEN	EEC		1	MSS	p.R130G	10,89682884,C,G	0.524	0.753	Missense	high			
2049	PTEN	EEC		1	MSI-High	p.I135fs	89682900			Frame_Shift_Ins				
2051	PTEN	EEC		1	MSI-High	p.R130Q	10,89682885,G,A	0.132	0.671	Missense	high			
2051	PTEN	EEC		1	MSI-High	p.E157fs	89682965			Frame_Shift_Del				
2054	PPP2R1A	ESC		N/A (3)	MSS	p.S256F	19,57408135,C,T	0.273	0.641	Missense	medium			
2054	TP53	ESC		N/A (3)	MSS	p.D148fs	7519205			Frame_Shift_Del				
2066	ARID1A	EEC		2	MSS	p.S1320Y	1,26972750,C,A	0.286	0.579	Missense	low			
2066	BRAF	EEC		2	MSS	p.S419Y	7,140129348,G,T	0.267	0.447	Missense				
2066	CTNNB1	EEC		2	MSS	p.M553V	3,41250766,A,G	0.211	0.530	Missense				
2066	CTNNB1	EEC		2	MSS	p.S37F	3,41241117,C,T	0.304	0.780	Missense	high			
2066	PIK3CA	EEC		2	MSS	p.R38C	3,180399419,C,T	0.233	0.571	Missense	medium			
2066	PIK3CA	EEC		2	MSS	p.T1025S	3,180434712,A,T	0.316	0.666	Missense	low	Validated		
2066	PTEN	EEC		2	MSS	p.R142W	10,89682920,C,T	0.438	0.486	Missense	medium			

ID	Gene	Original diagnosed subtype	Review Subtype	Grade	MSI Status	AA variant	Location (hg18)	Frequency	Probability	Type	Func. Impact	Sanger Validated	Normal available	Grade 3 Solid vs. Cytologic Atypia
2066	PTEN	EEC		2	MSS	p.R130Q	10,89682885,G,A	0.474	0.710	Missense	high			
2070	PIK3CA	EEC		2	MSI-High	p.E970K	3,180430830,G,A	0.417	0.688	Missense				
2070	PIK3CA	EEC		2	MSI-High	p.R88Q	3,180399570,G,A	0.343	0.707	Missense	medium			
2070	PTEN	EEC		2	MSI-High	p.N212_splice	89701995			Splice_Site				
2073	ARID1A	Carcinosarcoma		N/A (3)	MSS	p.A54fs	26895641			Frame_Shift_Ins				
2073	KRAS	Carcinosarcoma		N/A (3)	MSS	p.G12D	12,25289551,C,T	0.727	0.827	Missense	high			
2073	PTEN	Carcinosarcoma		N/A (3)	MSS	p.R130*	10,89682884,C,T	0.869	0.701	Truncating				
2073	TP53	Carcinosarcoma		N/A (3)	MSS	p.R273H	17,7517845,C,T	0.765	0.768	Missense	high			
2075	PTEN	EEC		2	MSS	p.R130G	10,89682884,C,G	0.250	0.634	Missense	high			
2076	PTEN	EEC_		1	MSS	p.R130L	10,89682885,G,T	0.371	0.660	Missense	high			
2080	PPP2R1A	ESC		N/A (3)	MSS	p.P179R	19,57407783,C,G	0.500	0.704	Missense	medium			
2080	TP53	ESC		N/A (3)	MSS	p.S241C	17,7518284,G,C	1.000	0.872	Missense	high			
2085	CTNNB1	EEC		1	MSS	p.S45P	3,41241140,T,C	0.333	0.450	Missense	medium			
2085	PTEN	EEC		1	MSS	p.V317fs	89710778			Frame_Shift_Del				
2087	PIK3CA	Carcinosarcoma		N/A (3)	MSS	p.H1047R	3,180434779,A,G	0.459	0.663	Missense	low			
2087	TP53	Carcinosarcoma		N/A (3)	MSS	p.A159P	17,7519180,C,G	0.375	0.577	Missense	high			
2088	PIK3CA	EEC		2	MSS	p.Y1021C	3,180434701,A,G	0.600	0.777	Missense	medium	Validated		
2088	PTEN	EEC		2	MSS	p.V317fs	89710778			Frame_Shift_Del				
2111	TP53	Carcinosarcoma		N/A (3)	MSS	p.H214R	17,7518933,T,C	0.250	0.637	Missense	medium			
2112	no mut	EEC		2	MSI-High	no mut								
2113	ARID1A	EEC		1	MSI-High	p.Q1650*	1,26974253,C,T	0.259	0.626	Truncating				
2113	PIK3CA	EEC		1	MSI-High	p.R88Q	3,180399570,G,A	0.271	0.730	Missense	medium			
2113	PIK3CA	EEC		1	MSI-High	p.H1047Y	3,180434778,C,T	0.266	0.807	Missense	low	Validated		
2113	PTEN	EEC		1	MSI-High	p.R130G	10,89682884,C,G	0.256	0.750	Missense	high			
2114	PIK3CA	EEC		2	MSI-High	p.H1047R	3,180434779,A,G	0.292	0.623	Missense	low	Validated		

ID	Gene	Original diagnosed subtype	Review Subtype	Grade	MSI Status	AA variant	Location (hg18)	Frequency	Probability	Type	Func. Impact	Sanger Validated	Normal available	Grade 3 Solid vs. Cytologic Atypia
2114	PTEN	EEC		2	MSI-High	p.Y176*	10,89701890,T,G	0.536	0.695	Truncating				
2114	PTEN	EEC		2	MSI-High	p.N340fs	89710848			Frame_Shift_Del				
2114	TP53	EEC		2	MSI-High	p.R273C	17,7517846,G,A	0.222	0.484	Missense	high			
2121	ARID1A	EEC		2	MSI-High	p.T1969I	1,26978882,C,T	0.070	0.641	Missense				
2121	ARID1A	EEC		2	MSI-High	p.N114K	1,26895823,C,G	0.500	0.681	Missense				
2121	CTNNB1	EEC		2	MSI-High	p.L539S	3,41250725,T,C	0.118	0.787	Missense	high			
2121	PTEN	EEC		2	MSI-High	p.R130G	10,89682884,C,G	0.272	0.810	Missense	high			
2124	ARID1A	EEC		2	MSS	p.K1382	1,26973449,A,T	0.161	0.595	Truncating				
2124	ARID1A	EEC		2	MSS	p.G1449fs	26973651			Frame_Shift_Ins				
2124	PTEN	EEC		2	MSS	p.R130G	10,89682884,C,G	0.120	0.538	Missense	high			
2124	PTEN	EEC		2	MSS	p.V216fs	89707603			Frame_Shift_Del				
2127	PTEN	EEC		2	MSS	SPLICE_SITE_ACCEPTOR	89701853,A,G	0.375	0.531	SPLICE_SITE_ACCEPTOR				
2127	PTEN	EEC		2	MSS	p.C136R	10,89682902,T,C	0.250	0.660	Missense	high			
2129	ARID1A	EEC		1	MSI-High	p.Y471*	1,26930292,C,A	0.298	0.632	Truncating				
2129	PTEN	EEC		1	MSI-High	p.R130G	10,89682884,C,G	0.345	0.654	Missense	high			
2134	PIK3CA	EEC		1	MSS	p.R617W	3,180420155,C,T	0.714	0.895	Missense	medium	Validated		
2134	PTEN	EEC		1	MSS	p.G20E	10,89614265,G,A	0.471	0.629	Missense	medium			
2134	PTEN	EEC		1	MSS	p.E7*	10,89614225,G,T	0.500	0.730	Truncating				
2135	PPP2R1A	EEC		1	MSS	p.S219L	19,57408024,C,T	0.667	0.824	Missense	medium			
2137	PIK3CA	EEC		1	MSI-High	p.H1047R	3,180434779,A,G	0.313	0.625	Missense	low			
2140	CTNNB1	EEC		2	MSI-High	p.G34V	3,41241108,G,T	0.308	0.687	Missense	medium			
2140	PIK3CA	EEC		2	MSI-High	p.E110del	180399631			In_Frame_Del				
2140	PTEN	EEC		2	MSI-High	p.L318fs	89710783			Frame_Shift_Ins				
2141	ARID1A	EEC		2	MSI-High	p.Q520R	1,26930438,A,G	0.385	0.524	Missense				
2141	ARID1A	EEC		2	MSI-High	p.N1070fs	26970208			Frame_Shift_Del				
2141	PTEN	EEC		2	MSI-	p.I101S	10,89682798,T,G	0.290	0.637	Missense				

ID	Gene	Original diagnosed subtype	Review Subtype	Grade	MSI Status	AA variant	Location (hg18)	Frequency	Probability	Type	Func. Impact	Sanger Validated	Normal available	Grade 3 Solid vs. Cytologic Atypia
					High									
2141	PTEN	EEC		2	MSI-High	p.R130G	10,89682884,C,G	0.463	0.638	Missense	high			
2144	ARID1A	EEC		2	MSS	p.W1023*	1,26966947,G,A	0.135	0.545	Truncating				
2144	KRAS	EEC		2	MSS	p.G13D	12,25289548,C,T	0.293	0.731	Missense	high			
2144	PTEN	EEC		2	MSS	p.R130*	10,89682884,C,T	0.115	0.821	Truncating				
2146	PTEN	EEC		1	MSS	p.L25S	10,89614280,T,C	0.250	0.442	Missense	high			
2146	PTEN	EEC		1	MSS	p.C218*	10,89707609,C,A	0.235	0.448	Truncating				
2146	PTEN	EEC		1	MSS	p.Y315*	10,89710774,T,G	0.167	0.576	Truncating				
2209	PTEN	EEC		2	MSS	p.Q171*	10,89701873,C,T	0.286	0.504	Truncating				
2209	PTEN	EEC		2	MSS	p.V317fs	89710778			Frame_Shift_Del				
2210	ARID1A	EEC		2	MSS	p.Q1473*	1,26973722,C,T	0.133	0.810	Truncating				
2210	ARID1A	EEC		2	MSS	p.F1103fs	26970306			Frame_Shift_Del				
2210	PTEN	EEC		2	MSS	p.K269*	10,89710634,A,T	0.294	0.436	Truncating				
2211	BRAF	EEC		1	MSI-High	p.R671Q	7,140086196,C,T	0.545	0.582	Missense	medium			
2211	PIK3CA	EEC		1	MSI-High	p.E263	3,180401996,G,T	0.200	0.354	Truncating				
2211	PIK3CA	EEC		1	MSI-High	p.N345K	3,180404247,T,A	0.357	0.465	Missense	medium			
2211	PTEN	EEC		1	MSI-High	p.R130Q	10,89682885,G,A	0.250	0.552	Missense	high			
2215	TP53	Carcinosarcoma		N/A (3)	MSS	p.R280G	17,7517825,T,C	0.895	0.840	Missense	high			
2225	ARID1A	EEC		1	MSS	p.E1799*	1,26978371,G,T	0.284	0.773	Truncating				
2226	KRAS	EEC		1	MSI-High	p.A146T	12,25269829,C,T	0.286	0.616	Missense	high			
2228	ARID1A	EEC		1	MSS	p.R1989L	1,26978942,G,T	0.097	0.775	Missense	medium			
2228	CTNNB1	EEC		1	MSS	p.N206H	3,41241949,A,C	0.139	0.791	Missense				
2228	PIK3CA	EEC		1	MSS	p.L339F	3,180404227,C,T	0.190	0.655	Missense	medium	Validated		
2228	PIK3CA	EEC		1	MSS	p.R88Q	3,180399570,G,A	0.254	0.741	Missense	medium			
2228	PTEN	EEC		1	MSS	p.E7	10,89614225,G,T	0.227	0.625	Truncating				
2231	ARID1A	EEC		1	MSS	p.P120S	1,26895839,C,T	0.545	0.745	Missense	low			
2231	PIK3CA	EEC		1	MSS	p.E545K	3,180418785,G,A	0.500	0.419	Missense	low	Validated		
2231	PTEN	EEC		1	MSS	p.A328fs	89710812			Frame_Shift_Del				
2246	ARID1A	EEC		1	MSI-High	p.P726fs	26960478			Frame_Shift_Del				
2246	PIK3CA	EEC		1	MSI-High	p.R88Q	3,180399570,G,A	0.200	0.571	Missense	medium			
2246	PIK3CA	EEC		1	MSI-	p.R108H	3,180399630,G,A	0.353	0.729	Missense	medium			

ID	Gene	Original diagnosed subtype	Review Subtype	Grade	MSI Status	AA variant	Location (hg18)	Frequency	Probability	Type	Func. Impact	Sanger Validated	Normal available	Grade 3 Solid vs. Cytologic Atypia
					High									
2246	TP53	EEC		1	MSI-High	p.E298K	17,7517771,C,T	0.304	0.731	Missense	medium			
2247	ARID1A	EEC		1	MSI-High	p.C2163fs	26979464			Frame_Shift_Ins				
2247	CTNNB1	EEC		1	MSI-High	p.T41A	3,41241128,A,G	0.353	0.582	Missense	medium			
2247	PPP2R1A	EEC		1	MSI-High	p.H87Y	19,57401117,C,T	0.486	0.661	Missense	low			
2247	PTEN	EEC		1	MSI-High	p.P95L	10,89682780,C,T	0.800	0.772	Missense	medium			
2250	PTEN	Carcinosarcoma		N/A (3)	MSS	p.E7*	10,89614225,G,T	0.485	0.706	Truncating				
2252	ARID1A	EEC		2	MSI-High	p.N1070fs	26970208			Frame_Shift_Del				
2252	CTNNB1	EEC		2	MSI-High	p.655_656 AA>A	41253093			In_Frame_Del				
2252	PIK3CA	EEC		2	MSI-High	p.R38H	3,180399420,G,A	0.360	0.656	Missense	medium			
2252	PTEN	EEC		2	MSI-High	p.E242*	10,89707679,G,T	0.810	0.800	Truncating				
2258	ARID1A	EEC		2	MSI-High	p.N201fs	26896083			Frame_Shift_Del				
2258	BRAF	EEC		2	MSI-High	p.P403fs	140129395			Frame_Shift_Del				
2258	PTEN	EEC		2	MSI-High	p.C136Y	10,89682903,G,A	0.761	0.791	Missense	high			
2260	CTNNB1	EEC		1	MSS	p.S37C	3,41241117,C,G	0.259	0.666	Missense	high			
2260	PIK3CA	EEC		1	MSS	p.E542K	3,180418776,G,A	0.333	0.417	Missense	low	Validated		
2260	PTEN	EEC		1	MSS	p.D92E	10,89682772,C,A	0.833	0.821	Missense	medium			
2271	ARID1A	Carcinosarcoma		N/A (3)	MSS	p.R1461	1,26973686,C,T	0.367	0.531	Truncating				
2271	ARID1A	Carcinosarcoma		N/A (3)	MSS	p.C884fs	26962283			Frame_Shift_Del				
2271	KRAS	Carcinosarcoma		N/A (3)	MSS	p.G12V	12,25289551,C,A	0.588	0.798	Missense	high			
2294	ARID1A	EEC		1	MSS	p.Q464*	1,26930269,C,T	0.463	0.598	Truncating				
2294	PIK3CA	EEC		1	MSS	p.Q75H	3,180399532,A,C	0.529	0.671	Missense	low			
2294	PTEN	EEC		1	MSS	p.L112V	10,89682830,C,G	0.519	0.664	Missense	medium			
2305	TP53	ESC		N/A (3)	MSS	p.S241fs	7518282			Frame_Shift_Del				
2310	ARID1A	EEC		1	MSI-High	p.G2087R	1,26979235,G,A	0.574	0.796	Missense	medium			
2310	KRAS	EEC		1	MSI-	p.G12A	12,25289551,C,G	0.308	0.616	Missense	high			

ID	Gene	Original diagnosed subtype	Review Subtype	Grade	MSI Status	AA variant	Location (hg18)	Frequency	Probability	Type	Func. Impact	Sanger Validated	Normal available	Grade 3 Solid vs. Cytologic Atypia
					High									
2310	PIK3CA	EEC		1	MSI-High	p.R88Q	3,180399570,G,A	0.433	0.672	Missense	medium			
2310	PTEN	EEC		1	MSI-High	p.R130G	10,89682884,C,G	0.341	0.689	Missense	high			
2311	TP53	EEC		2	MSS	p.D281E	17,7517820,G,T	0.533	0.772	Missense	high			
2319	PIK3CA	EEC		2	MSS	p.C420R	3,180410674,T,C	0.370	0.655	Missense	medium			
2319	PTEN	EEC		2	MSS	p.K13T	10,89614244,A,C	0.551	0.743	Missense	high			
2391	PIK3CA	ESC		N/A (3)	MSS	p.Q546R	3,180418789,A,G	0.833	0.784	Missense	low			
2391	TP53	ESC		N/A (3)	MSS	p.R273C	17,7517846,G,A	0.750	0.872	Missense	high			
2405	CTNNB1	EEC		1	MSS	p.S37A	3,41241116,T,G	0.444	0.739	Missense	high			
2405	PTEN	EEC		1	MSS	p.R130G	10,89682884,C,G	0.943	0.813	Missense	high			
2416	PPP2R1A	Carcinosarcoma		N/A (3)	MSS	p.P179R	19,57407783,C,G	0.778	0.836	Missense	medium			
2416	TP53	Carcinosarcoma		N/A (3)	MSS	p.R280T	17,7517824,C,G	0.857	0.926	Missense	high			
2417	ARID1A	EEC		1	MSS	p.R1276*	1,26972534,C,T	0.385	0.714	Truncating				
2417	PTEN	EEC		1	MSS	p.R233*	10,89707652,C,T	0.778	0.899	Truncating				
2430	PIK3CA	EEC		2	MSS	p.R88Q	3,180399570,G,A	0.250	0.686	Missense	medium			
2430	PTEN	EEC		2	MSS	p.R130L	10,89682885,G,T	0.447	0.617	Missense	high			
2430	PTEN	EEC		2	MSS	p.L182*	10,89701907,T,G	0.350	0.737	Truncating				
2431	ARID1A	EEC		2	MSI-High	p.R1721	1,26978137,C,T	0.364	0.682	Truncating				
2431	ARID1A	EEC		2	MSI-High	p.G1847fs	26978517			Frame_Shift_Del				
2431	CTNNB1	EEC		2	MSI-High	p.D32H	3,41241101,G,C	0.452	0.407	Missense	medium			
2431	PIK3CA	EEC		2	MSI-High	p.M16I	3,180399355,G,A	0.208	0.760	Missense	medium			
2431	PTEN	EEC		2	MSI-High	p.R130*	10,89682884,C,T	0.438	0.640	Truncating				
2431	PTEN	EEC		2	MSI-High	p.L23fs	89614274			Frame_Shift_Ins				
2435	ARID1A	EEC		1	MSS	p.Y1506*	1,26973823,T,G	0.389	0.728	Truncating				
2435	ARID1A	EEC		1	MSS	p.I1635fs	26974208			Frame_Shift_Ins				
2435	CTNNB1	EEC		1	MSS	p.S37Y	3,41241117,C,A	0.293	0.726	Missense	high			
2435	PTEN	EEC		1	MSS	E545K	3,180418785,G,A	0.200	0.316	Missense		Not Validated		
2435	PTEN	EEC		1	MSS	p.I168fs	89701864			Frame_Shift_Del				
2437	TP53	ESC		N/A	MSS	p.R273C	17,7517846,G,A	0.833	0.882	Missense	high			

ID	Gene	Original diagnosed subtype	Review Subtype	Grade	MSI Status	AA variant	Location (hg18)	Frequency	Probability	Type	Func. Impact	Sanger Validated	Normal available	Grade 3 Solid vs. Cytologic Atypia
				(3)										
2465	TP53	Carcinosarcoma		N/A (3)	MSS	p.R248Q	17,7518263,C,T	0.474	0.722	Missense	high			
2489	PPP2R1A	Mixed_clear_cell_and_ESC		N/A (3)	MSS	p.W257C	19,57408139,G,T	0.625	0.638	Missense	medium			
2489	TP53	Mixed_clear_cell_and_ESC		N/A (3)	MSS	p.R248W	17,7518264,G,A	1.000	0.881	Missense	high			
2558	PPP2R1A	Carcinosarcoma		N/A (3)	MSS	p.S256F	19,57408135,C,T	0.500	0.635	Missense	medium			
2558	PTEN	Carcinosarcoma		N/A (3)	MSS	p.110_111 QW>R	89682824			In_Frame_ Del				
2558	TP53	Carcinosarcoma		N/A (3)	MSS	p.P322fs	7517605			Frame_Shift_Del				
2575	ARID1A	Mixed clear_cell (80%)_ESC_(20%)		N/A (3)	MSS	p.R1879W	1,26978611,C,T	0.750	0.675	Missense				
2575	TP53	Mixed clear_cell (80%)_ESC_(20%)		N/A (3)	MSS	p.H179Y	17,7519120,G,A	0.857	0.819	Missense	high			
1099G	TP53	ESC		3	MSS	p.C176F	17,7519128,C,A	0.346	0.638	Missense	high			

Table B.4 All endometrial carcinoma mutation data

ID	Subtype	PTEN IHC	p53 IHC	ER IHC	P16 IHC	PR IHC	ARID1A	PTEN	PIK3CA	KRAS	PPP2R1A	TP53	CTNNB1	BRAF	PPP2R5C
92	High-Grade EEC	1	2	1	0	0	0	0	0	1	0	1	0	0	0
148	High-Grade EEC	1	2	1	1	0	1	1	0	0	0	1	0	0	0
181	Low-Grade EEC	0	1	1	0	1	0	1	1	0	0	0	0	0	0
220	Serous Carcinoma	0	1	0	0	0	1	1	1	0	0	0	0	1	0
454	Low-Grade EEC	0	1	1	0	1	1	1	1	0	0	0	0	0	0
458	Low-Grade EEC	0	1	1	0	1	1	1	1	0	0	0	1	0	0
465	Low-Grade EEC	0	1	1	0	0	1	1	1	1	1	1	0	0	0

ID	Subtype	PTEN IHC	p53 IHC	ER IHC	P16 IHC	PR IHC	ARID1A	PTEN	PIK3CA	KRAS	PPP2R1A	TP53	CTNNB1	BRAF	PPP2R5C
472	Serous Carcinoma	1	2	1	1	0	0	0	1	0	1	1	0	0	0
474	Low-Grade EEC	0	1	1	0	0	0	0	0	0	0	0	0	0	0
477	Low-Grade EEC	0	1	1	0	0	1	1	0	0	0	0	0	0	0
478	Low-Grade EEC	1	1	1	0	1	1	1	1	0	1	0	1	0	0
501	Low-Grade EEC	0	1	1	0	1	0	1	0	1	0	0	0	1	0
511	Low-Grade EEC	0	2	1	0	1	0	0	0	0	1	1	0	0	0
531	Low-Grade EEC	1	1	1	0	1	0	0	0	1	0	0	0	0	0
538	Low-Grade EEC	1	1	1	0	0	1	1	0	0	0	0	0	0	0
570	Low-Grade EEC	0	1	1	0	1	0	1	1	0	0	0	1	0	0
575	Low-Grade EEC	NA	NA	1	0	0	0	0	1	0	0	0	1	0	0
577	Low-Grade EEC	0	NA	1	0	1	0	1	1	0	1	1	0	0	0
578	Low-Grade EEC	0	1	1	0	1	0	0	1	0	0	0	0	0	0
584	Low-Grade EEC	0	2	1	0	1	1	1	0	1	1	0	0	0	0
585	Undifferentiated	1	1	0	0	0	0	0	0	0	0	0	0	0	0
587	Low-Grade EEC	0	1	1	0	1	1	1	1	0	0	0	0	0	0
588	Low-Grade EEC	1	1	1	0	1	0	1	1	0	1	0	0	0	0
607	High-Grade EEC	0	1	1	0	0	1	1	1	0	0	0	0	1	0
608	Low-Grade EEC	0	NA	1	0	1	1	1	1	0	0	1	0	0	0
611	Low-Grade EEC	0	2	1	1	NA	0	0	0	0	0	1	0	0	0
612	Low-Grade EEC	0	1	1	0	1	1	1	0	0	0	0	1	0	0
615	Low-Grade EEC	1	1	1	0	1	1	1	1	0	0	0	0	0	0
625	Low-Grade EEC	0	1	1	0	1	1	1	0	0	0	0	1	0	0
632	Low-Grade EEC	0	1	1	0	1	1	1	1	1	0	0	0	0	0
640	Low-Grade EEC	0	1	1	0	1	1	1	0	0	0	0	1	0	0
642	Low-Grade EEC	1	2	1	0	1	0	0	0	0	0	0	0	0	0
645	Low-Grade EEC	1	1	1	0	1	1	1	0	1	0	0	0	0	0
647	Low-Grade EEC	NA	1	NA	NA	NA	1	1	0	0	0	0	0	0	0
653	Low-Grade EEC	1	1	1	0	1	1	1	0	0	0	0	0	0	0
658	Low-Grade EEC	0	1	1	0	1	0	1	0	0	0	0	1	0	0
659	Low-Grade EEC	1	1	1	NA	1	1	1	0	1	0	0	0	0	0
661	High-Grade EEC	0	1	1	0	1	1	1	1	0	0	0	0	0	0
668	Low-Grade EEC	0	1	1	0	1	0	1	1	0	0	0	1	0	0
672	Low-Grade EEC	1	1	1	0	1	0	0	0	0	0	0	1	0	0
674	Low-Grade EEC	NA	NA	1	1	1	1	1	0	1	0	0	0	0	0
699	High-Grade EEC	0	2	1	0	1	1	1	1	0	0	1	0	0	1
700	Low-Grade EEC	0	1	1	0	1	0	1	1	1	1	0	0	0	0
701	Low-Grade EEC	0	1	1	0	1	1	0	1	1	0	0	1	0	0

ID	Subtype	PTEN IHC	p53 IHC	ER IHC	P16 IHC	PR IHC	ARID1A	PTEN	PIK3CA	KRAS	PPP2R1A	TP53	CTNNB1	BRAF	PPP2R5C
707	Low-Grade EEC	0	NA	1	0	0	1	1	0	0	0	0	1	0	0
712	High-Grade EEC	1	2	1	0	0	1	1	1	0	0	1	1	0	0
721	Low-Grade EEC	1	1	1	0	1	0	1	0	0	0	0	0	0	0
733	Low-Grade EEC	1	NA	1	0	0	0	1	1	0	0	0	0	0	0
737	Serous Carcinoma	1	2	0	1	0	0	0	1	0	0	1	0	0	0
742	Mixed Carcinoma	1	1	1	0	1	0	0	0	0	0	1	1	0	0
745	Low-Grade EEC	1	1	1	0	1	0	1	0	0	0	0	1	0	0
750	Low-Grade EEC	0	1	1	0	1	0	1	0	1	0	0	0	0	0
771	Low-Grade EEC	0	1	1	0	1	1	1	0	0	0	0	1	0	0
772	Low-Grade EEC	0	1	1	0	1	1	1	0	0	0	0	1	0	0
778	Low-Grade EEC	1	1	1	0	1	1	1	1	0	0	0	1	0	0
780	Low-Grade EEC	0	1	1	0	1	0	1	1	0	0	0	1	0	0
795	Serous Carcinoma	1	2	1	1	0	0	0	1	0	1	1	0	0	0
799	Low-Grade EEC	0	1	1	0	1	0	0	0	0	0	0	0	0	0
804	High-Grade EEC	0	1	1	0	1	0	1	0	0	0	0	1	0	0
806	Low-Grade EEC	0	1	1	1	1	0	0	0	1	0	0	0	0	0
807	Serous Carcinoma	1	2	1	1	0	0	0	1	0	1	1	0	0	0
810	Low-Grade EEC	1	1	1	0	1	0	1	1	0	0	0	1	0	0
815	Low-Grade EEC	1	1	1	0	1	1	1	1	0	0	0	0	0	0
819	Low-Grade EEC	0	2	1	1	0	0	0	0	0	0	0	0	0	0
823	High-Grade EEC	0	1	1	0	1	0	1	1	0	0	0	0	0	0
824	Low-Grade EEC	0	1	1	0	1	0	1	0	0	0	0	1	0	0
831	Low-Grade EEC	1	1	1	0	1	0	1	1	0	0	0	0	0	0
832	Low-Grade EEC	0	1	1	0	1	0	1	0	0	0	0	0	0	0
839	High-Grade EEC	1	NA	0	0	0	1	1	1	0	0	0	0	0	0
841	Serous Carcinoma	1	1	0	0	0	1	0	1	1	1	0	0	0	0
843	Low-Grade EEC	0	NA	1	0	1	1	1	1	0	1	1	0	0	0
844	Low-Grade EEC	1	1	1	0	0	0	1	1	0	0	0	1	1	0
849	Carcinosarcoma	0	2	1	1	1	0	1	0	0	0	1	0	0	0
852	High-Grade EEC	1	1	1	1	0	1	1	0	1	0	1	0	0	0
858	High-Grade EEC	1	1	1	0	1	1	1	1	0	0	0	1	1	0
863	Low-Grade EEC	1	1	1	0	1	1	1	0	0	0	1	0	0	0
872	Low-Grade EEC	0	1	1	0	1	1	1	1	0	0	0	0	0	0
874	Low-Grade EEC	1	1	1	0	1	0	1	0	0	0	1	0	0	0
876	Low-Grade EEC	0	1	1	0	0	1	1	1	0	0	0	0	0	0
879	Low-Grade EEC	0	1	1	1	0	1	1	0	0	0	0	0	0	0
882	Low-Grade EEC	1	1	1	0	1	0	0	0	0	0	0	0	0	0

ID	Subtype	PTEN IHC	p53 IHC	ER IHC	P16 IHC	PR IHC	ARID1A	PTEN	PIK3CA	KRAS	PPP2R1A	TP53	CTNNB1	BRAF	PPP2R5C
883	High-Grade EEC	1	1	1	0	1	0	1	0	0	0	0	0	0	0
887	Low-Grade EEC	1	NA	1	0	1	1	0	1	0	0	0	0	0	0
888	Mixed Carcinoma	1	2	0	0	0	1	0	1	1	1	0	0	0	0
892	Serous Carcinoma	1	0	1	1	0	0	0	0	0	1	1	0	0	0
895	Low-Grade EEC	0	2	1	0	1	0	0	0	0	0	1	0	0	0
896	Serous Carcinoma	0	2	0	1	0	0	0	0	0	0	0	0	0	0
913	Low-Grade EEC	0	1	1	0	1	1	1	1	0	0	1	0	0	0
918	Low-Grade EEC	0	1	1	0	1	0	1	1	0	0	0	0	0	0
920	Low-Grade EEC	0	1	1	0	1	0	0	0	0	0	0	0	0	0
926	Low-Grade EEC	0	1	1	0	1	1	1	0	0	1	0	0	0	0
928	Low-Grade EEC	0	1	1	0	1	0	1	1	0	0	0	1	0	0
931	Low-Grade EEC	1	1	1	0	1	1	1	1	0	0	0	0	0	0
936	Low-Grade EEC	0	1	1	0	0	0	0	0	0	0	0	0	0	0
938	High-Grade EEC	0	1	1	0	1	1	1	1	0	0	0	1	0	0
939	High-Grade EEC	0	1	1	0	1	0	1	0	0	0	0	1	0	0
941	Low-Grade EEC	1	1	1	0	1	0	0	0	0	0	0	0	0	0
947	High-Grade EEC	0	1	0	0	0	0	1	0	0	0	0	0	0	0
955	High-Grade EEC	1	1	0	0	0	1	1	1	0	0	0	0	0	0
957	High-Grade EEC	0	1	0	0	0	1	1	0	1	0	0	0	0	0
960	Low-Grade EEC	0	1	1	0	1	1	0	0	0	0	0	1	0	0
965	Low-Grade EEC	0	1	1	0	1	0	0	0	0	0	0	0	0	0
977	Serous Carcinoma	1	0	1	1	0	0	0	1	0	1	0	0	0	0
983	Low-Grade EEC	0	1	1	0	1	1	1	1	0	0	0	0	0	0
987	Low-Grade EEC	1	1	1	0	1	0	0	0	0	0	0	0	0	0
996	High-Grade EEC	1	1	1	0	0	0	1	1	0	0	0	0	0	0
998	Low-Grade EEC	0	1	1	0	1	0	0	0	0	0	0	0	0	0
1000	Low-Grade EEC	1	1	1	0	1	1	1	1	0	0	0	0	0	0
1002	Low-Grade EEC	1	1	1	0	1	0	0	0	0	0	0	0	0	0
1004	Low-Grade EEC	0	1	1	0	1	0	1	0	0	0	0	1	0	0
1007	Low-Grade EEC	0	1	1	0	1	0	0	0	0	0	0	0	0	0
1009	Serous Carcinoma	1	1	0	0	0	0	0	0	0	0	0	0	0	0
1010	Undifferentiated	1	1	1	1	0	0	1	1	0	0	1	0	0	0
1015	Low-Grade EEC	0	1	1	0	1	1	1	1	1	0	0	0	0	0
1020	Low-Grade EEC	0	1	1	0	1	0	1	1	0	0	0	0	0	0
1024	High-Grade EEC	0	1	1	0	1	1	1	1	1	0	0	0	0	0
1030	Serous Carcinoma	1	2	0	1	0	0	0	0	0	1	1	0	0	0
1034	Low-Grade EEC	0	2	1	1	1	0	1	0	0	0	1	0	0	0

ID	Subtype	PTEN IHC	p53 IHC	ER IHC	P16 IHC	PR IHC	ARID1A	PTEN	PIK3CA	KRAS	PPP2R1A	TP53	CTNNB1	BRAF	PPP2R5C
1040	Low-Grade EEC	0	1	1	0	1	0	0	0	0	0	0	0	0	0
1046	Low-Grade EEC	0	1	1	0	0	0	1	0	0	0	0	1	0	0
1047	Serous Carcinoma	NA	2	NA	NA	NA	0	0	0	0	1	1	0	0	0
1055	Low-Grade EEC	0	1	1	0	1	0	1	0	0	0	0	1	0	0
1058	High-Grade EEC	0	1	0	0	0	1	1	0	1	0	0	0	0	0
1059	Serous Carcinoma	0	2	1	1	0	0	0	0	0	0	1	0	0	0
1069	Low-Grade EEC	1	2	1	0	1	1	1	1	0	1	1	0	0	0
1073	Low-Grade EEC	0	1	1	0	1	1	1	0	0	0	0	1	0	0
1074	High-Grade EEC	1	1	1	0	1	1	1	1	0	1	0	0	0	0
1075	Low-Grade EEC	1	1	1	0	1	0	1	1	0	0	0	1	0	0
1081	Serous Carcinoma	1	0	0	1	0	0	0	0	0	0	0	0	0	0
1082	Serous Carcinoma	1	2	1	1	0	0	0	0	0	0	1	0	0	0
1086	High-Grade EEC	1	1	0	0	0	1	1	1	1	0	0	0	0	0
1087	Low-Grade EEC	1	1	1	0	1	0	0	0	0	0	0	0	0	0
1090	High-Grade EEC	0	1	0	1	0	1	1	0	0	0	1	0	0	0
1094	High-Grade EEC	0	2	0	0	0	1	1	1	1	1	1	1	0	1
1095	High-Grade EEC	0	NA	1	0	0	0	1	1	0	0	0	0	0	0
1099	Low-Grade EEC	0	1	1	0	1	1	1	0	0	0	0	0	0	0
1100	High-Grade EEC	1	0	0	1	0	0	0	1	0	0	1	0	0	0
1102	High-Grade EEC	0	1	1	0	1	0	1	0	0	0	0	0	0	0
1104	Low-Grade EEC	1	1	1	0	1	0	0	0	0	0	0	0	0	0
1109	High-Grade EEC	1	1	1	0	0	1	1	1	0	1	0	0	0	0
1111	High-Grade EEC	0	1	1	1	0	0	0	0	0	0	0	0	0	0
1118	Serous Carcinoma	1	2	1	0	0	0	0	1	0	1	1	0	0	0
1119	Undifferentiated	1	1	0	0	0	1	1	1	0	0	0	1	0	0
1120	Serous Carcinoma	1	1	1	0	1	1	0	1	1	0	0	0	0	0
1134	Low-Grade EEC	0	1	1	0	1	1	0	1	1	0	0	0	0	0
1135	Low-Grade EEC	0	1	1	0	1	1	0	0	0	0	0	0	0	0
1142	Low-Grade EEC	0	1	1	0	1	0	1	0	0	0	0	0	0	0

Table B.5 Endometrial carcinoma mutation data with immunohistochemistry scores

For mutation data; 1=presence of mutation, 0=no mutation detected, For PTEN, PR, ER, P16 IHC: 1=protein expression, 0=no protein expression. For p53 IHC: 1=normal expression, 0=loss of expression (nonsense or deletion mutations), 2= protein overexpression (missense mutations).

ID	Histology	C-Myc IHC Score	Gene	Chr	Genomic location (hg19)	Ref	Variant	Depth	Transcript ID (RefGene)	Type	Amino Acid Change	Allele Ratio	Validation
472	ESC	1	PPP2R1A	chr19	52714547	C	A	4748	NM_014225	Missense	T102K	0.362	Validated
472	ESC	1	PPP2R1A	chr19	52716323	C	T	14356	NM_014225	Missense	S256F	0.537	Validated
711	ESC	2	FBXW7	chr4	153249385	G	A	6356	NM_033632	Missense	R465C	0.194	Validated
711	ESC	2	TP53	chr17	7577545	T	C	2487	NM_000546	Missense	M246V	0.560	Validated
737a	ESC	1	FBXW7	chr4	153247289	G	A	3461	NM_033632	Missense	R505C	0.107	Validated
737a	ESC	1	TP53	chr17	7577538	C	T	4962	NM_000546	Missense	R248Q	0.517	Validated
795a	ESC	2	TP53	chr17	7577565	T	G	4461	NM_000546	Missense	N239T	0.519	Validated
795a	ESC	2	PPP2R1A	chr19	52716323	C	T	11838	NM_014225	Missense	S256F	0.491	Validated
807	ESC	1	TP53	chr17	7577551	C	A	4302	NM_000546	Missense	G244C	0.768	Validated
807	ESC	1	PPP2R1A	chr19	52715971	C	G	5177	NM_014225	Missense	P179R	0.573	Validated
849	ESC	2	TP53	chr17	7577097	C	G	5653	NM_000546	Missense	D281H	0.403	Validated
852	ESC	2	TP53	chr17	7607687	T	-		NM_000546	Frameshift			Validated
892a	ESC	0	PPP2R1A	chr19	52715982	C	T	5983	NM_014225	Missense	R183W	0.334	Validated
977a	ESC	0	PPP2R1A	chr19	52716323	C	T	11711	NM_014225	Missense	S256F	0.404	Validated
1030	ESC	1	TP53	chr17	7577095	G	T	4284	NM_000546	Missense	D281E	0.367	Validated
1030	ESC	1	PPP2R1A	chr19	52715971	C	G	3840	NM_014225	Missense	P179R	0.257	Validated
1034a	ESC	1	TP53	chr17	7577538	C	T	8924	NM_000546	Missense	R248Q	0.325	Validated
1047	ESC	1	TP53	chr17	7577120	C	T	5090	NM_000546	Missense	R273H	0.419	Validated
1047	ESC	1	PPP2R1A	chr19	52715971	C	T	3950	NM_014225	Missense	P179L	0.209	Validated
1118	ESC	0	TP53	chr17	7577570	C	T	6497	NM_000546	Missense	M237I	0.275	Validated
1118	ESC	0	PPP2R1A	chr19	52715971	C	G	3413	NM_014225	Missense	P179R	0.166	Validated
1833	ESC	1	TP53	chr17	7577121	G	A	5710	NM_000546	Missense	R273C	0.645	Validated
1847	ESC	1	TP53	chr17	7578259	A	C	4736	NM_000546	Missense	V197G	0.051	Validated
1921	ESC	1	FBXW7	chr4	153247294	G	A	3835	NM_033632	Missense	A503V	0.398	Validated
1921	ESC	1	TP53	chr17	7578266	T	A	5799	NM_000546	Missense	I195F	0.777	Validated
1942	ESC	1	FBXW7	chr4	153250883	G	A	3300	NM_033632	Nonsense	R393X	0.085	Validated
1967	ESC	1	TP53	chr17	7577094	G	A	5584	NM_000546	Missense	R282W	0.194	Validated
2011	ESC	1	TP53	chr17	7577538	C	T	6269	NM_000546	Missense	R248Q	0.930	Validated
2011	ESC	1	PPP2R1A	chr19	52715971	C	T	3048	NM_014225	Missense	P179L	0.453	Validated
2027	ESC	0	TP53	chr17	7577121	G	A	5275	NM_000546	Missense	R273C	0.539	Validated
2050	ESC	2	FBXW7	chr4	153249462	G	A	7580	NM_033632	Missense	T439I	0.258	Validated

ID	Histology	C-Myc IHC Score	Gene	Chr	Genomic location (hg19)	Ref	Variant	Depth	Transcript ID (RefGene)	Type	Amino Acid Change	Allele Ratio	Validation
472	ESC	1	PPP2R1A	chr19	52714547	C	A	4748	NM_014225	Missense	T102K	0.362	Validated
2050	ESC	2	TP53	chr17	7578263	G	A	6061	NM_000546	Nonsense	R196X	0.250	Validated
2050	ESC	2	PPP2R1A	chr19	52715971	C	G	4018	NM_014225	Missense	P179R	0.263	Validated
2064	ESC	1	TP53	chr17	7578452	T	TGGCG CG	9441	NM_000546	Insertion		0.425	Validated
2076	ESC	1	TP53	chr17	7577539	G	A	6904	NM_000546	Missense	R248W	0.455	Validated
2076	ESC	1	PPP2R1A	chr19	52716323	C	T	10789	NM_014225	Missense	S256F	0.203	Validated
2157	ESC	2	FBXW7	chr4	153268138	G	A	4839	NM_033632	Nonsense	R224X	0.403	Validated
2157	ESC	2	TP53	chr17	7577538	C	T	7241	NM_000546	Missense	R248Q	0.413	Validated
2157	ESC	2	PPP2R1A	chr19	52714526	C	T	3454	NM_014225	Missense	S95L	0.682	Validated
2157	ESC	2	PPP2R1A	chr19	52716081	G	A	1001	NM_014225	Missense	E216K	0.239	Validated
2214	ESC	2	FBXW7	chr4	153249384	C	T	6519	NM_033632	Missense	R465H	0.095	Validated
2214	ESC	2	PPP2R1A	chr19	52715982	C	T	4228	NM_014225	Missense	R183W	0.309	Validated
2242a	ESC	0	TP53	chr17	7577539	G	A	6172	NM_000546	Missense	R248W	0.813	Validated
2242a	ESC	0	PPP2R1A	chr19	52715971	C	G	3427	NM_014225	Missense	P179R	0.592	Validated
2297	ESC	1	TP53	chr17	7576903	A	AG	1074	NM_000546	Frameshift		0.416	Validated
2297	ESC	1	TP53	chr17	7578199	A	T	1120	NM_000546	Missense	V217E	0.421	Validated
3088	ESC	0	TP53	chr17	7577538	C	T	273	NM_000546	Missense	R248Q	0.604	Validated
1082	ESC	1	TP53	chr17	7578517	G	A	6884	NM_000546	Missense	A138V	0.393	Validated
2415a	ESC	0	TP53	chr17	7578474	C	CG	20124	NM_000546	Frameshift		0.432	Validated
2415a	ESC	0	PPP2R1A	chr19	52714543	G	A	6465	NM_014225	Missense	E101K	0.208	Validated
3219	ESC	0	TP53	chr17	7577121	G	A	6886	NM_000546	Missense	R273C	0.477	Validated
3047	ESC	0	TP53	chr17	7579470	CG	C	7372	NM_000546	Frameshift		0.384	Validated
3000	ESC	1	FBXW7	chr4	153244092	G	A	6752	NM_033632	Missense	R689W	0.199	Validated
3000	ESC	1	FBXW7	chr4	153247168	T	C	7327	NM_033632	Missense	Y545C	0.327	Validated
3000	ESC	1	TP53	chr17	7577548	C	T	6221	NM_000546	Missense	G245S	0.488	Validated
2426	ESC	2	FBXW7	chr4	153247366	C	T	587	NM_033632	Missense	R479Q	0.315	Validated
2426	ESC	2	TP53	chr17	7578406	C	T	230	NM_000546	Missense	R175H	0.626	Validated
2426	ESC	2	PPP2R1A	chr19	52716323	C	T	1175	NM_014225	Missense	S256F	0.301	Validated
2498	ESC	1	TP53	chr17	7578211	C	G	1161	NM_000546	Missense	R213P	0.117	Validated
2498	ESC	1	PPP2R1A	chr19	52716323	C	T	1368	NM_014225	Missense	S256F	0.157	Validated
3030	ESC	2	TP53	chr17	7577538	C	T	978	NM_000546	Missense	R248Q	0.575	Validated

ID	Histology	C-Myc IHC Score	Gene	Chr	Genomic location (hg19)	Ref	Variant	Depth	Transcript ID (RefGene)	Type	Amino Acid Change	Allele Ratio	Validation
472	ESC	1	PPP2R1A	chr19	52714547	C	A	4748	NM_014225	Missense	T102K	0.362	Validated
3030	ESC	2	TP53	chr17	7578268	A	C	1624	NM_000546	Missense	L194R	0.300	Validated
ESC001	ESC	0	TP53	chr17	7578236	A	G	7068	NM_000546	Missense	Y205H	0.354	Validated
ESC001	ESC	0	PPP2R1A	chr19	52715971	C	G	4342	NM_014225	Missense	P179R	0.653	Validated
ESC002	ESC	0	TP53	chr17	7578419	C	A	4725	NM_000546	Nonsense	E171X	0.998	Validated
ESC002	ESC	0	PPP2R1A	chr19	52716323	C	A	8999	NM_014225	Missense	S256Y	0.491	Validated
ESC003	ESC	1	PPP2R1A	chr19	52716327	G	C	144	NM_014225	Missense	W257C	0.792	Validated
ESC004	ESC	2	TP53	chr17	7577538	C	T	4365	NM_000546	Missense	R248Q	0.537	Validated
ESC004	ESC	2	PPP2R1A	chr19	52715983	G	A	5129	NM_014225	Missense	R183Q	0.449	Validated
ESC005	ESC	1	PPP2R1A	chr19	52715971	C	G	4496	NM_014225	Missense	P179R	0.707	Validated
ESC006	ESC	2	FBXW7	chr4	153249384	C	T	5827	NM_033632	Missense	R465H	0.140	Validated
ESC006	ESC	2	TP53	chr17	7578535	T	C	4280	NM_000546	Missense	K132R	0.658	Validated
ESC006	ESC	2	PPP2R1A	chr19	52716323	C	T	8652	NM_014225	Missense	S256F	0.399	Validated
ESC007	ESC	0	TP53	chr17	7578508	C	T	9750	NM_000546	Missense	C141Y	0.218	Validated
ESC008	ESC	2	FBXW7	chr4	153250931	T	C	4467	NM_033632	Missense	K377E	0.082	Not validated
ESC008	ESC	2	FBXW7	chr4	153332540	T	C	5774	NM_033632	Missense	H139R	0.232	Not validated
ESC009	ESC	2	TP53	chr17	7577508	T	C	4677	NM_000546	Missense	E258G	0.800	Validated
ESC009	ESC	2	PPP2R1A	chr19	52715971	C	T	4762	NM_014225	Missense	P179L	0.989	Validated
ESC010	ESC	1	PPP2R1A	chr19	52716323	C	T	10383	NM_014225	Missense	S256F	0.235	Validated
ESC011	ESC	2	TP53	chr17	7577128	A	C	3608	NM_000546	Missense	F270L	0.164	Validated
ESC012	ESC	0	TP53	chr17	7579713	T	C	859	NM_000546	Missense	E28G	0.282	Not validated
ESC012	ESC	0	PPP2R1A	chr19	52715971	C	G	3439	NM_014225	Missense	P179R	0.102	Validated
ESC013	ESC	1	TP53	chr17	7578265	A	G	6218	NM_000546	Missense	I195T	0.936	Validated
ESC014	ESC	1	TP53	chr17	7578467	T	G	4535	NM_000546	Missense	T155P	0.829	Validated
ESC014	ESC	1	PPP2R1A	chr19	52715971	C	T	5322	NM_014225	Missense	P179L	0.521	Validated
ESC015	ESC	1	FBXW7	chr4	153247366	C	T	7318	NM_033632	Missense	R479Q	0.369	Validated
ESC015	ESC	1	TP53	chr17	7579349	A	C	4506	NM_000546	Missense	F113C	0.147	Validated
ESC016	ESC	1	TP53	chr17	7574002	C	G	4678	NM_000546	Missense	R342P	0.370	Validated
ESC017	ESC	2	TP53	chr17	7579494	TG	T	4208	NM_000546	Frameshift		0.386	Not validated
ESC017	ESC	2	PPP2R1A	chr19	52716323	C	T	7891	NM_014225	Missense	S256F	0.613	Validated
ESC018	ESC	0	FBXW7	chr4	153249391	T	A	7609	NM_033632	Missense	T463S	0.090	Validated

ID	Histology	C-Myc IHC Score	Gene	Chr	Genomic location (hg19)	Ref	Variant	Depth	Transcript ID (RefGene)	Type	Amino Acid Change	Allele Ratio	Validation
472	ESC	1	PPP2R1A	chr19	52714547	C	A	4748	NM_014225	Missense	T102K	0.362	Validated
ESC018	ESC	0	TP53	chr17	7578508	C	T	8914	NM_000546	Missense	C141Y	0.661	Validated
ESC019	ESC	2	TP53	chr17	7577097	C	G	109	NM_000546	Missense	D281H	0.734	Validated
ESC020	ESC	2	PPP2R1A	chr19	52715971	C	G	4	NM_014225	Missense	P179R	0.500	Validated
ESC021	ESC	0	TP53	chr17	7578459	G	GAC	4897	NM_000546	Frameshift		0.176	Validated
ESC022	ESC	2	TP53	chr17	7577517	A	G	3615	NM_000546	Missense	I255T	0.996	Validated
ESC022	ESC	2	PPP2R1A	chr19	52716323	C	T	9990	NM_014225	Missense	S256F	0.298	Validated
ESC023	ESC	0	TP53	chr17	7577547	C	T	6425	NM_000546	Missense	G245D	0.552	Validated
ESC023	ESC	0	PPP2R1A	chr19	52716323	C	T	13684	NM_014225	Missense	S256F	0.222	Validated
ESC024	ESC	2	TP53	chr17	7577551	C	T	5154	NM_000546	Missense	G244S	0.607	Validated
ESC024	ESC	2	PPP2R1A	chr19	52716325	T	G	10084	NM_014225	Missense	W257G	0.297	Validated
ESC025	ESC	1	FBXW7	chr4	153332630	T	C	9048	NM_033632	Missense	D109G	0.083	Not validated
ESC025	ESC	1	TP53	chr17	7577538	C	T	6465	NM_000546	Missense	R248Q	0.722	Validated
ESC026	ESC	1	FBXW7	chr4	153247240	A	T	11910	NM_033632	Missense	F521Y	0.047	Not validated
ESC026	ESC	1	FBXW7	chr4	153332877	G	A	15195	NM_033632	Nonsense	Q27X	0.737	Validated
ESC027	ESC	1	TP53	chr17	7578196	A	C	17954	NM_000546	Missense	V218G	0.782	Validated
ESC028	ESC	1	TP53	chr17	7577121	G	A	6533	NM_000546	Missense	R273C	0.235	Not validated
ESC029	ESC	1	TP53	chr17	7577099	C	G	4980	NM_000546	Missense	R280T	0.588	Validated
ESC030	ESC	1	TP53	chr17	7578265	A	G	8684	NM_000546	Missense	I195T	0.853	Validated
ESC031	ESC	1	TP53	chr17	7577559	G	A	4524	NM_000546	Missense	S241F	0.147	Not validated
ESC032	ESC	0	TP53	chr17	7578395	G	T	4000	NM_000546	Missense	H179N	0.559	Validated

Table B.6 All mutation table for endometrial serous targeted gene sequencing

For C-Myc IHC staining score is the H-score binarized: 2= H score>60, 1= H-score <60, 0-no staining.

B.3 **Supplemental Figures**

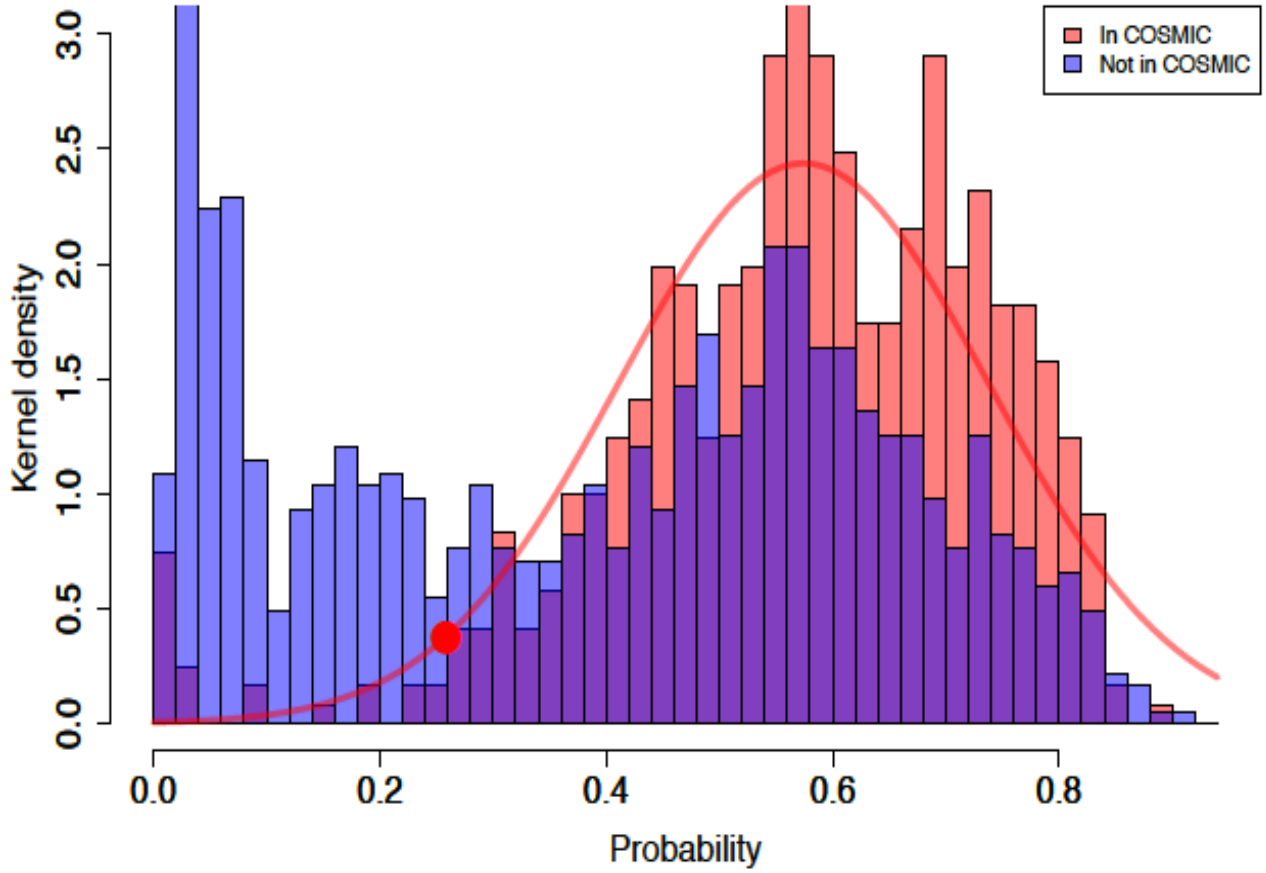

Figure B.1 A histogram of the probability distribution of the predicted SNV positions.
SNVs found in COSMIC (red), have higher probabilities than those not in COSMIC (blue). The threshold cutoff for selecting positive SNVs was set at 0.2588 as indicated by the red circle. All mutations to the left of the red circle were considered false positives and not considered in the data set.

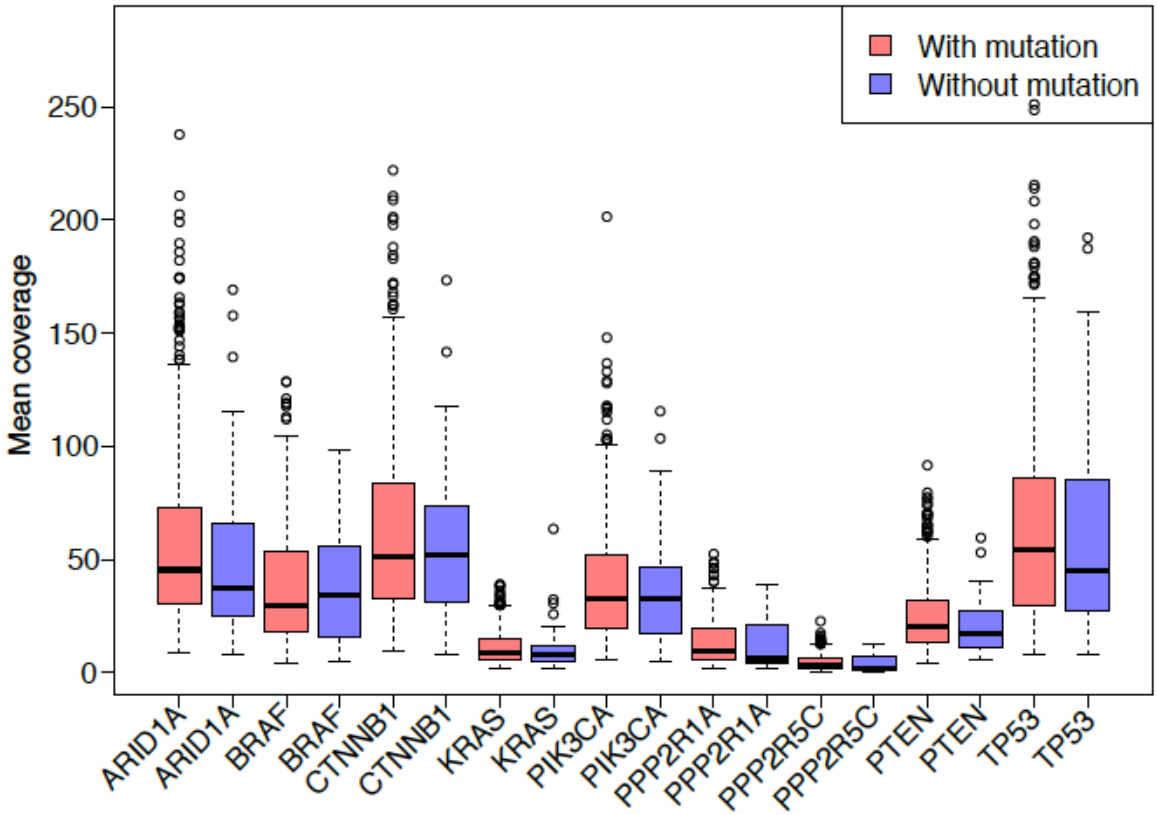

Figure B.2 Boxplots of the mean-coverage of each gene in the cases with and without mutations
Cases with mutations (red) and without mutations (blue), with mean-coverage defined as the number of reads covering each coding position of a gene. The cases with and without mutations have similar coverage; therefore it is unlikely these cases are not false negatives in the genes analyzed. It can be noted that *KRAS, PPP2R1A* and *PPP2R5C* have relatively lower coverage. However both *PPP2R1A* and *PPP2R5C* have lower coverage due to not being sequenced in 64 cases. Previously validated somatic *PPP2R1A* mutations were added in subsequent analysis.

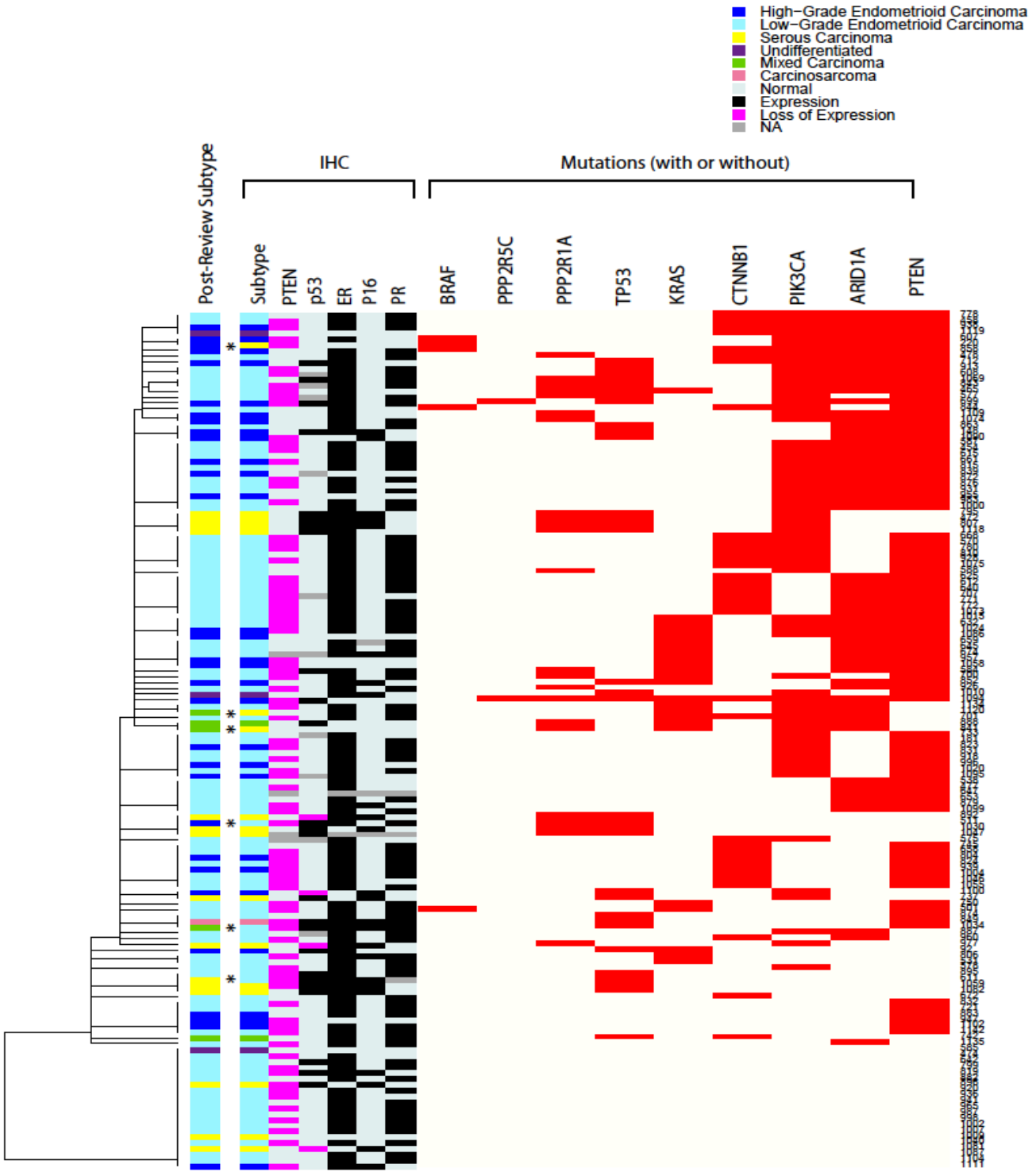

Figure B.3 Endometrial unsupervised hierarchical mutation clustering analysis aids in visualizing mutational outliers.

There are 147 cases clustered based on binarized mutation status in 9 genes, alongside IHC protein expression of 6 genes with histological subtypes based on data from Table B.4. Mutational outliers indicated by (*). The post-review classifications of outliers are shown in a new subtype panel.

Appendix C Chapter 4 Supplemental Table

ID	Gene	Original diagnosed subtype	Grade	AA variant	Location (hg18)	Indel Genotype	Frequency	Probability	Type	Func. Impact	Sanger Validated	Notes
12	CTNNB1	OEC		p.S37A	3,41241116,T,G		0.173	0.676	Missense	high	Validated	
12	PIK3CA	OEC		p.H1047R	3,180434779,A,G		0.298	0.682	Missense	low	Validated	
146	KRAS	OEC		p.G12D	12,25289551,C,T		0.792	0.815	Missense	high	Validated	
146	PIK3CA	OEC		p.H1047R	3,180434779,A,G		0.325	0.696	Missense	low	Validated	
156	ARID1A	OEC		p.G1178S	1,26971703,G,A		0.441	0.469	Missense	low		
156	CTNNB1	OEC		p.S33A	3,41241104,T,G		0.429	0.670	Missense	medium	Validated	
156	KRAS	OEC		p.G13C	12,25289549,C,A		0.229	0.344	Missense	high	Validated	
156	PTEN	OEC		p.R130*	10,89682884,C,T		0.782	0.617	Truncating		Validated	
242	PIK3CA	OEC		p.R93W	3,180399584,C,T		0.167	0.280	Missense	medium	Validated	
255	CTNNB1	OEC		p.S33C	3,41241105,C,G		0.135	0.825	Missense	medium	Validated	
281	KRAS	OEC		p.G12S	12,25289552,C,T		0.873	0.678	Missense	high	Validated	
281	PPP2R1A	OEC		p.W257G	19,57408137,T,G		0.297	0.468	Missense	medium	Validated	
334	ARID1A	OEC			26973919	*/-GCCAACCACGAAGGCTCGTGGCCTTCCCATGGCACAC			Frame_Shift_Del			
334	CTNNB1	OEC		p.G34R	3,41241107,G,C		0.303	0.493	Missense	medium		
334	PIK3CA	OEC		p.C901F	3,180430521,G,T		0.400	0.432	Missense	medium		
404	KRAS	OEC		p.G12V	12,25289551,C,A		0.353	0.439	Missense	high	Validated	
410	KRAS	OEC		p.G12V	12,25289551,C,A		0.316	0.319	Missense	high	Validated	
410	PIK3CA	OEC		p.N345K	3,180404247,T,A		0.346	0.298	Missense	medium		
437	CTNNB1	OEC		p.G34R	3,41241107,G,A		0.198	0.609	Missense	medium		
437	PIK3CA	OEC		p.K111E	3,180399638,A,G		0.137	0.378	Missense	medium		
448	KRAS	OEC		p.G12V	12,25289551,C,A		0.226	0.497	Missense	high	Validated	
554	CTNNB1	OEC		p.S33C	3,41241105,C,G		0.556	0.765	Missense	medium	Validated	
555	CTNNB1	OEC		p.G34V	3,41241108,G,T		0.181	0.622	Missense	medium	Validated	
555	KRAS	OEC		p.G12V	12,25289551,C,A		0.298	0.415	Missense	high	Validated	
579	CTNNB1	OEC		p.S33Y	3,41241105,C,A		0.366	0.772	Missense	medium	Validated	
629	ARID1A	OEC		p.E896*	1,26962317,G,T		0.139	0.646	Truncating			

ID	Gene	Original diagnosed subtype	Grade	AA variant	Location (hg18)	Indel Genotype	Frequency	Probability	Type	Func. Impact	Sanger Validated	Notes
629	PTEN	OEC		p.D326G	10,89710806,A,G		0.213	0.410	Missense	high		
629	PTEN	OEC		p.L139V	10,89682911,T,G		0.177	0.583	Missense	high	Not Validated	
629	PTEN	OEC		p.R173C	10,89701879,C,T		0.161	0.695	Missense	high		
629	PTEN	OEC		p.R335*	10,89710832,C,T		0.212	0.444	Truncating			
662	CTNNB1	OEC		p.G34V	3,41241108,G,T		0.543	0.616	Missense	medium	Validated	
752	CTNNB1	OEC		p.S33F	3,41241105,C,T		0.243	0.572	Missense	medium	Validated	
782	ARID1A	OEC		p.V2244G	1,26979707,T,G		0.058	0.272	Missense	low		
782	ARID1A	OEC		p.Y215*	1,26896126,C,A		0.438	0.724	Truncating			
782	CTNNB1	OEC		p.T41I	3,41241129,C,T		0.397	0.617	Missense	medium	Validated	
782	PIK3CA	OEC		p.H1047R	3,180434779,A,G		0.491	0.660	Missense	low	Validated	
783	ARID1A	OEC		p.A938S	1,26965378,G,T		0.143	0.464	Missense	low		
783	ARID1A	OEC			26978517	*/-G			Frame_Shift_Del			
783	PIK3CA	OEC		p.R88Q	3,180399570,G,A		0.141	0.481	Missense	medium	Validated	
783	PTEN	OEC		p.R130G	10,89682884,C,G		0.406	0.585	Missense	high		
785	KRAS	OEC		p.G12D	12,25289551,C,T		0.250	0.359	Missense	high	Validated	
785	PIK3CA	OEC		p.E545K	3,180418785,G,A		0.444	0.464	Missense	low	Validated	
864	PIK3CA	OEC		p.E39K	3,180399422,G,A		0.059	0.282	Missense	medium	Not Validated	
864	PIK3CA	OEC		p.L339I	3,180404227,C,A		0.115	0.496	Missense	medium	Validated	
877	CTNNB1	OEC		p.S33A	3,41241104,T,G		0.260	0.768	Missense	medium	Validated	
877	PTEN	OEC		p.R130G	10,89682884,C,G		0.434	0.562	Missense	high	Validated	
921	ARID1A	OEC		p.Q1835*	1,26978479,C,T		0.261	0.818	Truncating			
921	CTNNB1	OEC		p.G34V	3,41241108,G,T		0.234	0.688	Missense	medium	Validated	
921	PIK3CA	OEC		p.H1047R	3,180434779,A,G		0.134	0.770	Missense	low	Validated	
921	PPP2R1A	OEC		p.P179R	19,57407783,C,G		0.153	0.491	Missense	medium	Validated	
921	TP53	OEC		p.R273H	17,7517845,C,T		0.210	0.715	Missense	high	Validated	
949	ARID1A	OEC		p.R1989*	1,26978941,C,T		0.318	0.546	Truncating			
949	ARID1A	OEC		p.Y1389H	1,26973470,T,C		0.370	0.559	Missense	medium		
949	PIK3CA	OEC		p.R88Q	3,180399570,G,A		0.333	0.446	Missense	medium	Validated	
949	PPP2R1A	OEC		p.R183W	19,57407794,C,T		0.381	0.728	Missense	medium	Validated	
949	PTEN	OEC		p.E299*	10,89710724,G,T		0.500	0.621	Truncating			
949	PTEN	OEC		p.F341V	10,89710850,T,G		0.412	0.410	Missense	medium		

ID	Gene	Original diagnosed subtype	Grade	AA variant	Location (hg18)	Indel Genotype	Frequency	Probability	Type	Func. Impact	Sanger Validated	Notes
1019	CTNNB1	OEC		p.H36P	3,41241114,A,C		0.333	0.581	Missense	medium	Validated	
1065	ARID1A	OEC		p.V2244G	1,26979707,T,G		0.072	0.310	Missense	low		
1065	CTNNB1	OEC		p.W383R	3,41249901,T,A		0.286	0.485	Missense	medium		
1065	KRAS	OEC		p.Q61H	12,25271542,T,G		0.895	0.592	Missense	high	Validated	
1170	ARID1A	OEC		p.Q567*	1,26930578,C,T		0.750	0.888	Truncating			
1170	KRAS	OEC		p.G12V	12,25289551,C,A		0.550	0.657	Missense	high	Validated	
1170	PPP2R1A	OEC		p.S256Y	19,57408135,C,A		0.450	0.612	Missense	medium	Validated	
1186	TP53	OEC		p.N239S	17,7518290,T,C		0.758	0.689	Missense	high	Validated	
1214	CTNNB1	OEC		p.S37C	3,41241117,C,G		0.304	0.791	Missense	high	Validated	
1283	CTNNB1	OEC		p.S37F	3,41241117,C,T		0.388	0.478	Missense	high	Validated	
1283	PIK3CA	OEC		p.E545A	3,180418786,A,C		0.310	0.554	Missense	low	Validated	
1283	PTEN	OEC		p.R130G	10,89682884,C,G		0.608	0.570	Missense	high	Validated	
1286	PPP2R1A	OEC		p.R183W	19,57407794,C,T		0.343	0.592	Missense	medium	Validated	
1287	KRAS	OEC		p.G12V	12,25289551,C,A		0.224	0.548	Missense	high	Validated	
605	TP53	OEC		p.S183*	17,7519107,G,C		0.911	0.729	Truncating		Validated	
1328	CTNNB1	OEC	1	p.S37F	3,41241117,C,T				Missense	high	Validated	tested only for CTNNB1
1339	CTNNB1	OEC	1	p.G34R	3,41241107,G,C				Missense	medium	Validated	tested only for CTNNB1
1351	CTNNB1	OEC	2	p.S37F	3,41241117,C,T				Missense	high	Validated	tested only for CTNNB1
1372	CTNNB1	OEC	1	p.S37F	3,41241117,C,T				Missense	high	Validated	tested only for CTNNB1
1440	CTNNB1	OEC	2	no mut							Validated	tested only for CTNNB1
1443	CTNNB1	OEC	1	p.T41I	3,41241129,C,T				Missense	medium	Validated	tested only for CTNNB1
1469	CTNNB1	OEC	2	p.S33C	3,41241105,C,G				Missense	medium	Validated	tested only for CTNNB1
1472	CTNNB1	OEC	1	no mut							Validated	tested only for CTNNB1
1477	CTNNB1	OEC	2	p.G34R	3,41241107,G,C				Missense	medium	Validated	tested only for CTNNB1
1486	CTNNB1	OEC	1	p.S33C	3,41241105,C,G				Missense	medium	Validated	tested only for CTNNB1
1500	CTNNB1	OEC	2	no mut							Validated	tested only for CTNNB1
1578	CTNNB1	OEC	1	no mut							Validated	tested only for CTNNB1

ID	Gene	Original diagnosed subtype	Grade	AA variant	Location (hg18)	Indel Genotype	Frequency	Probability	Type	Func. Impact	Sanger Validated	Notes
1782	CTNNB1	OEC	1	no mut							Validated	tested only for CTNNB1
1905	CTNNB1	OEC	2	no mut							Validated	tested only for CTNNB1
1909	CTNNB1	OEC	2	no mut							Validated	tested only for CTNNB1
1911	CTNNB1	OEC	1	no mut							Validated	tested only for CTNNB1
62	CTNNB1	OEC	1	no mut							Validated	tested only for CTNNB1
1450	CTNNB1	OEC		p.S33C	3,41241105,C,G				Missense	medium	Validated	tested only for CTNNB1
1367	CTNNB1	OEC		no mut							Validated	tested only for CTNNB1
1848	CTNNB1	OEC		no mut							Validated	tested only for CTNNB1

Table C.7 Ovarian endometrioid carcinoma mutation data

All endometrial mutation data can be found in Appendix B Table B.3.

Appendix D Molecular Profiling of Endometrial Carcinosarcomas

D.1 Abstract

Uterine carcinosarcoma is a clinically aggressive uterine malignancy that contains a mix of carcinoma and sarcoma components. We performed targeted next-generation sequencing of 27 uterine cancer and sarcoma genes together with immunohistochemical analyses of selected genes in 30 uterine carcinosarcomas. This included 13 cases where the distinct carcinoma and sarcoma components were sequenced separately and 10 cases where the metastatic tumors were analyzed in addition to the primary tumors. We identified non-synonymous somatic mutations in 90% of the tumours, with 27 of 30 (90%) of all carcinosarcomas harboring *TP53* alterations. The most commonly mutated signaling pathway was the PI3K pathway (67%) with mutations identified in *PIK3CA, PTEN, PIK3R1*, and *PIK3R2*. Mutations in *FBXW7, PPP2R1A, ARID1A* and *KRAS* were also demonstrated in a small subset of cases. In cases where the different histologic components were separately analyzed, most of the mutations identified were present in both the carcinoma and sarcoma components, indicating a common origin for the two components. Furthermore, the same *TP53* alterations and/or PI3K pathway mutations seen in the primary tumors were also identified in the metastatic tumours. Overall, carcinosarcomas exhibited heterogeneous molecular features that resemble the heterogeneity seen in endometrial carcinomas, with some showing endometrioid carcinoma-like and others showing serous carcinoma-like mutation profiles. Our results provide insights into the oncogenesis of uterine carcinosarcoma and identify targetable mutations that represent early oncogenic events. The findings of the different molecular types of uterine carcinosarcoma that parallel the different molecular types in endometrial carcinoma may have future treatment implications with targeted therapies.

D.2 Materials and Methods

Patient Samples

The tumour samples analyzed in this study were acquired from tissue repositories from the VGH archives and the BC Cancer Agency OvCaRe Tumour Biobank. All patients were approached for written informed consent, before undergoing surgery; to donate tissue surplus to

diagnostic requirements plus a blood sample, for use in a research ethics board (REB) approved research protocol. All Formalin fixed paraffin blocks (FFPE) and H&E slides were reviewed by a gyneacological pathologist to determine the carcinoma, sarcoma and metastatic FFPE tumour blocks used for DNA extraction. Germline DNA from buffy coat or FFPE blocks containing non-tumour normal DNA were used to determine somatic status of the tumour mutations.

DNA Extractions

Fixed formalin paraffin FFPE blocks were identified to include the carcinoma, sarcoma, mixed, and normal components, and then separately cored (3-4 cores at 0.6 mm). Each component was extracted for DNA using the Qiagen FFPE kit as per manufacturers protocols. In a total of 15 cases, DNA was isolated from the carcinoma and sarcoma components and sequenced separately. In 15 cases the different components were not easily isolated for separate extractions. In 10 cases the metastatic tumour was also available for sequencing. Flash frozen tumour samples for each case were identified and cryosectioned for DNA extraction using the Gentra Puregene kit. If available, normal DNA from buffy coat was also extracted. All DNA was quantified using the Invitrogen Qubit flurometer using Molecular Probes broad range Qubit quantification kit.

Discovery Targeted Sequencing and Analysis

An Illumina custom Truseq amplicon panel (version 1) was designed using Illumina Design studio software to amplify 175bp libraries. This included 1519 amplicons in 27genes that are important in endometrial cancer [2, 42]: *ABCC9, AKT1, AKT2, AKT3, ARHGAP35 (GRLF1), CCND1, CHD4, CTCF, CSMD3, EP300, FGFR2, KRAS, MAP3K4, MED12, ARID1A, CTNNB1, PTEN, PIK3CA, PIK3R1, PIK3R2, POLE, PPP2R1A, FBXW7, SPOP, TP53, TSPYL2, ZFHX3*. The Illumina Truseq custom library prep was utilized using 250ng of starting DNA for FFPE DNA. The Illumina protocol was followed for library preparation (includes sample PCR and barcoding), however the protocol was modified for pooling and normalization. Before library pooling, libraries were quantified using the Qubit spectrometer, then pooled at equal concentrations. Each library pool was then quantified for amplifiable products using the KAPA Illumina SYBR qPCR quantification kit using the ABI7900 fast real-time instrument. Final libraries were denatured at 10-13nM with spiked-in 1% PhiX V3 library. Each pool was run on

the Illumina MiSeq using 300 cycle version 2 kits. All bam and VCF files were generated using Illumina MiSeq reporter. Analysis was performed using the VCF files generated by the somatic variant caller 3.2.3.0, then filtered based on reads passing filter, non-synonymous, somatic mutations with >5% variant allele frequency. All potential mutations were then manually interrogated and filtered using the Integrated Genome Viewer (IGV).

Mutation Validations

All non-synonymous somatic mutations, (except for *CSMD3*), underwent secondary validation using either Fluidigm 48X48 Access Arrays, then barcoded and sequenced on a MiSeq, or by Sanger sequencing. In brief, primer sets were designed using Primer 3 to amplify the specific mutations, and tagged with CS1 (5'-ACACTGACGACATGGTTCTACA-3') and CS2 (5'-TACGGTAGCAGAGACTTGGTCT-3') sequencing tags. PCR products (150-200bp) were generated using the Fluidigm 48X48 Access Arrays, as per manufacturers protocol, with input of 100ng for FFPE derived DNA, and 50ng for high-quality DNA from buffy coat or frozen tumour DNA. DNA barcodes (10bp) with Illumina cluster-generating adapters were added to the libraries post-Fluidigm harvest as previously described [174], then purified using Agencourt AMpure XP beads (Beckman Coulter), pooled and quantified as described for the TruSeq custom targeted panel discovery sequencing. In total, 96 samples were pooled and sequenced using a MiSeq 300 cycle V2 kit on the Illumina MiSeq for ultra-deep validations. Analysis was performed as described for discovery targeted panel sequencing. Sanger sequencing was performed if the amplicon of interest failed sequencing in the MiSeq run. This was performed and analyzed as previously described [1], however CS1 and CS2 primers were used as a universal sequencing primers on the ABI 3130xl (Applied Biosystems).

D.3 **Carcinosarcoma Mutation Profiles Figure**

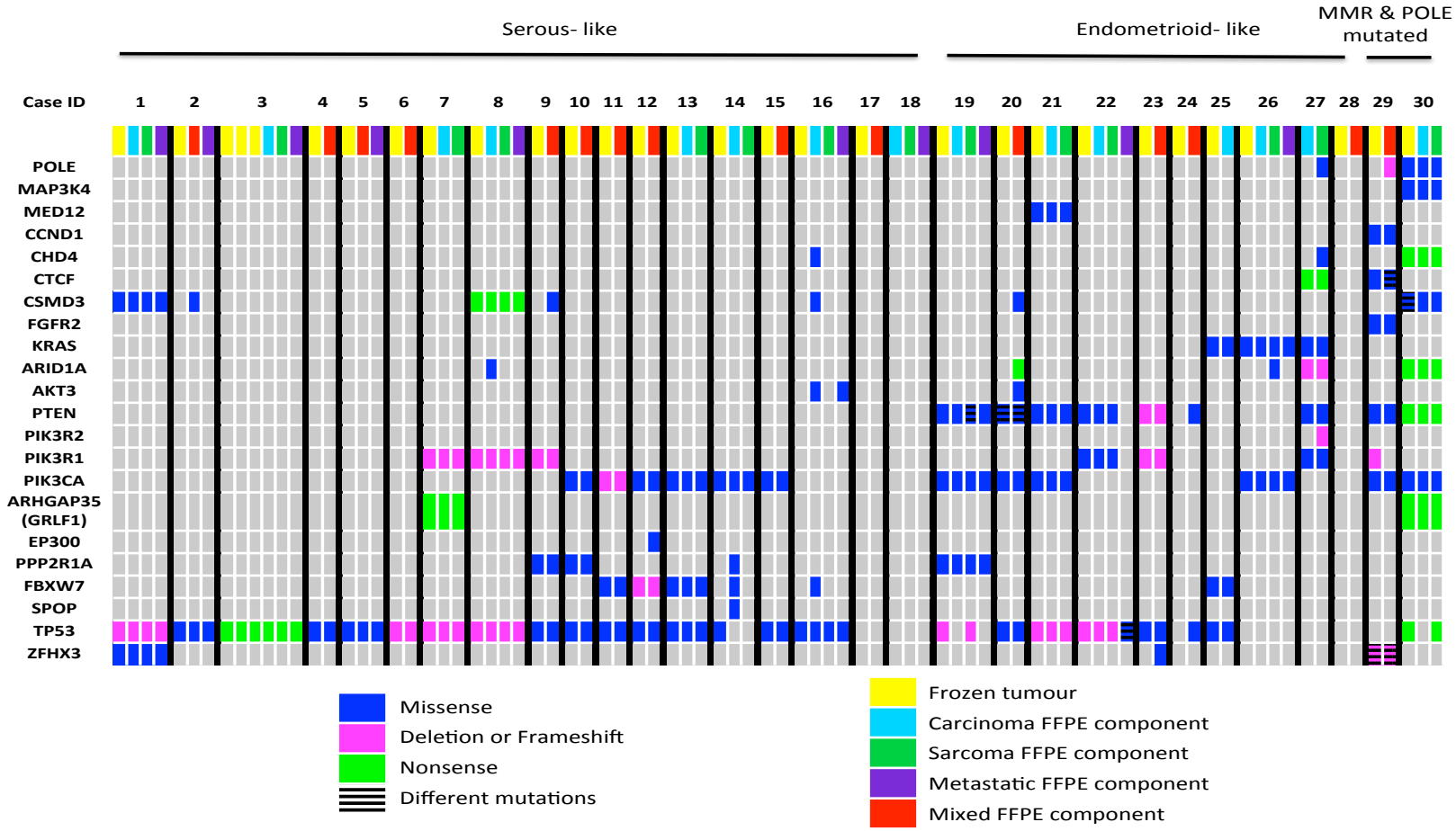

Figure D.4 Uterine carcinosarcoma mutation profiles
The columns separated by black bars indicate a tumour group from one patient. The rows indicate genes that were sequenced with coloured boxes indicating a somatic mutation present, and grey boxes indicate no mutation was identified. The cases 1-18 show a serous-like mutation profile, cases 19-28 show an endometrioid-like mutation profile, and cases 29 and 30 are MMR and POLE mutated cases respectively.

Appendix E *POLE* Mutations in Endometrial Carcinomas

E.1 Materials and Methods

Patient Samples

Patient samples were identified from five endometrial tumour tissue microarrays (TMA) (n=440). The tumour samples analyzed in this study were acquired from tissue repositories from the VGH archives and the BC Cancer Agency OvCaRe Tumour Biobank. All patients were approached for written informed consent, before undergoing surgery, to donate tissue surplus to diagnostic requirements plus a blood sample, for use in a research ethics board (REB) approved research protocol. DNA was extracted from available flash frozen tumours or formalin fixed paraffin embedded (FFPE) tumour blocks. If both FFPE and flash frozen tumours were available for the case, then DNA was extracted from the flash frozen tumours. To determine somatic status, the normal DNA was either extracted from available buffy coat or representative normal FFPE blocks.

DNA extractions

DNA from fresh frozen tumours and DNA from buffy coat were extracted with the Qiagen Gentra Puregene kit (Qiagen) as per manufacturers protocols. The FFPE tumours and normal were extracted using the Qiagen FFPE kit as per manufacturers protocols. All DNA was quantified using the Qubit fluorometer kit (Life Technologies).

Targeted Sequencing and Analysis

Targeted primers were designed to cover the *POLE* exonuclease domains exons 9-14, and synthesized by IDT Technologies. All primers were tested and re-synthesized if no amplification product was present. In brief, primer sets were designed using Primer 3 to amplify the specific gene regions, and tagged with CS1 (5'-ACACTGACGACATGGTTCTACA-3') and CS2 (5'-TACGGTAGCAGAGACTTGGTCT-3') sequencing tags. PCR products (150-200bp) were amplified using the Fluidigm 48X48 Access Arrays, as per manufacturers protocol, with input of 100ng for FFPE derived DNA, and 50ng for high-quality DNA from buffy coat or frozen tumour DNA. DNA barcodes (10bp) with Illumina cluster-generating adapters were added to the libraries post-Fluidigm harvest as previously described [174], and cleaned-up using Agencourt

AMpure XP beads (Beckman Coulter). Barcoded PCR product pools were then quantified using the high sensitivity DNA assay and Qubit fluorometer (Life Technologies) and pooled to one total library by normalizing to equal amounts of PCR product. In total, 96 samples were pooled, denatured according to Illumina standard protocols, and sequenced using a MiSeq 300 cycle V2 kit on the Illumina MiSeq for ultra-deep validations. Uni-directional barcode sequencing was performed. All bam and VCF files were generated using Illumina MiSeq reporter. Analysis was performed using the VCF files generated by the somatic variant caller 3.2.3.0, then filtered based on reads passing filter, non-synonymous, and >5% variant allele frequency. All potential mutations were then manually interrogated and filtered using the Integrated Genome Viewer (IGV). For validations, repeat Fluidigm-MiSeq sequencing was performed along with select Sanger sequencing, however CS1 and CS2 primers were used as a universal sequencing primers on the ABI 3130xl Genetic Analyzer (Applied Biosystems) and analyzed as previously described [1]. Normal DNA was also sequenced to check somatic status. All validated tumour *POLE* mutations were bi-directionally sequenced twice at minimum, and once in the normal to validate somatic or germline status.

E.2 **Results**

Histology	Grade	POLE mutated	POLE wild-type
Endometrioid	1	7 (18%)	117
	2	6 (15%)	62
	3	19 (49%)	104
Serous		3 (8%)	77
Clear Cell		1 (3%)	0
Undifferentiated		1 (3%)	0
Mixed carcinomas		2 (5%)	7
Total 406 tumours		39 (9.6%)	367

Table E.8 The histology distribution of *POLE* mutated endometrial carcinoma
The percentage indicated in the *POLE* mutated column indicates the percent of each histology with respect to the total *POLE* mutated cases.

Appendix F PPP2R1A-IP Mass Spectrometry Peptide Identifications

Protein Name	Protein ID	Sequence	Parental Pool 1	Parental Pool 2	Parental Pool 3	Mutant Pool 1	Mutant Pool2	Mutant Pool 3	Het Pool 1	Het Pool 2	Het Pool 3	IgG Ctl Pool 1	IgG Ctl Pool 2	IgG Ctl Pool 3
PPP2R1A	P30153	aAASHk			6.38E+03			5.41E+03			8.02E+03			
PPP2R1A	P30153	aAASHk			1.31E+04			1.67E+04			3.53E+04			1.29E+04
PPP2R1A	P30153	aAASHk			1.44E+04			1.79E+04			8.90E+03			
PPP2R1A	P30153	aAASHk			1.71E+04			1.63E+04			2.51E+04			8.24E+03
PPP2R1A	P30153	aAASHk			2.77E+04			2.94E+04			5.36E+04			1.48E+03
PPP2R1A	P30153	aAASHk		4.56E+04			3.33E+04			1.82E+04			9.83E+02	
PPP2R1A	P30153	aAASHk		4.65E+04			2.75E+04			1.92E+04			7.51E+03	
PPP2R1A	P30153	aAASHk	5.59E+03			6.09E+03			7.26E+03			1.30E+03		
PPP2R1A	P30153	aAASHk	2.13E+04			3.20E+04			2.24E+04			7.35E+03		
PPP2R1A	P30153	aAASHk	2.63E+04			2.73E+04			2.83E+04			9.63E+02		
PPP2R1A	P30153	aAASHk	3.18E+04			2.51E+04			3.09E+04					
PPP2R1A	P30153	aAASHk	3.98E+04			1.58E+04			2.12E+04			1.00E+03		
PPP2R1A	P30153	aAASHk	1.46E+05			1.03E+05			1.03E+05			4.14E+03		
PPP2R1A	P30153	aAASHk	2.24E+05			1.68E+05			1.67E+05			5.64E+03		
PPP2R1A	P30153	aAASHk			4.72E+04			3.90E+04			5.84E+04			1.08E+03
PPP2R1A	P30153	aAASHk			8.12E+04			6.86E+04			1.30E+05			1.84E+04
PPP2R1A	P30153	aAASHk		2.81E+04			2.05E+04			1.47E+04				
PPP2R1A	P30153	aAASHk		6.18E+04			4.46E+04			1.29E+04			1.11E+03	
PPP2R1A	P30153	aAASHk		9.64E+04			6.15E+04			3.81E+04			9.78E+03	
PPP2R1A	P30153	aVESLR		8.45E+05			6.20E+05			1.67E+05			9.77E+04	
PPP2R1A	P30153	aVESLR	1.88E+06			8.56E+05			1.34E+06			5.64E+04		
PPP2R1A	P30153	aVGPEITk			4.36E+05			5.26E+05			2.37E+05			8.89E+04
PPP2R1A	P30153	aVGPEITk			1.04E+06			8.60E+05			1.30E+06			1.37E+04
PPP2R1A	P30153	aVGPEITk		5.21E+05			3.38E+05			2.00E+05			2.31E+04	
PPP2R1A	P30153	aVGPEITk	2.60E+06			1.55E+06			1.34E+06			3.71E+04		
PPP2R1A	P30153	aVGPEITk			1.75E+05			1.18E+05			1.56E+05			1.66E+04
PPP2R1A	P30153	aVGPEITk			3.49E+05			2.32E+05			2.77E+05			1.15E+04
PPP2R1A	P30153	aVGPEITk		3.95E+05			2.47E+05			6.28E+04			1.47E+04	
PPP2R1A	P30153	aVGPEITk	3.72E+05			2.15E+05			2.52E+05			6.50E+03		
PPP2R1A	P30153	aVGPEITk	4.73E+05			1.79E+05			2.26E+05			9.43E+03		
PPP2R1A	P30153	dcEAEVR			1.31E+03			8.47E+02						

Protein Name	Protein ID	Sequence	Parental Pool 1	Parental Pool 2	Parental Pool 3	Mutant Pool 1	Mutant Pool2	Mutant Pool 3	Het Pool 1	Het Pool 2	Het Pool 3	IgG Ctl Pool 1	IgG Ctl Pool 2	IgG Ctl Pool 3
PPP2R1A	P30153	dcEAEVR			2.87E+04			2.60E+04			2.78E+04			1.15E+03
PPP2R1A	P30153	dcEAEVR			6.45E+04			1.13E+05			1.35E+05			3.52E+04
PPP2R1A	P30153	dcEAEVR			8.81E+04			8.89E+04			1.98E+05			3.81E+04
PPP2R1A	P30153	dcEAEVR			9.48E+04			9.74E+04			1.27E+05			2.40E+04
PPP2R1A	P30153	dcEAEVR			1.13E+05			9.53E+04			1.61E+05			6.18E+03
PPP2R1A	P30153	dcEAEVR			1.33E+05			1.08E+05			1.83E+05			1.09E+04
PPP2R1A	P30153	dcEAEVR			1.51E+05			1.40E+05			1.97E+05			5.83E+03
PPP2R1A	P30153	dcEAEVR			1.58E+05			1.64E+05			3.23E+05			4.03E+04
PPP2R1A	P30153	dcEAEVR			2.07E+05			1.92E+05			2.92E+05			3.53E+04
PPP2R1A	P30153	dcEAEVR			2.40E+05			1.99E+05			3.21E+05			1.82E+04
PPP2R1A	P30153	dcEAEVR		3.70E+04			2.38E+04			1.64E+04			5.93E+03	
PPP2R1A	P30153	dcEAEVR		1.71E+05			1.09E+05			5.74E+04			1.75E+04	
PPP2R1A	P30153	dcEAEVR		4.40E+05			2.40E+05			8.26E+04			1.62E+04	
PPP2R1A	P30153	dcEAEVR		7.20E+05			3.39E+05			2.20E+05			4.59E+04	
PPP2R1A	P30153	dcEAEVR		8.29E+05			4.42E+05			2.38E+05			5.81E+04	
PPP2R1A	P30153	dcEAEVR	9.01E+03			1.57E+04			8.16E+03			1.88E+03		
PPP2R1A	P30153	dcEAEVR	1.74E+04			2.01E+04			1.20E+04			1.89E+03		
PPP2R1A	P30153	dcEAEVR	3.16E+04			4.69E+04			1.82E+04			9.13E+03		
PPP2R1A	P30153	dcEAEVR	3.97E+04			2.88E+04			3.13E+04			2.16E+03		
PPP2R1A	P30153	dcEAEVR	4.05E+04			5.72E+04			3.99E+04			5.79E+03		
PPP2R1A	P30153	dcEAEVR	6.83E+04			2.13E+05			6.68E+04			5.73E+04		
PPP2R1A	P30153	dcEAEVR	7.76E+04			2.03E+05			6.52E+04			4.33E+04		
PPP2R1A	P30153	dcEAEVR	1.21E+05			1.24E+05			8.58E+04			6.33E+04		
PPP2R1A	P30153	dcEAEVR	2.29E+05			1.57E+05			1.34E+05			5.35E+03		
PPP2R1A	P30153	dcEAEVR	2.61E+05			1.92E+05			1.51E+05			8.32E+03		
PPP2R1A	P30153	dcEAEVR	2.82E+05			1.13E+05			1.67E+05			5.67E+03		
PPP2R1A	P30153	dcEAEVR			3.22E+04			2.24E+04			2.81E+04			
PPP2R1A	P30153	dcEAEVR			2.00E+05			2.45E+05			1.12E+05			7.85E+03
PPP2R1A	P30153	dcEAEVR			2.45E+05			1.92E+05			3.34E+05			1.19E+04
PPP2R1A	P30153	dcEAEVR			4.07E+05			2.69E+05			3.51E+05			5.19E+03
PPP2R1A	P30153	dcEAEVR			5.41E+05			4.87E+05			8.11E+05			3.36E+04
PPP2R1A	P30153	dcEAEVR		8.47E+04			5.60E+04			3.63E+04			4.91E+03	
PPP2R1A	P30153	dcEAEVR		1.25E+05			7.97E+04			5.85E+04			3.87E+04	

Protein Name	Protein ID	Sequence	Parental Pool 1	Parental Pool 2	Parental Pool 3	Mutant Pool 1	Mutant Pool2	Mutant Pool 3	Het Pool 1	Het Pool 2	Het Pool 3	IgG Ctl Pool 1	IgG Ctl Pool 2	IgG Ctl Pool 3
PPP2R1A	P30153	dcEAEVR		1.32E+05			8.03E+04			6.17E+04			3.06E+04	
PPP2R1A	P30153	dcEAEVR		1.36E+05			1.06E+05			6.05E+04			3.09E+04	
PPP2R1A	P30153	dcEAEVR		2.04E+05			1.12E+05			6.82E+04			1.75E+04	
PPP2R1A	P30153	dcEAEVR		2.23E+05			1.21E+05			7.54E+04			6.61E+03	
PPP2R1A	P30153	dcEAEVR		2.88E+05			1.98E+05			9.96E+04			1.09E+04	
PPP2R1A	P30153	dcEAEVR		2.96E+05			1.50E+05			9.78E+04			2.86E+04	
PPP2R1A	P30153	dcEAEVR		4.48E+05			2.45E+05			7.72E+04			1.58E+04	
PPP2R1A	P30153	dcEAEVR	6.54E+04			4.67E+04			5.67E+04			1.23E+03		
PPP2R1A	P30153	dcEAEVR	1.40E+05			8.87E+04			1.04E+05			1.78E+03		
PPP2R1A	P30153	dcEAEVR	1.71E+05			1.28E+05			1.27E+05			7.73E+03		
PPP2R1A	P30153	dcEAEVR	1.79E+05			1.12E+05			1.38E+05			1.61E+03		
PPP2R1A	P30153	dcEAEVR	2.52E+05			1.67E+05			2.03E+05			3.46E+03		
PPP2R1A	P30153	dcEAEVR	1.09E+06			7.07E+05			6.41E+05			1.73E+04		
PPP2R1A	P30153	dEcPEVR			6.55E+04			4.35E+04			6.78E+04			1.10E+03
PPP2R1A	P30153	dEcPEVR			1.13E+05			1.09E+05			1.30E+05			4.36E+04
PPP2R1A	P30153	dEcPEVR		9.18E+04			1.17E+05			8.69E+04			5.91E+04	
PPP2R1A	P30153	dEcPEVR		2.05E+05			1.30E+05			9.87E+04			4.17E+04	
PPP2R1A	P30153	dEcPEVR	4.13E+03			9.96E+03			5.54E+03			1.50E+03		
PPP2R1A	P30153	dEcPEVR	7.66E+03			1.11E+04			9.37E+03			5.54E+03		
PPP2R1A	P30153	dEcPEVR	1.89E+04			3.70E+04			1.66E+04			1.14E+04		
PPP2R1A	P30153	dEcPEVR	2.25E+04			6.02E+04			2.80E+04			1.32E+04		
PPP2R1A	P30153	dEcPEVR	3.48E+04			9.61E+04			4.27E+04			1.62E+04		
PPP2R1A	P30153	dEcPEVR	3.88E+04			9.59E+04			4.29E+04			2.24E+04		
PPP2R1A	P30153	dEcPEVR	8.16E+04			9.74E+04			1.08E+05			1.52E+04		
PPP2R1A	P30153	dEcPEVR	8.31E+04			9.98E+04			6.26E+04			1.16E+04		
PPP2R1A	P30153	dEcPEVR	1.08E+05			1.16E+05			7.78E+04			1.95E+04		
PPP2R1A	P30153	dEcPEVR	1.08E+05			1.45E+05			9.44E+04			4.48E+04		
PPP2R1A	P30153	dEcPEVR			8.80E+04			8.37E+04			1.14E+05			1.72E+04
PPP2R1A	P30153	dEcPEVR			1.03E+05			1.16E+05			1.46E+05			6.97E+03
PPP2R1A	P30153	dEcPEVR			1.23E+05			1.32E+05			1.66E+05			9.00E+03
PPP2R1A	P30153	dEcPEVR			1.29E+05			1.28E+05			5.83E+04			5.64E+03
PPP2R1A	P30153	dEcPEVR			1.38E+05			1.21E+05			1.88E+05			4.15E+03
PPP2R1A	P30153	dEcPEVR			1.66E+05			1.15E+05			1.51E+05			1.70E+03

Protein Name	Protein ID	Sequence	Parental Pool 1	Parental Pool 2	Parental Pool 3	Mutant Pool 1	Mutant Pool2	Mutant Pool 3	Het Pool 1	Het Pool 2	Het Pool 3	IgG Ctl Pool 1	IgG Ctl Pool 2	IgG Ctl Pool 3
PPP2R1A	P30153	dEcPEVR			1.78E+05			1.57E+05			2.60E+05			1.38E+04
PPP2R1A	P30153	dEcPEVR		4.50E+04			3.49E+04			3.59E+04			2.38E+04	
PPP2R1A	P30153	dEcPEVR		1.01E+05			7.40E+04			4.82E+04			4.85E+03	
PPP2R1A	P30153	dEcPEVR		1.74E+05			1.22E+05			7.78E+04			9.64E+03	
PPP2R1A	P30153	dEcPEVR		2.63E+05			1.31E+05			7.19E+04			1.42E+04	
PPP2R1A	P30153	dEcPEVR		3.24E+05			1.76E+05			4.22E+04			9.35E+03	
PPP2R1A	P30153	dEcPEVR		1.03E+06			4.49E+05			3.15E+05			5.34E+04	
PPP2R1A	P30153	dEcPEVR	5.39E+03			2.46E+04			1.16E+04			4.64E+03		
PPP2R1A	P30153	dEcPEVR	1.28E+04			1.29E+04			8.79E+03			3.97E+03		
PPP2R1A	P30153	dEcPEVR	1.62E+04			5.00E+04			2.17E+04			1.36E+04		
PPP2R1A	P30153	dEcPEVR	4.09E+04			4.71E+04			3.05E+04			4.65E+03		
PPP2R1A	P30153	dEcPEVR	4.26E+04			1.34E+05			5.50E+04			2.57E+04		
PPP2R1A	P30153	dEcPEVR	6.89E+04			6.95E+04			5.13E+04			8.57E+03		
PPP2R1A	P30153	dEcPEVR	7.00E+04			6.63E+04			7.74E+04			2.21E+03		
PPP2R1A	P30153	dEcPEVR	7.50E+04			8.80E+04			8.70E+04			8.16E+03		
PPP2R1A	P30153	dEcPEVR	2.34E+05			1.03E+05			1.05E+05			3.15E+03		
PPP2R1A	P30153	dNTIEHLLPLFLA QLk			1.05E+03			3.45E+03			3.85E+03			8.82E+02
PPP2R1A	P30153	dNTIEHLLPLFLA QLk			7.27E+03			7.78E+03			9.07E+03			2.31E+03
PPP2R1A	P30153	dNTIEHLLPLFLA QLk			1.64E+03			2.45E+03			2.15E+03			
PPP2R1A	P30153	dNTIEHLLPLFLA QLk			2.09E+03			4.42E+03			4.95E+03			1.35E+03
PPP2R1A	P30153	dNTIEHLLPLFLA QLk			4.54E+03			1.16E+04			7.46E+03			
PPP2R1A	P30153	dNTIEHLLPLFLA QLk			5.90E+03			1.97E+04			1.07E+04			
PPP2R1A	P30153	dNTIEHLLPLFLA QLk			7.35E+03			1.04E+04			1.92E+04			2.22E+03
PPP2R1A	P30153	dNTIEHLLPLFLA QLk			1.93E+04			2.84E+04			4.68E+04			3.81E+03
PPP2R1A	P30153	dNTIEHLLPLFLA QLk		5.47E+03			3.88E+03			4.12E+03			1.27E+03	
PPP2R1A	P30153	dNTIEHLLPLFLA QLk		3.07E+04			3.37E+04			7.24E+03			2.02E+03	
PPP2R1A	P30153	dNTIEHLLPLFLA QLk		6.73E+04			3.47E+04			2.25E+04			2.07E+03	
PPP2R1A	P30153	dNTIEHLLPLFLA QLk		9.09E+04			4.70E+04			2.88E+04			5.24E+03	

Protein Name	Protein ID	Sequence	Parental Pool 1	Parental Pool 2	Parental Pool 3	Mutant Pool 1	Mutant Pool2	Mutant Pool 3	Het Pool 1	Het Pool 2	Het Pool 3	IgG Ctl Pool 1	IgG Ctl Pool 2	IgG Ctl Pool 3
PPP2R1A	P30153	dNTIEHLLPLFLAQLk	1.98E+03			1.89E+03			1.64E+03					
PPP2R1A	P30153	dNTIEHLLPLFLAQLk	1.00E+04			1.14E+04			1.15E+04					
PPP2R1A	P30153	dNTIEHLLPLFLAQLk	3.47E+04			3.12E+04			2.75E+04					
PPP2R1A	P30153	dNTIEHLLPLFLAQLk	4.50E+04			3.25E+04			3.12E+04			9.41E+02		
PPP2R1A	P30153	eAATSNLk		7.12E+05			3.35E+05			2.32E+05			3.47E+04	
PPP2R1A	P30153	eAATSNLk	3.27E+05			2.71E+05			2.97E+05			8.16E+03		
PPP2R1A	P30153	eAATSNLk	3.58E+05			1.49E+05			1.83E+05			1.14E+04		
PPP2R1A	P30153	eAATSNLk			6.02E+04			4.50E+04			8.03E+04			5.65E+03
PPP2R1A	P30153	eAATSNLk			6.02E+04			6.66E+04			2.91E+04			9.75E+03
PPP2R1A	P30153	eAATSNLk			1.71E+05			1.75E+05			7.73E+04			1.34E+04
PPP2R1A	P30153	eAATSNLk			1.97E+05			1.87E+05			3.32E+05			1.14E+04
PPP2R1A	P30153	eAATSNLk			2.99E+05			2.09E+05			3.25E+05			6.48E+03
PPP2R1A	P30153	eAATSNLk			4.73E+05			4.12E+05			7.39E+05			6.14E+03
PPP2R1A	P30153	eAATSNLk			4.75E+05			4.23E+05			7.66E+05			2.58E+04
PPP2R1A	P30153	eAATSNLk			5.62E+05			5.10E+05			9.57E+05			2.65E+04
PPP2R1A	P30153	eAATSNLk		1.09E+05			7.39E+04			4.59E+04			7.69E+03	
PPP2R1A	P30153	eAATSNLk		2.23E+05			1.63E+05			1.17E+05			2.86E+04	
PPP2R1A	P30153	eAATSNLk		2.26E+05			1.66E+05			1.23E+05			1.31E+04	
PPP2R1A	P30153	eAATSNLk		3.20E+05			1.80E+05			4.46E+04			1.64E+04	
PPP2R1A	P30153	eAATSNLk		3.71E+05			1.84E+05			1.34E+05			2.40E+04	
PPP2R1A	P30153	eAATSNLk		5.91E+05			3.97E+05			2.79E+05			2.84E+04	
PPP2R1A	P30153	eAATSNLk		7.08E+05			3.44E+05			2.59E+05			3.86E+04	
PPP2R1A	P30153	eAATSNLk		7.62E+05			3.80E+05			2.89E+05			4.29E+04	
PPP2R1A	P30153	eAATSNLk	1.55E+04			3.61E+04			3.88E+04			5.44E+03		
PPP2R1A	P30153	eAATSNLk	1.14E+05			9.31E+04			9.38E+04			5.53E+03		
PPP2R1A	P30153	eAATSNLk	1.34E+05			1.04E+05			1.12E+05			1.76E+03		
PPP2R1A	P30153	eAATSNLk	1.57E+05			1.59E+05			1.98E+05			8.05E+03		
PPP2R1A	P30153	eAATSNLk	4.47E+05			3.62E+05			5.50E+05					
PPP2R1A	P30153	eAATSNLk	4.90E+05			1.98E+05			2.50E+05			9.62E+03		
PPP2R1A	P30153	eAATSNLk	8.25E+05			7.05E+05			7.66E+05			2.13E+04		
PPP2R1A	P30153	eAATSNLk	1.36E+06			1.09E+06			1.24E+06			2.44E+04		
PPP2R1A	P30153	eAATSNLkk			1.67E+04			1.48E+04			2.92E+04			7.37E+03

Protein Name	Protein ID	Sequence	Parental Pool 1	Parental Pool 2	Parental Pool 3	Mutant Pool 1	Mutant Pool2	Mutant Pool 3	Het Pool 1	Het Pool 2	Het Pool 3	IgG Ctl Pool 1	IgG Ctl Pool 2	IgG Ctl Pool 3
PPP2R1A	P30153	eAATSNLkk		9.90E+03			1.28E+04			5.58E+03			2.07E+03	
PPP2R1A	P30153	eAATSNLkk		1.20E+04			2.67E+04			1.62E+04			1.53E+04	
PPP2R1A	P30153	eAATSNLkk	3.96E+03			2.75E+04			1.28E+04			5.54E+03		
PPP2R1A	P30153	eAATSNLkk			4.67E+04			3.86E+04			1.12E+05			
PPP2R1A	P30153	eAATSNLkk		4.94E+04			3.87E+04			2.01E+04			1.15E+04	
PPP2R1A	P30153	eAATSNLkk		2.13E+05			2.44E+05			1.40E+05			1.18E+05	
PPP2R1A	P30153	eAATSNLkk	4.88E+04			1.34E+05			5.28E+04			1.31E+04		
PPP2R1A	P30153	eAATSNLkk	5.97E+04			2.32E+05			7.68E+04			3.20E+04		
PPP2R1A	P30153	eFcENLSADcR			9.60E+02			9.34E+02						
PPP2R1A	P30153	eFcENLSADcR			1.63E+05			1.62E+05			3.53E+05			1.81E+04
PPP2R1A	P30153	eFcENLSADcR	1.64E+04			1.57E+04			1.70E+04			2.00E+03		
PPP2R1A	P30153	eFcENLSADcR	2.87E+05			2.02E+05			1.74E+05			5.64E+03		
PPP2R1A	P30153	eFcENLSADcR			9.46E+02						7.63E+02			
PPP2R1A	P30153	eFcENLSADcR			4.38E+03			3.68E+03			8.45E+03			
PPP2R1A	P30153	eFcENLSADcR			6.37E+03			4.97E+03			2.32E+03			1.04E+03
PPP2R1A	P30153	eFcENLSADcR			2.18E+04			1.44E+04			1.88E+04			
PPP2R1A	P30153	eFcENLSADcR			3.08E+04			2.66E+04			6.20E+04			4.07E+03
PPP2R1A	P30153	eFcENLSADcR			3.46E+04			1.90E+04			1.36E+04			
PPP2R1A	P30153	eFcENLSADcR			3.97E+04			5.47E+04			9.02E+04			1.69E+04
PPP2R1A	P30153	eFcENLSADcR			5.12E+04			5.77E+04			2.90E+04			1.08E+03
PPP2R1A	P30153	eFcENLSADcR			6.18E+04			1.17E+05			1.44E+05			2.40E+04
PPP2R1A	P30153	eFcENLSADcR			6.52E+04			8.80E+04			1.88E+05			1.88E+04
PPP2R1A	P30153	eFcENLSADcR			9.65E+04			8.68E+04			1.40E+05			5.59E+03
PPP2R1A	P30153	eFcENLSADcR			4.42E+05			3.82E+05			7.05E+05			1.36E+04
PPP2R1A	P30153	eFcENLSADcR			4.55E+05			3.86E+05			6.46E+05			7.78E+03
PPP2R1A	P30153	eFcENLSADcR		5.19E+03			1.96E+03			1.44E+03				
PPP2R1A	P30153	eFcENLSADcR		1.24E+04			7.86E+03			4.38E+03				
PPP2R1A	P30153	eFcENLSADcR		1.91E+04			1.54E+04			8.37E+03			5.18E+03	
PPP2R1A	P30153	eFcENLSADcR		6.28E+04			3.49E+04			2.74E+04			4.21E+03	
PPP2R1A	P30153	eFcENLSADcR		7.55E+04			4.47E+04			2.77E+04			6.53E+03	
PPP2R1A	P30153	eFcENLSADcR		8.93E+04			4.49E+04			2.71E+04			5.72E+03	
PPP2R1A	P30153	eFcENLSADcR		1.01E+05			7.04E+04			4.21E+04			1.58E+04	
PPP2R1A	P30153	eFcENLSADcR		1.79E+05			8.43E+04			5.09E+04			4.83E+03	

Protein Name	Protein ID	Sequence	Parental Pool 1	Parental Pool 2	Parental Pool 3	Mutant Pool 1	Mutant Pool2	Mutant Pool 3	Het Pool 1	Het Pool 2	Het Pool 3	IgG Ctl Pool 1	IgG Ctl Pool 2	IgG Ctl Pool 3
PPP2R1A	P30153	eFcENLSADcR		1.96E+05			1.17E+05			7.79E+04			6.43E+03	
PPP2R1A	P30153	eFcENLSADcR		2.03E+05			1.19E+05			3.44E+04			7.05E+03	
PPP2R1A	P30153	eFcENLSADcR		2.43E+05			1.81E+05			1.14E+05			2.51E+04	
PPP2R1A	P30153	eFcENLSADcR		2.55E+05			1.19E+05			7.06E+04			8.74E+03	
PPP2R1A	P30153	eFcENLSADcR	2.12E+04			1.59E+04			1.76E+04			8.59E+02		
PPP2R1A	P30153	eFcENLSADcR	3.04E+04			2.79E+04			2.32E+04					
PPP2R1A	P30153	eFcENLSADcR	1.25E+05			9.51E+04			7.25E+04			1.27E+03		
PPP2R1A	P30153	eFcENLSADcR	1.51E+05			9.82E+04			1.20E+05			1.23E+03		
PPP2R1A	P30153	eFcENLSADcR	1.53E+05			1.01E+05			8.81E+04			2.36E+03		
PPP2R1A	P30153	eFcENLSADcR	1.62E+05			1.11E+05			9.62E+04			1.65E+03		
PPP2R1A	P30153	eFcENLSADcR	1.78E+05			1.22E+05			9.76E+04			1.41E+03		
PPP2R1A	P30153	eFcENLSADcR	1.79E+05			3.05E+05			1.66E+05			8.44E+03		
PPP2R1A	P30153	eFcENLSADcR	2.02E+05			1.42E+05			1.17E+05					
PPP2R1A	P30153	eFcENLSADcR	2.14E+05			7.37E+04			1.16E+05					
PPP2R1A	P30153	eFcENLSADcR	2.17E+05			1.54E+05			1.73E+05			7.42E+03		
PPP2R1A	P30153	eLVSDANQHVk		6.21E+05			3.68E+05			2.33E+05			2.18E+04	
PPP2R1A	P30153	eLVSDANQHVk			9.09E+03			1.15E+04			7.18E+03			1.50E+03
PPP2R1A	P30153	eLVSDANQHVk			1.44E+04			1.10E+04			1.25E+04			
PPP2R1A	P30153	eLVSDANQHVk			1.64E+04			9.62E+03			8.85E+03			
PPP2R1A	P30153	eLVSDANQHVk			2.38E+04			2.26E+04			2.65E+04			
PPP2R1A	P30153	eLVSDANQHVk			1.07E+05			8.90E+04			1.34E+05			4.50E+03
PPP2R1A	P30153	eLVSDANQHVk			1.25E+05			9.64E+04			1.65E+05			6.94E+03
PPP2R1A	P30153	eLVSDANQHVk			1.43E+05			1.06E+05			1.83E+05			
PPP2R1A	P30153	eLVSDANQHVk			2.18E+05			1.76E+05			3.32E+05			5.06E+04
PPP2R1A	P30153	eLVSDANQHVk			2.40E+05			1.78E+05			3.04E+05			1.31E+03
PPP2R1A	P30153	eLVSDANQHVk			5.24E+05			4.62E+05			6.41E+05			8.98E+03
PPP2R1A	P30153	eLVSDANQHVk			6.79E+05			5.21E+05			9.03E+05			
PPP2R1A	P30153	eLVSDANQHVk		7.94E+04			5.12E+04			3.24E+04			7.48E+03	
PPP2R1A	P30153	eLVSDANQHVk		9.40E+04			5.87E+04			3.84E+04			5.83E+03	
PPP2R1A	P30153	eLVSDANQHVk		1.13E+05			3.88E+04			2.49E+04			1.33E+03	
PPP2R1A	P30153	eLVSDANQHVk		1.70E+05			1.68E+05			1.47E+05			8.26E+04	
PPP2R1A	P30153	eLVSDANQHVk		2.24E+05			1.11E+05			6.85E+04			2.39E+04	
PPP2R1A	P30153	eLVSDANQHVk		2.77E+05			1.63E+05			1.06E+05			4.11E+04	

Protein Name	Protein ID	Sequence	Parental Pool 1	Parental Pool 2	Parental Pool 3	Mutant Pool 1	Mutant Pool2	Mutant Pool 3	Het Pool 1	Het Pool 2	Het Pool 3	IgG Ctl Pool 1	IgG Ctl Pool 2	IgG Ctl Pool 3
PPP2R1A	P30153	eLVSDANQHVk		4.02E+05			2.36E+05			1.44E+05			1.20E+04	
PPP2R1A	P30153	eLVSDANQHVk		4.96E+05			2.17E+05			1.34E+05			1.54E+04	
PPP2R1A	P30153	eLVSDANQHVk		1.52E+06			8.98E+05			5.69E+05			4.47E+04	
PPP2R1A	P30153	eLVSDANQHVk	1.23E+04			9.62E+03			1.04E+04			1.08E+03		
PPP2R1A	P30153	eLVSDANQHVk	3.70E+04			2.20E+04			2.67E+04					
PPP2R1A	P30153	eLVSDANQHVk	4.83E+04			5.10E+04			5.00E+04			3.14E+03		
PPP2R1A	P30153	eLVSDANQHVk	7.48E+04			4.66E+04			6.11E+04					
PPP2R1A	P30153	eLVSDANQHVk	1.28E+05			1.34E+05			1.08E+05			1.20E+04		
PPP2R1A	P30153	eLVSDANQHVk	1.52E+05			1.32E+05			1.15E+05			8.87E+03		
PPP2R1A	P30153	eLVSDANQHVk	2.31E+05			1.65E+05			1.92E+05			1.32E+04		
PPP2R1A	P30153	eLVSDANQHVk	3.22E+05			2.14E+05			2.10E+05			5.38E+03		
PPP2R1A	P30153	eLVSDANQHVk	3.33E+05			2.70E+05			3.03E+05			4.10E+04		
PPP2R1A	P30153	eLVSDANQHVk	4.37E+05			1.85E+05			3.15E+05			7.68E+03		
PPP2R1A	P30153	eLVSDANQHVk	4.54E+05			2.88E+05			4.02E+05			6.96E+03		
PPP2R1A	P30153	eLVSDANQHVk	4.93E+05			2.90E+05			4.06E+05			5.65E+03		
PPP2R1A	P30153	eLVSDANQHVk	4.98E+05			3.67E+05			3.49E+05			1.14E+04		
PPP2R1A	P30153	eNVIMSQILPcIk			3.98E+03			7.47E+03			2.09E+04			1.46E+03
PPP2R1A	P30153	eNVIMSQILPcIk			1.05E+05			6.01E+04			1.44E+05			1.09E+03
PPP2R1A	P30153	eNVIMSQILPcIk			1.68E+05			8.94E+04			2.27E+05			
PPP2R1A	P30153	eNVIMSQILPcIk			2.74E+05			1.47E+05			3.69E+05			
PPP2R1A	P30153	eNVIMSQILPcIk		9.23E+04			6.98E+04			3.10E+04			4.04E+03	
PPP2R1A	P30153	eNVIMSQILPcIk		1.45E+05			2.92E+04			1.98E+04			1.44E+03	
PPP2R1A	P30153	eNVIMSQILPcIk		2.15E+05			1.74E+05			7.45E+04			1.02E+04	
PPP2R1A	P30153	eNVIMSQILPcIk		3.06E+05			2.45E+05			9.98E+04			1.22E+04	
PPP2R1A	P30153	eNVIMSQILPcIk	2.90E+04			8.88E+03			9.09E+03					
PPP2R1A	P30153	eNVIMSQILPcIk	8.44E+04			2.86E+04			3.46E+04			5.46E+03		
PPP2R1A	P30153	eNVIMSQILPcIk	9.99E+04			2.09E+05			1.36E+05			1.80E+03		
PPP2R1A	P30153	eNVIMSQILPcIk	1.18E+05			2.41E+05			1.52E+05			1.45E+03		
PPP2R1A	P30153	eWAHATIIPk		1.53E+06			7.38E+05			3.39E+05			4.13E+04	
PPP2R1A	P30153	eWAHATIIPk			5.77E+04			8.18E+04			2.01E+05			7.95E+03
PPP2R1A	P30153	eWAHATIIPk			4.87E+05			3.26E+05			9.22E+05			
PPP2R1A	P30153	eWAHATIIPk		3.90E+05			2.79E+05			1.75E+05			1.73E+04	
PPP2R1A	P30153	eWAHATIIPk		1.39E+06			6.62E+05			2.94E+05			3.06E+04	

Protein Name	Protein ID	Sequence	Parental Pool 1	Parental Pool 2	Parental Pool 3	Mutant Pool 1	Mutant Pool2	Mutant Pool 3	Het Pool 1	Het Pool 2	Het Pool 3	IgG Ctl Pool 1	IgG Ctl Pool 2	IgG Ctl Pool 3
PPP2R1A	P30153	eWAHATIIPk	1.40E+04			2.66E+04			2.24E+04			5.65E+03		
PPP2R1A	P30153	eWAHATIIPk	2.63E+04			2.59E+04			3.55E+04			2.24E+03		
PPP2R1A	P30153	eWAHATIIPk	2.24E+05			1.50E+05			2.80E+05			5.00E+03		
PPP2R1A	P30153	eWAHATIIPk	5.69E+05			5.76E+05			8.43E+05			1.27E+04		
PPP2R1A	P30153	eWAHATIIPk	5.78E+05			5.87E+05			8.80E+05			1.42E+04		
PPP2R1A	P30153	fTELQk			3.15E+05			2.77E+05			4.13E+05			8.42E+03
PPP2R1A	P30153	fTELQk			3.23E+05			3.86E+05			1.66E+05			1.73E+04
PPP2R1A	P30153	fTELQk	3.13E+05			1.33E+05			1.73E+05			2.24E+03		
PPP2R1A	P30153	fTELQk	3.65E+05			2.11E+05			2.44E+05			6.86E+03		
PPP2R1A	P30153	fTELQk	6.25E+05			4.16E+05			3.64E+05			1.43E+04		
PPP2R1A	P30153	fTELQk	7.32E+05			4.91E+05			4.25E+05			1.33E+04		
PPP2R1A	P30153	fTELQk			3.70E+05			3.31E+05			4.75E+05			9.53E+03
PPP2R1A	P30153	fTELQk		7.54E+05			3.72E+05			2.05E+05			3.91E+04	
PPP2R1A	P30153	fTELQk		8.61E+05			4.39E+05			2.32E+05			2.88E+04	
PPP2R1A	P30153	hMLPTVLR			1.15E+05			1.07E+05			2.13E+05			8.40E+04
PPP2R1A	P30153	hMLPTVLR			1.52E+05			1.65E+05			2.06E+05			7.52E+04
PPP2R1A	P30153	hMLPTVLR			3.91E+05			3.10E+05			1.96E+05			2.47E+04
PPP2R1A	P30153	hMLPTVLR		1.29E+05			8.09E+04			1.13E+04			6.10E+03	
PPP2R1A	P30153	hMLPTVLR	1.69E+05			5.96E+04			5.44E+04			1.86E+03		
PPP2R1A	P30153	hMLPTVLR			6.00E+04			6.44E+04			1.98E+04			4.40E+03
PPP2R1A	P30153	hMLPTVLR			1.53E+05			1.21E+05			1.09E+05			5.97E+04
PPP2R1A	P30153	hMLPTVLR		8.79E+04			4.92E+04			1.41E+04			5.22E+03	
PPP2R1A	P30153	hMLPTVLR		2.30E+05			1.21E+05			3.69E+04			1.18E+04	
PPP2R1A	P30153	hMLPTVLR	2.81E+05			1.30E+05			1.20E+05			1.37E+04		
PPP2R1A	P30153	iGPILDNSTLQSEVkPILEk			3.09E+04			4.80E+04			1.22E+04			4.51E+03
PPP2R1A	P30153	iGPILDNSTLQSEVkPILEk			4.17E+04			5.82E+04			8.17E+04			2.20E+04
PPP2R1A	P30153	iGPILDNSTLQSEVkPILEk			4.59E+04			5.87E+04			5.02E+04			1.36E+04
PPP2R1A	P30153	iGPILDNSTLQSEVkPILEk			4.74E+04			2.36E+04			1.32E+04			1.04E+03
PPP2R1A	P30153	iGPILDNSTLQSEVkPILEk			8.20E+04			1.14E+05			3.01E+04			4.05E+03
PPP2R1A	P30153	iGPILDNSTLQSEVkPILEk			2.14E+05			1.09E+05			5.98E+04			4.55E+03
PPP2R1A	P30153	iGPILDNSTLQSEV			1.46E+06			9.92E+05			6.02E+05			4.55E+04

Protein Name	Protein ID	Sequence	Parental Pool 1	Parental Pool 2	Parental Pool 3	Mutant Pool 1	Mutant Pool2	Mutant Pool 3	Het Pool 1	Het Pool 2	Het Pool 3	IgG Ctl Pool 1	IgG Ctl Pool 2	IgG Ctl Pool 3
		kPILEk												
PPP2R1A	P30153	iGPILDNSTLQSEV kPILEk			2.26E+06			1.61E+06			8.58E+05			7.95E+04
PPP2R1A	P30153	iGPILDNSTLQSEV kPILEk		4.57E+04			2.54E+04			1.25E+04			5.27E+03	
PPP2R1A	P30153	iGPILDNSTLQSEV kPILEk		8.51E+04			5.55E+04			1.23E+04			1.21E+04	
PPP2R1A	P30153	iGPILDNSTLQSEV kPILEk		9.71E+04			4.35E+04			2.14E+04			5.77E+03	
PPP2R1A	P30153	iGPILDNSTLQSEV kPILEk		1.27E+05			6.53E+04			9.23E+03			2.41E+03	
PPP2R1A	P30153	iGPILDNSTLQSEV kPILEk		1.80E+05			7.74E+04			3.80E+04			9.31E+03	
PPP2R1A	P30153	iGPILDNSTLQSEV kPILEk		4.90E+05			2.05E+05			1.00E+05			2.78E+04	
PPP2R1A	P30153	iGPILDNSTLQSEV kPILEk		1.03E+06			3.38E+05			1.40E+05			4.50E+04	
PPP2R1A	P30153	iGPILDNSTLQSEV kPILEk		1.22E+06			3.95E+05			1.78E+05			4.77E+04	
PPP2R1A	P30153	iGPILDNSTLQSEV kPILEk		1.56E+06			5.45E+05			2.27E+05			7.01E+04	
PPP2R1A	P30153	iGPILDNSTLQSEV kPILEk	5.21E+04			1.34E+04			2.05E+04			1.48E+03		
PPP2R1A	P30153	iGPILDNSTLQSEV kPILEk	1.03E+05			2.33E+04			3.51E+04			1.91E+03		
PPP2R1A	P30153	iGPILDNSTLQSEV kPILEk	1.09E+05			2.35E+04			4.43E+04			2.06E+03		
PPP2R1A	P30153	iGPILDNSTLQSEV kPILEk	1.18E+05			3.22E+04			4.71E+04			1.47E+03		
PPP2R1A	P30153	iGPILDNSTLQSEV kPILEk	2.16E+05			4.08E+04			7.72E+04			2.90E+03		
PPP2R1A	P30153	iGPILDNSTLQSEV kPILEk	2.25E+05			5.30E+04			5.65E+04			6.72E+03		
PPP2R1A	P30153	iGPILDNSTLQSEV kPILEk	2.29E+05			6.42E+04			6.92E+04			9.90E+03		
PPP2R1A	P30153	iGPILDNSTLQSEV kPILEk	2.74E+05			6.45E+04			5.70E+04			6.79E+03		
PPP2R1A	P30153	iGPILDNSTLQSEV kPILEk	2.81E+05			5.57E+04			9.59E+04			4.52E+03		
PPP2R1A	P30153	iGPILDNSTLQSEV kPILEk	2.97E+05			6.61E+04			1.09E+05			7.68E+03		
PPP2R1A	P30153	iGPILDNSTLQSEV kPILEk	5.06E+05			7.23E+04			1.10E+05			2.86E+03		
PPP2R1A	P30153	lAGGDWFTSR			1.26E+03			1.24E+03			1.97E+03			
PPP2R1A	P30153	lAGGDWFTSR		1.08E+04			7.77E+03			4.03E+03			2.25E+03	

Protein Name	Protein ID	Sequence	Parental Pool 1	Parental Pool 2	Parental Pool 3	Mutant Pool 1	Mutant Pool2	Mutant Pool 3	Het Pool 1	Het Pool 2	Het Pool 3	IgG Ctl Pool 1	IgG Ctl Pool 2	IgG Ctl Pool 3
PPP2R1A	P30153	lAGGDWFTSR	1.23E+04			1.02E+04			7.92E+03			8.74E+02		
PPP2R1A	P30153	lAGGDWFTSR	1.70E+04			1.03E+04			1.01E+04			1.16E+03		
PPP2R1A	P30153	lAGGDWFTSR			1.82E+03			1.86E+03			1.70E+03			1.45E+03
PPP2R1A	P30153	lAGGDWFTSR			2.45E+03			4.11E+03			1.06E+04			1.85E+03
PPP2R1A	P30153	lAGGDWFTSR		8.93E+04			4.14E+04			2.43E+04			5.76E+03	
PPP2R1A	P30153	lAGGDWFTSR		1.30E+05			7.00E+04			4.30E+04			6.82E+03	
PPP2R1A	P30153	lAGGDWFTSR	5.76E+03			1.35E+03			1.92E+03					
PPP2R1A	P30153	lAGGDWFTSR	7.05E+04			2.97E+04			5.08E+04			1.41E+03		
PPP2R1A	P30153	lAGGDWFTSR	8.37E+04			1.18E+05			7.82E+04			1.37E+04		
PPP2R1A	P30153	lAIIEYMPLLAGQ LGVEFFDEk			2.04E+03			8.63E+03			4.54E+03			4.40E+03
PPP2R1A	P30153	lAIIEYMPLLAGQ LGVEFFDEk	1.47E+03			6.73E+03			1.86E+03			2.32E+03		
PPP2R1A	P30153	lAIIEYMPLLAGQ LGVEFFDEk	3.77E+04			1.97E+04			2.73E+04					
PPP2R1A	P30153	lAIIEYMPLLAGQ LGVEFFDEk	4.86E+04			2.95E+04			3.37E+04			2.36E+03		
PPP2R1A	P30153	lGEFAk			3.51E+05			2.06E+05			1.77E+05			9.71E+03
PPP2R1A	P30153	lGEFAk		3.42E+05			1.98E+05			1.14E+05			1.93E+04	
PPP2R1A	P30153	lGEFAk		3.85E+05			3.44E+05			7.97E+04			9.69E+04	
PPP2R1A	P30153	lGEFAk	2.93E+05			2.73E+05			2.10E+05			3.18E+04		
PPP2R1A	P30153	lGEFAk	3.98E+05			1.54E+05			2.63E+05			9.93E+03		
PPP2R1A	P30153	lNIISNLDcVNEVI GIR			8.87E+02			1.13E+03			4.28E+03			
PPP2R1A	P30153	lNIISNLDcVNEVI GIR			9.35E+02			1.76E+03			7.57E+03			1.44E+03
PPP2R1A	P30153	lNIISNLDcVNEVI GIR			1.17E+03			1.93E+03			3.96E+03			1.44E+03
PPP2R1A	P30153	lNIISNLDcVNEVI GIR			1.25E+03			1.16E+03			1.10E+03			8.88E+02
PPP2R1A	P30153	lNIISNLDcVNEVI GIR			1.40E+03			4.70E+03			9.23E+03			1.71E+03
PPP2R1A	P30153	lNIISNLDcVNEVI GIR			1.44E+03			1.81E+03			4.82E+03			9.07E+02
PPP2R1A	P30153	lNIISNLDcVNEVI GIR			2.14E+03			3.96E+03			8.23E+03			3.70E+03
PPP2R1A	P30153	lNIISNLDcVNEVI GIR			1.43E+04			4.18E+04			1.94E+04			1.31E+03
PPP2R1A	P30153	lNIISNLDcVNEVI GIR			1.69E+04			1.64E+04			2.39E+04			
PPP2R1A	P30153	lNIISNLDcVNEVI			2.45E+04			3.22E+04			6.81E+04			2.38E+03

Protein Name	Protein ID	Sequence	Parental Pool 1	Parental Pool 2	Parental Pool 3	Mutant Pool 1	Mutant Pool2	Mutant Pool 3	Het Pool 1	Het Pool 2	Het Pool 3	IgG Ctl Pool 1	IgG Ctl Pool 2	IgG Ctl Pool 3
		GIR												
PPP2R1A	P30153	lNIISNLDcVNEVIGIR			5.10E+04			6.52E+04			1.11E+05			5.65E+03
PPP2R1A	P30153	lNIISNLDcVNEVIGIR		1.77E+03			5.17E+03			1.94E+03				
PPP2R1A	P30153	lNIISNLDcVNEVIGIR		2.08E+03			2.31E+03			1.93E+03			1.67E+03	
PPP2R1A	P30153	lNIISNLDcVNEVIGIR		2.20E+03			4.10E+03			1.96E+03			1.56E+03	
PPP2R1A	P30153	lNIISNLDcVNEVIGIR		2.42E+03			8.68E+03			8.11E+03			5.34E+03	
PPP2R1A	P30153	lNIISNLDcVNEVIGIR		3.83E+03			5.41E+03			3.90E+03			2.01E+03	
PPP2R1A	P30153	lNIISNLDcVNEVIGIR		4.35E+03			1.35E+04			8.93E+03			7.31E+03	
PPP2R1A	P30153	lNIISNLDcVNEVIGIR		4.41E+03			8.30E+03			4.91E+03			1.64E+03	
PPP2R1A	P30153	lNIISNLDcVNEVIGIR		4.65E+03			8.88E+03			7.48E+03			7.22E+03	
PPP2R1A	P30153	lNIISNLDcVNEVIGIR		4.84E+03			5.02E+03			6.05E+03			3.75E+03	
PPP2R1A	P30153	lNIISNLDcVNEVIGIR		6.65E+03			5.41E+03			2.03E+03				
PPP2R1A	P30153	lNIISNLDcVNEVIGIR		6.66E+03			9.20E+03			5.28E+03			4.65E+03	
PPP2R1A	P30153	lNIISNLDcVNEVIGIR		7.62E+03			5.68E+03			5.20E+03				
PPP2R1A	P30153	lNIISNLDcVNEVIGIR		1.24E+04			2.36E+04			1.46E+04			1.63E+04	
PPP2R1A	P30153	lNIISNLDcVNEVIGIR		1.52E+04			3.06E+04			1.65E+04			1.52E+04	
PPP2R1A	P30153	lNIISNLDcVNEVIGIR		1.70E+04			2.10E+04			1.64E+04			9.23E+03	
PPP2R1A	P30153	lNIISNLDcVNEVIGIR		2.61E+04			2.64E+04			1.64E+04			6.87E+03	
PPP2R1A	P30153	lNIISNLDcVNEVIGIR		5.67E+04			4.55E+04			2.59E+04			7.12E+03	
PPP2R1A	P30153	lNIISNLDcVNEVIGIR		9.45E+04			7.42E+04			4.80E+04			1.03E+04	
PPP2R1A	P30153	lNIISNLDcVNEVIGIR	8.68E+02			2.12E+03			1.34E+03			1.05E+03		
PPP2R1A	P30153	lNIISNLDcVNEVIGIR	2.07E+03			5.60E+03			2.07E+03			8.74E+02		
PPP2R1A	P30153	lNIISNLDcVNEVIGIR	2.20E+03			1.29E+04			5.72E+03			2.40E+03		
PPP2R1A	P30153	lNIISNLDcVNEVIGIR	2.27E+03			2.46E+03			4.03E+03			9.85E+02		

Protein Name	Protein ID	Sequence	Parental Pool 1	Parental Pool 2	Parental Pool 3	Mutant Pool 1	Mutant Pool2	Mutant Pool 3	Het Pool 1	Het Pool 2	Het Pool 3	IgG Ctl Pool 1	IgG Ctl Pool 2	IgG Ctl Pool 3
PPP2R1A	P30153	lNIISNLDcVNEVIGIR	2.40E+03			4.10E+03			2.14E+03					
PPP2R1A	P30153	lNIISNLDcVNEVIGIR	3.88E+03			8.67E+03			5.99E+03			8.77E+02		
PPP2R1A	P30153	lNIISNLDcVNEVIGIR	4.32E+03			7.11E+03			7.07E+03			1.33E+03		
PPP2R1A	P30153	lNIISNLDcVNEVIGIR	4.62E+03			2.12E+04			9.98E+03			5.88E+03		
PPP2R1A	P30153	lNIISNLDcVNEVIGIR	5.04E+03			5.61E+03			4.22E+03					
PPP2R1A	P30153	lNIISNLDcVNEVIGIR	5.30E+03			9.99E+03			5.94E+03			1.22E+03		
PPP2R1A	P30153	lNIISNLDcVNEVIGIR	5.33E+03			7.25E+03			7.97E+03					
PPP2R1A	P30153	lNIISNLDcVNEVIGIR	5.61E+03			1.26E+04			8.55E+03			1.08E+03		
PPP2R1A	P30153	lNIISNLDcVNEVIGIR	5.83E+03			8.33E+03			5.41E+03					
PPP2R1A	P30153	lNIISNLDcVNEVIGIR	6.45E+03			8.55E+03			5.69E+03			9.88E+02		
PPP2R1A	P30153	lNIISNLDcVNEVIGIR	7.89E+03			1.56E+04			8.63E+03			2.06E+03		
PPP2R1A	P30153	lNIISNLDcVNEVIGIR	9.21E+03			1.45E+04			8.72E+03			2.10E+03		
PPP2R1A	P30153	lNIISNLDcVNEVIGIR	9.85E+03			1.13E+04			1.11E+04					
PPP2R1A	P30153	lNIISNLDcVNEVIGIR	9.85E+03			1.13E+04			1.11E+04					
PPP2R1A	P30153	lNIISNLDcVNEVIGIR	2.65E+04			2.27E+04			1.96E+04					
PPP2R1A	P30153	lNIISNLDcVNEVIGIR	1.18E+05			9.80E+04			1.22E+05			1.55E+03		
PPP2R1A	P30153	lNIISNLDcVNEVIGIR	1.37E+05			1.23E+05			1.14E+05			2.13E+03		
PPP2R1A	P30153	lNIISNLDcVNEVIGIR	1.87E+05			1.65E+05			1.45E+05			2.81E+03		
PPP2R1A	P30153	lNIISNLDcVNEVIGIR				1.59E+03			9.47E+02					
PPP2R1A	P30153	lNIISNLDcVNEVIGIR				1.59E+03			9.47E+02					
PPP2R1A	P30153	lSTIALALGVER			1.51E+04			2.75E+04			3.54E+04			1.80E+04
PPP2R1A	P30153	lSTIALALGVER			3.99E+03			1.27E+04			9.96E+03			
PPP2R1A	P30153	lSTIALALGVER			1.23E+04			1.63E+04			2.25E+04			8.29E+03
PPP2R1A	P30153	lSTIALALGVER		1.48E+04			1.80E+04			5.39E+03				
PPP2R1A	P30153	lSTIALALGVER		2.67E+04			3.26E+04			2.32E+04			1.04E+04	

Protein Name	Protein ID	Sequence	Parental Pool 1	Parental Pool 2	Parental Pool 3	Mutant Pool 1	Mutant Pool2	Mutant Pool 3	Het Pool 1	Het Pool 2	Het Pool 3	IgG Ctl Pool 1	IgG Ctl Pool 2	IgG Ctl Pool 3
PPP2R1A	P30153	lSTIALALGVER		9.20E+04			8.36E+04			6.41E+04			1.15E+04	
PPP2R1A	P30153	lSTIALALGVER	8.51E+03			1.16E+04			1.21E+04			6.88E+03		
PPP2R1A	P30153	lSTIALALGVER	9.62E+03			2.30E+04			2.81E+04					
PPP2R1A	P30153	lSTIALALGVER	2.78E+04			1.74E+04			2.71E+04					
PPP2R1A	P30153	lSTIALALGVER	4.53E+04			3.49E+04			4.68E+04					
PPP2R1A	P30153	lSTIALALGVER	9.55E+04			6.91E+04			9.74E+04					
PPP2R1A	P30153	lSTIALALGVER	1.16E+05			8.82E+04			1.20E+05					
PPP2R1A	P30153	lTQDQDVDVk			3.38E+05			2.21E+05			1.05E+05			7.84E+03
PPP2R1A	P30153	lTQDQDVDVk			1.19E+06			8.20E+05			4.67E+05			4.75E+04
PPP2R1A	P30153	lTQDQDVDVk	3.09E+05			5.46E+04			1.01E+05			5.42E+03		
PPP2R1A	P30153	lTQDQDVDVk	3.11E+05			1.85E+05			1.28E+05			3.45E+04		
PPP2R1A	P30153	lTQDQDVDVk	1.35E+06			2.59E+05			2.96E+05			2.82E+04		
PPP2R1A	P30153	lTQDQDVDVk			2.22E+04			8.39E+03			5.31E+03			
PPP2R1A	P30153	lTQDQDVDVk			8.45E+04			4.83E+04			4.18E+04			6.37E+03
PPP2R1A	P30153	lTQDQDVDVk			1.90E+05			1.77E+05			4.44E+04			7.31E+03
PPP2R1A	P30153	lTQDQDVDVk			3.05E+05			3.11E+05			7.85E+04			1.66E+04
PPP2R1A	P30153	lTQDQDVDVk			1.40E+06			9.58E+05			4.57E+05			3.21E+04
PPP2R1A	P30153	lTQDQDVDVk			1.61E+06			1.12E+06			5.40E+05			4.35E+04
PPP2R1A	P30153	lTQDQDVDVk		2.82E+05			1.79E+05			9.88E+04			5.24E+04	
PPP2R1A	P30153	lTQDQDVDVk		3.36E+05			1.53E+05			7.41E+04			2.37E+04	
PPP2R1A	P30153	lTQDQDVDVk		4.01E+05			1.76E+05			3.27E+04			1.12E+04	
PPP2R1A	P30153	lTQDQDVDVk		4.11E+05			1.45E+05			6.50E+04			2.24E+04	
PPP2R1A	P30153	lTQDQDVDVk		5.00E+05			2.34E+05			4.10E+04			1.66E+04	
PPP2R1A	P30153	lTQDQDVDVk		8.73E+05			2.84E+05			1.21E+05			2.75E+04	
PPP2R1A	P30153	lTQDQDVDVk	4.93E+05			1.07E+05			1.53E+05			6.51E+03		
PPP2R1A	P30153	lTQDQDVDVk	4.96E+05			1.20E+05			1.73E+05			1.35E+04		
PPP2R1A	P30153	lTQDQDVDVk	7.17E+05			1.69E+05			2.43E+05			9.72E+03		
PPP2R1A	P30153	lTQDQDVDVk	7.82E+05			1.03E+06			6.15E+05			1.62E+05		
PPP2R1A	P30153	lTQDQDVDVk	2.10E+06			8.31E+05			6.07E+05			1.71E+05		
PPP2R1A	P30153	lTQDQDVDVk	2.58E+06			9.36E+05			7.05E+05			1.67E+05		
PPP2R1A	P30153	mAGDPVANVR			9.63E+04			9.81E+04			1.57E+05			4.71E+04
PPP2R1A	P30153	mAGDPVANVR			1.02E+05			8.06E+04			1.52E+05			4.17E+04
PPP2R1A	P30153	mAGDPVANVR			1.13E+06			6.20E+05			4.03E+05			5.31E+04

Protein Name	Protein ID	Sequence	Parental Pool 1	Parental Pool 2	Parental Pool 3	Mutant Pool 1	Mutant Pool2	Mutant Pool 3	Het Pool 1	Het Pool 2	Het Pool 3	IgG Ctl Pool 1	IgG Ctl Pool 2	IgG Ctl Pool 3
PPP2R1A	P30153	mAGDPVANVR	2.41E+04			1.74E+04			1.14E+04			3.89E+03		
PPP2R1A	P30153	mAGDPVANVR			5.66E+04			7.06E+04			2.40E+04			4.57E+03
PPP2R1A	P30153	mAGDPVANVR			2.21E+05			2.01E+05			2.71E+05			8.16E+04
PPP2R1A	P30153	mAGDPVANVR			1.98E+06			1.09E+06			6.97E+05			7.17E+04
PPP2R1A	P30153	mAGDPVANVR		4.03E+04			2.31E+04			6.08E+03			3.70E+03	
PPP2R1A	P30153	mAGDPVANVR		5.37E+04			1.02E+05			7.73E+04			6.48E+04	
PPP2R1A	P30153	mAGDPVANVR		6.74E+04			1.55E+05			1.32E+05			8.46E+04	
PPP2R1A	P30153	mAGDPVANVR		1.10E+05			1.16E+05			1.35E+05			7.85E+04	
PPP2R1A	P30153	mAGDPVANVR		1.26E+05			1.02E+05			9.95E+04			6.81E+04	
PPP2R1A	P30153	mAGDPVANVR	1.40E+04			2.94E+04			2.27E+04			1.59E+04		
PPP2R1A	P30153	mAGDPVANVR	1.83E+04			6.20E+03			6.14E+03					
PPP2R1A	P30153	mAGDPVANVR	1.93E+04			1.46E+05			6.31E+04			1.96E+04		
PPP2R1A	P30153	mAGDPVANVR	2.00E+04			5.82E+04			4.95E+04			1.82E+04		
PPP2R1A	P30153	mAGDPVANVR	4.58E+05			3.41E+05			2.22E+05			8.69E+04		
PPP2R1A	P30153	nEDVQLR			5.72E+03			2.37E+03			3.92E+03			
PPP2R1A	P30153	nEDVQLR			1.66E+05			1.61E+05			2.32E+05			3.74E+04
PPP2R1A	P30153	nEDVQLR			6.34E+05			4.32E+05			7.07E+05			2.53E+04
PPP2R1A	P30153	nEDVQLR		9.67E+05			5.37E+05			3.14E+05			7.44E+04	
PPP2R1A	P30153	nEDVQLR		1.43E+06			1.31E+06			8.24E+05			3.05E+05	
PPP2R1A	P30153	nEDVQLR	1.69E+05			1.41E+05			1.52E+05			8.89E+03		
PPP2R1A	P30153	nEDVQLR	3.81E+05			4.57E+05			6.46E+05			4.31E+04		
PPP2R1A	P30153	nEDVQLR		7.29E+05			5.04E+05			1.39E+05			4.51E+04	
PPP2R1A	P30153	nEDVQLR		1.14E+06			6.64E+05			3.88E+05			1.52E+05	
PPP2R1A	P30153	nEDVQLR		1.59E+06			1.23E+06			7.58E+05			1.01E+05	
PPP2R1A	P30153	nEDVQLR		2.00E+06			1.44E+06			8.90E+05			8.53E+04	
PPP2R1A	P30153	nEDVQLR	1.49E+05			1.64E+05			2.32E+05			1.11E+04		
PPP2R1A	P30153	nEDVQLR	7.24E+05			6.50E+05			6.86E+05			4.39E+04		
PPP2R1A	P30153	nEDVQLR	3.00E+06			2.33E+06			2.79E+06			4.62E+04		
PPP2R1A	P30153	nLcSDDTPmVR			2.85E+04			1.61E+04			1.82E+04			3.90E+03
PPP2R1A	P30153	nLcSDDTPmVR		1.72E+04			1.67E+04			1.23E+04			8.36E+03	
PPP2R1A	P30153	nLcSDDTPMVR		2.11E+04			1.85E+04			1.09E+04			7.59E+03	
PPP2R1A	P30153	nLcSDDTPmVR		1.42E+05			8.73E+04			5.45E+04			3.52E+04	
PPP2R1A	P30153	nLcSDDTPmVR	2.00E+04			1.59E+04			2.15E+04					

Protein Name	Protein ID	Sequence	Parental Pool 1	Parental Pool 2	Parental Pool 3	Mutant Pool 1	Mutant Pool2	Mutant Pool 3	Het Pool 1	Het Pool 2	Het Pool 3	IgG Ctl Pool 1	IgG Ctl Pool 2	IgG Ctl Pool 3
PPP2R1A	P30153	nLcSDDTPmVR	3.47E+04			2.40E+04			2.08E+04			1.63E+03		
PPP2R1A	P30153	nLcSDDTPmVR	4.61E+04			3.27E+04			3.19E+04			3.87E+03		
PPP2R1A	P30153	nLcSDDTPmVR	5.64E+04			6.77E+04			5.25E+04			1.77E+04		
PPP2R1A	P30153	nLcSDDTPmVR			2.61E+04			3.01E+04			1.44E+04			1.62E+03
PPP2R1A	P30153	nLcSDDTPMVR			2.97E+04			2.25E+04			2.84E+04			3.41E+03
PPP2R1A	P30153	nLcSDDTPmVR			3.52E+04			2.82E+04			3.88E+04			1.18E+04
PPP2R1A	P30153	nLcSDDTPmVR			4.53E+04			5.11E+04			6.98E+04			2.89E+04
PPP2R1A	P30153	nLcSDDTPmVR			5.37E+04			2.62E+04			3.03E+04			2.11E+03
PPP2R1A	P30153	nLcSDDTPMVR			1.87E+05			2.13E+05			4.73E+05			6.46E+04
PPP2R1A	P30153	nLcSDDTPMVR			2.35E+05			2.67E+05			1.15E+05			1.27E+04
PPP2R1A	P30153	nLcSDDTPMVR			2.79E+05			1.97E+05			2.48E+05			4.43E+04
PPP2R1A	P30153	nLcSDDTPMVR			4.38E+05			2.25E+05			1.74E+05			1.11E+04
PPP2R1A	P30153	nLcSDDTPMVR			5.32E+05			2.86E+05			3.03E+05			1.81E+04
PPP2R1A	P30153	nLcSDDTPmVR		6.39E+04			3.52E+04			1.79E+04				
PPP2R1A	P30153	nLcSDDTPmVR		6.92E+04			3.29E+04			2.19E+04			6.40E+03	
PPP2R1A	P30153	nLcSDDTPMVR		1.11E+05			5.05E+04			2.78E+04			7.55E+03	
PPP2R1A	P30153	nLcSDDTPMVR		1.58E+05			8.59E+04			5.33E+04			2.04E+04	
PPP2R1A	P30153	nLcSDDTPMVR		1.87E+05			1.29E+05			3.15E+04			1.94E+04	
PPP2R1A	P30153	nLcSDDTPMVR		1.97E+05			9.92E+04			5.91E+04			1.16E+04	
PPP2R1A	P30153	nLcSDDTPMVR		2.75E+05			1.33E+05			8.63E+04			1.38E+04	
PPP2R1A	P30153	nLcSDDTPMVR		3.27E+05			1.50E+05			8.64E+04			2.58E+04	
PPP2R1A	P30153	nLcSDDTPMVR		3.60E+05			1.95E+05			5.17E+04			1.17E+04	
PPP2R1A	P30153	nLcSDDTPMVR		5.13E+05			2.60E+05			1.51E+05			2.21E+04	
PPP2R1A	P30153	nLcSDDTPMVR		8.40E+05			3.64E+05			2.26E+05			5.13E+04	
PPP2R1A	P30153	nLcSDDTPMVR		1.42E+06			5.79E+05			3.34E+05			6.24E+04	
PPP2R1A	P30153	nLcSDDTPmVR	2.10E+04			4.43E+04			4.43E+04			9.76E+03		
PPP2R1A	P30153	nLcSDDTPMVR	3.64E+04			3.83E+04			2.89E+04			8.32E+03		
PPP2R1A	P30153	nLcSDDTPmVR	3.81E+04			2.50E+04			3.25E+04			1.44E+03		
PPP2R1A	P30153	nLcSDDTPmVR	4.30E+04			2.84E+04			4.70E+04					
PPP2R1A	P30153	nLcSDDTPMVR	1.25E+05			8.87E+04			9.30E+04			8.14E+03		
PPP2R1A	P30153	nLcSDDTPMVR	1.28E+05			6.49E+04			7.50E+04			2.25E+03		
PPP2R1A	P30153	nLcSDDTPMVR	1.57E+05			5.64E+04			1.18E+05			1.51E+03		
PPP2R1A	P30153	nLcSDDTPMVR	1.85E+05			7.29E+04			1.30E+05			1.56E+03		

Protein Name	Protein ID	Sequence	Parental Pool 1	Parental Pool 2	Parental Pool 3	Mutant Pool 1	Mutant Pool2	Mutant Pool 3	Het Pool 1	Het Pool 2	Het Pool 3	IgG Ctl Pool 1	IgG Ctl Pool 2	IgG Ctl Pool 3
PPP2R1A	P30153	nLcSDDTPMVR	2.18E+05			9.11E+04			1.53E+05					
PPP2R1A	P30153	nLcSDDTPMVR	3.32E+05			2.39E+05			2.23E+05			2.11E+04		
PPP2R1A	P30153	nLcSDDTPMVR	3.67E+05			1.68E+05			2.10E+05			1.12E+04		
PPP2R1A	P30153	nLcSDDTPMVR	5.00E+05			2.14E+05			2.82E+05			1.08E+04		
PPP2R1A	P30153	nLcSDDTPMVR	5.30E+05			1.86E+05			3.89E+05					
PPP2R1A	P30153	qAAEDk			1.97E+05			2.14E+05			2.94E+05			2.53E+04
PPP2R1A	P30153	qAAEDk			4.09E+05			4.99E+05			2.05E+05			2.09E+04
PPP2R1A	P30153	qAAEDk		5.31E+05			2.44E+05			1.51E+05			2.30E+04	
PPP2R1A	P30153	qAAEDk		5.80E+05			3.34E+05			1.62E+05			5.53E+04	
PPP2R1A	P30153	qAAEDk		8.49E+05			4.67E+05			1.39E+05			3.43E+04	
PPP2R1A	P30153	qAAEDk	3.61E+06			2.15E+06			1.78E+06			4.70E+04		
PPP2R1A	P30153	qAAEDk		3.42E+06			1.55E+06			8.58E+05			1.21E+05	
PPP2R1A	P30153	qAAEDk	2.35E+05			1.35E+05			1.55E+05			8.15E+03		
PPP2R1A	P30153	qAAEDk	5.29E+05			2.08E+05			2.51E+05			7.11E+03		
PPP2R1A	P30153	qAAEDk	1.66E+06			9.35E+05			1.15E+06			2.74E+04		
PPP2R1A	P30153	qLSQSLLPAIVEL AEDAk			3.81E+03			2.06E+03			6.07E+03			
PPP2R1A	P30153	qLSQSLLPAIVEL AEDAk			5.68E+03			9.28E+03			1.34E+04			1.20E+03
PPP2R1A	P30153	qLSQSLLPAIVEL AEDAk			6.91E+03			1.01E+04			5.07E+03			
PPP2R1A	P30153	qLSQSLLPAIVEL AEDAk			1.97E+04			2.57E+04			1.46E+04			
PPP2R1A	P30153	qLSQSLLPAIVEL AEDAk			1.97E+04			2.57E+04			1.46E+04			
PPP2R1A	P30153	qLSQSLLPAIVEL AEDAk			3.88E+04			3.62E+04			7.63E+04			3.06E+03
PPP2R1A	P30153	qLSQSLLPAIVEL AEDAk			6.23E+04			3.94E+04			8.83E+04			
PPP2R1A	P30153	qLSQSLLPAIVEL AEDAk			8.44E+04			6.21E+04			1.46E+05			
PPP2R1A	P30153	qLSQSLLPAIVEL AEDAk			1.75E+05			1.54E+05			3.24E+05			4.78E+03
PPP2R1A	P30153	qLSQSLLPAIVEL AEDAk			4.27E+05			3.77E+05			7.77E+05			
PPP2R1A	P30153	qLSQSLLPAIVEL AEDAk		1.47E+03			1.61E+03			1.04E+03				
PPP2R1A	P30153	qLSQSLLPAIVEL AEDAk		5.19E+03			8.12E+03			6.29E+03			8.60E+02	
PPP2R1A	P30153	qLSQSLLPAIVEL AEDAk		1.14E+04			8.98E+03			8.31E+03			1.46E+03	

Protein Name	Protein ID	Sequence	Parental Pool 1	Parental Pool 2	Parental Pool 3	Mutant Pool 1	Mutant Pool2	Mutant Pool 3	Het Pool 1	Het Pool 2	Het Pool 3	IgG Ctl Pool 1	IgG Ctl Pool 2	IgG Ctl Pool 3
PPP2R1A	P30153	qLSQSLLPAIVEL AEDAk		1.91E+04			1.80E+04			1.52E+04			2.27E+03	
PPP2R1A	P30153	qLSQSLLPAIVEL AEDAk		2.52E+04			1.50E+04			7.31E+03				
PPP2R1A	P30153	qLSQSLLPAIVEL AEDAk		2.84E+04			2.30E+04			1.80E+04			5.50E+03	
PPP2R1A	P30153	qLSQSLLPAIVEL AEDAk		2.86E+04			1.95E+04			7.58E+03				
PPP2R1A	P30153	qLSQSLLPAIVEL AEDAk		7.94E+04			3.84E+04			3.90E+04			3.97E+03	
PPP2R1A	P30153	qLSQSLLPAIVEL AEDAk		1.31E+05			9.25E+04			8.51E+04			2.18E+03	
PPP2R1A	P30153	qLSQSLLPAIVEL AEDAk		2.36E+05			1.60E+05			1.35E+05			6.20E+03	
PPP2R1A	P30153	qLSQSLLPAIVEL AEDAk		2.44E+05			1.48E+05			1.66E+05				
PPP2R1A	P30153	qLSQSLLPAIVEL AEDAk		3.86E+05			2.04E+05			1.71E+05			2.07E+04	
PPP2R1A	P30153	qLSQSLLPAIVEL AEDAk		5.42E+05			3.65E+05			3.44E+05			1.74E+04	
PPP2R1A	P30153	qLSQSLLPAIVEL AEDAk		9.04E+05			4.57E+05			4.23E+05			3.82E+04	
PPP2R1A	P30153	qLSQSLLPAIVEL AEDAk	1.15E+03			1.25E+03			2.21E+03					
PPP2R1A	P30153	qLSQSLLPAIVEL AEDAk	1.31E+03			1.43E+03			4.59E+03					
PPP2R1A	P30153	qLSQSLLPAIVEL AEDAk	1.50E+03			1.62E+03			4.53E+03					
PPP2R1A	P30153	qLSQSLLPAIVEL AEDAk	1.60E+03			1.80E+03			2.24E+03					
PPP2R1A	P30153	qLSQSLLPAIVEL AEDAk	1.64E+03			1.27E+03			2.17E+03					
PPP2R1A	P30153	qLSQSLLPAIVEL AEDAk	1.81E+03			2.26E+03			3.96E+03					
PPP2R1A	P30153	qLSQSLLPAIVEL AEDAk	1.87E+03			3.73E+03			4.27E+03					
PPP2R1A	P30153	qLSQSLLPAIVEL AEDAk	2.01E+03			5.85E+03			5.45E+03					
PPP2R1A	P30153	qLSQSLLPAIVEL AEDAk	2.23E+03			4.23E+03			8.18E+03					
PPP2R1A	P30153	qLSQSLLPAIVEL AEDAk	3.86E+03			1.97E+03			4.61E+03					
PPP2R1A	P30153	qLSQSLLPAIVEL AEDAk	3.90E+03			6.22E+03			8.46E+03					
PPP2R1A	P30153	qLSQSLLPAIVEL AEDAk	5.24E+03			4.38E+03			7.26E+03					

Protein Name	Protein ID	Sequence	Parental Pool 1	Parental Pool 2	Parental Pool 3	Mutant Pool 1	Mutant Pool2	Mutant Pool 3	Het Pool 1	Het Pool 2	Het Pool 3	IgG Ctl Pool 1	IgG Ctl Pool 2	IgG Ctl Pool 3
PPP2R1A	P30153	qLSQSLLPAIVEL AEDAk	5.49E+03			5.69E+03			1.01E+04					
PPP2R1A	P30153	qLSQSLLPAIVEL AEDAk	5.83E+03			4.91E+03			9.30E+03					
PPP2R1A	P30153	qLSQSLLPAIVEL AEDAk	6.64E+03			7.79E+03			9.10E+03					
PPP2R1A	P30153	qLSQSLLPAIVEL AEDAk	6.75E+03			8.21E+03			1.07E+04					
PPP2R1A	P30153	qLSQSLLPAIVEL AEDAk	6.77E+03			9.33E+03			1.56E+04					
PPP2R1A	P30153	qLSQSLLPAIVEL AEDAk	6.96E+03			7.33E+03			5.53E+03					
PPP2R1A	P30153	qLSQSLLPAIVEL AEDAk	7.04E+03			9.30E+03			1.04E+04					
PPP2R1A	P30153	qLSQSLLPAIVEL AEDAk	7.20E+03			9.09E+03			1.18E+04			1.14E+03		
PPP2R1A	P30153	qLSQSLLPAIVEL AEDAk	7.28E+03			1.18E+04			1.49E+04					
PPP2R1A	P30153	qLSQSLLPAIVEL AEDAk	7.49E+03			1.07E+04			1.60E+04					
PPP2R1A	P30153	qLSQSLLPAIVEL AEDAk	1.05E+04			1.30E+04			1.22E+04			2.00E+03		
PPP2R1A	P30153	qLSQSLLPAIVEL AEDAk	1.14E+04			1.31E+04			1.90E+04					
PPP2R1A	P30153	qLSQSLLPAIVEL AEDAk	1.64E+04			2.02E+04			2.27E+04			3.66E+03		
PPP2R1A	P30153	qLSQSLLPAIVEL AEDAk	1.86E+04			2.45E+04			2.43E+04			2.04E+03		
PPP2R1A	P30153	qLSQSLLPAIVEL AEDAk	2.81E+04			3.34E+04			3.57E+04			1.36E+03		
PPP2R1A	P30153	qLSQSLLPAIVEL AEDAk	3.64E+04			1.86E+04			2.73E+04					
PPP2R1A	P30153	qLSQSLLPAIVEL AEDAk	5.15E+04			2.79E+04			4.34E+04					
PPP2R1A	P30153	qLSQSLLPAIVEL AEDAk	5.15E+04			2.79E+04			4.34E+04					
PPP2R1A	P30153	qLSQSLLPAIVEL AEDAk	5.21E+04			2.58E+04			3.43E+04					
PPP2R1A	P30153	qLSQSLLPAIVEL AEDAk	7.90E+04			8.80E+04			1.02E+05			2.87E+03		
PPP2R1A	P30153	qLSQSLLPAIVEL AEDAk	1.02E+05			9.20E+04			1.11E+05			1.28E+03		
PPP2R1A	P30153	qLSQSLLPAIVEL AEDAk	3.27E+05			3.09E+05			5.61E+05					
PPP2R1A	P30153	qLSQSLLPAIVEL AEDAk	3.58E+05			3.10E+05			3.99E+05			6.09E+03		

Protein Name	Protein ID	Sequence	Parental Pool 1	Parental Pool 2	Parental Pool 3	Mutant Pool 1	Mutant Pool2	Mutant Pool 3	Het Pool 1	Het Pool 2	Het Pool 3	IgG Ctl Pool 1	IgG Ctl Pool 2	IgG Ctl Pool 3
PPP2R1A	P30153	qLSQSLLPAIVEL AEDAk	5.43E+05			4.64E+05			6.05E+05					
PPP2R1A	P30153	qLSQSLLPAIVEL AEDAk	5.49E+05			5.09E+05			9.52E+05					
PPP2R1A	P30153	qLSQSLLPAIVEL AEDAk	7.75E+05			7.11E+05			1.28E+06					
PPP2R1A	P30153	sEIIPmFSNLASDE QDSVR	1.01E+05			6.13E+04			5.28E+04			6.07E+03		
PPP2R1A	P30153	sEIIPMFSNLASDE QDSVR			1.50E+04			1.43E+04			1.39E+04			
PPP2R1A	P30153	sEIIPmFSNLASDE QDSVR			2.00E+04			1.13E+04			1.19E+04			1.32E+03
PPP2R1A	P30153	sEIIPMFSNLASDE QDSVR			2.60E+04			7.66E+04			4.63E+04			3.87E+03
PPP2R1A	P30153	sEIIPMFSNLASDE QDSVR			3.18E+04			1.59E+04			1.44E+04			1.17E+03
PPP2R1A	P30153	sEIIPMFSNLASDE QDSVR			3.96E+04			2.14E+04			1.96E+04			1.60E+03
PPP2R1A	P30153	sEIIPmFSNLASDE QDSVR			7.71E+04			3.81E+04			5.37E+04			6.45E+03
PPP2R1A	P30153	sEIIPmFSNLASDE QDSVR			1.18E+05			5.78E+04			5.81E+04			6.84E+03
PPP2R1A	P30153	sEIIPMFSNLASDE QDSVR			1.83E+05			1.62E+05			1.52E+05			1.57E+04
PPP2R1A	P30153	sEIIPmFSNLASDE QDSVR			2.00E+05			9.39E+04			1.01E+05			1.19E+04
PPP2R1A	P30153	sEIIPMFSNLASDE QDSVR			3.62E+05			1.65E+05			1.63E+05			4.95E+03
PPP2R1A	P30153	sEIIPMFSNLASDE QDSVR			3.82E+05			1.73E+05			1.75E+05			7.05E+03
PPP2R1A	P30153	sEIIPMFSNLASDE QDSVR		8.31E+02			1.46E+03							
PPP2R1A	P30153	sEIIPmFSNLASDE QDSVR		6.11E+03			1.92E+03			1.19E+03				
PPP2R1A	P30153	sEIIPMFSNLASDE QDSVR		2.77E+04			9.19E+03			5.17E+03			9.49E+02	
PPP2R1A	P30153	sEIIPmFSNLASDE QDSVR		3.19E+04			1.53E+04			1.19E+04			6.08E+03	
PPP2R1A	P30153	sEIIPMFSNLASDE QDSVR		3.83E+04			1.24E+04			6.11E+03				
PPP2R1A	P30153	sEIIPMFSNLASDE QDSVR		3.97E+04			2.01E+04			9.56E+03			2.36E+03	
PPP2R1A	P30153	sEIIPMFSNLASDE QDSVR		8.26E+04			1.11E+05			3.42E+04			7.95E+03	
PPP2R1A	P30153	sEIIPMFSNLASDE QDSVR		8.64E+04			3.62E+04			1.77E+04			3.23E+03	

Protein Name	Protein ID	Sequence	Parental Pool 1	Parental Pool 2	Parental Pool 3	Mutant Pool 1	Mutant Pool2	Mutant Pool 3	Het Pool 1	Het Pool 2	Het Pool 3	IgG Ctl Pool 1	IgG Ctl Pool 2	IgG Ctl Pool 3
PPP2R1A	P30153	sEIIPmFSNLASDE QDSVR		9.48E+04			3.83E+04			2.46E+04			8.15E+03	
PPP2R1A	P30153	sEIIPmFSNLASDE QDSVR		1.25E+05			5.94E+04			3.20E+04			1.01E+04	
PPP2R1A	P30153	sEIIPMFSNLASDE QDSVR		5.53E+05			1.68E+05			9.68E+04			1.37E+04	
PPP2R1A	P30153	sEIIPMFSNLASDE QDSVR		5.81E+05			1.82E+05			1.02E+05			1.68E+04	
PPP2R1A	P30153	sEIIPMFSNLASDE QDSVR		7.25E+05			3.08E+05			1.47E+05			2.89E+04	
PPP2R1A	P30153	sEIIPMFSNLASDE QDSVR		1.91E+06			8.55E+05			4.15E+05			7.53E+04	
PPP2R1A	P30153	sEIIPmFSNLASDE QDSVR	1.31E+04			8.36E+03			9.07E+03			1.85E+03		
PPP2R1A	P30153	sEIIPMFSNLASDE QDSVR	1.87E+04			6.03E+03			8.14E+03					
PPP2R1A	P30153	sEIIPMFSNLASDE QDSVR	1.87E+04			6.03E+03			8.14E+03					
PPP2R1A	P30153	sEIIPmFSNLASDE QDSVR	3.24E+04			1.06E+04			1.99E+04			1.10E+03		
PPP2R1A	P30153	sEIIPMFSNLASDE QDSVR	3.45E+04			2.45E+04			3.65E+04			4.55E+03		
PPP2R1A	P30153	sEIIPMFSNLASDE QDSVR	3.66E+04			9.21E+03			1.75E+04					
PPP2R1A	P30153	sEIIPMFSNLASDE QDSVR	3.91E+04			1.98E+04			2.06E+04			1.39E+03		
PPP2R1A	P30153	sEIIPMFSNLASDE QDSVR	6.21E+04			3.72E+04			4.23E+04			8.74E+03		
PPP2R1A	P30153	sEIIPMFSNLASDE QDSVR	7.05E+04			3.40E+04			3.60E+04					
PPP2R1A	P30153	sEIIPmFSNLASDE QDSVR	1.55E+05			4.65E+04			8.85E+04			3.93E+03		
PPP2R1A	P30153	sEIIPMFSNLASDE QDSVR	2.32E+05			1.21E+05			1.28E+05					
PPP2R1A	P30153	sEIIPMFSNLASDE QDSVR	3.11E+05			1.30E+05			1.63E+05					
PPP2R1A	P30153	sEIIPMFSNLASDE QDSVR	5.46E+05			1.31E+05			2.44E+05			1.35E+04		
PPP2R1A	P30153	tDLVPAFQNLMk		4.68E+05			2.91E+05			1.30E+05			1.73E+04	
PPP2R1A	P30153	tDLVPAFQNLMk			2.01E+04			3.58E+04			1.75E+04			1.21E+03
PPP2R1A	P30153	tDLVPAFQNLMk			5.00E+04			4.18E+04			8.97E+04			
PPP2R1A	P30153	tDLVPAFQNLMk			7.26E+04			6.98E+04			1.32E+05			1.53E+03
PPP2R1A	P30153	tDLVPAFQNLMk			7.70E+04			1.10E+05			5.32E+04			4.95E+03
PPP2R1A	P30153	tDLVPAFQNLmk			7.79E+04			6.53E+04			1.09E+05			5.61E+03

Protein Name	Protein ID	Sequence	Parental Pool 1	Parental Pool 2	Parental Pool 3	Mutant Pool 1	Mutant Pool2	Mutant Pool 3	Het Pool 1	Het Pool 2	Het Pool 3	IgG Ctl Pool 1	IgG Ctl Pool 2	IgG Ctl Pool 3
PPP2R1A	P30153	tDLVPAFQNLmk			1.28E+05			1.15E+05			1.79E+05			1.48E+04
PPP2R1A	P30153	tDLVPAFQNLMk			1.43E+05			1.04E+05			1.74E+05			5.23E+03
PPP2R1A	P30153	tDLVPAFQNLmk			2.19E+05			1.95E+05			3.31E+05			1.54E+04
PPP2R1A	P30153	tDLVPAFQNLMk			4.65E+05			4.30E+05			8.07E+05			
PPP2R1A	P30153	tDLVPAFQNLMk			5.83E+05			5.71E+05			1.04E+06			
PPP2R1A	P30153	tDLVPAFQNLMk		5.94E+04			5.20E+04			1.01E+04			1.56E+03	
PPP2R1A	P30153	tDLVPAFQNLMk		9.61E+04			7.77E+04			4.68E+04			1.15E+04	
PPP2R1A	P30153	tDLVPAFQNLMk		1.58E+05			1.32E+05			2.45E+04			5.98E+03	
PPP2R1A	P30153	tDLVPAFQNLMk		2.30E+05			1.58E+05			9.31E+04			1.24E+04	
PPP2R1A	P30153	tDLVPAFQNLMk		2.55E+05			2.07E+05			1.23E+05			2.92E+04	
PPP2R1A	P30153	tDLVPAFQNLMk		2.58E+05			1.51E+05			7.06E+04			8.09E+03	
PPP2R1A	P30153	tDLVPAFQNLMk		5.24E+05			3.26E+05			1.61E+05			3.09E+04	
PPP2R1A	P30153	tDLVPAFQNLMk		6.05E+05			3.81E+05			1.73E+05			3.26E+04	
PPP2R1A	P30153	tDLVPAFQNLMk	1.14E+05			1.07E+05			1.01E+05			1.83E+03		
PPP2R1A	P30153	tDLVPAFQNLMk	1.15E+05			1.01E+05			1.08E+05			4.47E+03		
PPP2R1A	P30153	tDLVPAFQNLMk	1.30E+05			7.11E+04			8.66E+04			1.27E+03		
PPP2R1A	P30153	tDLVPAFQNLMk	1.41E+05			1.29E+05			1.44E+05			6.76E+03		
PPP2R1A	P30153	tDLVPAFQNLMk	1.58E+05			8.55E+04			1.03E+05			2.25E+03		
PPP2R1A	P30153	tDLVPAFQNLMk	1.65E+05			1.68E+05			1.51E+05			6.61E+03		
PPP2R1A	P30153	tDLVPAFQNLMk	2.17E+05			2.20E+05			2.14E+05			1.50E+04		
PPP2R1A	P30153	tDLVPAFQNLMk	2.75E+05			2.71E+05			2.41E+05			1.17E+04		
PPP2R1A	P30153	tDLVPAFQNLMk	3.48E+05			3.28E+05			3.04E+05			8.41E+03		
PPP2R1A	P30153	tSAcGLFSVcYPR	3.89E+04			6.01E+04			7.43E+04			1.39E+04		
PPP2R1A	P30153	tSAcGLFSVcYPR			4.81E+03			1.37E+04			7.29E+03			
PPP2R1A	P30153	tSAcGLFSVcYPR			4.86E+03			4.19E+03			1.85E+03			9.56E+02
PPP2R1A	P30153	tSAcGLFSVcYPR			7.98E+03			2.49E+04			1.27E+04			2.14E+03
PPP2R1A	P30153	tSAcGLFSVcYPR			1.71E+04			1.47E+04			7.57E+03			
PPP2R1A	P30153	tSAcGLFSVcYPR			2.93E+04			1.85E+04			2.15E+04			2.35E+03
PPP2R1A	P30153	tSAcGLFSVcYPR			4.10E+04			3.95E+04			4.80E+04			5.45E+03
PPP2R1A	P30153	tSAcGLFSVcYPR			5.91E+04			4.02E+04			9.23E+04			1.15E+04
PPP2R1A	P30153	tSAcGLFSVcYPR			6.25E+04			5.23E+04			7.03E+04			8.89E+03
PPP2R1A	P30153	tSAcGLFSVcYPR			7.96E+04			5.35E+04			6.66E+04			9.69E+03
PPP2R1A	P30153	tSAcGLFSVcYPR		1.60E+04			1.33E+04			5.21E+03				

Protein Name	Protein ID	Sequence	Parental Pool 1	Parental Pool 2	Parental Pool 3	Mutant Pool 1	Mutant Pool2	Mutant Pool 3	Het Pool 1	Het Pool 2	Het Pool 3	IgG Ctl Pool 1	IgG Ctl Pool 2	IgG Ctl Pool 3
PPP2R1A	P30153	tSAcGLFSVcYPR		2.76E+04			1.51E+04			5.60E+03				
PPP2R1A	P30153	tSAcGLFSVcYPR		3.75E+04			5.16E+04			3.31E+04			3.88E+04	
PPP2R1A	P30153	tSAcGLFSVcYPR		3.79E+04			5.69E+04			3.98E+04			2.77E+04	
PPP2R1A	P30153	tSAcGLFSVcYPR		3.79E+04			3.10E+04			1.91E+04			1.30E+04	
PPP2R1A	P30153	tSAcGLFSVcYPR		4.24E+04			3.59E+04			1.69E+04			9.75E+03	
PPP2R1A	P30153	tSAcGLFSVcYPR		4.59E+04			3.86E+04			1.28E+04			2.37E+03	
PPP2R1A	P30153	tSAcGLFSVcYPR		5.87E+04			6.85E+04			4.16E+04			3.35E+04	
PPP2R1A	P30153	tSAcGLFSVcYPR		6.10E+04			3.53E+04			2.37E+04			1.08E+04	
PPP2R1A	P30153	tSAcGLFSVcYPR	7.49E+03			5.14E+03			6.42E+03					
PPP2R1A	P30153	tSAcGLFSVcYPR	1.62E+04			3.25E+04			4.00E+04			4.32E+03		
PPP2R1A	P30153	tSAcGLFSVcYPR	2.16E+04			3.79E+04			3.15E+04			9.08E+03		
PPP2R1A	P30153	tSAcGLFSVcYPR	2.25E+04			6.04E+04			3.56E+04			1.06E+04		
PPP2R1A	P30153	tSAcGLFSVcYPR	2.26E+04			1.77E+04			2.56E+04			1.86E+03		
PPP2R1A	P30153	tSAcGLFSVcYPR	2.55E+04			1.65E+04			2.78E+04			1.50E+03		
PPP2R1A	P30153	tSAcGLFSVcYPR	2.90E+04			1.14E+05			6.20E+04			2.04E+04		
PPP2R1A	P30153	tSAcGLFSVcYPR	1.08E+05			8.76E+04			8.51E+04			1.08E+04		
PPP2R1A	P30153	tSAcGLFSVcYPR	1.98E+05			1.19E+05			1.34E+05			6.35E+03		
PPP2R1A	P30153	vLAMSGDPNYLHR		3.43E+05			2.11E+05			6.82E+04			2.73E+04	
PPP2R1A	P30153	vLAMSGDPNYLHR	1.65E+04			4.05E+04			1.93E+04			6.33E+03		
PPP2R1A	P30153	vLAmSGDPNYLHR			2.18E+04			4.55E+04			8.45E+04			2.12E+04
PPP2R1A	P30153	vLAMSGDPNYLHR			5.24E+04			4.30E+04			7.70E+04			5.48E+03
PPP2R1A	P30153	vLAMSGDPNYLHR			6.18E+04			6.38E+04			1.12E+05			6.70E+03
PPP2R1A	P30153	vLAMSGDPNYLHR			6.39E+04			5.71E+04			1.05E+05			4.27E+03
PPP2R1A	P30153	vLAMSGDPNYLHR			6.91E+04			1.19E+05			5.14E+04			1.01E+04
PPP2R1A	P30153	vLAMSGDPNYLHR			9.96E+04			9.33E+04			1.73E+05			1.02E+04
PPP2R1A	P30153	vLAMSGDPNYLHR			1.66E+05			1.66E+05			2.93E+05			1.26E+04
PPP2R1A	P30153	vLAMSGDPNYLHR		5.66E+04			6.50E+04			2.95E+04			2.51E+04	
PPP2R1A	P30153	vLAMSGDPNYLHR		6.44E+04			7.03E+04			1.42E+04			1.31E+04	
PPP2R1A	P30153	vLAMSGDPNYLH		6.62E+04			4.33E+04			2.65E+04			8.97E+03	

Protein Name	Protein ID	Sequence	Parental Pool 1	Parental Pool 2	Parental Pool 3	Mutant Pool 1	Mutant Pool2	Mutant Pool 3	Het Pool 1	Het Pool 2	Het Pool 3	IgG Ctl Pool 1	IgG Ctl Pool 2	IgG Ctl Pool 3
		R												
PPP2R1A	P30153	vLAMSGDPNYLHR		1.19E+05			1.11E+05			5.93E+04			2.91E+04	
PPP2R1A	P30153	vLAMSGDPNYLHR		1.20E+05			9.54E+04			3.91E+04			2.80E+04	
PPP2R1A	P30153	vLAMSGDPNYLHR		3.75E+05			2.47E+05			9.01E+04			4.63E+04	
PPP2R1A	P30153	vLAMSGDPNYLHR	3.04E+04			3.96E+04			2.34E+04			2.29E+03		
PPP2R1A	P30153	vLAMSGDPNYLHR	3.76E+04			7.51E+04			3.93E+04			1.55E+04		
PPP2R1A	P30153	vLAMSGDPNYLHR	4.07E+04			2.88E+04			2.63E+04			1.43E+03		
PPP2R1A	P30153	vLAMSGDPNYLHR	8.81E+04			5.61E+04			7.81E+04			9.57E+03		
PPP2R1A	P30153	vLAMSGDPNYLHR	8.91E+04			6.77E+04			6.66E+04			4.76E+03		
PPP2R1A	P30153	vLAMSGDPNYLHR	1.99E+05			2.20E+05			1.34E+05			1.85E+04		
PPP2R1A	P30153	vLELDNVk			2.06E+05			2.17E+05			9.26E+04			9.73E+03
PPP2R1A	P30153	vLELDNVk			3.56E+05			3.68E+05			1.71E+05			1.66E+04
PPP2R1A	P30153	vLELDNVk			4.17E+05			2.67E+05			2.50E+05			1.19E+04
PPP2R1A	P30153	vLELDNVk			4.21E+05			2.78E+05			2.52E+05			9.20E+03
PPP2R1A	P30153	vLELDNVk			8.80E+05			5.56E+05			5.08E+05			2.99E+04
PPP2R1A	P30153	vLELDNVk		3.57E+05			1.84E+05			4.43E+04			9.39E+03	
PPP2R1A	P30153	vLELDNVk		4.85E+05			2.54E+05			1.35E+05			1.77E+04	
PPP2R1A	P30153	vLELDNVk		6.56E+05			3.47E+05			1.88E+05			2.57E+04	
PPP2R1A	P30153	vLELDNVk		8.27E+05			3.34E+05			2.00E+05			3.49E+04	
PPP2R1A	P30153	vLELDNVk		8.47E+05			3.39E+05			1.97E+05			3.27E+04	
PPP2R1A	P30153	vLELDNVk	1.88E+05			7.86E+04			1.28E+05					
PPP2R1A	P30153	vLELDNVk	5.62E+05			2.11E+05			3.80E+05			1.04E+04		
PPP2R1A	P30153	vLELDNVk	6.33E+05			2.40E+05			3.26E+05			9.04E+03		
PPP2R1A	P30153	vLELDNVk	7.09E+05			2.63E+05			3.34E+05			1.04E+04		
PPP2R1A	P30153	vLELDNVk			1.43E+05			9.48E+04			1.04E+05			1.35E+04
PPP2R1A	P30153	vLELDNVk			1.49E+05			9.43E+04			8.88E+04			1.14E+04
PPP2R1A	P30153	vLELDNVk			4.51E+05			2.48E+05			1.90E+05			9.45E+03
PPP2R1A	P30153	vLELDNVk			6.23E+05			2.93E+05			2.77E+05			1.96E+04
PPP2R1A	P30153	vLELDNVk		3.01E+05			1.99E+05			1.20E+05			4.06E+04	
PPP2R1A	P30153	vLELDNVk		5.34E+05			2.94E+05			6.79E+04			1.80E+04	

Protein Name	Protein ID	Sequence	Parental Pool 1	Parental Pool 2	Parental Pool 3	Mutant Pool 1	Mutant Pool2	Mutant Pool 3	Het Pool 1	Het Pool 2	Het Pool 3	IgG Ctl Pool 1	IgG Ctl Pool 2	IgG Ctl Pool 3
PPP2R1A	P30153	vLELDNVk		1.04E+06			5.70E+05			3.07E+05			5.20E+04	
PPP2R1A	P30153	vLELDNVk		2.21E+06			9.30E+05			5.09E+05			8.38E+04	
PPP2R1A	P30153	vLELDNVk	1.83E+05			8.70E+04			9.44E+04			6.21E+03		
PPP2R1A	P30153	vLELDNVk	2.19E+05			1.13E+05			1.18E+05			9.39E+03		
PPP2R1A	P30153	vLELDNVk	3.38E+05			1.44E+05			2.11E+05			2.12E+03		
PPP2R1A	P30153	vLELDNVk	4.08E+05			1.53E+05			2.07E+05			5.61E+03		
PPP2R1A	P30153	vLELDNVk	5.62E+05			2.02E+05			3.98E+05			4.82E+03		
PPP2R1A	P30153	vLELDNVk	6.11E+05			2.48E+05			4.27E+05			1.50E+04		
PPP2R1A	P30153	vLELDNVk	6.31E+05			2.28E+05			4.31E+05			1.11E+04		
PPP2R1A	P30153	vLELDNVk	1.26E+06			4.64E+05			8.73E+05			1.22E+04		
PPP2R1A	P30153	vLELDNVk	1.69E+06			6.73E+05			8.61E+05			3.85E+04		
PPP2R1A	P30153	yFAQEALTVLSLA		1.03E+04			6.03E+03			1.09E+03				
PPP2R1A	P30153	yMVADk			2.41E+05			1.46E+05			1.81E+05			7.14E+03
PPP2R1A	P30153	yMVADk			3.02E+05			3.43E+05			1.69E+05			1.70E+04
PPP2R1A	P30153	yMVADk	3.50E+05			2.02E+05			2.36E+05			2.48E+04		
PPP2R1A	P30153	yMVADk		3.31E+05			1.84E+05			9.57E+04			1.15E+04	
PPP2R1A	P30153	yMVADk		3.92E+05			2.31E+05			1.26E+05			5.07E+04	
PPP2R1A	P30153	yMVADk		4.09E+05			2.41E+05			7.09E+04			2.68E+04	
PPP2R1A	P30153	yMVADk	1.99E+05			1.00E+05			1.21E+05			5.27E+03		
PPP2R1A	P30153	yMVADk	5.04E+05			2.28E+05			2.97E+05			1.40E+04		
PPP2CA	P67775	eLDQWIEQLNEck			1.97E+04			3.22E+04			4.72E+04			
PPP2CA	P67775	eLDQWIEQLNEck			2.33E+04			8.94E+04			4.16E+04			
PPP2CA	P67775	eLDQWIEQLNEck			1.24E+05			4.44E+05			2.07E+05			3.29E+03
PPP2CA	P67775	eLDQWIEQLNEck			1.59E+05			2.09E+05			2.52E+05			1.50E+03
PPP2CA	P67775	eLDQWIEQLNEck			1.84E+05			2.48E+05			2.97E+05			
PPP2CA	P67775	eLDQWIEQLNEck			3.69E+05			6.45E+05			9.21E+05			1.38E+04
PPP2CA	P67775	eLDQWIEQLNEck			4.35E+05			7.63E+05			1.07E+06			1.67E+04
PPP2CA	P67775	eLDQWIEQLNEck			4.60E+05			8.14E+05			1.16E+06			
PPP2CA	P67775	eLDQWIEQLNEck			4.95E+05			8.51E+05			1.23E+06			
PPP2CA	P67775	eLDQWIEQLNEck		8.62E+03			6.21E+03			1.35E+03				
PPP2CA	P67775	eLDQWIEQLNEck		5.23E+04			3.96E+04			1.73E+04			1.02E+03	
PPP2CA	P67775	eLDQWIEQLNEck		5.96E+04			3.97E+04			2.05E+04			1.75E+03	
PPP2CA	P67775	eLDQWIEQLNEck		8.91E+04			7.13E+04			3.42E+04			1.20E+04	

Protein Name	Protein ID	Sequence	Parental Pool 1	Parental Pool 2	Parental Pool 3	Mutant Pool 1	Mutant Pool2	Mutant Pool 3	Het Pool 1	Het Pool 2	Het Pool 3	IgG Ctl Pool 1	IgG Ctl Pool 2	IgG Ctl Pool 3
PPP2CA	P67775	eLDQWIEQLNEck		2.13E+05			1.62E+05			1.74E+05			1.12E+04	
PPP2CA	P67775	eLDQWIEQLNEck		2.94E+05			1.86E+05			2.06E+05			1.72E+04	
PPP2CA	P67775	eLDQWIEQLNEck		3.86E+05			2.94E+05			3.17E+05			1.58E+04	
PPP2CA	P67775	eLDQWIEQLNEck		4.17E+05			3.06E+05			3.26E+05			2.22E+04	
PPP2CA	P67775	eLDQWIEQLNEck		4.84E+05			3.19E+05			3.44E+05			2.35E+04	
PPP2CA	P67775	eLDQWIEQLNEck		5.10E+05			3.16E+05			3.32E+05			2.50E+04	
PPP2CA	P67775	eLDQWIEQLNEck		6.04E+05			4.57E+05			5.08E+05			2.48E+04	
PPP2CA	P67775	eLDQWIEQLNEck		8.59E+05			5.35E+05			5.75E+05			4.95E+04	
PPP2CA	P67775	eLDQWIEQLNEck	7.23E+03			1.03E+04			1.80E+04					
PPP2CA	P67775	eLDQWIEQLNEck	1.92E+04			3.38E+04			6.55E+04					
PPP2CA	P67775	eLDQWIEQLNEck	6.42E+04			9.26E+04			1.40E+05					
PPP2CA	P67775	eLDQWIEQLNEck	7.25E+04			1.40E+05			1.80E+05					
PPP2CA	P67775	eLDQWIEQLNEck	8.67E+04			1.49E+05			1.94E+05			4.71E+03		
PPP2CA	P67775	eLDQWIEQLNEck	9.42E+04			1.72E+05			3.43E+05					
PPP2CA	P67775	eLDQWIEQLNEck	1.21E+05			2.18E+05			3.00E+05					
PPP2CA	P67775	eLDQWIEQLNEck	1.70E+05			2.99E+05			6.02E+05					
PPP2CA	P67775	eLDQWIEQLNEck	1.94E+05			3.29E+05			6.74E+05					
PPP2CA	P67775	eLDQWIEQLNEck	2.08E+05			3.69E+05			7.83E+05					
PPP2CA	P67775	eLDQWIEQLNEck	2.82E+05			5.08E+05			7.03E+05					
PPP2CA	P67775	eLDQWIEQLNEck	3.06E+05			5.88E+05			7.82E+05					
PPP2CA	P67775	qLSESQVk			1.90E+05			3.09E+05			4.51E+05			
PPP2CA	P67775	qLSESQVk			2.70E+05			4.67E+05			6.64E+05			8.40E+03
PPP2CA	P67775	qLSESQVk			3.20E+05			5.42E+05			7.62E+05			
PPP2CA	P67775	qLSESQVk		1.09E+05			6.80E+04			8.03E+04			1.27E+04	
PPP2CA	P67775	qLSESQVk		4.01E+05			3.17E+05			3.32E+05			3.83E+04	
PPP2CA	P67775	qLSESQVk		9.51E+05			5.81E+05			6.38E+05			4.40E+04	
PPP2CA	P67775	qLSESQVk	1.51E+05			2.81E+05			5.21E+05			1.97E+03		
PPP2CA	P67775	qLSESQVk	2.37E+05			4.68E+05			6.18E+05			1.36E+04		
PPP2CA	P67775	qLSESQVk			1.02E+05			1.30E+05			1.61E+05			2.11E+03
PPP2CA	P67775	qLSESQVk			3.95E+05			6.20E+05			8.90E+05			
PPP2CA	P67775	qLSESQVk		1.36E+05			1.05E+05			1.16E+05			9.12E+03	
PPP2CA	P67775	qLSESQVk		1.97E+05			1.45E+05			1.59E+05			8.96E+03	
PPP2CA	P67775	qLSESQVk		9.15E+05			5.54E+05			5.59E+05			4.47E+04	

Protein Name	Protein ID	Sequence	Parental Pool 1	Parental Pool 2	Parental Pool 3	Mutant Pool 1	Mutant Pool2	Mutant Pool 3	Het Pool 1	Het Pool 2	Het Pool 3	IgG Ctl Pool 1	IgG Ctl Pool 2	IgG Ctl Pool 3
PPP2CA	P67775	qLSESQVk	4.09E+04			7.42E+04			1.33E+05					
PPP2CA	P67775	qLSESQVk	5.42E+04			9.07E+04			1.73E+05					
PPP2CA	P67775	qLSESQVk	1.64E+05			2.37E+05			3.33E+05					
PPP2CA	P67775	qLSESQVk	2.79E+05			5.10E+05			7.01E+05					
PPP2CA	P67775	qLSESQVk	3.29E+05			6.16E+05			8.21E+05					
PPP2CA	P67775	qLSESQVk	3.95E+05			7.03E+05			9.72E+05					
PPP2CA	P67775	sLcEk		3.04E+05			2.58E+05			2.70E+05			4.42E+04	
PPP2CA	P67775	sLcEk		5.25E+05			4.02E+05			3.86E+05			2.73E+04	
PPP2CA	P67775	sLcEk	1.30E+05			2.47E+05			4.13E+05			1.77E+04		
PPP2CB	P62714	eLDQWVEQLNEck			2.20E+03			9.32E+03			7.46E+03			
PPP2CB	P62714	eLDQWVEQLNEck			2.53E+04			4.50E+04			8.00E+04			2.60E+03
PPP2CB	P62714	eLDQWVEQLNEck			2.56E+04			3.76E+04			7.59E+04			8.40E+03
PPP2CB	P62714	eLDQWVEQLNEck			5.38E+04			1.47E+05			1.11E+05			
PPP2CB	P62714	eLDQWVEQLNEck			9.42E+04			1.26E+05			2.42E+05			
PPP2CB	P62714	eLDQWVEQLNEck			1.09E+05			1.12E+05			2.06E+05			
PPP2CB	P62714	eLDQWVEQLNEck			1.20E+05			1.51E+05			3.21E+05			1.51E+03
PPP2CB	P62714	eLDQWVEQLNEck		8.72E+03			8.52E+03			3.79E+03				
PPP2CB	P62714	eLDQWVEQLNEck		6.97E+04			5.63E+04			6.90E+04			4.17E+03	
PPP2CB	P62714	eLDQWVEQLNEck		1.13E+05			1.19E+05			1.17E+05			6.66E+04	
PPP2CB	P62714	eLDQWVEQLNEck		1.53E+05			1.16E+05			1.36E+05			8.25E+03	
PPP2CB	P62714	eLDQWVEQLNEck		1.89E+05			1.35E+05			1.47E+05			3.72E+04	
PPP2CB	P62714	eLDQWVEQLNEck		2.09E+05			1.28E+05			1.60E+05			1.57E+04	
PPP2CB	P62714	eLDQWVEQLNEck		2.24E+05			1.69E+05			8.60E+04			7.80E+03	
PPP2CB	P62714	eLDQWVEQLNEck	4.42E+03			8.02E+03			7.89E+03					
PPP2CB	P62714	eLDQWVEQLNEck	3.28E+04			4.53E+04			9.19E+04					
PPP2CB	P62714	eLDQWVEQLNEck	6.25E+04			8.21E+04			1.39E+05					
PPP2CB	P62714	eLDQWVEQLNEck	7.88E+04			1.14E+05			1.93E+05					
PPP2CB	P62714	eLDQWVEQLNEck	1.30E+05			1.77E+05			3.20E+05					
PPP2CB	P62714	eLDQWVEQLNEck	1.42E+05			1.56E+05			2.06E+05			3.17E+03		
PPP2CB	P62714	qLNENQVR			1.36E+04			3.76E+04			2.69E+04			
PPP2CB	P62714	qLNENQVR			9.10E+04			8.01E+04			1.52E+05			
PPP2CB	P62714	qLNENQVR			1.03E+05			1.28E+05			2.47E+05			1.90E+03
PPP2CB	P62714	qLNENQVR			1.10E+05			1.36E+05			2.69E+05			1.79E+03

Protein Name	Protein ID	Sequence	Parental Pool 1	Parental Pool 2	Parental Pool 3	Mutant Pool 1	Mutant Pool2	Mutant Pool 3	Het Pool 1	Het Pool 2	Het Pool 3	IgG Ctl Pool 1	IgG Ctl Pool 2	IgG Ctl Pool 3
PPP2CB	P62714	qLNENQVR		5.92E+04			5.12E+04			2.89E+04			5.56E+03	
PPP2CB	P62714	qLNENQVR		6.88E+04			5.44E+04			6.54E+04			2.91E+03	
PPP2CB	P62714	qLNENQVR		8.65E+04			7.01E+04			7.52E+04			5.37E+03	
PPP2CB	P62714	qLNENQVR		1.82E+05			1.12E+05			1.37E+05			4.44E+03	
PPP2CB	P62714	qLNENQVR		2.66E+05			1.75E+05			2.10E+05			2.25E+04	
PPP2CB	P62714	qLNENQVR	3.37E+04			4.50E+04			4.89E+04			4.29E+03		
PPP2CB	P62714	qLNENQVR	4.52E+04			6.14E+04			1.08E+05			1.03E+03		
PPP2CB	P62714	qLNENQVR	5.08E+04			6.00E+04			9.62E+04			1.22E+03		
PPP2CB	P62714	qLNENQVR	7.09E+04			1.11E+05			1.30E+05			3.14E+03		
PPP2CB	P62714	qLNENQVR	1.43E+05			1.85E+05			2.26E+05			1.79E+03		
PPP2R2A	E5RFR9	dITLEASR	1.33E+03			5.07E+03			1.50E+04					
PPP2R2A	E5RFR9	dITLEASR			8.81E+03			1.08E+04			2.30E+04			5.17E+03
PPP2R5C	H0YJU0	eVMFLNELEEILD VIEPSEFVk	5.50E+03			1.96E+03			8.35E+03					
PPP2R5C	H0YJU0	eVMFLNELEEILD VIEPSEFVk		1.20E+04			4.40E+03			4.27E+03			1.15E+03	
PPP2R5C	H0YJU0	eVMFLNELEEILD VIEPSEFVk			2.04E+03			3.84E+03			7.19E+03			
PPP2R5D	Q14738-2	eSSLTEPVIVGLLk		6.85E+04			4.13E+04			4.88E+04			2.73E+04	
PPP2R5D	Q14738-3	eSSLTEPVIVGLLk			9.16E+03			1.00E+04			2.42E+04			6.11E+03
PPP2R5D	Q14738	eSSLTEPVIVGLLk	1.04E+04			1.60E+04			3.28E+04			4.32E+03		
PPP2R5D	Q14738	eSSLTEPVIVGLLk	1.36E+03			7.05E+03			8.32E+03			9.86E+02		
PPP2R5D	Q14738-2	eSSLTEPVIVGLLk		1.20E+05			2.15E+04			6.74E+04			1.27E+04	
PPP2R5D	Q14738-2	eSSLTEPVIVGLLk		8.77E+03			1.32E+03			5.67E+03			1.38E+03	
PPP2R5D	Q14738-3	eSSLTEPVIVGLLk			5.48E+04			3.41E+04			1.47E+05			3.21E+03
PPP2R5D	Q14738-3	eSSLTEPVIVGLLk			2.36E+04			1.42E+04			5.19E+04			1.36E+03
PPP2R5D	Q14738	eVMFLNELEEILD VIEPSEFSk	1.07E+04			1.67E+03			1.48E+04					
PPP2R5D	Q14738	eVMFLNELEEILD VIEPSEFSk	1.07E+04			1.67E+03			1.48E+04					
PPP2R5D	Q14738	eVmFLNELEEILD VIEPSEFSk	1.67E+03						4.07E+03					
PPP2R5D	Q14738-2	eVMFLNELEEILD VIEPSEFSk		1.40E+04			4.03E+03			4.63E+03				

Protein Name	Protein ID	Sequence	Parental Pool 1	Parental Pool 2	Parental Pool 3	Mutant Pool 1	Mutant Pool2	Mutant Pool 3	Het Pool 1	Het Pool 2	Het Pool 3	IgG Ctl Pool 1	IgG Ctl Pool 2	IgG Ctl Pool 3
PPP2R5D	Q14738-2	eVMFLNELEEILDVIEPSEFSk		1.40E+04			4.03E+03			4.63E+03				
PPP2R5D	Q14738	rPSNSTPPPTQLSk	8.67E+04			7.11E+04			2.54E+05			6.92E+03		
PPP2R5D	Q14738	rPSNSTPPPTQLSk	5.83E+03			9.43E+03			2.04E+04			1.17E+03		
PPP2R5D	Q14738	rPSNSTPPPTQLSk	2.93E+04			1.84E+04			1.21E+05			1.42E+03		
PPP2R5D	Q14738-2	rPSNSTPPPTQLSk		1.52E+05			1.10E+05			1.32E+05			7.79E+04	
PPP2R5E	Q16537-2	dVPSSEQPELFLk	4.82E+03			8.81E+03			1.74E+04			8.93E+02		
PPP2R5E	Q16537-2	dVPSSEQPELFLk		5.78E+03			1.12E+04			8.65E+03			4.61E+03	
PPP2R5E	Q16537-2	dVPSSEQPELFLk			1.52E+04			1.24E+04			1.82E+04			1.79E+03
PPP2R5E	Q16537-2	fLESQEFQPSIAk	2.20E+04			1.78E+04			7.97E+04			1.76E+03		
PPP2R5E	Q16537-2	fLESQEFQPSIAk		4.93E+03			6.78E+03			8.58E+03			5.66E+03	
PPP2R5E	Q16537-2	fLESQEFQPSIAk			1.22E+03			1.86E+03			4.95E+03			
PPP2R5E	Q16537-2	fLESQEFQPSIAk			1.00E+04			8.27E+03			1.37E+04			1.40E+03
PPP2R5E	Q16537-2	fLESQEFQPSIAk			1.22E+03			1.86E+03			4.95E+03			
PPP2R4	A6PVN9	eSVGNSTR	2.09E+03			1.67E+04			1.12E+04			2.38E+03		
PPP2R4	A6PVN9	eSVGNSTR		1.12E+04			1.96E+04			1.46E+04			1.34E+04	
PPP2R4	A6PVN9	eSVGNSTR		5.20E+03			5.70E+03			5.50E+03			4.12E+03	
PPP2R4	A6PVN8	eSVGNSTR			1.56E+04			2.90E+04			4.12E+04			1.42E+04
PPP2R4	A6PVN9	hFVDEk		3.21E+05			3.62E+05			2.54E+05			3.59E+05	
PPP2R4	A6PVN9	hFVDEk		1.40E+05			2.24E+05			1.70E+05			1.44E+05	
PPP2R4	A6PVN9	lVALLNTLDR	2.43E+03			1.85E+04			1.28E+04			4.64E+03		
PPP2R4	A6PVN9	vDDQIAIVFk	1.97E+04			6.64E+04			3.93E+04			2.84E+04		
PPP2R4	A6PVN9	vDDQIAIVFk	7.39E+03			2.79E+04			1.88E+04			6.51E+03		
PPP2R4	A6PVN8	vSEAIEk			1.95E+04			1.92E+04			3.60E+04			1.23E+04
PPP2R4	A6PVN9	vSEAIEk	1.38E+04			7.37E+04			6.33E+04			1.26E+04		
PPP2R4	A6PVN8	wIDETPPVDQPSR			3.33E+04			4.60E+04			8.72E+04			2.57E+04
PPP2R4	A6PVN8	wIDETPPVDQPSR			2.11E+04			2.39E+04			2.90E+04			1.05E+04
PPP2R4	A6PVN9	wIDETPPVDQPSR	1.81E+04			7.55E+04			4.02E+04			1.51E+04		

Protein Name	Protein ID	Sequence	Parental Pool 1	Parental Pool 2	Parental Pool 3	Mutant Pool 1	Mutant Pool2	Mutant Pool 3	Het Pool 1	Het Pool 2	Het Pool 3	IgG Ctl Pool 1	IgG Ctl Pool 2	IgG Ctl Pool 3
PPP2R4	A6PVN9	wIDETPPVDQPSR	1.02E+04			4.70E+04			3.81E+04			1.01E+04		
PPP2R4	A6PVN9	wIDETPPVDQPSR		1.24E+04			2.24E+04			1.83E+04			1.59E+04	
SET	Q01105-2	eFHLNESGDPSSk			1.43E+04			4.97E+04			5.00E+04			1.04E+04
SET	Q01105-3	eFHLNESGDPSSk	1.06E+05			4.03E+05			6.61E+04			1.52E+05		
SET	Q01105-3	eFHLNESGDPSSk		5.97E+04			1.62E+05			3.36E+04			5.58E+04	
SET	Q01105-2	eFHLNESGDPSSk			9.32E+04			4.45E+05			4.71E+05			5.13E+04
SET	Q01105-2	eFHLNESGDPSSk			6.22E+04			2.93E+05			3.21E+05			3.66E+04
SET	Q01105-2	eFHLNESGDPSSk			1.89E+04			2.89E+05			8.43E+04			1.82E+04
SET	Q01105-3	eFHLNESGDPSSk	1.00E+05			3.92E+05			6.79E+04			1.40E+05		
SET	Q01105-3	eFHLNESGDPSSk	3.35E+04			1.40E+05			4.99E+04			4.26E+04		
SET	Q01105-3	eFHLNESGDPSSk	1.13E+05			3.02E+05			8.22E+04			1.55E+05		
SET	Q01105-3	eFHLNESGDPSSk		1.30E+05			3.14E+05			9.18E+04			1.38E+05	
SET	Q01105-3	eFHLNESGDPSSk		5.41E+04			8.14E+04			5.42E+04			3.83E+04	
SET	Q01105-3	eFHLNESGDPSSk		2.92E+04			9.30E+04			3.60E+04			4.38E+04	
SET	Q01105-2	eQQEAIEHIDEVQNEIDR			2.47E+04			1.31E+05			1.21E+05			2.12E+04
SET	Q01105-2	eQQEAIEHIDEVQNEIDR			1.59E+04			9.48E+04			9.01E+04			1.59E+04
SET	Q01105-2	eQQEAIEHIDEVQNEIDR			2.46E+04			1.04E+05			7.86E+04			1.05E+04
SET	Q01105-2	eQQEAIEHIDEVQNEIDR			1.86E+04			1.66E+05			5.74E+04			1.52E+04
SET	Q01105-3	eQQEAIEHIDEVQNEIDR	5.61E+04			1.96E+05			3.82E+04			8.58E+04		
SET	Q01105-3	eQQEAIEHIDEVQNEIDR	1.30E+05			3.92E+05			7.71E+04			1.70E+05		
SET	Q01105-3	eQQEAIEHIDEVQNEIDR	3.05E+04			1.23E+05			3.19E+04			4.14E+04		
SET	Q01105-3	eQQEAIEHIDEVQNEIDR	9.10E+03			3.88E+04			1.05E+04			1.30E+04		
SET	Q01105-3	eQQEAIEHIDEVQNEIDR	6.98E+04			2.55E+05			6.89E+04			8.50E+04		
SET	Q01105-3	eQQEAIEHIDEVQNEIDR	2.93E+04			9.71E+04			1.54E+04			2.84E+04		

Protein Name	Protein ID	Sequence	Parental Pool 1	Parental Pool 2	Parental Pool 3	Mutant Pool 1	Mutant Pool2	Mutant Pool 3	Het Pool 1	Het Pool 2	Het Pool 3	IgG Ctl Pool 1	IgG Ctl Pool 2	IgG Ctl Pool 3
SET	Q01105-3	eQQEAIEHIDEVQNEIDR		8.67E+04			2.26E+05			9.85E+04			1.08E+05	
SET	Q01105-3	eQQEAIEHIDEVQNEIDR		3.82E+04			1.11E+05			4.59E+04			5.04E+04	
SET	Q01105-3	eQQEAIEHIDEVQNEIDR		2.22E+04			6.18E+04			2.89E+04			2.94E+04	
SET	Q01105-3	eQQEAIEHIDEVQNEIDR		5.75E+04			1.56E+05			2.25E+04			4.57E+04	
SET	Q01105-2	iDFYFDENPYFENk			2.18E+04			3.58E+04			5.79E+04			1.39E+04
SET	Q01105-2	iDFYFDENPYFENk			1.84E+04			9.67E+04			8.27E+04			1.71E+04
SET	Q01105-2	iDFYFDENPYFENk			3.45E+04			1.65E+05			1.56E+05			2.83E+04
SET	Q01105-2	iDFYFDENPYFENk			3.35E+04			1.50E+05			9.81E+04			1.77E+04
SET	Q01105-2	iDFYFDENPYFENk			2.12E+04			9.88E+04			6.41E+04			1.25E+04
SET	Q01105-2	iDFYFDENPYFENk			1.45E+04			1.30E+05			4.13E+04			1.42E+04
SET	Q01105-2	iDFYFDENPYFENk			1.01E+03			1.64E+04			6.17E+03			8.86E+02
SET	Q01105-3	iDFYFDENPYFENk	8.87E+04			3.00E+05			4.65E+04			1.29E+05		
SET	Q01105-3	iDFYFDENPYFENk	6.40E+04			2.20E+05			3.37E+04			8.96E+04		
SET	Q01105-3	iDFYFDENPYFENk	1.11E+05			3.81E+05			5.39E+04			1.63E+05		
SET	Q01105-3	iDFYFDENPYFENk	8.88E+04			2.92E+05			4.45E+04			1.27E+05		
SET	Q01105-3	iDFYFDENPYFENk	5.45E+04			1.91E+05			4.92E+04			8.02E+04		
SET	Q01105-3	iDFYFDENPYFENk	6.61E+04			2.30E+05			5.32E+04			9.95E+04		
SET	Q01105-3	iDFYFDENPYFENk	7.65E+04			2.83E+05			6.04E+04			1.11E+05		
SET	Q01105-3	iDFYFDENPYFENk	2.69E+04			9.48E+04			2.02E+04			4.03E+04		
SET	Q01105-3	iDFYFDENPYFENk	7.89E+04			2.29E+05			3.68E+04			8.90E+04		
SET	Q01105-3	iDFYFDENPYFENk	1.44E+04			4.02E+04			6.88E+03			1.75E+04		
SET	Q01105-3	iDFYFDENPYFENk		1.18E+05			2.79E+05			8.21E+04			1.47E+05	
SET	Q01105-3	iDFYFDENPYFENk		4.63E+04			1.13E+05			3.66E+04			5.96E+04	

Protein Name	Protein ID	Sequence	Parental Pool 1	Parental Pool 2	Parental Pool 3	Mutant Pool 1	Mutant Pool2	Mutant Pool 3	Het Pool 1	Het Pool 2	Het Pool 3	IgG Ctl Pool 1	IgG Ctl Pool 2	IgG Ctl Pool 3
SET	Q01105-3	iDFYFDENPYFENk		1.24E+05			3.04E+05			8.75E+04			1.61E+05	
SET	Q01105-3	iDFYFDENPYFENk		7.73E+04			1.92E+05			5.38E+04			1.08E+05	
SET	Q01105-3	iDFYFDENPYFENk		5.16E+04			1.70E+05			4.36E+04			6.88E+04	
SET	Q01105-3	iDFYFDENPYFENk		4.58E+04			1.44E+05			3.70E+04			6.35E+04	
SET	Q01105-3	iDFYFDENPYFENk		8.12E+04			2.54E+05			7.21E+04			1.12E+05	
SET	Q01105-3	iDFYFDENPYFENk		3.55E+04			1.10E+05			2.74E+04			4.77E+04	
SET	Q01105-3	iDFYFDENPYFENk		3.66E+04			9.67E+04			1.42E+04			3.16E+04	
SET	Q01105-2	lNEQASEEILk			5.98E+03			2.37E+04			9.37E+03			1.11E+04
SET	Q01105-2	lNEQASEEILk			1.06E+05			6.29E+05			5.43E+05			1.04E+05
SET	Q01105-2	lNEQASEEILk			2.00E+04			1.19E+05			1.08E+05			1.53E+04
SET	Q01105-2	lNEQASEEILk			9.50E+04			5.63E+05			5.01E+05			6.51E+04
SET	Q01105-2	lNEQASEEILk			2.94E+04			1.70E+05			1.64E+05			2.54E+04
SET	Q01105-2	lNEQASEEILk			6.34E+04			3.01E+05			2.30E+05			3.82E+04
SET	Q01105-2	lNEQASEEILk			6.76E+03			6.64E+04			2.36E+04			7.98E+03
SET	Q01105-2	lNEQASEEILk			2.36E+04			2.15E+05			7.31E+04			2.61E+04
SET	Q01105-3	lNEQASEEILk	5.64E+04			2.24E+05			4.45E+04			6.93E+04		
SET	Q01105-3	lNEQASEEILk	5.52E+04			2.34E+05			3.09E+04			8.19E+04		
SET	Q01105-3	lNEQASEEILk	1.17E+05			4.50E+05			8.74E+04			1.48E+05		
SET	Q01105-3	lNEQASEEILk	1.03E+05			4.43E+05			8.15E+04			1.57E+05		
SET	Q01105-3	lNEQASEEILk	7.38E+04			3.07E+05			8.39E+04			1.05E+05		
SET	Q01105-3	lNEQASEEILk	3.32E+04			1.56E+05			3.94E+04			5.12E+04		
SET	Q01105-3	lNEQASEEILk	9.05E+04			3.80E+05			1.02E+05			1.30E+05		
SET	Q01105-3	lNEQASEEILk	3.92E+04			1.42E+05			2.41E+04			4.91E+04		

Protein Name	Protein ID	Sequence	Parental Pool 1	Parental Pool 2	Parental Pool 3	Mutant Pool 1	Mutant Pool2	Mutant Pool 3	Het Pool 1	Het Pool 2	Het Pool 3	IgG Ctl Pool 1	IgG Ctl Pool 2	IgG Ctl Pool 3
SET	Q01105-3	lNEQASEEILk	5.96E+04			2.36E+05			4.28E+04			5.35E+04		
SET	Q01105-3	lNEQASEEILk		1.70E+05			4.06E+05			1.74E+05			2.20E+05	
SET	Q01105-3	lNEQASEEILk		2.40E+05			5.36E+05			2.37E+05			3.06E+05	
SET	Q01105-3	lNEQASEEILk		9.44E+04			2.01E+05			9.08E+04			1.02E+05	
SET	Q01105-3	lNEQASEEILk		6.33E+04			1.67E+05			6.84E+04			7.86E+04	
SET	Q01105-3	lNEQASEEILk		1.16E+05			3.34E+05			1.33E+05			1.44E+05	
SET	Q01105-3	lNEQASEEILk		8.90E+04			2.37E+05			1.06E+05			1.25E+05	
SET	Q01105-3	lNEQASEEILk		2.49E+04			6.95E+04			1.28E+04			2.24E+04	
SET	Q01105-3	lNEQASEEILk		7.83E+04			2.13E+05			4.05E+04			6.35E+04	
SET	Q01105-2	mMSAPAAk			4.45E+04			5.09E+04			9.16E+04			3.94E+04
SET	Q01105-2	sSQTQNk			1.13E+04			1.44E+05			5.40E+04			7.13E+03
SET	Q01105-3	sSQTQNk	1.68E+04			6.83E+04			1.35E+04			1.92E+04		
SET	Q01105-3	sSQTQNk	1.67E+03			8.62E+03			2.34E+03			1.48E+03		
SET	Q01105-3	sSQTQNk	2.48E+04			7.95E+04			1.16E+04			3.43E+04		
SET	Q01105-3	sSQTQNk		2.23E+04			4.57E+04			2.35E+04			3.22E+04	
SET	Q01105-3	sSQTQNk		2.76E+04			7.22E+04			2.57E+04			3.35E+04	
SET	Q01105-3	sSQTQNk		3.79E+03			1.45E+04			4.53E+03			5.65E+03	
SET	Q01105-3	sSQTQNk		3.43E+03			1.50E+04			2.24E+03			5.79E+03	
SET	Q01105-3	sSQTQNk		3.68E+04			1.38E+05			2.29E+04			5.34E+04	
SET	Q01105-3	sSQTQNk	6.26E+03			2.56E+04			5.28E+03			9.65E+03		
SET	Q01105-2	sTElk			1.97E+04			6.66E+04			6.76E+04			1.01E+04
SET	Q01105-3	sTElk		9.13E+04			2.67E+05			4.13E+04			8.47E+04	
SET	Q01105-3	sTElk		3.95E+04			1.29E+05			4.64E+04			5.85E+04	

Protein Name	Protein ID	Sequence	Parental Pool 1	Parental Pool 2	Parental Pool 3	Mutant Pool 1	Mutant Pool2	Mutant Pool 3	Het Pool 1	Het Pool 2	Het Pool 3	IgG Ctl Pool 1	IgG Ctl Pool 2	IgG Ctl Pool 3
SET	Q01105-3	sTEIk		9.53E+04			3.35E+05			1.35E+05			1.42E+05	
SET	Q01105-2	vEVTEFEDIk			1.44E+05			7.17E+05			6.32E+05			1.13E+05
SET	Q01105-2	vEVTEFEDIk			3.48E+04			2.07E+05			1.71E+05			3.03E+04
SET	Q01105-2	vEVTEFEDIk			9.99E+04			5.95E+05			5.41E+05			9.22E+04
SET	Q01105-2	vEVTEFEDIk			1.89E+04			1.10E+05			9.03E+04			1.66E+04
SET	Q01105-2	vEVTEFEDIk			8.59E+04			4.20E+05			3.00E+05			5.17E+04
SET	Q01105-2	vEVTEFEDIk			9.64E+02			4.70E+03			1.87E+03			9.47E+02
SET	Q01105-2	vEVTEFEDIk			3.04E+04			2.78E+05			8.31E+04			3.07E+04
SET	Q01105-2	vEVTEFEDIk			1.63E+04			1.44E+05			4.63E+04			1.72E+04
SET	Q01105-2	vEVTEFEDIk			1.48E+04			1.52E+05			4.55E+04			1.46E+04
SET	Q01105-3	vEVTEFEDIk	3.30E+05			1.25E+06			2.05E+05			4.59E+05		
SET	Q01105-3	vEVTEFEDIk	5.99E+04			2.29E+05			3.92E+04			8.82E+04		
SET	Q01105-3	vEVTEFEDIk	6.77E+04			2.62E+05			4.20E+04			9.81E+04		
SET	Q01105-3	vEVTEFEDIk	1.20E+05			5.14E+05			9.38E+04			2.01E+05		
SET	Q01105-3	vEVTEFEDIk	9.91E+04			3.94E+05			9.79E+04			1.36E+05		
SET	Q01105-3	vEVTEFEDIk	3.52E+04			1.77E+05			4.79E+04			6.53E+04		
SET	Q01105-3	vEVTEFEDIk	2.92E+04			9.31E+04			1.62E+04			3.39E+04		
SET	Q01105-3	vEVTEFEDIk	2.55E+04			8.58E+04			1.66E+04			3.33E+04		
SET	Q01105-3	vEVTEFEDIk		1.46E+05			3.12E+05			1.51E+05			1.88E+05	
SET	Q01105-3	vEVTEFEDIk		1.02E+05			2.33E+05			9.39E+04			1.40E+05	
SET	Q01105-3	vEVTEFEDIk		1.10E+05			2.21E+05			9.33E+04			1.34E+05	
SET	Q01105-3	vEVTEFEDIk		9.25E+04			2.15E+05			8.99E+04			1.18E+05	
SET	Q01105-3	vEVTEFEDIk		1.68E+05			5.11E+05			1.86E+05			2.35E+05	

Protein Name	Protein ID	Sequence	Parental Pool 1	Parental Pool 2	Parental Pool 3	Mutant Pool 1	Mutant Pool2	Mutant Pool 3	Het Pool 1	Het Pool 2	Het Pool 3	IgG Ctl Pool 1	IgG Ctl Pool 2	IgG Ctl Pool 3
SET	Q01105-3	vEVTEFEDIk		3.35E+04			9.75E+04			3.98E+04			4.41E+04	
SET	Q01105-3	vEVTEFEDIk		3.79E+04			9.65E+04			1.21E+04			2.72E+04	
SET	Q01105-3	vEVTEFEDIk		3.51E+04			8.18E+04			1.20E+04			2.71E+04	
IGBP1	P78318	eASTSNSSR		1.39E+03			1.90E+03			1.93E+03				
IGBP1	P78318	eASTSNSSR			5.52E+03			6.67E+03			1.35E+04			4.35E+03
IGBP1	P78318	sAVESGQADDER	1.71E+03			1.08E+04			8.64E+03			8.50E+02		
IGBP1	P78318	sAVESGQADDER	1.24E+04			2.45E+04			3.23E+04			6.93E+03		
IGBP1	P78318	sAVESGQADDER		1.91E+04			3.07E+04			2.88E+04			2.27E+04	
IGBP1	P78318	sAVESGQADDER		7.84E+03			1.56E+04			1.26E+04			9.80E+03	
IGBP1	P78318	sAVESGQADDER			3.86E+03			3.94E+03			5.97E+03			1.40E+03
PPME1	Q9Y570	lPSRPPLPGSGGSQSGAk	2.58E+04			1.49E+05			9.02E+04			1.94E+04		
PPME1	Q9Y570	lPSRPPLPGSGGSQSGAk	3.56E+04			1.29E+05			1.20E+05			1.96E+04		
PPME1	Q9Y570	lPSRPPLPGSGGSQSGAk			9.22E+03			1.42E+04			2.37E+04			6.52E+03
PPME1	Q9Y570	nIESAR	1.87E+04			6.40E+04			6.98E+04			1.46E+04		
PPME1	Q9Y570	nIESAR		3.72E+04			8.38E+04			6.81E+04			4.18E+04	
PPME1	Q9Y570	nIESAR			4.52E+04			6.36E+04			9.48E+04			2.15E+04
PPME1	Q9Y570	nPEDLSAETMAk	2.12E+03			9.52E+03			1.63E+04			2.00E+03		
PPME1	Q9Y570	nPEDLSAETMAk			2.17E+04			3.51E+04			8.47E+04			1.48E+04
PPME1	Q9Y570	nPEDLSAETMAk			8.70E+03			9.44E+03			1.25E+04			1.44E+03
PPME1	Q9Y570	qcEGITSPEGSk	2.04E+04			5.27E+04			6.79E+04			9.91E+03		
PPME1	Q9Y570	qcEGITSPEGSk	5.73E+03			1.90E+04			3.13E+04			1.79E+03		
PPME1	Q9Y570	qcEGITSPEGSk		3.47E+04			3.67E+04			3.38E+04			2.27E+04	
PPME1	Q9Y570	qcEGITSPEGSk		1.99E+04			2.37E+04			2.25E+04			1.68E+04	
PPME1	Q9Y570	qcEGITSPEGSk		1.82E+04			2.31E+04			2.48E+04			1.17E+04	
PPME1	Q9Y570	qcEGITSPEGSk			1.41E+04			2.54E+04			4.16E+04			8.86E+03
PPME1	Q9Y570	qcEGITSPEGSk			5.19E+03			7.68E+03			1.17E+04			1.84E+03
PPME1	Q9Y570	sHGETk	2.12E+03			8.50E+03			1.18E+04			8.66E+02		
PPME1	Q9Y570	sHGETk		1.22E+04			1.58E+04			1.16E+04			1.20E+04	
PPME1	Q9Y570	sIVEGIIEEEEEDEEGSESISk		9.59E+03			1.22E+04			3.39E+03			4.67E+03	
PPME1	Q9Y570	sIVEGIIEEEEEDEEGSESISk			1.14E+04			1.48E+04			1.86E+04			4.72E+03

Protein Name	Protein ID	Sequence	Parental Pool 1	Parental Pool 2	Parental Pool 3	Mutant Pool 1	Mutant Pool2	Mutant Pool 3	Het Pool 1	Het Pool 2	Het Pool 3	IgG Ctl Pool 1	IgG Ctl Pool 2	IgG Ctl Pool 3
PPME1	Q9Y570	sIVEGIIEEEEEDE EGSESISk			4.27E+03			1.21E+04			7.30E+03			2.16E+03
PPME1	Q9Y570	sLENAIEWSVk		2.03E+04			7.35E+04			6.05E+04			2.71E+04	
PPME1	Q9Y570	sLENAIEWSVk			1.53E+04			1.74E+04			6.09E+04			8.27E+03

Table F.9 Peptide list used for *PPP2R1A* immunoprecipitation mass spectrometry quantitation